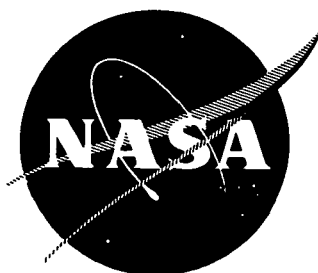JULY 1972

APPLICATIONS TECHNOLOGY SATELLITE ADVANCED MISSION STUDY

FINAL REPORT

Contract No. NAS 3-14359

HUGHES

HUGHES AIRCRAFT COMPANY
SPACE AND COMMUNICATIONS GROUP

Hughes Ref. No. C2266 • SCG 20498R

1. Report No. NASA CR 120872	2. Government Accession No.	3. Recipient's Catalog No.
4. Title and Subtitle Applications Technology Satellites Advanced Mission Study		5. Report Date
		6. Performing Organization Code
7. Author(s) L. M. Gould		8. Performing Organization Report No.
		10. Work Unit No.
9. Performing Organization Name and Address Hughes Aircraft Company Space and Communications Group P. O. Box 92919 Los Angeles, California 90009		
		11. Contract or Grant No. NAS 3-14359
		13. Type of Report and Period Covered Contractor Report
12. Sponsoring Agency Name and Address National Aeronautics and Space Administration Washington, D. C. 20546		
		14. Sponsoring Agency Code

15. Supplementary Notes

Project Manager, Robert E. Alexovich,   Division,
NASA Lewis Research Center, Cleveland, Ohio

16. Abstract

Three spacecraft configurations were designed for operation as a high powered synchronous communications satellite. Each spacecraft includes a 1 kw TWT and a 2 kw Klystron power amplifier feeding an antenna with multiple shaped beams. One of the spacecraft is designed to be boosted by a Thor-Delta launch vehicle and raised to synchronous orbit with electric propulsion. The other two are inserted into a elliptical transfer orbit with an Atlas Centaur and injected into final orbit with an apogee kick motor. Advanced technologies employed in the several configurations include tubes with multiple stage collectors radiating directly to space, multiple-contoured beam antennas, high voltage rollout solar cell arrays with integral power conditioning, electric propulsion for orbit raising and on-station attitude control and station-keeping, and liquid metal slip rings.

17. Key Words (Suggested by Author(s)) Communication Satellite Electric Propulsion High Power Transmitters	18. Distribution Statement Unclassified - Unlimited

19. Security Classif. (of this report) Unclassified	20. Security Classif. (of this page) Unclassified	21. No. of Pages	22. Price*

CONTENTS

i

CONTENTS (Continued)

FIGURES

FIGURES (Continued)

FIGURES (Continued)

FIGURES (Continued)

TABLES

TABLES (Continued)

1. INTRODUCTION AND SUMMARY

1.1 INTRODUCTION

The Applications Technology Satellites Advanced Mission Study (ATS/AMS) was directed toward the design of alternative synchronous orbit spacecraft concepts capable of carrying high powered communications and related technology experiments. This study was initiated on 19 January 1971, and was originally scheduled to be completed in approximately a seven month period. However, the period of performance was extended by a contract change which added the task of the preliminary design of a large-aperture lens antenna. The engineering design effort was completed in mid-February, 1972.

1.2 MISSION OBJECTIVES

The communications experiments to be performed with the advanced mission spacecraft were abstracted from the contract statement of work and are summarized as follows:

- The simultaneous operation of two high-power, 12-GHz transmitters,* one capable of delivering at least one kilowatt of RF power and the other capable of delivering up to two kilowatts. Both transmitters must also be capable of operation at output levels as low as 6 db below their saturation level.

- The simultaneous transmission over two or more contoured antenna beams shaped to illuminate predetermined geographic areas on the earth's surface.

- Demonstrating the use of the high power transmitters and contoured beams in a variety of broadcast and information networking systems servicing small user terminals.

---

*The initial study objective was to include one transmitter with an output of at least one kilowatt. The additional two kilowatt transmitter should properly be identified as a selected candidate from the list of potential experiments considered for this mission.

In addition to the communications experiments, the following advanced technologies were to be considered and are included in each of the configuration baseline designs, either as primary spacecraft subsystems or as experiments:

- High voltage solar arrays, with bus voltages of up to 15 kilovolts.

- Liquid Metal Slip Rings

- Electric Propulsion for orbit raising and/or on-station attitude control and stationkeeping.

Other potential experiments were identified, as listed in Table 1-1. Selected experiments were to be incorporated into the spacecraft designs to the extent that their excess payload capacity permitted. However, after including the two-kilowatt transmitter, none of the baseline spacecraft configurations had sufficient weight margins* to consider the inclusion of additional experiments.

TABLE 1-1. POTENTIAL EXPERIMENTS

- K-Band Satellite-to-Satellite Communications Link

- Optical Satellite-to-Satellite Communications Link (CO_2 Laser)

- VHF Synchronous Satellite to Low Altitude Satellite Link

- High Frequency (30-60 GHz) data relay

- Optical Communications between Spacecraft and Ground

- Optical Beacon for Spacecraft Tracking

- Environmental and/or Attitude Sensors

- Liquid Metal Bearings

---

*Recently received data on improved performance of the Atlas/Centaur launch vehicle now indicate some additional weight margin for the baseline configurations using this launch vehicle.

1.3 BASELINE SPACECRAFT CONFIGURATIONS

In accordance with the contract statement of work, three spacecraft configurations were to be designed. After initial configuration definition, it was possible to select launch vehicles and upper stage combinations, as summarized later in this section. The selected propulsion systems for the three configuration groups, identified as A, B and C, are:

- Configuration A, a Thor-Delta three-stage (2914) launch vehicle for insertion into transfer orbit with electric propulsion for orbit raising to final synchronous station.

- An Atlas Centaur launch vehicle with an apogee kick motor for synchronous injection for Configuration B.

- An Atlas Centaur for boosting to transfer orbit and electric propulsion for orbit raising to synchronous station for Configuration C. The latter approach (Configuration C) was essentially a back-up for Configuration A in the event the first propulsion system could not deliver sufficient payload to achieve mission objectives.

After it was established that the Thor-Delta/Electric Propulsion system would provide adequate payload, it was directed that the C Configuration group be dropped from further consideration and that emphasis be placed upon three vehicles carrying essentially identical communications subsystems. After looking at several variants in each of the groups, the selected baseline configurations now include one from Group A (A-1), and two from Group B (B-1 and B-5), each of which is described below. One of the configurations in the B Group was further modified to incorporate the lens antenna.

1.3.1 Spacecraft Configuration A-1

The A-1 baseline configuration is the only one which uses electric propulsion for achieving synchronous station and for performing attitude control and stationkeeping functions once on synchronous station. An artist's concept of the A-1 spacecraft is shown in Figure 1-1.

It is boosted into an elliptical transfer orbit with a Thor-Delta 2914 launch vehicle which requires an elongated fairing to accommodate the spacecraft's solar panels. After separation from the booster and separation rates have been nulled, the solar panels are unfurled and the required attitude for low-thrust orbit raising is acquired. Orbit raising, using three 30-cm mercury bombardment ion engines, takes about 80 days to achieve synchronous orbit.

On-station, the vehicle is oriented with its longitudinal axis parallel to the earth's polar axis (top-to-bottom in Figure 1-1). The solar panels are deployed about an axis which lies in orbit plane, and are free to rotate about this axis so that the panels are always normal to the sun line-of-site (LOS).

POWER AMPLIFIER

ANTENNA
FEED ASSEMBLY

EARTH SENSOR

1.83 m PARABOLIC
REFLECTOR

ROLL-OUT
SOLAR PANEL

LIQUID METAL
SLIP RING
ASSEMBLY

5 cm ION ENGINES

30 cm ION ENGINES

TT&C ANTENNA

SEPARATION WEIGHT   624 Kg

INITIAL STATION
WEIGHT   570 Kg

TIME TO STATION   80 DAYS

2.6 m

23.8 m

2.14 m
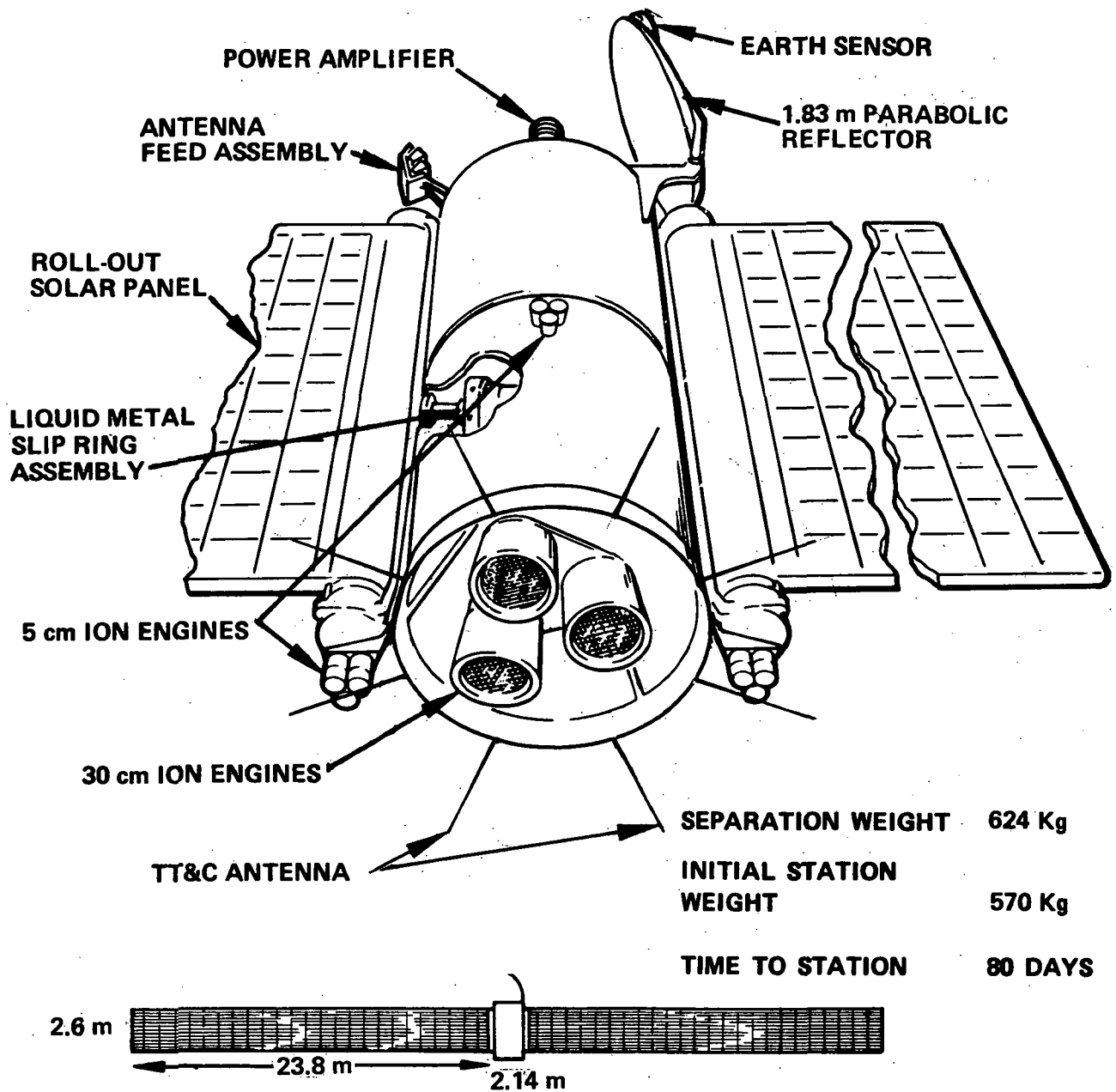
Figure 1-1. Spacecraft A-1

The spacecraft body, to which the solar panels are attached, rotates once per year to present a constant aspect toward the sun. The communications platform, shown at the top of the spacecraft in Figure 1-1, rotates one revolution per day with respect to the spacecraft body, thereby maintaining the antenna boresite earth-oriented.

The communications platform is coupled to the spacecraft with a single liquid metal slip ring (LMSR) assembly. The two roll-out solar cell arrays are coupled to the spacecraft with a dual LMSR assembly. Other major components are identified in Figure 1-1.

The communications platform houses the Communications Subsystem, which is comprised of a repeater and an antenna assembly. The Antenna Subsystem includes a 1.83 m. diameter offset section of a parabolic reflector and a cluster of feed horns located about the focal point of the reflector. The offset reflector was chosen to minimize blockage from the feed cluster. The reflector is stowed during launch and may be deployed after separation from the booster or upon arriving on station.

The repeater power amplifiers (one 1-kilowatt TWT and one 2-kilowatt klystron) are mounted on the communications platform with their collectors exposed, as shown in Figure 1-1, so that their large thermal dissipation can be radiated directly to space.

Attitude control and stationkeeping maneuvers are accomplished by intermittent operation of three clusters of 30-cm ion engines. North-South (N-S) stationkeeping velocity increments are provided by the two south facing clusters mounted below the solar panels, operating at a duty cycle of about 1/6 ($\pm 30^{\circ}$ about an orbit nodal crossing). East-West (E-W) stationkeeping is performed by the third cluster, shown on the side of the spacecraft body in Figure 1-1, operating at a duty cycle of about 1/8 during periods when the N-S clusters are off. Continuous control of attitude is maintained by three reaction wheels and a three-axis gyro attitude reference. A sun sensor and an earth sensor are used to determine absolute attitude for periodic updating of the gyro reference.

Overall spacecraft weight and power budgets are summarized in Table 1-2. The on-station dry weight of 560 Kg includes a contingency of 42 Kg, which is generally considered quite low at this stage of design. However, for a spacecraft raised to final orbit with a low-thrust propulsion system, it is possible to trade off spacecraft weight against end-of-life (EOL) solar array power and orbit raising time by varying the parameters of the initial transfer orbit at the time the vehicle is launched. This flexibility, which does not exist for chemically injected spacecraft, justifies the use of somewhat lower contingency factors than with conventional propulsion systems.

About 9 Kg of mercury are expended for on-station attitude control and stationkeeping, and about 55 Kg for orbit raising. Allowing an additional 37 Kg for the attached fitting, the resultant booster payload is 661 Kg.

TABLE 1-2.   CONFIGURATION A-1 WEIGHT
AND POWER SUMMARIES

Weight	Kilograms	(Pounds)
Basic Spacecraft Plus Payload	518.0	(1,140)
Contingency	42.0	(92)
Spacecraft Dry Weight	560.0	(1,232)
ACS Expendables	9.1	(20)
Weight into Sync Orbit	569.1	(1,252)
Orbit Raising Expendables	54.5	(120)
Separation Weight	623.6	(1,372)
Attach Fitting	37.3	(60)
Thor-Delta Payload (Elliptic Transfer Orbit)[*]	661	(1,432)

Power	Kilowatts
Beginning of Life (1 A.U.)	10.2
End of Life (1.02 A.U. 0° Sun Angle, 0.65 Radiation Degradation Factor)	6.5
Required	6.0

[*]Apogee altitude of 31,900 kilometers, perigee altitude 555 kilometers.

Parameters of the elliptical transfer orbit with this booster payload are given in the footnote of Table 1-2 (factors leading to the selection of this orbit are summarized in Section 1.6).

The spacecraft requires 6 kilowatts for normal daylight operation. The solar panels are designed with an initial capability of 10.2 kilowatts, degrading to an EOL output of 6.5 kilowatts at summer solstice after five years of operation, leaving a margin of 500 watts. Most of the panel degradation occurs during that portion of the orbit raising period when the spacecraft repeatedly passes through the Van Allen radiation belts.

1-6

The principal spacecraft subsystems are identified in Table 1-3. Since most of the subsystems are the same or very similar for all three baseline configurations, their descriptions are all summarized in Section 1.4, following the discussion of the other baseline spacecraft.

1.3.2 Spacecraft Configurations B-1 and B-5

The spacecraft shown in Figure 1-2 is illustrative of both the B-1 and the B-5 baseline configurations. The two configurations differ in the technologies employed in their subsystems.

Both are launched into a near-synchronous apogee elliptical transfer orbit with an Atlas/Centaur launch vehicle and injected into synchronous orbit with an apogee kick motor (AKM) whose performance is optimized to match that of the launch vehicle.

As indicated in the illustration, the on-station orientation of the spacecraft is such that the solar panels are deployed along an axis parallel to the earth's polar axis, and the panels are free to rotate about this axis so as to remain pointed toward the sun. (Since the panels have only one degree of freedom relative to the orbit, they experience an annual cyclic variation relative to the sun LOS due to the inclination of the earth's axis relative to the ecliptic.)

The spacecraft body, which includes the communications subsystem, is nominally oriented with its longitudinal axis tangential to the orbit and rotates once per day so as to maintain the antenna boresight toward its designated target on the earth's surface.

As in the A-1 Configuration, the solar panels are coupled to the spacecraft body with a double-ended slip ring assembly. Conventional ring-brush slip rings, low voltage solar cell arrays, and conventional power conditioning

TABLE 1-3. PRINCIPAL SUBSYSTEMS
ATS/AMS SPACECRAFT

- Communications

- Attitude Control and Stationkeeping

- Orbit Raising

- Electrical Power

- Thermal Control

- Telemetry and Command

are employed in the B-1 Configuration. B-5 utilizes LMSRs and high voltage solar panels with integrated power conditioning.

The communications subsystem for both the B-1 and the B-5 space-craft is the same as that for A-1; however, the launch vehicle fairing for the B configurations permits the 1.83 m. diameter antenna reflector to be rigidly fixed to the spacecraft. The power amplifiers are mounted on opposite faces of the spacecraft, one of which is visible in Figure 1-2.

INITIAL STATION WEIGHT   895 Kg
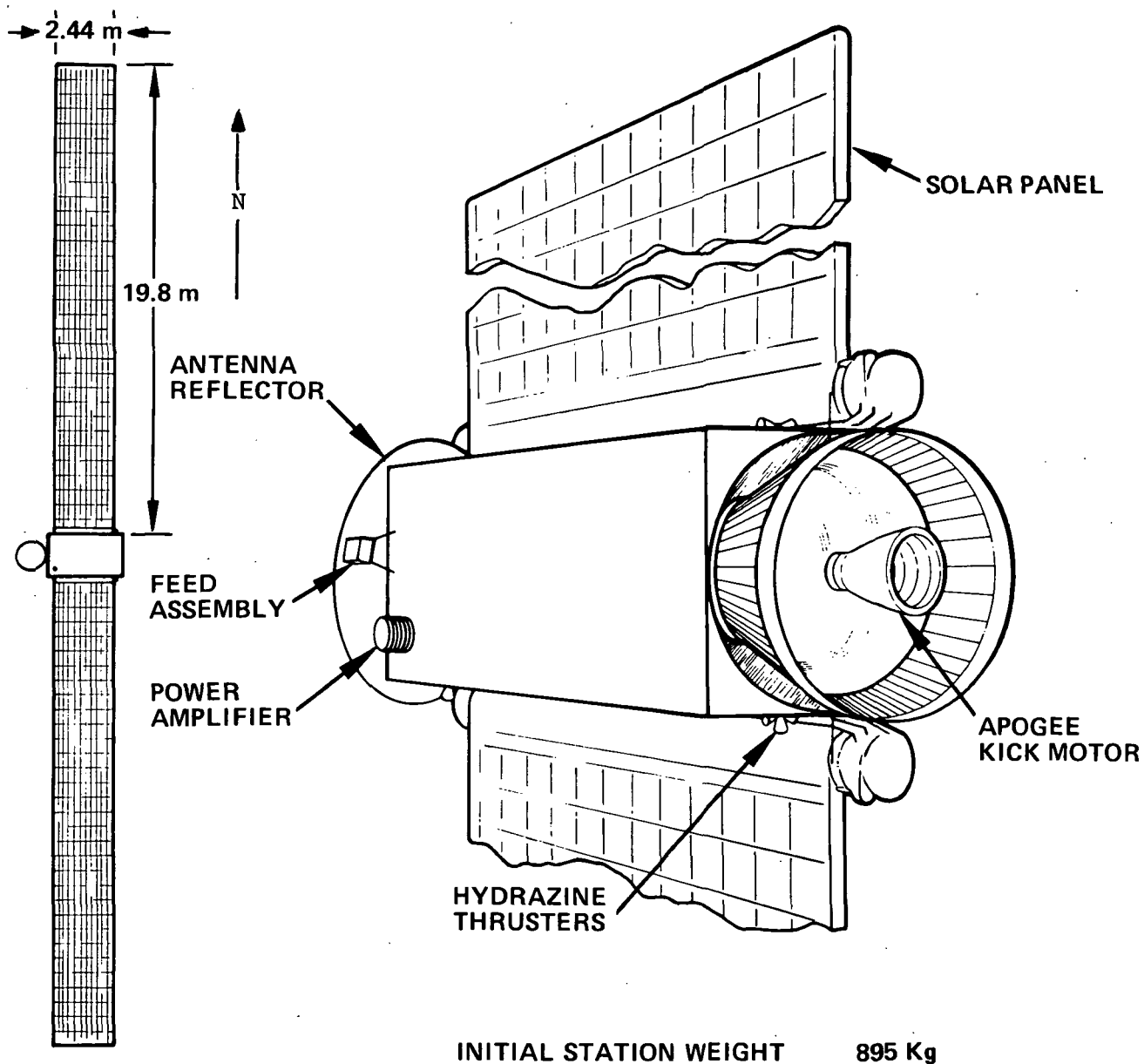
Figure 1-2.   Spacecraft B-1 or B-5

The Attitude Control and Stationkeeping subsystems are the same for both B spacecraft, and are functionally similar to that described for Configuration A-1. The principal difference between the A and B baselines is the use of a Hydrazine Reaction Control System (N_2H_2 RCS) in the B baselines in place of the clusters of 30-cm ion engines used in Configuration A-1.

1.3.3 Spacecraft Configuration B-1A

The B-1A Configuration, illustrated in Figure 1-3, is a modification of the B-1 design incorporating the 2.44 meter lens antenna designed during the final phase of the study. A 2.44 meter diameter lens antenna is about the largest which can be accommodated within the diameter of the Intelsat IV fairing without folding of the lens and deploying the lens and/or the feed assembly. The fairing must also be extended about 1.8 to 2.5 meters to accommodate this size antenna.

The boresite axis of the antenna is canted relative to the spacecraft axes requiring that the on-station orientation of the satellite be rotated (about the solar panel axis) with respect to the orientation of the B-1 or B-5 spacecraft. This necessitated a corresponding canting of the RCS thrust axis for E-W stationkeeping. Otherwise, this configuration is essentially identical to that of the B-1 spacecraft; the same changes could equally be applied to Configuration B-5.

Weight and power estimates are shown in Table 1-4 together with those of the B-1 and B-5 spacecraft.
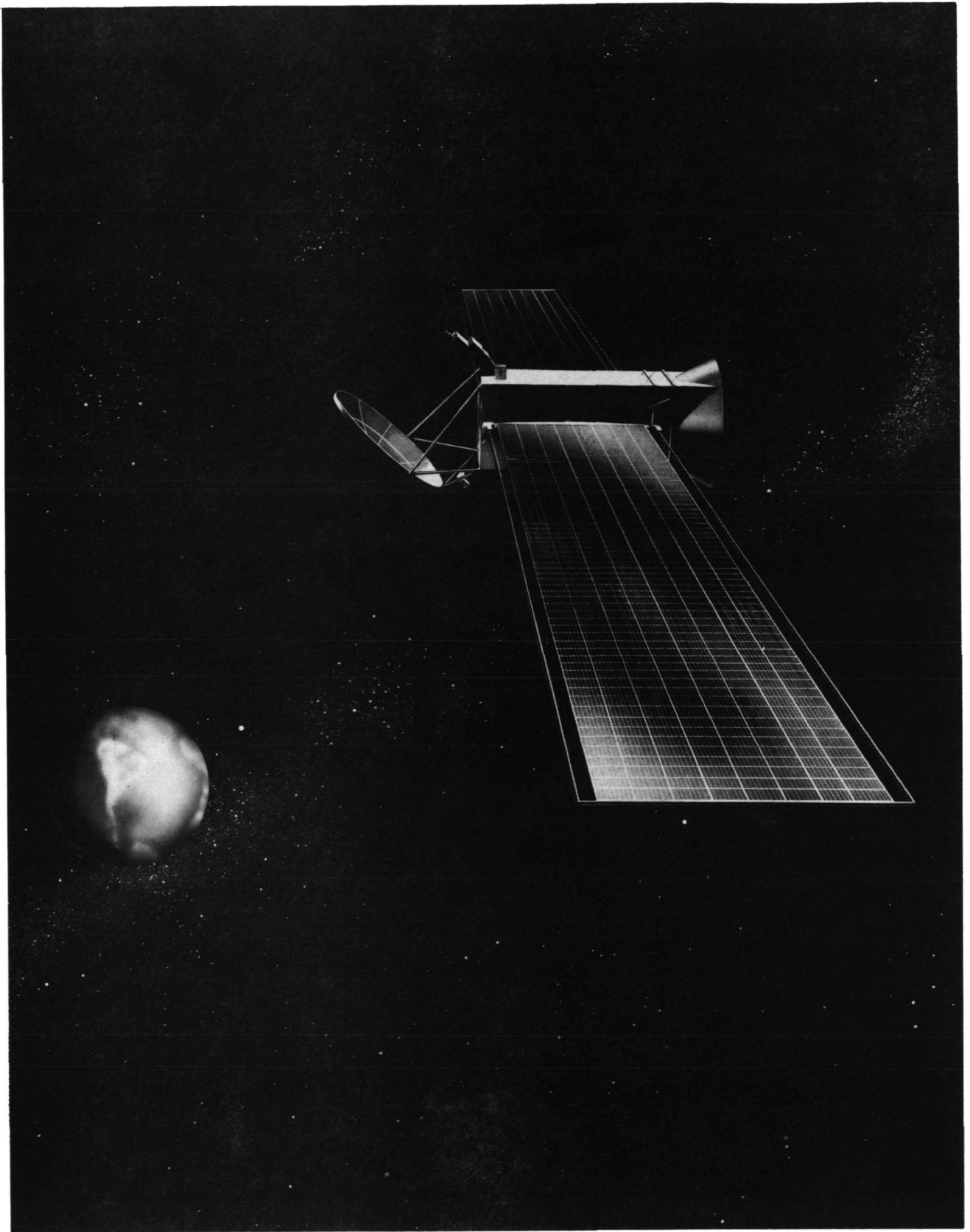
Figure 1-3. Spacecraft Configuration B-1A

TABLE 1-4. B SPACECRAFT BASELINE WEIGHT AND POWER SUMMARIES

	B-1	B-5	B-1A
Weight	Kilograms (Pounds)		
Basic Spacecraft Plus Payload	516 (1135)	480 (1055)	528 (1160)
Contingency or Additional P/L Capability	209 (460)	245 (540)	186 (410)
	725	725	714
Spacecraft Dry Weight	(1595)	(1595)	(1570)
ACS Expendables	170 (375)	170 (375)	168 (370)
	895	895	882
Atlas-Centaur Payload*	(1970)	(1970)	(1940)
Power	Kilowatts		
Beginning of Life (1 A.U.)	8.0		
End of Life (1.02 A.U. 23° Angle, 0.85 Radiation Degradation Factors)	6.0		
Power Required	5.6		

*Net payload into synchronous orbit. For B-1A, with an extended shroud, the decrease of payload into synchronous orbit is estimated at 13.6 Kg.

1.4 SUBSYSTEM AND TRADEOFF SUMMARIES

The implementation tradeoffs performed during the study which strongly influenced the spacecraft configurations are summarized in Table 1-5. The most significant of these, booster selection, is specifically discussed below. Others are included in the subsystem summaries, where relevant.

TABLE 1-5. ATS/AMS CONFIGURATION TRADEOFF SUMMARY

Tradeoff	Advantages	Disadvantages
Booster Selection		
a. Thor-Delta/electric propulsion	• Low Cost	• Long orbit raising time (80 days) • Higher risk • Development of electric thrusters required • Lowest recurring cost
b. Atlas Centaur/standard apogee motor	• Reliable, low risk • Short orbit raising time • No development	• No weight margin for baseline
c. Atlas Centaur/optimum apogee motor	• Maximum payload capability • Allows completely conventional approach, lowest risk	• Highest recurring cost • Minor development required
High Voltage Versus Low Voltage Solar Panels		
a. High voltage with integral power conditioning	• Lower spacecraft weight • Better spacecraft thermal integration	• Development required • Higher cost • Lower reliability, higher risk • Greater spacecraft integration problems • More S/C commands required
b. Low voltage panels with conventional power	• Proven approach • Lower cost • Ease of manufacture and test • Simpler design	• Heavier spacecraft weight • More thermal integration problems
N-S Versus E-W of Solar Panels		
a. N-S panels	• Enables use of both north and south faces as thermal radiators • Can perform the communication mission with one rotating joint • Principal solar torque is cyclic thus saving ACS fuel • No interference in LOS to earth for sensors	• Loss of power during summer and winter solstice • Restricts use of electric propulsion for attitude control and stationkeeping due to plume impingement
b. E-W panels	• Power advantage during solstices • Electric thrusters can be body mounted for ACS	• Thermal radiator is restricted to north end for transmitter waste heat • Requires two rotating joints to perform communication mission • Small interference in earth sensor LOS
Foldout vs Rollout Solar Panels		
a. Foldout	• Potentially small weight saving • Can be used as thermal shield during transfer orbit on B-1 and B-5	• Deployment difficult to control in lengths of interest
b. Rollout	• Smooth deployment process • Compact storage on drum • Easier to mechanize retraction if desired	• More complex
Conventional vs Liquid Metal Sliprings		
a. Conventional	• Developed technology • Proven reliability • Lower cost	• High friction torque • Electrical noise • Wear debris
b. Liquid Metal	• Low resistance and power loss • Negligible electrical noise • No wearout mode • Stick-slip friction replaced by negligible viscous friction	• Need for temperature control of assembly • Maintain (prelaunch) inert environment • Higher cost • Higher risk

TABLE 1-5. (continued)

Tradeoff	Advantages	Disadvantages
Electric vs Hydrazine Thrusters for RCS		
a. Electric thruster	• Finer granularity in control • Significant weight saving	• Development required • Not fully space proven
b. Hydrazine RCS	• Proven reliability • Off the shelf system available	• Potential spacecraft/solar panel dynamic interactions • Heavier weight
High vs Low Collector Temperatures		
a. High temperature	• Waste heat removed by direct radiation, lower spacecraft radiator weight • Larger overall RF powers possible	• Greater difficulty in obtaining vacuum seals at high temperatures • Local protection required for other spacecraft hardware
b. Low temperature	• Proven design • Space experience available	• Total spacecraft RF limited from a thermal standpoint • Creator thermal radiator weight

1.4.1 Propulsion System Selection

At the outset of this study, it was established that the baseline spacecraft designs would include at least one configuration which used electric propulsion to achieve synchronous orbit from a chemically injected transfer orbit, and at least one configuration which utilized an all-chemical propulsion subsystem for achieving final orbit. Specific launch vehicles and apogee kick motors to be considered were also cited in the statement of work. However, before the propulsion selection could be performed, it was necessary to make preliminary spacecraft configuration designs to provide volumetric and weight constraints on the propulsion system. This effort resulted in the requirement for a minimum on-station payload requirement[*] of about 570 Kg for a low-thrust orbit raising mission and about 525 Kg for one using an AKM.

The principal propulsion system candidates are listed in Table 1-6, together with pertinent cost and performance data. Beyond the minimum mission constraints, the primary factors influencing the selection, in order of priority, are cost, status of hardware, and development risk.

As indicated in Table 1-6, the Thor-Delta booster with electric propulsion was selected for the A-1 spacecraft. Although high in development risk, in that electric propulsion is still in the development stage, it represents a substantially lower cost propulsion system than any of the alternatives.

---

[*]This requirement is based upon a minimum mission capability which did not include the second high power transmitter included in the final baseline designs.

TABLE 1-6. PROPULSION SYSTEM TRADEOFF PARAMETERS

	Thor-Delta 2914 Electric Propulsion	Atlas-Centaur SVM 4 Apogee Motor	Atlas-Centaur Optimum Apogee Motor	Atlas-Centaur Electric Propulsion	Titan 3C
L/V Cost [1]	6 M[2]	16 M	16 M	16 M[2]	22 M
Payload into Synchronous Transfer Orbit	775 Kgs (1550 lbs)		2050 Kgs[3] (4100 lbs)	2050 Kgs[3] (4100 lbs)	
Payload into Synchronous Orbit	630 Kgs (1252 lbs)	725 Kgs (1450 lbs)	985 Kgs (1970 lbs)	1458 Kgs (3200 lbs)	1720 Kgs (3433 lbs)
Development Required	Electric Propulsion	None	Apogee Motor	Electric Propulsion	None
Orbit Raising Time	80 days	1 day	1 day	120 days	1 day
Spacecraft Designs:					
Baseline	A-1		B-1, B-5		
Other	A-2, A-3	B0, B2-B4		C1-C2	

[1] Recurring cost, in 1971 dollars.

[2] The cost of electric propulsion plus the added solar panels required in excess of that needed for on-station operation must be added for comparing total system cost. For the Thor-Delta 2914 (Configuration A-1), this is about \$2M, and for the Atlas-Centaur (Configuration C-1), about \$6.5M.

[3] 3-sigma capability as obtained recently from General Dynamics. The resultant on-station payload (985 Kgs) is about 140 Kgs more than was used during the study for performance of the Atlas-Centaur with an optimum AKM.

The Atlas/Centaur with an optimized AKM was selected for the B baseline configurations. The use of a new AKM has a small development risk, as well as additional development cost over the use of the existing SVM-4 apogee motor, but was preferred because of the poor match between the SVM-4 and the Atlas/Centaur capability. Should one of the alternate B configurations indicated in Table 1-6 ultimately be selected, the performance with the SVM-4 may be adequate.

The Atlas/Centaur with electric propulsion and the Titan IIIC both provided substantially more capability than is required, and the Titan was ruled out for this reason as well as for its high cost. The Atlas/Centaur-electric propulsion combination was initially selected for the C spacecraft configuration in the event that the Thor-Delta would not provide sufficient capability for the mission. However, as indicated earlier, all of the C configurations were dropped from further consideration when it was established that Configuration A would support the minimum mission plus a second high power transmitter.

1.4.2 Communications Subsystem

The communications subsystem design, common to all of the baseline spacecraft configurations, is shown in the functional diagram of Figure 1-4. As is evident from the diagram, it is essentially a two-channel repeater. However, depending upon the configuration of the switching networks and the frequency filters, selectable by ground command, it can be operated in a number of modes to support a variety of broadcast and networking applications. The principal operating modes are defined below, following the discussion of the principal elements of the subsystem.

1.4.2.1 Antenna Subsystem

The baseline antenna design, shown conceptually in Figure 1-5, consists of a 1.8 meter diameter section of a paraboloidal reflector with a focal length of 1.8 meters, an assembly of feed horns clustered in the vicinity of the focal point of the reflector, and associated switches and electronics for selecting the desired elements of the feed assembly (not shown in Figure 1-5). As indicated in the illustration, the multiple feed assembly consists of nine horns. Two of these are dedicated to the Hawaiian and Alaskan beams, and the other seven, in various combinations, are used to generate the four time zone beams as well as a 48 state beam.

The antenna beam dimensions and performance (at beam edge) are given below in Table 1-7.

TABLE 1-7. ANTENNA BEAM PERFORMANCE

		Gain (Off Axis)
Eastern Time Zone	$2\text{-}1/2^{\circ} \times 3^{\circ}$	33 dB
Central Time Zone	$3\text{-}1/2^{\circ} \times 3\text{-}1/2^{\circ}$	31 dB
Mountain Time Zone	$3^{\circ} \times 3^{\circ}$	32 dB
Pacific Time Zone	$2^{\circ} \times 3^{\circ}$	34 dB
48 States	$7^{\circ} \times 3\text{-}1/2^{\circ}$	28 dB
Alaska	$2^{\circ} \times 1^{\circ}$	38 dB
Hawaii	$1^{\circ} \times 1^{\circ}$	41 dB

Figure 1-4. Communications Subsystem Functional Diagram

TOP VIEW ASSEMBLY

| 1 | 2 | 3 | 4 | 5 | 6 | 7 | | A | H |

TIME ZONES   E   1 AND 2   48 STATES   1 - 7
             C   2, 3 AND 4
             M   4, 5 AND 6
             P   6, 7

1.83 m DIA SECTION OF PARABOLOID

MULTIPLE FEED ASSEMBLY

HAWAII

ALASKA

── 1.83 m FOCAL LENGTH ──

SPACECRAFT
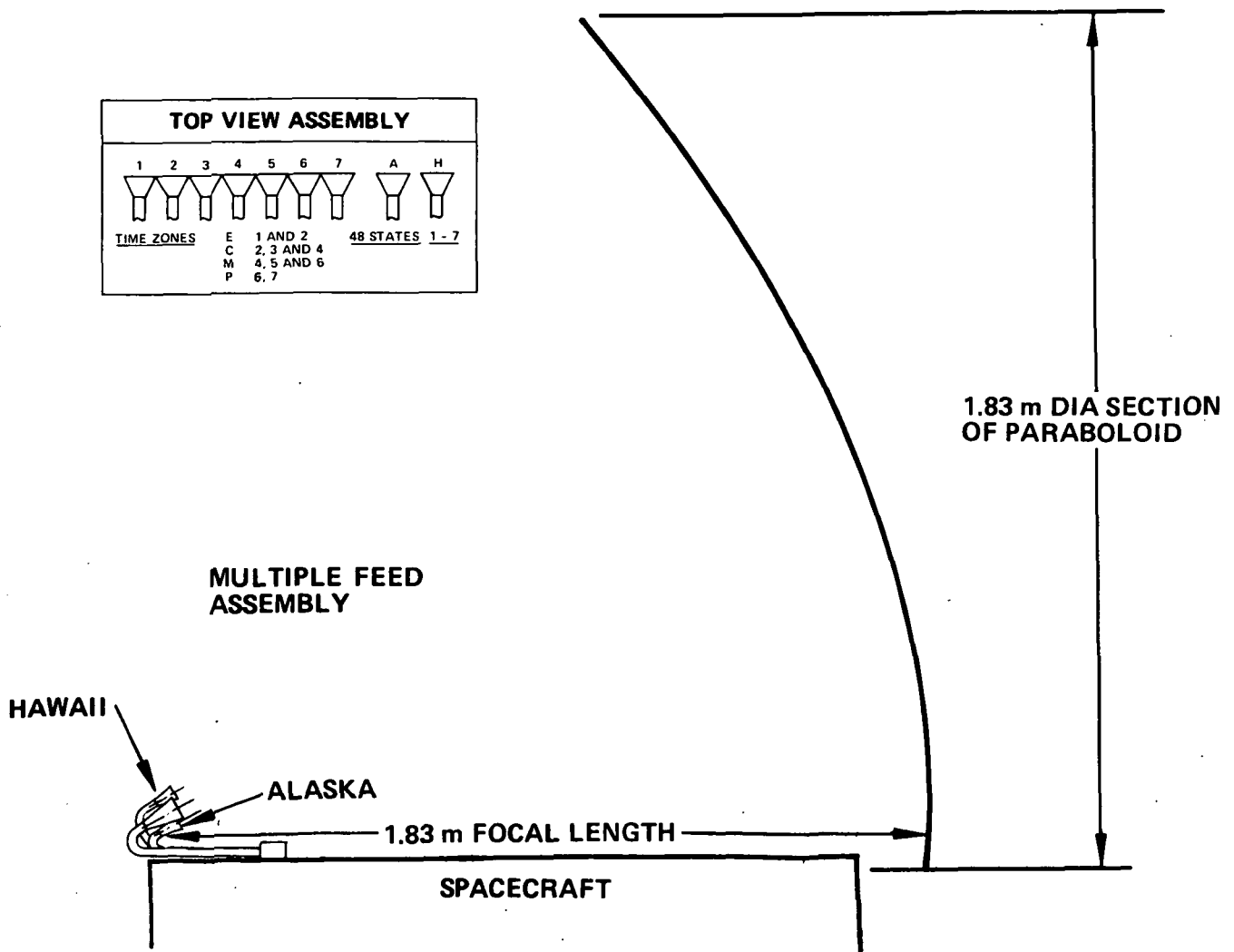
Figure 1-5. Parabolic Antenna Configuration

1.4.2.2 Repeater Subsystem

The repeater subsystem consists of switching networks, receivers, frequency converters, band and channel filters, signal processing, and high power transmitters. Referring to the functional diagram, Figure 1-4, signals from any one of the antenna beams can be switched into the upper channel, whereas only the signals from the Pacific Time Zone beam, the Central Time Zone beam, or the 48 states beam can be selected for the lower channel. The signals are then downconverted to the transmit frequency and band pass filtered before being separated into information channels. The information channels are recombined in a sumer and amplified in the high power transmitters; the upper channel contains the wide band one-kilowatt TWT

(500 MHz BW) and the lower channel contains the narrower band two-kilowatt klystron (120 MHz BW).

1.4.2.3 Operating Modes

Early in the study, a tentative frequency band allocation for the two basic channels was made, as shown in Figure 1-4. It was assumed that each channel would have a bandwidth (BW) of 100 MHz, which might be further divided into two 50-MHz channels. This allocation, together with the flexibility of configuring the paths through the repeater, permit a wide variety of experiments. The principal operating modes, and examples of how they might be employed, are described below.

Through-Put Broadcast Mode. In this mode, the repeater would be configured to pass the received signal from the selected receive beam for each channel directly through the corresponding channel to the transmit antenna. Nominally, the selected transmit beam would illuminate the same region from which the receive signal arrived, but other transmit beams may be selected.

For direct broadcast operation to minimally sized ground terminals, the received signal would consist of a single channel (presumably TV), and the repeater would be set to drive the power amplifiers so as to obtain full power output. Alternative operation in this mode, for servicing somewhat larger terminals, would permit multiple carrier operation. In this case the power amplifiers would be driven so that their total output power was up to 6 dB below their saturated level.

Frequency Reuse Mode. In the frequency reuse mode, the repeater may be configured in any of its possible operating modes subject to the constraint that the receive and transmit antenna beams are appropriately selected. In particular, if the two channels operate at the same receive frequency and at the same transmit frequency, the antenna beams must be spatially separated so that neither pair of receive and transmit beams sees significant signal strength from the other pair of receive and transmit beams. For example, the lower channel may be set to service the Pacific Time Zone and the upper channel to the Eastern Time Zone, both zones using the same uplink and downlink frequencies.

Crossed Information Channels. In the crossed information channel mode, it is assumed that each of the selected receive signals contains at least two information channels, one in the upper half of the channel bandwidth and one in the lower half. (The information channels in each half-BW may be single carrier and/or multiple carrier.) As the signal passes through the repeater, the information in the lower half-BW would be outputted on the same channel on which it is received, whereas the information on the upper half-BW may be directed either to its own channel's power amplifier or to the alternate channel of the repeater, as indicated in the functional diagram of Figure 1-4. Depending upon the structure of the information channels, and the particular experiment being performed, either or both of the power amplifiers may be operated at saturated or reduced power levels.

1.4.2.4 Lens Antenna

A lens antenna configuration was studied to determine the feasibility and performance of this antenna type for the ATS/AMS objectives. Both eight-foot diameter and twelve-foot diameter lens designs were investigated. The 2.44 meter diameter lens will fit into a 2.84 meter diameter dynamic envelope without interference. The 3.66 meter lens requires folding of the lens and deployment of the lens and/or the feed assembly to satisfy fairing constraints.

Figure 1-6 shows the general arrangement of the 2.44 meter diameter antenna. Figures 1-7 and 1-8 show details of the lens aperture and the feed network, respectively. The weights are estimated to be 27.2 Kg for the lens and 2.7 Kg for the feed package.
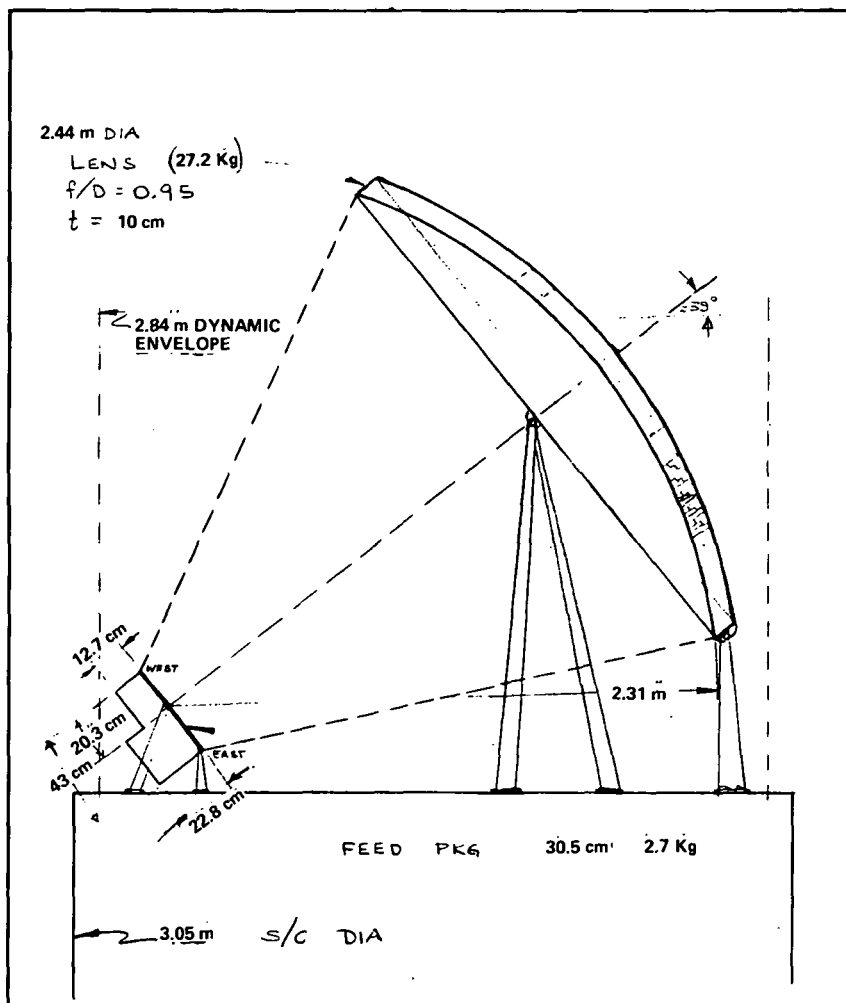
Figure 1-6. General Arrangement 2.44 Meter
Diameter Lens Antenna

DETAIL A

DETAIL B

EARTH

LENS AXIS
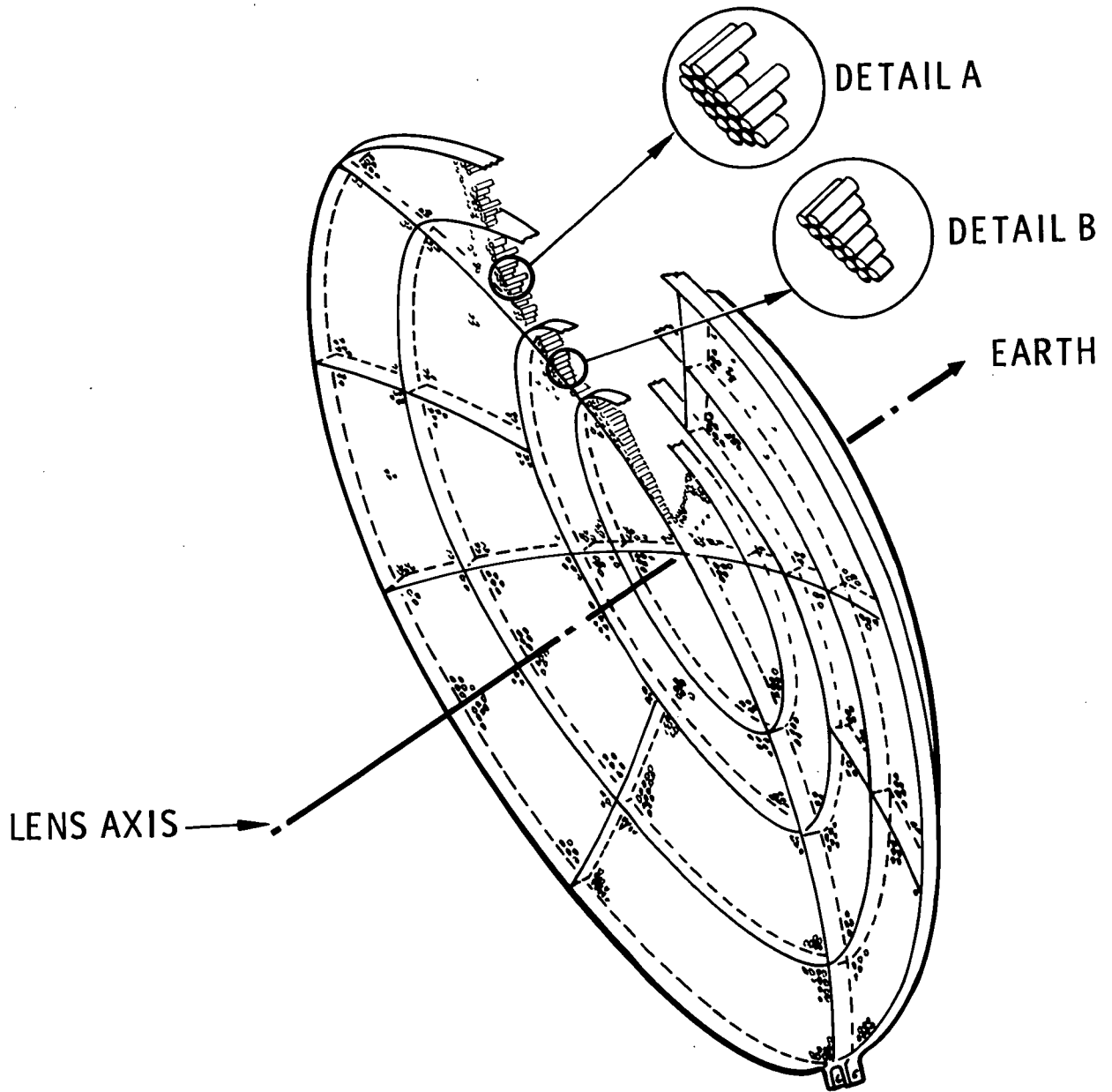
Figure 1-7. Antenna Lens
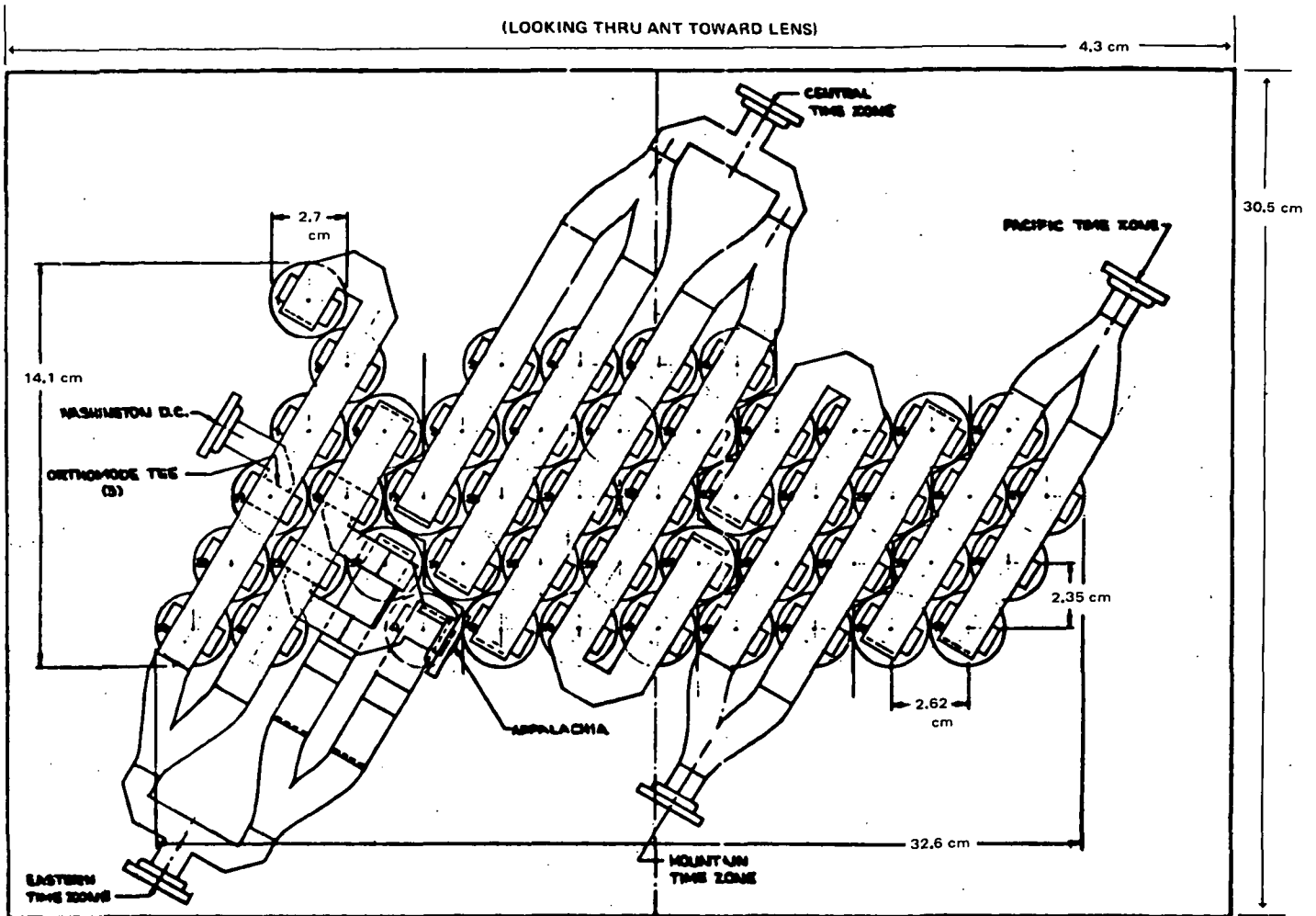
Figure 1-8. 2.44 Meter Diameter Lens Antenna Feed

Shaped beams for all four time zones were calculated using a computer program for both the eight-foot and the twelve-foot designs at 11.95 GHz. Both provided well behaved patterns with minimal ripple. Over approximately 95 percent of each time zone, the twelve-foot design provided a minimum gain of 37 dB and the eight-foot design was about 3 dB lower. Figure 1-9 shows a typical time zone pattern.

The sidelobe performance of the eight-foot diameter antenna was calculated for the Eastern Time Zone beam to determine the amount of isolation which could be achieved in frequency reuse experiments. The gain in the Mountain Time Zone was determined to be at least 30 dB below the peak in the Eastern Time Zone.

While the lens cell design was not optimized for broad band performance, a computation of a receive spot beam at 14.5 GHz showed that approximately a 32 dB gain could be achieved in the direction of a station in the vicinity of Washington, D. C. Although this investigation demonstrated
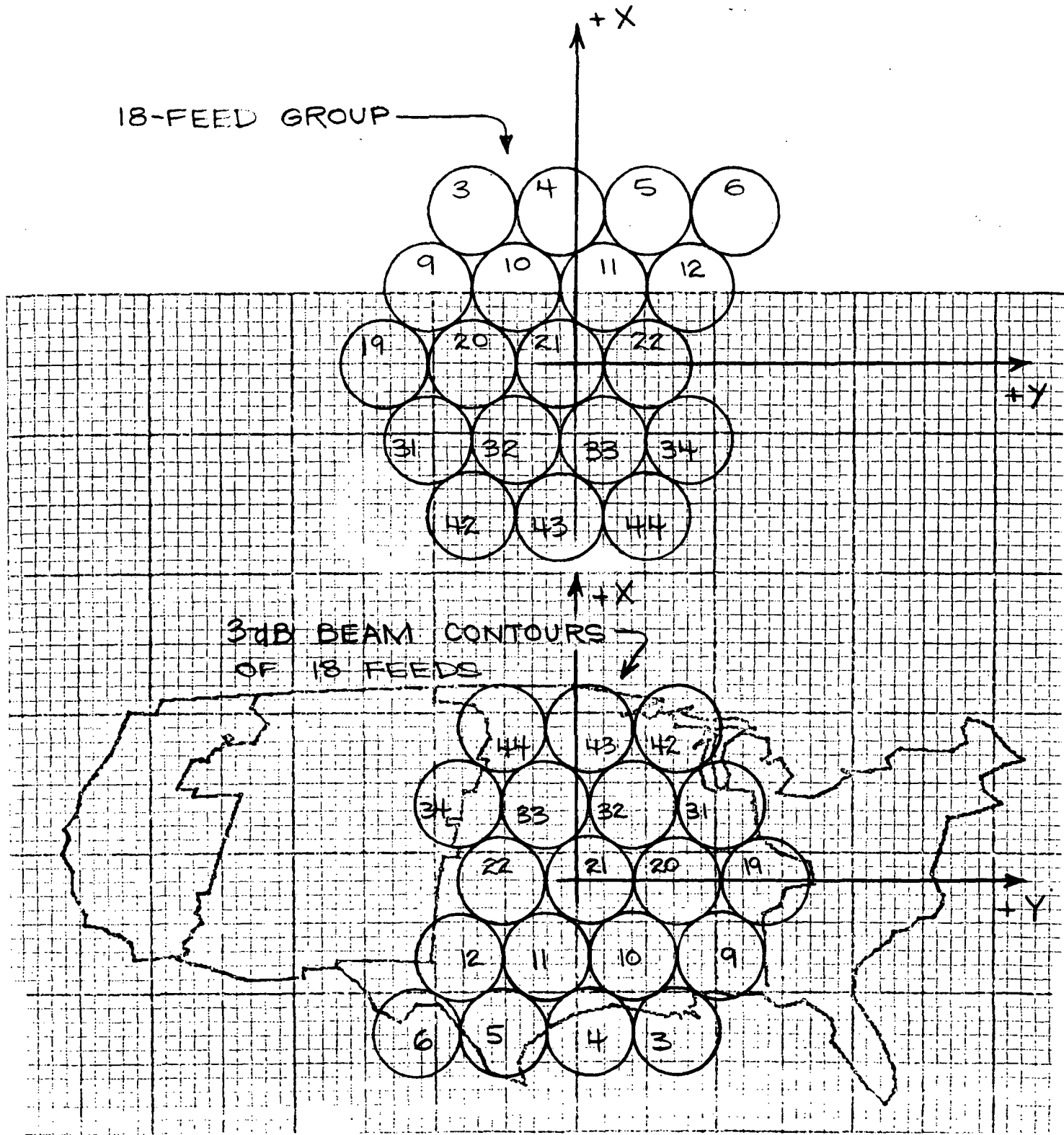
Figure 1-9. Feed Horn and 3-dB Contour Level Arrangements
of Feed Group Covering Central Time Zone:
2.44 Meter Diameter Lens

that useful gain could be achieved at this frequency, multi-moding in the lens cell elements was indicated. This problem needs to be addressed in a more detailed design study.

Techniques to improve and extend the preliminary lens antenna design were considered, including the use of other waveguide cell designs. Mechanical design and fabrication techniques were evaluated in deriving weight estimates and packaging of the feed configuration.

1.4.3 Attitude Control and Stationkeeping Subsystem (AC&SS)

The AC&SS senses the vehicle attitude and provides torques and velocity increments as needed to maintain the vehicle attitude and trajectory within specified tolerances. The on-station functional requirements are essentially the same for all configurations; however, for the period between booster separation and the achievement of synchronous station, the requirements for the electrically propelled A-1 spacecraft and the chemically injected B configurations are obviously different. Qualitative functional requirements for both types of spacecraft are given in Table 1-8.

The baseline AC&SS design concept is similar for all three classes of spacecraft configuration (A, B, and C), as summarized in Table 1-9. The baseline design approach was selected after tradeoff studies considering a number of actuation and sensing alternatives, as summarized below. Specific component selection varies for each of the spacecraft configurations, as listed in Tables 1-10 through 1-12, for configurations A, B and C, respectively. Except for the ion engines, all of the hardware has been flight qualified and proven on prior programs.

1.4.3.1 Actuator Alternatives

Trajectory correction can be accomplished only by expulsion of mass from the spacecraft, and the selection of ion engines was dictated for Configuration A-1 by weight constraints. For the B Configurations, a hydrazine reaction control system (N_2H_2 RCS) was selected because of the objectives to use proven technology for basic housekeeping functions and to avoid contamination problems associated with the use of ion engines on a spacecraft with N-S solar panels.

Conceptually, the simplest attitude control approach is to use mass-expulsion elements directly for developing the required torques. However, the cyclic variation of some of the attitude perturbations would result in excessive fuel consumption if the perturbations were corrected by direct thrusting. Other operational constraints discussed in detail in the body of the report also make direct thrust unattractive for attitude control. The alternative is to use one of several momentum storage techniques. These include reaction wheels or control moment gyros (CMGs) in a spacecraft with nominally zero momentum, or a single large reaction wheel which provides gyroscopic stiffness to the spacecraft. The latter approach is unattractive when orbit raising by electric propulsion because excessive fuel would be required to precess the spacecraft's momentum vector through the periodic

TABLE 1-8. AC&SS FUNCTIONS DURING MISSION PHASES

ORBIT RAISING PHASE.   (Configuration A-1 with Electric Propulsion)

- Yo-yo despin after separation from booster.

- Null tipoff rate using reaction wheels, rate gyros.

- Reorientation to desired attitude after panel deployment.

- ΔV added for orbit raising; attitude control performed via thrust vectoring and reaction wheels.

- Attitude reference provided by gyros updated periodically by command.

- Attitude determination by ground processing of earth and sun sensor data.

TRANSFER ORBIT.   (B-Configurations with AKM Injection)

- Orient spacecraft to desired attitude for AKM burn.

- Spin spacecraft to desired attitude for AKM burn.

- Despin (yo-yo) after AKM burn.

ON-ORBIT PHASE.

- Reorientation maneuver to acquire on-station attitude.

- Continuous attitude control and sensing provided by reaction wheels and gyros.

- Gyro drift periodically updated by command, using ground-processed sun and earth sensor data.

- Stationkeeping, N-S and E-W, using electric thrusters (Configuration A) or hydrazine thrusters (Configuration B).

- Maintain control during eclipse - wheels and gyros maintain desired orientation.

- Backup control and sensing provided by thrusters and earth and sun sensors.

TABLE 1-9. AC&SS BASELINE DESIGN APPROACH

Vehicle Configuration	A-1 or C-1	B1 or B5
Continuous Attitude Control	Three single-axis momentum wheels	
Continuous Altitude Reference	Three single-axis rate integrating gyros	
Absolute Attitude Reference	One two-axis Earth sensor and one two-axis sun sensor	
Momentum Dumping and Stationkeeping	Three clusters* of 5-cm ion engines (w/thrust throttling and deflection)	Eight pulsed hydrazine thrusters (single thread design)**
Control Electronics	Matched to specific implementation for each configuration.	
Antenna Pointing Control	Motor, position encoder and electronics for precise orientation of Antenna	(Inherent in control of spacecraft attitude)

*A single engine in any cluster is operated at any given time. Multiple engines are required to provide five-year mission life and reliability.

**Eight additional thrusters are required to provide redundancy.

TABLE 1-10. AC&SS HARDWARE SUMMARY CONFIGURATION A-1

Unit	Quantity	Unit Weight	Size	Power
Gyros	3	1.6 Kg each	900 cm^3 each	9.5W
Wheels	3	3.46 Kg each	16.5 cm OD x 7.6 cm high	9.5W Stall each / 3.0W Avg each
Sun Sensor	1	1.52 Kg (including Electronics)	5.1 cm x 7.6 cm x 6.35 cm / 5.1 cm x 15.2 cm x 6.35 cm	3 W
Earth Sensor	1	3.27 Kg (including Electronics)	19.0 cm dia x 17.8 cm	1.6W
Control Electronics	1	5.45 Kg		18W
		25.2*		60.1W

*Single thread design

TABLE 1-11. AC&SS HARDWARE SUMMARY - CONFIGURATION B

Unit	Quantity	Unit Weight	Size	Power
Gyros	3	1.6 Kg each	900 cm^3 each	9.5W each
Wheels	· 3	2 x 3.46 Kg 1 x 4.55 Kg	16.5 cm OD x 7.6 cm 25.7 cm OD x 10.9 cm	2 x 3W Avg 1 x 4W Avg
Sun Sensor	1	1.52 Kg (including Electronics)	5.1 cm x 7.6 cm x 6.35 cm 5.1 cm x 15.2 cm x 6.35 cm	3W
Earth Sensor	1	3.27 Kg (including Electronics)	19.0 dia x 17.8 cm	1.6W
Control	1	5.9 Kg		18W
		26.8 Kg*		6.1.W

*Single thread design; probable standby redundancy in gyros, electronics.

TABLE 1-12. AC&SS HARDWARE SUMMARY - CONFIGURATION C-1

Unit	Quantity	Unit Weight	Size	Power
Gyros	3	1.6 Kg each	900 cm^3 each	9.5W each
Wheels	3	6.81 Kg each	30.5 cm OD x 12.1 cm	62W Stall each 7.5W Avg each
Sun Sensor	1	1.52 Kg (including Electronics)	5.1 cm x 7.6 cm x 6.35 cm 5.1 cm x 1.5 cm x 6.35 cm	3W
Earth Sensor	1	3.27 Kg (including Electronics)	19.0 cm dia x 17.8 cm	1.6W
Control Electronics	1	6.81 Kg		24W
		36.7 Kg*		79.6W

*Single thread design; probable standby redundancy in gyros, electronics.

large attitude changes required during the orbit raising period. The multiple reaction wheel design was selected because it provides a low torque level over a large dynamic range of momentum storage, which is compatible with both the orbit raising and on-station requirements for the A Configuration. CMGs are relatively unattractive because they do not have the large dynamic range which is required.

For the B Configurations, the large reaction wheel with gyroscopic stiffness has some advantage, but the reaction wheel approach was selected because it appears to be more compatible with the spaced pulse usage of the hydrazine thrusters.

1.4.3.2 Sensor Alternatives

The uses of star, earth and sun sensors were considered as primary references for this mission. Star sensors were rejected because of their relative complexity, and, for the A-1 Configuration, their incompatibility for supporting both orbit raising and on-station operations. Earth and sun sensor combinations have been used in many prior applications with comparable accuracy requirements and were selected for the baseline design.

As in the case of the actuators, the primary sensors conceivably could be used to provide a continuous reference. However, the sun sensor is inoperative during eclipse periods. This requires an alternative reference for at least one axis to permit reacquisition of spacecraft orientation. Performance of this function with earth sensor data alone would require an extensive amount of on-board data processing to provide the required accuracy. Alternatively, precision gyroscopes with proven reliability are available which can provide a continuous reference and require only infrequent periodic drift correction. Updating would be available by ground command using processed telemetered data from the primary earth and sun sensors. A three-gyro approach has been selected as the baseline design.

1.4.4 Electric Propulsion Systems Summary

Electric propulsion systems were considered as possible alternatives for two major mission functions, namely, on-station attitude control and stationkeeping (AC/SK) and synchronous orbit injection by slow orbit raising. The design analyses for these systems considered all major propulsion subsystems as well as their integration into the overall spacecraft. The major subsystems included the thrust devices and propellant feed systems, the propellant reservoirs, and the power conditioning and control systems. The special power conditioning and controls for the orbit raising propulsion system are described in the spacecraft power system discussion. The major guidelines of the design analyses were (1) employ Hg bombardment ion thrusters, (2) establish system reliability as an important design criterion, and (3) minimize program cost by considering, wherever possible, componets and systems presently under development.

1.4.4.1 Attitude Control and Station-Keeping Ion Thruster Subsystems

The attitude control and station-keeping approach chosen for the ATS/AMS spacecraft configuration employs deflectable beam ion thrusters in combination with reaction wheels. The specific control mode is designed to (1) satisfy N-S and E-W station-keeping requirements, (2) correct for solar pressure (i.e., C.P.-C.M.* solar torque and orbital eccentricity build-up), and (3) augment reaction wheel attitude control via thrust vectoring. With the chosen control mode, the N-S station-keeping is unidirectional (i.e., north pointing thrust vector) and performed during a 60 degree sector of the orbit at a time of maximum correction influence. Two thrusters, firing simultaneously and separated by the diameter of the spacecraft base plate, are used for the N-S correction. In this configuration, and with the use of thrust vectoring, reduction of the 3-axis reaction wheel system energy is accomplished during station-keeping thrusting. Finally, E-W station-keeping is provided by firing a third thruster (identical in design to the N-S thrusters) periodically during the orbit (but not during N-S station-keeping) to compensate for solar pressure and earth triaxiality effects. Thus, complete AC/SK control is achieved with three thruster stations. Furthermore, by proper placement of these stations (e.g., see Figure 4.4-17) no spacecraft surface extends beyond the thruster ion beam exit plane. In this way, no impingement or deposition of either neutral particles (propellant or sputtered material) or ions on the spacecraft is possible.

As shown in Figure 1-10 each station is equipped with three separate ion thruster units which share a common liquid mercury feed system. Only one thruster per station is needed to fulfill mission thrust requirements, while two redundant thrusters per station insure high propulsion reliability with minimal mass penalty since the mercury reservoir constitutes the major mass contribution of the thruster system. The individual thruster units which have a mass of 0.7 Kg each are adapted directly from the existing SIT-5 thruster system shown in Figure 1-11.

At a given thruster station, each of the thruster units operate independently of the other two. Propellant flowrate to the individual thruster is regulated by a separate phase separator or vaporizer which provides the necessary rate of vapor flow to the discharge chamber while preventing direct transmission of liquid mercury. Electrical isolation from the mercury supply is provided by separate high-voltage isolator subassemblies located downstream of the propellant vaporizers. Each thruster includes a thrust-vectorable ion-extraction system which is capable of high angle ($>10^{\circ}$) thrust vector control by electrostatic deflection.

---

*Center of Pressure offset from the Center of Mass
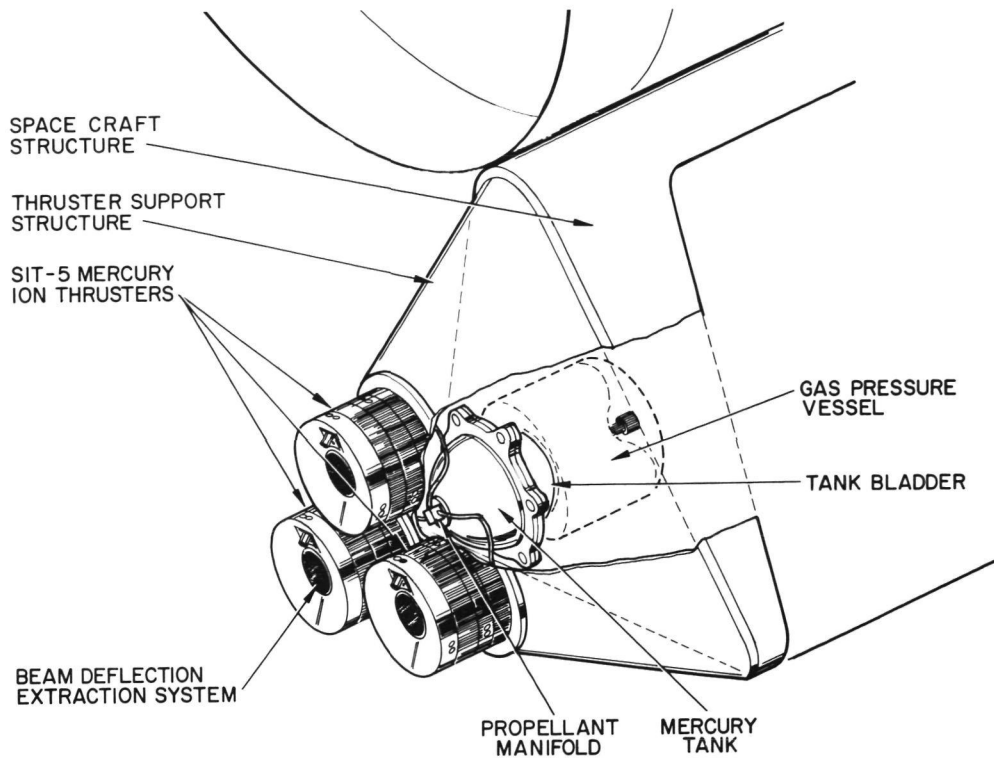
Figure 1-10.   Attitude Control and Stationkeeping
Thruster Station

SPACE CRAFT
STRUCTURE

THRUSTER SUPPORT
STRUCTURE

SIT-5 MERCURY
ION THRUSTERS

GAS PRESSURE
VESSEL

TANK BLADDER

BEAM DEFLECTION
EXTRACTION SYSTEM

PROPELLANT
MANIFOLD

MERCURY
TANK
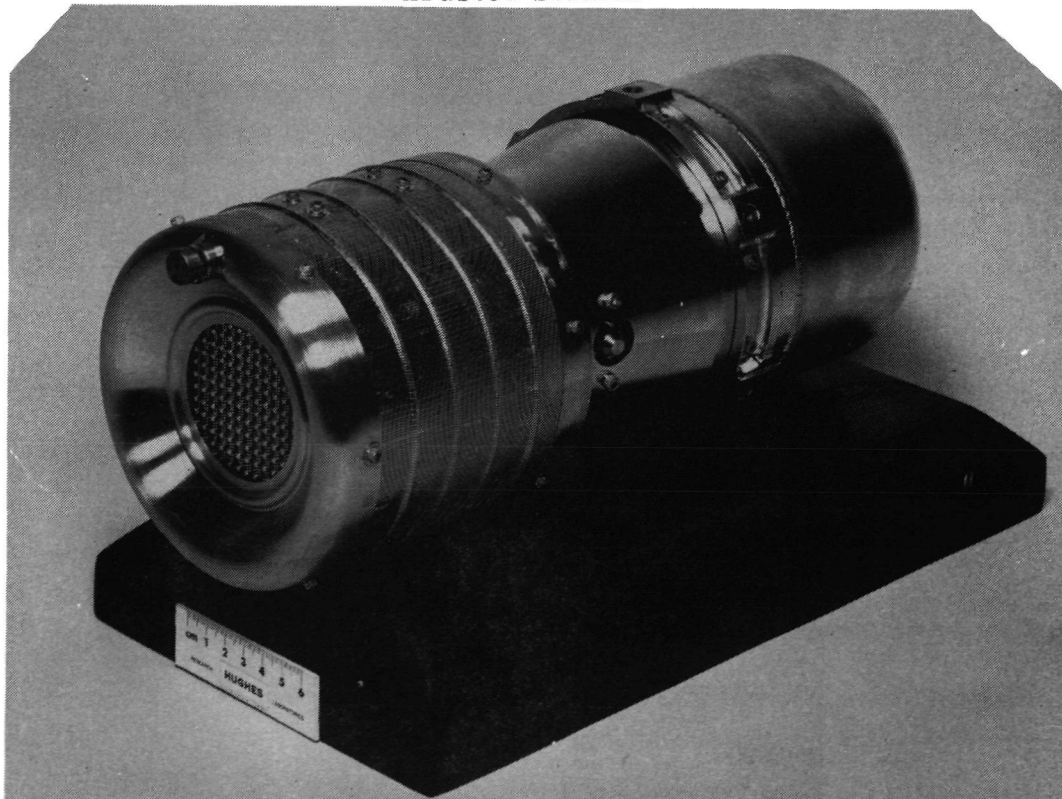
Figure 1-11.   SIT-5 Thruster and Reservoir System

Each element of the SIT-5 system has been flight qualified by extensive test programs. Earlier models of both the thruster unit and the thrust-vectorable ion-extraction system have demonstrated their capability for booster launch by a rigorous series of shock and vibration tests.

A summary of the specifications of the complete on-station ion thruster attitude control and station-keeping subsystem for spacecraft configuration A-1 is given in Table 1-13. As indicated the total system weight for five year operation, including three thruster stations, propellant, power conditioning and controls, and switching matrix, is 13.7 Kg. Furthermore, the peak power requirement is 290 W (i.e., two stations operating simultaneously). Finally, the system described in Table 1-13 is a conservative extension of SOA hardware to be flight tested on the Canadian Technology Satellite scheduled for launch in April 1975.

TABLE 1-13. ATTITUDE CONTROL AND STATION KEEPING
ION THRUSTER SYSTEM SPECIFICATIONS

- PROPULSION SYSTEM DEFINITION
  - Thruster Stations = 3 (2 N-S, 1 E-W)
  - Reservoirs = 1/station
  - System Weight = 13.7 Kg
  - Propellant Weight = 9.1 Kg

- THRUSTER STATION
  - Thrusters/Station = 1 operation/2 standby
  - Reservoirs/Station = 1
  - Input Power = 145 watts
  - Thruster Diameter = 5 cm
  - Effective Specific Impulse = 4100 sec
  - Weight (less propellant) = 2.45 Kg

- POWER CONDITIONING, SWITCHING & THRUSTER CONTROLS
  - PC&C Units = 3
  - Efficiency ≥85%
  - Switching Matrix = 1
  - Minimum PC&C to operate = 2 of 3
  - Weight = 6.35 Kg

1.4.4.2 Orbit Raising Ion Thruster Subsystem

The design of the orbit raising ion thruster subsystem for the ATS/AMS must satisfy the overall propulsion system design point established by the flight dynamics analyses. The specific design point information generated by these analyses include (1) the initial solar panel power level and its variation with time (2) the propellant mass, and (3) the specific impulse. For the proposed orbit raising profile the initial power level was 7.2 kW, the Hg propellant requirement was 54.5 Kg, and the optimum specific impulse was 3500 sec. Based on this design point and on an analysis of reliability-power matching - weight tradeoffs, a modularized thruster array consisting of three 30-cm thruster modules, only two of which would operate at any one time, was chosen.

As indicated the thruster and feed system module is a 3.6 kW, 30-cm Hg bombardment ion thruster operating at 3500 sec effective specific impulse. Each thruster is equipped with a movable screen electrode thrust vectoring system (presently under development-contract No. NAS 3-15385). Thus, 3-axis spacecraft orientation control can be provided by the prime propulsion system during orbit raising. A photograph of a 30-cm flight-configured thruster is shown in Figure 1-12.
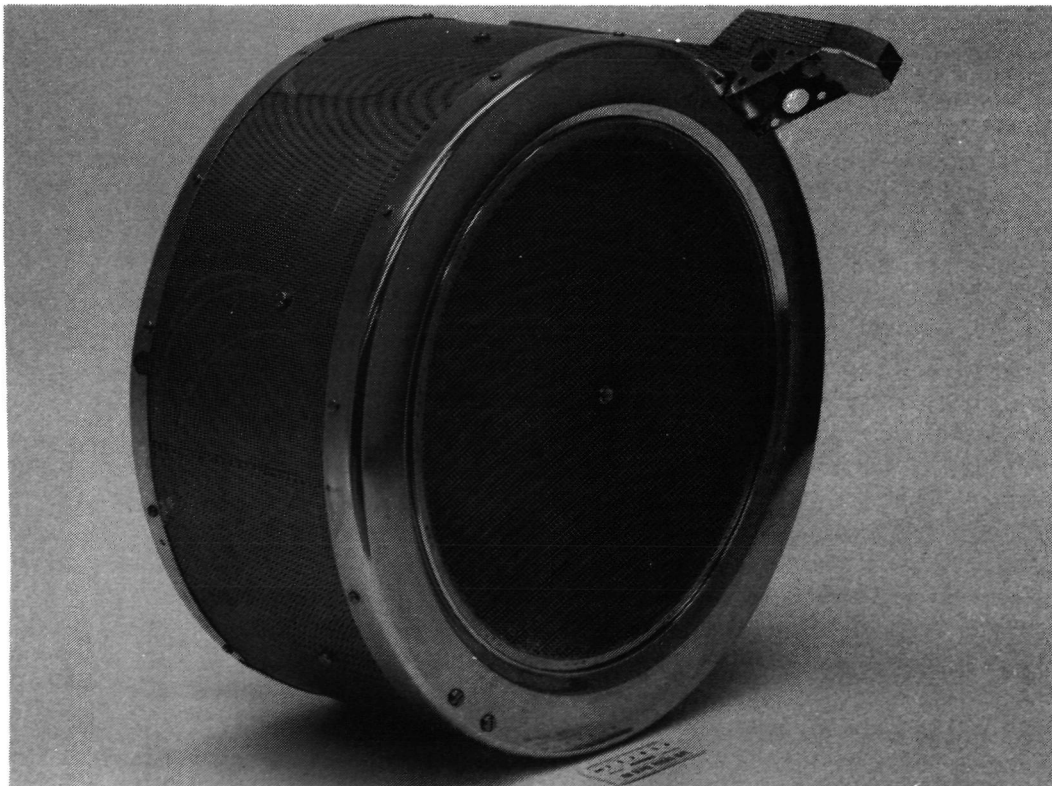
Figure 1-12. Hughes 30-cm Thruster
and Feed System Module

The mechanical integration of the three 30-cm thruster modules and single Hg propellant reservoir is relatively straightforward. As shown in Figure 1-13 each thruster is mounted to a thruster array shelf and canted such that its thrust vector is through the spacecraft center-of-mass. In order to minimize thrust loss (i.e., perpendicular thrust components) the cant angle is minimized by placing the thruster modules in a triangular array. This design also minimizes the overall array envelope and simplifies the spacecraft structural design at the spacecraft separation plane. The spherical metal Hg reservoir of the type used for the NASA/LeRC SERT-II test flight is mounted directly to the equipment shelf from which structural supports emanate to both the thruster shelf and the sides of the spacecraft. In this way the major propulsion system weight (viz. the propellant reservoir) is rigidly mounted to the spacecraft.

In spacecraft configuration A-1, the thruster and reservoir array are electrically integrated with a High Voltage Solar Array (HVSA). During thruster operation the HVSA is configured to provide screen, accelerator, discharge and keeper starting power directly to two of the three thrusters in the thruster array. Regulation and sequential control of this power is
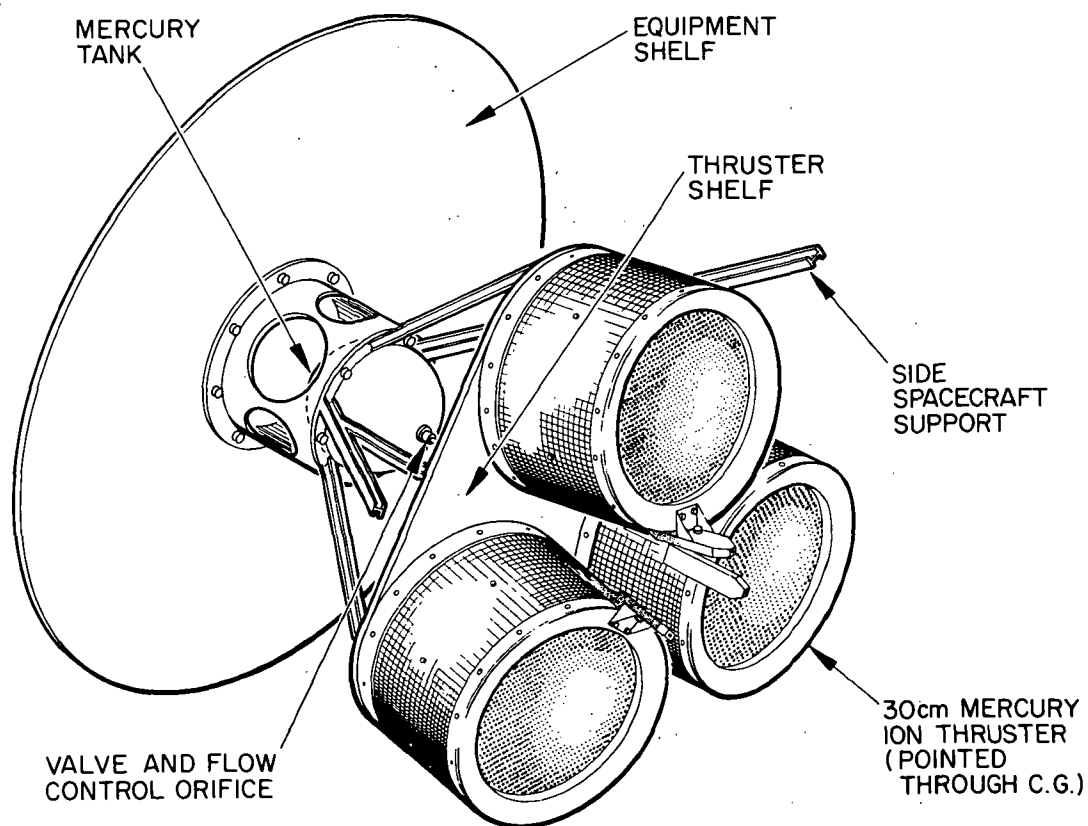
Figure 1-13. Orbit Raising Thruster Array

performed by the on-board HVSA control electronics which issue digital control commands to the regulation and reconfiguration circuitry based on the general operational format required for the 30-cm thruster, the sensed thruster voltages and currents, and the thruster system command signals (preheat, startup, thrust level, etc.) received from the spacecraft command distribution electronics.

Additional conventional power conditioning operating from the 28 VDC bus provides conditioned low voltage power for heaters, vaporizers and keepers (at the run level) and for powering the movable screen beam deflection system. In order to conserve weight this power conditioning is designed to power only two thrusters, hence transfer switching is included to allow rerouting the power to the standby thruster in the event of a failure.

Two dimensional beam deflection of each operating thruster is accomplished with analog thrust vector control signals received from the attitude control electronics. These signals act as variable set point references in individual deflection supply control loops.

The orbit raising thrust/attitude programmer which is up-dated once each day, both directly and indirectly controls the operation of the thruster system. It directly establishes the thruster on-off thrust profile by initiating start-up and shut-down, and by setting beam current magnitude. It indirectly determines the beam deflection (thrust vector) angles with the spacecraft attitude profile issued to the attitude control electronics.

Maximum power tracking circuitry similar to that suggested for ion propulsion systems powered with conventional power conditioning and a low voltage solar array (i.e., in numerous previous Solar Electric Propulsion (SEP) interplanetary spacecraft studies) is incorporated as part of the HVSA control logic with a negligible increase in weight.

Implementation of the tracker would be restricted to individual screen supplies which consist of configured solar cell power blocks. Since the thruster power use profile does not utilize the total maximum power during the earlier portions of the orbit raising mission, the tracker would actually function more as a monitor of power available to aid in determining allowable thrust/attitude programmer up-date levels.

The proximity of the commanded operating point (beam current level) to the maximum power point of the combined power blocks would be determined by injecting a low amplitude-low frequency dither signal into the beam current control loop. Then, by electronically monitoring the sensed screen voltage and current (already required for other control functions) an assessment of the operating point's position on the I-V characteristics would be made. This would establish whether a commanded beam current level could be achieved or what reserve existed between the commanded level and the maximum level.

An analysis of the magnetic and electric fields generated by the orbit raising system showed that no deleterious effects would result with any experiments associated with the mission. Furthermore, based on SERT II flight results, no radio frequency interference in the spacecraft communication bands is expected. Finally, no particle (neutral or ion) impingement or deposition is possible since, as with the AC/SK thrusters, the orbit raising thrusters are positioned such that no spacecraft structures exist downstream of the ion beam exit plane.

A summary of the specifications of the complete orbit raising ion thruster subsystem, including thruster array and propellant reservoir, is given in Table 1-14. As indicated the total system weight including propellant is 75 Kg. The system requires a total initial power of 7.2 kW. By use of redundancy techniques system reliability is increased to levels greater than 0.99. Finally, the system design is based on a 30-cm thruster module which is scheduled for a 6000 hr life test during 1972 (NASA Contract No. NAS 3-15523).

1.4.5 Electrical Power Subsystem

The electrical power subsystem designs for spacecraft configurations A-1, B-1 and B-5 are principally impacted by the end of life conditioned power required by the communication subsystem. The 1-kw traveling wave tube (TWT) and the 2-kw klystron, which are common to the three configurations, represent a load power demand of approximately 5 kw when both are operating simultaneously at saturation drive levels. Another major factor in the design effort involved the power requirements for a mercury bombardment ion propulsion system to be used for orbit raising. By comparison, the combined power requirements of other auxiliary subsystems, attitude control, orientation mechanisms, etc., are routine in nature and can be implemented in a manner typical of present spacecraft.

For each of the baseline spacecraft configurations, a corresponding power subsystem design was developed to satisfy total mission requirements. Trade studies were performed to judiciously select the best design approach from competing alternatives. To a large degree, the approaches chosen for electrical power subsystem implementation have contributed to making the spacecraft configurations uniquely different from each other.

In the A-1 configuration, a larger solar array is necessary because of degradation which would be experienced in the orbit raising phase of the mission, and an East-West orientation is required to avoid impingement from the ion thruster exhaust. The B-5 configuration resembles the B-1 in that the solar arrays for each deploy North-South and are approximately equal in size; but B-5, like A-1, is designed for high voltage and contains integral power conditioning, while the B-1 array and conditioning designs employ conventional technology.

TABLE 1-14. ORBIT-RAISING SUBSYSTEM DESIGN SPECIFICATIONS

PROPULSION SUBSYSTEM DEFINITION

- Thruster Array = 2 operating/1 standby

- Reservoir = 1

- Auxiliary Power Conditioning = 2.27 Kg

- System Weight = 20.4 Kg

- System Reliability ≥ 0.99

- Propellant Weight = 54.5 Kg

RESERVOIR

- Spherical Diameter = 21.2 cm

- Weight = 1.68 Kg

- Reliability ≥ 0.999

THRUSTER CHARACTERISTICS

Input Power	3.6 kW
Diameter	30 cm
Effective Specific Impulse	3500 sec
Mass Utilization	90%
Electrical Efficiency	85%
Beam Current Range	1.9 ±0.05A
Thrust Vector Technique	Movable screen electrode
Thrust Vector Capability	+10 degrees, 2 axes
Thruster Weight (including housing, feedlines, isolators, mounting interface, bulkhead-thruster cabling and movable screen mechanism)	5.5 Kg

The mission requirements analysis of Section 2 led to design analysis and tradeoffs in Section 3. A summary of each configuration's power requirements for on-station operations is shown in Table 1-15. The power requirements for Configuration A-1 during orbit raising were dominated by the peak demand for the ion thrusters of 7.2 kw; but the sizing for the 10.2 kw solar array is determined by the on-orbit power demand of 6 kw plus the radiation degradation during the orbit raising. Further tradeoffs were conducted on each of the power subsystem assemblies in Section 4.5 and are summarized in the following sections.

TABLE 1-15. BASELINE POWER BUDGETS

Subsystem	Normal Operation			Eclipse Operation
	A-1	B-1/B-1A	B-5	
	←——— (watts) ———→			
Communications				
Repeater	———— 100 ————			
One 1 kw TWT (0.53E)	———— 1885 ————			12*
One 2 kw Klystron (0.66E)	———— 3000 ————			18*
Power Matching/Conditioning	———— 490 ————			
Power Electronics and Distribution	———— 45 ————			10
Attitude Control	———— 55 ————			55
TT&C	———— 20 ————			20
Subtotals	5595	5595	5595	115
Electric RCS (5 cm Eng)	290			
Orientation Mechanism	20	10	10	10
Thermal Control	80	10	50	
Total	5985	5615	5655	125
*Cathode heaters on half-power				

1.4.5.1 Power Subsystem Configurations

Descriptions of the power subsystems for each of the baseline
spacecraft configurations are summarized from the results of the many
tradeoffs and design iterations conducted during the study.

Configuration A-1 Power Subsystem. A power management block
biagram of the electrical power subsystem for spacecraft configuration A-1
is shown in Figure 1-14. The rollout solar array is divided into two sections.
The high voltage solar array (HVSA) section, which constitutes approximately
90 percent of the total array power, provides screen, accelerator, discharge
and keeper starting power for the ion thrusters during orbit raising. Upon
arrival on station, the array power is rerouted through reconfiguration
switches to the 1-kw TWT and 2-kw klystron to provide the range of cathode
and collector electronic voltages required.

The low voltage solar array section provides a nominal 28 v power
bus for energy storage for the attitude control and stationkeeping (AC/SK)
5-cm ion thrusters and for the various housekeeping functions. In addition,
during the orbit raising phase low voltage bus power is used to meet various
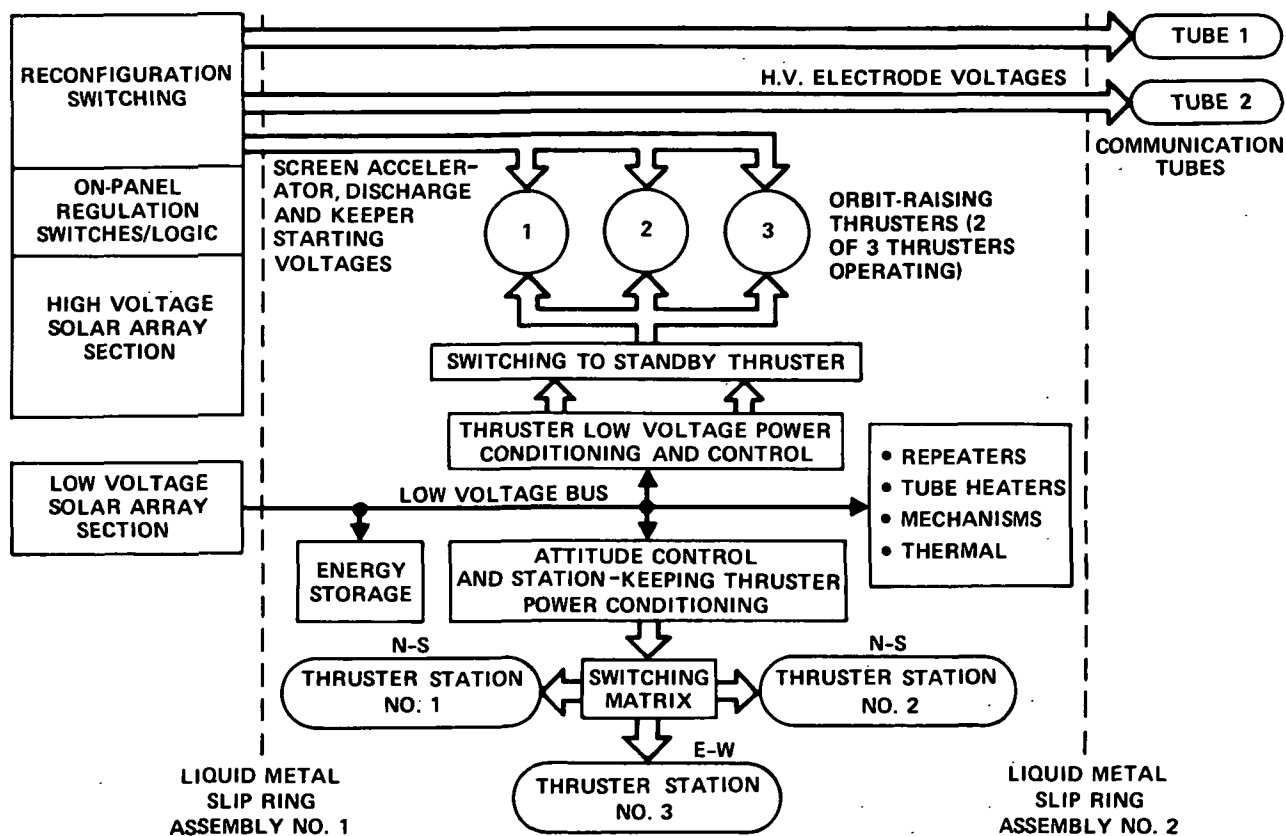
Figure 1-14. Power Management Block Diagram,
Spacecraft Configuration A-1

low voltage - low power needs of the orbit raising thrusters. This approach is a more appropriate implementation for these low voltage - high current supplies than using an extension of the HVSA concept to provide this power since the number of sliprings and array/spacecraft cable runs would be greatly increased.

Because of the wide range of spacecraft orientations possible during orbit raising and the requirement for E-W panel orientation on-station to allow body mounting of the AC/SK ion thrusters, two slipring assemblies are required. Liquid metal sliprings were selected for the A-1 configuration.

Energy storage is provided by two 6-ampere hour nickel cadmium batteries.

Configuration B-1 Power Subsystem. The power management block diagram of the electrical power subsystem for spacecraft configuration B-1 is shown in Figure 1-15. The solar array is again divided into two sections; one section provides a medium voltage bus for the TWT and klystron conventional power conditioning and the other section functions as a low voltage bus for housekeeping, energy storage, and auxiliary use.
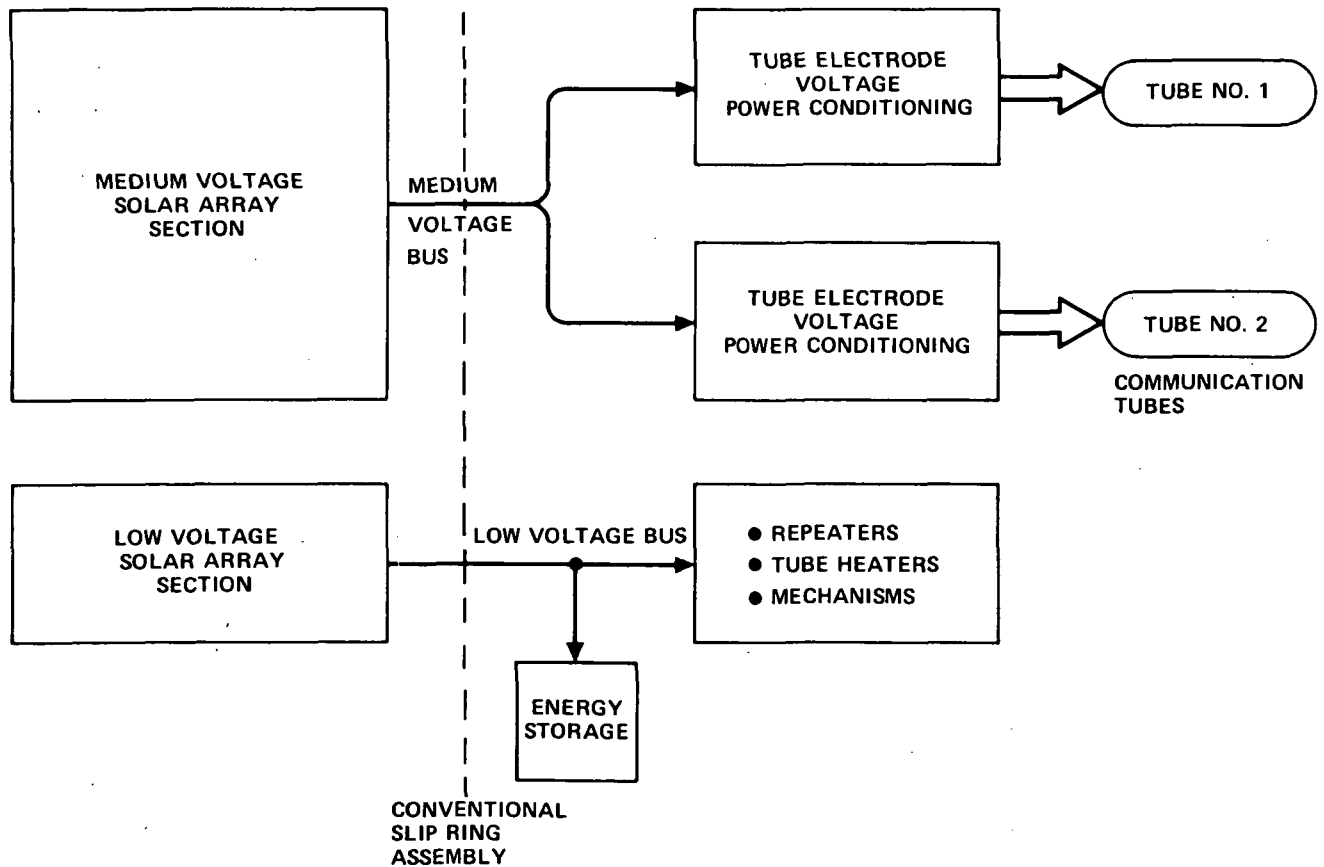
Figure 1-15. Power Management Block Diagram, Spacecraft Configuration B-1

The selection of a medium voltage bus for powering the communication subsystem leads to a substantial saving in the projected specific weight of the power conditioning, and to improved efficiency which becomes extremely important at the power levels required.

Direct chemical spacecraft injection and N-S orientation of the solar panel lead to the necessity of a single slipring assembly. Since spacecraft configuration B-1 was chosen to represent a more conservative and conventional spacecraft approach, a standard brush-on ring assembly was selected for implementation.

Again, energy storage is provided by two 6-ampere hour nickel cadmium batteries.

Configuration B-5 Power Subsystem. The power management block diagram for configuration B-5, shown in Figure 1-16, is essentially the same as that for configuration B-1 with the exception that a high voltage solar array with integral power conditioning replaces the medium voltage bus and the conventional power conditioning. A single liquid metal slipring assembly provides power transfer between the N-S oriented solar array and the spacecraft body, and two 6-ampere hour nickel cadmium batteries provide energy storage.
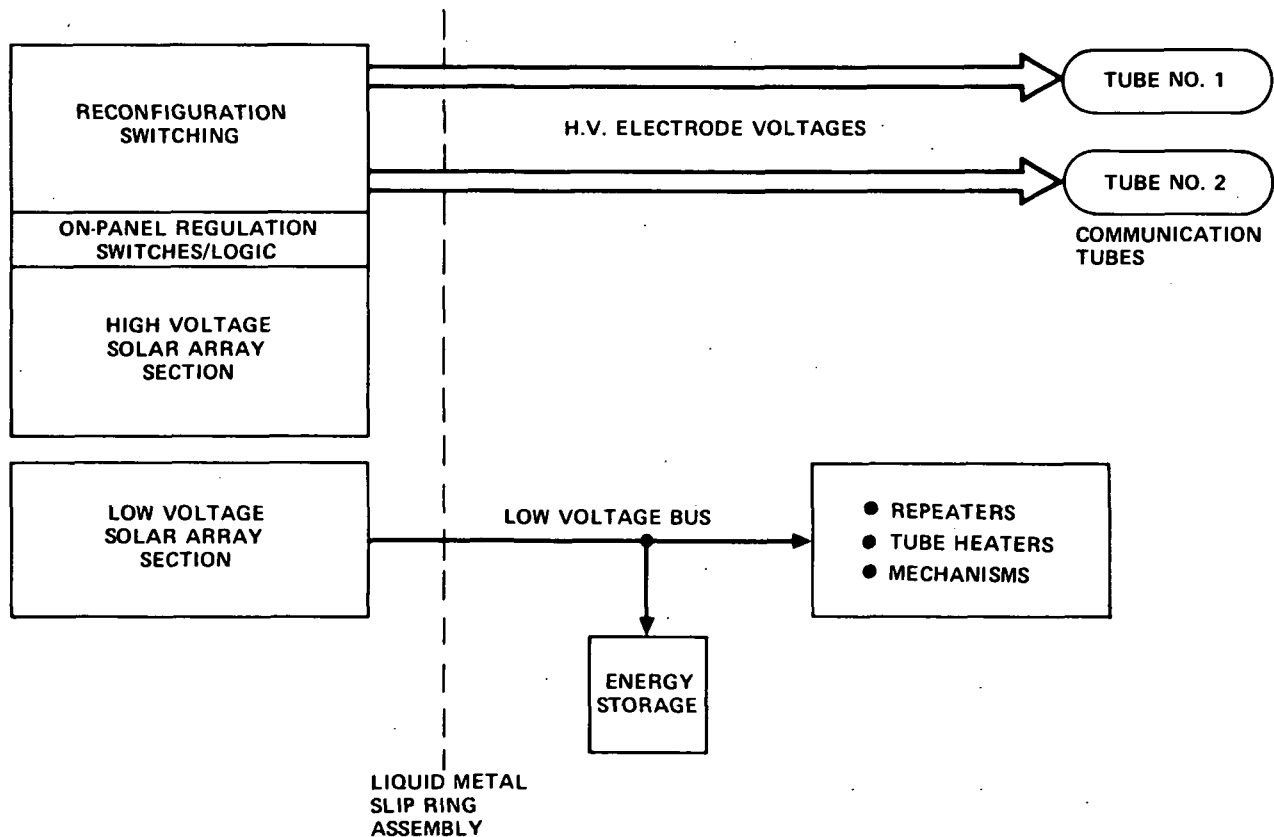
Figure 1-16. Power Management Block Diagram, Spacecraft Configuration B-5

1.4.5.2 Solar Arrays

In Typical spacecraft designs, the solar array represents a significant portion of the total weight. In multi-kilowatt spacecraft, such as the ATS/AMS, a departure from conventional designs is essential if severe weight penalties are to be avoided. Tradeoff analysis has indicated an advantage for either foldout or rollout arrays which are oriented to the sun. Further analysis has favored the rollout concept over the foldout because of weight and stabilization advantages. The technology for rollout systems of the power rating required for ATS/AMS has recently been demonstrated by the Air Force with the Hughes-developed FRUSA (Flexible Roll-Up Solar Array). For these reasons, a FRUSA derivative was selected for each of the three spacecraft configurations. The principal difference in the ATS/AMS arrays and FRUSA is the lighter weight solar cells with bonded covers chosen for ATS/AMS.

Array Arrangement and Sizing. The general arrangement of the chosen solar array consists of two rollout deployment drums, each carrying single panels of equal size and symmetrically attached to the spacecraft in either an E-W or N-S panel axis orientation.

The rollout drum storage technique was chosen after evaluation of other storage configurations, in particular, flat folding of flexible substrate arrays in "accordian" fashion. Structural weight of the flat fold storage package was not seen to offer significant advantage over the drum when all parts of the required mechanism system were taken into account. Most importantly, the uncontrolled nature of the deployment of flat folded arrays is considered a serious deficiency in any but impractically small sizes. Based on experience with FRUSA, the predictable and controlled deployment possible with drum storage is an important feature. Because of this, the drum design has been used as baseline on all spacecraft configurations.

The sizing of the arrays was based upon on-orbit load requirements of 5.5 to 6.0 kilowatts, 5-year degradation of cell output and solstice irradiation levels. This equates to a beginning of life power level of 8 kw for configurations B-1 and B-5 and 10.2 kw for A-1. A summary of array parameters for the three baseline spacecraft is presented in Table 1-16.

High Voltage Solar Array. Recent LeRC and Hughes studies on high voltage solar arrays (HVSA) have indicated the feasibility and superior performance associated with HVSA's. The principal features are the improved specific weight, efficiency and reliability inherent in the integral power conditioning functions performed by the array as compared with conventional power conditioning operating with a low voltage array.

Efficiency in a HVSA load conditioning can approach 99 percent when ideal matching with the load is achieved. The particular operating features of the 1-kw TWT and 2-kw klystron amplifiers preclude this ideal match but high overall efficiency can be obtained with appropriate mixes of 1 x 2 cm and

TABLE 1-16. ARRAY SYSTEM SUMMARY

	Spacecraft Configuration		
	A-1	B-1	B-5
Orbit Raising/ Direct Injection	OR	DI	DI
Low Voltage/ High Voltage	HV	LV	HV
Panel/Sun Orientation	Fully oriented	±23-1/2°	±23-1/2°
Power Requirement (watts)	5985	5615	5655
End of Life Nominal Output, Constraining Season (kW)	6.5	6.0	6.0
Beginning of Life Nominal Output Oriented Median Solar Intensity (kW)	10.2	8.0	8.0
Total Array Area (m²)	124	92.0	96.5
Total Array Weight Including Deployment and Storage Mech but not orientation (Kg)	138	107	115
Substrate Thickness (microns)	76 Kapton	25.4 fiberglass 25.4 Kapton	76 Kapton
Single Panel Length (m)	23.8	18.9	19.8
Single Panel Width (m)	2.59	2.44	2.44

2 x 2 cm cell strings. In-depth analysis of loads and power supply configurations for HVSA's is reported in Section 4.5.3. The weight increase in the A-1 and B-5 arrays for integral power conditioning is approximately 13.6 Kg but this approach permits an overall system weight saving of 36.4 Kg when compared to the conventional B-1 system.

1.4.5.3 Power Conditioning

Of the three selected baseline designs, only configuration B-1 employs conventional power conditioning for the communication tubes. The power conditioning designs for both orbit raising ion thrusters and communication tubes were investigated in considerable depth during the study. These two types of loads dominate the power demand for the extended total class of configurations considered and are therefore the determining factor in the choice of the bus voltage when conventional power conditioning is used.

To have a fair comparison between conventional power conditioning and the advanced high voltage solar array concept, competitive power conditioning designs at the specific power levels of interest should be generated which more accurately represent what could be achieved within existing technology. In generating and evaluating the conventional power conditioning configurations, past design experience in low power communication tube flight power supplies and in high power ion thruster flight prototype transistorized power conditioning was combined to arrive at design having attractive specific weight, efficiency and reliability specifications.

In order to apply proper consideration to all the interrelated factors affecting the power conditioning design, detailed designs of the power supplies for the 1-kw TWT and 2-kw klystron amplifiers were accomplished. The end results of these design studies is shown in Table 1-17. The conservative value of 110 pounds chosen for the ATS/AMS baseline is based upon a 50 percent contingency factor. This accounts for details which could interact with the overall spacecraft design to increase the weight.

TABLE 1-17. TWT AND KLYSTRON POWER CONDITIONING SPECIFICATIONS

Item	Calculated Estimates	ATS/AMS Baseline
Weight (Kg)	33.6	50
Efficiency (percent)	91.4	90
Radiating Panel Area (m^2)	1.17	1.2
5-year Reliability	0.96	0.96

1.4.5.4 Power Transfer

Five means of transferring electrical power and electrical signals across rotating joints in spacecraft were considered during the study:

1) Conventional brush-on-ring assemblies

2) Flex cables with fast return

3) Rotary transformers

4) Non-sliding rotary electrical connectors

5) Liquid metal sliprings

For the baseline spacecraft configurations, power transfer is constrained by the requirements for continuous rotation, relatively high currents, and the need to transfer power at very high voltages in some spacecraft configurations.

The tradeoff analyses for the use of the above five methods reduced the candidates to two, namely, the conventional sliprings and the liquid metal sliprings. The advantages and disadvantages of these two approaches were outlined in Table 1-5.

Conventional sliprings were chosen for configuration B-1. The slipring design for the solar array orientation mechanism of configuration B-1 is dominated by the large shaft which connects the two halves of the array through the body of the spacecraft. This shaft is likely to be 7.6 cm or greater in diameter and the sliprings must be mounted outside the shaft. It is estimated that the sliprings will have a diameter of 10.2 cm. For mounting locations on the end of a shaft, the diameter could be reduced to just enough to bring out the leads, to about 5.1 cm or less. The weight of the required 24 ring assemblies is about 6.8 Kg and the overall weight, including shafts, bearings, etc., is about 18.2 Kg.

Liquid metal sliprings (LMSR) were chosen for configurations A-1 and B-5.

LMSR design is also dominated by the through shaft. The weight of individual sliprings is determined by the same needs for electrical conductivity, dimensional stability and manufacturability. Sliprings for use with liquid metal cannot be made of silver, gold, copper, aluminum or beryllium because of the severe chemical reaction with gallium. Stainless steel, nickel and refractory metals such as tungsten and molybdenum are suitable. Therefore, despite the very low contact resistance, no great weight saving can be expected. The usual design of a LMSR utilizes a rotor and a stator ring for each line, and thus might be heavier for a given number of line functions than conventional sliprings. Liquid metal brush designs are being studied to reduce weight and complexity, and to increase environmental resistance.

The LMSR for the ATS/AMS can be accommodated with 116 rings, a ring complement which has been designed on another LeRC contract. The weight of the ring assemblies would be approximately 5.9 Kg out of the overall mechanism target weight of 18.2 Kg

Gallium is used in the liquid metal sliprings because of its low vapor pressure. Mercury has excessive evaporation. The 302°K Freezing point of gallium is convenient to allow freezing for retention during launch. The surface tension of 735 dynes/cm allows retention during orbital conditions and testing. Although the need for continuing studies into liquid metal slip ring operational characteristics is evident, the initial promise of low friction and electrical noise makes them an attractive candidate for this application.

1.4.5.5 Energy Storage

The energy storage system provides power during the launch phase prior to solar panel deployment, power for housekeeping operation during eclipse, and additional power for peak load requirements to the low voltage bus during sunlight operation such as igniting squibs, etc. The demand varies from a few watts during the launch phase to approximately 125 watts during the on-orbit eclipse operation. For the spacecraft configuration A-1, the solar panels are deployed within one hour of liftoff so the total energy consumed before deployment is less than required for on-orbit eclipse operation. For the B-1 and B-5 spacecraft, however, the launch and transfer orbit lasts approximately six hours and imposes a moderate constraint on energy storage. The equipment operating during this time will be minimized to make the total energy requirement approximately an equivalent to an on-orbit eclipse period.

The above requirements can best be satisfied for a 5-year mission lifetime with nickel-cadmium battery cells. These cells have been proved on many previous missions. They are available in reliably sealed individual cells with rugged electrode construction.

Based on the requirements of the baseline spacecraft configurations, a battery system composed of two 6-ampere-hour nickel-cadmium batteries appears adequate. This system can supply all mission needs at a depth of discharge of approximately 50 percent which permits a 5-year life to be achieved. Charging of the batteries is accomplished with the low voltage solar panel section, achieving a lightweight, reliable approach to providing a constant charge current.

1.4.5.6 Power Subsystem Weight Summary

The weights of individual electrical power subsystem units for the three baseline spacecraft configurations are presented in Table 1-18.

TABLE 1-18. POWER SUBSYSTEM WEIGHT SUMMARY (Kg)

Unit	Configuration		
	A-1	B-1	B-5
High Voltage Solar Array	138		115
Integral Power Conditioning	14.1		12.7
Low Voltage Solar Array		112	
Communications Conventional Power Conditioning	4.55	54.5	4.55
AC&S Ion Thruster Power Conditioning	6.45		
Orbit Raising Ion Thruster Power Conditioning	2.27		
Liquid Metal Sliprings	45.5		22.7
Conventional Sliprings		18.2	
Batteries and Electronics	22.7	22.7	22.7
Orientation Electronics	6.8	6.8	6.8
TOTALS	240	210	184

1.4.6 Thermal Control

The primary objectives of the thermal design effort during the study were to establish workable methods for handling the very high system power dissipations and for maintaining proper thermal environments for critical components during all phases of the mission. The study has been successful in establishing feasible designs for each spacecraft configuration.

1.4.6.1 Requirements

The orbital environment imposed identical requirements on all configurations considered and solutions were essentially identical for like sub-systems. Solar irradiation was the only significant external source of heating and deep space offered a heat sink in all other directions; Earth's effects are negligible. The north and south faces of the spacecraft were generally available for heat radiation, with due consideration required for the $\pm 23^\circ$ excursions of the Sun above and below the orbital plane. During equinox the loss of solar radiation due to eclipsing occurs over a period of 45 days for durations of up to 72 minutes per day.

The thermal environment during transfer to synchronous orbit is unique to each of the two basic configurations and impose special requirements on launch windows, attitude control and thermal control. The major factor affecting the thermal design in this period is the choice of orbit raising propulsion; conventional apogee motor insertion requiring only a few hours of transfer orbit operations while the solar/electric propulsion requires about 3 months to complete synchronous orbit insertion.

Unique temperature control requirements were associated with the RF power amplifiers, the liquid metal sliprings and the ion engines. The requirements and solutions for electronics, attitude control and power conditioning were generally typical of past practice.

1.4.6.2 Thermal Design

The maximum heat dissipation load to be radiated from the spacecraft, exclusive of the power amplifier collectors, varied among the configurations from approximately 1.5 to 2 kilowatts. Most of this heat is radiated in approximately equal amounts from north and south facing radiators. Several design options for direct radiating collectors were analyzed and the preliminary choice was for use of a sealed envelope radiator covering the entire collector assembly. Heat pipes were selected for transferring heat from the amplifier cavities to the equipment radiator and for heat distribution within radiators.

Freezing and thawing of the Gallium in the liquid metal sliprings is accomplished by on-pad precooling prior to launch, bulk spacecraft temperature during coast periods, and active heating during orbital operations.

It was found that temperature control for the ion thrusters could be maintained within limits by proper spacing between the thrusters in the cluster and by thermally isolating the cluster from the main spacecraft body.

Thermal designs for configurations A-1 and C-1 are essentially identical, as are the designs for B-1 and B-5. The key thermal control features employed in each of these four designs are summarized in Table 1-19.

1.4.6.3 Conclusions

Although the design approaches varied as a result of the significant complexity presented by the electric propulsion, high voltage arrays, and liquid metal sliprings, the differences in weight and development difficulty were not sufficient to affect the configuration selection process. Overall conclusions were that:

1) High temperature, direct radiating TWT and klystron collector designs are essential. (The radiator area available in the various configurations is not sufficient to handle the approximately 2 kw of thermal dissipation and maintain reasonable ambient temperatures.)

TABLE 1-19. KEY THERMAL FEATURES

	Configuration			
	A-1	B-1	B-5	C-1
Transfer orbit	a) 200 watts of active heating b) 40 watts of continuous	Ejectable radiator covers	Ejectable radiator covers	a) 400 watts of active heating b) 40 watts of LMSR heating
On-orbit operations	Use excess system power for active heating when tubes are operated in the backed-off mode	Passive	Passive	Use excess system power for active heating when tubes are operated in the backed-off mode
	80 watts of continuous LMSR heating (2 assemblies)	10 watts RCS heating	a) 10 watts active RCS heating b) 40 watts LMSR heating	80 watts of LMSR heating (2 assemblies)
Power system demands, watts	240	10	50	440
Thermal Control Weight (kg / lb)				
● Apogee motor insulation		0.9 / 2	0.9 / 2	
● Low temperature insulation	2.6 / 6	3.6 / 8	3.6 / 8	3.6 / 8
● High temperature insulation (ion engines and tube collectors)	4.5 / 10	0.9 / 2	0.9 / 2	4.5 / 10
● RCS heaters		1.4 / 3	1.4 / 3	
● LMSR heaters	0.9 / 2		0.5 / 1	0.9 / 2
● Second surface mirror radiator finish	2.3 / 5	6.8 / 15	4.5 / 10	3.6 / 8
● Internal paint	1.4 / 3	1.4 / 3	1.4 / 3	1.4 / 3
TOTAL	11.8 / 26	14.1 / 31	12.3 / 27	14.1 / 31

2) Large amounts of localized power dissipation (with saturated tube operation) within the spacecraft require the use of heat pipes to provide adequate energy distribution. Particularly significant thermal loads are the RF output switches, filters and lines, which result in 590 watts of thermal dissipation for 3 kw of RF output, and must be temperature controlled to stay in the range from 273 to 338°K.

3) On-orbit temperature control when tubes are operating below saturation can be provided through active heating without penalizing the power system design. The operating characteristics of the multistage collector tubes are such that ample power becomes available for active temperature control purposes when the tubes are operated in a backed off mode.

4) Transfer orbit temperature control can be provided through active heating for the electric propulsion configurations. Ejectable radiator covers are required for the apogee motor configurations, since prime power is not available.

1.4.7 Tracking, Telemetry and Command (TT&C) Subsystem

Estimated telemetry and command requirements for this mission are similar to those for many other spacecraft and can be satisfied with a conventional design approach. The VHF TT&C Subsystem is essentially the same for all spacecraft configurations and has been designed to be compatible with the existing STADAN system currently in operation by NASA. A functional diagram of the subsystem is shown in Figure 1-17. As indicated in the block diagram, commands are processed in a central decoder and transferred to remote local decoders for execution. Similarly, telemetry signals are sampled in remote multiplexers, all of which feed a central encoder which converts all analog signals to eight-bit digital words. The Central encoder also time division multiplexes (TDM) all of the data into a
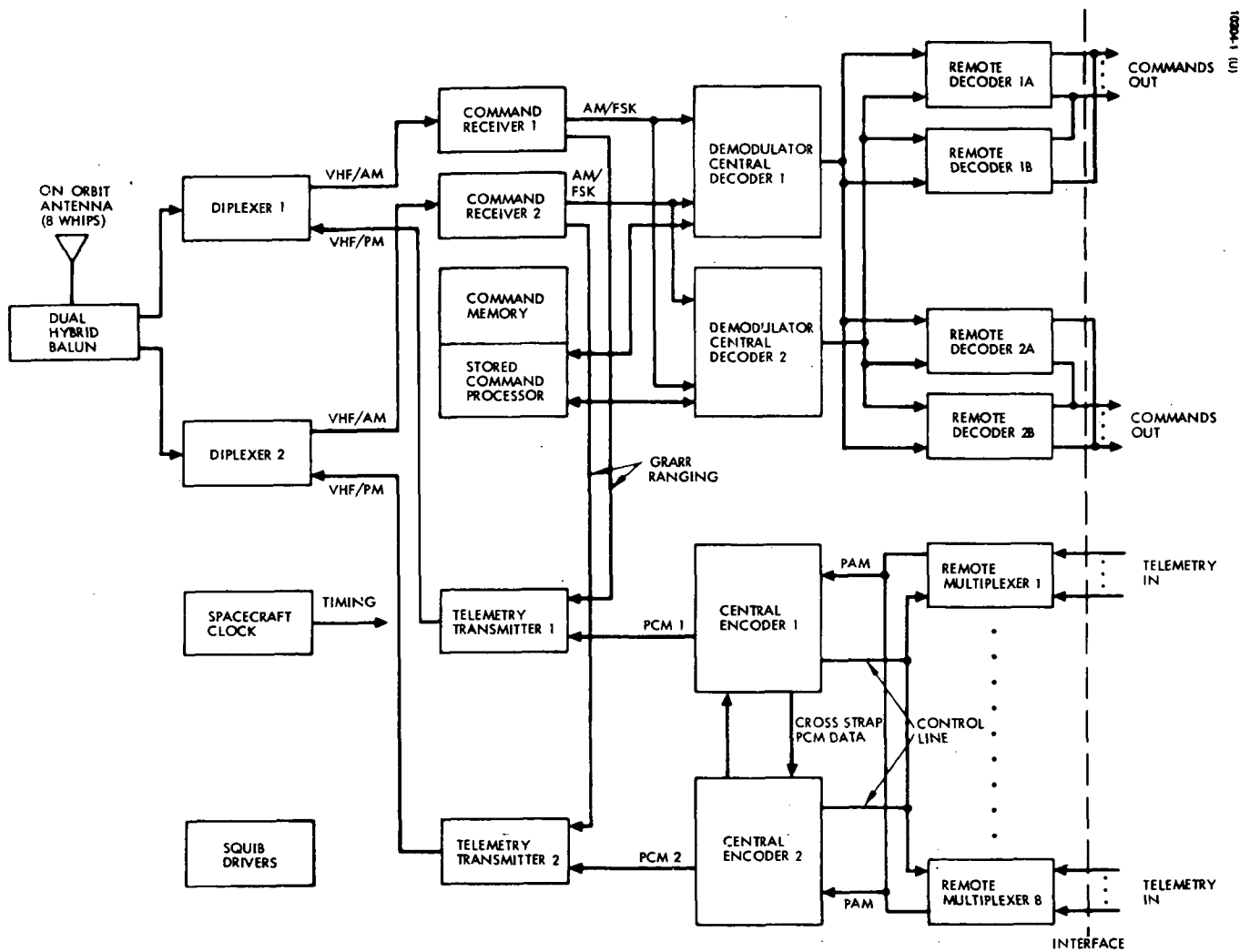
Figure 1-17. TT&C Block Diagram

PCM bit stream, which is then bi-phase modulated onto a carrier before entering the telemetry transmitter. The transmitter can operate in either a non-coherent mode, at a frequency originating in the spacecraft, or in a coherent mode, where its frequency is derived from the frequency of the received command signal. In the coherent mode, the command receiver/ telemetry transmitter acts as a GRARR* transponder to provide accurate ranging information for purposes of orbit determination. As indicated in the block diagram, full redundancy is employed to ensure high reliability.

The principal difference between implementation concepts for the different spacecraft configurations is in the Command Memory/Stored Command Processor. For configuration A-1, this unit must store at least one days worth of commands for the orbit-raising attitude and thrust profiles. On-station requirements are about the same for all configurations.

The hardware employed is largely existing. In a few cases, slight modifications from existing designs (employed in the OSO program) are required. However, no new development is foreseen.

1.5 MISSION PROFILE

The ATS/AMS spacecraft mission occurs in three phases, namely prelaunch operations, launch and injection into synchronous orbit, and on-orbit operations, each of which is described below.

1.5.1 Prelaunch Operations

The spacecraft would arrive at the launch facility (ETR) in a partially disassembled state following final acceptance at the manufacturing facility. After reassembly and optical alignment procedures have been completed, a functional test of all spacecraft subsystems will be performed and the results compared with prior test data to ensure that no damage has resulted in the intervening period. Standard prelaunch procedures are generally applicable; special operating constraints are described below.

Power Amplifiers - Depending upon the final design of the power amplifier tube collectors, continuous operation may not be permitted unless provision is made for cooling the collectors. In this case, full tests may be performed before the spacecraft is encapsulated in the fairing. Thereafter, pulsed operation will permit verification of functional operation.

Ion Engines - Functional tests are limited to verification of power conditioning and switching circuitry. Full operation cannot be performed because of contamination and facility constraints.

---

*The Goddard Range and Range Rate System.

Solar Cell Arrays - Special tables will be required to verify the panel deployment mechanisms. Functional testing will be constrained to portions of the panel at a time as it is not feasible to simultaneously illuminate the entire panel area. If high voltage arrays are employed, precautions must be taken to ensure that voltages developed during testing do not exceed values limited by the atmospheric environment.

Liquid Metal Sliprings - The liquid metal (Gallium) must be kept frozen and in an inert environment prior to launch to minimize contamination of the Gallium. Therefore, no functional testing of the LMSRs is feasible before post-launch separation from the booster.

1.5.2 Launch and Injection to Synchronous Station

Launch and post-launch operations are essentially the same as for any synchronous satellite. In the case of a low-thrust upper stage, the orbit raising period is essentially similar to an extended "transfer orbit," and will require support from the STADAN system for about 3 months. However, the spacecraft TT&C subsystem has sufficient capacity to store commands for at least a 24-hour period, and ground support is required for only a few minutes each day.

1.5.3 On-Station Operations

After arriving on station, a functional test will be performed on all operative spacecraft subsystems, using telemetered data for verification of operation. It is assumed that a dedicated ground terminal will be provided to this mission; such a terminal must be equipped to operate at the communications frequency (14.0 to 14.5 GHz on the up-link and 11.7 to 12.2 GHz on the down-link). It should also be capable of handling TT&C functions, or be colocated with a TT&C ground terminal so that various experimental configurations can be commanded and monitored in real time operations. After functional tests have been completed, the spacecraft is ready for performing the desired communications experiments.

1.6 TRAJECTORY CONSIDERATIONS

Two fundamentally different launch profiles have been considered in this study. The launch vehicle for the A configuration is a Thor-Delta 2914. The launch injection into transfer orbit is similar to that for the all-chemical injection. However, the orbit raising to synchronous station is done over approximately a 3-month period with low-thrust ion propulsion. A conventional all-chemical injection has been utilized with the B configuration launch vehicles, where the launch vehicle is an Atlas-Centaur. All-chemical injection has become essentially a routine operation and therefore will not be analyzed in depth.

1.6.1 All-Chemical Launch and Injection

The launch and transfer orbit injection for reaching synchronous orbit are similar with either chemical or low-thrust ion propulsion. Figure 1-18 shows a typical launch and transfer orbit injection for the Thor-Delta launch vehicle. Liftoff takes place at a time compatible with launch window constraints. Following liftoff, the first stage and a partial burn of the second stage places the spacecraft into a 28.5 degree inclined parking orbit 8.9 minutes after liftoff. After a 15.5 minute coast in the parking orbit, the second stage is restarted. This second burn of the second stage and the entire third stage inject the spacecraft into a 28-degree inclined transfer orbit about 26 minutes after liftoff. The trajectory for Atlas-Centaur is similar.

Synchronous injection with an apogee kick motor is shown schematically in Figure 1-19. The apogee kick motor is fired to circularize the orbit and remove the inclination. Firing is done at one of the first few apogees, and is usually planned to occur at that apogee which is closest to the desired station location of the satellite to minimize the time of drift to the desired station.

Configurations B-1 and B-5 have been optimized to perform the all-chemical mission with the Atlas-Centaur launch vehicle and an optimum solid motor for final orbit injection.
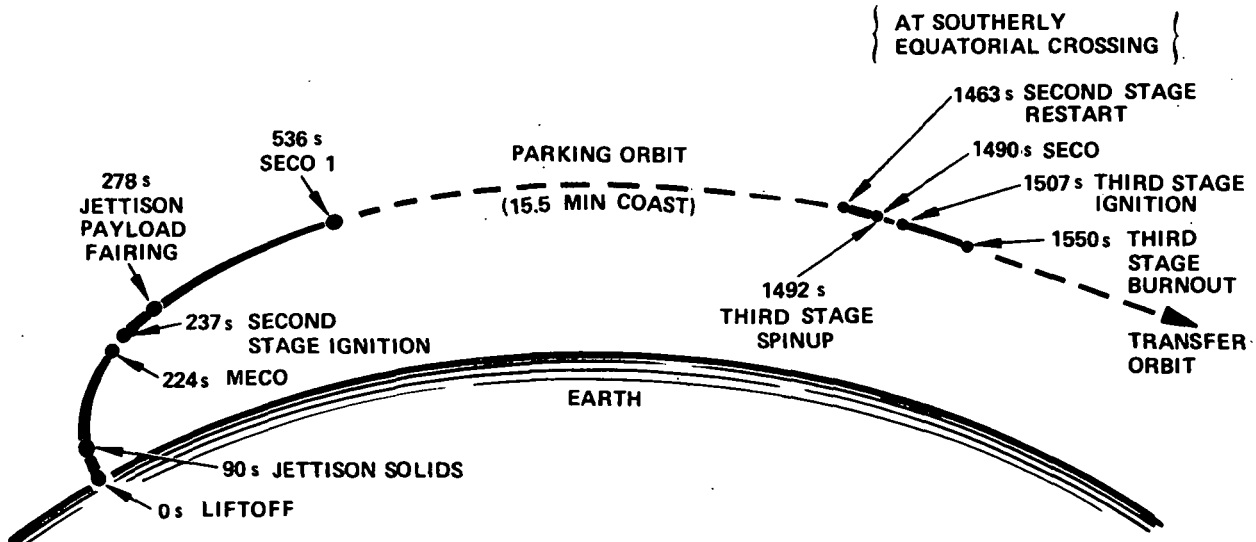
Figure 1-18. Typical Parking and Transfer Orbit Injection
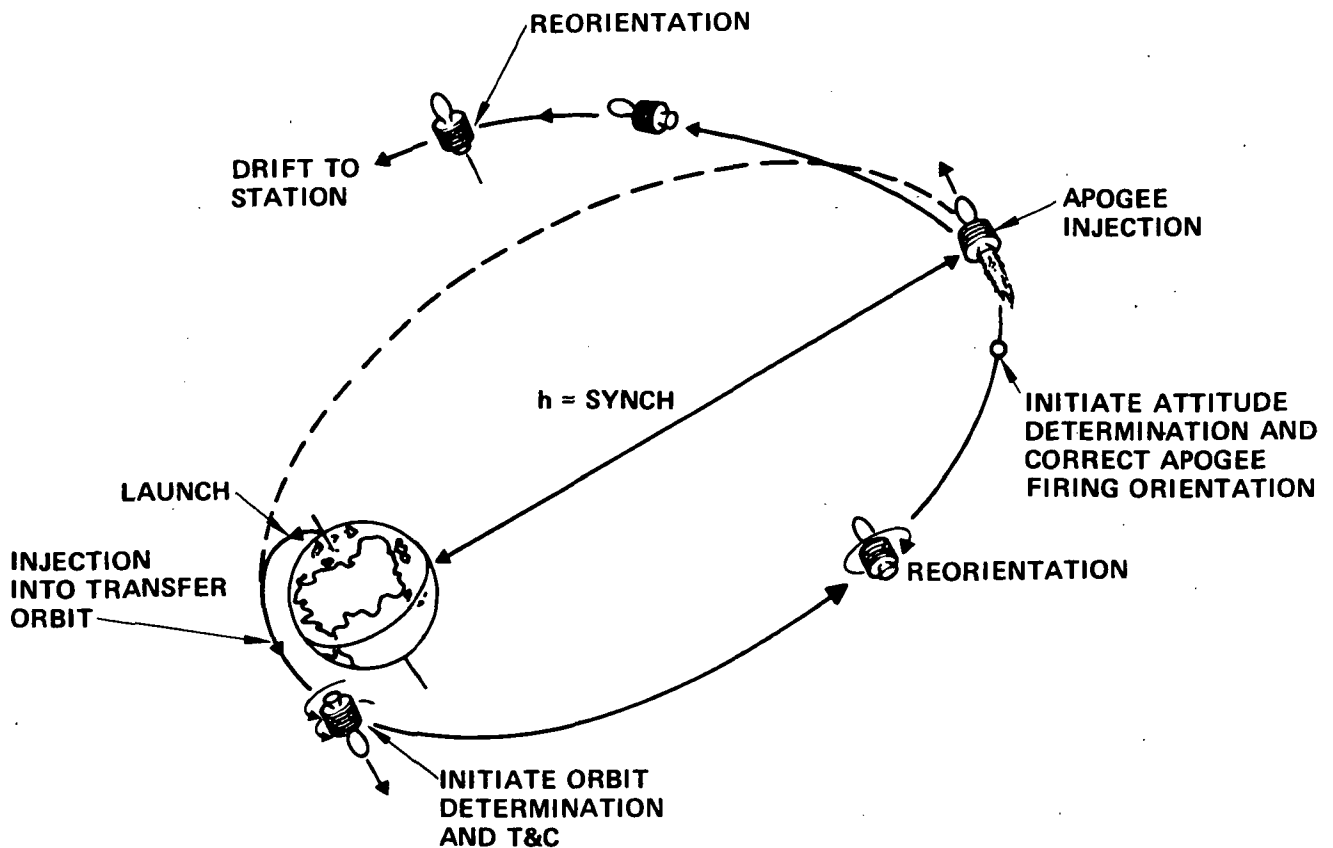
Figure 1-19. Synchronous Injection with Apogee Kick Motor

1.6.2 Orbit Raising with Low-Thrust Propulsion

The general approach to the low-thrust orbit raising analysis has been one of determining the constraints and relationships which circumscribe practical trajectories. Among the many variables which determine an optimum trajectory and solar-electric system design are the solar array degradation which accrues as the orbit is slowly raised through the radiation belts and thrust/attitude profiles which are most efficient in terms of both maneuver duration and payload ratio. Software has been developed at Hughes for treating this complex problem and for optimizing both the trajectory and the propulsion system design.

Detailed analysis of the tradeoffs in selection of the low-thrust trajectory and system design specifications are presented in Section 3.3. It was found that the Thor-Delta 2914 launch vehicle had sufficient performance in combination with a range of possible solar-powered low-thrust propulsion systems to insert the necessary payload. Selection of starting perigee and apogee values for the orbit raising phase was based on payload and spacecraft optimizations. The lowest possible perigee was desirable but this minimum was limited by aerodynamic drag effects to about 555 kilometers. A high initial

apogee, in the neighborhood of synchronous orbit altitude, was found to be advantageous because it reduces the solar cell degradation and also the time of the orbit raising maneuver. Figure 1-20 helps to illustrate how the orbit raising time is reduced with higher initial apogees and how matching the solar power to the orbital mission requirements (about 6 kw) also affects the orbit raising duration. Plane changing from 28 degrees to zero can also be accomplished in an optimal way during the orbit raising maneuver.

Further optimization of the propulsion system involved the design and sizing of the solar array and the optimization of ion thruster parameters such as specific impulse, thrust level, reliability, thrust vector control and throttling. Final details of this design optimization are discussed in Section 4.4 for the ion propulsion and Section 4.5 for the power system.

A baseline value of 10.2 kw for initial rated solar panel power was chosen for the A-1 configuration. With this initial power and the effects of radiation degradation with increasing orbit raising durations, a payload injection estimate can be made in terms of initial apogee radius. A variation of injected mass with initial apogee radius is shown in Figure 1-21. For final injected mass approaching 600 kg, the maximum apogee should be less than 6 earth radii. Table 1-20 indicates the selected baseline trajectory parameters. Much latitude in the design of the orbit raising mission and resulting spacecraft payload performance is possible when the solar-electric orbit raising is used; this is in sharp contrast to the essentially single point performance result with all-chemical propulsion when the booster and apogee motor is specified.
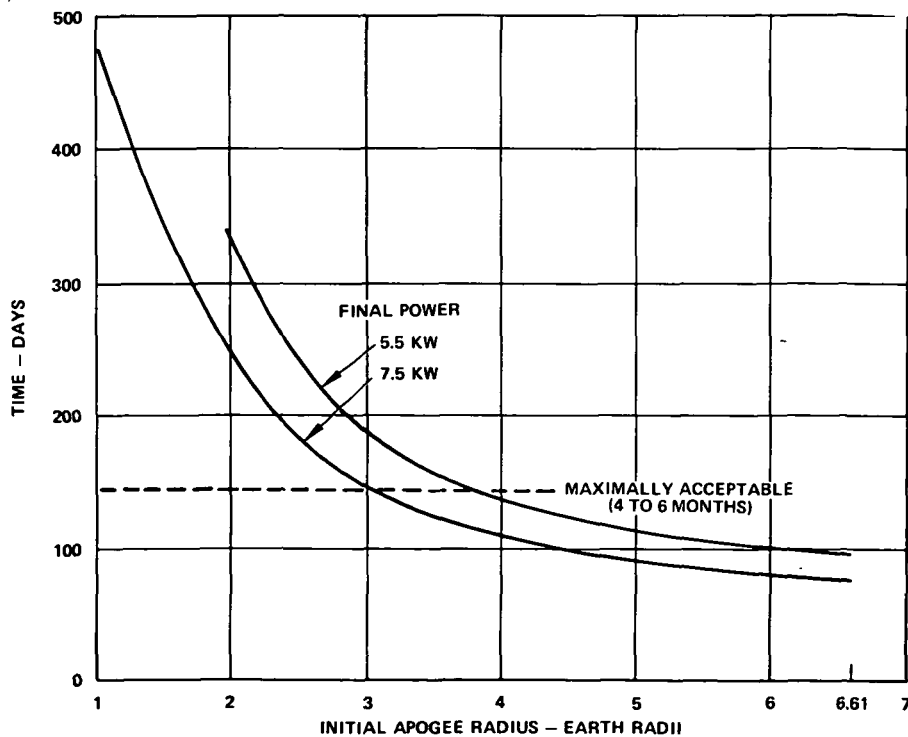
Figure 1-20. Orbit Raising Time
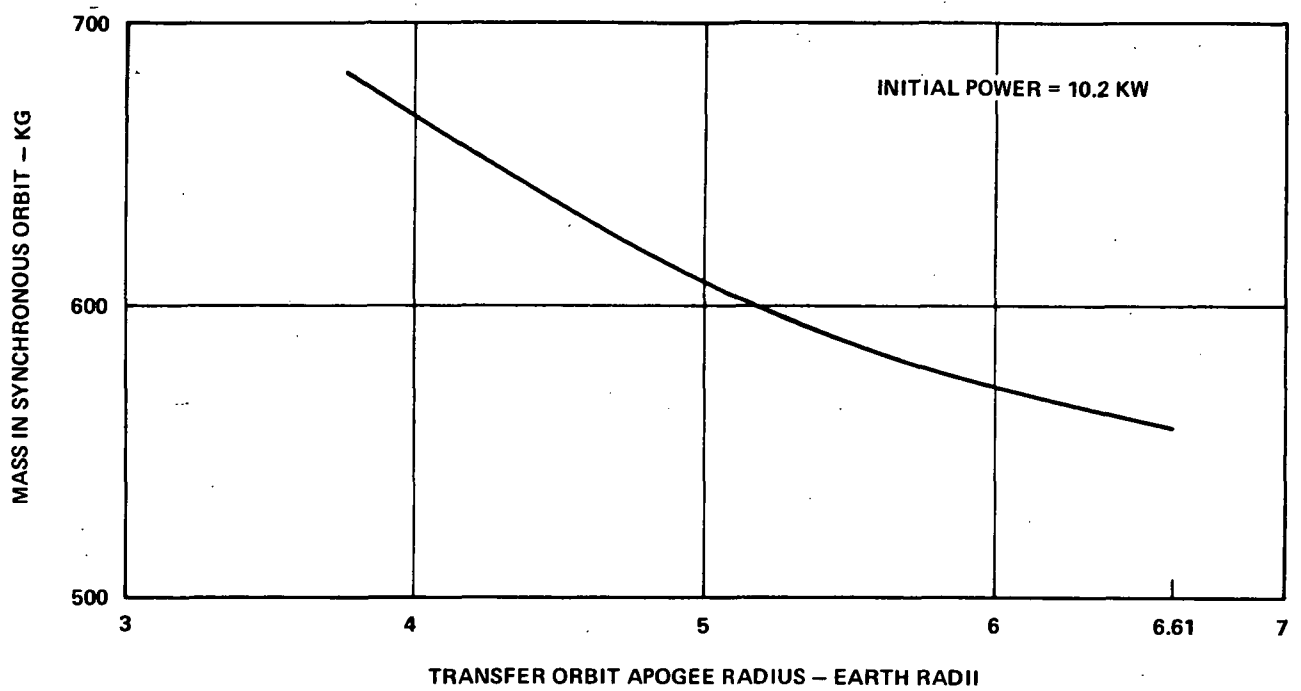
Figure 1-21.   A-1 Configuration Orbited Mass Capability

TABLE 1-20.   BASELINE TRANSFER TRAJECTORY
PARAMETERS

Apogee altitude	= 17,200 n.mi	= 31,900 km	
Perigee altitude	= 300 n.mi.	= 555 km	
Inclination	= 28 degrees		
80-day orbit raising time			
45-minute coast at perigee			

1.7 PROGRAM PLAN

An ATS/AMS program plan has been prepared to provide a schedule for program implementation and a gross estimate of resource requirements.

Section 5 provides a discussion on the Master Phasing Schedule, the facility requirements and the estimated cost. It is estimated that the ATS/AMS program can be executed in a thirty-month time span. The Master Phasing Schedule has been prepared using January 1974 as a program start date and July 1976 as launch date.

An initial analysis indicates that the facilities requirements necessary to perform the ATS/AMS program can be met with some specialized subsystem and system facilities and some modifications to the existing test facilities.

The program cost totals shown in Table 1-21 have been derived by having the responsible engineering activities prepare their best estimates of how long and how much it would take to perform their portion of the ATS/AMS program.

TABLE 1-21. ATS/AMS COST COMPARISON
(Dollars in Millions at Sales Price)

Description	A-1	B-1	B-5
Spacecraft Development	57.5	52.2	53.8
Thor Delta (2914) Launch Vehicle	6.0		
Atlas-Centaur Launch Vehicle		16.0	16.0
Total Program Cost	63.5	68.2	69.8
Recurring Cost for each Additional Spacecraft (including L/V)*	20.4	29.0	29.5
Recurring Cost Delta (Relative to A-1)		+8.6	+9.1
1971 Dollars			
*Assuming a user procurement of eight operational spacecraft			

1.8 CONCLUSIONS

The ATS Advanced Mission Study established the feasibility of configuring synchronous satellites capable of carrying high power transmitters outputting up to 3 kilowatts of RF power into an antenna with mulitple shaped beams.

The three baseline spacecraft configurations significantly vary with respect to each other in their usage of new technologies. However, preliminary estimates of the program cost for the development of a single flight vehicle with a refurbished prototype as a back-up flight vehicle are all about the same magnitude for the different baselines. Recurring costs for additional spacecraft, including launch vehicles, favors the A-1 configuration if it is to be applied to a multi-spacecraft operational application employing on-station payloads requiring large amounts of prime power (upwards of several kilowatts).

Depending upon the spacecraft condiguration ultimately selected, the following technology areas require further development which should be initiated in advance of the spacecraft procurement:

- Ion Engines

- Orbit-raising Trajectory Optimization

- High Power TWTs and/or Klystrons

- Contoured Multiple Beam Antennas

- High Voltage Solar Cell Arrays with Integral Power Conditioning

- Liquid Metal Sliprings and Bearings

- Dynamic Analysis (simulation) of Interactions between Large Solar Cell Arrays and Spacecraft Attitude Control

2. MISSION REQUIREMENTS AND OPERATIONS

Specific spacecraft design objectives, initially derived from the contract Statement of Work* and modified by direction from NASA and/or the iteration of requirements and design instructions as the study proceeded, are discussed in the first part of this section. The second part identifies and briefly discusses a variety of experiments potentially applicable as candidates for any unused spacecraft payload capability. Finally, Section 2.3 covers mission operations, commencing with pre-launch operations at the launch site and continuing through on-station operations.

2.1 SPACECRAFT DESIGN OBJECTIVES

The ATS Advanced Mission (ATS-H) Spacecraft is intended to demonstrate a variety of communication experiments when positioned in geostationary orbit. The primary objectives include the operation of high power 12 GHz (1 kw or more) transmitters and a contoured antenna pattern for the demonstration of the operation of information networking systems servicing small user terminals. Much of the high power spacecraft technology being developed by Lewis Research Center (LeRC) is directly applicable to these objectives. These include high power transmitting tubes, shaped-beam antennas, high voltage solar arrays, ion thruster systems, and liquid metal sliprings. Launch of this spacecraft is projected for 1976, thus allowing completion of the development of most of the required technology prior to the start of the spacecraft procurement.

2.1.1 Primary Experiments

The ATS/AM spacecraft should incorporate a number of experiments, defined below, which are considered as primary to the mission.

High Power 12 GHz Transmitters

Provide amplification of microwave signals to power levels of 1.0 kw or more in the frequency band of 11.7 to 12.2 GHz, using a tube which employs a high temperature collector (up to 1273°K) for direct heat rejection of electrical power dissipated in the tube. The amplifiers for this mission shall be one or more klystrons and/or TWTs with efficiencies of 50 percent or greater.

---

*The original Statement of Work, as amended by Supplemental Agreement No. 1 to this contract, is included in Appendix A to this report.

These tubes will be integrated into the spacecraft in such a fashion that they may be vented to space vacuum after launch, if so desired. The tubes shall be driven with an angle modulated signal, with their output signals ranging from saturated to 6 dB below saturation. In addition, the tubes should be able to withstand continuous operation in a zero drive condition.

Illumination by Contoured Antenna Patterns*

Provide controlled illumination of desired areas on earth by space-borne antennas having selectable contoured patterns. This antenna, in conjunction with the high power repeater, will enable communications to and from multiple small ground terminals.

Networking of Small Ground Terminals

The communications subsystem shall include the ability to perform as an active repeater in a variety of experiments demonstrating networking applications employing small user terminals. In performing these experiments, transmissions to the spacecraft will be made in frequency range of 14.0 to 14.5 GHz** and retransmitted from the spacecraft in the frequency range of from 11.7 to 12.2 GHz.

Hi-Voltage Solar Cell Arrays

Power is to be obtained from chains of photovoltaic elements, biased to levels of 5, 10, and 15 kilovolts with respect to ground. The high voltage solar panel technology being developed by LeRC will be considered for operational use as the prime solar panel power. The overall spacecraft electrical subsystem design should utilize the space vacuum environment for high voltage insulation wherever possible. (This experiment shall not be required if high voltage arrays are used as the primary power source.)

Liquid Metal Sliprings

Use of gallium liquid metal slipring for transfer of power across a rotational joint will be demonstrated, either as a separate experiment or as an integral element of the electrical power subsystem.

---

*Illumination of controlled areas of the earth with contoured beams having radii or curvature varying from 0.004 radian to 0.1 radian became a revised design objective with the execution of supplemental agreement No. 1 to the contract.

**At the time this study was initiated, it was anticipated that transmission from the ground to the ATS/AMS spacecraft would be in a 13 GHz band. This was subsequently revised to 14 GHz as a result of adopted frequency allocations.

2.1.2 Spacecraft Subsystems

The principal spacecraft subsystems are identified in Table 2-1. The key requirements for each of these subsystems are discussed in the following paragraphs. In addition, constraints are imposed on their design depending upon the specific vehicle configuration being considered. These constraints, consisting primarily of weight and geometric limitations, are derived from booster payload and dynamic envelope considerations. Their impact on subsystem design is covered in more detail in the Spacecraft Descriptions and Subsystem Design, Sections 3 and 4 respectively.

2.1.2.1 Communications Subsystem

The Communications Subsystem is shown functionally in Figure 2-1; it is comprised of the antenna and the repeater subsystems, each of which are separately discussed below. As indicated in the diagram, the antenna subsystem must be capable of receiving and transmitting on a selected combination of beams from among the total number it is capable of illuminating. The repeater, in turn, takes the selected incoming signals, processes them to form the desired output signals, and amplifies them in power amplifiers capable of developing RF signals at the 1 to 2 kilowatt level. Both the input and output beam selectors are shown as straddling the two subsystems, as this function is likely to be partially implemented in each subsystem.

The overall communications subsystem is the principal direct element of the spacecraft employed in the primary experiements of demonstrating high power radiation, controlled illumination of selected earth areas, and networking of small user terminals.

TABLE 2-1. PRINCIPAL SUBSYSTEMS OF ATS/AMS SPACECRAFT

Communications
Antenna
Repeater
Attitude Control and Stationkeeping
Orbit Raising
Electrical Power
Thermal Control
Telemetry and Command
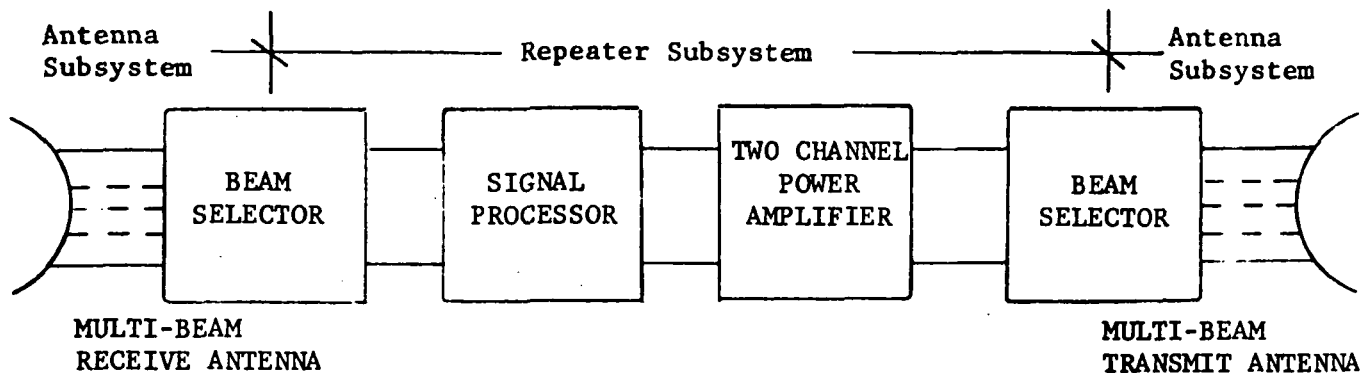
Figure 2-1. Communication Subsystem Functions

2. 1. 2. 2 Antenna Subsystem

Based upon the original Statement of Work, and upon discussions with NASA/LeRC personnel, the original design objective for the antenna subsystem was for the controlled illumination of desired areas of the earth. Specifically, shaped multibeam illumination was desired, with major beam dimensions of up to 7 degrees, minor beam dimensions as small as one-half degree, and having a ratio of major to minor beam dimensions not exceeding three. The initial design goal was that this subsystem be capable of forming the following beams, any two of which could be illuminated simultaneously:

1) The contiguous area comprising the 48 states as a single area.

2) The four sub-areas corresponding to the time-zone regions of the 48 states.

3) Hawaii

4) Alaska

One experiment to be performed while simultaneously illuminating two non-contiguous areas is frequency reuse; this might be done by simultaneously transmitting different information channels to the Eastern and to the Mountain or Pacific time zones over the same frequency band.

Contract Amendment No. 1 changed the design objectives for the antenna subsystem, primarily by defining a requirement for contouring the beams in terms of radii of curvature (from 0.004 to 0.1 radian). Its purpose is to achieve the illumination of areas more closely fitting the desired geographic regions. The areas defined in Figure 2-2 are representative of typically desired illumination contours.

The four continental United States time zones, Figure 2-2(a), are one such group of representative areas for which contoured beams are desired. A second set corresponding to cultural regions is shown in
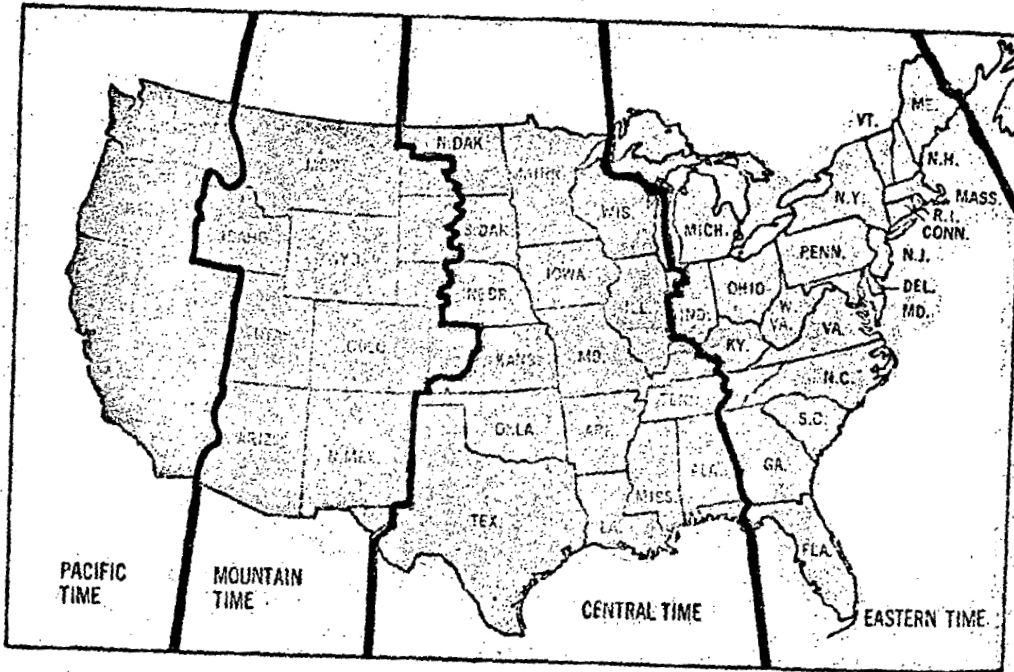
Ground Station Symbol Legend:

+   Public Broadcast System (PBS)
        Originating Station

◊   PBS Storage Station

○   Special Region Service Station

✕   PBS/Office of Education (PBS/OE)
        Service Center

Figure 2-2(a).   Representative Antenna Illumination Areas
              (a) Continental Time Zones

Figure 2-2(b), which includes the Alaskan and Hawaiian regions as well as a division of the 48 continental states into five regions. Part "c" further identifies two regions for Special Region Service. In addition, the locations of a variety of ground terminals are superimposed on the maps of Figure 2-2. These include Public Broadcast System (PBS) Originating Stations, which are located so as to fall both within each of the time zones and the five cultural regions comprising the 48 states, PBS/Office of Education (PBS/OE) service centers, and several Special Region Service stations. As indicated, in many cases, a single site will comprise several or all of the ground station types.

In technical discussions with the NASA Project Manager relative to the revised statement of work, it was agreed that emphasis should be placed upon a lens antenna designed for transmitting over the band from 11.7 to 12.2 GHz and capable of illuminating the time zones of Figure 2-2(a), plus spot beams illuminating the Hawaiin-Alaskan regions. Also to be incorporated into the design was switching of feed array elements to illuminate the Appalachian Region shown in Figure 2-2(c).

The antenna pattern for the Eastern time zone will be developed to show side lobe levels across the other three time zones of Figure 2-2(a), as well as gain over the desired region of coverage. Only 3 dB contours will be required for the other three time zones.

Gain for an uplink transmission at 14.5 GHz from a fixed ground station on the eastern seaboard will also be calculated; it is nominally a worst case in its offset from the boresite axis of the lens.

2.1.2.3 Repeater Subsystem

Requirements for the repeater subsystem largely had to be developed as part of the study. Specific requirements imposed by the SOW (Appendix A) include the following:

- The microwave power amplifiers shall be Klystrons or travelling wave tubes (TWTs) with efficiencies of at least 50 percent (Paragraph 3.5).

- Angle modulation format shall be used, and the output signal level shall range from saturated to 6 dB below saturated (Paragraph 3.13).

- The spacecraft shall be of repeater type operation (Paragraph 3.14). This was interpreted as a frequency-translation type of repeater, and the spacecraft receive frequencies were assumed to be from 12.75 to 13.25 GHz, based upon the U.S. recommendations to the ITU World Administrative Radio Conference (WARC). Subsequent to the completion of the initial design effort on this study, the 1971 WARC recommendations provided a 500 MHz uplink band from 14.0 to 14.5 GHz. The shift in frequency does not represent a significant change to the repeater concept, although it obviously changes implementation details.
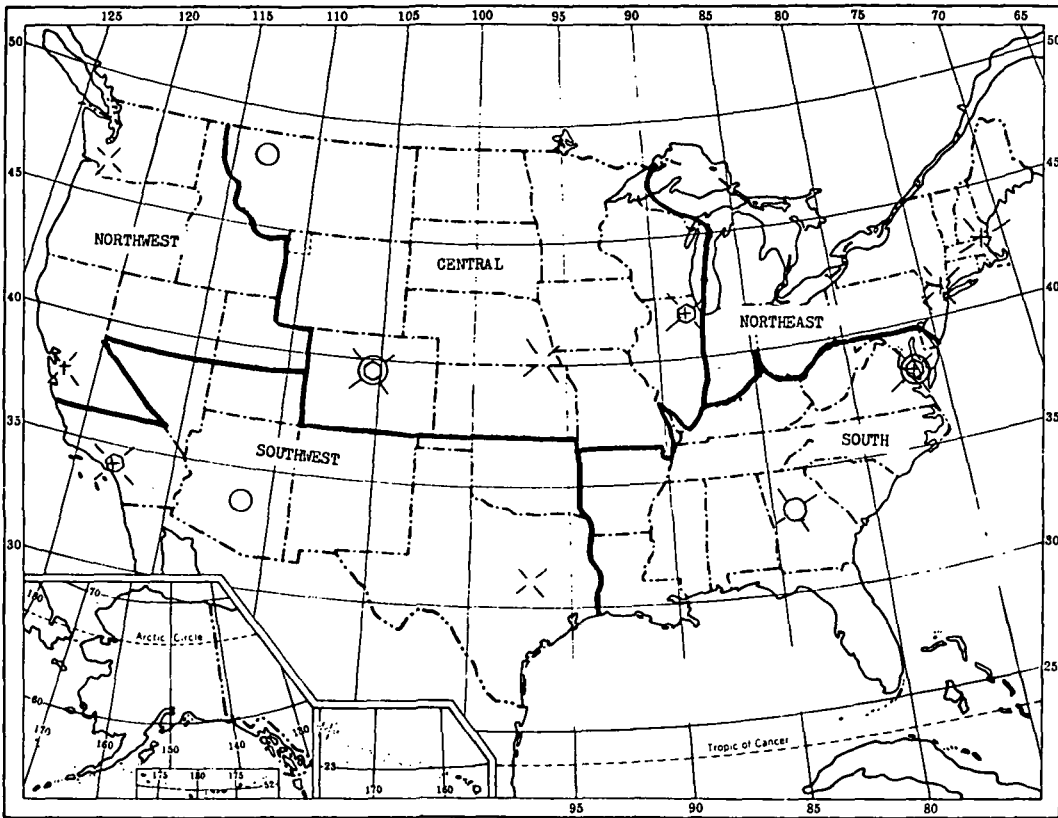
Figure 2-2(b). Representative Antenna Illumination Areas
(b) Cultural Regions
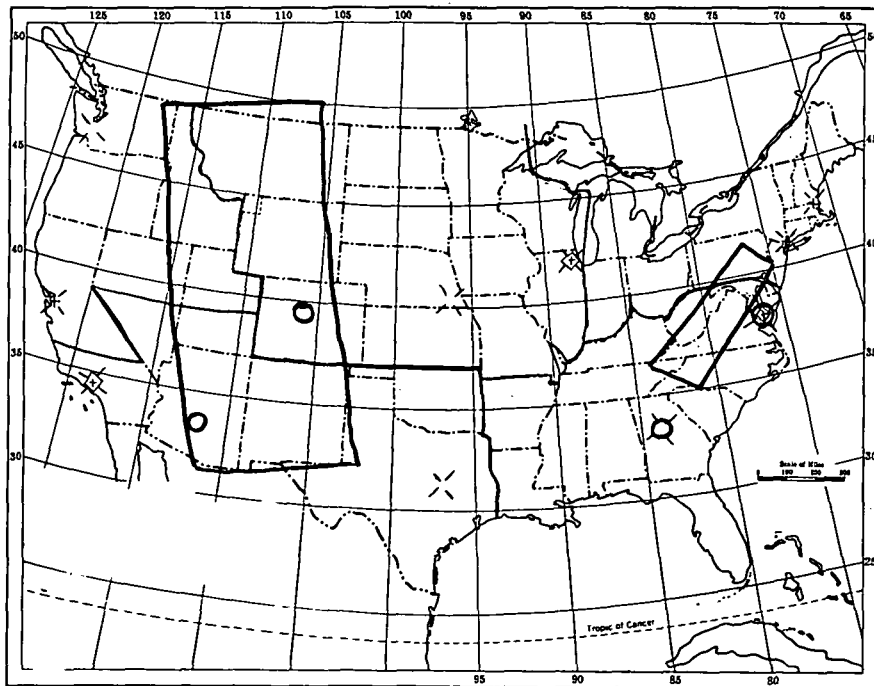
Figure 2-2(c). Representative Antenna Illumination Areas
(c) Special Regions

2-7

In technical discussions with the NASA/LeRC Project Manager and based upon preliminary configuration study results, it was further established that the repeater should include two power amplifiers, consisting of one TWT at one kilowatt, and one Klystron with a power level exceeding one kilowatt (two kilowatts desired). (As shown in Section 3.1, the three baseline spacecraft configurations all are capable of carrying the 1 kw TWT and a 2 kw Klystron.) The use of a Klystron for the higher level amplifier was predicated upon Klystrons having a greater efficiency than TWTs.

With two power amplifiers, the repeater is essentially a two-channel device, as shown conceptually in Figure 2-3. Outputs from two of the receive antenna ports would be selected by the input multiplexer. To provide operational flexibility, the filters would permit either of the received signals to be passed directly through the channel or split into two parts, one of which remains in the original channel and the other is diverted to the alternate channel. The two basic operating modes are shown in Figure 2-4, which portrays a particular manner in which each of the two modes may be operated. For the direct translation through the two channels, as shown in the upper portion of Figure 2-4, the indicated single wideband video carrier could equally be multiple carriers of narrower bandwidth, originating from one or more ground stations operating within the area illuminated by the selected receive antenna beam.

To provide additional flexibility, specifically directed towards a frequency reuse experiment, the TWT power amplifier will be designed to operate at two frequencies, namely, f_1 and f_2, as shown in Figure 2-3, whereas the Klystron need operate only at the single frequency, f_2. (The two frequency operation was assigned to the TWT because of their typically wider bandwidth than is available with Klystrons.)

Specific frequency allocations for power amplifiers were discussed with the NASA Project Manager during the period in which the lens antenna design was being performed. Because of its bandwidth limitations, it was established that the Klystron would have a bandwidth of 120 MHz at the top end of the transmit band, or from 12.08 to 12.20 GHz, as shown in Figure 2-5. Within the 120 MHz allocated, two 40 MHz channels are assumed.
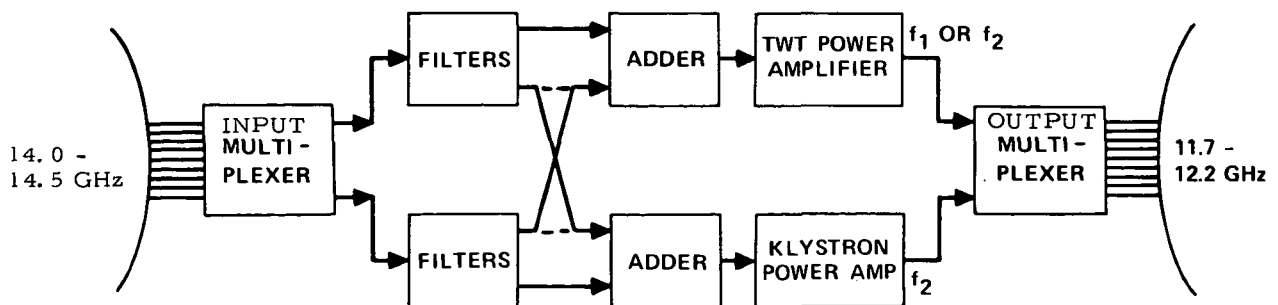
Figure 2-3. Multi-Mode Repeater Concept
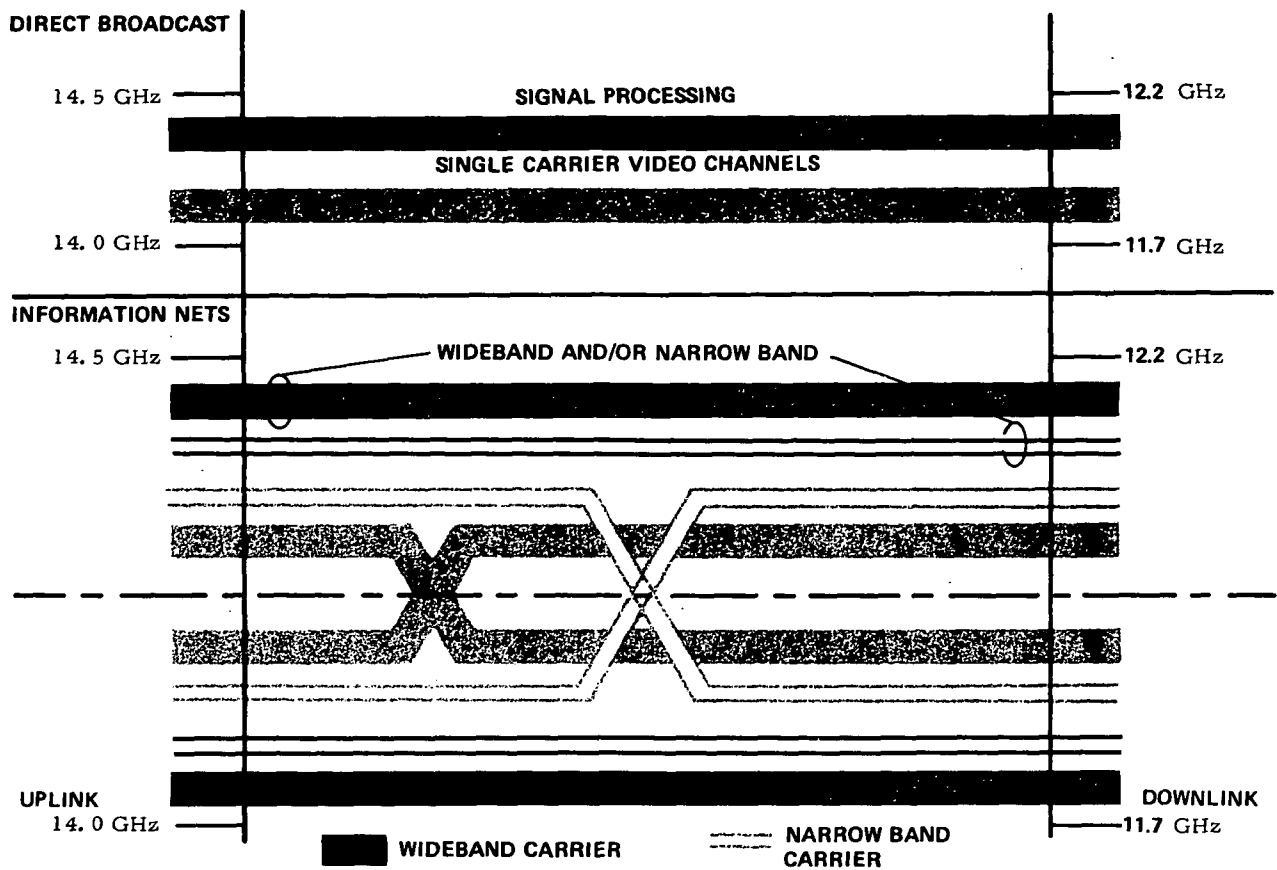
Figure 2-4. Typical Repeater Operating Modes
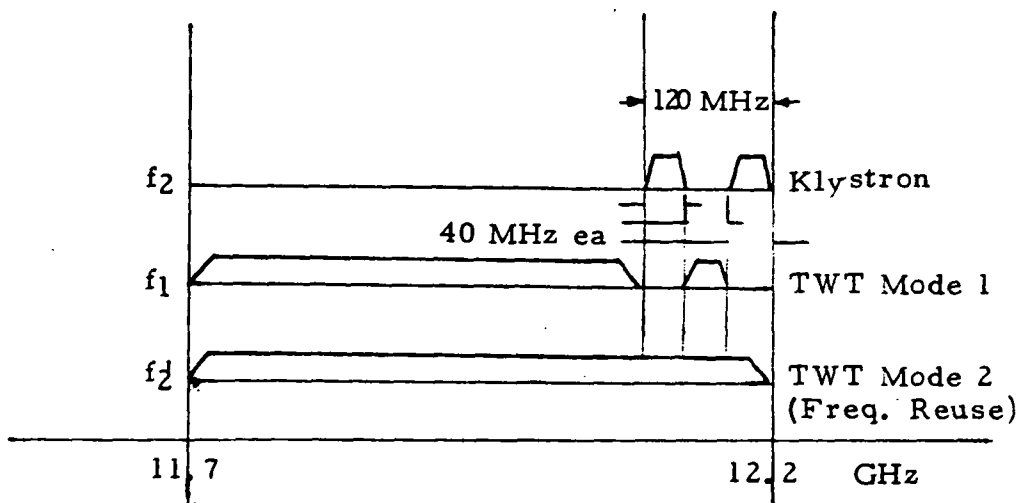
Figure 2-5. Power Amplifier Frequency Allocations

2-9

The 40 MHz separation between them assures that no intermodulation interference will lie within the occupied channel assignments.

Correspondingly, two modes were defined for the TWT, also shown in Figure 2-5. In mode 1, the two 40 MHz bands assigned for use to the Klystron would be filtered from the output of the TWT, whereas, in mode 2, the TWT is permitted to occupy the entire 500 MHz transmit band. Mode 2 is intended primarily for demonstration of frequency reuse. In the frequency reuse experiment, it is necessary to transmit the outputs of the two power amplifiers on antenna beams sufficiently separated to avoid side-lobe interference.

2.1.2.4 Attitude Control and Stationkeeping Subsystem

This subsystem shall consist of the hardware necessary to sense and maintain attitude control of the vehicle throughout the orbit raising phase as well as the on-orbit operation. It shall perform stationkeeping maneuvers on command and maintain pointing of the communications antenna. Station repositioning of the spacecraft (on command) shall be provided by this subsystem. The primary requirements are:

1) The spacecraft shall have the capability to maintain north-south and east-west stationkeeping to within ±0.2 degree and shall carry sufficient propellant to perform such stationkeeping for 5 years.

2) Attitude control shall be capable of maintaining antenna beam pointing to within ±0.2 degree in latitude and longitude relative to the subsatellite point and ±0.2 degree in rotation about the boresight axis.

3) The spacecraft shall have a ΔV of at least 30.5 m/sec for station repositioning capability.

4) Low-thrust (electric propulsion) as well as high-thrust (chemical propulsion) will be considered for injection from initial transfer orbit to synchronous orbit.

2.1.2.5 Electric Propulsion Subsystem

A. Electric propulsion shall be considered for raising the spacecraft orbit from an initial transfer orbit to a geostationary orbit. The engines for this purpose should be in the 20 cm to 30 cm range.

B. Electric propulsion for attitude control and stationkeeping will be considered. Engines in the 5 cm class should be considered.

C. Both mechanically and electrostatically steerable ion engines shall be considered.

2.1.2.6 Electrical Power Subsystem

The power source shall be an array of photovoltaic cells, supplemented by energy storage (batteries) to provide power during periods of solar eclipse for housekeeping functions and for operation of power amplifier cathode heaters at one half their nominal levels.

The following power system features will be considered:

● Use of rollout and foldout array configurations.

● Interaction of the array with spacecraft attitude control.

● Commonality of power conditioning to satisfy the requirements of the electric propulsion system (where used for orbit-raising) and the communications subsystem.

● Use of liquid metal and conventional sliprings for transfer of power across rotary joints.

2.1.2.7 Thermal Control Subsystem

● Direct radiation heat rejection techniques will be considered to control the temperature of the transmitter power amplifier.

● Operation of tubes with ten or more collectors operating at temperatures of up to $1273^{\circ}K$ will be considered.

● Open-envelope tube operation will be considered.

● Heating power required during eclipse periods shall be minimized.

● Spacecraft raw power of up to 10 kw will be considered in the thermal design.

2.1.2.8 Telemetry and Command

Sufficient telemetry and command channels shall be provided to handle all experimental as well as housekeeping needs throughout the mission lifetime. Memory for storing required attitude and thrust vectoring profiles for the electric thrusters will be required to permit intermittent operation of the ground link. As an objective, commands for orbit raising should not be required more frequently than once per day.

2.1.3 Applications of High Powered Communications Satellites

To aid in the determination of spacecraft performance requirements, a number of potential operational applications were considered. Source material was obtained from discussions with personnel from various agencies

and within Hughes and from selected literature.* Time and funding limitations of this study restricted this task to identifying those applications which appear particularly suitable to utilizing the technologies stressed in the ATS Advanced Mission Study, namely, high-powered transmitters operating at 12 GHz into a multiple shaped-beam antenna applied to networks of small user terminals. The primary classes of service suitable for these technologies include:

1) Direct broadcast applications - single video carrier (per repeater transmitter channel) for operation into very small user terminals of ETV/ITV to sparsely populated regions.

2) Distribution of requested data to small users - essentially a library function, where the user in a small community can request documents from a large data bank (Library of Congress, etc.). Requires narrow band communication to central bank with wide band distribution.

3) Data exchange systems - a variety of applications require multiple access and distribution of data on both wide band and narrow band channels simultaneously.

2.1.3.1 Potential Applications

A list of networking applications is shown in Table 2-2. This list was abstracted from data furnished by the NASA Project Manager for the ATS/AMS Study. Other applications considered are not specifically called out in the list of Tabl3 2-2 but are essentially similar to items identified therein and would fit into one or more of the classes included in the list.

In the area of Information Networks, most of the applications identified correspond to a calss that might be categorized as simultaneous multipoint to multi-point user operation.

In particular, Group IA, Regional Communications, is primarily concerned with providing communication links to remote sparsely populated areas. They can be serviced with a repeater operating over a relatively wide bandwidth with its transmitter backed off to permit simultaneous access of a large number of narrow band carriers, each carrying only a small number of voice channels. The use of high powered satellite transmitters are required because of the need to back off to provide quasi-linear operation while retaining sufficient power in each carrier to be able to service a small terminal.

---

*A literature search was performed at Hughes' request by the NASA Scientific and Technical Information Facility. The result, entitled "High Powered Communication Satellites," was appended to ATS/AMS Monthly Technical Narrative No. 1, dated 17 March 1971. A list of literature perused in the course of this study is attached as Appendix B.

TABLE 2-2. NETWORKING APPLICATIONS

I. INFORMATION NETWORKS

    A. Regional

        1. Alaska Communication Network

        2. Rural Regions Communication Networks (Appalachia, Rocky Mountain)

        3. Pacific Trust Territories

    B. Identified User (Government) Agency

        1. Biomedical Communications Network

        2. Post Office Corporation

        3. Possibilities: GSA, OE, Interior

    C. General Needs Networks

        1. Domestic Information Networks (MIT)

        2. Record, Business, Computer Data Networks

        3. Interactive TV Networks (Teleconferencing)

        4. Public Information Network (Libraries)

II. BROADCAST SYSTEMS

    A. Regional

        1. Alaska Educational Television/Instructional Television (ETV/ITV)

        2. Appalachia

        3. Rocky Mountain

    B. Special Audience/Purpose

        1. Disaster Warning

        2. U.S. Indian ETV/ITV

        3. Migrant Workers ETV/ITV

        4. Talking Books for the Blind

Groups IB and IC might be classed as institutional users requiring simultaneous two-way wide-band and narrow-band carriers. Another likely user group in the IB category is the law-enforcement data networks, some of which are currently being implemented on an experimental basis.

Both of these groups (IB and IC) tend to concentrate on the transmission of documents (printed page, photos, etc.), although straight digital data (computer nets) and live video (teleconferencing) are included. To be able to handle a great variety of users without being restrictive on their data formats, it was established that the spacecraft be equipped with a frequency translation repeater rather than a regenerative repeater, in which the incoming data is recovered at baseband before retransmission. (The regenerative repeater is attractive for certain digital data links where the data rate and format is fixed, in which case low error rates may be achieved at lower power levels than would be required in a frequency translation repeater.)

For the Broadcast Systems, the applications listed under IIA and the TV applications of IIB must provide live video to sparsely populated areas. The corresponding user terminals for these applications are categorized as "personal" receivers in that they must service individual families and/or very small communities. The desire to have a minimal cost, minimal maintenance receiver is paramount for these applications for the obvious reasons of their remoteness from large communities and the corresponding lack of highly trained service personnel. For operation in the 12 GHz band, it is speculated that the minimum practical antenna beamwidth is on the order of two to three degrees, or a maximum diameter of about 0.61 meters. It would be too difficult for this class of users to establish and maintain adequate alignment for a larger antenna with a correspondingly smaller beamwidth.

Some of the applications discussed in a general way in the preceding material are described somewhat more specifically below. In addition, some general concepts on "institutional" terminals will be discussed.

2.1.3.2 Direct Broadcast to Personal Receivers

Perhaps the most obvious application for high powered space transmitters, and certainly the application most frequently encountered in the literature, is that of direct broadcast of ETV/ITV to personal receivers. Although many of the studies have been devoted to servicing underdeveloped national areas, the concepts are equally applicable to domestic population groups in sparsely settled relatively inaccessible or remote areas of the United States. The ETV/ITV applications identified in Group II of Table 2-2 all fit into this category.

To support this application, it is desirable to maximize the effective radiated power from the spacecraft; to do this, antenna gain and transmitter power should be maximized. However, increased antenna gain results in reduced area coverage. A reasonable lower bound on area coverage for

domestic application is assumed to be one of the U.S. time zones.* If it is further assumed that the available transmitter power is one kilowatt,** then a typical link budget for video broadcast to a home receiver is shown in Table 2-3.

As indicated, the received signal-to-noise power results in picture quality of TASO Grade 2 (fine quality) for the median viewer. Although this is probably a very acceptable quality, a slight improvement in received carrier power (on the order of 1 to 2 dB) would result in a substantially improved picture quality. (This might be accomplished by designing for outage due to weather of up to 1 percent of the time, rather than up to 0.1 percent of the time. The reduced atmospheric attentuation would probably be in the order of 3-5 dB. The reduced loss could then be applied to the signal design to improve basic picture quality.)

2.1.3.3 Law Enforcement Networks

The need for extensive communications networks to support local, regional and national law enforcement agencies has become increasingly apparent in recent years. Although satellite communications links will not solve all of the needs for these agencies, it is a potential solution to a number of problems in this area. In particular, virtually every agency concerned with the apprehension of criminals and the prevention of crime has the need to request or transmit high resolution data to and from many related agencies. Although the traffic requirements may vary drastically with the nature of the agency or the community which it serves, all of the agencies must be capable of handling such data as fingerprints, mug-shots, photographs of stolen articles, etc. Satellites appear to be a natural medium for satisfying many of these requirements. High power technology is required because the communities which may tie into such networks potentially number in the thousands or tens of thousands. However, even though the number of users is large, they can support a substantially larger terminal than can the direct broadcast application described above. If one assumes the use of a terminal with a 2 meter diameter antenna, there is a 10 dB improvement due to antenna gain alone. Recognizing that such an institutional application will require that the transmitter operate in a multi-carrier mode, the RF power is likely to be backed off on the order of 3 dB. If it is assumed to be carrying two wideband carriers plus several narrow-band carriers, the power to each of the wideband channels is about 6 dB down relative to the single channel considered in the link calculations of Table 2-3, or the net carrier power is about 4 dB better than in the direct broadcast case. This is more than sufficient to design for very much higher video quality with the same or more severe outage requirements used in Table 2-3.

---

*Smaller regions of interest were defined relative to the new antenna design effort resulting from Contract Amendment No. 1. These are shown in Figure 2-2.

**These link budgets were calculated before the 2 kw Klystron was added to the repeater. Use of 2 kw essentially provides an additional margin of 3 dB.

TABLE 2-3. DIRECT-TO-USER TV BROADCAST

Transmitter Power (1 kw)*	30	dBw
Transmit RF Loss (in spacecraft)	-1	dB
Antenna Gain (3.5° x 3.5° Time Zone, at Beam Edge)	30	
Propagation Loss (Beam Axis at 37°N Latitude)	-205.6	
Atmospheric Attenuation (99.9% of Time	-3	
Receive Antenna Gain (0.61 m Diameter)	35.1	
Receive Antenna Pointing Loss (0.75°)	-0.5	
Receiver RF Loss	-1	
Received Carrier Power	-116	dBw
Receiver Noise Power Density (1200°K)	-197.8	dBw/Hz
IF Bandwidth (15 MHz)	71.8	dB-Hz
Receiver Noise Power	-126	dBw
Carrier/Noise Ratio	10	dB
FM Improvement Factor	5.5	
Pre-emphasis Improvement	3.0	
Noise Weighting Factor	10.2	
Peak-to-Peak/RMS Ratio	9.0	
Picture/Video Ratio	-3.0	
Peak-to-Peak Picture/ Weighted RMS Noise	34.7	dB

Note: 34.7 dB is equivalent to TASO 2 (50%).

*If a 2 kw transmitter is substituted, an additional 3dB margin
is available. This extra margin might well be distributed
amongst the RF losses and atmospheric attenuation allowance,
as these are estimated losses. Should this redistribution
prove to be conservative, the result would be improved picture
quality under adverse weather conditions.

Although the above discussion is in terms of video quality, it should be recognized that video is used primarily as a quality reference. In the case of law-enforcement communication nets, as in the case of many other applications, the end use of the data is not likely to be real-time video. In this application, the communication link may terminate in a high resolution reproducing machine or a digital computer memory.

2.1.3.4 Library Networks

Another application which might make effective use of satellite communications is the servicing of small community needs from large data banks. Even relatively large cities cannot provide the facilities of major libraries, such as the Library of Congress, but it is feasible that the contents of selected documents can be provided upon request to small communities over the country. In this case, the individual communities can time-share one or more narrow-band links for requesting data, and the central data bank would provide the data on one or more wideband links. Each of the requesting terminals would be alerted as to when its request would be fulfilled and record data directed to it; this data could then be replayed on a visual readout, or printed, depending upon the needs of the user. The wideband link requirements appear to be similar to those discussed above for the law-enforcement nets.

2.1.3.5 Other Considerations - User Terminals

As indicated in the discussion of Table 2-2, a multitude of other potential networking applications could be identified; however, it would not serve a useful function, for purposes of defining ATS/AMS spacecraft requirements, to define additional applications, nor to explore in greater detail the networks already identified. It is evident, at this point, that the spacecraft communications subsystem must provide no significant constraints on the user's ability to structure the information content of his communications signals; it must permit the user to selectively maximize the power available to a single channel as well as to share the available power amongst several channels in simultaneous operation.

Before recommending a specific repeater configuration for the spacecraft, a few words on user terminals are warranted. For the direct broadcast application, it was already indicated that the objective must be for a low initial procurement and installation cost as well as a low maintenance cost. Both installation and maintenance considerations suggest that the minimum beamwidth be on the order of 2 to 3 degrees, or a maximum diameter of about 0.61 m. Maintaining long-term antenna alignment on the order of about $3/4^o$ is estimated to be about the best that can be achieved without extensive installation costs and protection from climatic exposure.

For institutional terminals, larger antennas can be maintained. The order of 10 dB gain improvement obtained with a 2 meter ($\approx$6 feet) antenna relative to the direct broadcast receiver is probably sufficient for the greater capacity and quality required by the users of such terminals. Another consideration, however, is that most of the users of such terminals will be

relatively small communities which are also likely to have much lower traffic densities than larger communities. For such users, there would be significant economic advantage if the terminal, or most of it, could be time-shared amongst several types of user applications. From the foregoing discussion of law-enforcement and library networks, it is evident that their local receiver requirements are very similar; at most, the baseband equipment mist differ. Similarly, the same terminal could serve users receiving real-time video with only relatively small changes in terminal configuration.

A concept of the receiver portion of a small institutional terminal which could be shared amongst several networks is shown in Figure 2-6. (Although it is not an objective of this study to develop terminal design concepts, this discussion is included because of its influence on establishing spacecraft performance requirements.)

If this concept is implemented, it becomes desirable to coordinate the user networks so as to employ a somewhat standardized repeater channel. The only real limitation of such standardization is the bandwidth of individual channels, and this is not considered to be a severe restriction. Following this approach, the recommended channel bandwidth for a channelized repeater is 36 MHz, the same bandwidth currently employed by Comsat on the Intelsat IV commercial communications satellites. The potential impact that such a restriction might have on a typical user requirement is shown in the data of Table 2-4.

The Videofile Standard was established by Ampex for an internal data storage and retrieval system for the Los Angeles County Sheriff's Department; it appears that other agencies may employ the same approach if its
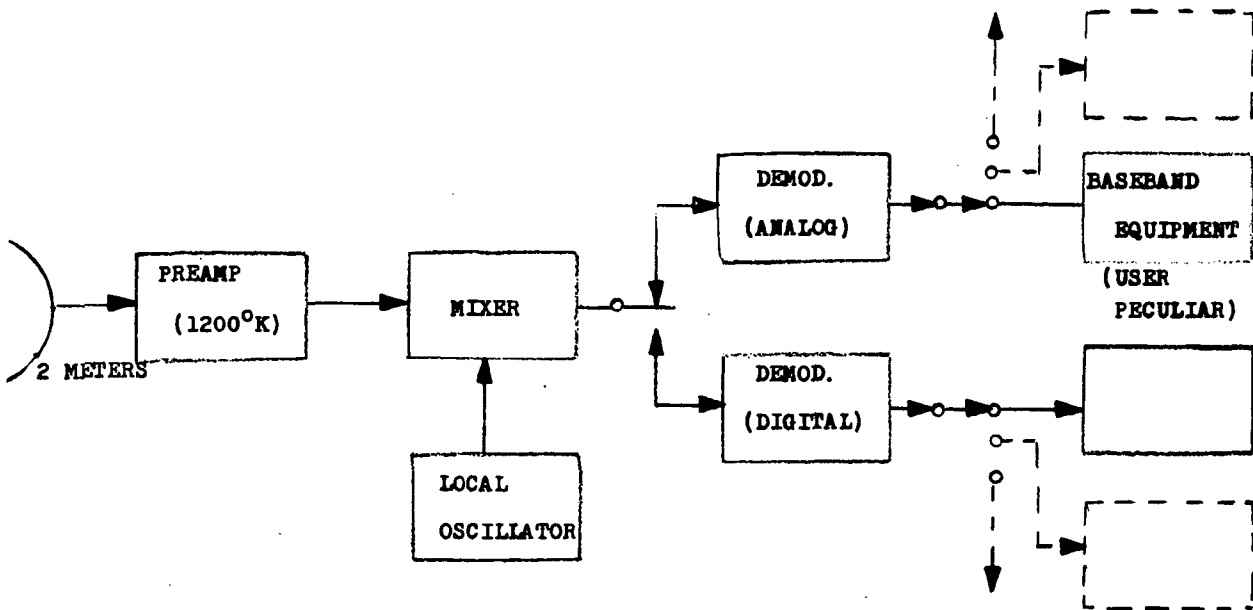
Figure 2-6. Multi-User Institutional Terminal-Receiver Concept

TABLE 2-4. COMPARISON OF VIDEO STANDARDS

	Ampex Videofile Standard	Broadcast Television Standard	TV Channel Compatible System
Nominal Scanning Standard (lines)	1,280	525	1,280
Active Lines per Frame	1,240	500	1,240
Video Bandwidth (MHz)	7.2	4.2	4.2
Frame Repetition Rate $(\sec^{-1})$	15	30	8.75
Interlace	None	2:1	None
Line Repetition Rate (Hz)	19,200	15,750	11,200
Active Line Time (μsec)	43	53.3	74.6
Aspect Ratio	8-1/2:11	4:3	8-1/2:11
Horizontal Resolutions* (lines)	620	450	620
Vertical Resolution** (lines)	870	350	870
Total Number of Picture Resolution Elements***	540,000	158,000	540,000

*Horizontal Resolution = Video bandwidth x active line time x 2

**Vertical Resolution = Number of active vertical lines x Kell factor (0.7)

***Total number of resolvable elements at about 50 percent amplitude = Horizontal resolution x vertical resolution

first application is successful. Should these come into widespread use, it is an almost certain requirement that the various users be able to access each other's data banks. Column 2 of Table 2-4 shows the corresponding commercial TV standards, and Column 3 shows how the videofile can be made compatible with video distribution channels merely by decreasing the frame rate to 8.75 per sec for inter-system transmission as compared to 15 per sec for intra-system operation.

2.1.3.6 Spacecraft Performance Requirements

It is recommended that a spacecraft communications subsystem for networking applications such as those described in the foregoing discussions should be comprised of a multi-channel frequency translation repeater in which each channel can independently be operated at full power with a single carrier or with multiple carriers at backed off power levels. In conjunction with direction from the NASA Project Manager for the ATS/AMS, it was established that the design objective for the ATS/AMS spacecraft be a two-channel repeater capable of accepting any one or two signals received from a multiple beam antenna. Each of the repeater channels has been allocated a bandwidth of 100 MHz,* subdivided as shown in Figure 2-7. The left or low-frequency half of the channel bandwidth is routed through the channel, whereas the right or high frequency half of the bandwidth is routed to the other repeater channel. The output of each repeater channel is then selectively routed to one of several antenna beams.

OUTPUT TO CHANNEL

|◄─── 1 (2) ──►|◄─── 2 (1) ──►|

N/B | N/B

W/B   W/B

|◄───── 100 MHz ─────►|

INPUT TO CHANNEL 1 (2)
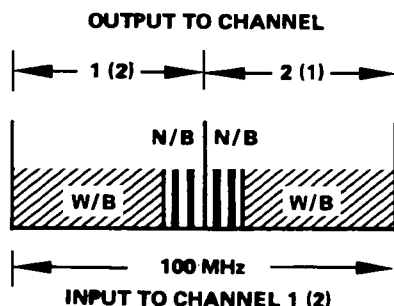
Figure 2-7. Originally
Proposed Spectral
Use of Repeater
Channel

---

*The channel bandwidth allocation of 100 MHz was made in the initial study. It provides for networking application indicated in the lower portion of Figure 2-4 and is essentially not imcompatible with the more recently . defined allocations illustrated in Figure 2-5.

Within each channel, provision will be incorporated for power limiting each of the subchannels shown in Figure 2-7, and attenuators will also be provided to control the distribution of output power amongst the subchannels as well as the total power output of the power amplifiers. More detail on performance has been included in Section 2.1.2 of this report.

2.2 EXPERIMENT SELECTION AND DEFINITION

One of the objectives of this study was the definition of additional experiments to complement the primary experiments defined in Section 2.1.1 to the extent permissible by spacecraft weight and power budgets. Additional experiments considered are listed below.

1) The incorporation of a second high power transmitter. Strong emphasis for incorporations of a second power amplifier, at a power level of up to 2 kilowatts, was directed by the NASA Project Manager, and it was agreed that other secondary experiments would not be further considered unless there was additional spacecraft capacity after this experiment was included. (As shown in the Spacecraft Description of Section 3, the inclusion of a 2 kilowatt Klystron in addition to a 1 kilowatt TWT left insufficient weight or power to consider the inclusion of any of the other experiments identified below.)

2) Satellite-to-satellite communications. * A number of concepts for satellite-to-satellite communication experiments were identified. These include:

● K-band satellite-to-satellite link, such as is being considered for the Tracking and Data Relay Satellite System (TDRSS). This would require the incorporation on the ATS/AMS spacecraft of a high gain tracking antenna and the active cooperation of another spacecraft similarly equipped.

● A laser CO_2 link, such as has been considered for earlier ATS missions. One such design is described in Item B of Appendix B.

● VHF data relay for communicating with low altitude satellites. Such a system was studied by Hughes under contract from NASA/GSFC (Item 74 of Appendix B).

● High frequency data relay (30-60 GHz). In-house studies at Hughes have considered these frequencies for various applications.

---

*Additional experiments numbered 2 and 3 were recommended for consideration in Section 3.16 of the contract Statement of Work.

3). Optical communications between spacecraft and earth and/or
   station sensing by optical methods.* A laser beacon tracker
   might be used for this, but no specific approach was investigated.

4) Environmental or attitude sensory systems. A variety of
   sensory systems could be considered, many of which might fall
   within the scope of other NASA programs. No specifics were
   investigated, as it was apparent that they could not be incorpo-
   rated into the spacecraft designs.

5) Liquid metal bearings. Such an experiment might be desirable
   as a supplement to liquid metal sliprings or in lieu of them if
   conventional sliprings are adopted in the final spacecraft
   configuration.

2.3 MISSION PROFILE

The ATS spacecraft mission can best be described by dividing it into
three parts; namely, Prelaunch Operations, Launch and Injection, and
On-Orbit Operations, each of which is described below.

2.3.1 Prelaunch Operations

Prelaunch support envisioned for the ATS/AM spacecraft will largely
utilize standard prelaunch procedures. The spacecraft will be shipped to the
launch facility in a partially disassembled condition following final acceptance
testing at the manufacturing facility. Normal caution in handling the equip-
ment will be exercised as will cleanliness and humidity protection. After
arrival at the launch facility, the spacecraft will be transported to an
assembly building for final assembly and checkout. As part of this sequence,
final optical alignment will be made of the various sensors, thrusters, and
the antenna boresight. Tests will be performed on all hardware to ascertain
if any damage occurred in shipping, and ensure functioning of all spacecraft
hardware prior to launch. This test will be a modified version of the system
test performed at the contractors plant. Data taken during this testing will
be compared with previous test data. Re-conditioning of the batteries will
be performed to bring them to full capacity. This will consist of discharge
at a slow rate and recharge at a normal rate, and finishing with a trickle
charge.

The reaction control system will be serviced to prepare for launch.
If it is hydrazine, the system will be loaded and pressurized to operating
conditions, if ion propulsion, the system will be loaded with mercury
propellant.

---

*Additional experiments numbered 2 and 3 were recommended for considera-
tion in Section 3.16 of the contract Statement of Work.

A number of special component prelaunch constraints will have to be observed. Special precautions may be required to protect the transport seals of the high power tube. If there is an ejectable case around the collectors, testing may be limited to a pulsed operation mode to ensure cool temperatures while the spacecraft is on the launch pad. At other times prior to encapsulation, external cooling can be provided, thus enabling more complete testing.

Precautions will be required to keep the gallium liquid metal slip-rings in a frozen state. In addition, an inert environment will be maintained whenever possible to further reduce the likelihood of contamination.

The solar cell arrays present handling problems. They will be unrolled for inspection and test in the final assembly building. This will necessitate a table of about 24.4 m in length as well as a portable light for testing. This will be available and can probably be shipped from the factory.

If the spacecraft employs ion thrusters, as in the A-1 configuration, it will be subjected to a limited prelaunch functional test which will checkout the power conditioning and switching circuits. No provision will be made to fully exercise the ion engines due to the likelihood of plume contamination.

None of the above constraints appear to pose any major implementation problems.

2.3.2 Launch and Injection

No special equipment is required by the ATS/AM spacecraft during the ascent phase; all equipment needed is currently available as a part of the NASA Satellite Tracking and Data Acquisition Network (STADAN). Ground facilities required from launch through on-orbit station acquisition are similar for both chemical and low thrust electric injection with the major difference between them being in the time required to support transfer to synchronous orbit. For an all-chemical configuration, injection into a synchronous orbit can be made within hours or days after launch, whereas low thrust electric propulsion will require up to several months. In either case, the spacecraft will be configured to use the existing STADAN stations, which offer sufficient coverage and flexibility to cover any selected trajectory.

1) Chemical Injection. For chemical injection, the bulk of the ground support occurs within hours or at most a few days after launch. During this time, the support consists of receiving spacecraft status and attitude data, and of sending commands for control of the spacecraft. Commands are typically required to control attitude during powered and unpowered phases, as well as for control of other spacecraft functions. The launch, transfer orbit injection, and synchronous orbit injection sequences are standard and have been employed many times to place synchronous satellites on station. These are described in greater detail in Section 3.3, Trajectory Considerations.

2) Ion Engine Orbit Raising. For the ion engine orbit raising
    mission, tracking data will be obtained from the GSFC-STADAN
    minitrack system by using residual telemetry transmitter power.
    Thus, orbit determination can be accomplished simultaneoulsy
    with data acquisition. In addition, each command receiver/
    telemetry transmitter combination functions as a GRARR trans-
    ponder, enabling accurate ranging to be obtained as needed to
    establish final synchronous orbit.

A spacecraft command memory and stored command processor must
be loaded by ground command approximately once per day with a thrust vec-
toring profile for the ion engines. These will be transmitted from a STADAN
station via the VHF link. The stored command capability could provide for
spacecraft operation for more than a day, if desired. All telemetry data
needed to determine spacecraft status and determination of the results of
spacecraft maneuvers can also be obtained via the VHF telemetry link to
STADAN stations. Details of the orbit raising profile are explained in
Section 3.3.

2.3.3 On-Orbit Operation

A representative user network configuration is shown in Figure 2-8.
Here, one control ground terminal is operating in conjunction with several
smaller terminals in a single network. While the configuration shown is
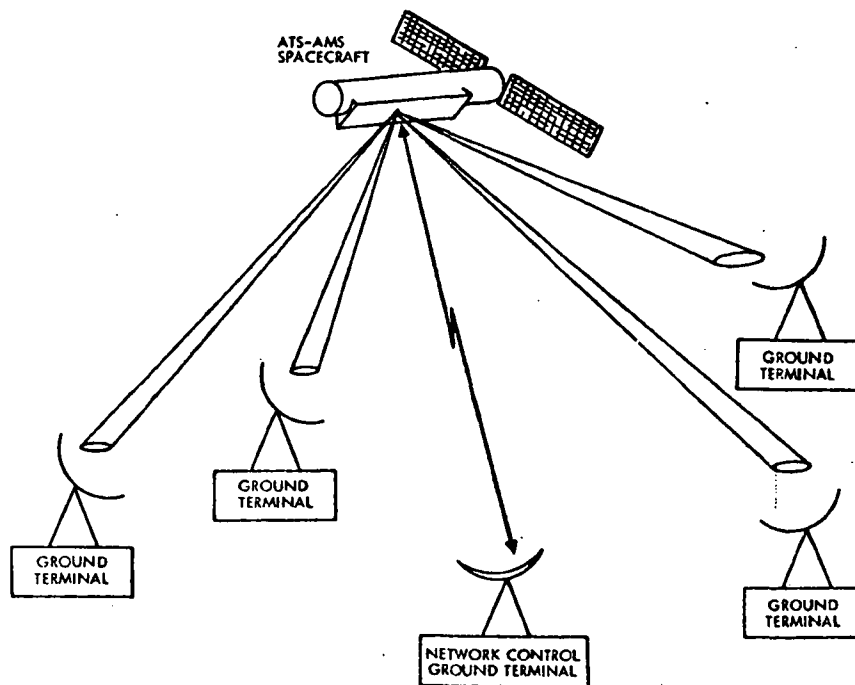
Figure 2-8. ATS/Advanced Mission Typical
Network Configuration

a broadcast operation, many other configurations are possible with both symmetric and asymmetric two-way links.

On-orbit evaluation is performed in accordance with an orbital test plan. The orbital test plan will define all tests, beginning at injection of the spacecraft into its final orbit and continuing until all aspects of system and spacecraft performance have been evaluated. The major items of the orbital evaluation are indicated below.

1) Initial Spacecraft and Communication System Checkout. The initial communication system checkout will be accomplished in steps. First, the spacecraft antenna would be positioned so that one of the receive and transmit beams are aimed at the ATS Advanced Mission ground control terminal. The antenna will be operated in single beam configuration for these initial tests. A known signal will be transmitted from the ground control terminal and monitored onboard the spacecraft. Since the communications transmitter will not have been activated, monitoring will be accomplished by spacecraft telemetry data relayed to the ground terminal via the spacecraft TT&C subsystem. Following the receiver checkout, the spacecraft's high power transmitter(s) will be energized. Voltages, currents, powers, and temperatures will be monitored in the spacecraft, and the wideband noise transmitted by the spacecraft will be monitored by the control ground terminal.

2) Initial Antenna Pattern Mapping. Repeater gain will be adjusted so that the wideband noise transmitted by the spacecraft transmitter will be of relatively low power. However, the signal will be strong enough to permit antenna mapping.

The center of one of the beams will be aimed at the ground control terminal, and the attitude of the spacecraft determined to within 0.1 degree. To perform antenna mapping, the spacecraft attitude will be varied so that the main beam and all of the strong sidelobes pass over the ground control terminal. Typically, the spacecraft would be pitched approximately +5 degrees, and then yawed from -10 to +10 degrees. The signal strength received on the ground will be recorded during this sweep. When the spacecraft has completed the yaw maneuver, the pitch angle will be decreased in steps, and the spacecraft yaw maneuver will be repeated. This sweeping will continue until the pitch has reached a -5 degree attitude, resulting in a complete antenna map for the selected beam.

3) System Calibration. System calibration is accomplished by comparing "repeated" signals with their originals. With the spacecraft repeater energized, a known signal is transmitted from the ground control terminal to the spacecraft, repeated by the spacecraft, and received at the ground control terminal. Simultaneously, the signal transmitted by the ground control terminal is attenuated and demodulated in the ground terminal, providing a known

or reference signal. Both the demodulated test signal from the spacecraft and the reference signal are applied to test equipment in the ground terminal. The pertinent measurements include:

a) Power loss/amplification of the repeater system

b) Signal delay

c) Frequency and phase stability, distortion

d) Image or spurious response

Figure 2-9 shows the basic arrangement for this calibration.

The ATS Advanced Mission spacecraft repeater must operate with multiple signals being received and transmitted. Upon completion of the single signal calibration, two known signals will be transmitted from the ground control terminal, repeated in the spacecraft, and received in the same ground terminal. The two signals will be monitored as previously described in the single signal calibration, with additional measurements performed on the multiple signals. Power dividing or sharing, and intermodulation effects will be determined during these multiple signal calibrations. Known signals will be added until the repeater has been loaded to its design capacity. The results will be compared with the analytical and prelaunch test data.

An optional step in system calibration can be to use several ground terminals to transmit and receive known signals. The spacecraft antenna is
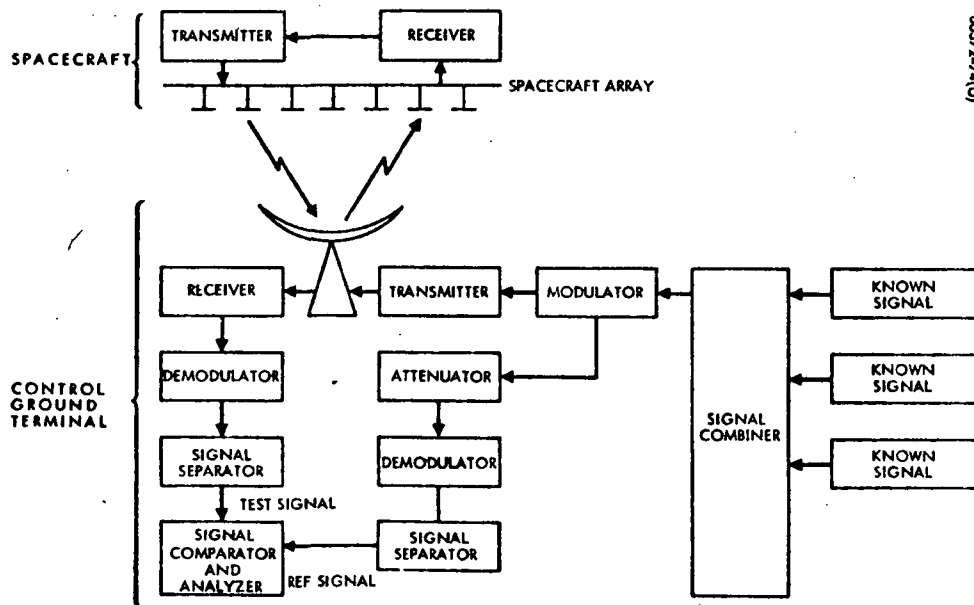
Figure 2-9. System Calibration

used to generate the multiple beam pattern and selected ground terminals will transmit known signals. The ground control terminal will monitor the spacecraft repeated signals and perform signal comparison and analysis using the original signals received on land lines. The number of ground terminals can be varied, depending upon their availability.

4) Information Networking System. An objective of the ATS Advanced Mission is the demonstration of information networking systems comprised of small ground terminals. Using the ground terminals required for the system calibration, networking systems can be demonstrated. The system shown in Figure 2-8 is typical of a broadcast networking system. To simulate a network for test purposes, portable stations that can be moved to remote locations are ideal. Each terminal will be electronically equivalent to a 1, 2 or 4 meter ground terminal, and able to transmit as well as receive. Each terminal will have spectrum and signal analyzers for monitoring transmitted and received signals. Known test signals will be used in initial demonstrations, but television, voice, and digital data may be used for later demonstrations.

5) Ground Terminals. Several basic types of ground terminals can be used for demonstration of the communications system. The first is the ground control terminal, probably a fixed installation at the Rosman, N. C., or Barstow, California, STADAN station. This terminal would control all of the operational tests and demonstrations performed by the communications system. It would contain X-band transmitting and receiving equipment and signal monitoring equipment. In addition, it would contain TT&C equipment for monitoring spacecraft telemetry data and transmitting commands to the spacecraft.

A second type of ground terminal is the small remote terminal. Mobility of such a terminal will permit placing the terminals at various locations, providing greater flexibility for a variety of networking tests. If only fixed sites are to be considered, the number of locations presently available in the United States may limit the extent of the networking experiments to be performed. Other ground terminals could be provided by obtaining the participation of potential operational users. Such users could provide realistic conditions for verification of the networking systems. Preliminary definitions of the first two types of terminals is contained below.

6) Ground Control Terminal. Figure 2-10 is a block diagram of the transmitting, receiving, and monitoring equipment in a typical control ground terminal.

The antenna might be about 6.1 m in diameter and mounted on an hour/angle declination type mount. It will be capable of receiving and transmitting through the same feed structure.

The transmitting subsystem consists of the modulators, upconverter, and transmitter capable of accepting signals from either a broad baseband input (0.3 to 10 MHz) or a 70 MHz modulated carrier. Present indications

PREAMPLIFIER — AMPLIFIER — DOWN CONVERTER — GROUP DELAY EQUALIZER — IF AMPLIFIERS AND FILTERS — DEMODULATOR — OUTPUT

11.7 TO 12.2 GHz

14.0 to 14.5 GHz

FEED AND DIPLEXER

NOISE SOURCE

TEST TRANSLATOR

RECEIVER PERFORMANCE MONITOR UP CONVERTER

TRANSMIT PERFORMANCE MONITOR DOWN CONVERTER

SIGNAL ANALYZERS

SPECTRUM ANALYZERS

KNOWN SIGNALS

DRIVE MOTORS

REMOTE CONTROL

5 kw POWER AMPLIFIER

RF AMPLIFIER — UP CONVERTER

GROUP DELAY EQUALIZER

MODULATOR

Figure 2-10.   Typical Ground Terminal Block Diagram

are that up to 5000 watts of RF power may be required under some circumstances when operating through the postulated 20-foot antenna. Output power will be variable so that the control ground terminal can duplicate the operating characteristics of a user terminal.

The ground terminal's usefulness for various experiments and missions requires attention to initial design of the receiving subsystem. The pre-amplifier will provide a low noise receiver capable of receiving signals from the spacecraft operating in a low power mode. The downconverters, equal-izers, IF amplifiers and filters and demodulators will provide the signal processing to accommodate the required wideband data outputs.

The ground terminal test translator subsystem contains the transmit performance monitor, receive performance monitor, RF loop translator, and frequency synthesizer. The transmit monitor provides the capability of frequency conversion of the 14 GHz carrier to a 70 MHz IF signal. The receive monitoring equipment must have the capability of allowing frequency conversion of the 70 MHz modulated signal to the input RF of the receiver. The RF loop translation equipment is required to translate the transmit fre-quency to the received frequency with the frequency offset being obtained from the station frequency standard. The transponder must have sufficient bandwidth with insignificant distortion characteristics. No frequency inver-sion will be permitted.

2-28

The signal analyzing subsystem will contain test equipment capable of monitoring the spectrum under consideration. Spectrum analyzers similar to the HP 851 system and network analyzers similar to the HP 8410 system will be used in this section of the ground terminal.

It is quite possible that the calibration ground terminal would also contain the TT&C equipment necessary to command and control the spacecraft. The communication system will require special commands. Commanding will be conducted in real time, permitting monitoring of the signals as the equipment is switched. Voltage current, power, and temperature of the spacecraft communications system will also be required at the ground calibration terminal, adding to the justification for the colocation of the TT&C and Communications terminal functions.

7) Small Remote Terminals. The small remote terminal contains the same basic 12 GHz receivers, 14 GHz transmitters, test translators, and monitoring equipment. However, the antennas will probably be somewhat smaller. The terminals may be used to simulate 1, 2 or 4 meter antennas. The receive side of the station would have bariable attenuation levels that could be switched to simulate different receiving terminals. Uplink power control could be used to simulate various user functions.

Telemetry monitoring and spacecraft commanding is probably not needed at these small terminals. Experiment requirements are not sufficiently defined to determine the number of terminals required.

2.3.4 Conclusion

The orbital support recommendations and ground terminal definition has been discussed and preliminary recommendations made. It is desirable to encourage potential users to define and participate in the networking experiments. Initial checkout and calibration of the system will precede these experiments, and can be accomplished largely by using existing ground stations, with appropriate RF equipment added for operation at the frequency bands employed in this mission.

3. SPACECRAFT DESCRIPTIONS

3.1 SPACECRAFT CONFIGURATIONS

A total of twelve configurations grouped into three classes were considered during the course of the study. Groups A and C use chemical propulsion for injection of the spacecraft into transfer orbit and low thrust electric propulsion systems for raising the orbit to synchronous station, whereas Group B uses chemical propulsion for synchronous injection.

Group A configurations utilize a Thor-Delta 2914 launch vehicle for injection into an elliptical transfer orbit with its apogee near synchronous latitude. Of three variants considered, the configuration designated as A-1 was selected as the baseline for this group.

Group B configurations use an Atlas-Centaur for injection into a similar transfer orbit and an apogee kick motor (AKM) for final injection. Of six variants originally considered, B-1 and B-5 were selected as baselines.

Another variant, designated B-1A, incorporates the lens antenna designed under Contract Amendment No. 1, in place of the parabolic antenna shown on configuration B-1. (This becomes the seventh variant in the B group. It is equally applicable as a variant to B-5.)

Group C also uses the Atlas-Centaur, plus clusters of 30 cm ion engines for synchronous injection. Of two Group C variants, configuration C-1 was the selected baseline until this group was dropped from further consideration at the direction of NASA when it was established that all of the baseline configurations should have essentially the same payload capability.

The baseline configurations A-1, B-1, B-1A, and B-5 are described below, followed by a review of the other configurations considered.

3.1.1 Configuration A-1

Of the baseline configurations, A-1 is the only one which uses electric propulsion for achieving geostationary orbit. An artist's sketch of this spacecraft is shown in Figure 3-1, and a detailed layout in Figure 3-2.

POWER AMPLIFIER

EARTH SENSOR

ANTENNA FEED ASSEMBLY

1.83 m PARABOLIC REFLECTOR

ROLL-OUT SOLAR PANEL

LIQUID METAL SLIP RING ASSEMBLY

5 cm ION ENGINES

30 cm ION ENGINES

TT&C ANTENNA

SEPARATION WEIGHT   624 Kg

INITIAL STATION WEIGHT   570 Kg

TIME TO STATION   80 DAYS

2.6 m

23.8 m

2.14 m
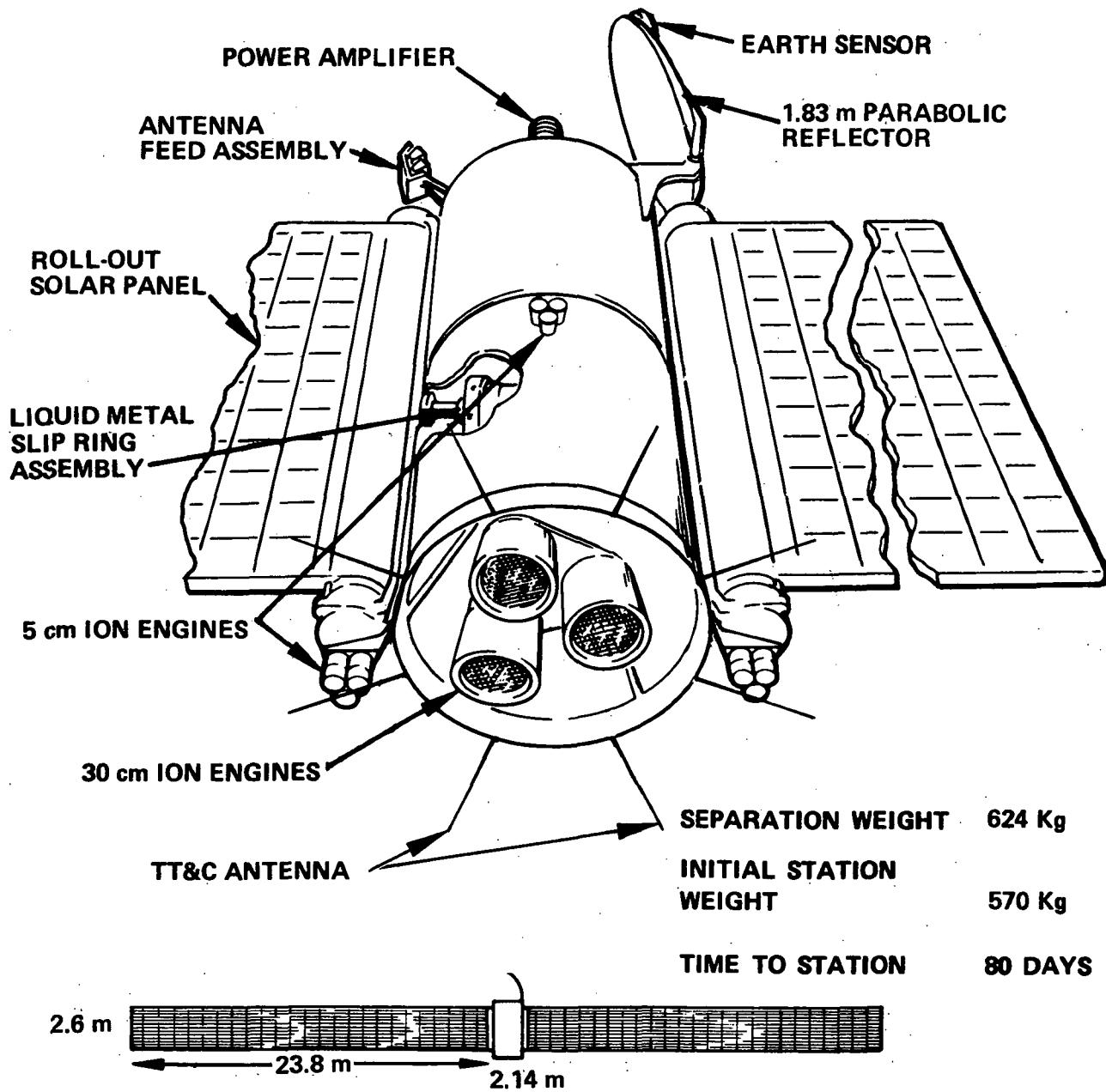
Figure 3-1.   Spacecraft A-1
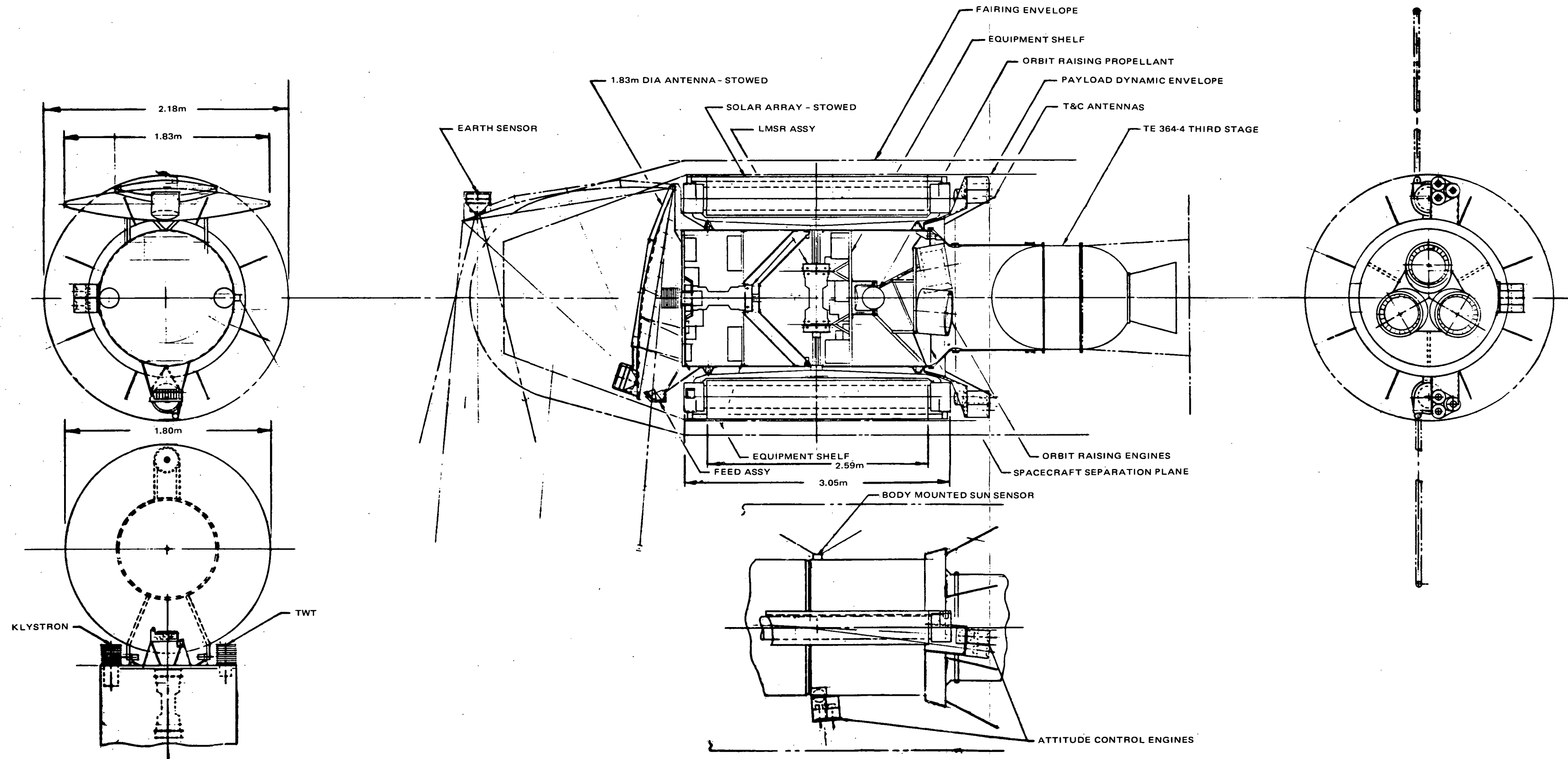
Figure 3-2. Spacecraft Configuration A-1

Boosted by a Thor-Delta 2914 launch vehicle, the spacecraft is encapsulated within a 2.4 meter (8 foot) diameter fairing, elongated by 0.61 meter (2 feet) relative to the current standard shroud*. The booster payload is 650 kg (1,432 pounds) into the selected elliptic transfer orbit**, and the separated spacecraft weight is 634 kg (1,372 pounds), as indicated in the weight and power summaries listed in Table 3-1. After about 80 days for orbit raising, the spacecraft arrives on station with a weight of 570 kg (1252 pounds), of which 9.1 kg (20 pounds) is propellant for attitude control and stationkeeping, and 42 kg (92 pounds) is contingency. Although the weight contingency is considered low at this stage of design (8 percent as compared to a design objective of 15 percent) it is sufficient to establish the feasibility of accomplishing a mission well in excess of the minimal requirements. A further consideration justifying a relatively low contingency allowance for this spacecraft is the felxibility gained in booster payload with an electric propulsion orbit raising system. Weight can be traded against orbit raising time and solar cell degradation. A discussion of this tradeoff capability appears in Section 3.3.

As may be seen in Figure 3-2, the spacecraft consists of three major elements, namely the spacecraft body, the solar panels, and the communications platform. The body is oriented, while on synchronous station, with one axis maintained parallel to the earth's polar axis and the solar panel axis n normal to the line of sight to the sun***. The solar panels are free to rotate so that their plane may be maintained normal to the sun line. The communications platform is free to rotate about the polar axis of the body so that the antenna can be earth oriented.

The communications platform and the solar panels are coupled to the spacecraft body via liquid metal slipring assemblies. A single ended assembly is used for the platform and a double ended one for the solar panels.

The solar panels are deployed after separation from the booster. As indicated in Table 3-1, they have an initial power output of 10.2 kilowatts at the nominal location of one astronomical unit (A.U.). They have an end of life capability at summer solstice (1.02 A.U.) of 6.5 kilowatts, leaving a power contingency of 500 watts after five years of operation. The degradation of the solar cells occurs primarily during the orbit raising period.

The communications platform contains the communications subsystem. The antenna reflector is stowed during launch. It is nominally deployed upon spacecraft separation, but a detailed thermal and operational analysis may indicate that it need not be deployed until the spacecraft arrives on station.

---

*According to the manufacturer, the shroud can be extended by several feet for only a nominal non-recurring cost.

**The selection of the transfer orbit is discussed in Section 3.3.

***This is frequently referred to as E-W orientation of the solar panels.

TABLE 3-1. CONFIGURATION A-1 WEIGHT AND POWER SUMMARIES

Weight	Kilograms	Pounds
Basic Spacecraft Plus Payload	518.0	1,140
Contingency	42.0	92
Spacecraft Dry Weight	560.0	1,232
ACS Expendables	9.1	20
Weight into Sync Orbit	569.1	1,252
Orbit Raising Expendables	54.5	120
Separation Weight	623.6	1,372
Attach Fitting	37.3	60
Thor-Delta Payload (Elliptic Transfer Orbit)*	661.0	1,432
Power		**Kilowatts**
Beginning of Life (1 A.U.)		10.2
End of Life (1.02 A.U. 0° Sun Angle, 0.65 Radiation Degradation Factor)		6.5
Required		6.0

*Apogee altitude of 31,900 kilometers, perigee altitude 555 kilometers.

The antenna reflector is a 1.83 meter diameter offset circular section of a paraboloid. Offsetting is required to reduce the blockage which would result from the feed assembly located at the focal point of the reflector. The feed is a multiple horn assembly capable of illuminating the four continental time zones, the 48 states, and Alaska and Hawaii.

The power amplifiers (one 1 kilowatt TWT and one 2 kilowatt klystron) are mounted on the platform so that their collectors protrude from the space-craft body, thereby permitting them to radiate directly into space.

An earth sensor is mounted near the top end of the reflector, viewing the earth through a cutout in the reflector. It is placed as far forward as

possible so as to minimize eclipsing of its earth view by the solar panels. The residual blockage by the solar panels does not significantly affect the performance of the sensor, nor does the viewing hole in the reflector significantly affect the antenna performance.

A three axis gyro assembly provides the basic attitude reference both during orbit raising and on-station operations. Drifts are corrected periodically by command based upon data telemetered from the onboard earth and sun sensors. During orbit raising, attitude control is maintained primarily by vectoring the thrust axis of the orbit raising 30 cm ion engines. The axis of the orbit raising engines are canted so as to have their nominal thrust axis through the spacecraft center of gravity. As a result of the canting, the spacecraft requires a separation plane diameter larger than the 0.93 m. mounting adapter standard for the third stage of the booster. A flared supplemental adapter is provided, with the separation plane located about 25.4 cm inside the spacecraft body.

The ion engines are augmented by reaction wheels. Once on station, the reaction wheels are used to maintain continuous attitude control, with three clusters of 5 cm ion engines used for stationkeeping and momentum dumping of the reaction wheels.

Principal characteristics of the A-1 spacecraft are summarized in Table 3-2.

3.1.2 Configurations B-1, B-1A, and B-5

The three Group B baseline configurations are all variants of the same basic spacecraft, illustrated in Figure 3-3. Launched by an Atlas Centaur with an Intelsat IV shroud and injected into synchronous orbit with an optimized apogee kick motor, the B-1 and B-5 spacecraft arrive on station with an initial weight of 895 kg (1970 pounds). (The B-1A configuration requires an extended shroud to accommodate the lens antenna, and would have an injected weight of about 880 kg (1940 pounds)).

A layout of the B-1 and B-5 spacecraft is shown in Figure 3-4. The two spacecraft differ from each other primarily in their power subsystems. B-1 uses low voltage solar cell arrays with conventional power conditioning, and uses conventional sliprings for power transfer from the solar panels to the spacecraft body. B-5 has high voltage arrays with integral power conditioning and liquid metal sliprings.

All of the B spacecraft are oriented, while on station, with their solar panel axes parallel to the earth's polar axis (N-S) and the panels are free to rotate about this axis so as to face the sun. The longitudinal axis of the B-1 or B-5 spacecraft body is posttioned tangential to the orbital velocity vector so that the antenna is properly boresighted. For the B-1A configuration, whose layout is shown in Figure 3-5, the spacecraft body is rotated away from the orbit tangent to accommodate the pointing of the antenna.

TABLE 3-2.   A-1 SPACECRAFT CHARACTERISTICS

PROPULSION

    Booster: Thor-Delta 2914

    Injection: Three 30-cm Hg bombardment ion engines

    Time to achieve station ≈ 80 days

COMMUNICATIONS

    Transmit   11.7-12.2 GHz

    Receive   14-14.5 GHz

    1 kw TWT

    2 kw klystron   } Collectors radiate directly to space

    Open envelope tube operation

    Antenna with multiple shaped beams

ATTITUDE CONTROL AND STATIONKEEPING

    Orbit Raising Operations (Attitude Control)

- Primary control by thrust vectoring of orbit raising engines
- Augmented by reaction wheels
- Attitude reference provided by precise rate integrating gyros
- Periodic update of gyros by earth and sun sensor data

    On-Orbit Operations (Attitude Control and Stationkeeping)

- Continuous control by reaction wheels
- Periodic dumping by three 5-cm Hg bombardment ion engines (Engine cluster used to achieve life and redundancy)
- Attitude reference by gyros with periodic update by command
- N-S and E-W stationkeeping provided by the ion engines
- On-board earth and sun sensors

POWER SUBSYSTEM

    Two roll-out solar panels approximately 2.59 x 25.8 meters

    High voltage configuration with integral power conditioning

    Liquid metal slipring assemblies (gallium)

    Conventional power conditioning for housekeeping functions

    Batteries for housekeeping during eclipse operation

2.44 m

N

19.8 m

ANTENNA
REFLECTOR

FEED
ASSEMBLY

POWER
AMPLIFIER

SOLAR PANEL

APOGEE
KICK MOTOR

HYDRAZINE
THRUSTERS

INITIAL STATION WEIGHT   895 Kg
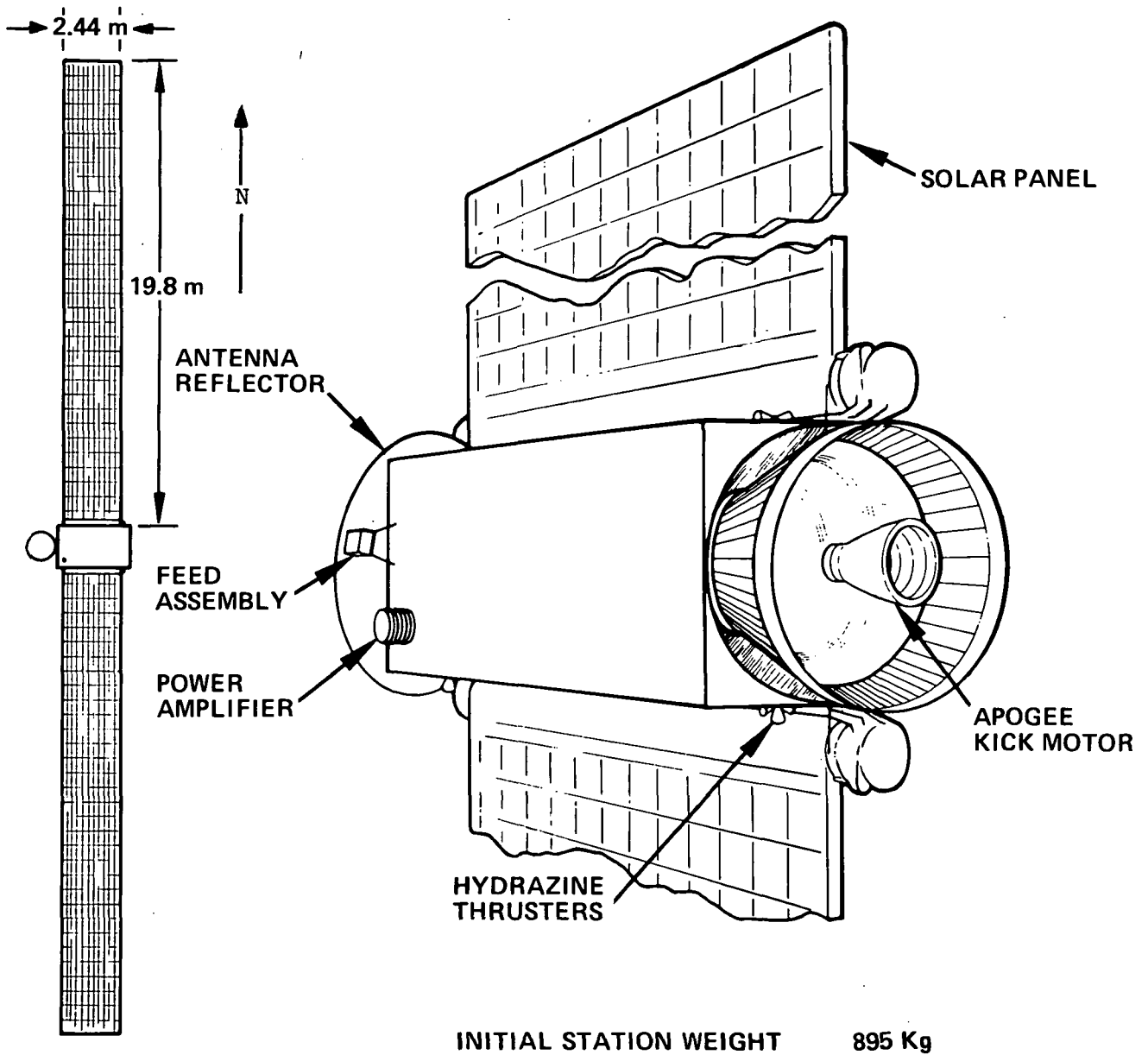
Figure 3-3.   Spacecraft B-1 or B-5

3-9

TWT

KLYSTRON

FAIRING ENVELOPE

PAYLOAD DYNAMIC ENVELOPE

EQUIPMENT SHELF

SOLAR ARRAY – STOWED

APOGEE MOTOR SEPARATION PLANE

BOOSTER SEPARATION PLANE

BOOSTER INTERFACE

1.83m DIA ANTENNA

N_2H_4 TANK

SLIP RING ASSY

ACS JETS

ANTENNA FEED ASSY

EARTH SENSOR

TT&C ANTENNA
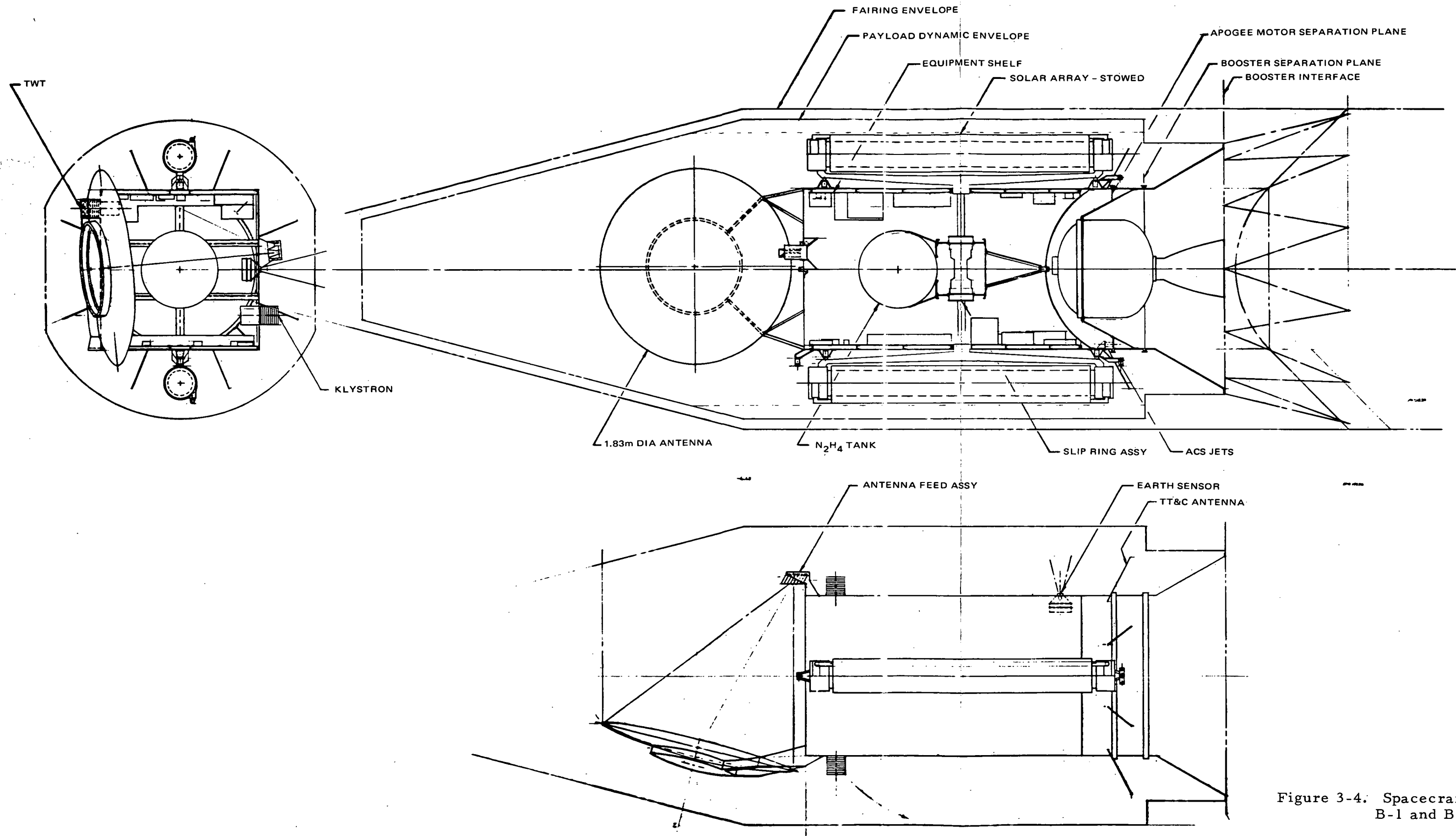
Figure 3-4. Spacecraft Configuration
B-1 and B-5

3-11

Preceding Page Blank
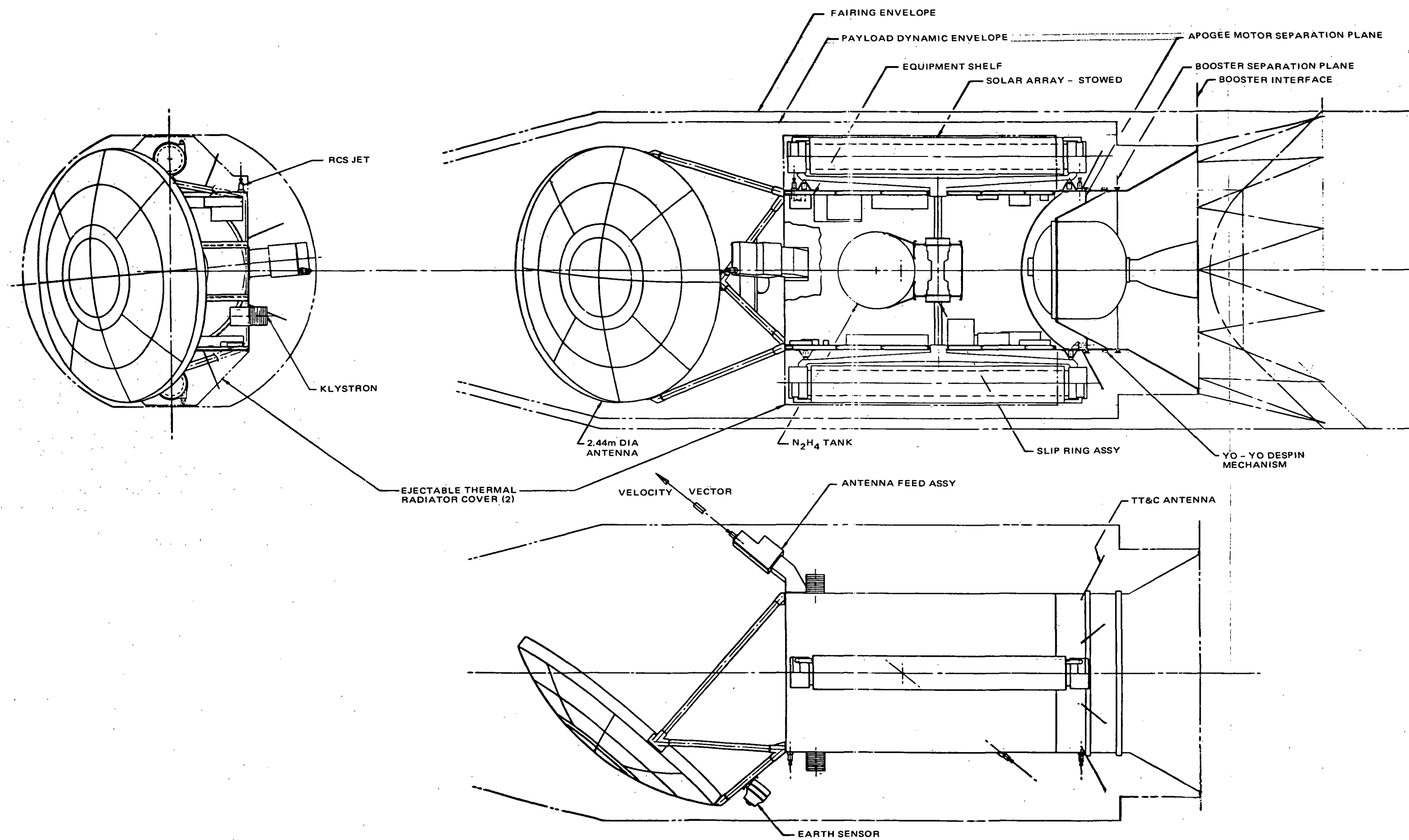
Figure 3-5. Spacecraft Configuration B-1A

Labels on figure:

RCS JET

KLYSTRON

EJECTABLE THERMAL RADIATOR COVER (2)

FAIRING ENVELOPE

PAYLOAD DYNAMIC ENVELOPE

EQUIPMENT SHELF

SOLAR ARRAY – STOWED

APOGEE MOTOR SEPARATION PLANE

BOOSTER SEPARATION PLANE

BOOSTER INTERFACE

2.44m DIA ANTENNA

N_2H_4 TANK

SLIP RING ASSY

YO – YO DESPIN MECHANISM

VELOCITY VECTOR

ANTENNA FEED ASSY

TT&C ANTENNA

EARTH SENSOR

Preceding Page Blank

The solar panels rotate once per year and the spacecraft body rotates once per day, maintaining their orientation towards the sun and earth respectively.

Weight and power summaries for the three baseline configurations are given in Table 3-3. The indicated weight contingencies are based upon improved booster performance*, with a resultant increase of payload into synchronous orbit of about 135 kg over that used when the configurations were defined. Allowing 15 percent for design contingency, 80 to 135 kg could be allocated to additional experiments.

For all three configurations, the communications subsystem is mounted on the spacecraft body. In B-1 and B-5, the antenna reflector is the same parabolic section used on Configuration A-1. However, in all of the B baselines, the antenna is rigidly attached to the spacecraft body and does not require deployment after launch. The collectors of the power amplifiers protrude through opposite faces of the spacecraft (Figure 3-3) permitting direct thermal radiation to space, and the north and south oriented faces of the body provide radiation surfaces for dissipating other thermal loads.

On station attitude control is maintained by a set of reaction wheels, as in the A-1 configuration. Stationkeeping and momentum dumping of the reaction wheels are accomplished with a hydrazine reaction control system (RCS). Eight 0.1 pound thrusters provide moments about three orthogonal axes, as well as north, east and west directed velocity increments, as shown in Figure 3-5 for the B-1A vehicle. (North-south stationkeeping may be performed with a unidirectional velocity increment, whereas east-west stationkeeping requires bi-directional thrusting.)

The impulsive operation of the jets poses a potential dynamic interaction with the large solar panels, but initial studies suggest that they can be bounded within acceptable limits.

The end of life power output (6 kilowatts) provides sufficient power, with a 400 watt margin, to permit continuous operation of the high power transmitters during sunlit periods over the design life of five years. During eclipse operation, batteries are provided to maintain housekeeping operations and reduced (half-power) excitation of the power amplifier cathode heaters.

Primary characteristics of the B family baselines are shown in Table 3-4.

A more detailed comparison of the power and weight budgets for all of the baseline configurations (A-1, B-1, B-1A, and B-5) are shown in Tables 3-5 and 3-6, respectively.

---

*The improved booster performance is indicated in Table 3-15.

Preceding Page Blank

TABLE 3-3. B SPACECRAFT BASELINE WEIGHT AND POWER SUMMARIES

	B-1	B-5	B-1A
Weight	Kilograms (Pounds)		
Basic Spacecraft Plus Payload	516 (1135)	480 (1055)	528 (1160)
Contingency or Additional P/L Capability	209 (460)	245 (540)	186 (410)
Spacecraft Dry Weight	725 (1595)	725 (1595)	714 (1570)
ACS Expendables	170 (375)	170 (375)	168 (370)
Atlas-Centaur Payload*	895 (1970)	895 (1970)	882 (1940)
Power	Kilowatts		
Beginning of Life (1 A.U.)	8.0		
End of Life (1.02 A.U. 23° Angle, 0.85 Radiation Degradation Factors)	6.0		
Power Required	5.6		

*Net payload into synchronous orbit. For B-1A, with an extended shroud, the decrease of payload into synchronous orbit is estimated at 13.6 kg.

TABLE 3-4.   B BASELINE CONFIGURATION CHARACTERISTICS

PROPULSION

    Booster: Atlas-Centaur

    Synchronous Injection: Optimized Apogee Kick Motor

COMMUNICATIONS

    Transmit   11.7 - 12.2 GHz

    Receive   14.0 - 14.5 GHz

    Power Amplifiers - 1 kw TWT + 2 kw klystron
    (Collectors radiate directly to space)

    Open envelope tube operation (on command)

    Shaped/Multi-beam antenna (B-1 and B-5 parabolic reflector.
    B-1A lens antenna)

ATTITUDE CONTROL AND STATIONKEEPING

    On-orbit Operation

        ● Continuous control by reaction wheels

        ● Periodic dumping by RCS jets (H_2N_4)

        ● N-S and E-W stationkeeping provided by the RCS jets

        ● Attitude reference by gyros with periodic update

        ● Sun and earth sensors

POWER SUBSYSTEM

    Two roll-out solar panels each approximately 2.44 x 18.9 meters

    Batteries for housekeeping during eclipse

	B-1	B-5
Solar Cell Arrays	Low Voltage	High Voltage
Sliprings	Conventional	Liquid Metal
Power-Conditioning	Conventional	Integral with Solar Panels

TABLE 3-5. BASELINE POWER BUDGETS

Subsystem	Normal Operation			Eclipse Operation
	A-1	B-1/B-1A	B-5	
	◄———— (watts) ————►			
Communications				
Repeater	———— 100 ————			
One 1 kw TWT (0.53E)	———— 1885 ————			12*
One 2 kw Klystron (0.66E)	———— 3000 ————			18*
Power Matching/Conditioning	———— 490 ————			
Power Electronics and Distribution	———— 45 ————			10
Attitude Control	———— 55 ————			55
TT&C	———— 20 ————			20
Subtotals	5595	5595	5595	115
Electric RCS (5 cm Eng)	290			
Orientation Mechanism	20	10	10	10
Thermal Control	80	10	50	
Total	5985	5615	5655	125
*Cathode heaters on half-power				

TABLE 3-6A. BASELINE WEIGHT BUDGETS (KILOGRAMS)

Subsystem	A-1	B-1	B-1A	B-5
Communications				
Repeater	37.2	37.2	37.2	37.2
One 1 kw TWT	13.6	13.6	13.6	13.6
One 2 kw Klystron	13.6	13.6	13.6	13.6
Power Conditioning	4.5	54.5		4.5
Antenna	15.9	15.9	27.2	15.9
Power (N-S or E-W)	E-W	N-S	N-S	N-S
High Voltage Solar Panels	152			127
Low Voltage Solar Panels				
Liquid Metal Sliprings	45			22.5
Conventional Sliprings		18.2	18.2	
Batteries and Electronics	22.7	22.7	22.7	22.7
Orientation Electronics	6.8	6.8	6.8	6.8
HV Solar Panel Experiment		2.4	2.4	
LM SR Experiment		6.8	6.8	
Attitude Control and Stationkeeping				
Sensors, Wheels, Etc.	31.8	31.8	31.8	31.8
Hydrazine RCS		25.0	25.0	25.0
Electric RCS	13.6			
TT&C	20.4	20.4	20.4	20.4
Thermal	11.4	13.6	13.6	11.4
Structure and Wire Harness	109.0	127.0	127.0	127.0
Orbit Raising Electric Propulsion	20.4			
Basic Spacecraft Plus P/L Weight	518	516	528	480

TABLE 3-6B. BASELINE WEIGHT BUDGETS (POUNDS)

Subsystem	A-1	B-1	B-1A	B-5
Communications				
Repeater	80	80	80	80
One 1 kw TWT	30	30	30	30
One 2 kw Klystron	30	30	30	30
Power Conditioning	10	120	120	10
Antenna	35	35	60	35
Power (N-S or E-W)	E-W	N-S	N-S	N-S
High Voltage Solar Panels	335			280
Low Voltage Solar Panels		235	235	
Liquid Metal Sliprings	100			50
Conventional Sliprings		40	40	
Batteries and Electronics	50	50	50	50
Orientation Electronics	15	15	15	15
HV Solar Panel Experiment		5	5	
LM SR Experiment		15	15	
Attitude Control and Stationkeeping				
Sensors, Wheels, etc.	70	70	70	70
Hydrazine RCS		55	55	55
Electric RCS	30			
TT&C	45	45	45	45
Thermal	25	30	30	25
Structure and Wire Harness	240	280	280	280
Orbit Raising Electric Propulsion	45			
Basic Spacecraft plus P/L Weight	1140	1135	1160	1055

3.1.3 Other Configurations

Group A Configurations

In the A family, the two other variants carried a payload of a single one kilowatt power amplifier with correspondingly smaller solar cell arrays and longer injection periods. Except for the size of the solar panels, they are all similar in appearance (Figure 3-1). The principal difference between the two alternates is that Configuration A-2 uses high voltage arrays with integral power conditioning, as in the A-1 baseline, whereas the A-3 uses low voltage arrays with conventional power conditioning. With the smaller payload, the basic weight of the alternates is less than that for the baseline, leaving a greater weight for contingency and the possible inclusion of other experiments. Table 3-7 summarizes the differences between the A variants and Table 3-8 summarizes subsystem weight allocations for all of the A group.

TABLE 3-7. COMPARISON OF GROUP A CONFIGURATIONS

	A-1	A-2	A-3
Orbit Raising Time (days)	80	120	120
Power Amplifiers			
1 kw TWT	x	x	x
2 kw Klystron	x		
Solar Cell Arrays			
High Voltage	x	x	
Low Voltage			x
High Voltage Experiment			x
Solar Panel Output (kilowatts)			
Initial (1 A.U.)	10.2	5.5	5.5
End of Life (1.02 A.U., 0.65 RDF*)	6.5	3.2	3.2
Weight - Kilograms (pounds)			
Basic Spacecraft plus Payload (on-station)	518 (1140)	443** (975)	478** (1055)
Contingency	42 (92)	120 (265)	84 (185)
*RDF is radiation degradation factor			
**Weights estimated using early orbit raising estimates, which were subsequently refined for A-1 but not the others.			

TABLE 3-8. WEIGHT BUDGETS - "A" SPACECRAFT FAMILY

Subsystem	A-1	A-2	A-3
	(kg)	(kg)	(kg)
Communications			
Repeater	36.4	36.4	36.4
One 1 kw TWT	13.6	13.6	13.6
One 2 kw Klystron	13.6		
Power Conditioning	9.1	6.8	22.8
Antenna	15.9	15.9	15.9
Power (N-S or E-W)	E-W	E-W	E-W
High Voltage Solar Panels	152	95.5	
Low Voltage Solar Panels			88.6
Liquid Metal Sliprings	45.5	45.5	
Conventional Sliprings			36.4
Batteries and Electronics	22.8	22.8	22.8
Orientation Electronics	6.8	6.8	6.8
HV Solar Panel Experiment			2.3
LM SR Experiment			6.8
Attitude Control and Stationkeeping			
Sensors, Wheels, etc.	31.8	31.8	31.8
Hydrazine RCS			
Electric RCS	11.4	11.4	11.4
TT&C	20.4	20.4	20.4
Thermal	11.4	9.1	9.1
Structure and Wire Harness	109	109	109
Orbit Raising Electric Propulsion	18.2	18.2	41.0
Basic Spacecraft Plus P/L Weight	518	443	480

Group B Configurations

A total of seven variants of the B family were considered, of which three (B-1, B-1A, and B-5) were described in Section 3.1.2. The key element of commonality amongst the various members of this group is the use of an Atlas-Centaur as the booster, the Intelsat IV shroud, and an AKM for injection into synchronous orbit. These and other features which are common to the members of this group are summarized in Table 3-9. The primary variations which distinguish the individual members are summarized in Table 3-10.

The B-0 configuration is essentially the same as that of the B-1 baseline, described previously. It differs in that an attempt was made to use the existing SVM-4 as the AKM which is poorly matched to the capability of the booster. With that AKM, there was no weight margin and was therefore considered to be an unacceptable design. B-1 achieved an acceptable weight margin by assuming that an optimum AKM would be available. B-2 was an alternate attempt at achieving adequate margin with the SVM-4 AKM, with the weight savings achieved by substituting clusters of 5 cm ion engines in place of the hydrazine RCS. This also necessitated the use of E-W oriented solar panels to avoid the need for placing ion engine thrusters at the end of one of the solar panels. B-3 and B-4 progressively utilize additional new technology to attain further weight reductions, as indicated in Table 3-10, which indicates the principal differences between the various members of the

TABLE 3-9. COMMON FEATURES OF B SPACECRAFT

Booster:	Atlas-Centaur with Intelsat IV Shroud
Synchronous Injection:	Apogee Kick Motor (SVM-4 or New)
Communications Subsystem:	One 1 kw TWT
	One 2 kw Klystron
	1.83 m Offset Parabolic Antenna with Multiple Feed Array*
Primary Power:	Roll-out Solar Cell Arrays
Batteries:	Housekeeping Functions

*B-1A incorporates a 2.44 meter diameter lens antenna

TABLE 3-10. B SPACECRAFT SUBSYSTEM VARIATIONS

Parameter		B-0	B-1	B-2	B-3	B-4	B-5
Apogee Kick Motor		SVM-4	New	SVM-4	SVM-4	SVM-4	New
HV Solar Panels							
Prime Power					x	x	x
Experiment Only		x	x	x			
Liquid Metal Sliprings							
Prime						x	x
Experiment Only		x	x	x	x		
Attitude Control Thrusters		Hydra-zine	Hydra-zine	Elec	Elec	Elec	Hydra-zine
Solar Panel Orientation		N-S	N-S	E-W	E-W	E-W	N-S
Basic S/C Weight plus Payload	kgs (lbs)	523 (1150)	523 (1150)	510 (1120)	486 (1070)	425 (1045)	486 (1070)
Contingency or Additional Payload Capability	kgs (lbs)	0	96 (205)	141 (310)	164 (360)	175 (385)	130 (285)

B family. B-5 is essentially the same as B-1, except for the use of high voltage arrays as the prime power source, rather than as an experiment. B-1 and B-5 were selected as the baselines because a basic objective for the B Spacecraft group was to emphasize conventional technology.

B-1A is the seventh variant of this group, added at the end of the study to incorporate the lens antenna design. It could equally be applied to B-5, with the same modifications as is required for B-1.

Weight allocations for the B group, down to the subsystem level, are summarized in Table 3-11.

Group C Configurations

Of the two variants in this group, Configuration C-1 was originally intended as the third spacecraft baseline. Placed into an elliptic transfer orbit by an Atlas-Centaur, and raised to synchronous orbit in about 120 days with a cluster of six 30 cm ion engines, the propulsion system is capable of deploying a spacecraft with a dry weight of approximately 1360 kg (3000 pounds). This spacecraft could carry a payload of four 1 kw power amplifiers for

TABLE 3-11A. CONFIGURATION B WEIGHT BUDGETS

Subsystem	B-0/B-1	B-2	B-3	B-4	B-5
	(kilograms)				
Communications					
Repeater	←————————		36.4		————————→
One 1-kw TWT	←————————		13.6		————————→
One 2-kw Klystron	←————————		13.6		————————→
Power Conditioning	54.5	54.5	9.1	9.1	9.1
Antenna	←————————		15.9		————————→
	(27.2)*				
Power (N-S or E-W)	N-S	E-W	E-W	E-W	N-S
High Voltage Solar Panels			129.5	129.5	129.5
Low Voltage Solar Panels					
Liquid Metal Sliprings	107	107		22.7	22.7
Conventional Sliprings	18.2	18.2	27.3		
Batteries and Electronics	←————————		22.7		————————→
Orientation Electronics	←————————		6.8		————————→
HV Solar Panel Experiment	2.3	2.3			
LM SR Experiment	18.2	18.2	18.2		
Attitude Control and Station-keeping, Sensors, Wheels, etc.	←————————		31.8		————————→
Hydrazine RCS	25.0				25.0
Electric RCS		11.4	11.4	11.4	
TT&C	←————————		20.4		————————→
Thermal	13.6	13.6	13.6	13.6	11.4
Structure and Wire Harness	127	127	127	127	127
Basic Spacecraft Plus P/L Weight	516 (528)*	502	486	475	486

*B-1A with 2.44 m. diameter lens antenna

TABLE 3-11B. WEIGHT BUDGETS (B SPACECRAFT FAMILY)

Subsystem	B-0/B-1	B-2	B-3	B-4	B-5
			(Pounds)		
Communications					
Repeater	←		80		→
One 1-kw TWT	←		30		→
One 2-kw Klystron	←		30		→
Power Conditioning	120	120	20	20	20
Antenna	←		35		→
	(60)*				
Power (N-S or E-W)	N-S	E-W	E-W	E-W	N-S
High Voltage Solar Panels			285	285	285
Low Voltage Solar Panels	270	235			
Liquid Metal Sliprings				50	50
Conventional Sliprings	40	40	60		
Batteries and Electronics	←		50		→
Orientation Electronics	←		15		→
HV Solar Panel Experiment	5	5			
LM SR Experiment	15	15	15		
Attitude Control and Station-keeping, Sensors, Wheels, etc.	←		70		→
Hydrazine RCS	55				55
Electric RCS		25	25	25	
TT&C	←		45		→
Thermal	←		30		→
Structure and Wire Harness	←		280		→
Basic Spacecraft Plus P/L Weight	1135 (1160)*	1105	1070	1045	1070

*B1-A with 8 foot diameter lens antenna

continuous sunlit operation, and enough batteries to provide for operating one of the power amplifiers during eclipse operation. Essentially similar to the A-1 configuration, the solar panels are deployed in the orbit plane (the nominal E-W orientation). They have an initial output of about 17 kw and an end of life output of about 10 kw. Key characteristics of the C-1 spacecraft are shown in Table 3-12 and its layout, while encapsulated within the shroud, is shown in Figure 3-6.

The C-2 configuration was initially considered as a backup to the A-1 had it proved unfeasible to loft sufficient payload with a Thor-Delta booster to accommodate the mission with electric propulsion orbit raising. It is essentially similar to the A-1 spacecraft, as may be seen in its layout shown in Figure 3-7. In the Intelsat IV shroud, the antenna is rigidly mounted and does not require deployment after separation. Otherwise, the communications payload is identical to that of A-1.

The other principal difference with respect to A-1 is the use of low voltage solar cell arrays with conventional power conditioning in place of the high voltage arrays with integral conditioning employed on the A-1 baseline.

Principal characteristics of the C-2 spacecraft are shown in Table 3-13.

3.2 CONFIGURATION TRADEOFFS

A number of tradeoffs were made during the study that have an impact on the overall spacecraft configuration. The most significant of these is the selection of the booster for placing the spacecraft into final position in synchronous orbit. This is discussed in Section 3.2.1.

Three major tradeoff selections involve the solar panels. First is the selection of high voltage solar cell arrays with integral power condition- ing as opposed to low voltage arrays with conventional power conditioning. Second is the orientation of the solar panels in the final orbit in which the choice is between panels which deploy in the north-south direction as opposed to deployment in the orbit plane (nominally the east-west direction). Third is the selection between rollout and foldout solar panels. These are all discussed in Section 3.2.2.

In regards to power transfer, several methods are discussed in the power subsystem section of this report. These include conventional brush and ring assemblies, flexible cables with fast return, rotary transformers, nonsliding rotary electrical connectors, and liquid metal sliprings. For the ATS/AM application, the choice was narrowed to conventional slipring versus liquid metal sliprings, as summarized in Section 3.2.3.

TABLE 3-12. PRIMARY CHARACTERISTICS - CONFIGURATION C-1

SPACECRAFT

- Sun-oriented portion supporting rollout solar panels (E-W)
- Earth-oriented portion supporting antenna
- Spacecraft dry weight approximately 1400 kilograms

PROPULSION

- Booster: Atlas-Centaur
- Orbit Raising - Six 30-cm Hg bombardment ion engines
- Time to achieve orbit, approximately 120 days

COMMUNICATIONS

- Transmit   11.7 - 12.2 GHz
- Receive   14.0 - 14.5 GHz
- Two 1-kw TWT   } Collectors radiate directly to space
- Two 1-kw klystron   }
- Open envelope tube operation
- Shaped/multi-beam antenna (1.83 diameter offset paraboloid)

ATTITUDE CONTROL AND STATIONKEEPING

- Orbit Raising Phase

  - Primary control by thrust vectoring of orbit-raising ion engines
  - Augmented by reaction wheels
  - Attitude reference provided by rate integrating gyros
  - Periodic update of gyros by earth and sun sensor data

- On-orbit Operation

  - Continuous control by reaction wheels
  - Periodic dumping by three clusters of 5-cm Hg bombardment ion engines
  - Gyro attitude reference with periodic update
  - N-S and E-W stationkeeping provided by the ion engines

POWER SUBSYSTEM

- Solar Panel Output

  - Beginning of life (1.0 A.U., 0° sun angle, 1.0 radiation   17.0 kw
    degradation factor)
  - End of life (1.02 A.U., 0°, 0.6 RDF)   10.0 kw

- Four rollout solar panels each approximately 2.44 x 21.0 meters
- High voltage solar cell array with integral power conditioning
- Liquid metal slipring assemblies (gallium)
- Minimum conventional power conditioning
- Batteries for one 1-kw power amplifier plus housekeeping during eclipse

SPACECRAFT WEIGHT (kilograms/pounds)

- Basic S/C weight plus payload   1008/2215
- Contingency or additional payload capability   425/ 935
- S/C dry weight   1433/3150
- ACS expendables   23/ 50
- Orbit raising propellant   135/ 300
- Adapter   46/ 100
- Atlas-Centaur payload   1638/3600

EARTH SENSOR
ELECTRONIC SHELF
SOLAR ARRAY - STOWED
LM SLIP RING ASSY
ELECTRONIC SHELF
FAIRING ENVELOPE (EXTENDED 2.05m)
PAYLOAD DYNAMIC ENVELOPE
ATTITUDE CONTROL ION THRUSTERS
SPACECRAFT SEPARATION PLANE
BOOSTER INTERFACE

TWT (2)

KLYSTRON (2)
THERMAL RADIATOR

ORBIT RAISING ION THRUSTERS
Hg PROPELLANT TANK

1.83m DIA ANTENNA
FEED ASSY
THERMAL RADIATOR
BODY MOUNTED SUN SENSOR

ATTITUDE CONTROL ION THRUSTERS

Figure 3-6. Spacecraft Configuration C-1

3-29

EARTH
SENSOR

THERMAL
RADIATOR

SOLAR
PANEL

ATTITUDE CONTROL
ION THRUSTERS

ELECTRONIC
SHELVES

TWT (1)
KLYSTRON (1)

FEED ASSEMBLY

LIQUID METAL
SLIP RINGS

ELECTRONIC
SHELVES

MERCURY
PROPELLANT TANK

ORBIT RAISING
ION THRUSTERS (3)
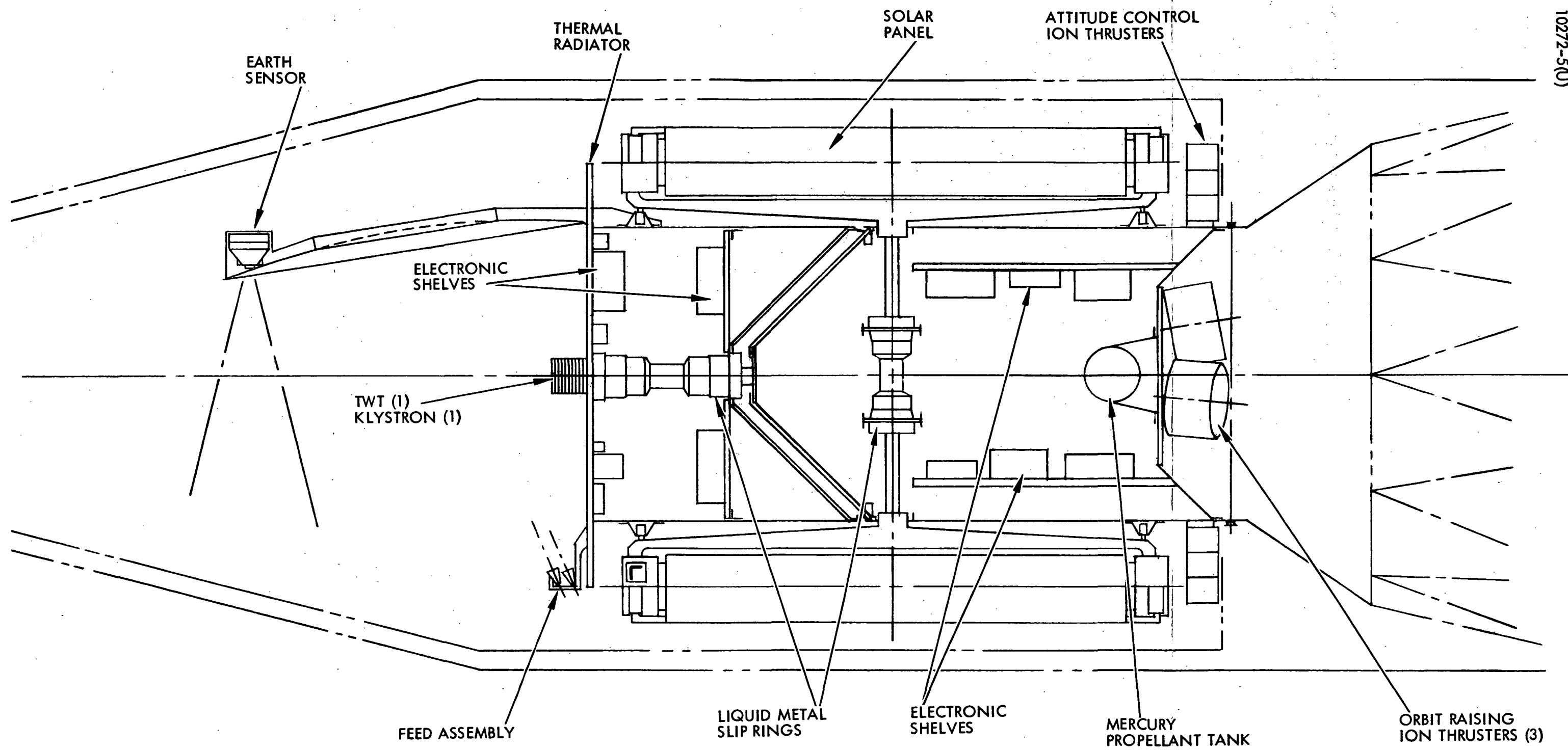
Figure 3-7. Spacecraft
Configuration C-2

3-31

Preceding Page Blank

TABLE 3-13. PRIMARY CHARACTERISTICS - CONFIGURATION C-2

SPACECRAFT

- Sun-oriented portion supporting rollout solar panels (E-W)
- Earth-oriented portion supporting antenna
- Spacecraft dry weight approximately 680 kilograms

PROPULSION

- Main Booster: Atlas-Centaur
- Orbit Raising - Three 30 cm Hg bombardment ion engines
- Time to achieve orbit, approximately 120 days

COMMUNICATIONS

- Transmit   11.7 - 12.2 GHz
- Receive   12.75 - 13.25 GHz
- One 1 kw TWT
- One 2 kw Klystron   } Collectors radiate directly to space
- One envelope tube operation
- Shaped/multi-beam antenna

ATTITUDE CONTROL AND STATIONKEEPING

- Orbit Raising Phase

  - Primary control by thrust vectoring of orbit-raising ion engines
  - Augmented by reaction wheels
  - Attitude reference provided by rate integrating gyros
  - Periodic update of gyros by earth and sun sensor data

- On-Orbit Operation

  - Continuous control by reaction wheels
  - Periodic dumping by three clusters of 5-cm Hg bombardment ion engines
  - Gyro attitude reference with periodic update
  - N-S and E-W stationkeeping provided by the ion engines

POWER SUBSYSTEM

- Solar Panel Output

  - Beginning of life (1.0 A.U., 0° sun angle, 1.0 radiation   10.5 kw
    degradation factor
  - End of life (1.02 A.U., 0°, 0.6 RDF)   6.1 kw

- Two rollout solar panels each approximately 2.44 x 24.7 meters
- Low voltage solar cell array
- Liquid metal slipring assemblies (gallium)
- Conventional power conditioning
- Batteries for housekeeping only during eclipse

SPACECRAFT WEIGHT (kilograms/pounds)

- Basic S/C weight plus payload   570/1255
- Contingency or additional payload capability   111/ 245
- Spacecraft dry weight   681/1500
- ACS expendables   11/ 25
- Orbit raising propellant   68/ 150
- Adapter   46/ 100
- Atlas-Centaur payload   806/1775

Other tradeoffs possible include the use of electric thrusters for attitude control and stationkeeping versus a hydrazine reaction control system (Section 3.3.4), and the use of a very hot collector system (1273°K) and direct heat radiation for the high power tubes versus the more standard way of running the collectors cooler and providing methods of conducting away the waste heat (Section 3.2.5).

All of the above tradeoffs are summarized in this section. Some are covered in more detail elsewhere in this report. Table 3-14 summarizes the important parameters of these tradeoffs.

3.2.1 Booster Selection

In the preceding discussion describing the various spacecraft configuration studies, it was shown that a minimum on-station spacecraft weight of about 570 kilograms (1250 pounds) is necessary with electric propulsion used for orbit raising, or about 525 kilograms (1150 pounds) with all chemical propulsion. The principal propulsion systems considered during this study which can deliver the indicated on-station payload are listed in Table 3-15. Other variants considered but not listed in Table 3-15 are mentioned in the following discussions.

Thor-Delta Family

Thor-Delta launch vehicles are applicable to this mission only when electric propulsion is used for achieving synchronous station. In addition to the three stage 2914 shown in Table 3-15, a two-stage variant, using the Burner II as the second stage, was also considered. It does not provide sufficient payload capacity and was dropped from further consideration.

The 2914 consists of a long tank Thor first stage with nine Castor II solids strapped on for thrust augmentation, a Titan transtage, and a spin stabilized solid third stage. The electric propulsion consists of three 30 cm ion engines as described previously (Section 3.1.1). This propulsion combination can place approximately, 558 kg into synchronous orbit, which is adequate for this mission. The cost is shown as $6 million for the basic booster, plus $2 million for electric propulsion. The electric propulsion costs include the solar panels in excess of the basic mission needs and for the ion engines. The power requirement for the high power communication tubes was shown to be about 5 to 5.5 kilowatts of usable power. Allowing for sun angle, sun intensity, power matching inefficiencies, and radiation degradation, the beginning of life power required for chemical injection is about 8 kw and about 10 kw for the Thor-Delta electrically propelled version. (The greater degradation occurs during the orbit raising period since the vehicle spends a long period in the Van Allen radiation belt.) The cost for this additional 2 kw of solar panel is about $1.5 million. The cost of the ion engines has been estimated at $1 million to $2 million. This brings the total propulsion cost to about $8 million. At this cost, it is $8 million to $9 million lower than that of any of the other boosters listed in Table 3-15. It is

TABLE 3-14. ATS/AMS CONFIGURATION TRADEOFF SUMMARY

Tradeoff	Advantages	Disadvantages
Booster Selection		
a. Thor-Delta/electric propulsion	• Low Cost	• Long orbit raising time (80 days) • Higher risk • Development of electric thrusters required • Lowest recurring cost
b. Atlas Centaur/standard apogee motor	• Reliable, low risk • Short orbit raising time • No development	• No weight margin for baseline
c. Atlas Centaur/optimum apogee motor	• Maximum payload capability • Allows completely conventional approach, lowest risk	• Highest recurring cost • Minor development required
High Voltage Versus Low Voltage Solar Panels		
a. High voltage with integral power conditioning	• Lower spacecraft weight • Better spacecraft thermal integration	• Development required • Higher cost • Lower reliability, higher risk • Greater spacecraft integration problems • More S/C commands required
b. Low voltage panels with conventional power	• Proven approach • Lower cost • Ease of manufacture and test • Simpler design	• Heavier spacecraft weight • More thermal integration problems
N-S Versus E-W of Solar Panels		
a. N-S panels	• Enables use of both north and south faces as thermal radiators • Can perform the communication mission with one rotating joint • Principal solar torque is cyclic thus saving ACS fuel • No interference in LOS to earth for sensors	• Loss of power during summer and winter solstice • Restricts use of electric propulsion for attitude control and stationkeeping due to plume impingement
b. E-W panels	• Power advantage during solstices • Electric thrusters can be body mounted for ACS	• Thermal radiator is restricted to north end for transmitter waste heat • Requires two rotating joints to perform communication mission • Small interference in earth sensor LOS
Foldout vs Rollout Solar Panels		
a. Foldout	• Potentially small weight saving • Can be used as thermal shield during transfer orbit on B-1 and B-5	• Deployment difficult to control in lengths of interest
b. Rollout	• Smooth deployment process • Compact storage on drum • Easier to mechanize retraction if desired	• More complex
Conventional vs Liquid Metal Sliprings		
a. Conventional	• Developed technology • Proven reliability • Lower cost	• High friction torque • Electrical noise • Wear debris
b. Liquid Metal	• Low resistance and power loss • Negligible electrical noise • No wearout mode • Stick-slip friction replaced by negligible viscous friction	• Need for temperature control of assembly • Maintain (prelaunch) inert environment • Higher cost • Higher risk

TABLE 3-14. (continued)

Tradeoff	Advantages	Disadvantages
Electric vs Hydrazine Thrusters for RCS		
a. Electric thruster	• Finer granularity in control • Significant weight saving	• Development required • Not fully space proven
b. Hydrazine RCS	• Proven reliability • Off the shelf system available	• Potential spacecraft/solar panel dynamic interactions • Heavier weight
High vs Low Collector Temperatures		
a. High temperature	• Waste heat removed by direct radiation, lower spacecraft radiator weight • Larger overall RF powers possible	• Greater difficulty in obtaining vacuum seals at high temperatures • Local protection required for other spacecraft hardware
b. Low temperature	• Proven design • Space experience available	• Total spacecraft RF limited from a thermal standpoint • Creator thermal radiator weight

TABLE 3-15. PROPULSION SYSTEM TRADEOFF PARAMETERS

	Thor-Delta 2914 Electric Propulsion	Atlas-Centaur SVM 4 Apogee Motor	Atlas-Centaur Optimum Apogee Motor	Atlas-Centaur Electric Propulsion	Titan 3C
L/V Cost [1]	6 M[2]	16 M	16 M	16 M[2]	22 M
Payload into Synchronous Transfer Orbit	775 Kgs (1550 lbs)		2050 Kgs[3] (4100 lbs)	2050 Kgs[3] (4100 lbs)	
Payload into Synchronous Orbit	630 Kgs (1252 lbs)	725 Kgs (1450 lbs)	985 Kgs (1970 lbs)	1458 Kgs (3200 lbs)	1720 Kgs (3433 lbs)
Development Required	Electric Propulsion	None	Apogee Motor	Electric Propulsion	None
Orbit Raising Time	80 days	1 day	1 day	120 days	1 day
Spacecraft Designs:					
Baseline	A-1		B-1, B-5		
Other	A-2, A-3	B0, B2-B4		C1-C2	

[1] Recurring cost, in 1971 dollars.

[2] The cost of electric propulsion plus the added solar panels required in excess of that needed for on-station operation must be added for comparing total system cost. For the Thor-Delta 2914 (Configuration A-1), this is about $2M, and for the Atlas-Centaur (Configuration C-1), about $6.5M.

[3] 3-sigma capability as obtained recently from General Dynamics. The resultant on-station payload (985 Kgs) is about 140 Kgs more than was used during the study for performance of the Atlas-Centaur with an optimum AKM.

the booster selected for the A spacecraft configurations, and Configuration A-1 has been designed to use the full payload capability of this booster. The shroud for this booster is shown in Figure 3-8. It provides a 2.18 meter diameter dynamic envelope for the spacecraft and an overall length of about 3.98 m forward of the third stage separation plane. Shroud length is a severe constraining factor in the A configuration, and it was necessary to extend the shroud as well as to allow the solar panels to protrude past the third stage separation plane.

The orbit raising time for this vehicle has been shown to be approximately 80 days, which is considered reasonable for a spacecraft with a 5-year mission.

DELTA PAYLOAD ENVELOPE
4 DIGIT SERIES VEHICLES

3J1-13029
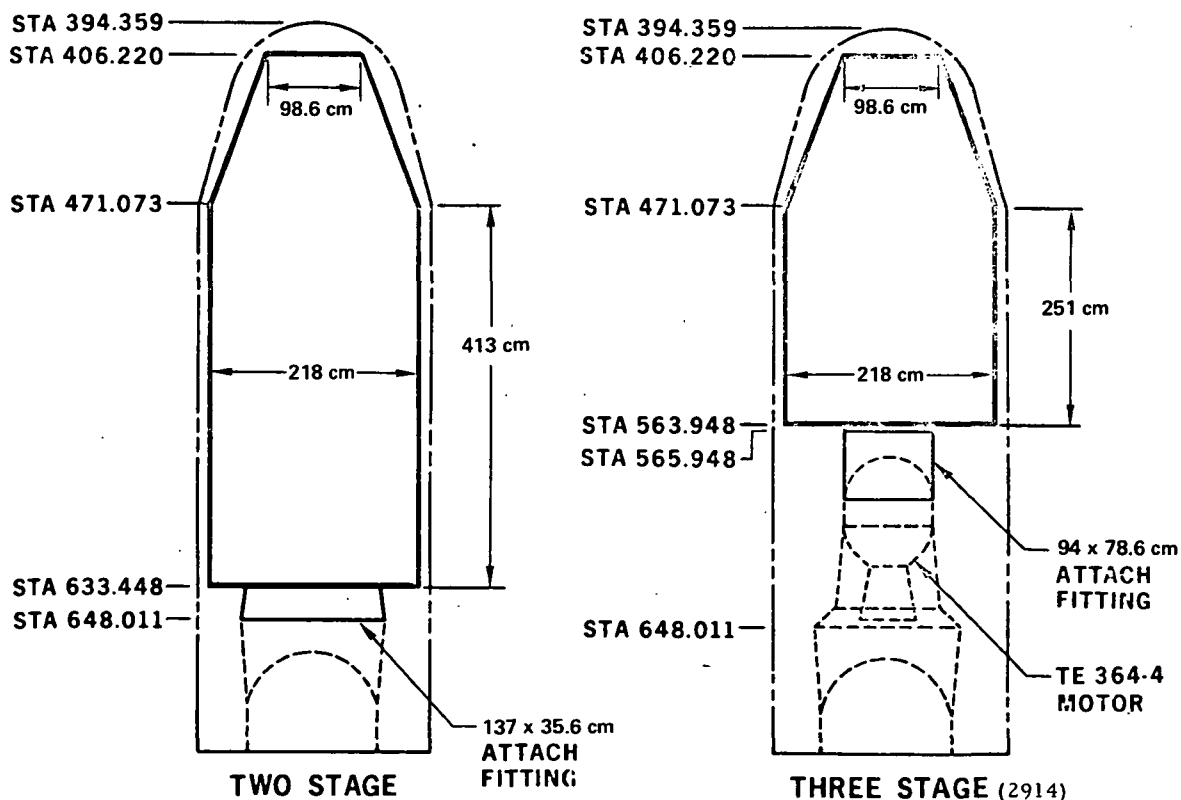
Figure 3-8. Thor Delta Payload Envelope (A Configurations)

PAYLOAD ENVELOPE
WITH INTELSAT IV NOSE FAIRING

SPLIT FAIRING
SPLIT BARREL
TRUSS ADAPTER
STUB ADAPTER

PAYLOAD ENVELOPE

A

CENTAUR D WITH
INTELSAT PAYLOAD
SUPPORT STRUCTURE &
FAIRING. (AC-25)

94.08
DIA.

A

30.00

15 FT.

27 FT.

35 FT.

STA.226.87

STA.146.90

STA.218.90

STA.193.90
FAIRING HINGE PLANE

FAIRING SPLIT LINE

+X

112.0
DIA.

-Y   +Y   102.0

-X

SECT. A-A
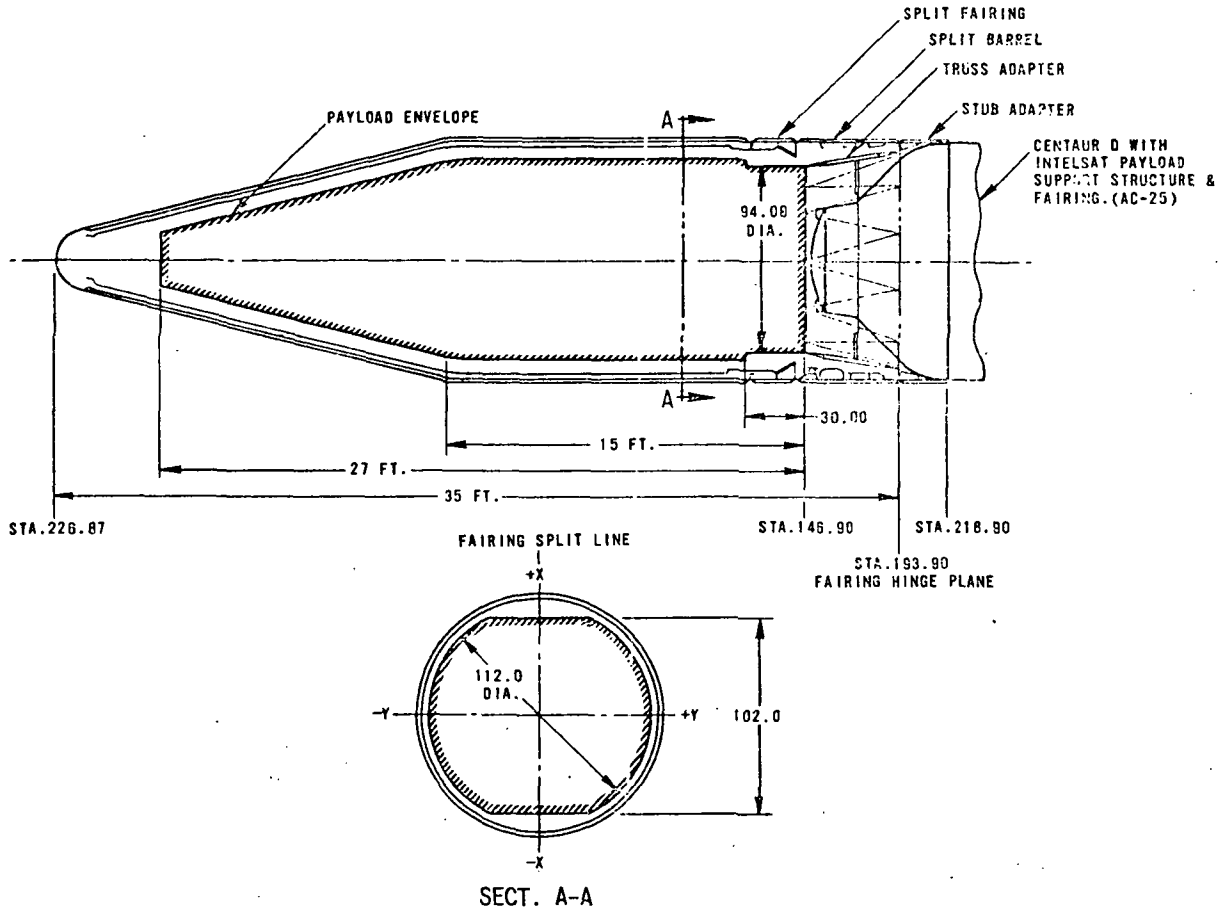
Figure 3-9. Atlas Centaur Fairing (For all "B" Configurations
Except B-1A)

PAYLOAD SUPPORT (INTELSAT IV FAIRING LENGTHENED 80 INCHES)

41.7 FEET
(WAS 35 FEET)

SPLIT
FAIRING

TRUSS

SPLIT
BARREL

102
(WAS 22)

52.0

47.0

HINGE PLANE

25.0

FIXED
ADAPTER
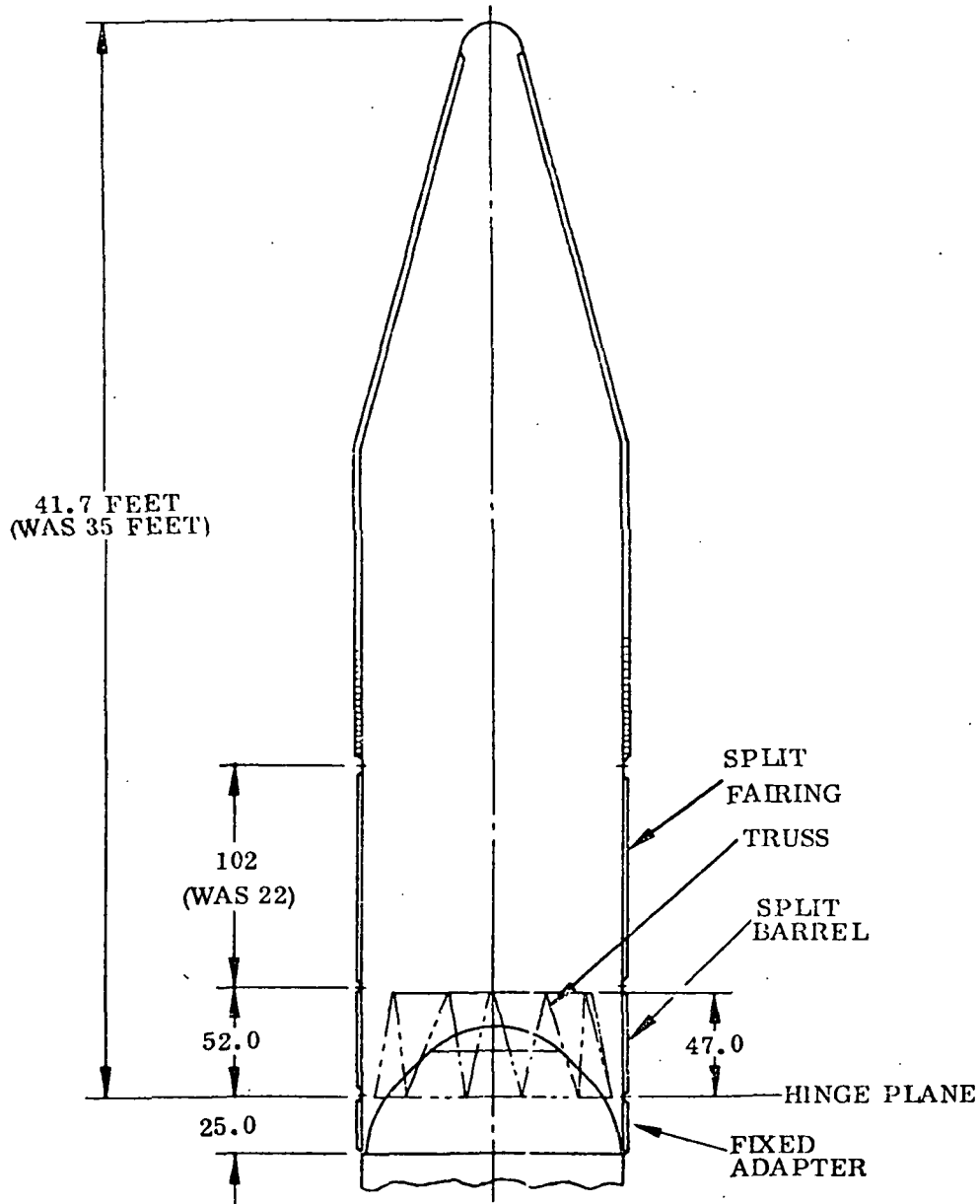
Figure 3-10. Extended Atlas Centaur Fairing
(For Configurations C-1 and B-1A)

3-39

Atlas-Centaur Systems

The Atlas-Centaur (A/C) launch vehicle has sufficient capacity for spacecraft injected into synchronous orbit with either an AKM, as used with all of the Group B configurations described previously, or with electric propulsion, as in the case of the Group C configurations.

Three variants using different AKMs were considered, two which are shown in Table 3-15. The third variant used a Burner II as the AKM. However, since the on-station payload with the Burner II (≈ 650 Kgs) is substantially less than that indicated for the Atlas-Centaur with an optimum AKM, and has about the same recurring costs, it was not considered a viable candidate.

The A/C with the AGC SVM-4 AKM is an attractive candidate in that it utilizes an existing AKM design and is likely to be somewhat less expensive than a new motor. However, it is poorly matched to the A/C capability*, and provides a substantially lower payload capability than does an optimum AKM. Nevertheless, it provides sufficient payload for some of the non-baseline configurations considered in the B group.

For the Group B baselines, the selected propulsion system included the optimized AKM. With either AKM, the fairing is the same as that used for the Intelsat IV. Its dynamic envelope is shown in Figure 3-9, which has sufficient volume to encapsulate all of the B spacecraft configurations except the B-1A with a 2.44 meter lens antenna. An elongated version of the same fairing, such as is shown in Figure 3-10 is required in this case.

The A/C is coupled with electric propulsion for injection of Group C spacecraft configurations. It has a large payload capability and can boost approximately 1370 kilograms into synchronous orbit. Although this capability is far in excess of that needed for this mission, it was selected for configurations C-1 and C-2. The C-1 configuration, using the full capability of the booster, approximates the maximum spacecraft that could be launched with a member of the Atlas-Centaur family**. The cost of this vehicle is shown as $17 million plus $6.5 million for electric propulsion and the solar panels needed in excess of that for a chemically injected spacecraft with the same payload.

The shroud utilized for this vehicle is shown in Figure 3-10. It allows a payload dynamic envelope of about 2.48 m in diameter and 10.25 m in length, 2.03 m longer than the standard fairing used by the Intelsat IV spacecraft

---

*The mismatch is even greater with the recently received upgraded performance data for the A/C.

**The synchronous orbit payload as indicated in Table 3-15 does not reflect the recently received upgrade in A/C performance. However, it is questionable that the shroud could be sufficiently extended to accommodate a significantly larger spacecraft.

(Figure 3-9). The longer fairing is required to house the 17 kw of solar panel for Configuration C-1. The orbit raising time for this vehicle is about 100 days.

Titan IIIC Family

The capability of the Titan IIIC is shown in Table 3-15 as 1720 kgs*. This is substantially more than is needed for the essential experiments defined in this study, and is substantially more expensive than the Atlas-Centaur family. This booster would be attractive only if it were not possible to get an all-chemical propulsion system on one of the members of the Atlas-Centaur family. In an operational system it may be attractive in that dually-launched spacecraft can be accommodated. However, for an experimental mission, the cost of the Titan IIIC is unattractive.

Conclusion

Based upon cost and delivered payload, the most desirable booster is the uprated Thor-Delta (2914) with orbit injection using electric propulsion, as in Configuration A-1. It can meet the basic requirements identified to date at a cost saving of some $8 million to $9 million over any other booster in Table 3-15. For larger payloads, or if all chemical propulsion is desired, a suitable booster can be found within the Atlas-Centaur family. The most promising of these is the Atlas-Centaur with a new apogee motor which has been used for the other two baseline spacecraft configurations (B-1 and B-5). The capability inherent in the Titan IIIC family is not needed to satisfy the current ATS/AMS requirements.

3.2.2 Power Subsystem Tradeoffs

High Voltage versus Low Voltage Solar Cell Arrays

The study and preliminary development of high voltage solar panels has been in progress for several years under the sponsorship and direction of NASA/LeRC with contracts being awarded to Hughes (NAS 3-8996) and other companies. Hughes has also supported development of this technology with internal funding. Working models have been built and tested to prove the feasibility of high voltage solar panels (HVSP) with integral power conditioning. However, development would result in a somewhat higher cost system relative to low voltage panels, which also require further development for high power applications.

The advantage of HVSPs is in lower spacecraft weight, since a significant saving is obtained by deletion of most of the conventional power conditioning, and in potentially simpler high voltage bus regulation for the high power

---

*Current estimate of the upgraded TIIIC.

tubes. Another advantage results from the elimination of the thermal dissipation associated with conventional power conditioning. Efficiency of solar panels is approximately the same, in that the 10 percent of the input power (500 watts) that would normally be dissipated as thermal load in the power conditioning would be power not drawn from HVSPs.

Low voltage solar panels (LVSP) offer a more conventional and proven approach. There would be fewer manufacturing and test constraints and the overall cost should be lower, but all at the expense of heavier spacecraft weight and more complex thermal integration.

For the three baseline spacecraft, HVSPs were selected for the A-1 and B-5 configurations, and LVSPs used for the B-1 configuration.

N-S Pointing Solar Panels versus E-W*

The choice of the orientation of the solar panel deployment axis is a major consideration in configuring the spacecraft. The use of N-S solar panels enables use of both the north and south faces as thermal radiators once on final orbit whereas the E-W panels have only the north face. Further, N-S panels require only one rotating interface between the solar panels and the spacecraft body. The E-W panels require two rotary interfaces, one for the solar panels, and one for the despun antenna, resulting in a more complex and costly design. The extra interface is useful during the solstice seasons in that E-W panels can be oriented normal to the sun direction. With N-S panels, the principal solar torque is cyclic, thus reducing attitude control fuel consumption. In addition, the N-S solar panels present no interference in LOS to the earth for the sensors, whereas the E-W solar panels result in some interference over a small portion of the orbit.

A major advantage of E-W solar panels (other than the orientation during solstice) is the ability to use electric thrusters for attitude control since they can be mounted on the spacecraft body. Body mounted electric thrusters used with N-S solar panels result in a plume impingement on the panels during N-S stationkeeping. Consideration was given to mounting the electric thrusters outboard of the N-S solar panels. However, it appears that with solar panels in the 18 to 25 meter length range, there would be significant problems in determining thrust direction. In addition, the weight of the thrusters plus fuel (approximately 7 Kg) would present a structural problem for the deployment of the light weight solar panels. Although it may be possible to resolve these problems, it was concluded that the use of electric thrusters for N-S stationkeeping is justified only with E-W panels.

E-W solar panels were selected for the A-1 spacecraft, and N-S solar panels for B-1 and B-5.

---

*E-W orientation is a nominal designation for panels with their axis in the orbit plane. The coincidence of the panel axes with E-W occurs twice per orbit.

Foldout versus Rollout Arrays

The accordian style or foldout rigid solar panels have merits but are heavier than rollout arrays. One advantage of foldout panels for the B-1 and B-5 configurations is the use of the panels as a thermal shield during the transfer orbit when the solar panels are not deployed and the internal spacecraft dissipation is very low. During this period, it is necessary to cover the thermal radiators (north and south) to keep the internal temperatures at an acceptable level (the spacecraft tends to get very cold). With the rollout solar panels, extra thermal covers would be required for the radiators. Deployment interactions are more significant with foldout panels for the large lengths used on these spacecraft, whereas the rollout panels feature a smooth deployment process. Storage for rollout solar panels is more compact and retraction is simpler to implement, should there be such a requirement.

Rollout solar panels are used in all three baseline configurations. *

Conventional versus Liquid Metal Sliprings

Conventional sliprings have been used on a number of spacecraft and have accumulated a history of reliability in space operation. Their principal disadvantage is in high friction torque and its possible degrading effect on spacecraft dynamics. However, this is not viewed as a major problem. Electrical noise and wearout debris are significant constraints on spacecraft with rapidly rotating interfaces, but for the ATS/AM application, they are not severe as the maximum rotation rate is on the order of one revolution per day.

Liquid metal sliprings (LMSR) have been under development for several years by NASA/LeRC and appear attractive for the ATS/AM application. They offer low resistance and power loss, negligible electrical noise, and elimination of the wearout mode. The stick slip friction of conventional brush and ring assemblies has been replaced by a negligible viscous friction. On the negative side, LMSR imposes a need for temperature control during the boost phase of the mission to maintain a frozen assembly and during eclipse conditions to maintain a thawed state. Difficulties imposed during assembly and handling include the maintenance of a strictly inert environment to prevent the formation of a surface film. The overall cost and development risk associated with LMSR would be higher than for conventional sliprings, although not prohibitive.

LMSR assemblies are used on the A-1 and B-5 baseline configurations, and conventional sliprings are used on the B-1.

---

*As of the writing of this report, a rollout solar array developed by Hughes has been successfully operated both as a space experiment and as a primary spacecraft power system.

Electric Thruster versus Hydrazine

Electric thrusters for use in attitude control and stationkeeping have the advantages of providing finer granularity in control and substantial savings in propellant weight relative to impulsive chemical thrusters. The impulsive thrust associated with the use of hydrazine RCS introduces a potential spacecraft/solar panel dynamic interaction problem.

Hydrazine systems offer well developed technology with off-the-shelf hardware which has been demonstrated in space.

A detailed quantiative analysis of the tradeoff factors is presented in Section 4.3, Attitude Control and Stationkeeping Subsystem.

For the baseline configurations, electric thrusters are used on the A-1 configuration, and hydrazine on the B-1 and B-5 configurations.

High versus Low Collector Temperatures

The use of high temperature collectors operating at temperatures of up to $1273^{\circ}K$, and radiating directly to space, has been selected for all three candidate spacecraft configurations. This offers a significant weight saving in thermal radiators and makes larger RF powers feasible. Powers of the magnitude present on the ATS/AM impose severe theremal constraints and careful design. The major disadvantages with hot collectors are the difficulty in maintaining vacuum seals at high temperatures, and the requirement for local thermal protection of other spacecraft hardware. The advantages of low temperature operation include proven design techniques. However, the large amounts of collector heat developed in each of the three spacecraft configurations make this technique undesirable, and justifies the use of high temperature collectors.

3.3 TRAJECTORY CONSIDERATIONS

Two fundamentally different launch profiles have been considered in this study. The launch vehicle for the A configuration is a Thor-Delta 2914. The launch injection into transfer orbit is similar to that for the all-chemical injection. However, the orbit raising to synchronous station is done over approximately a three month period with low-thrust ion propulsion. A conventional all-chemical injection has been utilized with the B configuration launch vehicles, where the launch vehicle is an Atlas-Centaur.

All chemical injection has been accomplished many times and therefore will not be discussed in detail. However, the trajectory considerations for injecting a spacecraft into a synchronous orbit utilizing low-thrust ion propulsion are not nearly as familiar and tradeoffs are discussed in more detail.

3.3.1 Launch Profile and Chemical Injection

The launch and transfer orbit injection are similar for synchronous injection with either chemical or low-thrust ion propulsion. Figure 3-11 shows a typical launch and transfer orbit injection for the Thor-Delta launch vehicle. Liftoff takes place at a time compatible with launch window constraints. Following liftoff, the first stage and a partial burn of the second stage places the spacecraft into a 28.5 degree inclined parking orbit 8.9 minutes after liftoff. After a 15.5 minute coast in the parking orbit, the second stage is restarted. This second burn of the second stage and the entire third stage inject the spacecraft into a 28 degree inclined transfer orbit about 26 minutes after liftoff.

Synchronous injection with an apogee kick motor is shown schematically in Figure 3-12. The apogee kick motor is fired to circularize the orbit and remove the inclination. Firing is done at one of the first few apogees, and is usually planned to occur at that apogee which is closest to the desired station location of the satellite to minimize the time of drift to the desired station.

3.3.2 Orbit Raising with Low-Thrust Propulsion

The general approach to the low-thrust orbit raising analysis has been one of determining the constraints and relationships which circumscribe practical trajectories. This has been done not only because it leads to valuable insight into the flight dynamics of the problem, but also because it is advantageous economically to perform detailed investigations only for those flight mechanics profiles which are shown to be desirable. The use of the "EPSTOP" computer program is particularly efficient for this purpose
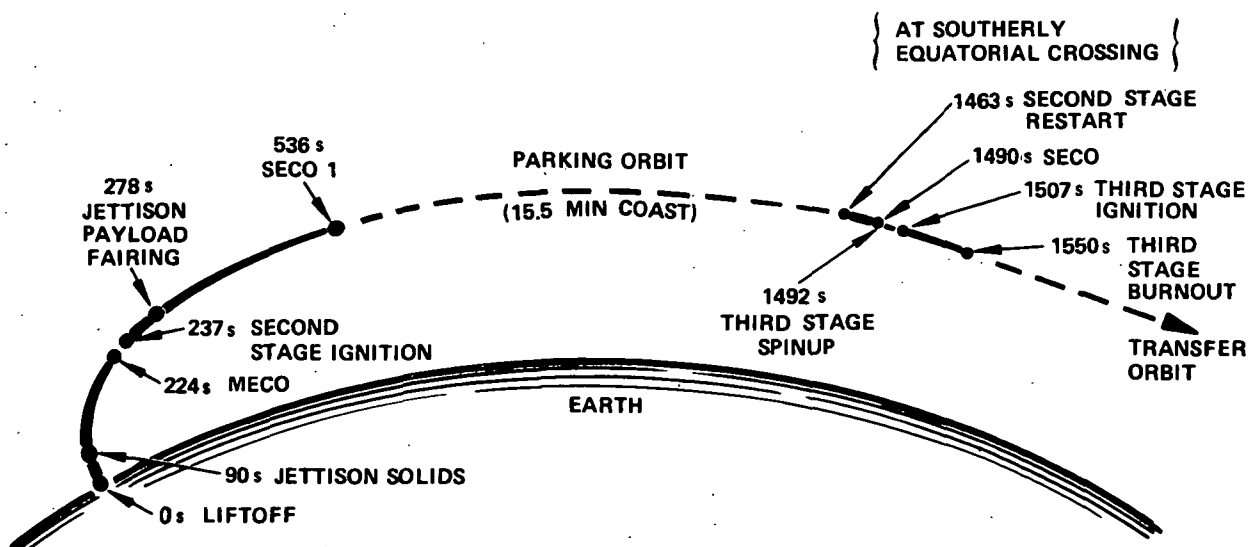
Figure 3-11. Typical Parking and Transfer Orbit Injection
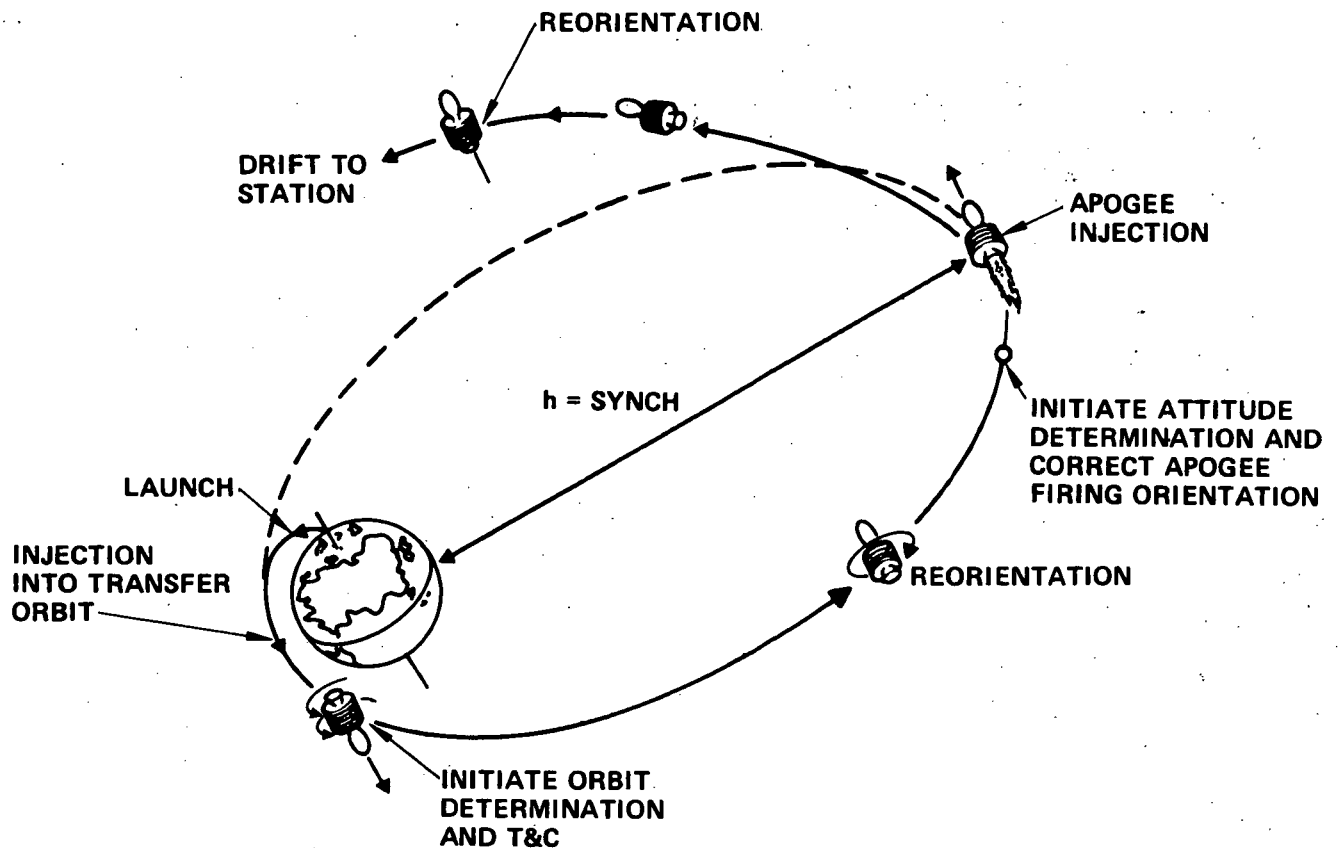
Figure 3-12. Synchronous Injection With Apogee Kick Motor

because it explicitly handles trajectory parameters (e.g., solar panel
radiation degradation, thrust attitude profile) which would otherwise require
considerable iteration for convergence or optimization.

A simplified block diagram of the orbit raising analysis process is
shown in Figure 3-13. Specifically, the items that lead to a proper evalua-
tion of injected mass and power are the initial conditions for the orbit
raising process, i.e., the transfer orbit and propulsion system design, and
an accurate modeling of the orbit raising trajectories. If these two functions
are properly performed, the values obtained for the injected mass and power
must be correct. Inevitably at this preliminary stage, uncertainties exists
in subsystems performance characteristics. These uncertainties appear to be
small with the exception of solar panel degradation due to radiation damage
in the Van Allen belts. More detailed testing of solar panel characteristics
and more accurate modeling of flux levels in the belts may be anticipated in
the future. Hopefully, the refined data will substantiate the information used
to date. However, even a significant change in these numbers will not invali-
date the general conclusions of the study, namely the considerable performance
advantage of orbit raising utilizing low-thrust propulsion with respect to all
chemical injection, and the conclusions regarding the type of transfer orbit
profile (i.e., eliptical versus circular) which is more desirable for the low-
thrust orbit raising mission.

```
┌─────────────────────┐      ┌─────────────────────┐      ┌─────────────────────┐
│                     │      │      OPTIMIZE       │      │                     │
│ INITIAL CONDITIONS  │      │     ACCURATELY      │      │   INJECTED MASS     │
│  ● TRANSFER ORBIT   │─────▶│      MODELED        │─────▶│    AND POWER        │
│                     │      │    TRAJECTORIES     │      │                     │
│                     │      │  (EPSTOP PROGRAM)   │      │                     │
└─────────────────────┘      └─────────────────────┘      └─────────────────────┘
```
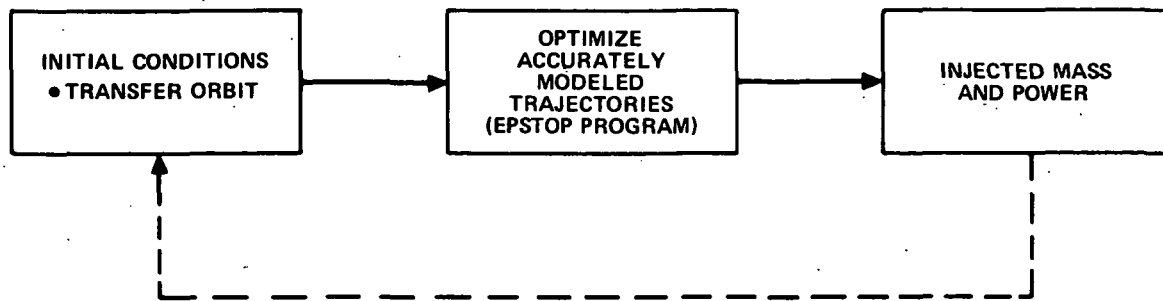
Figure 3-13.   Orbit Raising Analysis

3.3.2.1   Modelling of Subsystem Performance Characteristics

Modelling of subsystem performance characteristics is of primary importance in assuring an accurate representation of the trjaectory flight dynamics.   A brief disucssion of the modelling of the three significant subsystems. for the orbit raising analysis will be given, namely,

1)   Launch booster performance

2)   Solar panel degradation

3)   Ion propulsion system

Launch Booster Performance.   The basic performance characteristics of the upgraded Thor-Delta launch vehicle are shown in Figures 3-14 and 3-15.   Two versions were considered; the two-stage (2910) and the three-stage (2914).   The three-stage differs from the two-stage only in that it has a solid third-stage added on top of the basic two-stage vehicle.   Figure 3-14 shows the injected mass capability of these two launch vehicles (due east launch) into a low altitude circular orbit.   Since the upper third stage of the three-stage vehicle is a solid, intermediate altitude orbits cannot be obtained with the use of a Hohmann transfer, thereby requiring that these orbits be obtained with a direct injection maneuver.   This flight dynamics profile is very inefficient as injection altitude is increased.   Therefore, injected mass capability for the three-stage vehicle falls off very rapidly (much more rapidly than for the two-stage vehicle) as injection altitude is increased.   For this reason performance data is shown for the three-stage vehicle only at a single point, which is at injection at 185 km (100 n. mi.) circular altitude. The curve shows that even at this altitude the injected mass available with a two-stage version of the Thor vehicle is greater than that available with the three-stage, and for the reason just mentioned, this performance difference increases as the injection altitude is increased.   This effect of decreasing performance by adding additional stages to the vehicle may appear incongruous but it is not uncommon.   In effect, the addition of mass on a launch vehicle causes greatly increased gravity losses during the burning of the lower stages.   These losses may be large enough so that they cannot be overcome even if a significant portion of the added mass is an upper stage.   Since most of the United States launch vehicles were initially developed for weapon system
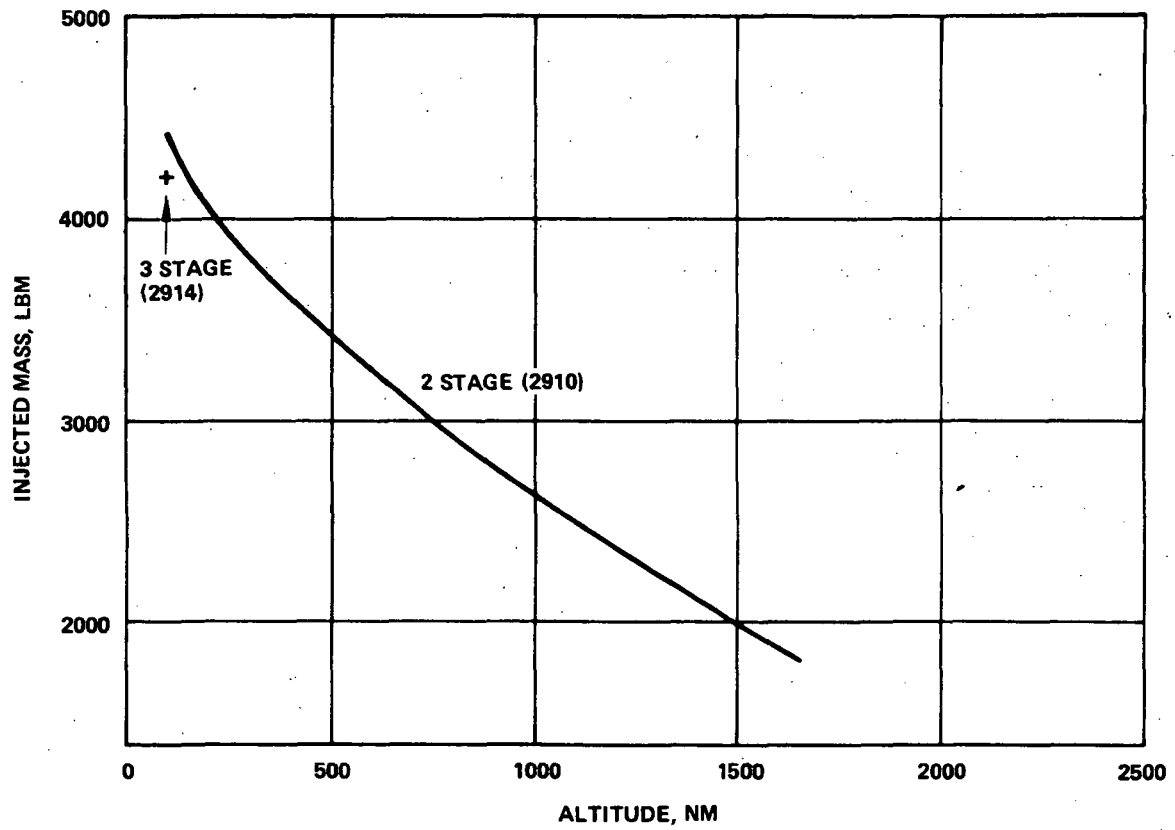
Figure 3-14.   Circular Transfer Orbit with Thor-Delta
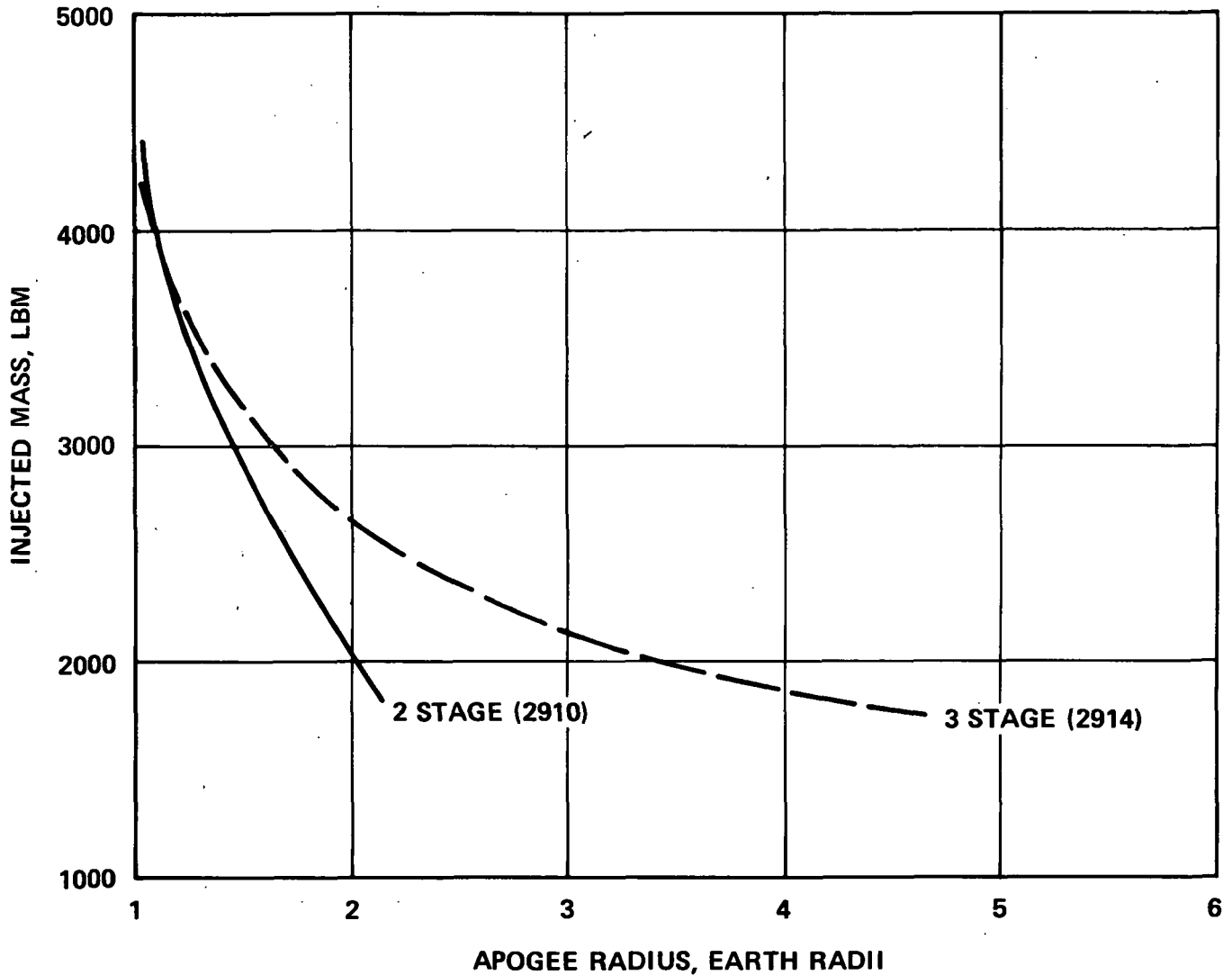
Figure 3-15.   Elliptical Transfer Orbit with Thor-Delta

delivery, they are sized for relatively light weight upper stages and the
phenomena just described has often been experienced.   When more total veloc-
ity is required from the launch vehicle, the injected mass capability goes
down and the use of an upper stage becomes more advantageous.   This is
shown in Figure 3-15, where injected mass is given as a function of apogee
radius for injection into an elliptical orbit with a 185 km (100 n. mi.) perigee.
Therefore, the version of the launch vehicle which is most advantageously
utilized depends upon the transfer orbit.   For injection into a low altitude
circular orbit, the two-stage version is preferred, whereas the three-stage
vehicle is more appropriate for injection into elliptical orbits.

The performance sensitivity to initial perigee altitude is shown in
Figure 3-16. This figure shows that the performance penalty for injecting
into a 555 km (300 n.mi.) perigee rather than a 185 km (100 n.mi.) perigee is
significant but not prohibitive. It is obviously preferable to use the lowest
initial perigee altitude which is compatible with other system requirements.

Solar Panel Degradation. Solar panel degradation comes from two
sources: protons in the Van Allen belts during orbit raising, and electrons
at synchronous altitudes during the lifetime of the mission (the electron flux
during the orbit raising process is negligible in comparison to the effect of
the protons). The integrated electron flux on station is assumed to be 2×10^{15}
equivalent 1 Mev electrons. This dosage has a relatively minor effect in
comparison to that which is incurred from the protons during the orbit raising
process. The computation of the solar cell degradation from proton flux is
indicated in Figure 3-17. The flux (both intensity and energy levels of parti-
cles) is a function of position. This flux, together with relative damage
coefficients (which are a function of solar cell characteristics), lead to an
equivalent flux intensity which can then be integrated to give the total integrated
flux as a function of time. This total integrated flux and the solar cell charac-
teristics are used to provide an estimate of the solar panel degradation. The
power which is available for low thrust propulsion is then a function of the
solar panel degradation; this available power effects the spacecraft accelera-
tion and therefore the spacecraft position at future times. This process is
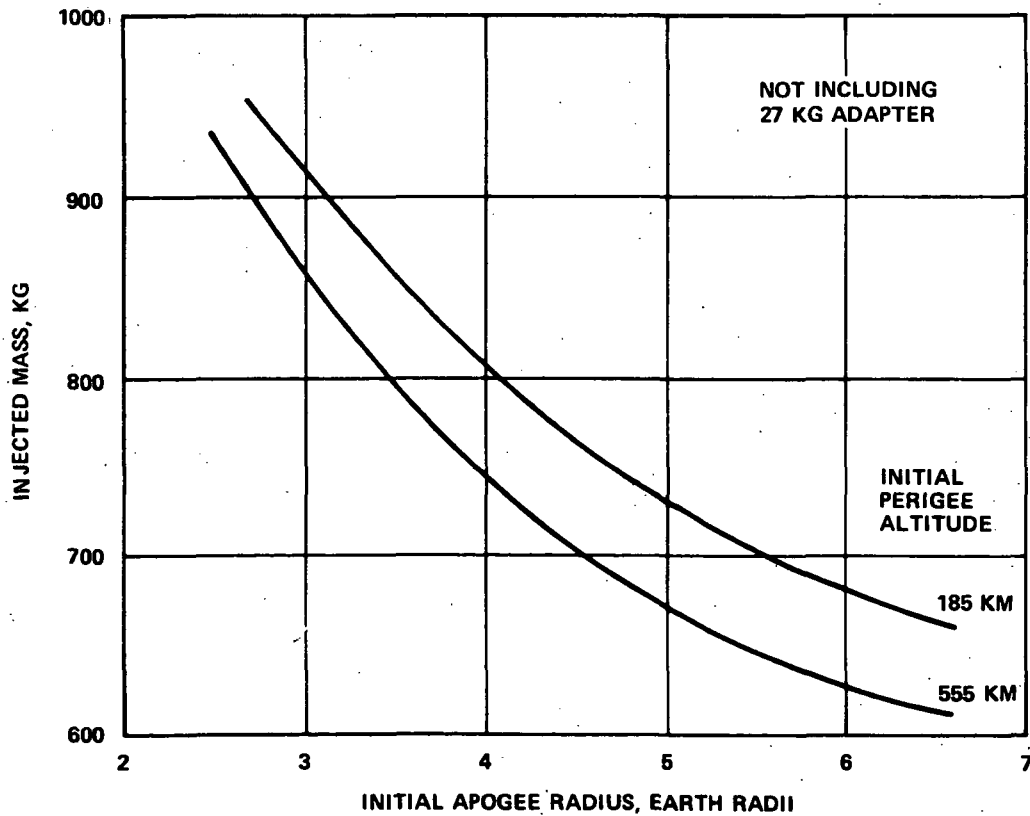
Figure 3-16. Sensitivity to Perigee Altitude
3-Stage Thor Delta (2914)
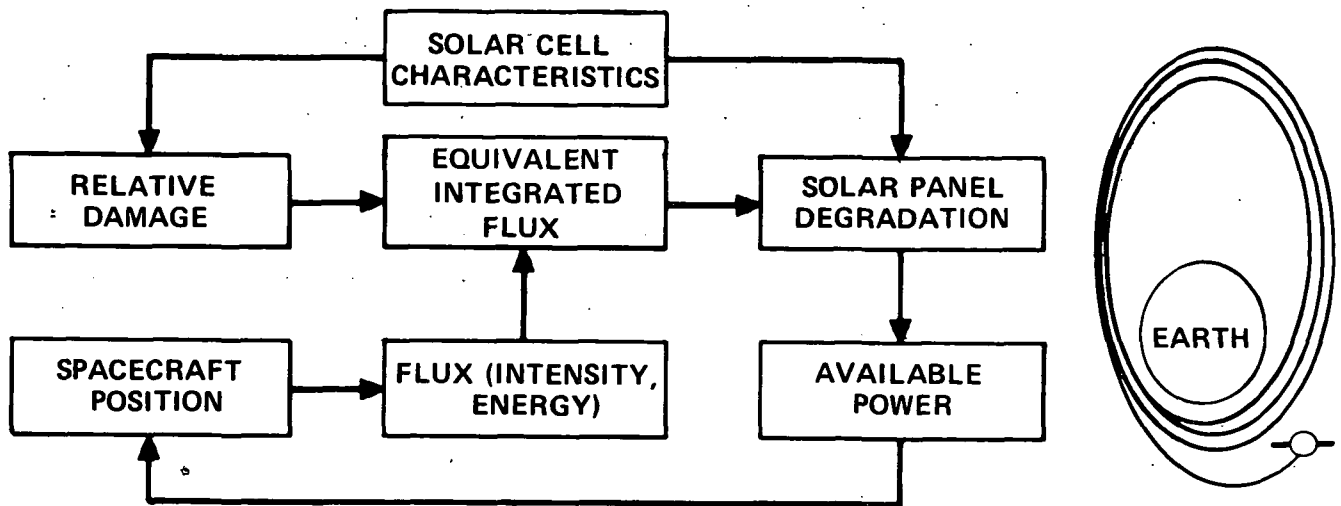
Figure 3-17. Computation of Solar Cell Degradation

performed continuously as the trajectory is integrated; the equivalent integrated flux is carried as one of the state variables in the trajectory integration. The proton flux model used is the NASA Goddard Model AP7. The relative damage coefficients were obtained from TRW studies (Report 99900-6547-R000). The solar panel degradation as a function of equivalent integrated flux and solar cell characteristics was taken from Heliotec cell test data.

Ion Propulsion System. Ion propulsion system modelling requires a proper representation of power available to the thrusters, thrust, mass, and reliability. The power available for thrust is not only a function of the solar panel design and the solar panel degradation, but also of the power conditioning efficiency and the housekeeping power. Although the magnitude of the house-keeping power may be constant, its percentage of the available output varies during the mission as the panel degrades and this must be properly accounted for. The thrust level is a function of the power available, the number of thruster modules utilized, and the characteristics of the individual thruster modules. The characteristics of the individual thruster modules include the physical size, the nominal (i.e., full power) operating characteristics, and penalties associated with throttling the thruster below full power input. Important nominal operating characteristics include power losses (from discharge, heaters, etc.), utilization efficiency, and the ion optics (which effect current density and specific impulse). Penalties for throttling include power loss due to power subsystem mismatch, and utilization efficiency loss, which reduces the effective specific impulse. The thruster characteristics which are utilized in this study produce the total propulsion system efficiency as a function of specific impulse as shown in Figure 3-18. Power matching losses are shown in Figure 3-19. The solid curve represents the beam power avail-able without power matching losses. The dashed curve indicates the actual beam power including these losses. The horizontal portion of the dashed line represents a period of time where all but one of the original thrusters (N-1) are operating at full power. On other points on the dashed curve, the thrusters which are operating are throttled back equally to some value less than the full power. The point where the dashed line and a solid line touch represents a
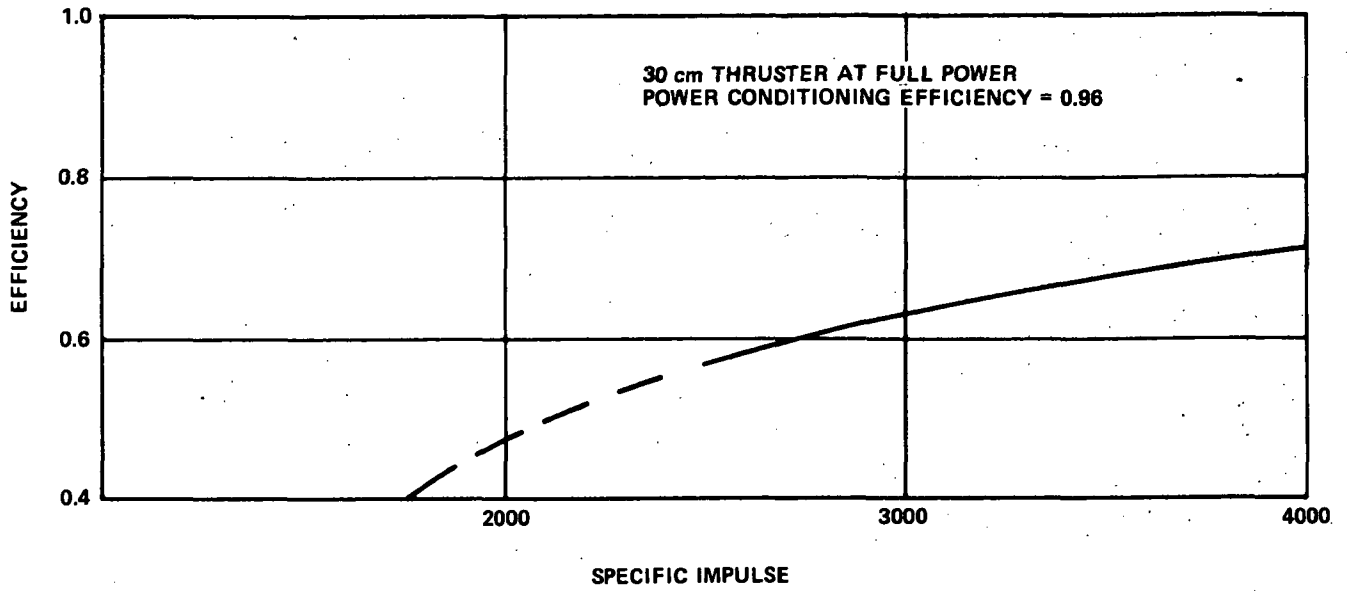
Figure 3-18. Total Electric Propulsion System Efficiency
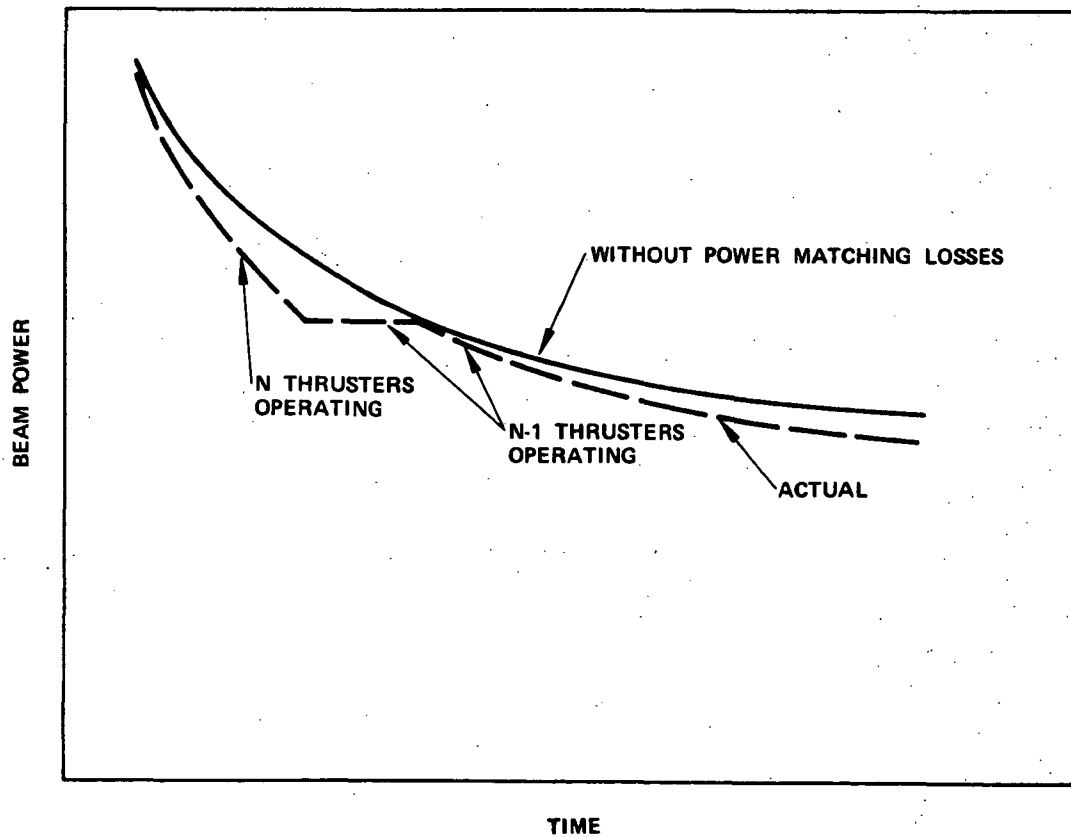
Figure 3-19. Matching Available Power to Thruster Input

perfect match in that the power available to the thrusters from the solar panel is just adequate to operate N-1 thrusters at full power. At points immediately before this in time, N-1 thrusters are operated at full power rather than N thrusters over-throttled because the latter alternative actually produces less beam power and therefore less thrust. The effect of utilization efficiency loss due to throttling is shown on Figure 3-20, where the ratio of effective specific impulse to full power effective specific impulse is shown as a function of thrust ratio for throttling at constant EV/ion. It is presumed that the neutralizer flow and the neutral flux remain constant during this throttling. It may be noted that one of the reasons for optimizing the propulsion system design is to obtain a configuration which will minimize the losses due to power matching and throttling.

The propulsion system mass must also be modelled. This mass is a direct function of power, rated specific impulse, thruster module size and reliability. The mass is an implicit function of the thrust losses; the indirect relationship is that both nominal power losses and those resulting from throt-tling influence propulsion system capability and therefore the "size" of the propulsion system required to perform the mission. For example, increased losses may be compensated by an increase in basic power level which influences the propulsion system mass through the direct relationships. It may be noted that the common assumption of constant specific mass is a poor one for most subsystems. Figure 3-21 illustrates a typical thruster module specific mass. This specific mass is a nonlinear function of power and specific impulse.
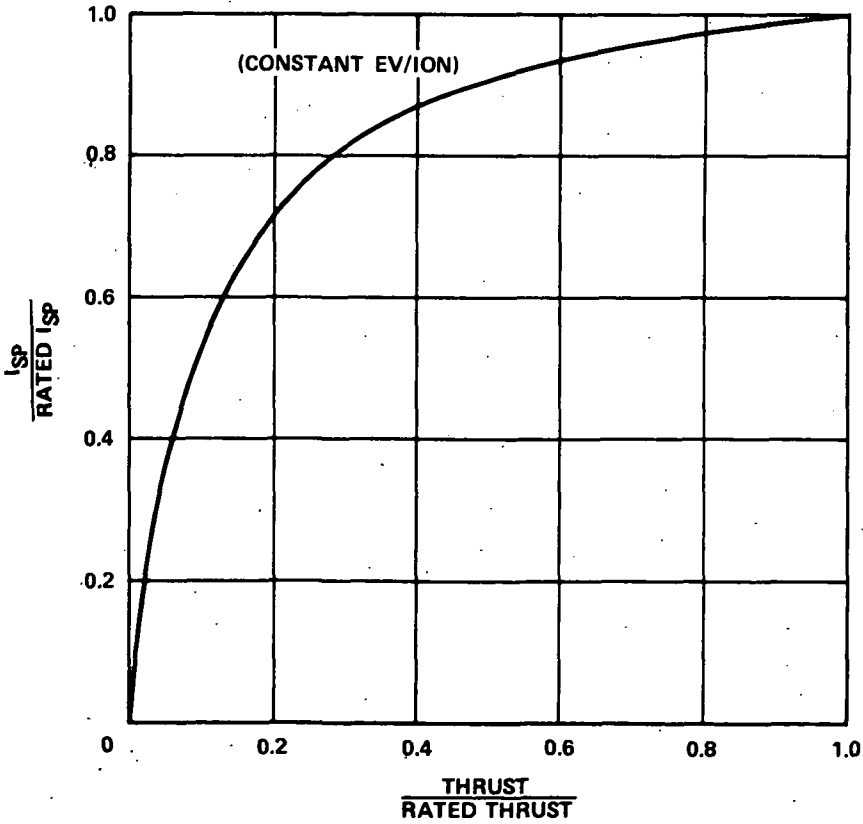
Figure 3-20. Mercury Bombardment Thruster
Throttling Characteristics
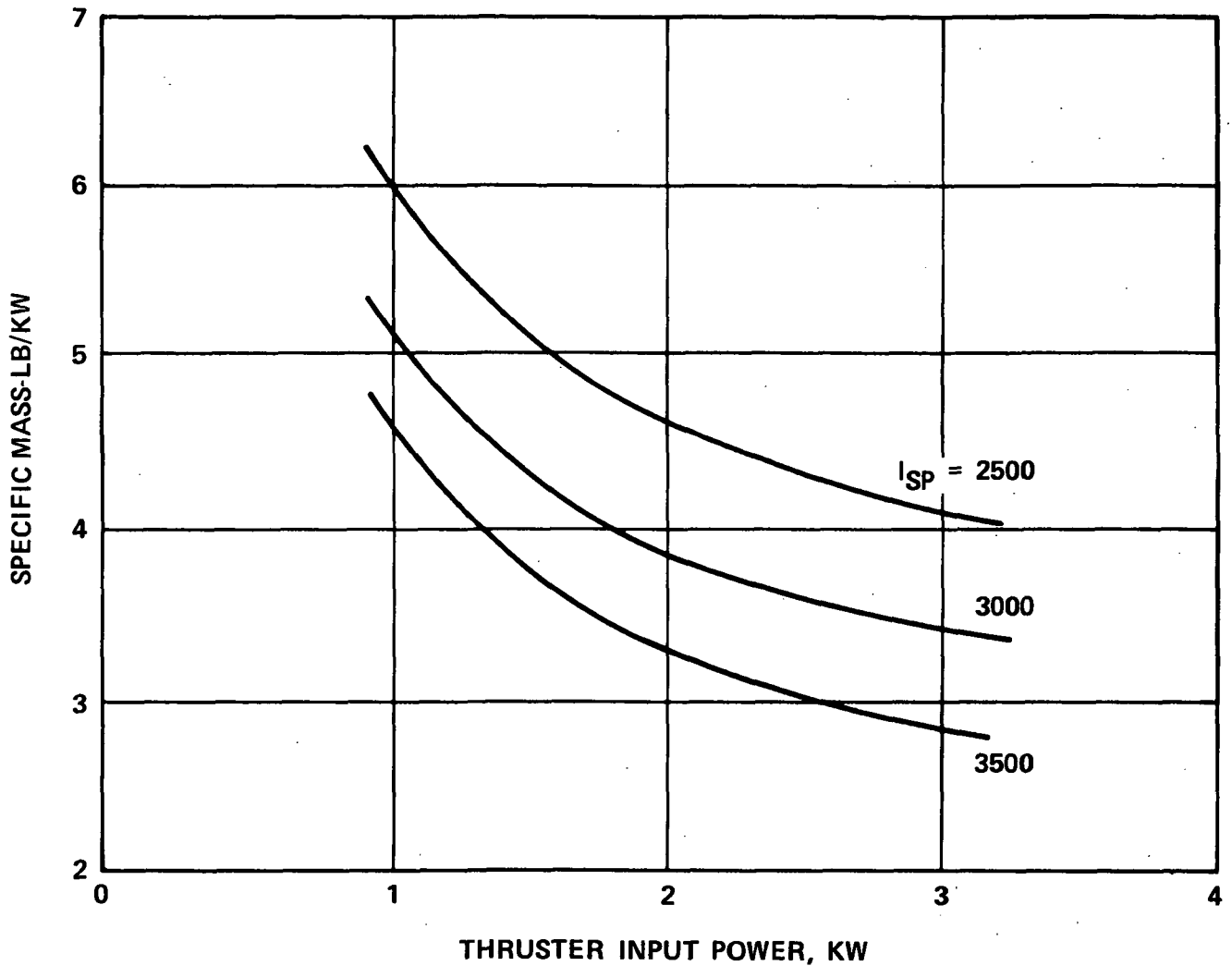
Figure 3-21. Thruster Module Specific Mass

The propulsion system reliability modelling assumes that random failures occur at constant failure rates. Propulsion system reliability is built up with the use of either standby or parallel redundancy. A previous study investigated thruster module failure rates. The results of this study are shown in Figure 3-22. Note that, although smaller diameter modules individually have smaller failure rates, this does not necessarily indicate that a system comprised of smaller modules will have a higher reliability than one comprised of larger modules. The mass-reliability tradeoffs for this mission are discussed elsewhere (Section 4.4). The failure rate for the high voltage solar panel was assumed to be 230×10^{-9} failures per hour in this study.

Although this failure rate appears satisfactory for the orbit raising mission, it is a function of the design and can be reduced at a slight mass penalty.
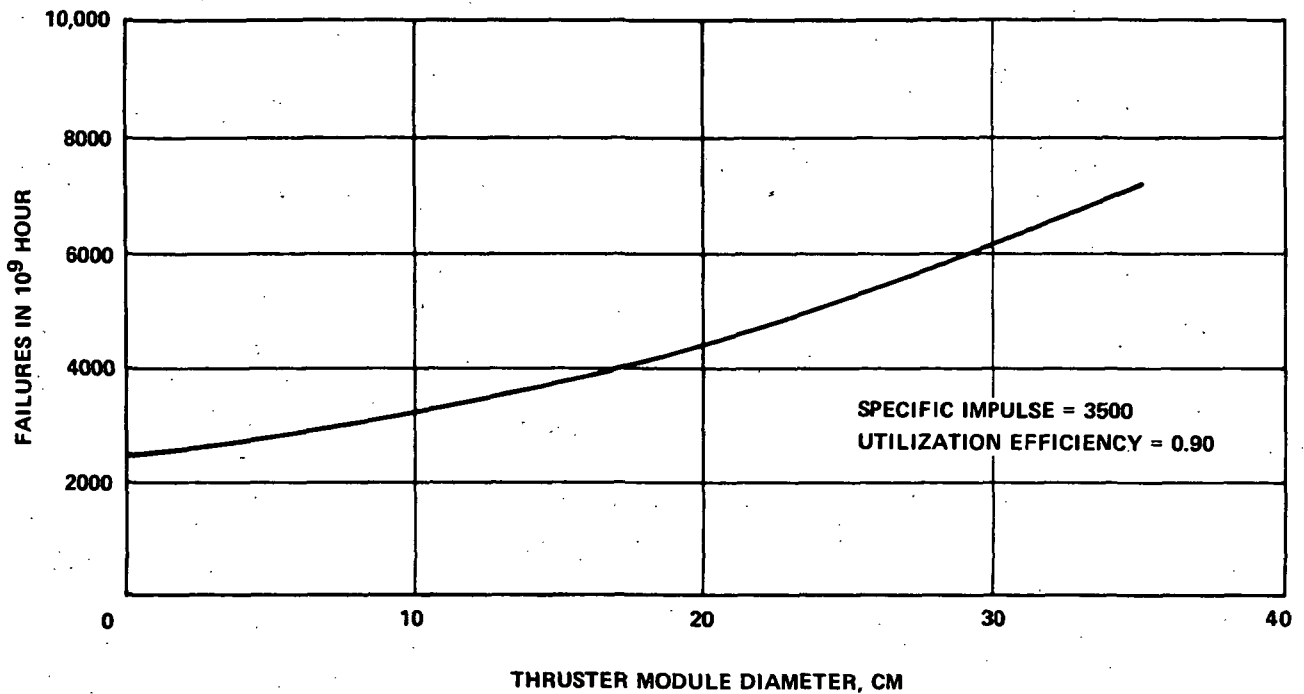
Figure 3-22. Thruster Module Failure Rate

3.3.2.2 Selection of Transfer Orbit Profile

Two aspects of the transfer orbit profile must be specified, namely the inclination and the dimensional elements (e.g., apogee and perigee). The transfer orbit inclination is very tightly constrained by practical considerations. The launch must be from Cape Kennedy at a latitude of 28.5 degrees, which becomes the practical lower limit on the inclination of the parking orbit. There is an optimum plane change at transfer orbit insertion. However, this is quite small, being less than 2 degrees with chemical orbit raising, and less than 1 degree with orbit raising utilizing low thruse propulsion. In either case, this is a minor performance consideration, and for practical purposes in the low thrust orbit raising analysis, the transfer orbit inclination can be considered to be fixed at 28 degrees.

Figure 3-23 schematically indicates possible transfer orbit profiles. The solid lines are a family of elliptical transfer orbits all with the same low altitude perigee and various apogees. Obviously, the total mass that a launch vehicle can inject into these orbits decreases as the apogee is increased. As indicated previously, it is most efficient to have the orbit perigee as low as is possible because of performance considerations. There is, therefore, only one family of viable elliptic orbits, specifically that family which has perigee at the lowest acceptable value. An alternative family of orbits is indicated by the dashed line. These orbits are initially circular at various altitudes. As before, an increase in the orbit altitude requires a reduction in the injected mass. It is possible to pick out pairs of orbits, one from each family, which have the same injected mass.
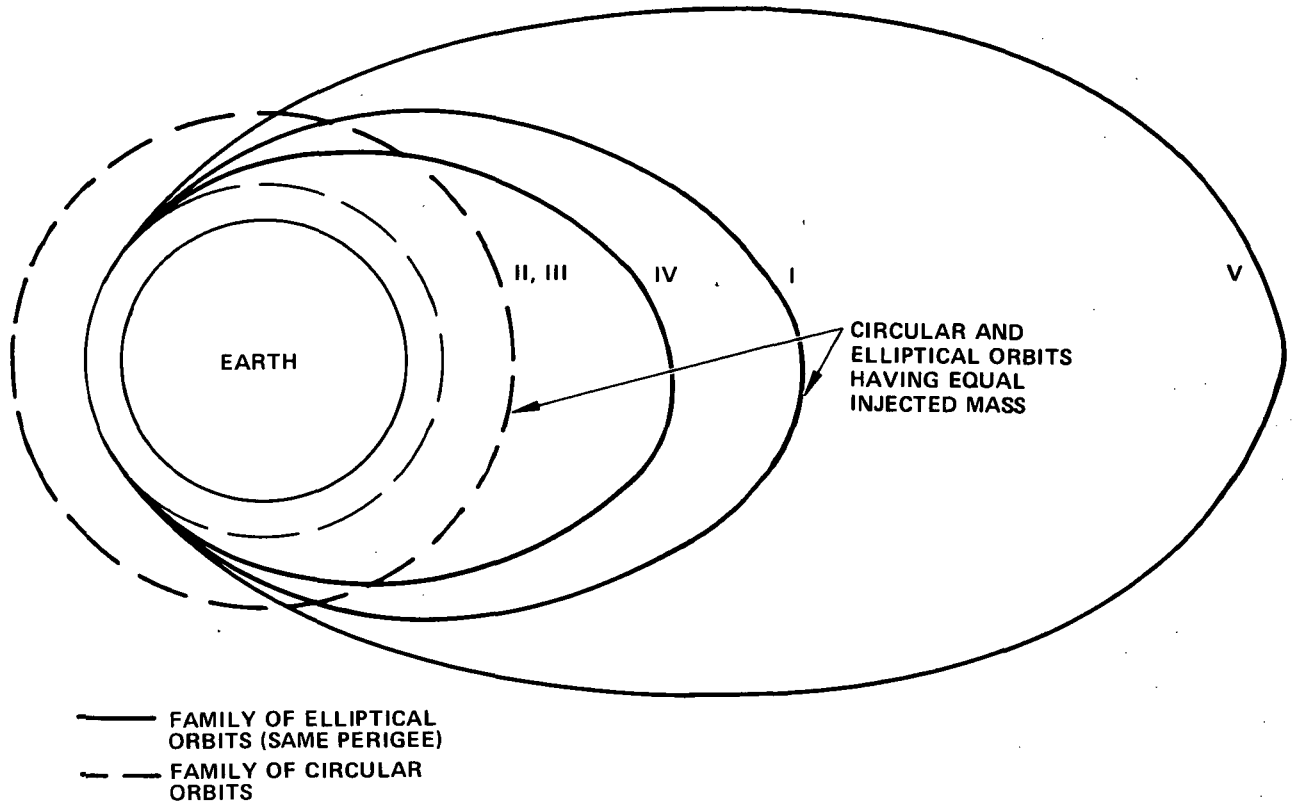
Figure 3-23. Possible Transfer Orbit Dimensional Elements

It happens that the best circular orbit altitude (presuming that the family of circular orbit profiles is used for the transfer orbit) is rather tightly constrained. It must be above about 550 km (300 n. mi.) to avoid serious control problems due to aerodynamic torque. Likewise the performance of Thor-Delta imposes an upper limit of about 3700 km (2000 n. mi.). The solar panel degradation is not influenced significantly by the choice of altitudes between these limits because there is a relatively low proton flux density below about 2800 km (1500 n. mi.) altitude. The orbit raising time is then not influenced by a greater degradation and therefore the thrust acceleration is the primary consideration in determining the orbit raising time. (The initial altitude is of secondary consideration because the time required to do orbit raising above 3700 km is much greater than the period required to achieve this altitude.) An initial circular orbit altitude of about 2800 km appears to be about the best choice that can be made for the ATS/AMS mission on the basis of orbited mass and power required (utilizing the Thor-Delta and an initially circular transfer orbit).

The tradeoffs between a 2800 km circular orbit and selected elliptical orbits are shown in Table 3-16. The baseline circular orbit is orbit No. 2. Comparing this with orbit No. 1, we note that the mass in synchronous orbit is identical but that the elliptical orbit requires much less initial power for the same final power, and has a much shorter orbit raising time.

TABLE 3-16. FASTER INJECTION WITH LESS SOLAR POWER FROM ELLIPTIC TRANSFER ORBIT

Orbit No.		1	2	3	4
Orbit Altitude	km (nm)	260 x 17,200 (140 x 9300)	2800 x 2800 (1500 x 1500)	2800 x 2800 (1500 x 1500) (l_{sp} = 2000)	260 x 11,550 (140 x 5700)
Mass in Synchronous Orbit - kg		770	770	610	920
Initial Rated Power - kw		11.3	16.7	15.7	16.7
Final Rated Power (Conservative) - kw		5.5	5.5	5.5	7.5
Orbit Raising Time - Days		150	290	230	170
l_{sp} = 3500 Except for Orbit 111					

Alternatively, the baseline circular orbit can be compared with orbit No. 4, which has the same initial power. In this case, we see that the eliptical orbit provides a substantial improvement in synchronous orbit mass, much higher final power, and a much shorter orbit raising time. We also note that increasing the thrust by decreasing the specific impulse (orbit No. 3) at a constant final power reduces the required initial power and the orbit raising time only slightly, but at a significant penalty in synchronous orbit mass. The performance differences between the elliptic and circular orbits are so large that there can be no doubt that the family of elliptical orbits is superior, for this mission, to the family of circular orbits. Therefore, subsequent mission analysis deals only with the family of elliptic transfer orbits.

The perigee altitude is constrained by the necessity of maintaining control during eclipse in the presence of aerodynamic moments. Although this makes it desirable to avoid eclipses near perigee, other considerations dictate the desirability of locating any eclipses at perigee. The required minimum perigee altitude is a function of the momentum storage capability in the spacecraft, and, as such, is a design tradeoff. A minimum perigee altitude of 550 km (300 miles) appears to be an appropriate baseline value, although further study might indicate that a somewhat lower value could be used. As indicated previously, raising the perigee to 550 km (300 n.mi.) from 185 km (100 n.mi.) incurs a penalty of approximately 50 kgs in a spacecraft mass injected into the transfer orbit.

The mass injected into synchronous orbit is shown as a function of initial apogee radius in Figure 3-24. Although low initial apogee radii provide relatively large values of injected mass, they introduce serious system penalties which makes the use of these trajectories unattractive. The first difficulty is indicated in Figure 3-25, which shows the orbit raising time as a function of initial apogee radius. Although the maximum acceptable orbit raising time is ill-defined, times in excess of 4 to 6 months are not expected to be acceptable. This indicates that for reasonable final power levels, the initial apogee radius of the transfer orbit should be at least three to four Earth radii. A second problem with low initial radii is illustrated in Figure 3-26. Orbits with low apogees spend substantially greater amounts of time in the high intensity Van Allen belts and the radiation damage to the solar panel is greatly increased. As a result, the initial power required to maintain a fixed final power is correspondingly increased. This is undesirable because the solar panels are relatively expensive, and the fitting of large panels into the spacecraft shroud presents significant design problems. Therefore, if the required spacecraft mass is so large that the booster cannot place it in an orbit with an initial apogee greater than about three Earth radii, it is desirable to either use a more powerful launch booster or to modify the spacecraft design.
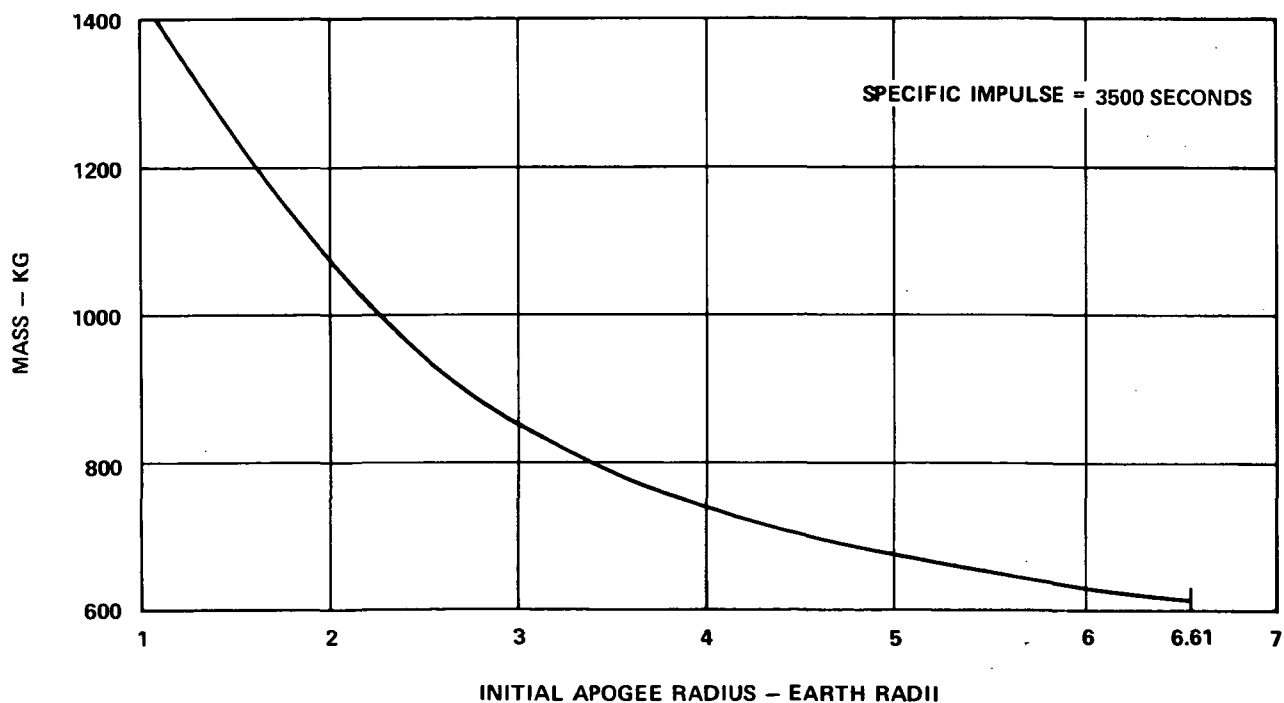
Figure 3-24. Mass Injected Into Synchronous Orbit
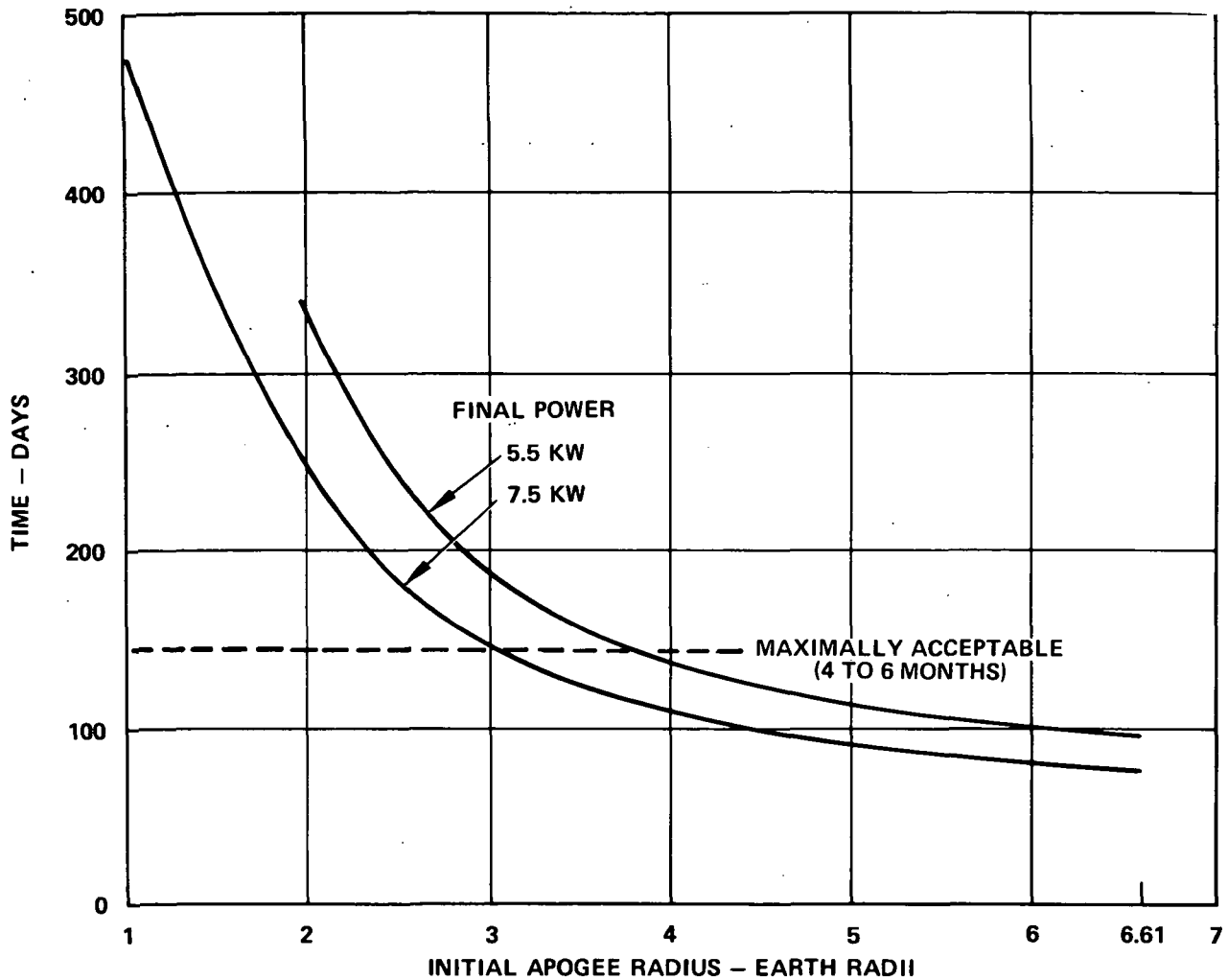
Figure 3-25. Orbit Raising Time

3.3.2.3 Propulsion System Optimization

The tradeoffs in solar cell selection are shown in Figure 3-27 for both a circular transfer orbit and an elliptical transfer orbit. In either case, the degradation is relatively insensitive to the thickness of the solar cell and the coverglass. However, the mass of the panel is considerably reduced when thinner solar cells are used (maintaining the same final power). For performance purposes, the best solar cell and coverglass is the minimum thickness which can be reasonably manufactured; at the present time this appears to be about 75 to 100 microns.
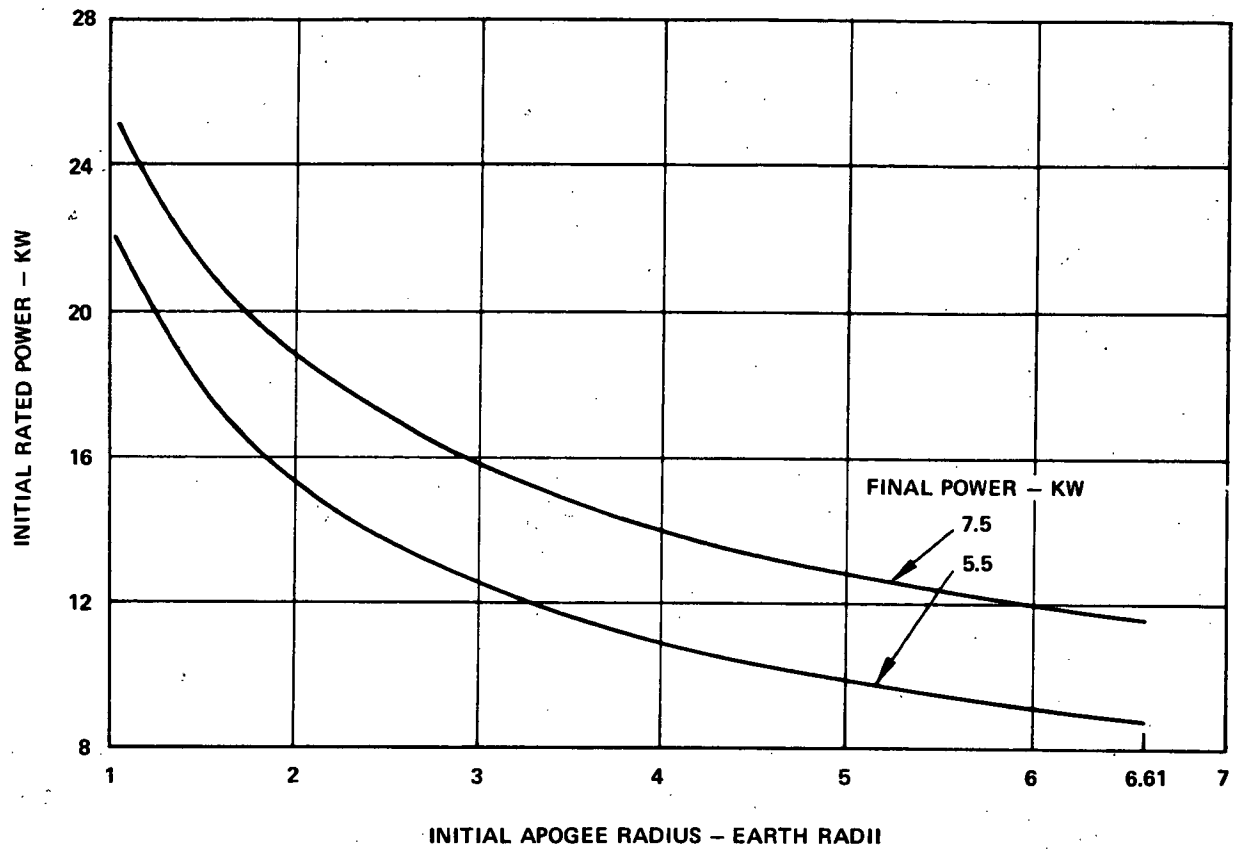
Figure 3-26.   Required Initial Power for Fixed Final Power
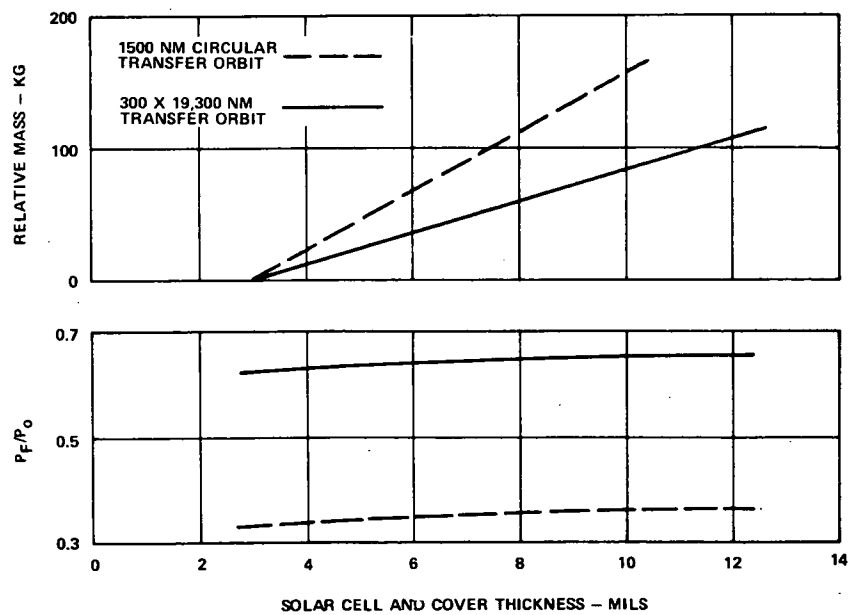
Figure 3-27.   Solar Cell Selection

The thrust attitude profile can be divided into two components for purposes of discussion; an out of plane component for inclination removal, and an in-plane component for orbit raising. Both components are continually varying as the inclination is removed continuously during the orbit raising process. The out-of-plane thrust attitude is a function of the orbital elements and is selected so as to maximize the injected mass. The in-plane thrust attitude is constrained to hold apogee altitude at or below synchronous altitude, and to raise perigee as rapidly as possible. Raising perigee rapidly minimizes the required thrusting time and propellant consumption, thereby maximizing injected mass. A typical thrust attitude profile for a highly elliptic orbit with the line of apsides at the line of nodes is shown in Figure 3-28. There will be a 45 minute coast at perigee during which time the spacecraft may be in eclipse. Figure 3-28 shows that the incorporation of this coast period avoids imposing a requirement for high rotational rates on the ACS.

Specific impulse optimization is shown in Figure 3-29 for a nominal end-of-life power of 5.8 kw and a propulsion system design with three 30-cm thrusters operated on a thrust profile which requires that the propulsion system reliability be greater than 0.99. The orbit raising time is minimized at a specific impulse of about 3,000 seconds, whereas the injected mass is maximized at a specific impulse of about 3,700 seconds. A compromise value of specific impulse of 3,500 has been selected as the baseline.
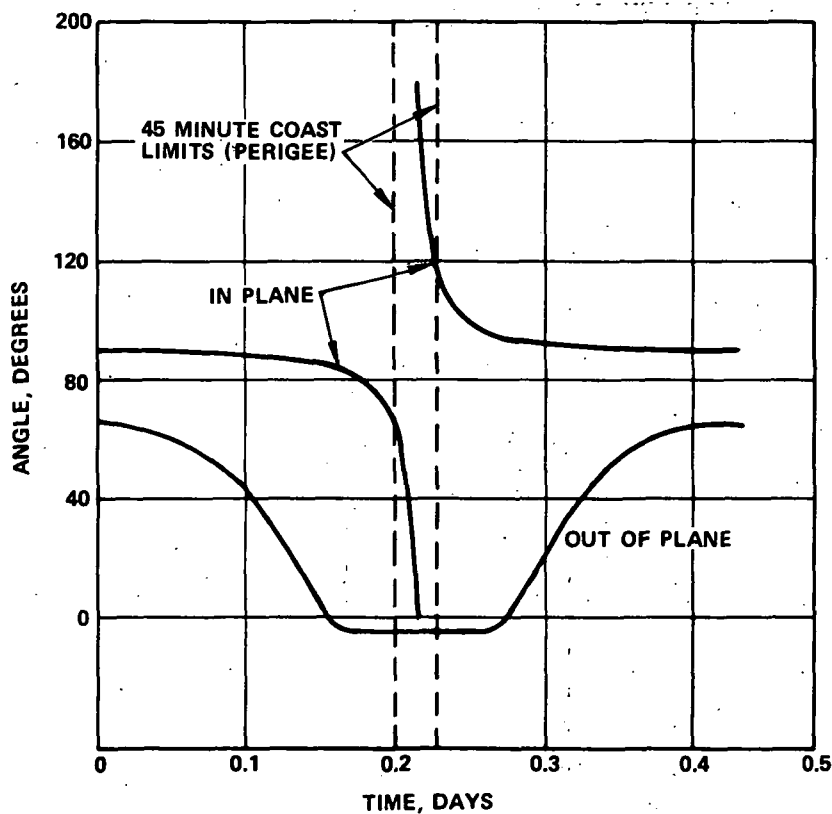
Figure 3-28. Typical Thrust Attitude Profile
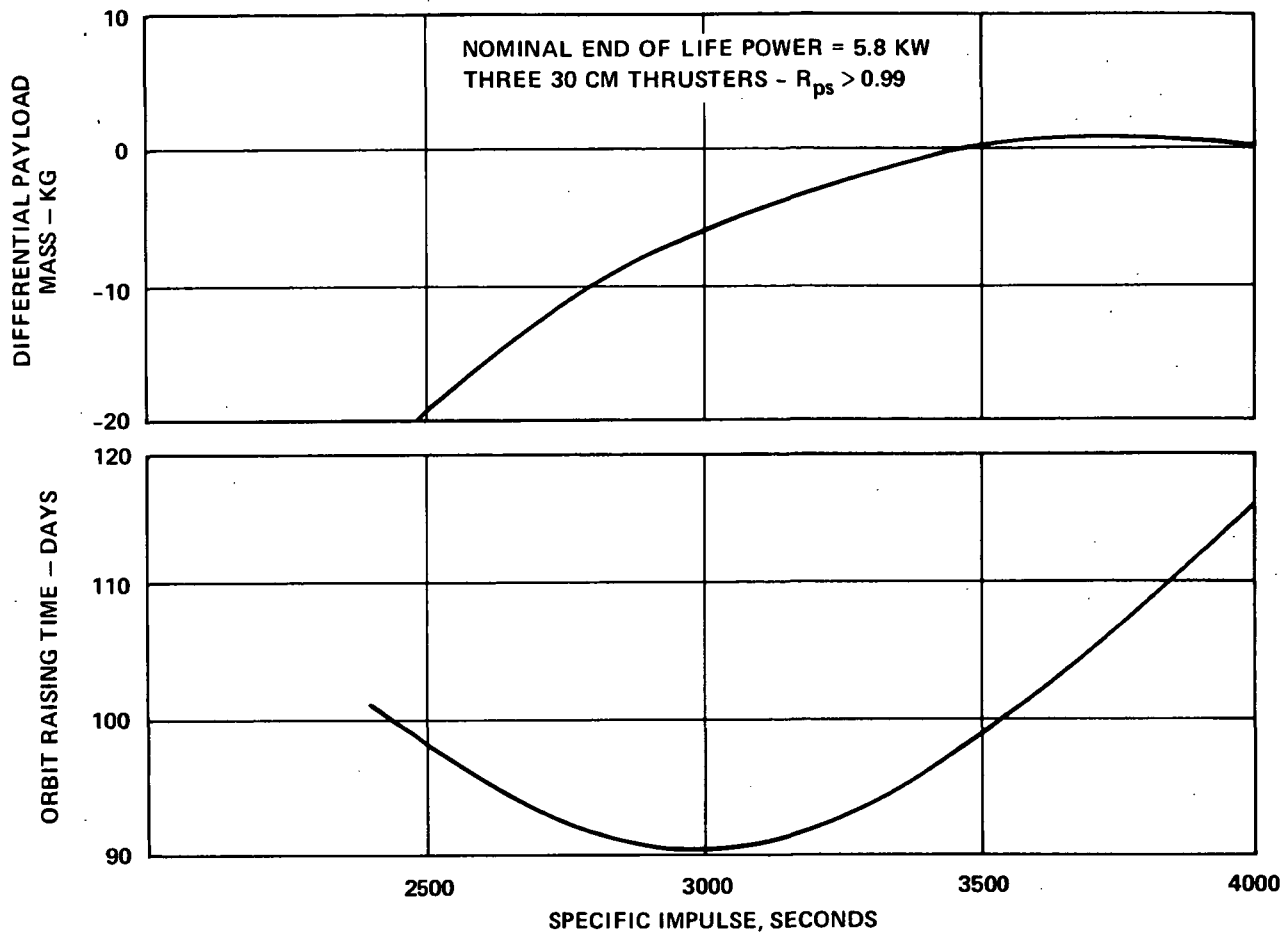
Figure 3-29. Specific Impulse Optimization

Initial solar panel power was a subject of considerable tradeoff
analysis during the study. However, a baseline value of 10.2 kw for initial
rated power has been selected primarily on the basis of satisfying the pay-
load fairing limitations. This power satisfies the mission requirements and
further increases can be accomplished only at the expense of increasing
design difficulty. The propulsion system design optimization is discussed in
Section 4.4.

3.3.2.4 A-1 Spacecraft Baseline Trajectory and Contingency

The A-1 spacecraft configuration on-station mass capability with a
Thor-Delta launch vehicle is shown in Figure 3-30. The mass in synchronous
orbit is shown as a function of transfer orbit apogee. Although lower orbit
apogee radii provide greater mass into synchronous orbit, this payload capa-
bility is provided at the expense of greater solar panel degradation. A com-
promise between orbited mass and end-of-life power must be made, as
represented by the related baseline trajectory. This baseline is summarized
in Table 3-17. The resulting 80-day orbit raising time is quite satisfactory.

INITIAL POWER = 10.2 KW

MASS IN SYNCHRONOUS ORBIT — KG

TRANSFER ORBIT APOGEE RADIUS — EARTH RADII
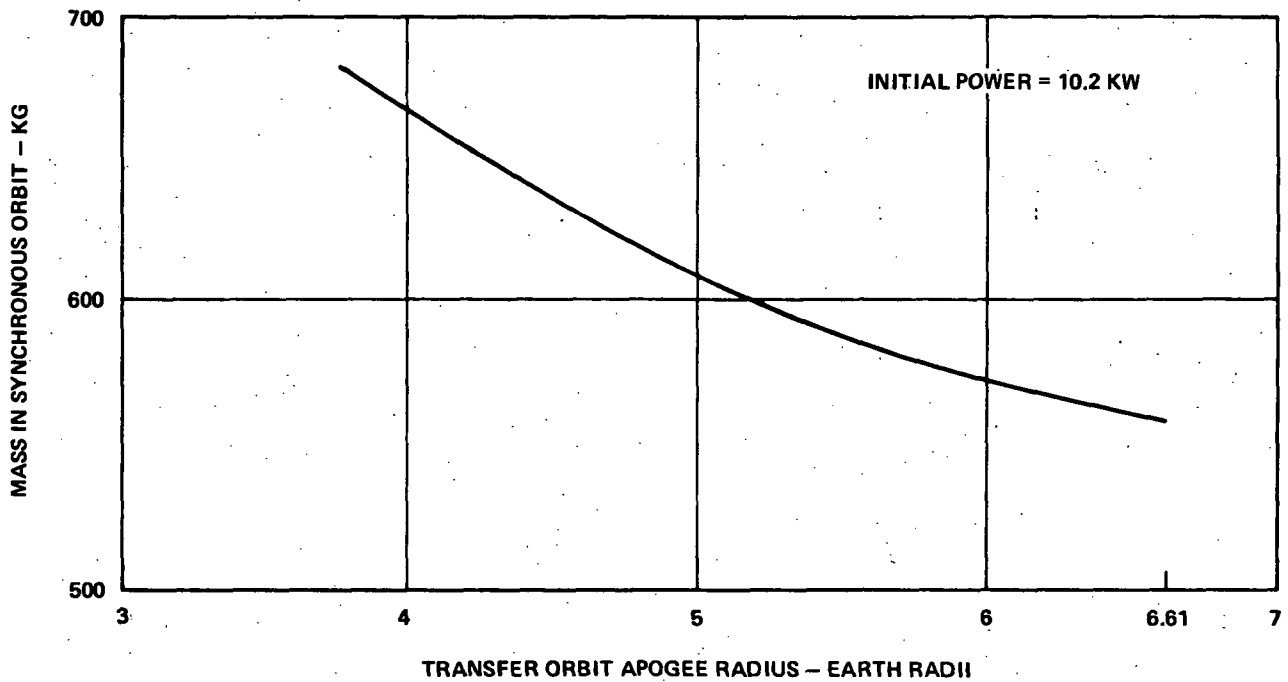
Figure 3-30. A-1 Configuration Orbited Mass Capability

TABLE 3-17. BASELINE TRANSFER TRAJECTORY PARAMETERS

Apogee altitude	=	17, 200 n. mi.	=	31, 900 km
Perigee altitude	=	300 n. mi.	=	555 km
Inclination	=	28 degrees		
80 day orbit raising time				
45 minute coast at perigee				

As mentioned previously, the 45 minute coast will be incorporated at the perigee of each orbit. If launch occurs at a time of year when eclipses occur, the orbit will be oriented so that the solar eclipse occurs during this period.

The basic mass-power tradeoff curve is shown in Figure 3-31. As indicated previously, an increase in orbited mass is accompanied by a decrease in end-of-life solar panel power. The available performance is obtained by varying the transfer orbit apogee and does not represent space-craft configuration change. The baseline design with the allocated contingencies in orbited mass and end-of-life power is a point on the available performance curve. The baseline design without contengencies is also shown on the figure. Other points on the available performance curve could have been
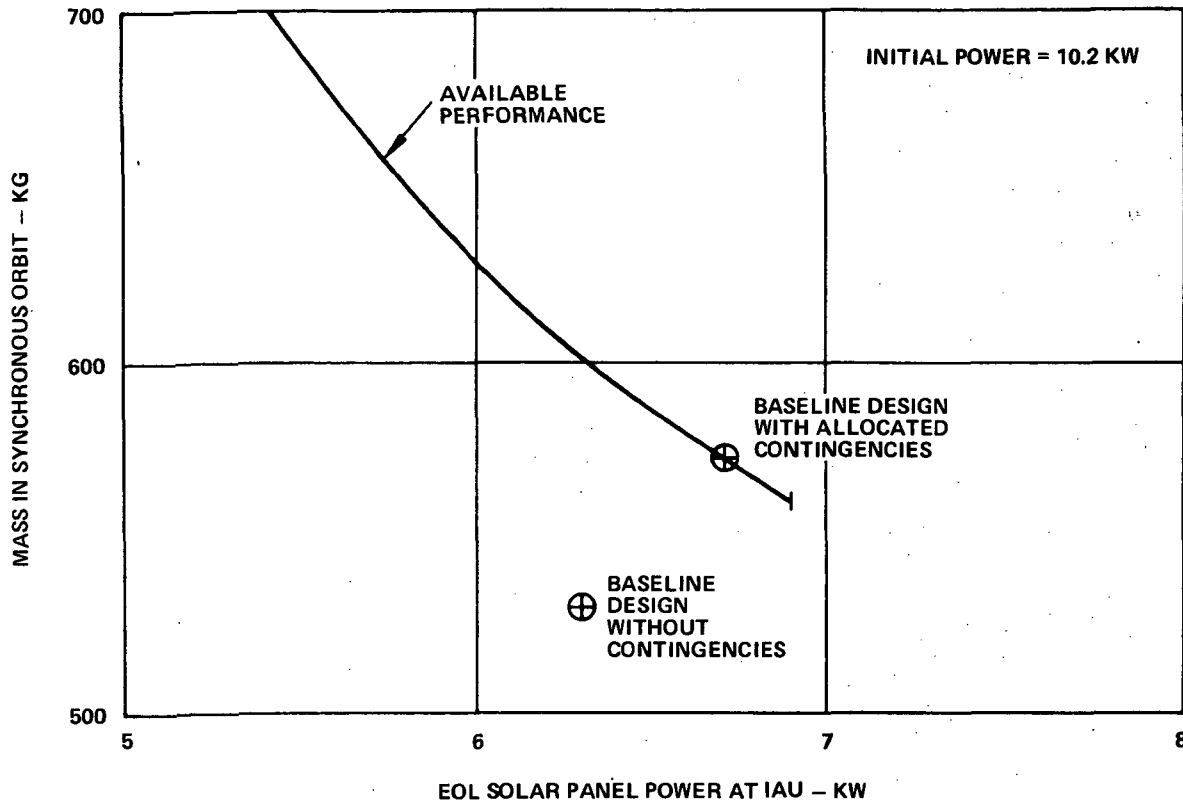
Figure 3-31. A-1 Configuration Basic Mass/Power Tradeoff

selected, representing a reallocation between the contingencies in mass and power. This flexibility represents a capability that does not exist with an all-chemical injection because mass contingency and power contingency must be allocated separately and are not interchangeable. With low-thrust raising, this flexibility is available at the time of alunch by varying the apogee of the transfer orbit, thereby injecting greater or lesser spacecraft mass and accepting the accompanying greater or lesser (respectively) solar panel degradation. At worst, the actual spacecraft mass may be substantially more than that which is planned, in which case it would still be possible to inject the spacecraft into synchronous orbit, although this might require a significant compromise in end-of-life power. For example, a 630 kg space-craft could be injected and achieve an end-of-life power of 6 kw at 1 AU. Although this would require compromises in the mission (e. g. , one of the planned operating tubes might have to be shut down), it would still be possible to inject the spacecraft into the desired orbit without redesign. This capa-bility does not exist with a chemically injected spacecraft.

Additional contingency is available with variation of the launch booster performance, as shown in Figure 3-32. The available performance shown in Figure 3-31 represents that available with a guaranteed performance booster (3), but operationally, almost all launch boosters will deliver performance in excess of the guaranteed minimum. This additional performance can then be used to achieve a higher apogee transfer orbit than would be provided by the guaranteed booster performance; the corresponding solar panel degrada-tion will be less, and the end-of-life power will be greater than planned.
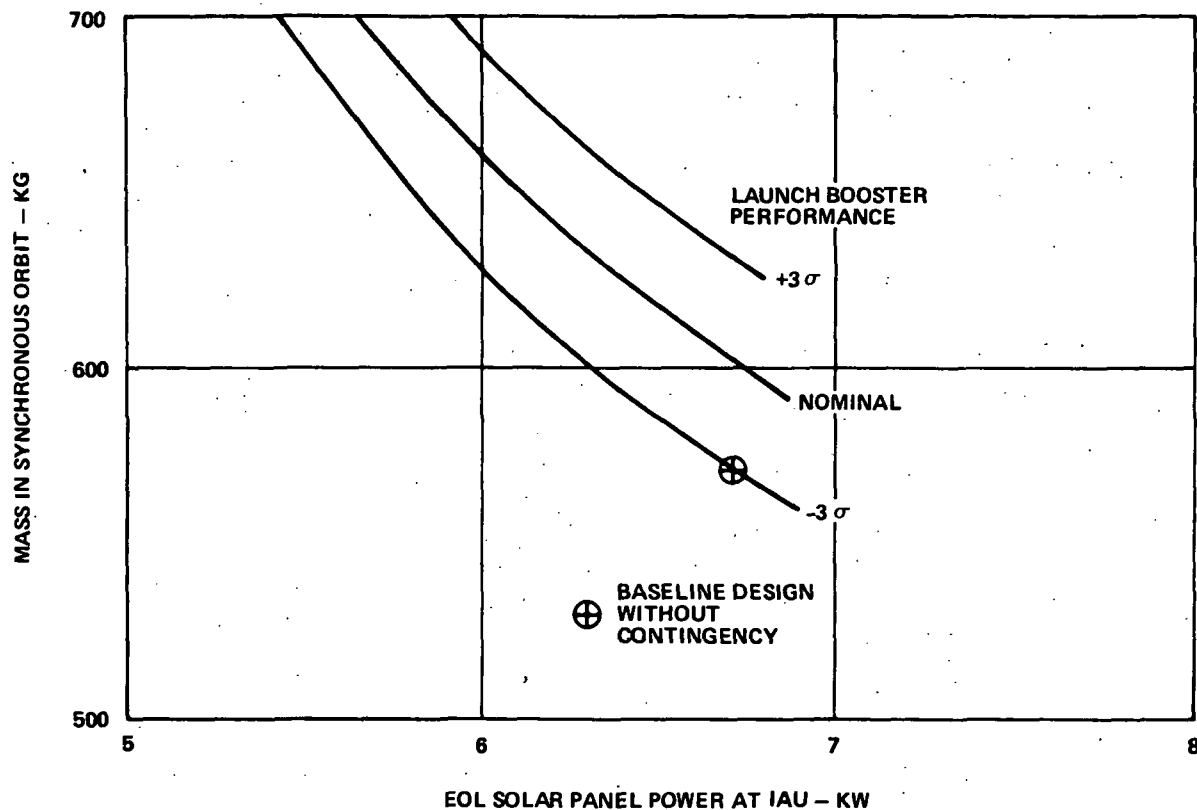
Figure 3-32. Additional Contingency with Variation
of Launch Booster Performance

For the previous example of a 630 kg spacecraft, a nominal booster would provide an end-of-life solar panel power of about 6.4 kw, and a very high performance booster would provide an end-of-life power of 6.8 kw. This indicates that, although it might be acceptable to give up end-of-life power in order to launch an overweight spacecraft without redesign, the sacrifice might, in fact, be only academic. A similar situation regarding the uncertainty in the solar cell degradation as is indicated in Figure 3-33. A conservative estimate has been used in the analysis, and if the degradation is actually less than the estimate, a corresponding increase in end-of-life power can be expected. These contingency situations are summarized in Table 3-18. If synchronous injection is achieved chemically with an AKM, separate and non-interchangeable performance pads are required on the launch vehicle, the kick state motor, and the solar panel degradation. However, if low-thrust propulsion is used for orbit raising, performance in excess of nominal on any of the subsystems can be utilized to increase the end-of-life power. In effect, therefore, only a single performance pad is needed for all of these subsystems taken together, resulting in a significant advantage for low thrust orbit raising.

Further system analysis and design for the orbit raising electronic propulsion system is presented in Section 4.2.2. The related power system and power conditioning design analysis is presented in Section 4.5.

3-65
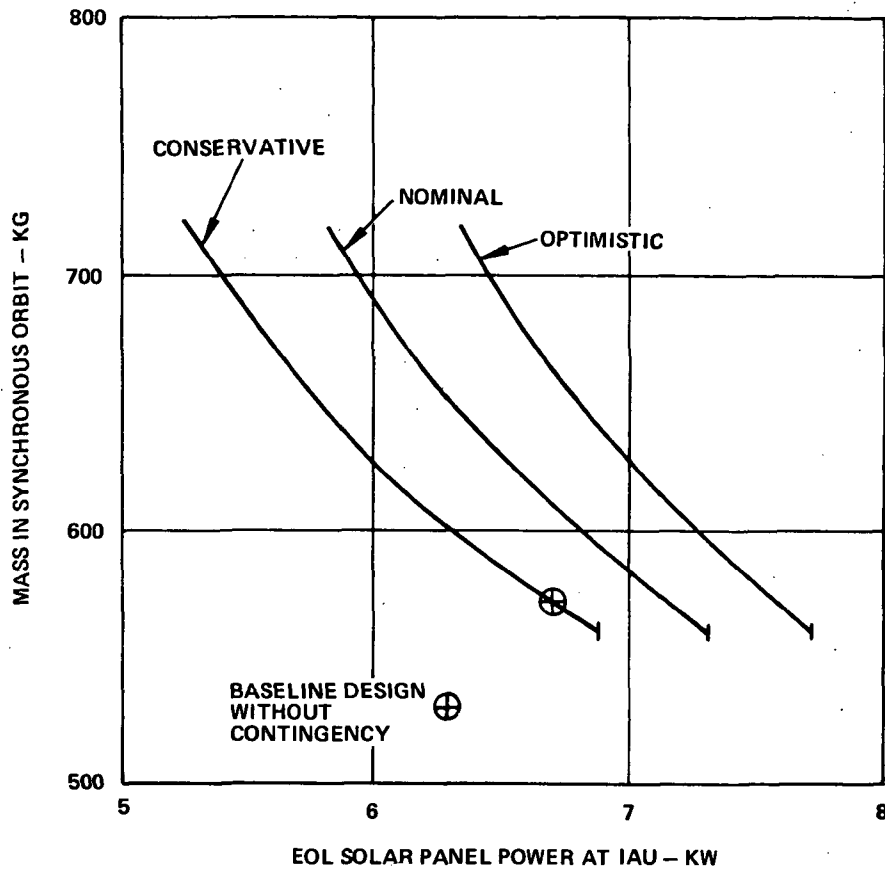
Figure 3-33. Additional Contingency Resulting From
Solar Cell Degradation Uncertainty

TABLE 3-18. QUALITATIVE CONTINGENCY CONSIDERATIONS

Synchronous Injection Technique	Launch Vehicle	Synchronous Injection Propulsion	Power
Apogee kick motor	3σ pad	3σ pad	3σ pad
Ion propulsion	One single performance pad		

4. SUBSYSTEM DESIGN

4.1 BASELINE COMMUNICATIONS SUBSYSTEM

The Communications Subsystem was designed after careful study of the spectrum of possible requirements discussed in Section 2.1.2.1. The design is therefore highly flexible in order to permit the selection of operational configurations for a variety of broadcast and networking experiments. It is comprised of two repeater chains, a multiple feedhorn assembly and high gain antenna, and a system of commandable switching networks, filters, limiters, and level controls. The repeater chains incorporate a wideband 1-kw TWT amplifier in one chain and a 2-kw klystron amplifier in the other.

4.1.1 Communications Performance

Some limitations were imposed on the degree of flexibility in the design in consideration of power efficiency and undue complexity. Switches, power dividers and other controls, which are applied after the kilowatt class spacecraft power amplifiers, tend to waste considerable power and require complex thermal control features for heat dissipation. For this reason, the possible output configurations which can be selected are fewer than the selectable input configurations. However, some constraint is also applied to the flexibility of the input switching network in order to keep the introduction of noise within reasonable bounds.

Seven individual receiving and transmitting beams are available. These beams are produced by one or more of the 9 feed horns so as to illuminate the four time zones of the forty-eight states, the forty-eight states together, Alaska and Hawaii. In Section 4.2, which follows this section, a separate design effort for a lens antenna with more complex feed horn clusters is described. The feed interconnect with the repeater would be essentially identical to the one treated in this section. Any one of the receiving beams can be connected to the TWT repeater chain while only the Central Time Zone, Pacific Time Zone and forty-eight state beams are available, one at a time, to the klystron repeater. Concurrently, the output of the TWT amplifier can be fed to either the Hawaii, Alaska, Eastern or Mountain beams while the klystron output can be fed to either the Central, Pacific or forty-eight state beams. The reasons for the differences between input and output choices for each of the repeater chains will become clearer

as the subsystem is further explained and have to do with the reduction of inter-beam interference and unnecessary redundancy and complexity while still meeting the system objectives.

Further flexibility is afforded by filtering to accommodate two separate frequency bands on both the up and down links. These bands, identified as bands A and B, were chosen early in the study to be comprised of 100 MHz of bandwidth each. They were also further subdivided for certain applications into 50 MHz components, each of which could further be separated into a 40 MHz wideband channel and two narrow band channels. The upper half of each 100 MHz band can also be cross switched between the separate repeater chains. The possible configurations of input beams, output beams, throughput frequency bands and cross channel frequency bands is illustrated in Figure 4.1-1. The variety of possible configuration combinations inherent in the design is more than adequate to permit experimental modes for throughput broadcasting, frequency reuse and crossed channel networks. Note that the TWT repeater can handle either the A or B frequency bands while the klystron chain accepts only band B.
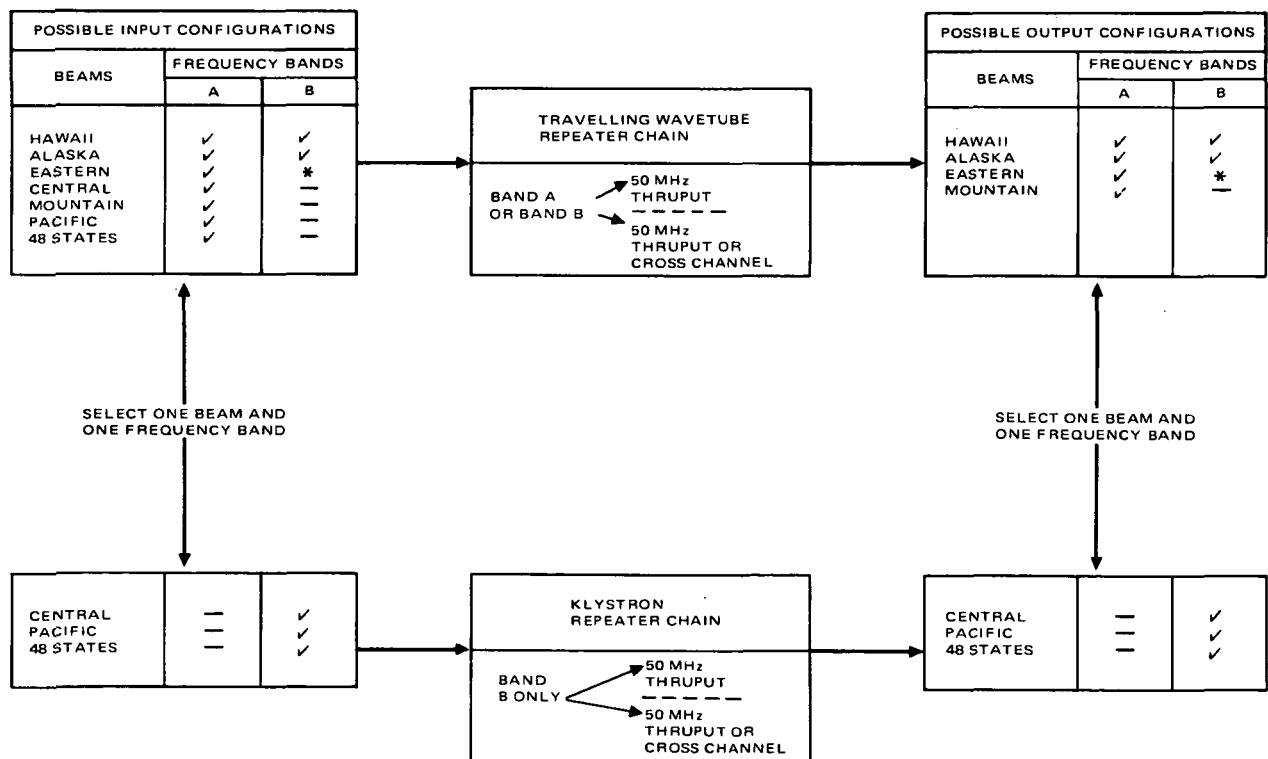
*IF THE EASTERN BEAM IS ASSIGNED BAND B IN THE TWT REPEATER, THE KLYSTRON REPEATER
MUST BE CONNECTED TO THE PACIFIC OUTPUT PORT TO AVOID INTERFERENCE BETWEEN
TWO ADJACENT BEAMS OPERATING ON THE SAME FREQUENCY BAND.

Figure 4.1-1. Possible Beam and Frequency Band Selections

A more detailed description of the subsystem's functional aspects is shown in Figure 4.1-2. Also shown in the figure is the frequency plan which was adopted early in the study. This plan comprises two 100-MHz bands located within the 500 MHz of bandwidth allocated for receiving and transmitting. Wider bandwidths than 100 MHz could obviously be implemented but it was felt that 100 MHz was a nominal value considering the bandwidth limitation of the klystron amplifier used in the lower repeater chain. The location of these two bands within the 500 MHz allocations would depend also on a thorough spur analysis and filter design study which were not practical to attempt at this point in the program definition.

In addition to the capability of selecting any of the 7 beams to input the upper repeater, there is the additional flexibility of selecting either band A or band B by choosing the downconverter local oscillator frequency. The lower repeater input accepts band B only. Following the band selection and filtering stages, the six individual frequency channels (two wide band and four narrow band) are separated by filtering and independently limited. Commandable attenuators are provided after each channel limiter to adjust the output level of each channel over a range sufficient to determine the operating point
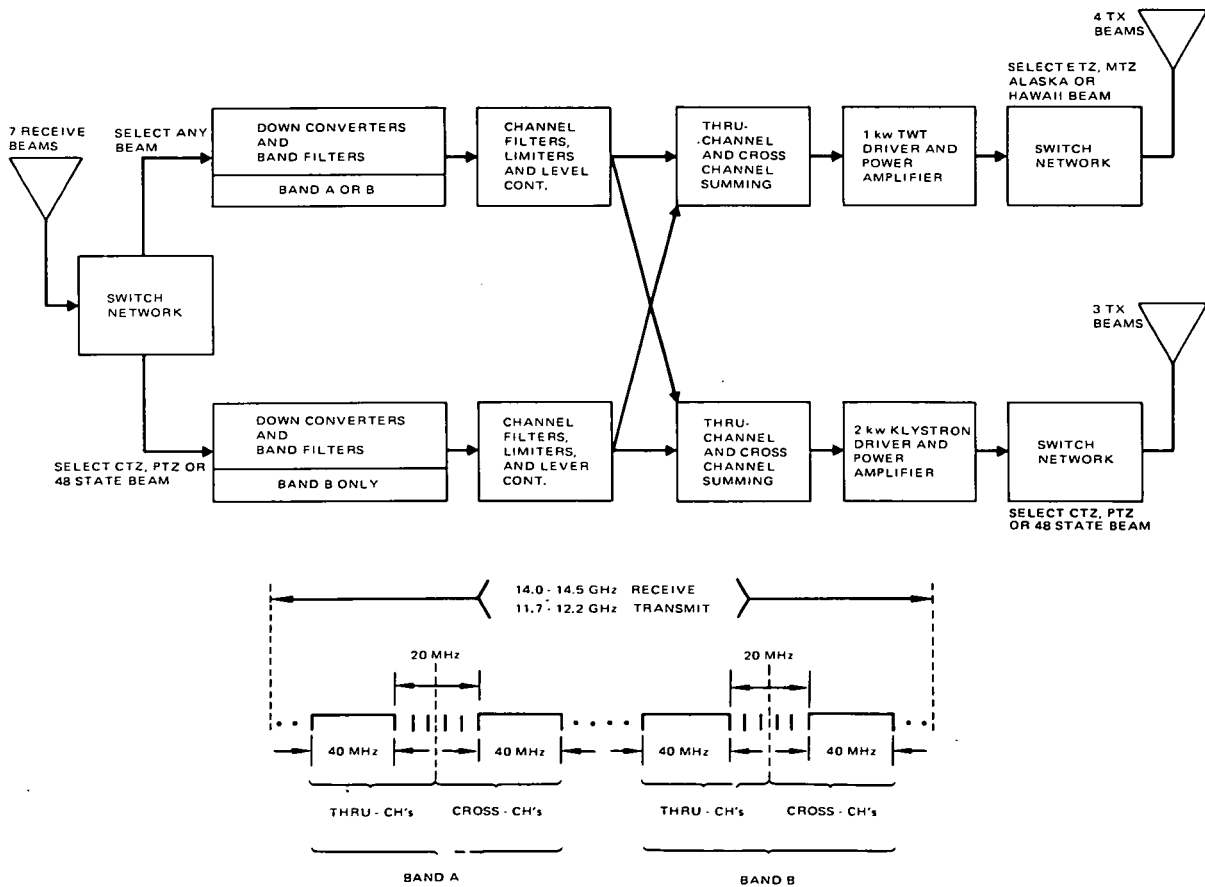
Figure 4.1-2. Communications Subsystem Functional Diagram

4.1-3

of the power amplifier (from saturation to 6 dB backoff) and to set the relative power of the carriers sharing a single amplifier.

From this point, the upper half of the frequency band appearing in each of the two repeater chains may be cross-connected to the identical space in the other repeater chain. This feature permits signals which originate in two different receiver beams to be transmitted via a common beam. The reconstructed bands in this case are then amplified by the driver and power amplifier combination in each repeater chain. The final operational selection is made at the output switching network where one of the four beams listed in the figure may be selected for the output of the TWT amplifier and one of the three beams shown may be selected at the output of the klystron amplifier.

There are a few precautions to be observed when configuring the communications subsystem for proper operation. Because the time zone beams for adjacent zones overlap, signals from adjacent zones must be assigned to separate frequency bands (A and B). It is also necessary to be aware of the effect of multiple carriers sharing a common power amplifier. While power sharing can be accomplished effectively by individually limited channels and adjustable level controls, this does not obviate the effect of the AM/PM conversion in the common driver and power amplifier. This effect is proportional to the ratio of the power of the carrier varied to the average power of all the carriers present. Thus, turning a video carrier on or off in the presence of narrow band data signals would cause transient phase shifts in the data carriers which could cause a burst of errors in those channels.

The performance of the communications subsystem for video and data circuits is summarized in Figures 4.1-3 and 4.1-4, respectively. Referring to the video performance, the curves show the relationships between the video signal bandwidth (limited to a maximum of 40 MHz) and a figure of merit which takes into account the spacecraft EIRP and the sensitivity of the receiving ground station. The parameter used in Figure 4.1-3 is television picture quality as defined by several standards. (See Appendix C for the derivation of these curves and a description of the picture quality standards.) The horizontal region between 65 and 68 dB corresponds to EIRP from the forty-eight state beam over the range of 1 to 2 kw of transmitter power. The diagonal line (C/N = 10 dB) is the detector threshold limit. Permissible operation would therefore fall within the shaded region and above. The 10 dB threshold, a nominal value for conventional threshold detection. Operation would be satisfactory except when losses exceed the allocated weather margin.

The multi-carrier digital data performance in Figure 4.1-4 illustrates the total information rate capacity for each of the beams when the system is shared between data channels and two video carriers. (Linear power amplifier operation is assumed at 4.5 dB backoff.) The Central Time Zone and the forty-eight state beams do not appear on the figure because they have insufficient EIRP to support simultaneous video and data channels with linear operation of the power amplifiers. Without video carriers, in an all-digital mode, all beams are bandwidth, not EIRP, limited.
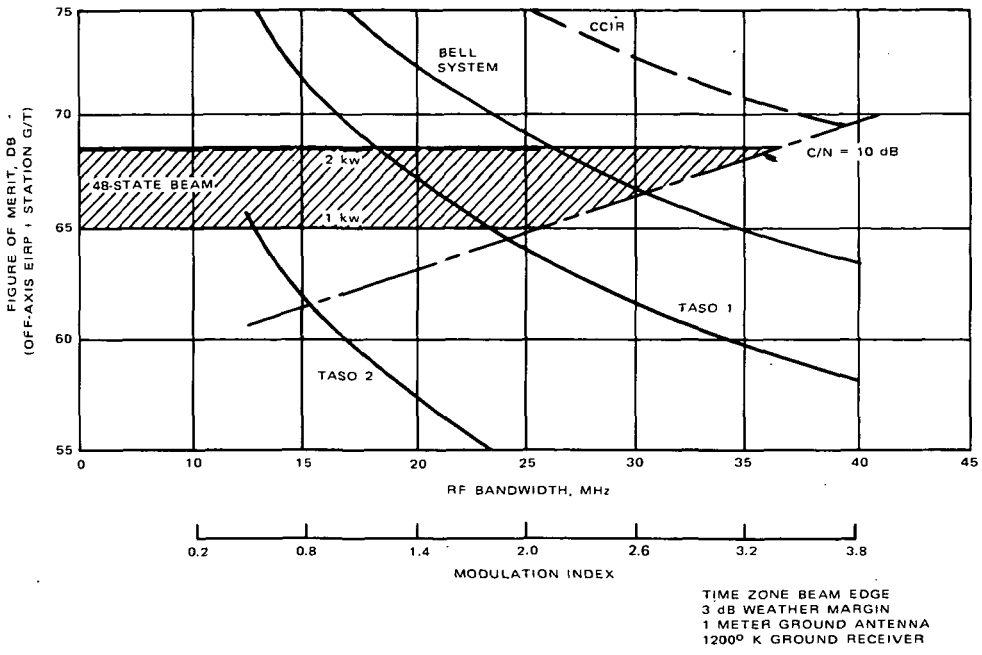
Figure 4.1-3. Direct Broadcast Video to Small Terminals

EARTH TERMINAL CHARACTERISTICS:
- ●COHERENT PHASE SHIFT KEYING
- ●BIT ERROR PROBABILITY = 10^{-5}
- ●SYSTEM NOISE TEMPERATURE = $1200°K$
- ●ANTENNA APERTURE = 1 METER
- ●BAND SHARED WITH 2 VIDEO CARRIERS
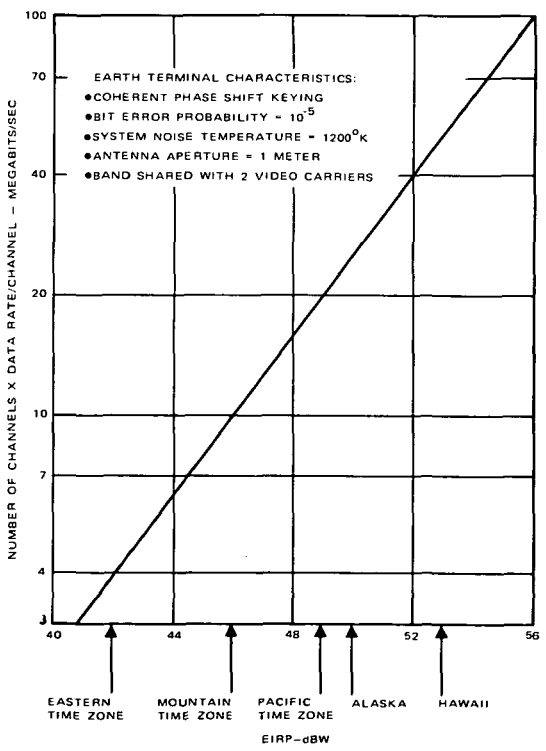
Figure 4.1-4. Multicarrier Networking of Digital Data

Figure 4.1-4 also shows that only the Eastern and Mountain Time Zone beams are EIRP constrained with two video carriers present as the maximum narrow band allocation is 20 MHz. With reasonable guard band assignments between channels, and quadriphase modulation, the maximum data rate for operation of four channels would be approximately 10 megabits.

4.1.4 Operating Modes

A description of system operating procedures and plans can be readily developed after specific mission plans have been developed. At this point in the planning process, a variety of program possibilities are under consideration. This dictates that operating concepts for the Communications Subsystem be treated in a flexible manner. The operating modes described below are only typical examples of how the subsystem can be employed. A number of other modes are also possible within the design concept.

Through-Put Broadcast Mode - In this mode, the repeater would be configured to pass the received signal from the selected receive beam for each channel directly through the corresponding channel to the transmit antenna. Nominally, the selected transmit beam would illuminate the same region from which the receive signal arrived, but other transmit beams may be selected.

For direct broadcast operation to minimally sized ground terminals, the received signal would consist of a single channel (presumably TV), and the repeater would be set to drive the power amplifiers so as to obtain full power output. Alternative operation in this mode, for servicing somewhat larger terminals, would permit multiple carrier operation, in which case the power amplifiers would be driven so that their total output power was up to 6 dB below their saturated level.

In this mode, the up and down beams can be employed in a number of pairs for both band A and band B. It is also possible to come up on one beam and one frequency and broadcast the information on a pair of down beams.

Frequency Reuse Mode - In the frequency reuse mode, the repeater may be configured in any of its possible operating modes subject to the constraint that the receive and transmit antenna beams are appropriately selected. In particular, if the two channels operate at the same receive frequency and at the same transmit frequency, the antenna beams must be spatially separated so that neither pair of receive and transmit beams sees significant signal strength from the other pair of receive and transmit beams. For example, the lower channel may be set to service the Pacific Time Zone and the upper channel to the Eastern Time Zone, both zones using the same uplink and downlink frequencies.

The necessary isolation for frequency reuse is achieved by a combination of -25 dB sidelobes and crossed, linear polarization. To achieve the maximum spectrum reuse capability among the seven beams, the switchable feed network would operate as illustrated in Figure 4.1-5. Examples of two
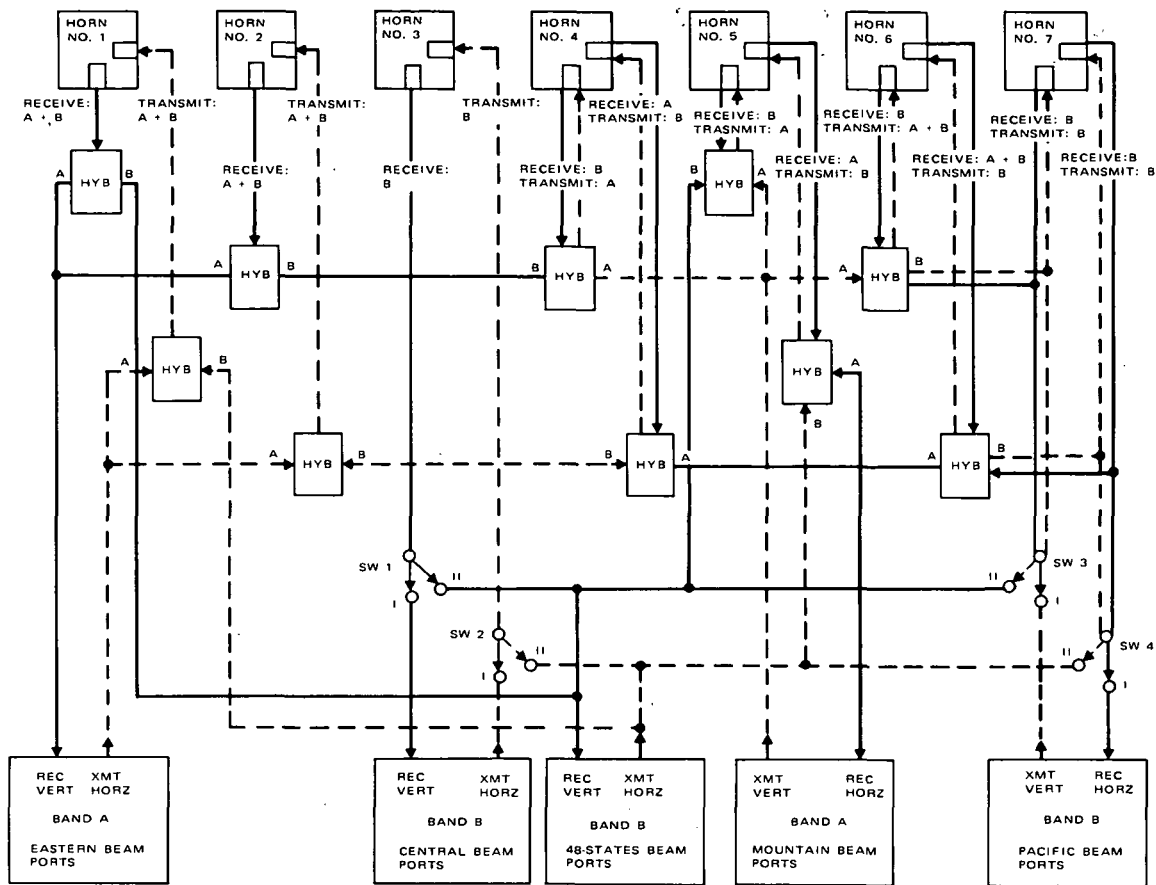
Figure 4.1-5. Composite Feed Arrangement

sets of frequency reuse possibilities made possible by the switching matrix shown in Figure 4.1-5 are listed in Table 4.1-1. These sets are referred to as Modes I and II. See Figure 4.1-6 for the horn groupings used to form the seven beams.

In Mode I, the receive signal in each time zone beam is cross-polarized to the transmit signal in that beam. Hence, the diplexing problem is alleviated both on the ground and in the spacecraft. The arrangement further provides cross-polarization in all cases where a frequency band is reused. Transmit-receive cross-polarization is also maintained in Mode II where two, non-adjacent time zones and a forty-eight state beam are provided.

If later study shows that the full baseline capability with switchable modes is not required, a single fixed network might be provided which greatly simplifies the design of the feeds and diplexers.

TABLE 4.1-1. ANTENNA BEAM CONFIGURATIONS FOR FREQUENCY REUSE

	Time Zone		Horn No.	Transmit		Receive	
				A	B	A	B
Mode I	Eastern (Band A		1	H		V	
			2	H	H	V	V
	Central (Band B)		3		H		V
			4	V	H	H	V
	Mountain (Band A)		5	V		H	
			6	V	V	H	H
	Pacific (Band B)		7		V		H
Mode II	Eastern (Band A)		1	H	H	V	V
			2	H	H	V	V
		48 States (Band B)	3		H		V
	Mountain (Band A)		4	V	H	H	V
			5	V	H	H	V
			6	V	H	H	V
			7		H		V

Figure 4.1-6. Parabolic Antenna Configuration

Crossed Information Channels - In the crossed information channel mode, it is assumed that each of the selected receive signals contains at least two information channels, one in the upper half of the channel bandwidth and one in the lower half. (The information channels in each half-BW may be single carrier and/or multiple carrier.) As the signal passes through the repeater, the information in the lower half-BW would be outputted on the same channel on which it is received, whereas the information on the upper half-BW may be directed either to its own channel's power amplifier or to the alternate channel of the repeater, as indicated in the functional diagram of Figure 4.1-2. Depending upon the structure of the information channels, and the particular experiment being performed, either or both of the power amplifiers may be operated at saturated or reduced power levels.

4.1.3 Antenna Design

The baseline antenna design was selected to satisfy the experiment performance requirements and the launch vehicle constraints, considering the objectives for simplicity and a minimal extension of the state of the art. The result is a configuration employing the 1.83 m diameter parabolidal section and 9-horn feed assembly shown in Figure 4.1-6. The figure also

indicates how the time zone and forty-eight state beams are formed by appropriate combinations of horns in the 7-horn cluster. The Alaska and Hawaii beams are each generated by separate offset horns. Figure 4.1-7 shows a typical time zone beam pattern. Table 4.1-2 lists the nominal performance for each of the 7 beams. The feed network is commandable so as to permit the selection of appropriate beams and frequencies for the various experiment modes.

SIMULTANEOUSLY FEEDING
TWO HORNS IN MAIN CLUSTER
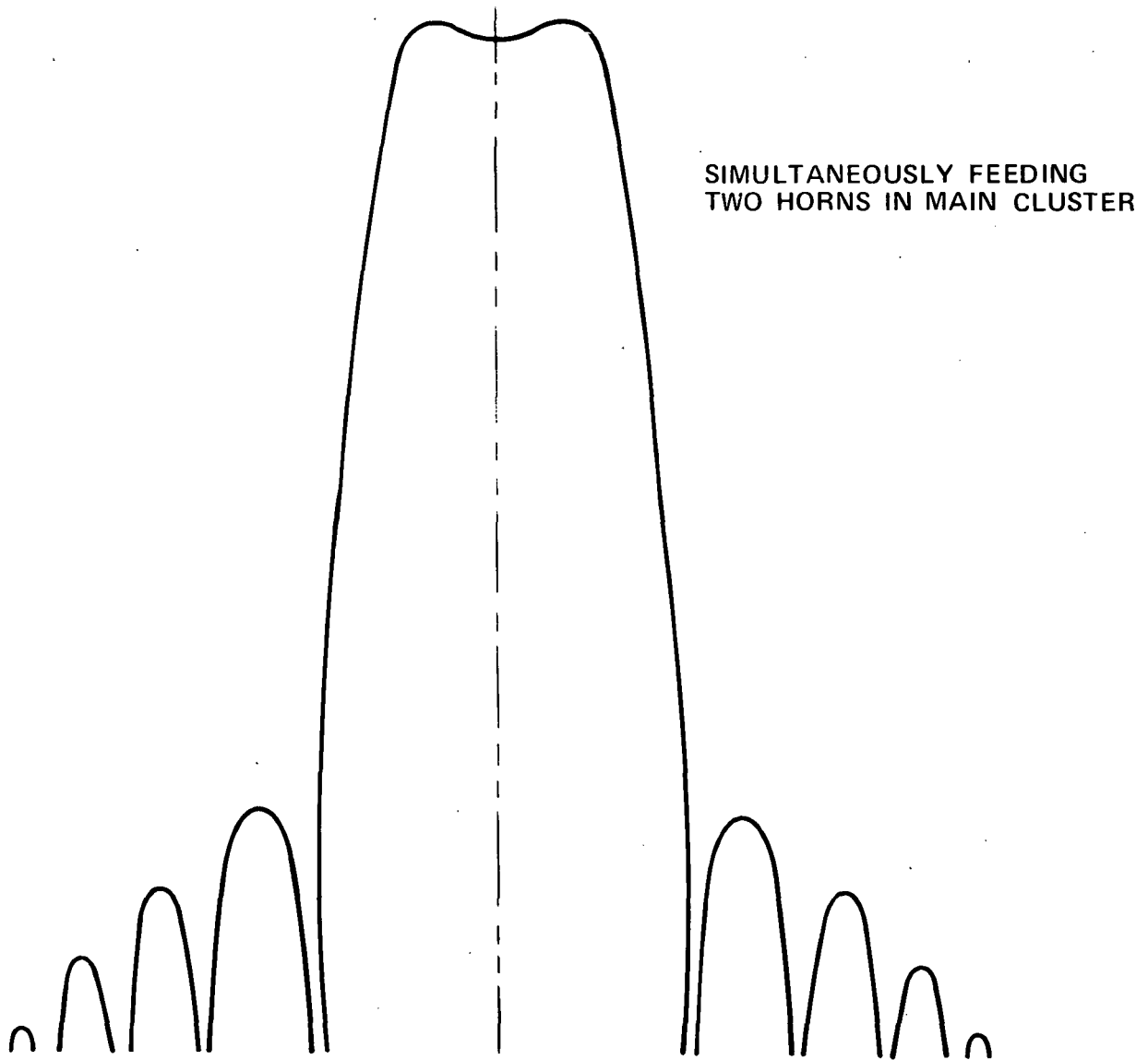
Figure 4.1-7. Typical Time Zone Beam Pattern

TABLE 4.1-2. ANTENNA BEAM PERFORMANCE

Beam	Dimension	Gain (Off Axis)
Eastern Time Zone	$2\text{-}1/2^{\circ} \times 3^{\circ}$	33 dB
Central Time Zone	$3\text{-}1/2^{\circ} \times 3\text{-}1/2^{\circ}$	31 dB
Mountain Time Zone	$3^{\circ} \times 3^{\circ}$	32 dB
Pacific Time Zone	$2^{\circ} \times 3^{\circ}$	34 dB
48 States	$7^{\circ} \times 3\text{-}1/2^{\circ}$	28 dB
Alaska	$2^{\circ} \times 1^{\circ}$	38 dB
Hawaii	$1^{\circ} \times 1^{\circ}$	41 dB

4.1.4 Repeater Design

The overall repeater block diagram is shown in Figure 4.1-8. To the left are the input ports from the 7 beams. These are followed by two-stage tunnel diode preamplifiers to establish the noise figure for the repeater before signal splitting. The switching network permits the connection of any of the beams to the upper repeater chain and a choice of the Central Time Zone, Pacific Time Zone or forty-eight state beams to the lower chain. Hybrids are used for signal splitting and latching ferrite switches for routing.

The input filters are broadband preselector filters; the upper filter is wide enough to pass both bands A and B in the input spectrum while the bottom filter is tailored to pass band B alone. Two downconverters are used in each repeater half; in the wideband channels (the middle two downconverters), the signals are translated directly to the output frequencies. The narrowband signals are translated to an IF of 100 to 200 MHz where the narrow band signals can be conveniently separated by filtering.

The wideband channels are separated by the diplexer after which they are individually limited. A four-channel multiplexer filter is used for the narrow band channels, each of which is also followed by an individual limiter. Commandable, stepped attenuators are used at the output of each limiter to set the power level of the signal in each channel when they are recombined.

The channel gain is set so that the channel limits on front end noise with no signal present. This minimizes the power required on the uplink to assure saturation of the channel. It also requires that any idle channel be turned off to prevent the noise power in that channel from taking power from desired signals in the power amplifier. As the wideband channel limiters
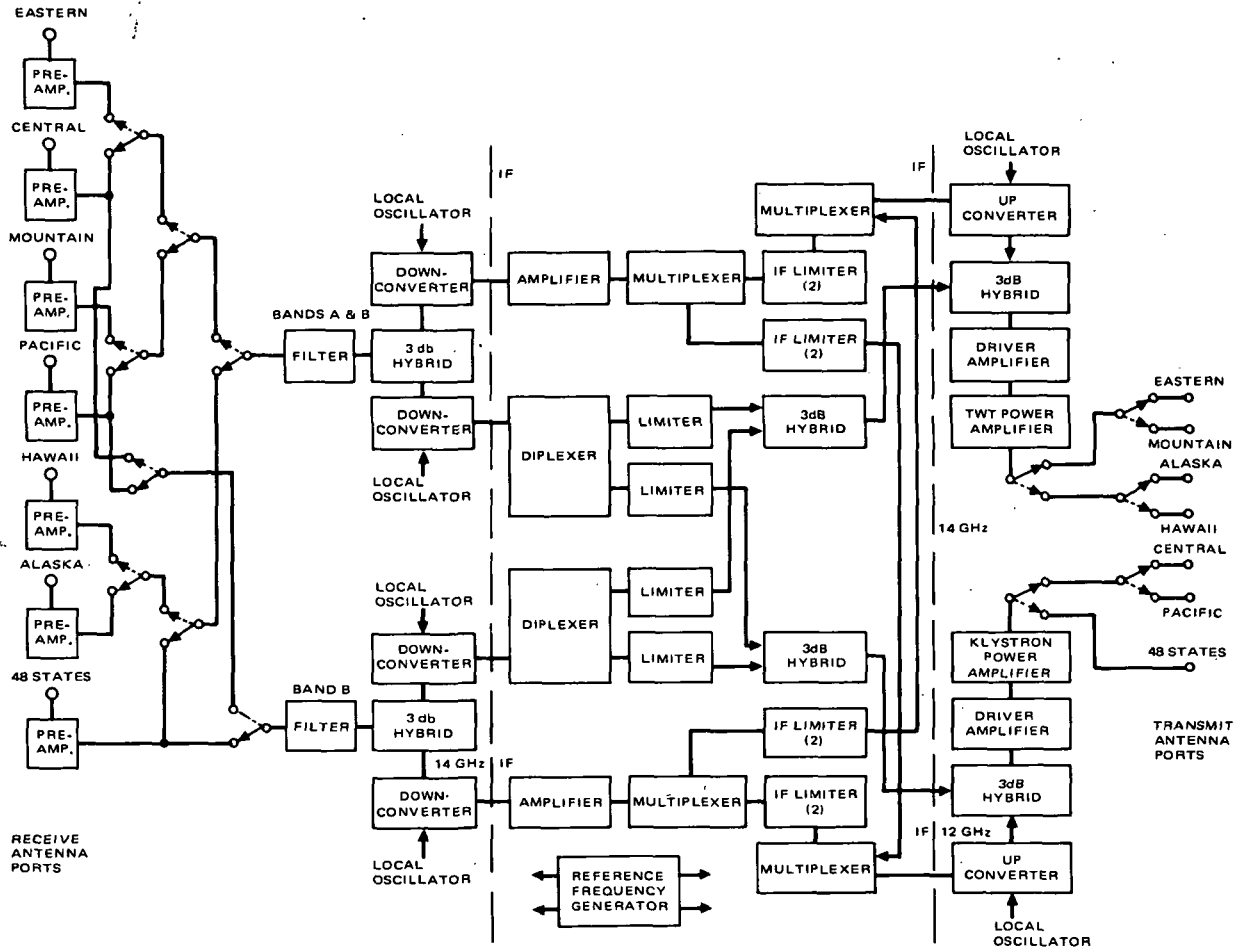
Figure 4.1-8. Repeater Block Diagram

would be comprised of several 5-port circulator tunnel diode stages, it will be sufficient to remove power from these stages to turn off the channel. Removing power would also be a convenient means for turning off the idle narrow band channels although it is necessary to assure that the semiconductor amplifier still presents a matched load to the multiplexer with power removed in order that the other filter ports are not disturbed.

Cross strapping the two repeater chains takes place following the channel limiters. The narrow band channels (at IF) are combined in a multiplexer and the wideband channels in a hybrid. The narrow band channel spectrums are then upconverted to the output frequency and combined with the two wideband signals in another hybrid. From there, each group (band A or B in the upper half and band B in the lower) is amplified by its driver and power amplifier. A 1-kw TWT amplifier is used in the upper half and a 2-kw klystron in the lower. Latching ferrite single-pole, double-throw switches are again used in the output switching network.

4.1-12

4.1.5 Power Amplifier Characteristics

Data on the performance and physical characteristics of 1 and 2-kilowatt TWT's and 1 and 2-kilowatt klystrons were furnished to the contractor by the NASA/LeRC Project Office. In some areas, additional data was provided to the study by personnel from the Electron Dynamics Division of Hughes.

Physical characteristics of the tubes, summarized in Table 4.1-3, were used in configuring the spacecraft.

The performance data furnished by LeRC was used for sizing and configuring the electrical power subsystem and establishing the dissipative loads for the thermal control design.

4.1.6 Weight and Power Budgets

The weight and power requirements for the baseline communications subsystems for Configurations A-1, B-1 and B-5 are assumed to be identical except for the additional weight requirement associated with the power conditioning on B-5, which uses low voltage arrays. Table 4.1-4 summarizes the weight and power for the major components of the subsystem.

TABLE 4.1-3. 12 GHz KLYSTRON AND TWT CHARACTERISTICS

	Klystron		TWT		Source of Data
	1 kw	2 kw	1 kw	2 kw	
Efficiency (with collector)	- 69%	- 69%	55% 51%	55% 51%	EDD* LeRC
Bandwidth (MHz)	- 40 (3 dB)	- 100 (3 dB)	500 160	160 160	EDD LeRC
Gain (dB)	40	40	40	40	
Weight (Kg): Tube	- 5.9	- 9.1	4.55 6.8	5.0 6.8	EDD LeRC
Collector	6.8	6.8	6.8	6.8	LeRC
Size: Tube	- 12.7 cm d x 17.8 cm	- 17.8 cm d x 17.8 cm	7.6 x 10.2 x 24.8 cm (mod. anode gun) 10.2 cm dia x 10.2 cm		EDD LeRC
Collector	30.5 cm max dia x 20.3 cm 17.8 cm dia x 17.8 cm		30.5 cm max dia x 20.3 cm 17.8 cm dia x 17.8 cm		EDD LeRC
Max Voltage (kV) Tube	- -7.4	- -6.9	-11, +5 -16	-11, +5 -16	EDD LeRC
Collector	- -11	- -10	-11 -16	-11 -16	EDD LeRC
*EDD is the Electron Dynamics Division of Hughes					

TABLE 4.1-4. COMMUNICATIONS SUBSYSTEM WEIGHT
AND POWER BUDGETS

Component	Weight		Power (watts)	
	(kilograms)	(pounds)	Normal	Eclipse
Repeater	37.2	82	100	-
One 1-kw TWT (0.53E)	13.6	30	1,885	12**
One 1-kw Klystron (0.66E)	13.6	30	3,000	18**
Power Conditioning	4.5*	10	490	-
Antenna	15.9	35	-	-
TOTALS	84.8	187	5,475	40

*On Configurations A-1 and B-5, the high voltage array permits this reduction of conventional power conditioning weight from the 54.5 kg required on Configuration B-1 which uses low voltage arrays.

**Cathode heaters on half-power.

4.2 LENS ANTENNA

4.2.1 Introduction and Summary

The purpose of the ATS/AMS lens antenna study was to investigate an attractive alternative design concept to that of the baseline and determine the following:

1. The gain coverage performance at the transmitting frequency of four individually shaped beams covering the four time zones of the United States.

2. The side lobe levels.

3. The gain at the receiving frequency.

4. A mechanical design.

The antenna consists of a waveguide lens and a feed package. The general arrangement of an 2.44 m diameter antenna is shown in Figure 4.2-1.
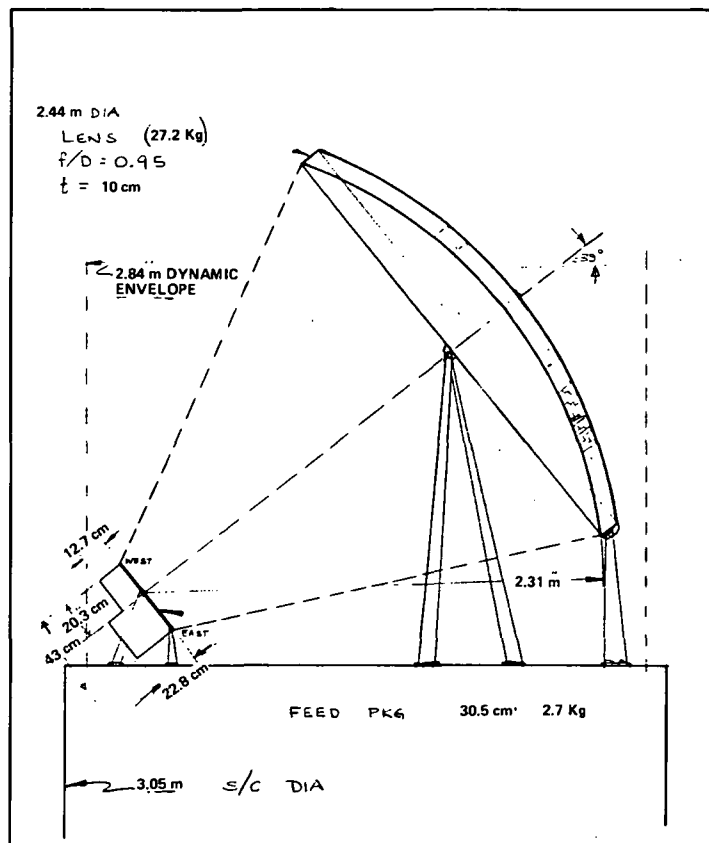
Figure 4.2-1. General Arrangement 2.44 Meter Diameter Lens Antenna

The lens is a variable thickness structure with a doubly concave surface and circular shape. Circular cylindrical waveguide cells arranged in a triangular lattice with their axes parallel to the lens axis form an egg-crate type structure that completely fills the circle. The antenna is similar to the one described by A. R. Dion and L. J. Ricardi (1). The principal difference between the Dion and the ATS/AMS antenna is that the former uses square waveguides in the lens and the latter uses circular waveguides. Circular waveguides were selected in order to simplify fabrication of the much larger lens for the ATS/AMS spacecraft. The feed package consists of feedhorns and a feed network.

The gain coverage performance was computed for two lens diameters. A 2.44 m diameter lens was selected as the minimum size required to match reasonable well the main lobes of the four radiation patterns to their respective time zones. The 2.44 m diameter was also satisfactory from a mechanical viewpoint because it could be attached rigidly to a 3.05 m diameter spacecraft in a 2.84 m diameter dynamic envelope. A 3.66 m diameter lens was selected as about the minimum increase in size required to show significant changes in coverage performance.

The lens was designed for the transmitting band center frequency of 11.95 GHz. Over the ±2 percent (500 MHz) transmitting band, the coverage is expected to decrease by less than 0.5 dB. Shaped beams for all four time zones were computed for both the 2.44 and 3.66 m lens diameters. As was expected, the coverage was better for the larger lens. The minimum gain over most (≈ 95 percent) of each time zone area is 37.0 dB for the 3.66 m lens and 34.0 dB for the 2.44 m lens. Also, the ripple is less for the larger lens.

Time and funding limitations did not permit optimization of the gain characteristics for the two lens antennas. However, as a first-cut analysis it is believed to portray very well the type of beam shaping that can be achieved with a large waveguide lens antenna.

The sidelobe level performance was computed only for the feed group illuminating the eastern time zone, and only for the 2.44 m diameter lens. For the frequency reuse operating mode, the mountain time zone is the one which is protected by minimizing sidelobes from the eastern time zone beam. The sidelobes in this region are at least 30 dB below the eastern time zone beam peak. The same general behavior can be expected for the beams covering the other time zones.

Since the bandwidth of the simply configured lens antenna is only about ±10 percent, the efficiency at the receiving frequency for a single feed will be considerably less than optimum. However, the gain computations made for

---

[1] A. R. Dion and L. J. Ricardi, "A Variable-Coverage Satellite Antenna System" Proc. IEEE, Vol. 52, pp 252-262, February 1971.

a typical single feed for the 2.44 m lens showed that the receiving gain at 14.5 GHz within one degree of the beam center will be greater than 29.0 dB. The gain computations also showed secondary lobes having comparable gain.

. A weight analysis was made only for the 2.44 m antenna. This analysis is summarized below.

Lens

Lens Waveguide Elements	15.40 Kg
Lens Structure	4.45
Adhesive	6.50
Miscellaneous	0.65
	27.2 Kg
Feed Package	2.7
Antenna Weight, Total	30.0 Kg

4.2.2 Electrical Performance of 2.44 m Diameter Lens Antenna

The Continental United States and Cuba, as viewed in the coordinate system of the satellite, is depicted in Figure 4.2-2. The azimuthal and elevation coordinates used in this figure, and denoted as ETA and ZETA respectively, are the same coordinates used in the computerprogram to calculate
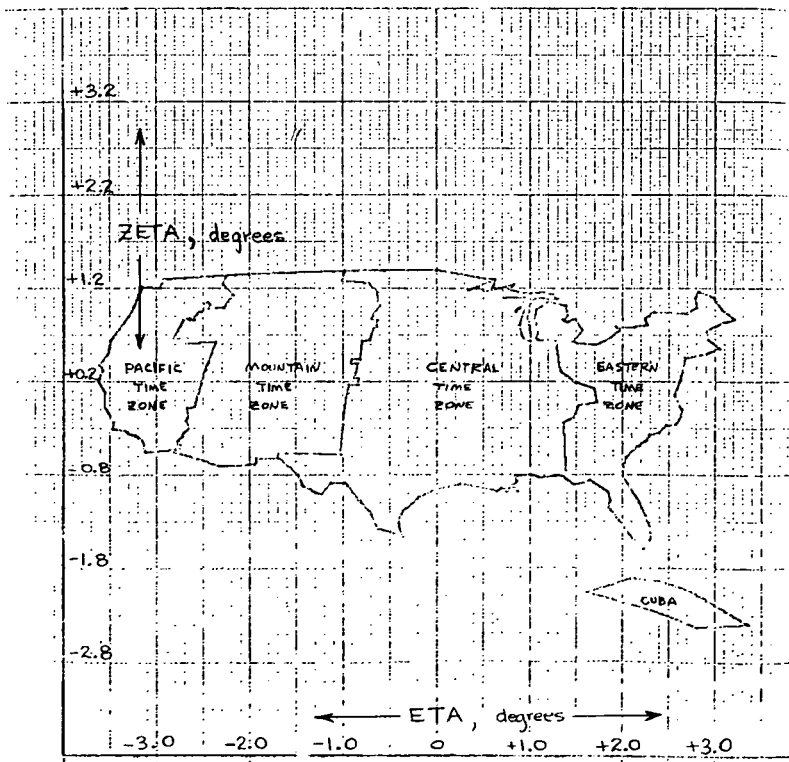
Figure 4.2-2. Angular Coordinate System of Lens Antenna and View of U.S.A. and Cuba From Synchronous Orbit: 2.44 m Diameter Lens

the far-field radiation patterns of the multiple feed lens antenna. Boundaries for the four United States time zones are plotted to enable the design of adjacent nonoverlapping feed group arrangements for the illumination of these zones.

A single feed horn illuminating an 2.44 m diameter lens will produce a half-power beamwidth of about 0.011 radian (0.63 degree) at the design frequency of 11.95 GHz. A group of circular feed horns that are closed-packed in a triangular lattice arrangement will produce overlapping beams. The resulting pattern will have a beam shape that approximates a constant power envelope of the beams of the feed group and a ripple that generally diminishes with an increase in the number of feeds. If seven of these feeds are selected to form the group shown in Figure 4.2-3, the seven individual antenna pencil beams will overlap at the 3-dB levels (as illustrated in the same figure) to produce a broad, irregular shaped beam that covers the major portion of the pacific time zone with the power level varying about 4 dB. The X-Y coordinates of the feed group are shown as viewed from behind the feed
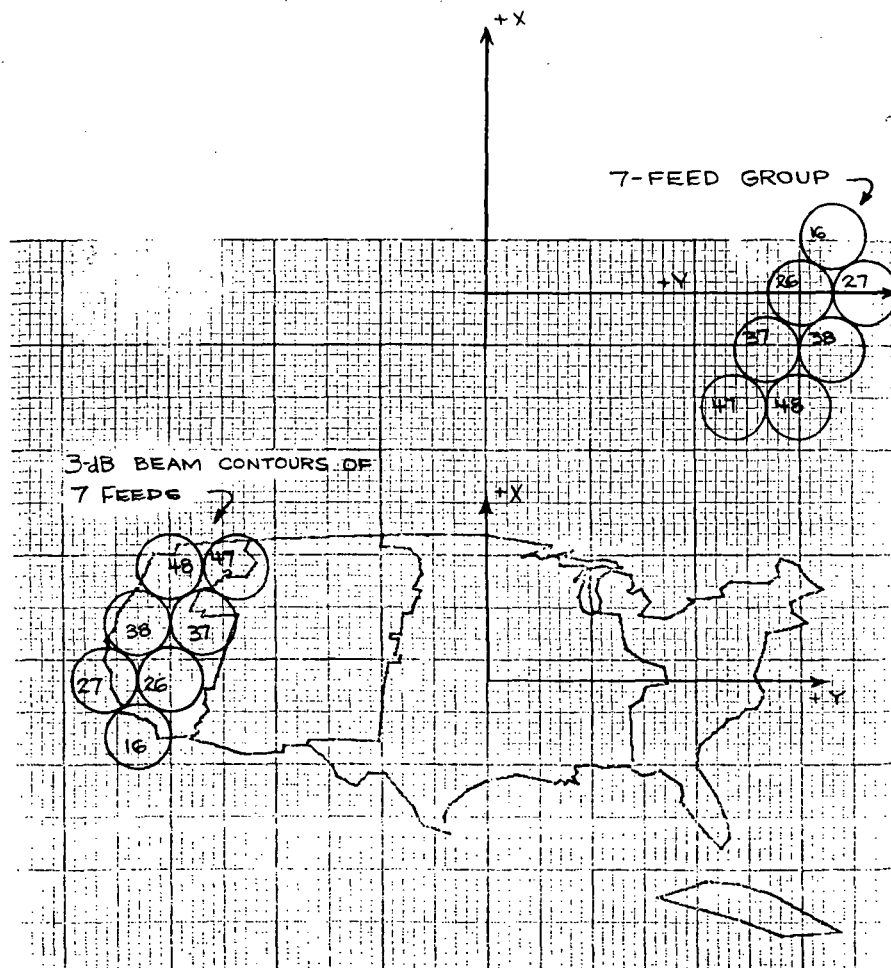
Figure 4.2-3. Feed Horn and 3-dB Contour Level Arrangements of Feed Group Covering Pacific Time Zone: 2.44 m Diameter Lens

4.2-4

looking along the lens axis towards the central time zone of the U.S. The
X axis corresponds to ETA = 0 degrees at 95 degrees longitude. The
satellite is in an equatorial plane with the lens axis (Z axis) pointing 5.8 deg-
rees north of the equatorial plane. ZETA is measured from this plane as
shown in Figure 4.2-2, so that ZETA = 0 degrees is the reference plane
corresponding to the plane of inclination of the lens axis relative to the
orbital plane.

The feed groups and their corresponding groups of beams with 3-dB
contour levels projected onto the other three time zones are shown in Figures
4.2-4, 4.2-5, and 4.2-6. Note that the X-Y coordinates are scaled in degrees
for the feed group; these angular displacements of the feeds measured from
the lens axis may be converted into displacement in inches by multiplying by
96.0·tan (angular displacement). The total number of feeds required to cover
all of the time zones is 48.
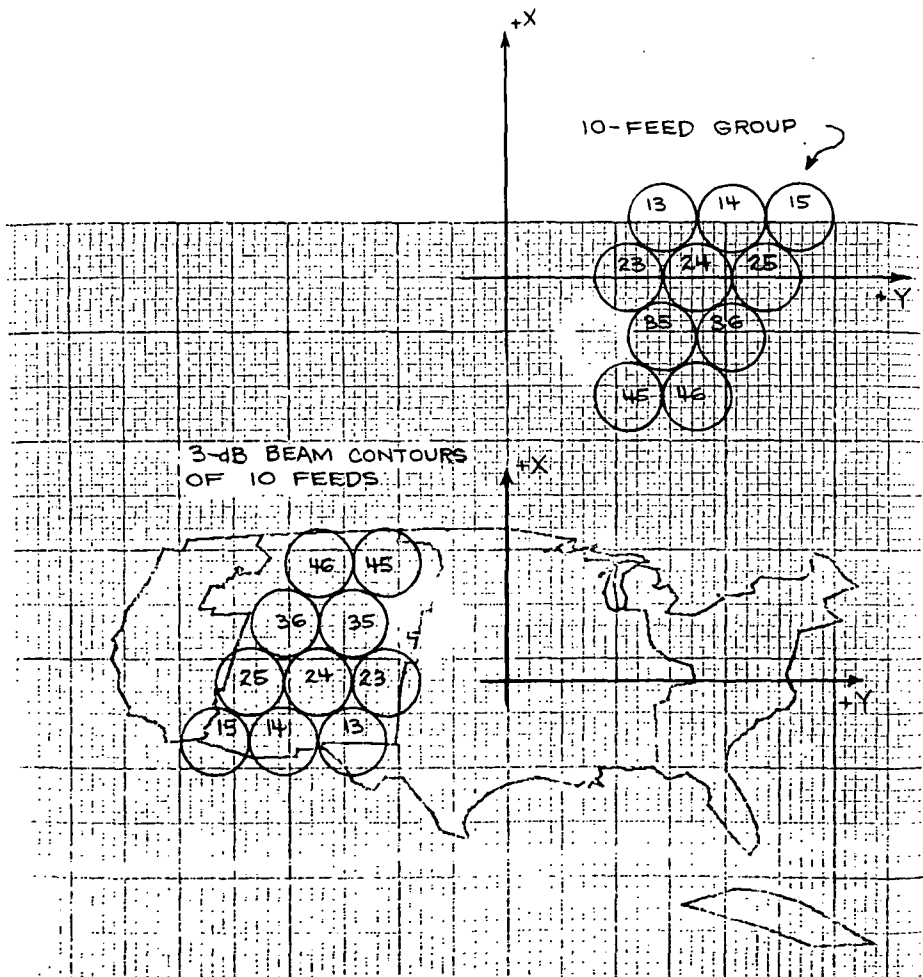
Figure 4.2-4. Feed Horn and 3-dB Contour Level Arrangements
of Feed Group Covering Mountain Time
Zone: 2.44 m Diameter Lens

4.2-5
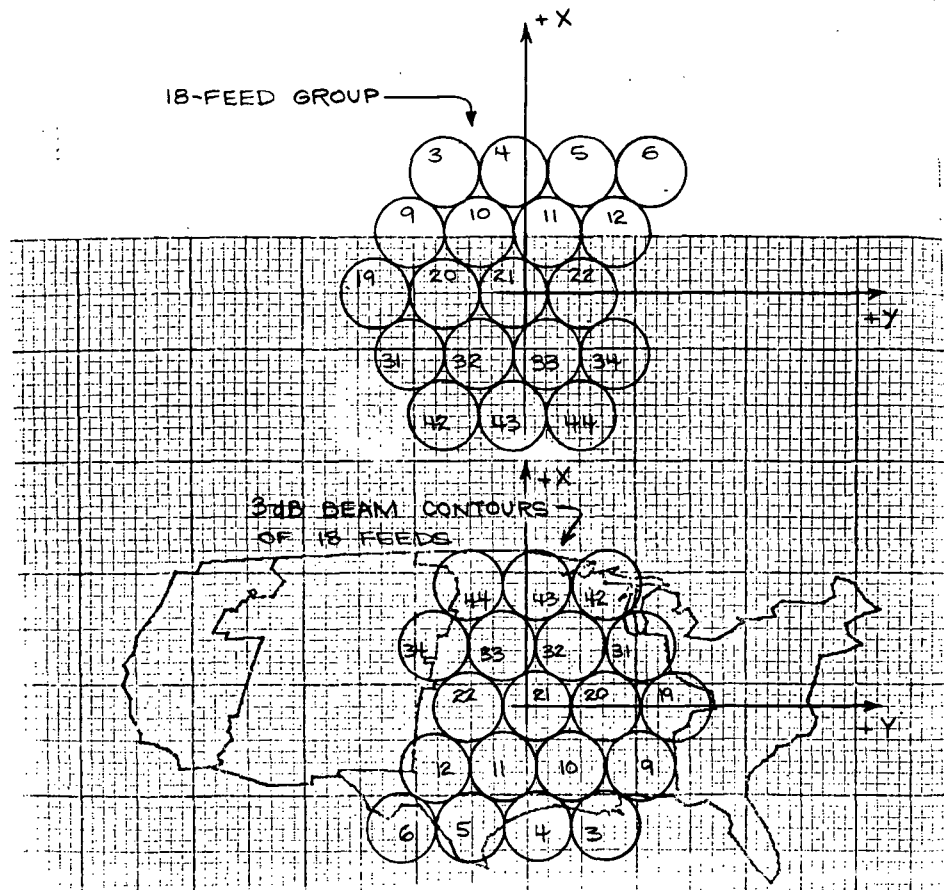
Figure 4.2-5. Feed Horn and 3-dB Contour
Level Arrangements of Feed Group Cover-
ing Central Time Zone: 2.44 m Diameter Lens
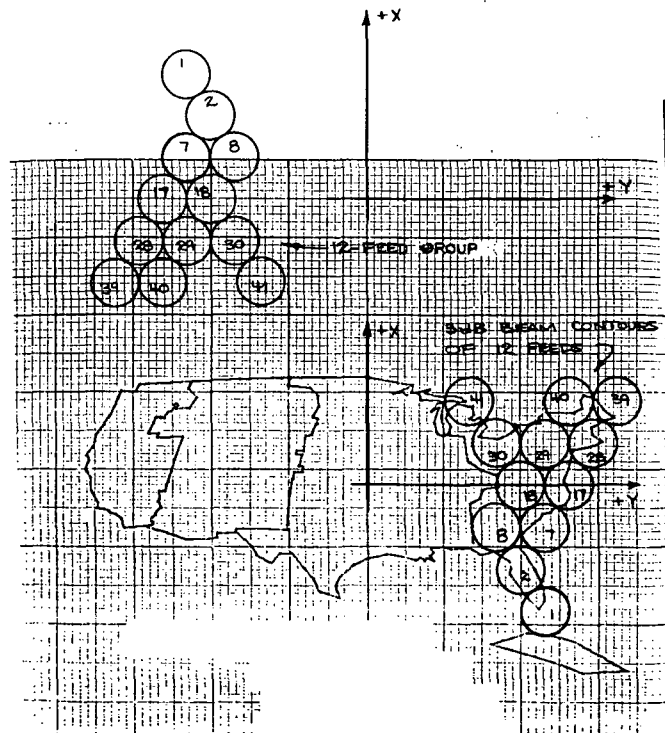
Figure 4.2-6. Feed Horn and 3-dB Contour
Level Arrangements of Feed Group Cover-
ing Eastern Time Zone: 2.44 m Diameter Lens

4.2-6

The theoretical power patterns expected from the lens feed group combinations were obtained with the use of a computer program Section 4. 2. 6). As shown in Figure 4. 2-7 through 4. 2-10, each pattern is presented as a group of several constant power levels (contours) overlaying its particular time zone, with 0 dB corresponding to peak gain. The peak gain is given so that the contours may be converted to constant gain contours. The peak includes an assumed dissipative loss of 0. 7 dB.

An examination of Figures 4. 2-7 through 4. 2-10 shows that the first cut at designing the feed gave a good match of the composite beam shape of each feed group and its respective time zone boundary. Each time zone can be seen to have a gain coverage of about 34. 0 dB or more.

The sidelobe performance of the beam covering the eastern time zone is shown in Figure 4. 2-11.

While the lens design selected for analysis did not include wideband operation, a check was made to determine whether a single feed element could provide useful gain for receiving at 14. 5 GHz at a spot. It was determined that this was feasible although the dispersive properties of the particular circular waveguide cell design caused considerable break up in the pattern, as shown in Figure 4. 2-12.

The beam provides a gain of 32. 5 dB at the target center (Washington, DC), which is down about 12 dB relative to the performance at the 11. 95 GHz design frequency (Figure 4. 2-10). This gain reduction is due principally to the break up of the beam (observe that much of the area in the figure is above a -3 dB contour) and would be significantly improved by a cell designed for wideband operation. (A discussion of this effect and appropriate measures to correct it are discussed in Section 4. 2. 4.)

4. 2. 3 Electrical Performance of 12-Foot Diameter Lens Antenna

The 3. 66 m diameter lens antenna is designed in the same manner as the 2. 44 m diameter lens antenna with the exception that the feed horns were arranged so that the individual antenna beams would have crossover levels of 4. 2 dB rather than 3 dB. This choice results in fewer feeds without degrading the beam shape nor significantly increasing the ripple. A single feed illuminating the 3. 66 m lens produces a 4. 2 dB beamwidth of about 0. 008 radian (0. 5 degree) at the down link frequency of 11. 96 GHz. Four feed group arrangements that provide coverage at the four time zones are shown individually with their corresponding group of overlapping beams in Figures 4. 2-13 to 4. 2-16. There are 74 feed horns in all.
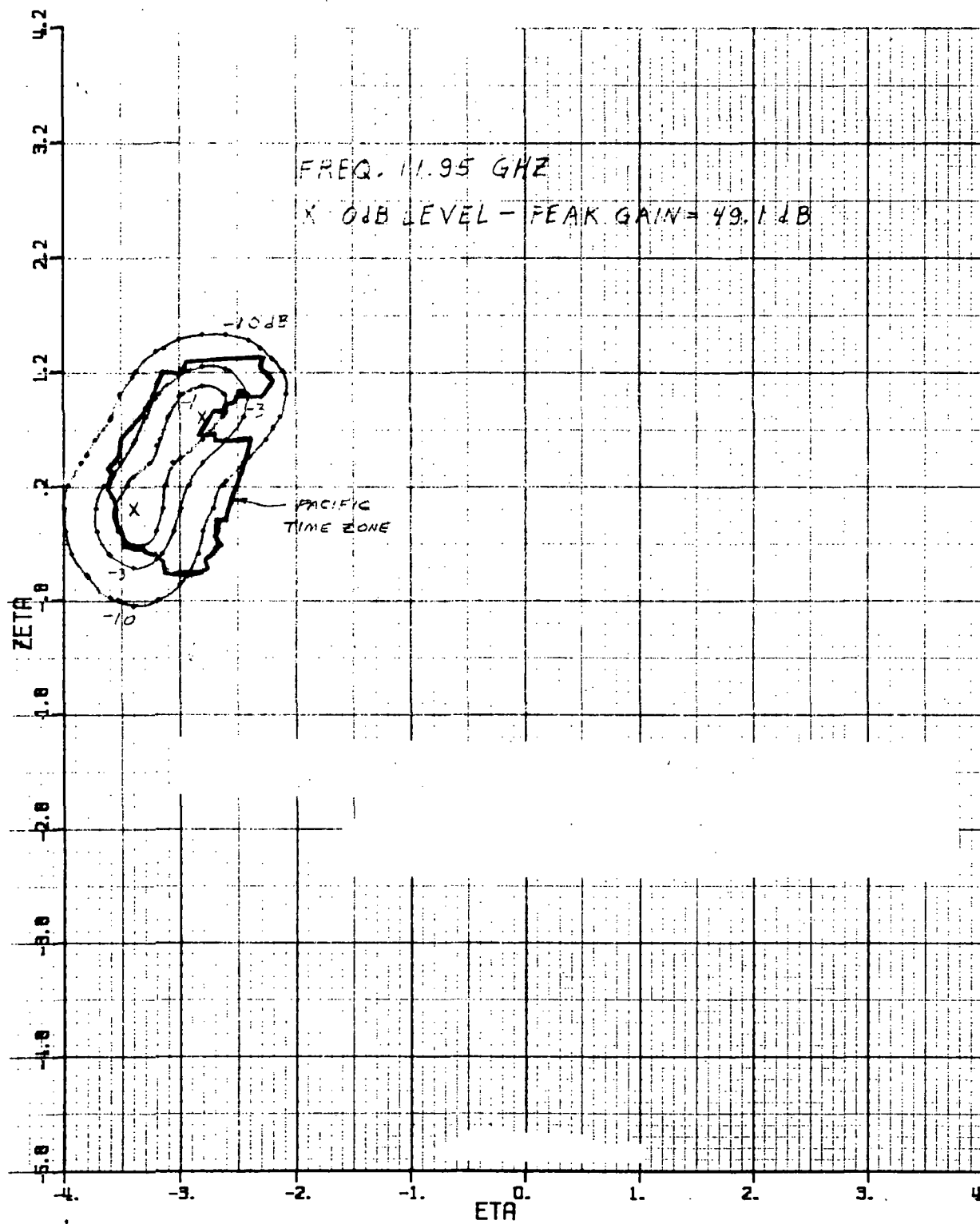
Figure 4.2-7. Contour Levels of Shaped Beam Radiation Pattern Covering
the Pacific Time Zone: 2.44 m Diameter Lens
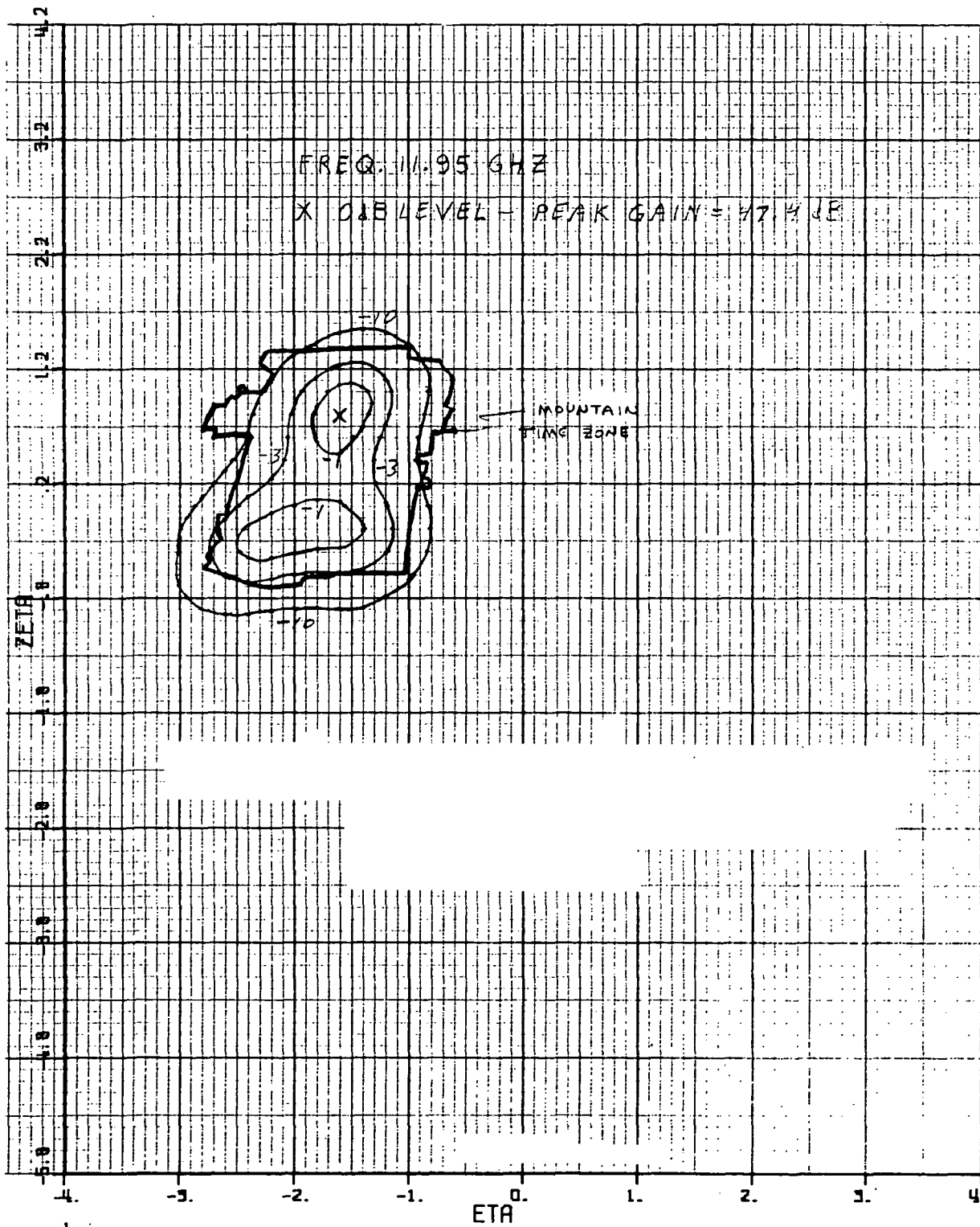
Figure 4.2-8. Contour Levels of Shaped Beam Radiation Pattern Covering
the Mountain Time Zone: 2.44 m Diameter Lens
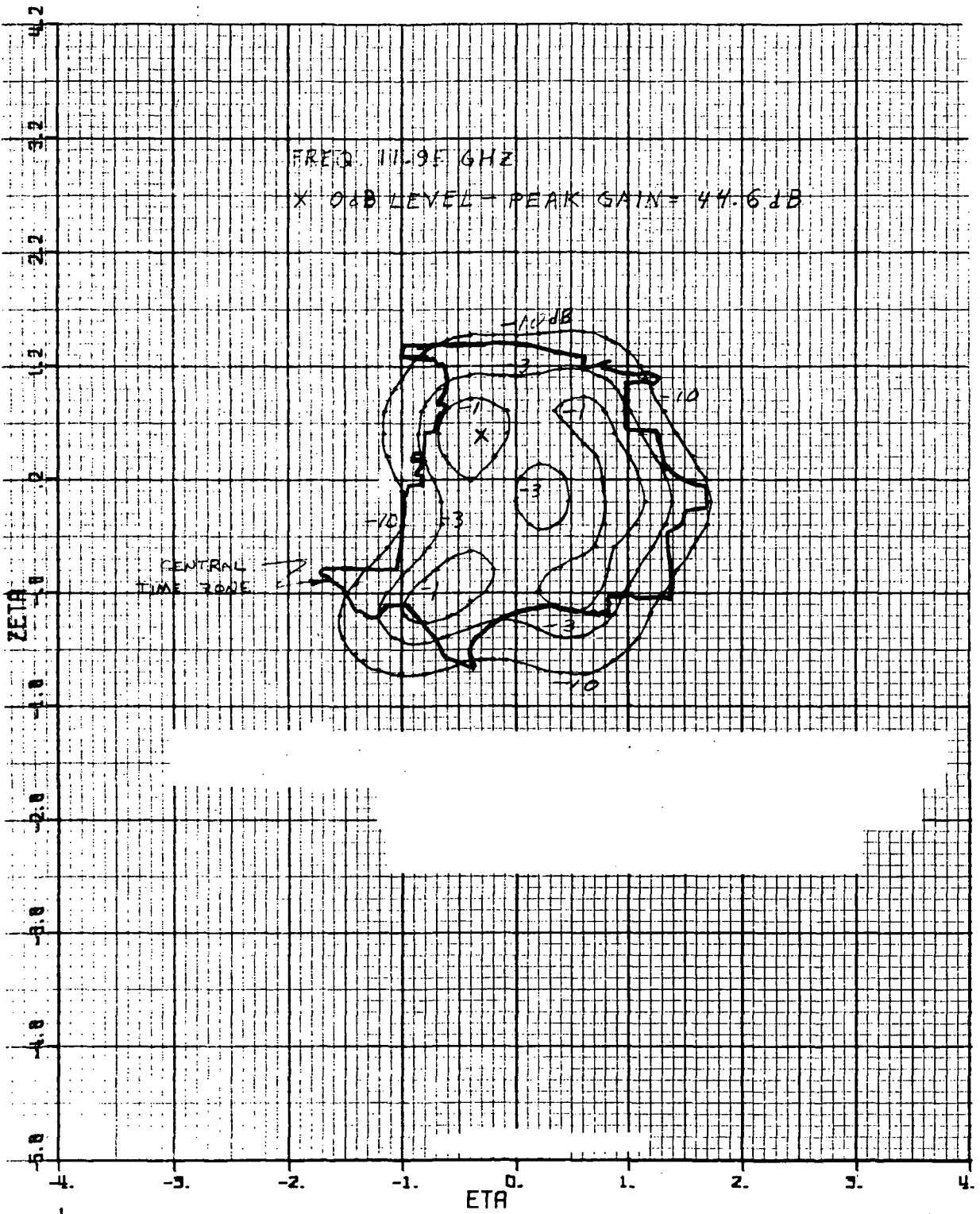
Figure 4.2-9. Contour Levels of Shaped Beam Radiation Pattern Covering
the Central Time Zone: 2.44 m Diameter Lens

4.2-10

FREQ. 11.95 GHZ

X 0 dB LEVEL — PEAK GAIN = 46.6 dB
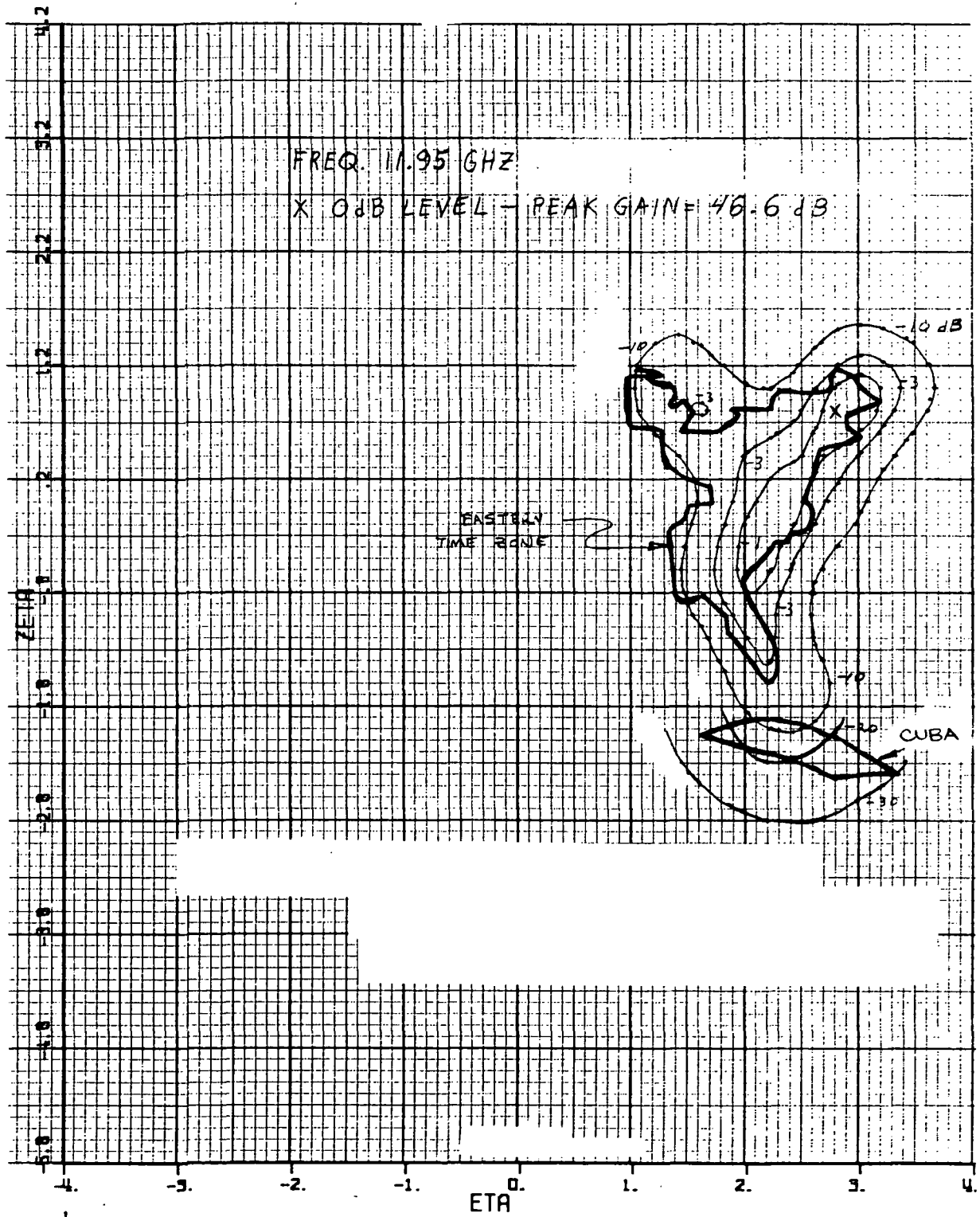
Figure 4.2-10. Contour Levels of Shaped Beam Radiation Pattern Covering
the Eastern Time Zone: 2.44 m Diameter Lens
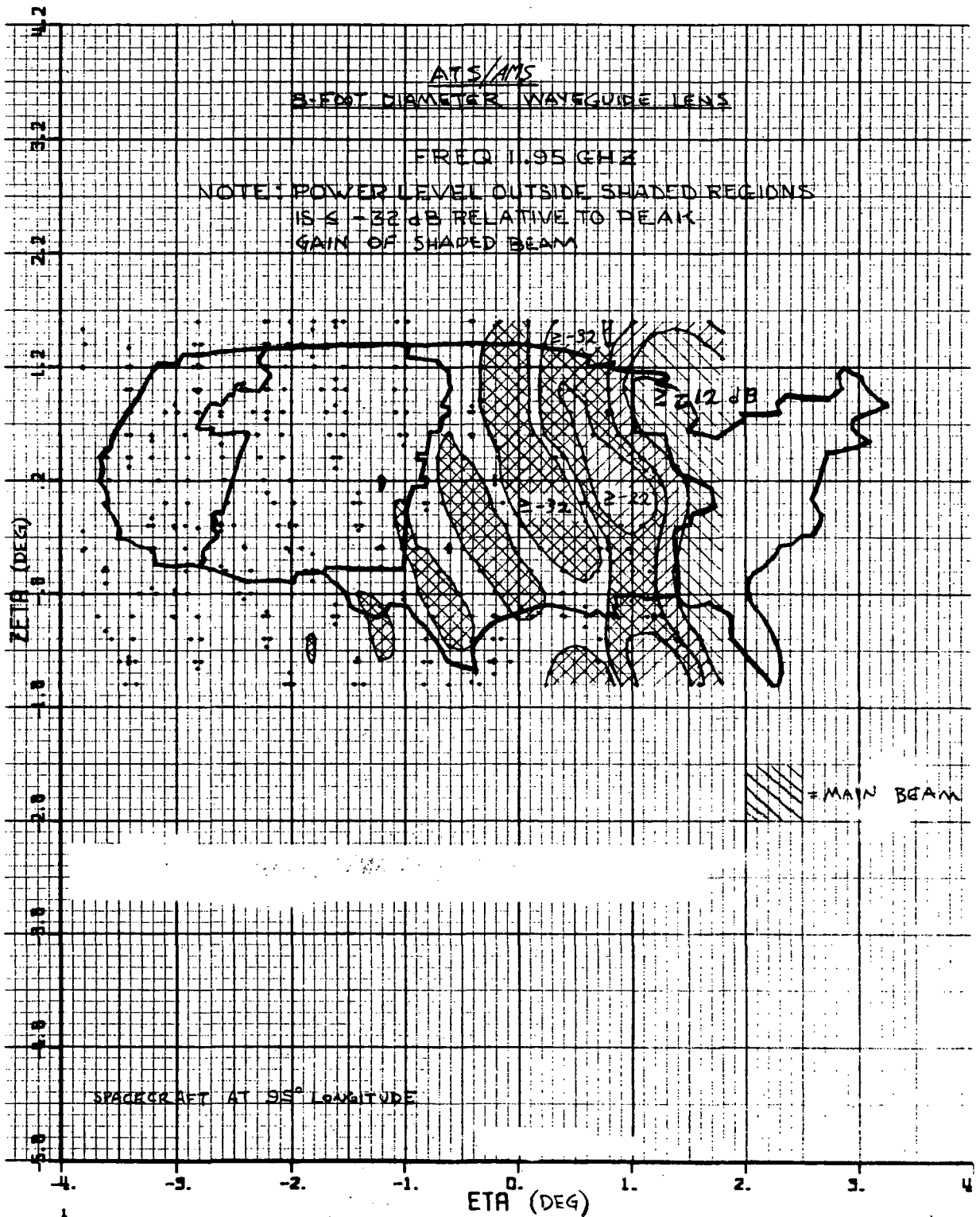
Figure 4.2-11. Side Lobe Contour Levels of Shaped Beam
Covering Eastern Time Zone
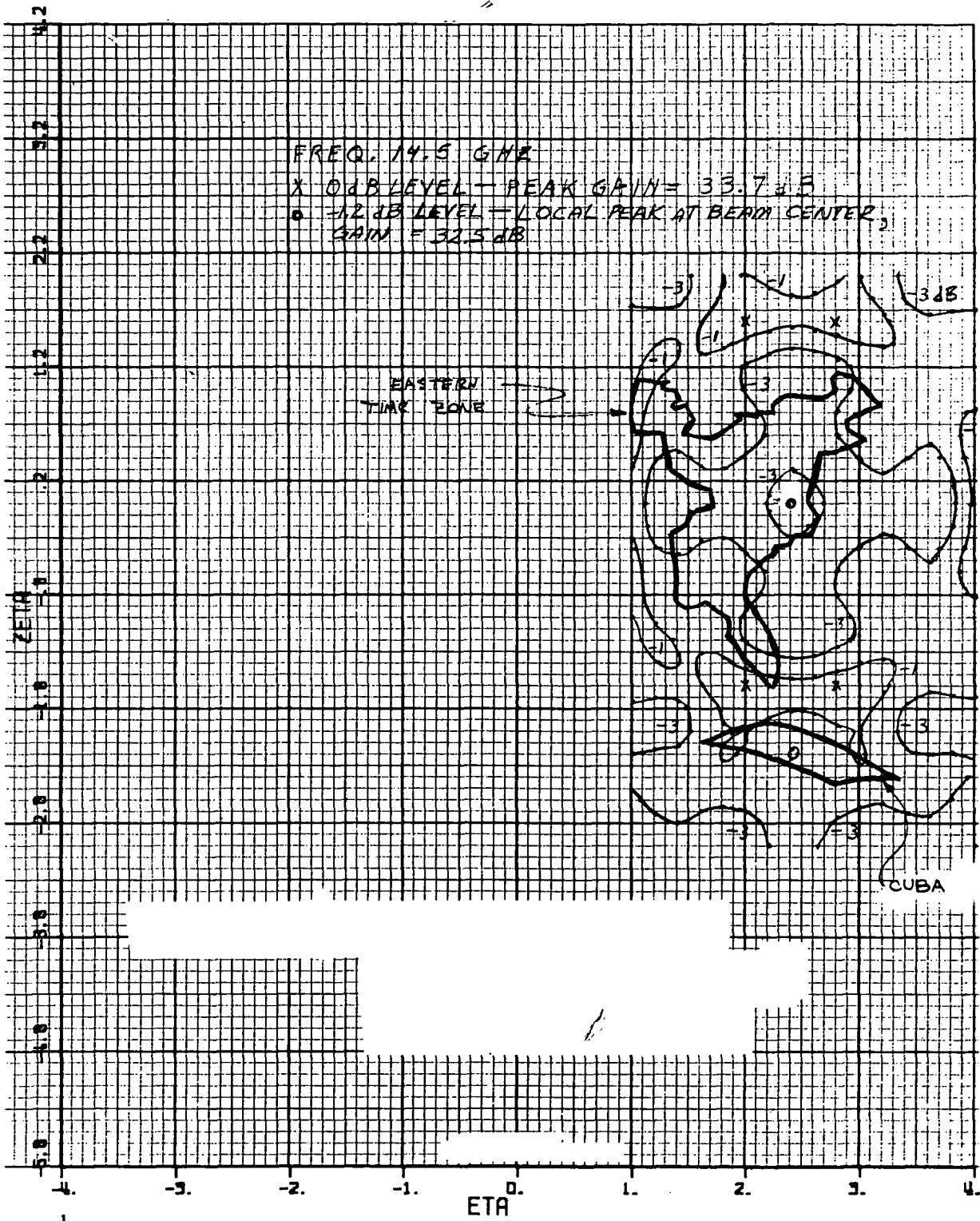
Figure 4.2-12.   Contour Levels of Single Feed Horn (No. 17) at
Receive Frequency: 2.44 m Diameter Lens
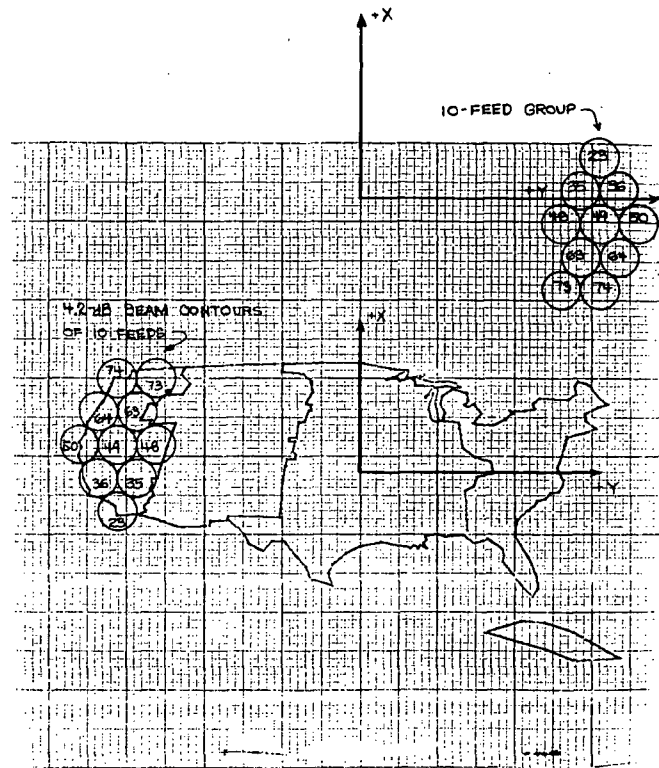
Figure 4.2-13. Feed Horn and 4.2-dB Contour
Level Arrangements of Feed Group Covering
Pacific Time Zone: 3.66 m Diameter Lens
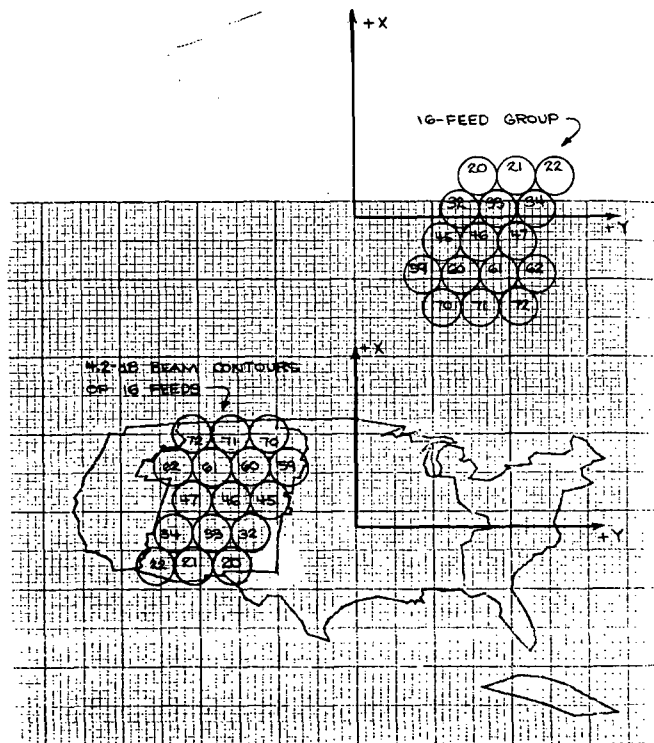
Figure 4.2-14. Feed Horn and 4.2-dB Contour
Level Arrangements of Feed Group Covering
Mountain Time Zone: 3.66 m Diameter Lens
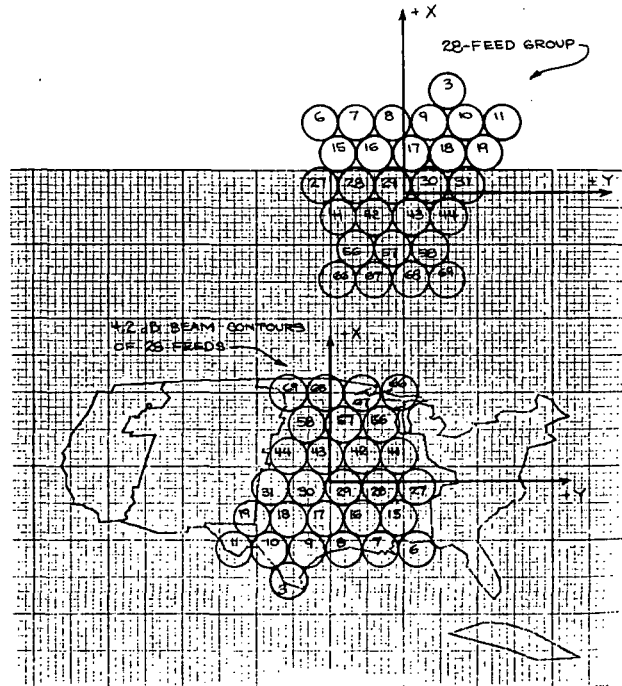
Figure 4.2-15. Field Horn and 4.2-dB Contour
Level Arrangements of Feed Group Covering
Central Time Zone: 3.66 m Diameter Lens
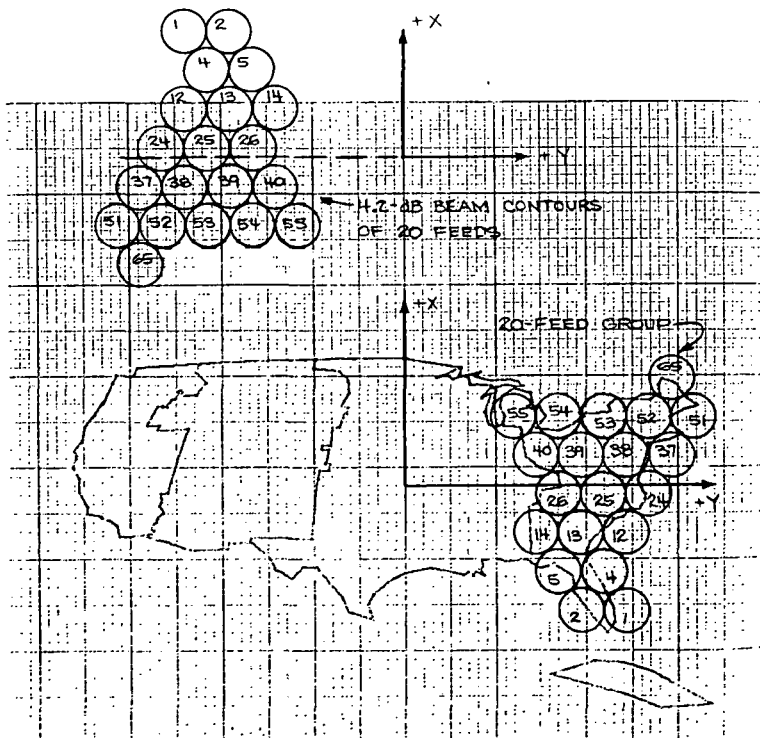
Figure 4.2-16. Feed Horn and 4.2-dB Contour
Level Arrangements of Feed Group Covering
Eastern Time Zone: 3.66 m Diameter Lens

4.2-15

The theoretical power patterns of each lens feed group are shown in Figures 4.2-17 to 4.2-20 as a contour plot of the -1, -3, and -10 dB power levels relative to the peak of 9 dB. The peak gain is given so that the contours may be converted to constant gain contours. The peak gain includes an assumed dissipative loss of 0.7 dB. As can be seen, the shaped beam of each feed group matches less than 2 dB) and small separation between the -3 and -10 dB contours. The matching of the time zone boundary is better with the 3.66 m antenna than with the 2.44 m. Each time zone can be seen to have a gain coverage over most (≈ 95 percent) of its area of about 37.0 dB or more, when illuminated by its respective feed group.

4.2.4 Lens Design Considerations

The diameter of the circular waveguide cells comprising the lens is selected such that the dominant TE_{11} mode will propagate efficiently at both ends of the operating band, 11.7 to 14.5 GHz. The index of refraction, μ, of the lens or lens cell corresponding to the TE_{11} mode, is related to the cell radius, a, by the relation

$$\mu = \sqrt{1 - (\lambda/3.41a)^2}$$

where μ is the free space wavelength. Because reflection of a wave incident on the lens increases above 12 percent as μTE_{11} decreases from 0.5, the latter value is chosen as the lower limit of μ at the lowest frequency. Thus a = 1.01 cm. At 14.5 GHz, $\mu TE_{11} = 0.802$; a $\mu TE_{11} \geq 0.642$ permits propagation of the TM_{01} mode and a $\mu \geq 0.798$ permits propagation of the TE_{21} mode. It is possible for either or both of these modes to be excited in a cell; further investigation is required to determine if a problem does exist. If necessary, ridges can be used in the circular guide to spread the cutoff frequencies of the dominant and higher order modes in order to solve this potential problem. Other means of suppressing the undesired modes can also be used.

Use of a mode suppression technique would result in an additional benefit. This benefit comes from the fact that each of these techniques reduces dispersion, that is, the variation in μ, resulting in broader band performance. Thus a higher gain and an improved beam shape could be achieved at 14.5 GHz.

4.2.5 Mechanical Design of 2.44 m Diameter Lens Antenna

A light weight, rigid rib and ring structure divides the lens into several zones as illustrated in Figure 4.2-21. The ribs and rings are 6.3 mm honeycomb sandwich plate. The circular waveguide cells are tubes with 100 micron wall thickness. These tube elements are epoxy coated and stacked to fill each zone. There are approximately 1400 waveguide cells. Three attachment points are provided for mounting the lens to the spacecraft. The weight of the lens is 27.2 Kg. (An engineering analysis for the weight determination is given in Tables 4.2-1, a, b, and c.)
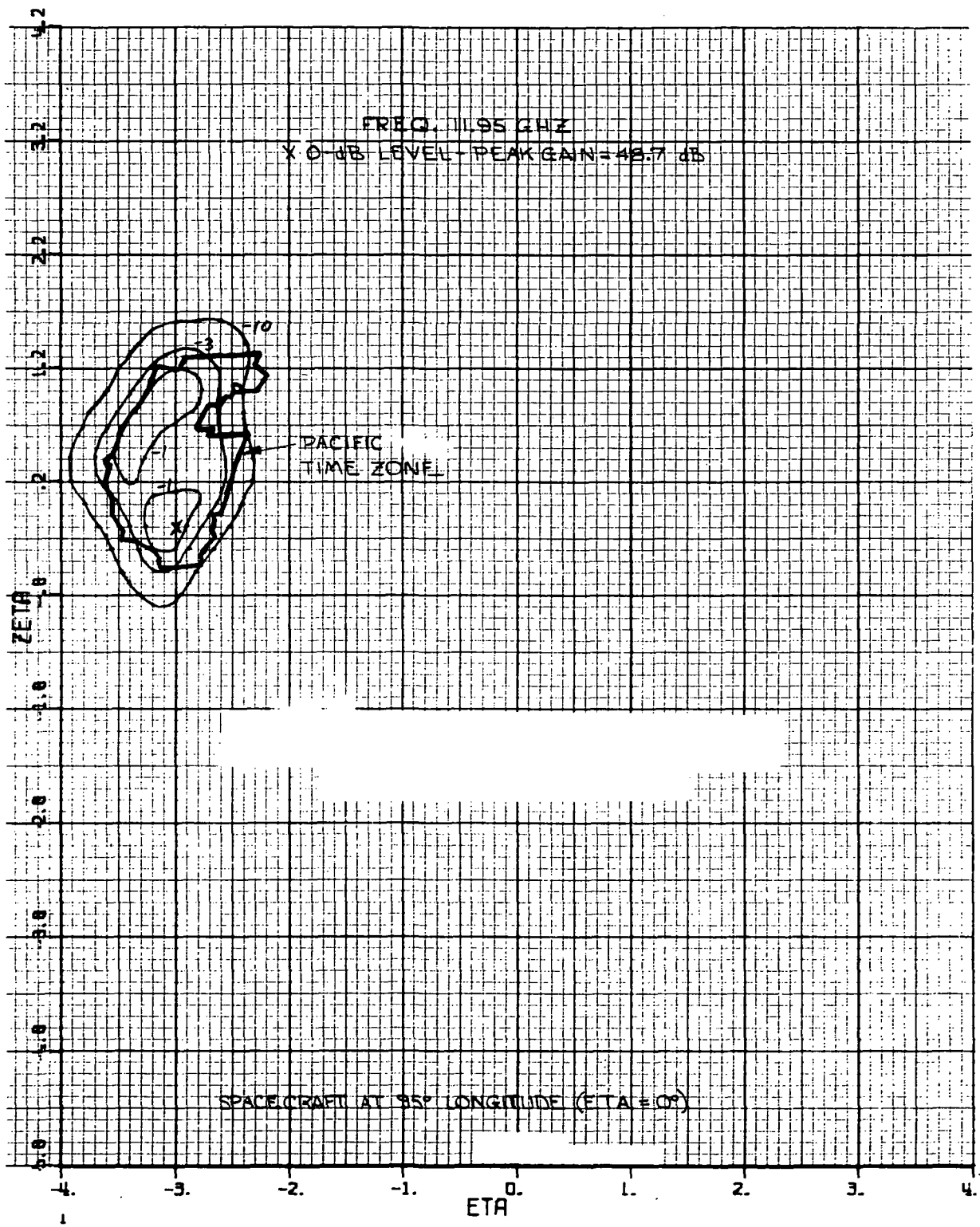
Figure 4.2-17. Contour Levels of Shaped Beam Covering
Pacific Time Zone: 3.66 m Diameter Lens

4.2-17
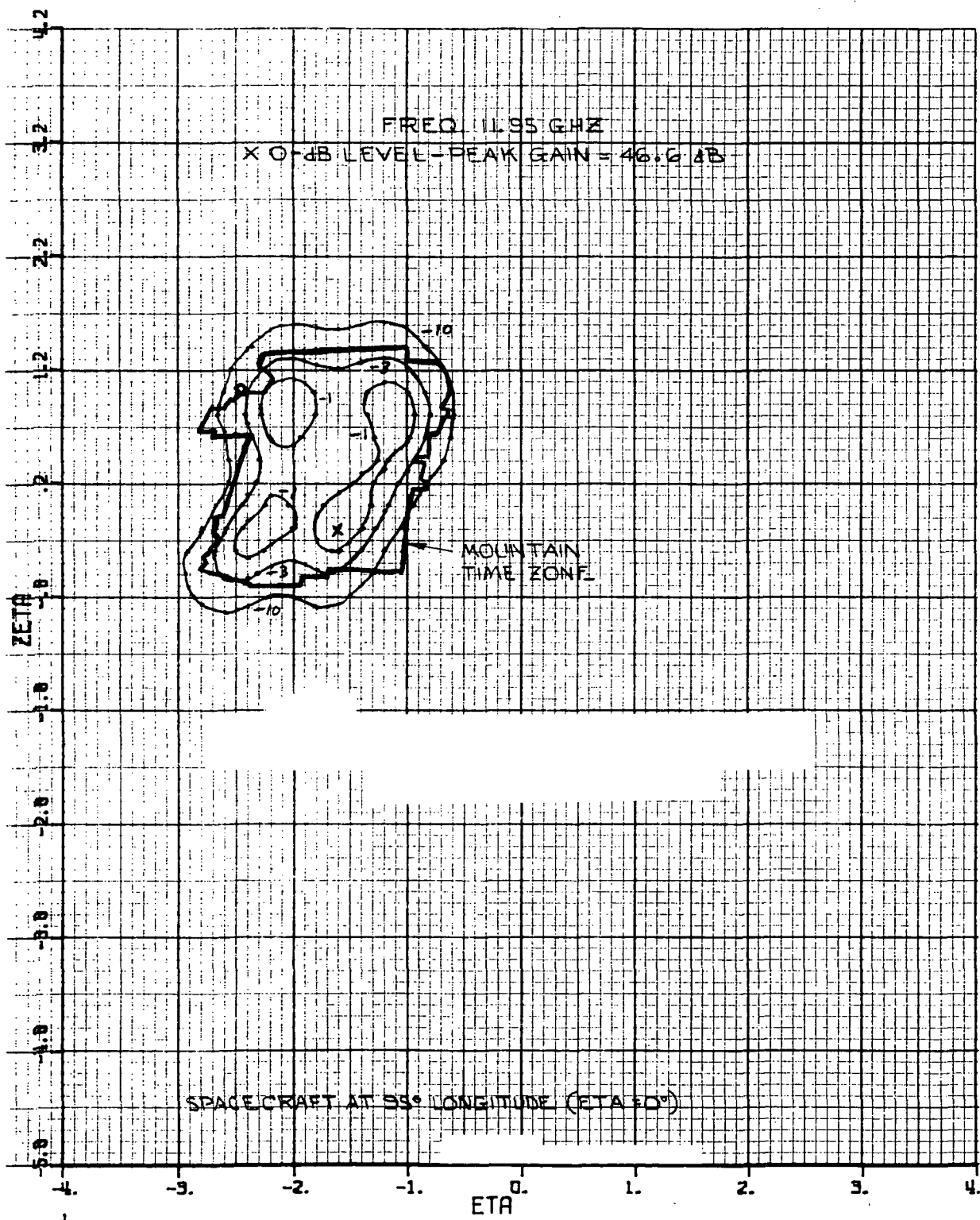
Figure 4.2-18. Contour Levels of Shaped Beam Covering
Mountain Time Zone: 3.66 m Diameter Lens

4.2-18
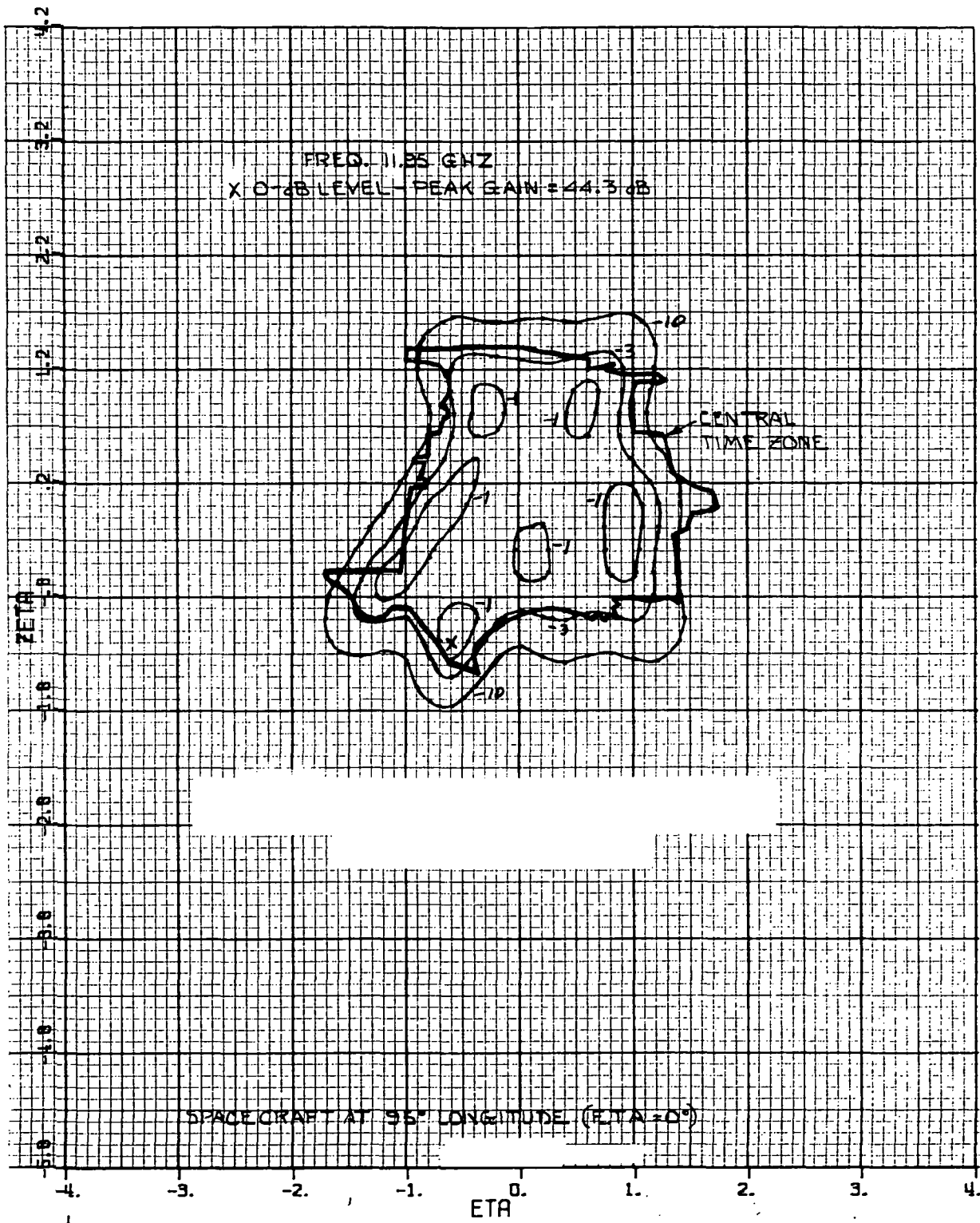
Figure 4.2-19. Contour Levels of Shaped Beam Covering
Central Time Zone: 3.66 m Diameter Lens
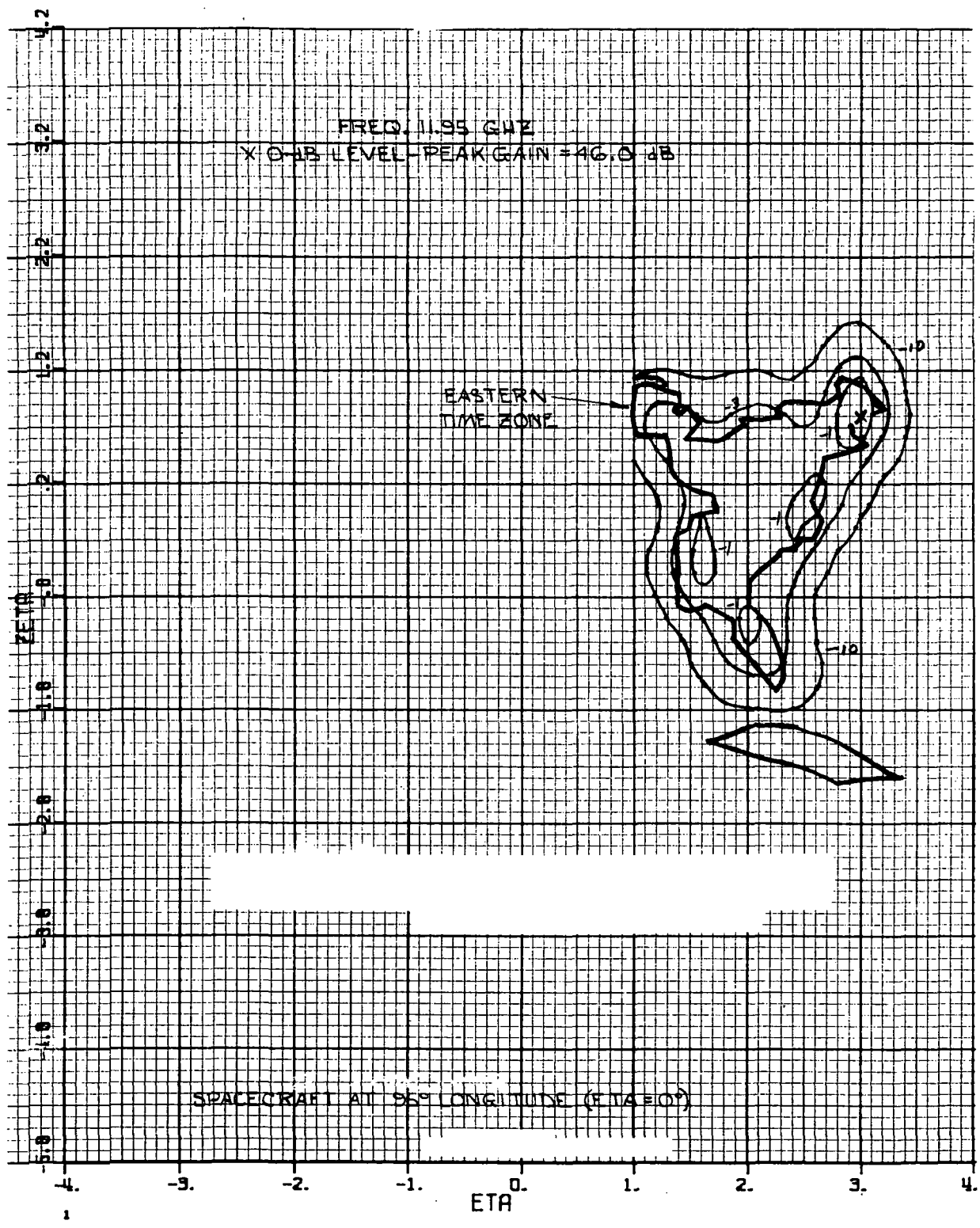
Figure 4.2-20. Contour Levels of Shaped Beam Covering
Eastern Time Zone: 3.66 m Diameter Lens

4.2-20

DETAIL A

DETAIL B

EARTH

LENS AXIS
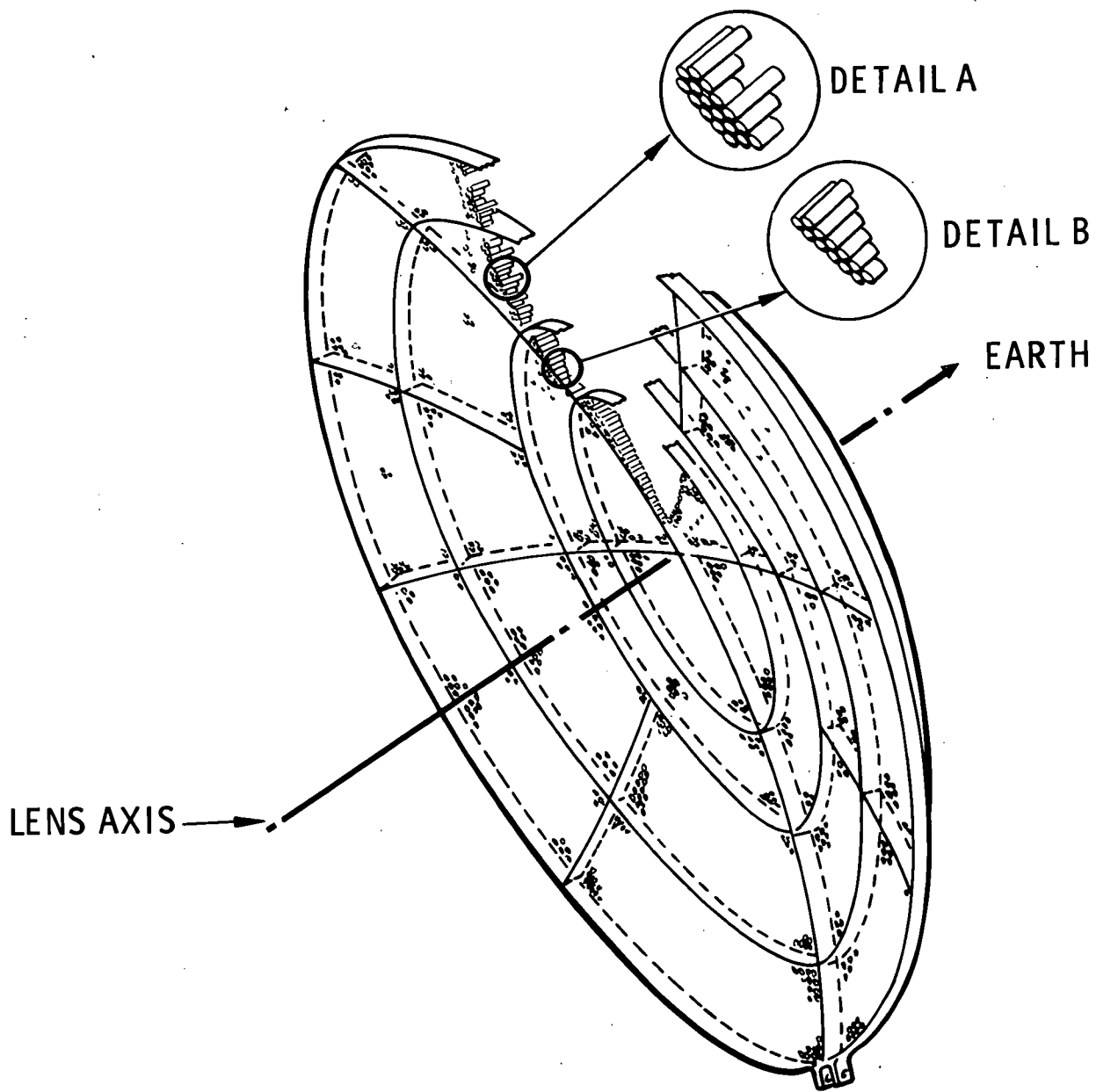
Figure 4.2-21. Antenna Lens

TABLE 4.2-1a. ATS/AMS FEED PACKAGE

Honeycomb Sandwich Plate Support Structure:

(0.635 cm thk w/0.010 cm thk Al covers)

$$\rho' = 2\,(.010)\,2.768 + .050\,(.635) + .059 = 0.1461\ \text{gm/cm}^2$$

Radial Elements:

$$\ell \approx 2\left\{232\left(2\,\sin^{-1}\frac{122}{232}\right)\left[2 - 2\,\sin^{-1}\frac{50.8}{232}\right]\right\}$$

$$= 800\ \text{cm} \quad @\ b = 10\ \text{cm} \quad A = 8,000\ \text{cm}^2 \quad W = 1.169\ \text{Kg}$$

Rings:

$$W = 0.1461\,(10)\,\pi\left[245 + 200 + 100 + 75\right] = 2.846\ \text{Kg}$$

$$\Sigma = 4.015 + 10\% \approx 4.42\ \text{Kg}$$

Lens W/G:

1.90 cm ID x 0.010 cm Al wall, 6.35 cm average length.

$$N \approx \frac{A}{\frac{\sqrt{3}}{2}D^2} \approx \frac{\pi\,(244)^2\,2}{4\,\sqrt{3}\,(1.92)^2}$$

$$N = 14,650; \quad W \rightarrow 14,650\ \pi\ 1.92\ (6.35)\ .010\ (2.768)$$

$$W = 15.532\ \text{Kg}$$

Adhesive:
$$W \approx 1.38\,\overset{\rho}{(.0076)}\,14,650\,\pi\,1.93\,\overset{t}{(6.35)} = 5.916\ \text{Kg} + 10\%,\ W = 6.51\ \text{Kg}$$

TABLE 4.2-1b. ATS/AMS FEED PACKAGE

Feed Horn, (Alum)

WR 75 W/G

2.13
2.60
2.70

1.90   4.83   1.27

(1) $\quad W \approx 48\ (2.768)\left\{\overset{H}{\pi}\left[(1.90)^2 + \overset{H}{(.234)^2}\right]^{1/2} \dfrac{\overset{D}{(2.18 + 2.65)}}{2}\overset{t}{(.05)^1}\right.$
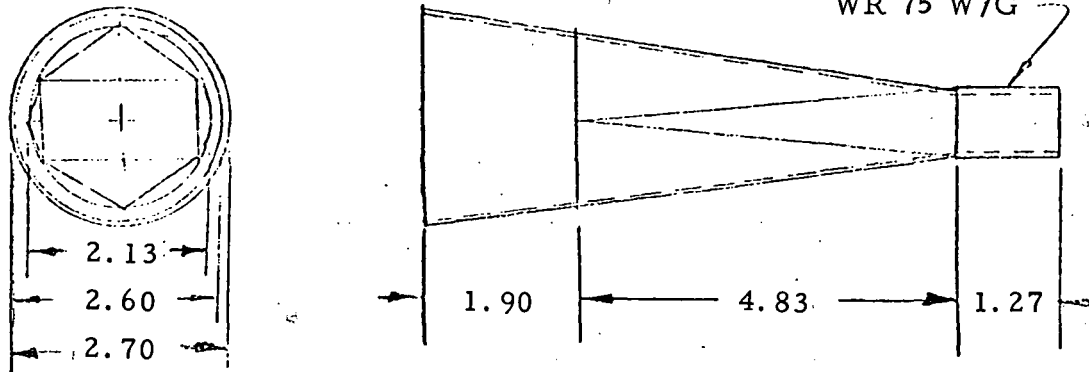
$\qquad + \left[\overset{H}{(4.83)^2} + (.584)^2\right]^{1/2}\left(\dfrac{\overset{A}{\pi 2.13\ (.0635) + 2\ (1.97 + 1.02).0635}}{2}\right)$

$\qquad + 1.27\ (.0635)\ 2\ (2.98)$

$\quad W = 132.9\left\{0.7407 + 1.9574 + 0.4806\right\} = 422\ \text{gm}$

Orthomode Tees: (3)

(2) $\quad W \approx 3(2.768)\left\{(1.97 + \overset{perm}{1.02})\ 2\left[6.35 + \overset{2}{1.40} + 3.81\right]\right\}\overset{t}{(.076)^2} = 44\ \text{gm}$

Horn/ W/G Support Plate

$\qquad$ 20 cm x 33 cm, 0.95 cm thk H.C. w/.0254 cm thk Al covers

$\qquad\qquad\qquad$ covers $\qquad$ corc $\qquad$ adhesive

(3) $\quad W = 20\ (33)\ 2\ (.0254)\ 2.768 + .050\ (.95) + .059 = 163\ \text{gm} + 20\% \rightarrow \approx 196\ \text{gm}$

$\qquad$ 30 cm W/G$_1$: $\quad W = 2\ (30)\ 2.768\overset{\rho}{\left[(2.03)(1.08) - \overset{A}{(1.90)(0.95)}\right]} = 64\ \text{gm}$

$\qquad$ 215 cm W/G$_2$: $\quad W = (215)\ 2.768\left[3.38\ (2.01) - 3.28\ (1.90)\right] \doteq 334\ \text{gm}$

$\qquad$ 8 Flanges @ 47.5 gm ea. = 380 gm.

TABLE 4.2-1c. ATS/AMS FEED PACKAGE

(4) Total W/G:

$$WT = 64 + 334 + 380 = 778 \text{ gm}$$

(5) W/G Switch: (1)

$$W = 635 \text{ gm}$$

Horn Aperture Support Plate:

$$A \approx 2 \ (25 + 38)(2.5) = 315 \text{ cm}^2$$

(6) $\quad W \approx \overset{A}{315} \ \overset{\rho}{(2.768)} \ \overset{t}{.452} = 133 \text{ gm}$

Misc. Brackets and Hdwe

(7) $\qquad W = 540 \text{ gm}$

38 cm

25 cm
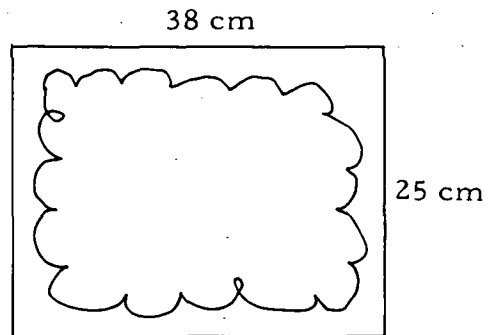
FEED WEIGHT SUMMARY

Item	Weight, Kgm
Feed Horns and Tees	0.466
Waveguide	0.778
Waveguide Switch	0.635
Support Structure	0.329
Misc. Hdwe/Brackets	0.540
Total	2.75

Nomenclature:

$\rho' = $ area density, gm/cm^2

$\rho = $ volume density, gm/cm^3

$\ell = $ length, cm

$W = $ weight, gm (kg)

$N = $ number of W/G elements in lens

$A = $ area, cm^2

The mechanical design of the lens lends itself to a straight forward fabrication procedure. The basic fabrication steps are:

1. Fabricate support structure

   a. Cut ribs from flat honeycomb sandwich plates.

   b. Lay up the 4 cylindrical sections.

   c. Assemble ribs and cylinders on spherical fixture.

   d. Cure assembly adhesives.

2. Fabricate Lens W/G elements

   a. Extrude (seamless) thin-wall tubing.

   b. Incorporate cutoff in final sizing die to give proper length tubes.

   c. Clean and adhesive coat tube element exterior.

   d. Assemble in support structure, on spherical fixture.

   e. Cure at room temperature.

The feed package for the 2.44 m lens antenna consists of 48 circular horns arranged in a triangular grid and 4 feed networks. The envelope enclosing all the horns is shaped like an inverted projection of the United States as viewed from a satellite in equatorial orbit. The 48 hours are separated into groups that most nearly cover the four time zones. The number of horns covering each time zone is shown below.

TIME ZONE	NUMBER OF HORNS
Pacific	7
Mountain	10
Central	19
Eastern	12

The horns for each time zone are combined through a feed network to a single terminal except for the eastern time zone. The eastern time zone feed cluster has two terminals, one for transmit and one for receive. A plan view of the feed network is shown in Figure 4.2-22.
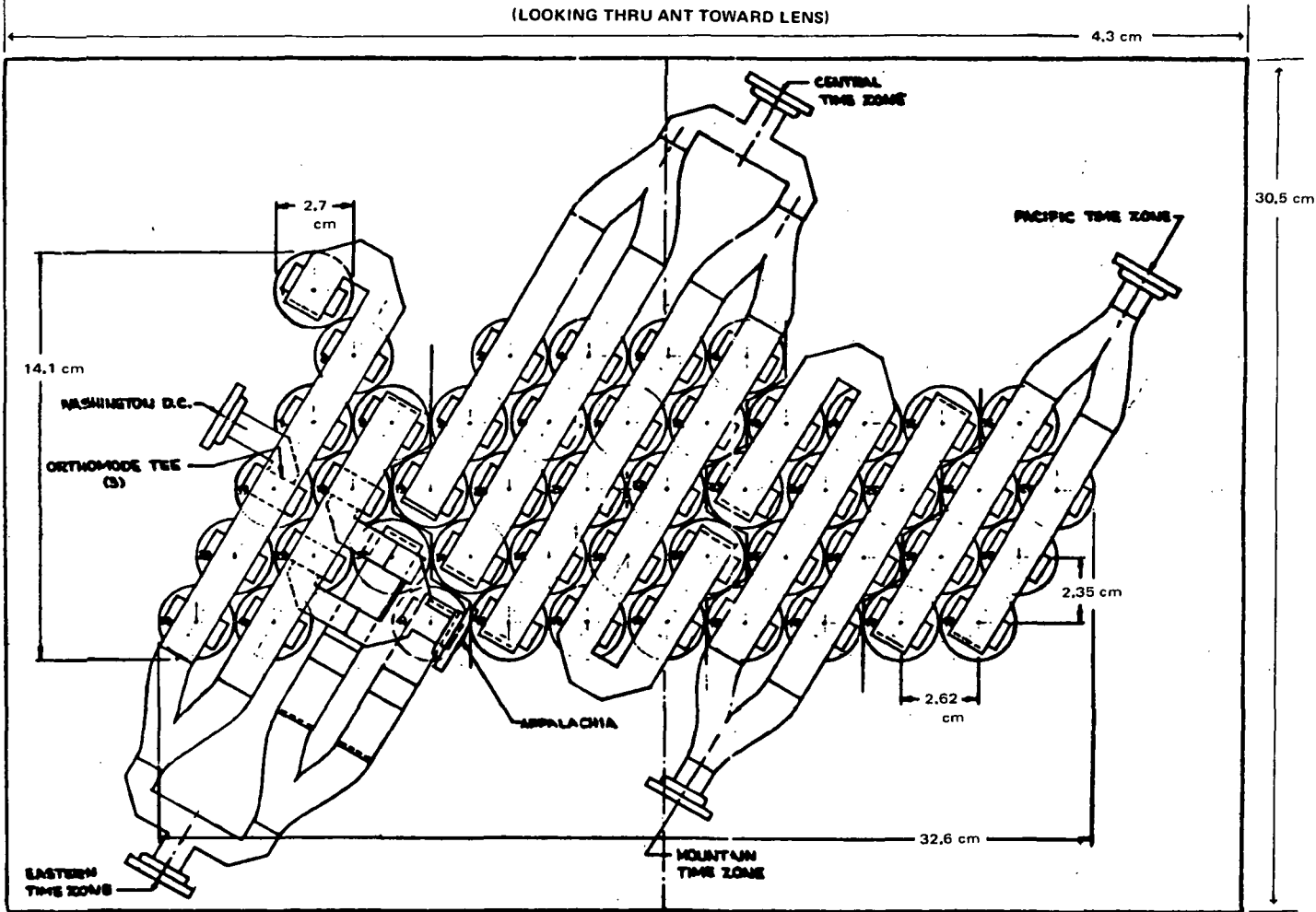
Figure 4.2-22. 2.44 Meter Diameter Lens Antenna Feed

        The feed networks for all time zones are similar except the one for
eastern zone which will be discussed later. A typical feed network for a
single time zone is described below. Each row of horns is fed from a wave-
guide standing wave array by slot coupling through the narrow wall of the
waveguide. The waveguide making up the array is sized to have a λg equal to
the spacing between horns so that the horns are fed in phase. The energy
is coupled from the waveguide array into the end of a rectangular waveguide,
then through a rectangular to round transition to the horn. The number of
waveguide arrays required for any time zone is an even number. The wave-
guide arrays are connected together through E-plan tees to a single terminal.

        The feed network for the eastern time zone has two variations. These
variations are a receiving capability for the Washington, D. C. area, and a
separate transmit beam for the Appalachia area. The receiving capability is
added to the single horn covering the Washington, D. C. area by placing an
orthomode tee between the horn and the circular to rectangular transition.
The sideport of the orthomode tee is connected to a receiver through a trans-
mit frequency reject filter which protects the receiver from the high trans-
mitted power. This arrangement enables this one horn to receive signals
from the ground that are polarized orthogonal to the transmit signals. The

4.2-26

other variation for the eastern time zone feed is a capability to transmit to the Appalachia area only, or to the entire eastern time zone by switching between appropriate horns. This is accomplished by placing an orthomode tee in the two horns covering the Appalachia area, as was done for the Washington, D.C. area horn. The outputs of the two orthomode tees are combined through an E-plane tee to form a single terminal. The polarization of the transmitted signal to the Appalachia area is orthogonal to the transmitted signal to the entire eastern time zone. The rectangular waveguide section of the remaining nine horns covering the eastern time zone are extended so that the rows of horns can be fed from standing wave arrays as in the feed networks of the other time zones. The single terminal from the twelve horns and the single terminal from the two Appalachia area horns are connected to an electromechanical waveguide switch, and a single transmit terminal comes off the third port of the switch. Figure 4.2-23 shows the eastern time zone feed network (without the waveguide switch and receiving port).
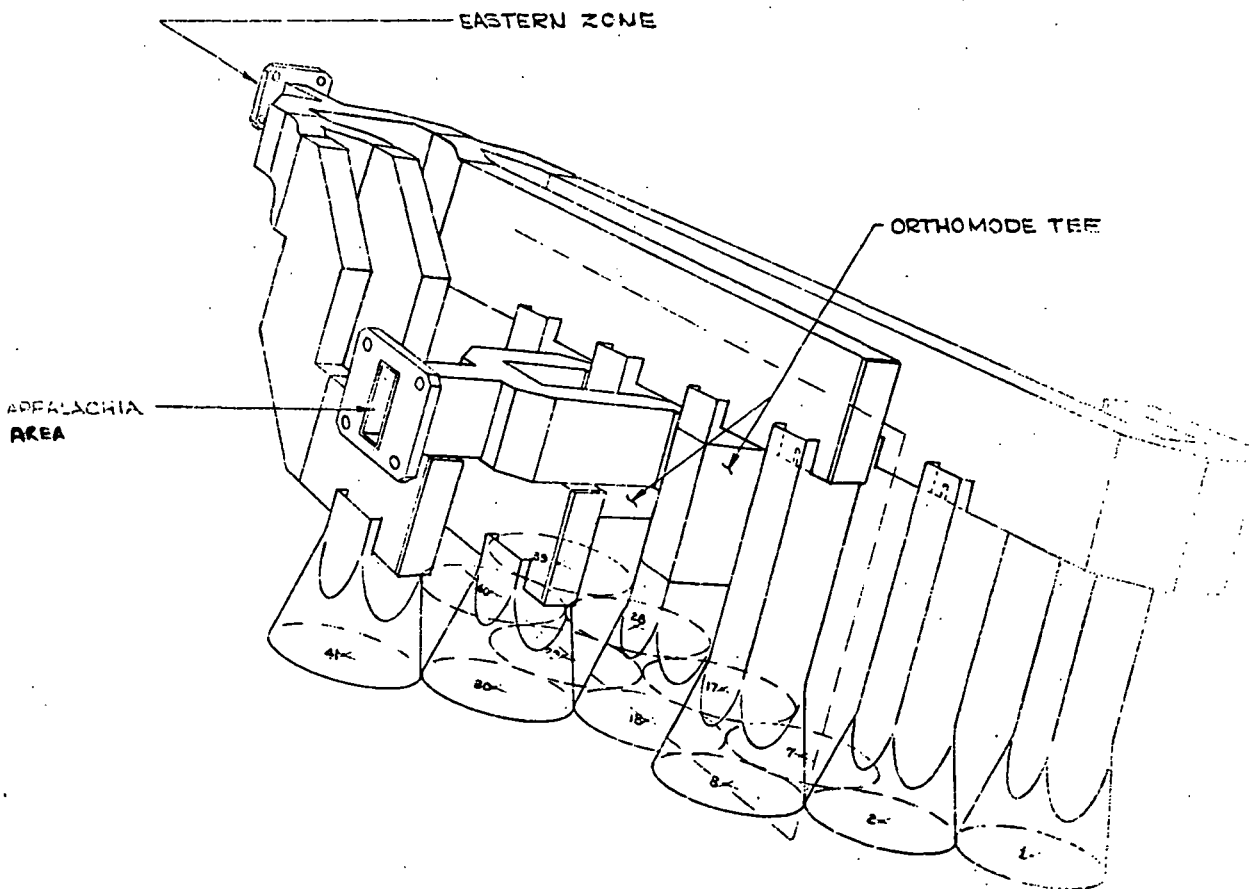
Figure 4.2-23. Feed Network — Eastern Time Zone

The horns and feed networks will be made from thin wall aluminum parts. The wall thickness will range between 0.5 to 0.6 mm. The weight of the complete feed package including the waveguide switch is 2.7 Kg.

4.2.6. Computer Program Used for ATS-H Lens Antenna Study

The dimensions of the waveguide lens, and the far-field radiation patterns of the lens when illuminated by various feed groups, were computed with the aid of a Fortran IV program written for the Honeywell 635 computer. The program is a modification of one provided to the Hughes Antenna Department by the M.I.T. Lincoln Laboratory and written for the IBM 7094 computer. The program assumes the lens is constructed from square waveguide cells. Although the ATS/AMS lens uses circular waveguide cells, it was felt that the square waveguides would adequately simulate the circular waveguides for determining the performance on a first-cut basis.

The lens geometry is determined from surface equations that satisfy the requirement that rays emanating from a point source feed offset from the lens axis will, after refraction by the lens, form a plane wave propagating in the direction parallel to the line joining the joint source to the center of the lens. These surface equations are a function of the index of refraction, which for a waveguide lens equals $\lambda/\lambda g$, and the constraint that within the lens the rays are parallel to the lens axis.

The far-field radiation pattern and gain is computed by considering the lens antenna as an array of open-ended waveguide radiators, the outer surface of the lens, and summing the far-field contribution of each waveguide radiator. The excitation of the waveguide radiators is determined in the following manner. The feeds are excited uniformly with each feed having the same assumed gain function. The excitation of the inner surface of the lens is determined by summing at each waveguide cell the field contribution from each feed, taking into account the path length between each feed and waveguide cell. The excitation at the outer surface of the lens is a transformation of the inner surface excitation through the path lengths of the individual waveguide cells.

The required input data are in two sets. One set is for the lens. This data includes the design wavelength, the operating wavelength, the lens diameter, the inside dimensions of the square waveguide cell, the wall thickness of the waveguide cell, the length of the center waveguide and the focal length to diameter ratio. The other set of input data is for the feed group. The feed group must have its feeds located symmetrically about an origin and the feed phase centers must lie in a plane perpendicular to the lens axis. An asymmetrical feed group is simulated by "turning-off" appropriate feeds in the symmetrical group. The feed horns are assumed to lie in a triangular lattice arrangement with all feeds touching. The feed group set of data includes the number of rows of feeds, the number of feeds per row, the spacing of feeds along each row, the isosceles angle factor (chosen to be 0.866 for an equilateral triangle), the number of active horns, the horns "turned-off" and the displacement of the center of the symmetrical feed group from the lens axis. The latter three design factors permit some freedom in shaping the beam of the feed array and in pointing the beam away from the lens axis.

The output of the program includes a printout of the length of each waveguide cell, the zoning of the lens (the outer surface is stepped at radii determined by the program in order to limit the lens thickness, and to increase its bandwidth), the power level normalized to 0 dB at the peak over a nearly rectangularly shaped solid angle, the peak gain and a Cal Comp plot of constant gain power level (dB contours).

4.3 ATTITUDE CONTROL AND STATIONKEEPING SUBSYSTEM

4.3.1 Introduction

. During the course of the study, emphasis was first placed upon the design of the A-1 configuration, followed by B and C, respectively. In defining the baseline design of the Attitude Control and Stationkeeping Subsystem (AC&SS), the same sequence was utilized. Since many of the tradeoff studies are the same for all three configurations, their descriptions are included in the discussion for Configuration A-1 and are not repeated in the descriptions for the B and C configurations. Where conclusions for B and C differ from those for A, the appropriate discussion will be referenced, and tradeoffs which are peculiar to configuration B or C will be covered in the corresponding discussions for the baseline subsystem designs.

Following the baseline design descriptions, there is a qualitative discussion of the dynamic interaction considerations for the ATS/AMS spacecraft.

4.3.2 AC&SS for Configuration A-1

4.3.2.1 Summary

The AC&SS provides the necessary sensing and actuation elements which control the spacecraft to its desired orientation accuracy and which perform the ΔV corrections to maintain the desired trajectory. The AC&SS must provide these functions during on-station operations as well as during the orbit-raising phase. As a result, strong design emphasis has been placed on the use of components which can be utilized in as many mission modes as practical, so as to minimize weight and power consumption, and to enhance reliability.

The baseline AC&SS design consists of the following:

1) Three momentum wheels to provide short-term control/stability

2) Deflectable electric propulsion thrusters to provide periodic momentum dumping and ΔV corrections

3) Three strapdown rate integrating gyros to provide short term, continuous attitude error sensing and

4) Earth and sun sensors which are used to update gyro drift via periodic commands derived from ground data processing.

This baseline design was selected after careful evaluation of sensing and actuation alternatives, along with considerations of interfaces with the overall spacecraft and other subsystems. The selected baseline design combines the short term stability and maneuverability advantages of a momentum storage system with the long term fuel efficiency of electric thrusters.

The specific functions performed by the AC&SS during the two mission phases are summarized in Table 4.3-1. The physical characteristics of the AC&SS hardware elements are summarized in Table 4.3-2. The total system weight is 25.2 Kg for a single thread design, and uses less than 60 watts average power. Redundant gyros and control electronics are a likely requirement to enhance reliability.

4.3.2.2 Functional Requirements

The functional requirements for the AC&SS during both mission phases are summarized in Table 4.3-3. The orbit raising portion of the mission will last approximately ninety days, and the AC&SS is to be designed to operate for a 5-year mission lifetime.

The requirements for on-station antenna beam pointing of ±0.2 degree in earth latitude and longitude results in a ±0.035 degree pointing accuracy requirement as measured about spacecraft axes (normal to the antenna boresight). This accuracy must be provided at the same time that N-S and/or E-W stationkeeping is taking place. Control during eclipse is also desirable to avoid the necessity for an acquisition maneuver following each eclipse period.

During orbit raising, the vehicle orientation must be varied over the orbit to provide the desired ΔV direction. Figure 4.3-1 illustrates representative in-plane and out-of-plane thrust directions required as a function of orbit position. The resultant maneuvers are required to optimize the ΔV utilization during the orbit raising phase.

4.3.2.3 Design and Implementation Alternatives

A number of design and implementation alternatives were examined in defining the baseline AC&SS design. The major factors which influenced the selection of the baseline design are summarized in Table 4.3-4. Environmental disturbance torques and thrust misalignment torques (during ΔV maneuvers) must be accommodated; in addition, the solar pressure force acting on the large projected area must be counteracted to avoid unacceptable orbit perturbations. Functional versatility is a highly desirable design feature; an AC&SS sensing and actuation complement performs multiple functions during both mission phases and minimizes the on-board weight and complexity.

Actuation Alternatives. Although sensing and actuation are closely related to one another to perform AC&SS functions, they are discussed separately here for convenience. Attractive actuation candidates for attitude control are summarized in Table 4.3-5, and consist of two general classes, namely:

1) Momentum storage with mass expulsion momentum removal

2) Primary (~continuous) control with mass expulsion. Other approaches such as interactions with ambient fields (solar

4.3-2

TABLE 4.3-1. AC&SS FUNCTIONS DURING MISSION PHASES

ORBIT RAISING PHASE

- Yo-yo despin after separation from booster.

- Tipoff rate nulled using reaction wheels, rate gyros.

- Reorientation to desired attitude performed after panel deployment.

- ΔV added for orbit raising; attitude control performed via thrust vectoring and reaction wheels.

- Attitude reference provided by gyros updated periodically by command.

- Attitude determination by ground processing of earth and sun sensor data.

ON-ORBIT PHASE

- Reorientation maneuver to acquire on-station attitude.

- Continuous attitude control and sensing provided by reaction wheels and gyros.

- Gyro drift periodically updated by command, using ground processed sun and earth sensor data.

- 1/6 duty cycle for N-S stationkeeping; thrusters are vectored to negate thrust misalignment. Low thrust provided to compensate for solar pressure force, moment.

- No loss of control during eclipse — wheels and gyros maintain desired orientation.

- Backup control and sensing provided by electric propulsion jets and earth and sun sensors.

TABLE 4.3-2. AC&SS HARDWARE SUMMARY

Unit	Quantity	Unit Weight	Size	Power
Gyros	3	1.6 Kg Each	900 cm^3	9.5 W Each
Wheels	3	3.5 Kg Each	16.5 cm OD x 7.6 cm High	9.5 W Stall Each 3.0 W Average Each
Sun Sensor	1	1.4 Kg (Including Electronics)	5.1 x 7.6 x 6.35 cm 5.1 x 15.3 x 6.35 cm	3 W
Earth Sensor	1	3.3 Kg (Including Electronics)	19 cm Dia x 17.8 cm	1.6 W
Control Electronics	1	5.5 Kg		
		25.2 Kg*		60.1 W

*Single thread design and control.

TABLE 4.3-3. STABILIZATION AND CONTROL FUNCTIONAL REQUIREMENTS

ORBIT RAISING PHASE

- Provide for initial acquisition, reorientation, reacquisition.
- Maintain attitude control to ±1.0 degree about each axis.
- Reorient vehicle as required to provide desired ΔV thrust direction.

ON-ORBIT PHASE

- Provide for antenna beam orientation ±0.2 degree in latitude and longitude; corresponding vehicle roll, pitch accuracy is ±0.035 degree; ±0.2 degree in yaw (earth referenced set).
- Provide for initial acquisition, reorientation capability.
- Provide ~ 2.14 mps/yr for E-W stationkeeping, ~ 51.5 mps for N-S stationkeeping; provide attitude control during ΔV operations.
- Counteract all environmental and thrust misalignment induced disturbance torques.
- Counteract the effects of solar pressure forces which act to perturb the orbit.

Figure 4.3-1. Typical Thrust Attitude Profile

TABLE 4.3-4. MAJOR FACTORS INFLUENCING AC&SS DESIGN
APPROACH

● Environmental Disturbance Torques

Cyclic momentum sizes momentum storage devices; secular momentum build-up rate sizes excess storage capacity (for a fixed dumping frequency) along with fuel required for dumping.

● Attitude Sensing During Orbit Raising

A versatile sensing complement is desired which can be used in both orbit raising and on-orbit modes.

● Attitude Control and Sensing During and Subsequent to Eclipse

Electric propulsion alone requires excessive energy storage (batteries); momentum storage (with appropriate sensing) alleviated the need for large acquisition maneuvers at the end of eclipse.

● Interaction Between ΔV Thrusters and Attitude Control

Disturbance torques due to ΔV thrust misalignments must be automatically compensated; simultaneous ΔV and attitude control generally required.

TABLE 4.3-5. ACTUATION ALTERNATIVES

1. Continuous control via electric propulsion	● Loss of control torque during eclipse requires reacquisition at sunrise ● Continuous computation of thrust deflection and thrust modulation commands required as a function of attitude error, desired ΔV ● Rate nulling and initial acquisition can take excessive time
2. Momentum storage with electric propulsion momentum dumping	● Allows continuous control during eclipse ● Provide redundancy — thrusters can be used as backup ● Normal mode allows (but not requires) ground computations associated with ΔV maneuvers, thruster deflections, etc., to null disturbance torques ● Momentum removal can usually be done in conjunction with ΔV maneuvers
3. Chemical propulsion with or without momentum storage	● Severe weight penalty for N-S stationkeeping ($\sim$105 Kg N_2H_2), or weight penalty for two types of propulsion ● Zero g propellant feed requires diaphragms or bladders ● Difficult to achieve small impulse bits for attitude control ● Large attitude disturbances caused by thrust misalignments — gyroscopic stiffness may be desirable

pressure, magnetic, etc.) do not provide sufficient control torques for this mission.

Continuous Control via Mass Expulsion. The use of primary (essentially continuous) control via electric propulsion is potentially attractive in that is conceptually represents the minimum complement of on-board hardware. The principal disadvantage is that the thrusters must be operated continuously, which poses a power problem during eclipse (or reacquisition at the end of eclipse), as well as requiring continuous computation of thrust levels and deflection to provide simultaneous torque and ΔV.

Primary control via a separate system, such as chemical propulsion, imposes the penalty of an additional system, or a large fuel penalty for a single system which performs both N-S stationkeeping and attitude control. Chemical propulsion also requires zero-g propellant feed diaphragms, which further increase the weight, cost and complexity. Chemical propulsion implies large torques and torque impulses, which induce correspondingly large attitude transients relative to those induced by electric propulsion. In many applications, precision pointing missions utilizing chemical thrusters such as Hydrazine (high I_{sp} compared to cold gas) require the use of gyroscopic stiffness in order to minimize attitude transients.

The disadvantages of continuous attitude control via either electric or chemical thrusters for this mission far outweigh the oversimplified (potential) advantage of minimal hardware; as a result, this alternative was rejected in favor of other alternatives after careful comparison of the respective qualitative and quantitative merits.

Momentum Storage Approach. The use of momentum storage devices (e.g., reaction wheels, CMG's, single large reaction wheel, etc.) provides a short-term attitude stabilization/attitude maneuver capability which is independent of mass-expelling thrusters. This approach permits the intermittent usage of the thrusters for momentum dumping and/or ΔV maneuvers; all or part of the computations may be performed on the ground to minimize on-board complexity.

There are two principal types of momentum storage approaches, namely, devices which store momentum with essentially zero net spacecraft momentum (reaction wheels, CMG's, etc.), and devices which store momentum while providing nonzero gyroscopic stiffness (such as momentum bias with a single large reaction wheel). For the Configuration A mission, spacecraft maneuvers are required during the orbit raising phase (see Figure 4.3-1); thus, the momentum bias approach is not attractive due to the fuel required for precession of the spin momentum or for the weight required with a large gimballed wheel. The zero momentum approach can perform these maneuvers with no fuel penalty. For this mission, low torque levels with a large momentum storage dynamic range is a requirement (no rapid maneuvers, small disturbance torques). Thus, the use of three reaction wheels is more attractive than the use of CMG's (which provide high torque with a low momentum storage dynamic range.) Momentum wheels are proven, having demonstrated long-life performance both in orbit (OAO, OGO, Nimbus, etc.) as well as over eight years of continuous operation in life testing.

The tradeoffs between chemical and electric thrusters for momentum dumping are essentially identical to those discussed previously for primary control. The high thrust/torque level and the low I_{sp} for both stationkeeping and momentum dumping, or the high weight penalty for a separate chemical system (momentum dumping only) combine to favor the use of a single electric propulsion system for both ΔV and momentum dumping functions.

Sensing Alternatives. Several attitude sensing candidates are summarized in Table 4.3-6.

Sun/Earth Sensing. Continuous use of sun and/or earth sensors represent a reasonably simple sensing concept. However, present earth sensor technology is such that accuracy on the order of 0.05 to 0.07 degree is the best attainable when used on a continuous basis at synchronous altitude. This accuracy is unacceptable unless relatively complex and sophisticated on-board filtering is used to estimate and remove bias and random errors. A more sophisticated sensor design (i.e., variable altitude edge tracking type) would be required for use during the orbit raising phase. During eclipse, the sun sensor loses its target, and reacquisition would be necessary, at least in one axis. Thus, continuous use of sun and earth sensor data does not meet mission attitude sensing objectives.

Star Sensors. Star sensors or star trackers provide more than sufficient accuracy, but at a relatively large increase in cost, weight and complexity. Either gimballed star trackers (e.g., similar in concept to those in use on OAO, etc.), or an oriented platform containing a cluster of fixed star sensors (e.g., the Hughes' STARS concept, currently under development[*]) would provide three-axis pointing information (inertial) on a continuous basis. Star acquisition, star identification and false and missing signals are difficulties typically associated with star sensors, and gyros are required to assure star acquisition; thus the on-board equipment complement is large. The vehicle orientation and star sensor location on the spacecraft make it difficult to utilize star sensing on a continuous basis during both mission phases. Although continuous star sensing/tracking will meet mission accuracy requirements, the disadvantages of cost, complexity, and inflexibility make this approach less attractive when compared to gyros updated by earth and sun sensor data.

Gyros Updated by Sun/Earth Data. Precision rate integrating gyros provide stable, continuous attitude information; however, auxiliary sensors must be provided to correct the gyros for long-term random drift effects. Earth sensors are not sufficiently accurate when utilized continuously as a primary sensing source. However, when the sun and earth data is telemetered to the ground and processed, the data is more than sufficiently accurate to update the gyros for drift once every several orbits. The ground data processing utilizes sophisticated estimation techniques (Kalman filtering) to

---

[*]IDC 4113.10.11, "Application of STARS to Precision Attitude Sensing and Control in Synchronous Orbit," by B. Klestadt, dated 2 April 1971, item 75 of Appendix B.

TABLE 4.3-6. SENSING ALTERNATIVES

1. Continuous use of Sun and Earth sensors	• Earth sensor accuracy on continuous basis not suitable (0.07 degree)
	• Loss of Sun sensor signal during eclipse requires reacquisition
	• Earth sensor use during orbit-raising requires variable altitude sensor
2. Continuous use of star sensors (STARS concept)	• Sun, Earth sensor required for initial star acquisition
	• Not usable during orbit raising due to geometry
	• Loss of torque during eclipse (no power) requires star acquisition followed by spacecraft LOS acquisition
	• To satisfy all mission phases, gyros, Sun sensor, Earth sensor, and STARS may all be required
3. Rate integrating gyros updated by Sun, Earth sensors	• Desired pointing accuracy can be achieved by using Earth sensor (or Earth and Sun sensors) only for update of gyro drift
	• Attitude error signals can be maintained during eclipse
	• Ground processing (gyro drift, etc.) minimizes onboard complexity (can be done onboard if desired)
	• Sun and Earth sensors can be used continuously as backup
	• Can be used for all mission modes — rate nulling, orbit raising sensing, on-orbit sensing

smooth noise and to remove biases. This substantially improves the raw earth sensor data by at least a factor of four or five about its single sample accuracy of 0.05 to 0.07 degree.

The gyros, earth sensors, and sun sensors are versatile and can be utilized during both mission phases. The gyros, used in a rate mode, serve to aid initial acquisition by providing spacecraft rate signals to be nulled. The gyros also provide for attitude sensing during eclipse and/or maneuvers, when sun or earth sensors may lose their targets. Available gyros have demonstrated both long life (e.g., 8×10^4 hours MTBF) and low random drift (10^{-3} deg/hr) in numerous flight applications.

The selected baseline sensing complement of gyros, earth sensors, and sun sensors combines the desired characteristics of maximum mission versatility, minimum on-board weight and complexity, and acceptable sensing accuracy for this application. These capabilities are achievable with available, flight-proven hardware elements.

Thruster Location Alternatives. The location of the 30-cm ion thrusters used during orbit raising is determined primarily by vehicle configuration and shroud constraints. As indicated in the description of spacecraft configurations A-1, the axes of the three clusters are oriented so that their nominal thrust direction passes through the vehicle center of gravity. Thus, there is no freedom for the attitude control design to influence the location or orientation of these thrusters. However, it should be noted that their thrust direction and magnitude are individually controlled so as to perform attitude maneuvers simultaneously with orbit raising.

Once on station, attitude control and stationkeeping are performed with clusters of 5 cm ion engineers. (Functionally, each cluster represents a single thruster. Multiple units are used to provide life and redundancy.) A number of possible arrangements are feasible. The tradeoffs are covered in the discussion of the electric propulsion subsystem, Section 4.4. The selected arrangements consists of 3 clusters, two are located at the south end of the vehicle (see Figure 3-1), just below the solar panel housings. The third is located on the side of the spacecraft body, at the nominal center of pressure of the solar force.

The pair of clusters at the south end of the vehicle provide the N-S stationkeeping ΔV, as well as momentum wheel dumping. Moments are generated by thrust vectoring and/or differential thrusting. The side cluster is used to offset the solar pressure constantly acting on the vehicle. Thrust magnitude control is used to compensate for any mismatch between predicted and actual solar pressure, and thrust deflection provides moments to correct for misalignment or environmental torques, and for momentum wheel dumping.

4.3.2.4 Baseline Design Description

Functional Operation. The baseline AC and SS consists of the following elements:

- 3 single-axis momentum wheels

- 3 stations of deflectable, throttleable ion engines

- 3 single-axis rate integrating gyros (strapdown)

- 1 two-axis earth sensor (fixed array)

- 1 two-axis sun sensor

- Control electronics for control logic, sensor data processing, wheel drive, etc.

- A motor, position encoder, and associated electronics to provide precision orientation of the antenna platform relative to the earth LOS.

Table 4.3-7 summarizes the functional use of these AC and SS components during the two mission phases.

Figure 4.3-2 illustrates a representative one-axis block diagram of the AC and SS subsystem. Error signals (E) generated by the gyro package (updated periodically by ground processing of earth, sun data) are processed to provide motor torque commands (T_{MC}) for each of the reaction wheels. Equal and opposite torques act on the spacecraft proper and the wheels (the wheels speed up and slow down to store the accumulated momentum due to disturbances), and their motor torques act on the vehicle so as to keep the error signals small in each axis in a closed loop fashion. Wheel speed is monitored (by a tachometer), and momentum is removed by commanding appropriate torques from the electric thrusters whenever a speed threshold is exceeded. In this manner, the wheel momentum storage capacity (wheel size, weight) is kept to a minimum while still maintaining short term control capability/stability independently of the electric thrusters.

Figures 4.3-3 and 4.3-4 illustrate the relative geometry of the spacecraft, orbit, and earth in each of the two mission phases. During the on-station phase, the No. 3 axis is normal to the orbit plane, and the antenna is rotated at one revolution per orbit (rpo) to maintain earth LOS, for a desired thrust vector in the orbit plane local vertical. The spacecraft is maneuvered to vary the in-plane and out of plane ΔV components during this mission phase.

During the orbit raising, the reaction wheels provide the required spacecraft maneuvers to orient the thrust direction of the cluster of 30-cm ion engines. The orientation profile is stored as a function of time (updated periodically) with the rate integrating gyros providing the attitude reference for these maneuvers. Earth and sun sensor data is processed on the ground

TABLE 4.3-7. SUMMARY OF BASELINE DESIGN APPROACH

	Orbit Raising Usage	On-Station Usage
Actuators		
3 Reaction Wheels	• Provide momentum storage • Perform acquisition and reorientation maneuvers as required	• Provide momentum storage • Perform acquisition and reorientation maneuvers as required
3 Electric Propulsion Stations, 2 Deflectable	• Vernier control (if necessary) — Primary mode is vector control of orbit raising complement	• Momentum dumping • E-W, N-S stationkeeping • Torque augmentation during ΔV maneuvers • Backup attitude control during failure mode
1 Motor/Encoder Set to Provide Precise Antenna Orientation (about 3 axis)	• Preprogrammed as required by spacecraft for proper ΔV positioning and/or thermal control	• Automatic "despin" of antenna at 1 rpd for precise earth pointing
Sensors		
3 Strapdown Rate/Rate Integrating Gyros	• Null separation rates (rate mode) • Initial acquisition after separation • Primary attitude reference (periodically updated)	• Initial acquisition • Primary attitude reference (updated by earth, sun data) • Attitude reference during loss of sun
Two-Axis Precision Sun Sensor	• Update gyro reference (2 axes) • Backup control sensor in event of gyro failure	• Update gyro reference (2 axes) • Backup control sensor in event of gyro failure
Two-Axis Earth Sensor	• Periodically update gyro for drift	• Periodically update gyro reference for drift • Backup control for gyro failure
Control Electronics Wheel Drive Electronics Sensor Processing Electronics Thruster Logic Electronics Antenna Positioner Electronics	• Provides all electronic functions for thruster actuation, wheel drive, etc.	• Provides all electronic functions for thruster actuation, wheel drive, etc.
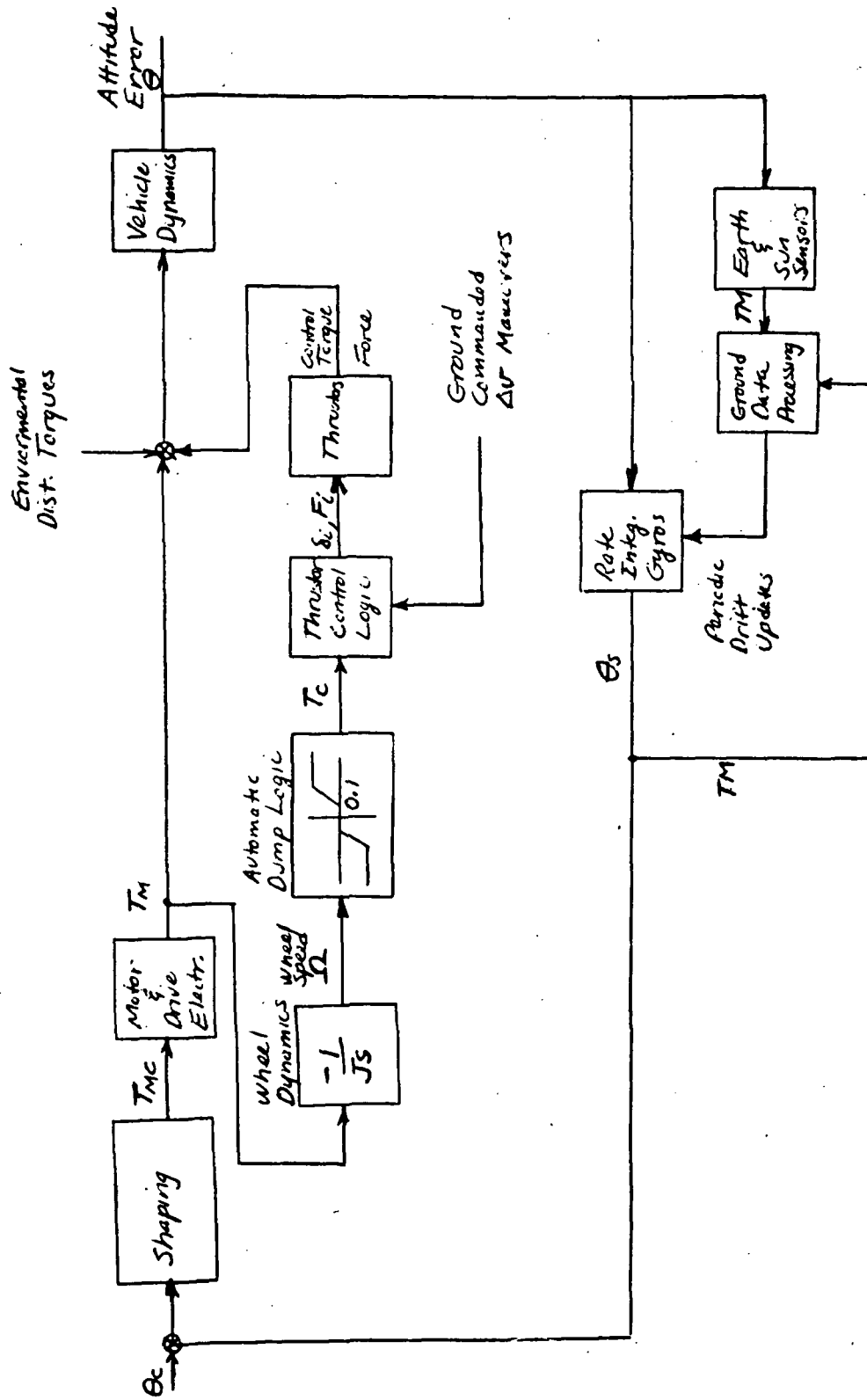
Figure 4.3-2. Representative Single Axis Functional Block Diagram

COORDINATE DEFINITION

FINAL SYNCHRONOUS ORBIT
GEOMETRY - A CONFIGURATION
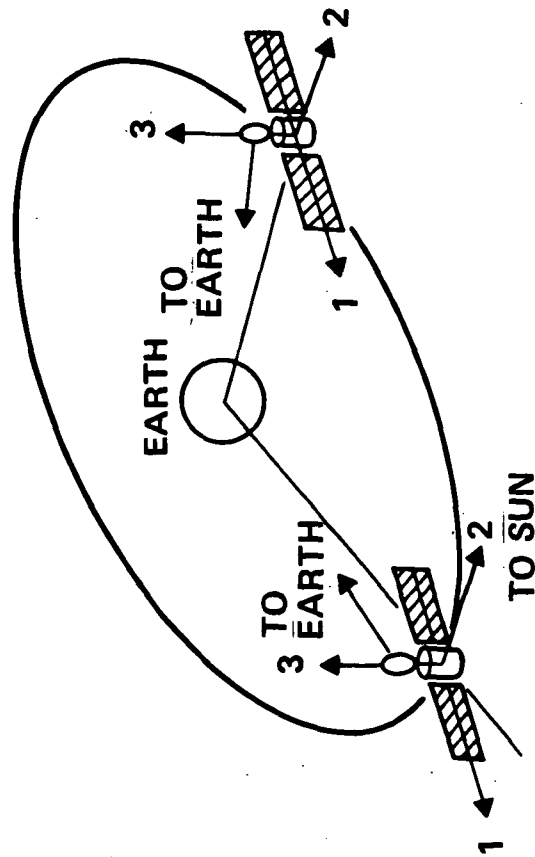
Figure 4.3-3. Representative Geometry of
Spacecraft in Final Synchronous Orbit

ORBIT RISING GEOMETRY AND
"B" CONFIGURATION "ON-STATION"
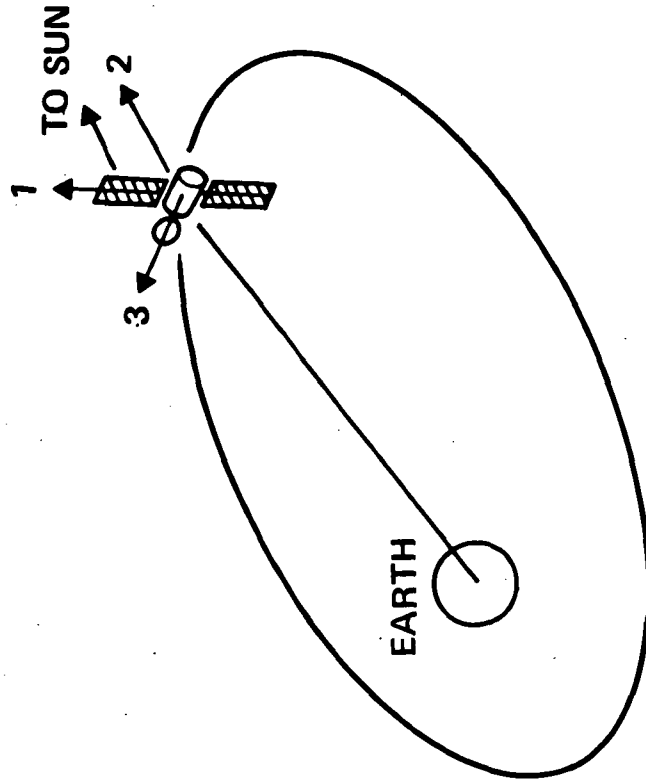
Figure 4.3-4. Representative Geometry of
Spacecraft During Orbit Raising Phase

4.3-14

and used every several orbits to command gyro drift updates (the ±1 degree pointing accuracy does not make this a frequent operation). Earth sensor data is taken in the vicinity of apogee in order to utilize a sensor with a small altitude range.

During thrusting, the thrust direction is vectored to counteract misalignments, disturbance torques, etc. This is accomplished by automatically commanding more expulsion torques (thrust deflection angles) proportional to wheel speeds above a small threshold (~ 0.1 maximum wheel speed). In this way, the wheel size is minimized without compromising the short term control capability (maneuverability) of the momentum wheel approach.

The wheel size requirements for the orbit raising phase are based upon the maximum expected environmental disturbance torques and the ability to operate for up to two hours around perigee without unloading.

On-station the operation of the AC and SS is somewhat similar to the orbit raising phase. Based upon tradeoffs of thruster location, fuel utilization efficiency, thruster duty cycle, etc., the ΔV and momentum operations using the smaller (5 cm) thrusters are performed on an intermittent basis. The attitude reference is still provided by the gyro package, updated every several orbits for drift correction by ground processing (smoothing) telemetered sun and earth sensor data.

The orientation of the three clusters of 5 cm electric thrusters on the spacecraft is illustrated in Figure 4.3-5. The two sets whose thrust axis is parallel to the No. 3 axis ("N-S" thrusters) provide N-S stationkeeping and all three axes of attitude control (momentum dumping) torque during the $\sim 1/6$ duty cycle of operation (±30 degrees about nodal crossing).

During this time, thrust deflections and/or differential throttling are commanded to, 1) continuously reduce wheel momentum (above 10 percent maximum wheel speed), 2) counteract the solar pressure force, and 3) generate the N-S ΔV. During the remaining 5/6 of the orbit, the thruster along the No. 2 axis is operated intermittently to counteract solar force ($\sim 1/8$ duty cycle), to dump accumulated momentum about the No. 1 and No. 3 axes ($\sim$ five times per orbit), and to provide E-W stationkeeping. The majority of the accumulated momentum is about the No. 1 and No. 3 axes. Should momentum accumulate about the 2 axis, the "N-S" thrusters are utilized for a short time for dumping. During this portion of the orbit, momentum dumping is not continuous, but occurs at a fixed wheel speed threshold (~ 80 percent of maximum wheel speed), and the logic is such that the wheel is driven to near the opposite threshold (e.g., $+0.8\ \omega_{max}$ goes to $-0.7\ \omega_{max}$). This approach minimizes required wheel size by taking advantage of the predominantly secular nature of the principal environmental disturbance, torque due to solar pressure.

Design and Performance Analysis

Environmental Disturbance Torques. The disturbance torques due to interactions of the vehicle with ambient fields dictate the momentum storage
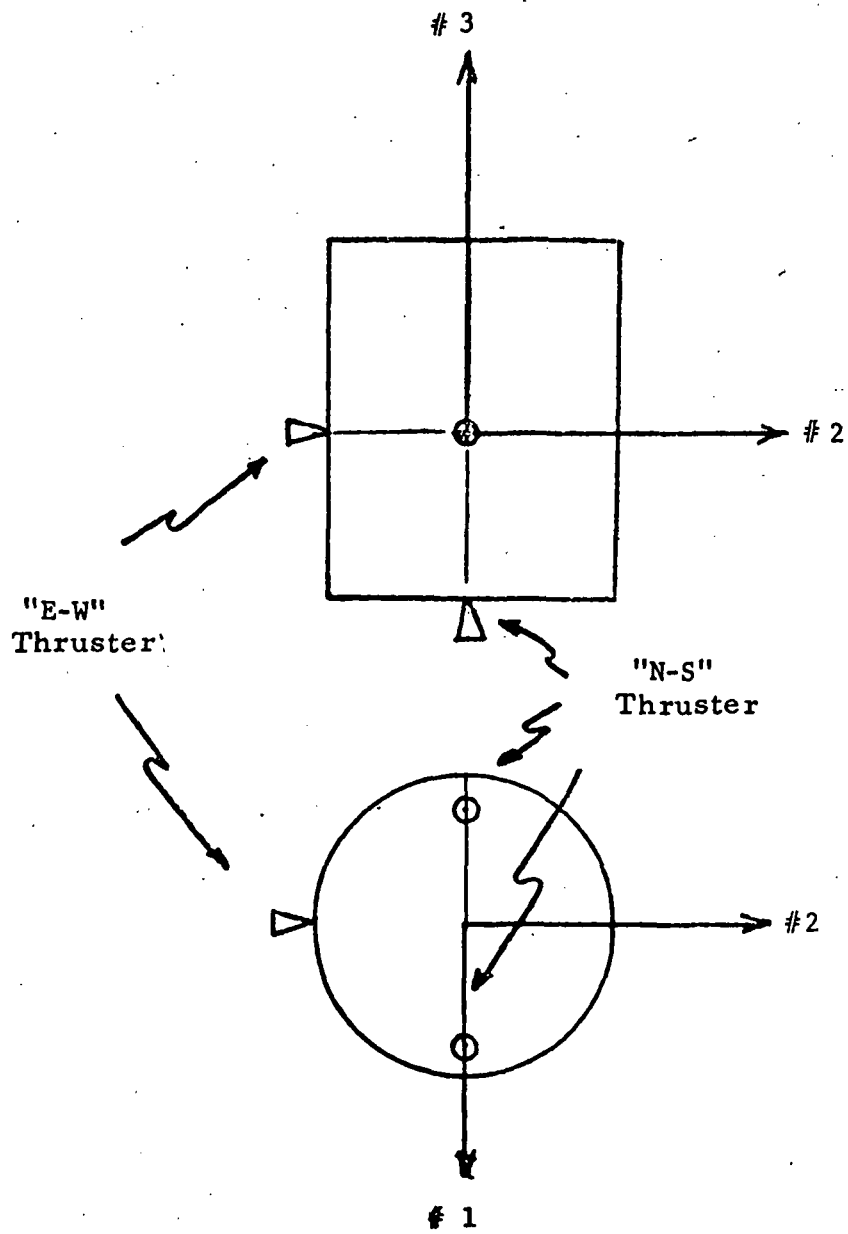
Figure 4.3-5. Location of "N-S" and "E-W" Thruster
on Spacecraft

and removal requirements for the system. The principal environmental disturbance torques are the following:

- Solar radiation pressure

- Gravity gradient

- Aerodynamics

- Magnetic field interactions

Other sources such as electric field interactions, outgassing, radiated antenna power torques, etc., are small by comparison to the principal effects listed above.

Representative values of the torques from each source were computed using the geometry of Figures 4.3-3 and 4.3-4, along with vehicle mass properties, inertias, etc. These torque values are summarized in Table 4.3-8 for the two mission phases. The torques are presented in body axes; these axes are nominally inertial (one rotation per year) for the on-station phase,

TABLE 4.3-8. ENVIRONMENTAL DISTURBANCE TORQUE SUMMARY

Source	T_1 (newton-meters)	T_2 (newton-meters)	T_3 (newton-meters)
A. ORBIT-RAISING			
Solar Pressure	1.44×10^{-4}	12.5×10^{-6}	12.5×10^{-6}
Aero (300 nm)	*	4.6×10^{-4}	*
Grav. Grad.	*	*	2.3×10^{-4}
Magnetic (1 amp-turn-ft^2)	*	4.47×10^{-6}	4.47×10^{-6}
B. ON-STATION			
Solar Pressure	1.44×10^{-4}	*	12.5×10^{-6}
Aero	*	*	*
Grav. Grad.	*	*	3.66×10^{-5}
Magnetic (1 amp-turn-ft^2)	2.04×10^{-8}	2.04×10^{-8}	*
*Small by comparison with other sources and/or components.			

and non-inertial during the orbit raising phase. Since momentum is removed essentially continuously during orbit raising, the slow motion of these axes may be neglected for approximate computation of momentum storage/removal requirements during this phase.

During orbit raising, the peak torques in the vicinity of perigee (550 km assumed) are the same order magnitude about each axis. Both gravity gradient torques and aerodynamic torques fall off rapidly with time as altitude increases, as illustrated in Figures 4.3-6 and 4.3-7. Accounting for this effect, the required momentum storage in each axis for two hour storage around perigee is summarized in Table 4.3-9. A 50 percent design margin is included to account for uncertainties in vehicle properties, attitude errors, maneuvers, etc.

During the on-station phase, the principal disturbing torque source is solar pressure, which is predominantly secular; a small cyclic component exists about the No. 1 axis due to variation in the sun projected area of the antenna over the orbit. The primary secular torque is about the No. 1 axis, with a smaller torque about the No. 3 axis due to assymetries in panel projected area and center of pressure shift (thermal bending, sun angle variation, etc.) Since momentum is dumped intermittently, except during N-S stationkeeping, the accumulated momentum must be stored for several hours or more to minimize the duty cycle of the "E-W" thruster. The baseline design assumes a four hour average period, with a biased removal logic such that the momentum is accumulated from peak to peak wheel capacity rather than from zero to peak.

Table 4.3-9 summarizes the wheel storage requirements for the on-station phase. Evaluation of these requirements (both phases) and available off the shelf units resulted in the selection of three identical wheels in each axis, each with a peak momentum storage capability of ± 1.59 newton-m-sec at 1250 rpm. This preliminary selection accommodates expected disturbances with a reasonable design margin.

Thruster Duty Cycle, Deflection, and Throttling Requirements. The use of the 5-cm electric thrusters to provide both attitude control torques and stationkeeping results in requirements for thrust throttling, thrust deflection, and thrust duty cycling. The nominal thrust level for each thruster is 4×10^{-3} newtons, and the deflection capability is ± 10 degrees. The following paragraphs summarize the development of the thruster usage requirements for the various on-station torque and ΔV requirements.

For N-S stationkeeping, two thrusters are utilized over approximately 1/6 of the orbit, centered about one nodal crossing, to provide effectively 51 mps/year at an average thrust level of 3.8×10^{-3} newton for each thruster. The thrusters are offset and canted relative to the No. 1 and No. 3 plane such that nominally both the solar force ($\sim 10^{-4}$ newton) and the solar torque ($\sim 10^{-4}$ newton meter) are cancelled; this geometry is illustrated in Figure 4.3-8. The expressions which determine the cant angle (θ_c) and the thruster offset (r_2) are
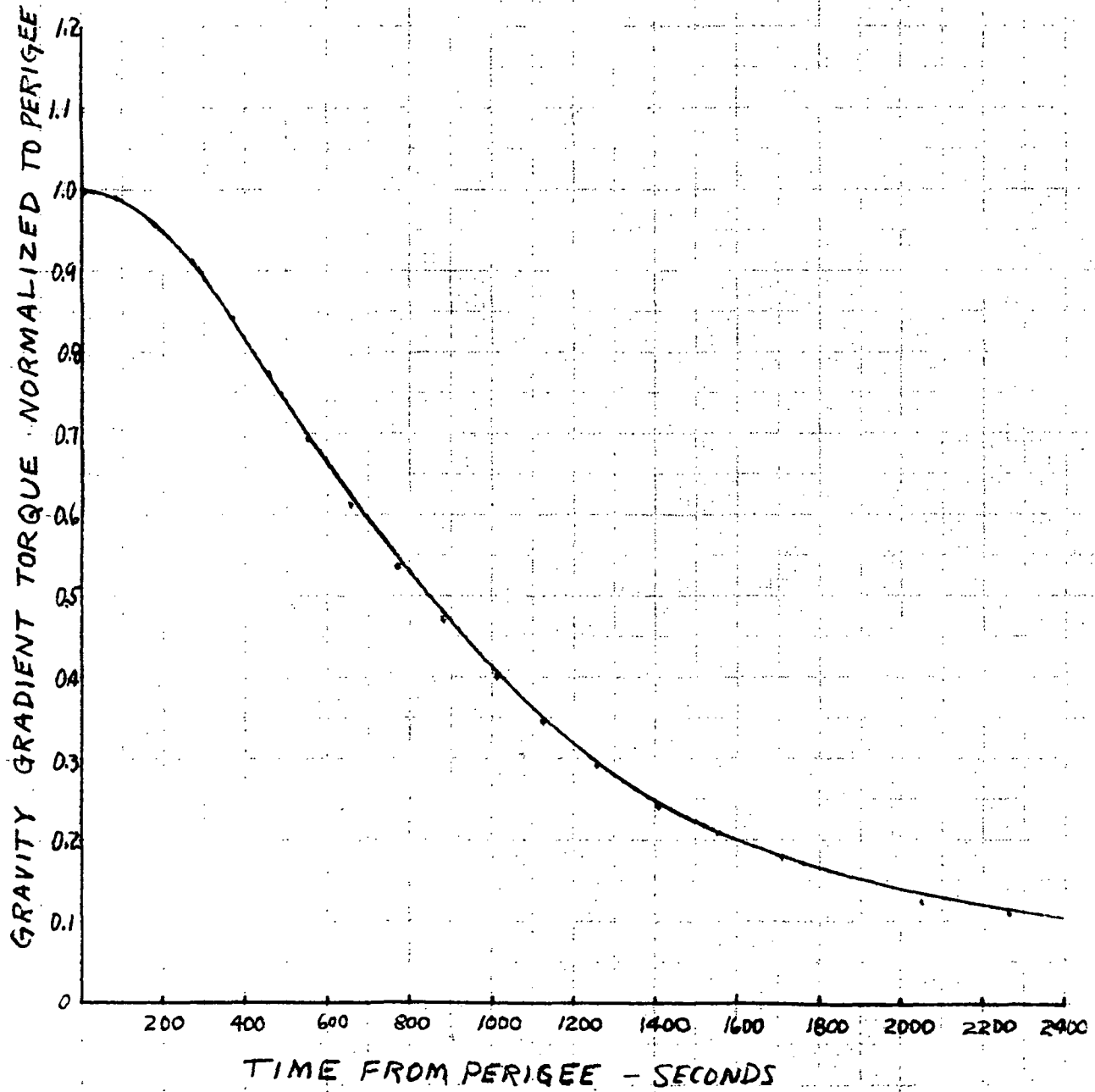
Figure 4.3-6. Normalized Gravity-Gradient Torque
vs Time from Perigee
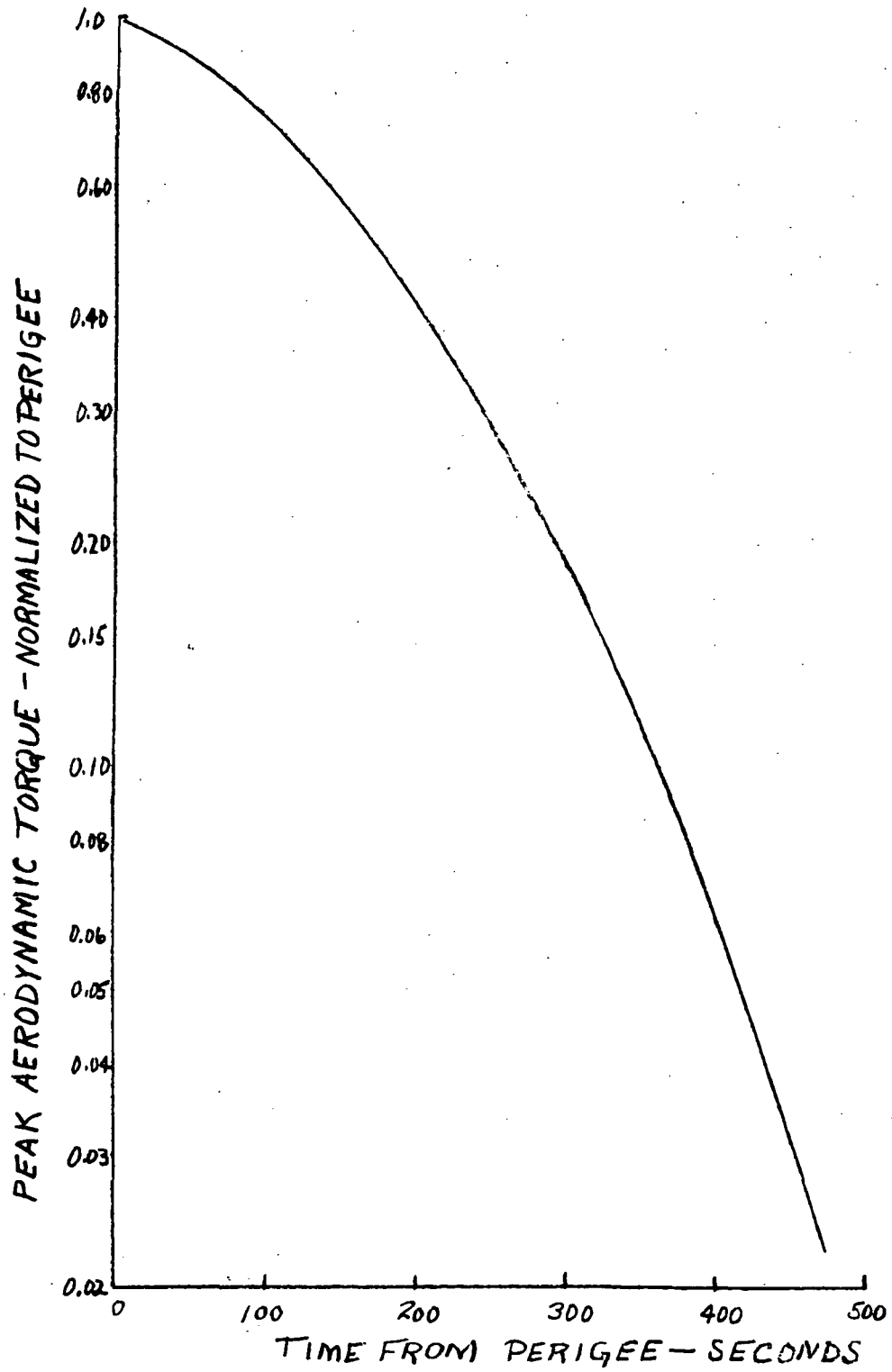
Figure 4.3-7. Normalized Aerodynamic Torque
vs Time from Perigee

TABLE 4.3-9. MOMENTUM STORAGE REQUIREMENTS

	No. 1 Axis Wheel (newton-meter-sec)	No. 2 Axis (newton-meter-sec)	No. 3 Axis (newton-meter-sec)
A. Orbit-Raising Phase (two hour accumulation, 1 axis normal to orbit plane)			
Solar Pressure	1.03	0.0894	0.0894
Aero-dynamics	—	0.274	—
Gravity Gradient	—	0.274	0.507
Magnetic	—	0.0095	0.0095
Sum	1.03	0.372	0.606
50% Margin for Maneuvers, etc.	0.516	0.186	0.303
Approximate Storage Req'mt.	1.55	0.558	0.909
B. On-Station Phase (4 hour accumulation with biased removal)			
Solar Pressure	±1.03	—	±0.0894
Aero-dynamics	—	—	—
Gravity Gradient	—	—	±0.263
Magnetic	—	—	—
Sum	±1.03	—	±0.352
50% Margin	±0.516	—	±0.176
Approximate Storage Req'mt.	±1.55	—	±0.528
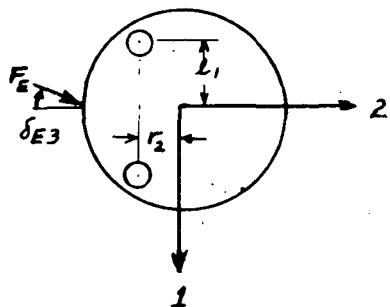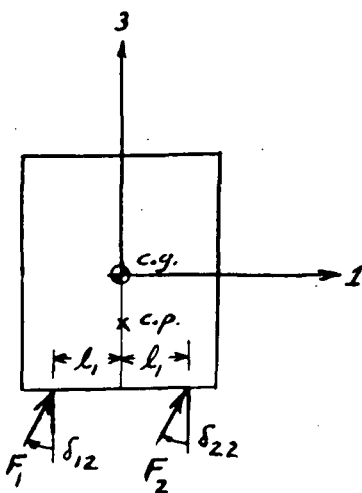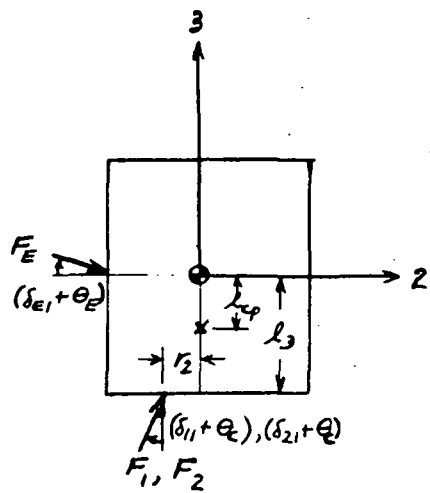
Figure 4.3-8. Thruster Deflection Geometry for Force and Torque Generation

$$\theta_c = \sin^{-1}\left(\frac{f_s}{F_1 + F_2}\right) = \sin^{-1}\left(\frac{0.1}{1.8}\right) = 3.24 \text{ degrees}$$

and

$$r_2 = (\ell_3 + \ell_{cp}) \tan \theta_c = 0.055 \text{ m.}$$

where

f_s = solar pressure force $\cong 4.45 \times 10^{-4}$ newton[*]

$F_1 + F_2$ = net thrust $\cong 8 \times 10^{-3}$ newton[*]

ℓ_3 = thruster to c.g. along No. 3 axis $\cong 1.3$ meter[*]

ℓ_{cp} = effective cp-cg offset $\cong -0.3$ meter[*]

The (linearized) expression, during N-S stationkeeping, defining torque and force in any direction are as follows:

1 axis
$$\begin{cases} f_1 \cong F_1 \delta_{12} + F_2 \delta_{22} \\ T_1 = F_1 (\delta_{11} + \theta_c) + F_2 (\delta_{21} + \theta_c) \ell_3 - (F_1 + F_2) r_2 \end{cases}$$

2 axis
$$\begin{cases} f_2 \cong F_1 (\delta_{11} + \theta_c) + F_2 (\delta_{21} + \theta_c) \\ T_2 \cong -(F_1 \delta_{12} + F_2 \delta_{22}) \ell_3 + (F_1 - F_2) \ell_1 \end{cases}$$

3 axis
$$\begin{cases} f_3 \cong F_1 + F_2 \\ T_3 \cong \left[F_1 (\delta_{11} + \theta_c) - F_2 (\delta_{21} + \theta_c)\right] \ell_1 + (F_1 \delta_{12} + F_2 \delta_{22}) r_2 \end{cases}$$

The torque capability in each axis, for a maximum thrust deflection of 10 degrees, assuming no thrust modulation, is as follows:

$$\Delta T_1 \text{ (max)} = \pm 1.83 \times 10^{-3} \text{ newton-meter}$$

$$T_2 \text{ (max)} = \pm 1.83 \times 10^{-3} \text{ newton-meter}$$

$$T_3 \text{ (max)} = \pm 0.91 \times 10^{-3} \text{ newton-meter}$$

---

[*]Representative values for configuration A-1.

These torques can be increased, if desired, by including thrust modulation (at the expense of some additional torque force coupling) however, thrust modulation is not essential. The control torque margin is seen to be over 13 to 1 in the worst case (No. 1 axis — Table 4.3-8).

During the 5/6 of the orbit period when N-S stationkeeping is not taking place, the "E-W" thruster (located on the minus No. 2 axis) operates at a duty cycle of about 1/8 to provide solar force balance, and about 1/70 for E-W stationkeeping. It also provides control torque about the No. 1 and No. 3 axes for momentum dumping. (The N-S thrusters must be used occasionally for dumping about the No. 2 axis.) This thruster (E-W) will be canted downward in the No. 2 - No. 3 plane such that the preprogrammed solar force thrustings also nominally cancel solar torque. Referrring to Figure 4.3-8, the cant angle is

$$\theta_{ec} = \sin^{-1}\left(\frac{f_s \ell_{cp}}{F_E \ell_2}\right) \frac{(10^{-4})(57.3)}{(0.9 \times 10^{-3})(2.4)} = 2.65 \text{ degrees}$$

The maximum control torque authority during this mission phase, δ_{max} (thrust deflection) = 10 degrees, is as follows:

$$\Delta T_1 \text{ (max)} = 1.02 \times 10^{-3} \text{ newton-meter}$$

$$T_2 \text{ (max)} = 1.83 \times 10^{-3} \text{ newton-meter}$$

$$T_3 \text{ (max)} = 1.02 \times 10^{-3} \text{ newton-meter}$$

The torque margin with the E-W thruster is over 7 to 1 in the worst case (No. 1 axis, Table 4.3-8).

Programmed inputs for the thruster forces (f_1, f_2, f_3) are computed on the ground and stored onboard for several orbits. The onboard computations for torque are automatic, and account for either zero or nonzero thrust commands. Torques can also be commanded from the ground in a backup mode. Nominally, with the canted thrusters, most of the on-station momentum dumping is performed in conjunction with stationkeeping, and is essentially "free" in terms of fuel consumption. A representative fuel budget is given in Table 4.3-10 for on-station operation. It is conservative in that momentum dumping fuel is separately added.

Hardware Implementation. Characteristics of the hardware elements which comprise the AC and SS subsystem are summarized below. All of the items described are available as off the shelf units requiring essentially no development (the onboard electronics package is, however, a special design, as in most missions). These elements represent a preliminary baseline selection. In most cases, the specific elements described are representative of several available candidates which could satisfy mission requirements.

TABLE 4.3-10. REPRESENTATIVE FUEL BUDGET (ON-STATION)

Source	Annual Requirement	Total Mission Requirement	Total Fuel Weight**
North-South Station-Keeping	54 mps*	270 mps	4.9
East-West Station-Keeping	2.14 mps	10.7 mps	0.18
Solar Force Compensation	19.2 mps	96 mps	1.77
Momentum Dumping	23..6 mps	118	2.18
Total	98 mps	496 mps	10 Kg Hg

*Includes $\sin\theta/\theta$ inefficiency for thrust over ± 30 degrees about nodal crossing.

**$m \cong 730$ Kg, average $I_{sp} = 4100$ sec

Momentum Wheels. The characteristics of the Bendix Advent Reaction Wheel, Type 1786070, are summarized in Table 4.3-11. This unit is one of a class of wheels which have been developed, tested and flown on spacecraft such as OGO, Nimbus, OAO, etc. The selected unit has a momentum storage capability of 1.6 n.m. at 1250 rpm; this is sufficient to meet the mission requirements (see Table 4.3-9). Its weight is 3.46 Kg. The variation of wheel weight versus wheel inertia (momentum storage capability) is illustrated in Figure 4.3-9 for wheels of this class. It is evident that there is a strong incentive to minimize wheel storage capacity.

The wheel is hermetically sealed but is designed to operate in the event the seal fails. It is filled with 98 percent helium and 2 percent oxygen at one-half atmospheric pressure to minimize lubricant depletion and to ensure cleanliness. The bearing lubrication design utilizes labyrinth seals and provides sufficient lubricant even in the event of loss of hermetic sealing. The bearings are 440C modified stainless steel, and are the deep groove inch series of the finest grade available. These designs have demonstrated very high reliability in test and in space — no OGO wheel failures have occurred in over four years of orbital life, and life tests have experienced no failures, with two OGO units still running after approximately eight years of operation.

The inside-out, two phase AC motor design is similar to a squirrel cage induction motor, eliminating the need for brushes or sliprings. The squirrel cage rotor is assembled as part of the flywheel or rotating member

TABLE 4.3-11. REACTION WHEEL DESIGN AND PERFORMANCE CHARACTERISTICS

General

Momentum at 1250 rpm	1.59 newton-meter-sec
Rotating Inertia	3.8 Kg cm^2
Unit Weight	3.45 Kg
Size	16.5 cm O.D. x 7.6 cm high
Mounting	4 lug, flat side heat sink
Temperature Range	283°K to 320°K

Motor

Stall Torque	$\geq$0.028 newton-meters
Total Stall Power	9.5 watts
Power Required	26 V, 400 Hz, 2 phase at 90°
Speed-Torque Linearity	20% minimum
Synchronous Speed	1500 rpm

Tachometer

Excitation	Permanent magnet
Tachometer Output (2 cycle/rev.)	4 volts/1000 rpm
Circuit Load per Phase	$\geq10^4$ ohm
Two-Phase Output	90 deg phase relationship
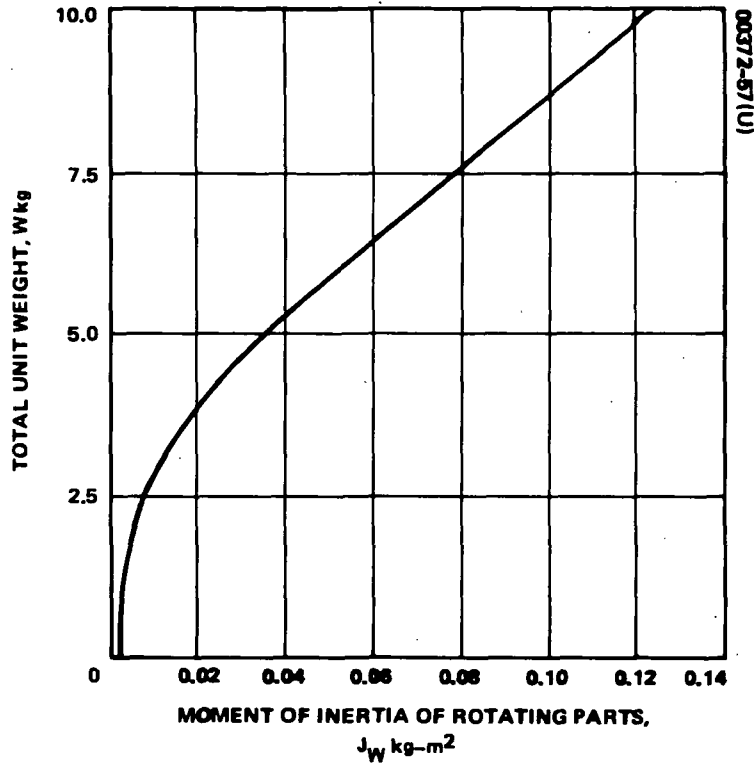
Figure 4.3-9. Momentum Wheel Weight
vs Rotating Parts Inertia

and its resistance is varied to produce the desired torque speed character-
istics. A torque characteristic which is essentially constant over the operat-
ing speed range is desirable and can be obtained since control authority is
required at any momentum level.

The two control phase windings of the motor are assembled as part of
the stationary member and are well insulated to completely isolate one from
the other. The remaining parts of the stationary member are constructed to
be lightweight but stiff, and provide a heat sink surface as well as the her-
metically sealed enclosure.

A design feature which may be incorporated, enhance reliability is
the use of brushless DC motors rather than the AC motor in the present unit
(recent vendor designs have incorporated this feature for other proposed
applications). These drive motors include a degree of redundancy via dual
windings, either of which can provide up to 70 percent of the rated torque.

Rate Integrating Gyros. Table 4.3-12 summarizes the design charac-
teristics of the Northrop Electronics Model G1-T rate integrating gyro. This
is an existing unit which has been employed primarily in the Minuteman Guid-
ance System.

TABLE 4.3-12. RATE INTEGRATING GYRO DESIGN AND PERFORMANCE SUMMARY

Volume	9 cm^3
Weight	1.59 Kg
Power	
Wheel (Running)	≤7.5 watts
Thermal Control Heater	≤3.5 watts average (5 W max)
Angular Momentum	1.85 x 10^6 gm-cm^2/sec
MBTF	80,000 hr
Drift Rates	
Non-g Sensitive*	0.1 deg/hr
Random	0.001 deg/hour (1σ)
Elastic Restraint	0.0003 deg/hr per sec about input axis
g-Sensitive (Trimmed)	<0.1 deg/hr/g
g^2-sensitive	<0.1 deg/hr/g^2
Motor Voltage	0.005 deg/hr/volt
Gyro Scale Factor	14 volts/rad
Torquer	
Max Command Rate	350 deg/hr
Scale Factor	5 deg/hr/ma
Linearity	<0.01 percent
Environment (Operating)	
Vibration	15 g (20-2000 Hz)
Acceleration	20 g
Shock (11 ms)	50 g

*Biased out by in-orbit calibration

The gyro unit derives its high performance (≤ 0.001 deg/hr-1σ random drift rate) from several unique construction features:

- Taut wire suspension on output axis

- Thermally symmetrical construction

- Fine mass unbalance adjust mechanism

- Highly stabilized and linear DC permanent magnet torquer

- Extremely stable hydrodynamic gas bearing proven under more than 2000 start-stop cycles and over drive to four times nominal rotor speed.

The gyros are hard-mounted to a common heat sink by means of a rigid support structure with builtin thermal impedances, thereby minimizing control heater power requirements. At maximum heat sink temperature, the 5-watt heater (per gyro) would have a maximum duty cycle of 10 percent; at minimum heat sink temperature, the maximum duty cycle is 70 percent (average power ≤ 3.5 watts).

The electronics for power conditioning, signal processing, and thermal control are included within the Hughes-supplied control electronics package. Periodic drift calibrations result in bias currents which are summed with command currents (representing ~ 1 rpo pitch rate) and pickoff voltage derived currents, which compensate for the small but known output axis restraint.

Attitude Sensors. The design characteristics of the earth and sun sensors are summarized in Table 4.3-13. The outputs of these devices are telemetered to the ground where they are processed and used to provide periodic commands to update gyro random drift. Both units are existing, qualified designs, and each provides two-axis sensing information.

The Quantic earth sensor uses a fixed thermocouple detector array and contains no moving parts. The sensor is designed to operate in a narrow band (± 370 Km) around synchronous altitude. It provides ± 0.05 to ± 0.07 degree accuracy and can be used with degraded accuracy over the altitude range of 30,000 Km to 40,000 Km. The sensor is located near the top of the antenna reflector (Figure 3-1).

The sun sensor also contains no moving parts and is mounted on the main portion of the spacecraft along with the wheels, electronics, gyros, and thrusters. It provides ~ 30 arc sec accuracy (~ 0.01 degrees), and is manufactured by the Adcole Corporation. This device is considerably more accurate than is required, and consideration could be given to lower accuracy devices utilizing silicon cells.

TABLE 4.3-13. ATTITUDE SENSOR DESIGN CHARACTERISTICS

Quantic Earth Horizon Sensor	Adcole Sun Sensor
Accuracy, ±0.07 degree	Accuracy, ±0.5 arcminute
Range pitch and roll, ±5 degrees	Field of view, ±5 degrees
Acquisition range, ±22 degrees	Power, 3 watts
Field of view, ±13.7 degrees	Size
Output time constant, 1.5 second	Sensor, 5.16 x 7.6 x 6.35 cm
MBTF = 533,000 hour	Electronics, 5.16 x 15.2 x 6.35 cm
Power, 1.6 watts	Weight
Size, 19 cm dia. x 17.8 cm	Sensor, 0.36 Kg
	Electronics, 1.0 Kg
Weight, 3.27 Kg	

Attitude Control Electronics. The attitude control electronics contains the logic and processing to perform the following functions:

- Wheel drive control

- Telemetry sensor processing

- Generation of gyro and wheel torque commands

- Thruster control logic (deflections, etc.)

- AC and SS telemetry and command functions

These functions are similar to those on other Hughes spacecraft, and the weight, power, and size estimates for the electronics unit, as listed in Table 4.3-2 were derived from scaling of similar units from other designs.

4.3.3 Attitude Control and Stationkeeping — Configuration B & C

4.3.3.1 Summary

The AC and S subsystems for Configuration B and C are similar to that for Configuration A in that momentum storage with mass expulsion momentum removal is included in all three baselines.

In Configurations B-1 and B-5, the ion engines are replaced by eight 0.44 N hydrazine thrusters (plus eight redundant thrusters) to perform ΔV and momentum dumping functions. Since the solar panels are oriented in a

N-S direction in the B baseline configurations, the principal disturbance torque (solar pressure) is cyclic rather than secular (as in Configurations A and C). For this reason, a larger wheel is used in one axis (solar panel axis) to accommodate cyclic momentum variations without dumping, thereby minimizing fuel consumption.

The wheel dumping logic for Configuration B is somewhat more complicated than for Configurations A and C, since the torque level is several orders of magnitude larger. Torque pulses for momentum unloading must be small, and spaced so that the resultant attitude transients do not exceed tolerances. The larger torque and acceleration levels also result in somewhat a greater susceptibility to problems due to interactions with the flexible dynamics of the solar array.

The sensing complement for Configuration B is identical to that for Configurations A and C.

Two of the three wheels are identical to those for A. The fuel load for Configuration B is substantially greater than for either A or C due to the much lower specific impulse obtainable in chemical propulsion systems.

Configuration C is merely a scaled up version of Configuration A, and the disturbance torques, momentum storage requirements, etc., scale accordingly. The baseline design for Configuration C therefore incorporates larger momentum wheels, and requires a greater fuel load for ΔV maneuvers and momentum dumping. The sensing complement for C is identical to that for A and B.

4.3.3.2 Functional Requirements

The functional requirements listed in Table 4.3-3 for Configuration A-1 are equally applicable to Configurations B and C.

4.3.3.3 Design and Implementation Tradeoffs

The design and implementation tradeoffs which were examined for Configuration A for the most part apply also to Configurations B and C. The use of momentum storage with mass expulsion momentum removal provides continuous stability and control during all mission modes and mission phases. Versatility and backup redundancy is inherent in both the sensing baseline (gyros periodically updated by sun, earth sensors) and the actuation baseline (wheels with momentum removal).

Configuration C is a larger version of Configuration A. The mission modes, etc., are identical. The desire to select an AC and SS implementation which can be used in all mission phases was a strong factor in the selection of the baseline approach, as it was for Configuration A.

The N-S orientation of the solar array plus the absence of an orbit raising mission phase for Configuration B resulted in the momentum bias stabilization approach (see actuation alternatives under Section 4.3.2.3)

becoming a more attractive candidate than it was for A or C. The gyroscopic stiffness of such an approach reduces pointing errors resulting from the larger control torques of the chemical thrusters (several orders of magnitude greater than for A or C). Nevertheless, momentum bias was finally rejected for Configuration B since the spaced pulse approach for momentum dumping proved to be reasonable with the baseline wheel sizes. In addition, the momentum bias wheel size necessary to accommodate the (cyclic) solar pressure disturbance torques within required pointing accuracy (spin axis drift) proved to be excessive unless frequent momentum removal via the thrusters took place. Thus, momentum storage wheels were selected for Configuration B as well as for Configuration A and C.

4.3.3.4 Baseline Design Summary

The baseline AC and CSs for Configurations B and C is summarized as follows:

	Configuration B	Configuration C
Actuation	• 3 single-axis momentum wheels	• 3 single-axis momentum wheels
	• Eight 0.44 N hydrazine thrusters	• 3 stations of deflectable ion engines
Sensing	• 3 single-axis rate integrating gyros	• 3 single-axis rate integrating gyros
	• 1 two-axis sun sensor	• 1 two-axis sun sensor
	• 1 two-axis earth sensor	• 1 two-axis earth sensor
Electronics	• 1 set of control electronics for wheel drive, sensor processing, jet selection and firing logic, etc.	• 1 set of control electronics for wheel drive, sensor processing, thruster control, etc.
Antenna Control	• Fixed antenna, no separate control required	• Single axis drive (motor, encoder, electronics, etc.) to orient panel to earth LOS

Geometry. The geometric relations of the orbit, spacecraft and earth for Configuration B is illustrated in Figure 4.3-10. The geometry for Configuration C is the same as that of Configuration A, shown in Figures 4.3-3 and 4.3-4. Configuration B is injected directly into synchronous orbit (via an apogee motor) and therefore does not experience an orbit-raising mission phase. During transfer orbit, the vehicle is spin stabilized. After apogee motor fire, the vehicle is despun (yo-yos), attitude acquisition and solar
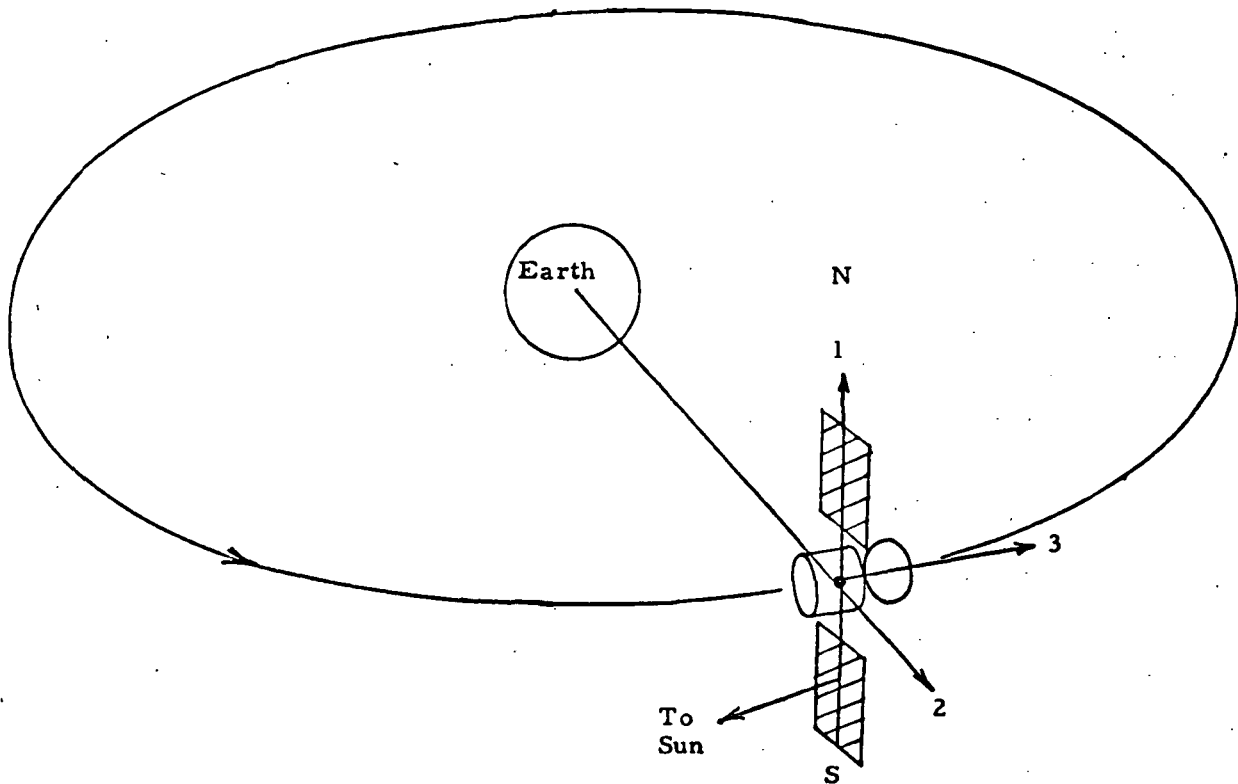
Figure 4.3-10. Representative Geometry — Configuration B

panel deployment takes place, and the mission begins. The antenna is fixed relative to the spacecraft and the solar panel array is unfurled about the No. 1 axis for sun pointing.

Configuration C arrives on station after an orbit raising phase of approximately three months. During this phase, the solar panels are oriented N-S (nominally), and the panel array is oriented to the sun by its control system. In synchronous orbit, the No. 3 axis is N-S, and the antenna must be rotated about this axis to point to the earth. The solar panels could be fixed, but are normally oriented about the No. 1 axis to compensate for the ±23.5 degree sun angle variation over a year.

Functional Operation. The single axis block diagram of Figure 4.3-2 represents the closed loop utilization of the various elements, just as described for Configuration A-1. In Configuration B, the logic for the selection of thrust deflection angle and thrust level is replaced by logic to select the appropriate thruster and thrust duration (pulse length and spacing).

Thruster Configuration. Figure 4.3-11 illustrates the nominal thruster locations for Configurations B-1 or B-5. The N-S thrusters are individually pulsed for momentum dumping while both are fired continuously for N-S stationkeeping. Intermittent turnoff of one jet permits dumping during N-S

4.3-33
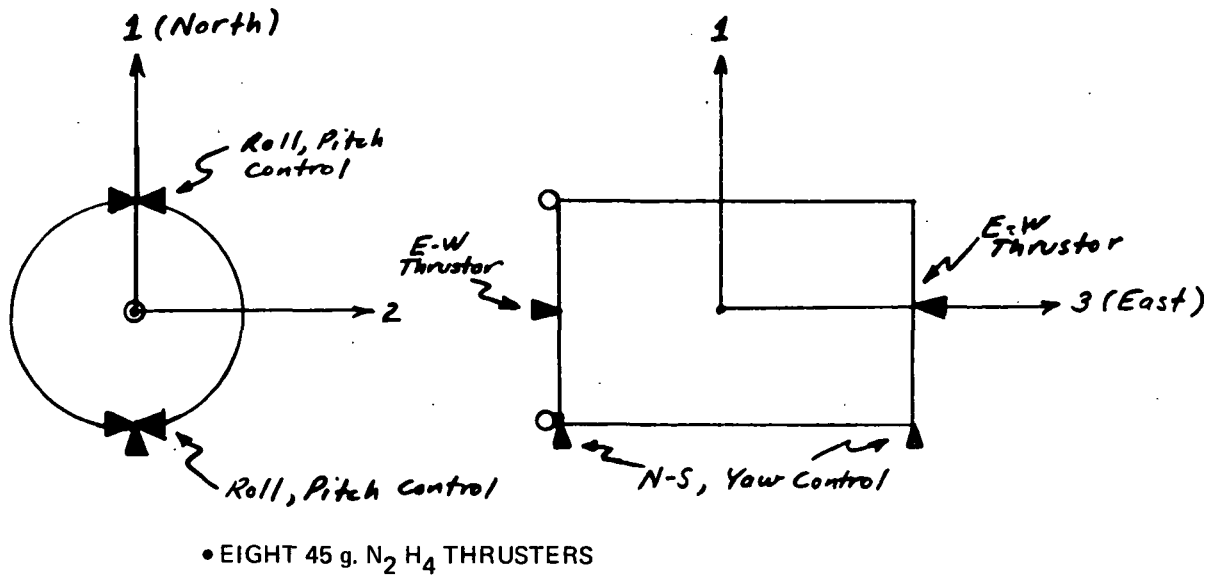
Figure 4.3-11. Thruster Location on Spacecraft, Configuration B

stationkeeping. The E-W jets thrust through the C.G., providing E-W station-keeping and solar force balancing. The remaining two pairs of jets provide torque about the No. 1 and No. 3 axes, including an initial spinup capability about the No. 3 axis before the apogee motor firing. Since the thrust levels are high in comparison to the ion thrusters on Configurations A and C (0.44 N versus 4 mN), duty cycles are low for all thrusting operations.

The orientation of the three clusters of 5-cm electric thrusters for Configuration C (and A) is illustrated in Figure 4.3-8. The two sets whose thrust axis is parallel to the No. 3 axis ("N-S" thrusters) provide N-S stationkeeping and all three axes of attitude control (momentum dumping) torques during their operation (±60 degrees about nodal crossing). During this time, thrust deflections and thrust modulations are commanded to, 1) continuously reduce wheel momentum (if it exceeds 10 percent of maximum wheel speed), 2) counteract the solar pressure force, and 3) generate the N-S thrust. During the remaining 2/3 of the orbit, the thruster along the No. 2 axis is operated intermittently to counteract solar force (~1/4 duty cycle), to dump accumulated momentum about the No. 1 and No. 3 axes (~five times per orbit), and to provide E-W stationkeeping. The majority of the accumulated momentum is about the No. 1 and No. 3 axes. Should excess-ive momentum accumulate about the No. 2 axis, the "N-S" thrusters are utilized for a short time to dump. During this portion of the orbit, momentum dumping is not continuous, but occurs at a fixed wheel speed threshold and the logic is such that the wheel is driven to approach the opposite threshold (e.g., +0.8 ω_{max} goes to -0.7 ω_{max}). This minimizes the required wheel size by taking advantage of the predominantly secular nature of the principal nature of the principal on-station environmental disturbance torque, solar pressure.

Disturbance Torques. The principal environmental disturbance torques acting on configurations B and C (on-station) are summarized in Table 4.3-14. These torques are used to size the wheel momentum storage requirements as well as to determine the fuel required for removing momentum accumulated due to secular torques. Note that the principal disturbance torque for Configuration B is cyclic about the No. 1 axis. To avoid unnecessary fuel consumption for removal of the cyclic momentum, a larger wheel size requirement for the No. 1 axis is ±2.7 N-m-s, which provides at least a 25 percent design margin. The storage requirements for the No. 2 and No. 3 axes are similar to those required for Configuration A.

For Configuration C, all torque sources are larger due to the larger vehicle. During orbit-raising, the principal torques are about the No. 2 axis (aerodynamics) and the No. 3 axis (gravity gradient). During the on-station phase, the principal torque is about the No. 1 axis; thus all three wheels were selected with equal storage capability. The required capability is ±3.8 N-m-s, including a 25 percent design margin. This allows for an average period of about 4 hours between momentum dumping operations.

Fuel Budgets. Representative fuel budgets are given in Tables 4.3-15 and 4.3-16 for Configurations B and C, respectively. Total fuel weight for Configuration B is seen to be quite large as compared to Configuration A or

TABLE 4.3-14. DISTURBANCE TORQUES

	T_1 (N-m)	T_2 (N-m)	T_3 (N-m)
Configuration B			
Solar Pressure	$1.68 \times 10^{-4*}$	$3.36 \times 10^{-5**}$	$3.36 \times 10^{-5**}$
Gravity Gradient	7.17×10^{-8}	3.95×10^{-6}	10.03×10^{-7}
Magnetics ($10a-t-ft^2$)	—	$10.0 \times 10^{-8*}$	$10.0 \times 10^{-8*}$
*Cyclic in inertial space **Secular in inertial space			
Configuration C (On-Station Phase)			
Solar Pressure	$3.36 \times 10^{-4**}$	—	$8.1 \times 10^{-5**}$
Gravity Gradient	10.76×10^{-7}	6.9×10^{-6}	$6.26 \times 10^{-5**}$
Magnetics ($100a-t-ft^2$)	$10.0 \times 10^{-7*}$	$10.0 \times 10^{-7*}$	—
*Secular **Cyclic			

TABLE 4.3-15. REPRESENTATIVE FUEL BUDGET
BUDGET — CONFIGURATION B

Source	Annual Requirement	Total Mission Requirement	Total Fuel Weight*
North-South Stationkeeping	51.5 mps	258 mps	85 Kg
East-West Stationkeeping	2.13 mps	10.7 mps	3.54 Kg
Solar Force Compensation	23.8 mps	120 mps	39.5 Kg
Momentum Dumping	1.89 mps	9.45 mps	3.13 Kg
Initial Station Acquisition	—	45.7 mps	15.2 Kg
Total	79.5 mps	444 mps	146 Kg

*m = 730 Kg, I_{sp} = 255 sec

TABLE 4.3-16. REPRESENTATIVE FUEL BUDGET
(ON-STATION) — CONFIGURATION C

Source	Annual Requirement	Total Mission Requirement	Total Fuel Weight**
North-South Stationkeeping	62.5 mps	312 mps	12.8 Kg
East-West Stationkeeping	2.13 mps	10.7 mps	0.45 Kg
Solar Force Compensation	21.3 mps	106.8 mps	4.36 Kg
Momentum Dumping	30.3 mps	152 mps	6.17 Kg
Total	116 mps	581 mps	23.8 Kg Hg

*Includes $\sin\theta/\theta$ inefficiency for thrust over ±60 degrees about nodal crossing.

**m ≅ 1640 Kg, average I_{sp} = 4100 sec.

C, due to the lower specific impulse of the chemical thrusters. The fuel weight required for Configuration C is larger than for A simply due to the larger vehicle size. It should be noted that on Configuration C (and A), solar force compensation and momentum dumping functions are performed in conjunction with N-S stationkeeping during 1/3 of the orbit with essentially no additional fuel expenditure.

Implementation Summary. The AC&SS hardware implementation for Configurations B and C are summarized in Tables 4.3-17 and 4.3-18 (exclusive of the propulsion system). Hardware descriptions of subsystem elements given in 4.3.2 are applicable to both Configurations B and C. The wheel utilized in the representative implementation for Configuration B (No. 1 axis) is the Bendix Model 1804270 (OAO Fine wheel, ±4.83 N-m-s).

4.3.4 Coupled Dynamic Interactions

Several types of coupled dynamic interactions can occur on spacecraft with large flexible solar arrays, namely,

1) Interactions between the flexible array dynamics and the vehicle attitude control system (ACS)

2) Interactions between the ACS and the array orientation control system

3) Interactions between the array orientation control system and the flexible array dynamics.

The latter two sources of coupled interactions have been carefully addressed at Hughes as part of the design and development effort associated with FRUSA*. The array control system has been designed such that interactions between it and the array dynamics are minimized and no instabilities can occur even for very low open-loop structural damping. Array motions are very slow, so that torque interactions between the two control systems are small and can easily be accommodated by the vehicle attitude control system. For Configurations B-1 and B-5, the array rate is essentially constant (once per day); for Configuration A-1, no array motion is necessary in final orbit, and slow (up to twice per day) cyclic motion is required during the orbit-raising phase.

The principal area of concern is the interaction between the vehicle Attitude Control System (ACS) and the flexible array. The low torque levels from the momentum wheels (all configurations) and the electric thrusters (Configuration A-1) are such that the flexible array dynamics will not be appreciably excited. The higher torque levels from the chemical thrusters (Configurations B-1, B-5) present a much higher excitation. However, proper selection of control loop parameters can result in closed loop damping

---

*Flexible Rolled-Up Solar Array.

TABLE 4.3-17. AC&S HARDWARE SUMMARY — CONFIGURATION B

Unit	Quantity	Unit Weight	Size	Power
Gyros	3	1.59 Kg each	900 cm^3 each	9.5 W each
Wheels	3	2 x 3.45 Kg	16.5 cm OD x 7.6 cm	2 x 3 W average
		1 x 4.54 Kg*	26.6 cm OD x 10.9 cm	1 x 4 W average
Sun Sensor	1	1.36 Kg (Including Electronics)	5.08 x 7.6 x 6.35 cm	3 W
Earth Sensor	1	3.27 Kg (Including Electronics)	19 cm dia. x 7.8 cm	1.6 W
Control Electronics	1	5.9 Kg		18 W
		26.8 Kg*		61.1 W

*Single thread design; probable standby redundancy in gyros, electronics

TABLE 4.3-18. AC&S HARDWARE SUMMARY — CONFIGURATION C

Unit	Quantity	Unit Weight	Size	Power
Gyros	3	1.59 Kg each	900 cm^3 each	9.5 W each
Wheels	3	6.8 Kg each	30.4 cm OD x 12.1 cm	62 W Stall each / 7.5 W average each
Sun Sensor	1	1.36 Kg (Including Electronics)	5.08 x 7.6 x 6.35 cm / 5.08 x 15.2 x 6.35 cm	3 W
Earth Sensor	1	3.27 Kg (Including Electronics)	19 cm dia. x 7.8 cm	1.6 w
Control Electronics	1	6.8 Kg		24 W
		36.6 Kg*		79.6 W

*Single thread design; probable standby redundancy in gyros, electronics

somewhat higher than the open loop structural damping. These basic design techniques are similar to those which have already been applied at Hughes in the synthesis of the array control loop.

An approximate design technique may be illustrated by an example which uses typical ATS/AMS parameters. A single axis block diagram is illustrated in Figure 4.3-12 with the wheels, shaping, and rigid body/flexible array dynamics.

The body dynamics (linearized) may be represented by the following transfer function

$$\left(\frac{\dot{\theta}}{T}\right) = \frac{1}{IS}\left(\frac{S^2 + \Omega_1^2}{\mu_1 S^2 + \Omega_1^2}\right)\left(\frac{S^2 + \Omega_2^2}{\mu_2 S^2 + \Omega_2^2}\right)\cdots\left(\frac{S^2 + \Omega_i^2}{\mu_i S^2 + \Omega_i^2}\right) \tag{1}$$

where open loop structural damping is conservatively ignored, and where:

> I = single axis rigid body (and array) inertia
>
> T = net applied torque about control axis of interest
>
> $\theta, \dot{\theta}$ = rotation, rotation rate of rigid body about control axis
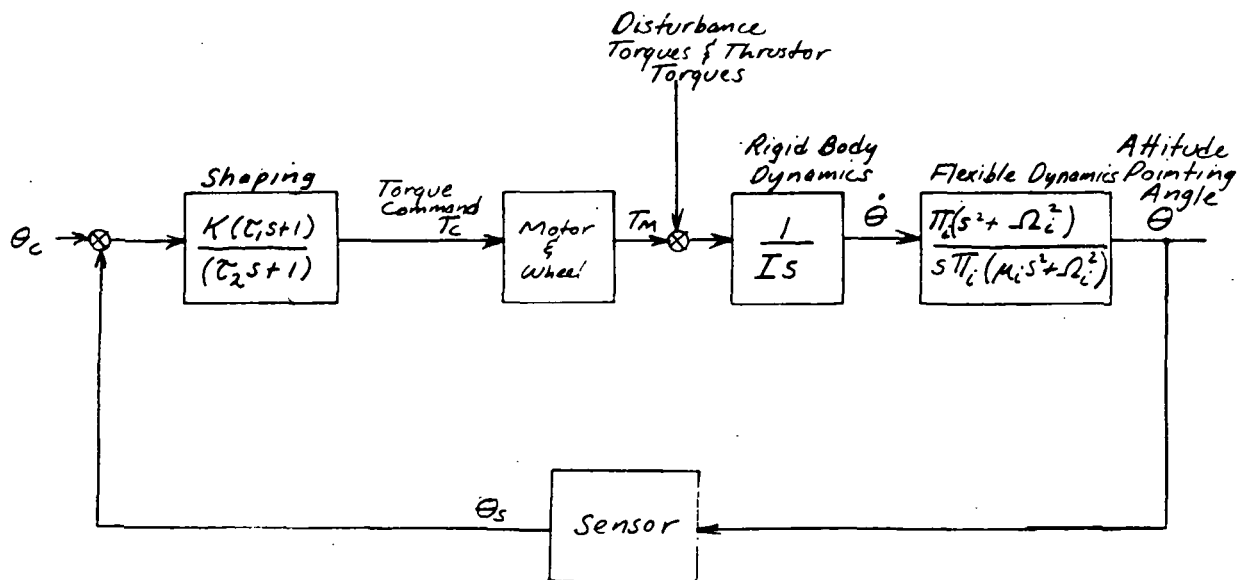
Figure 4.3-12. Simplified Single Axis Block Diagram Including Linearized Structural Dynamics (Array Flexibility)

Ω_i = frequency associated with the ith flexible mode (bending, torsional, etc.)

m_i = characteristic mass associated with the ith flexible mode

μ_i = characteristic inertia ratio of its mode = $\left(\dfrac{m_i \ell_i{}^2}{I}\right)$

The characteristic parameters associated with the various flexible modes of the array can be computed.[*] Results of a sample computation of the first bending mode as a function of array parameters is shown in Figure 4.3-13. In an actual design, many modes would be computed and utilized; however, for this example, only the first bending mode was utilized since it is the mode most difficult to stabilize.

The root locus of the system illustrated in Figure 4.3-12, including only rigid body dynamics, is illustrated in Figure 4.3-14. The loop gain as well as shaping parameters are selected consistent with desired closed loop response and damping characteristics as well as considerations such as mechanizational complexity, noise sensitivity, etc.
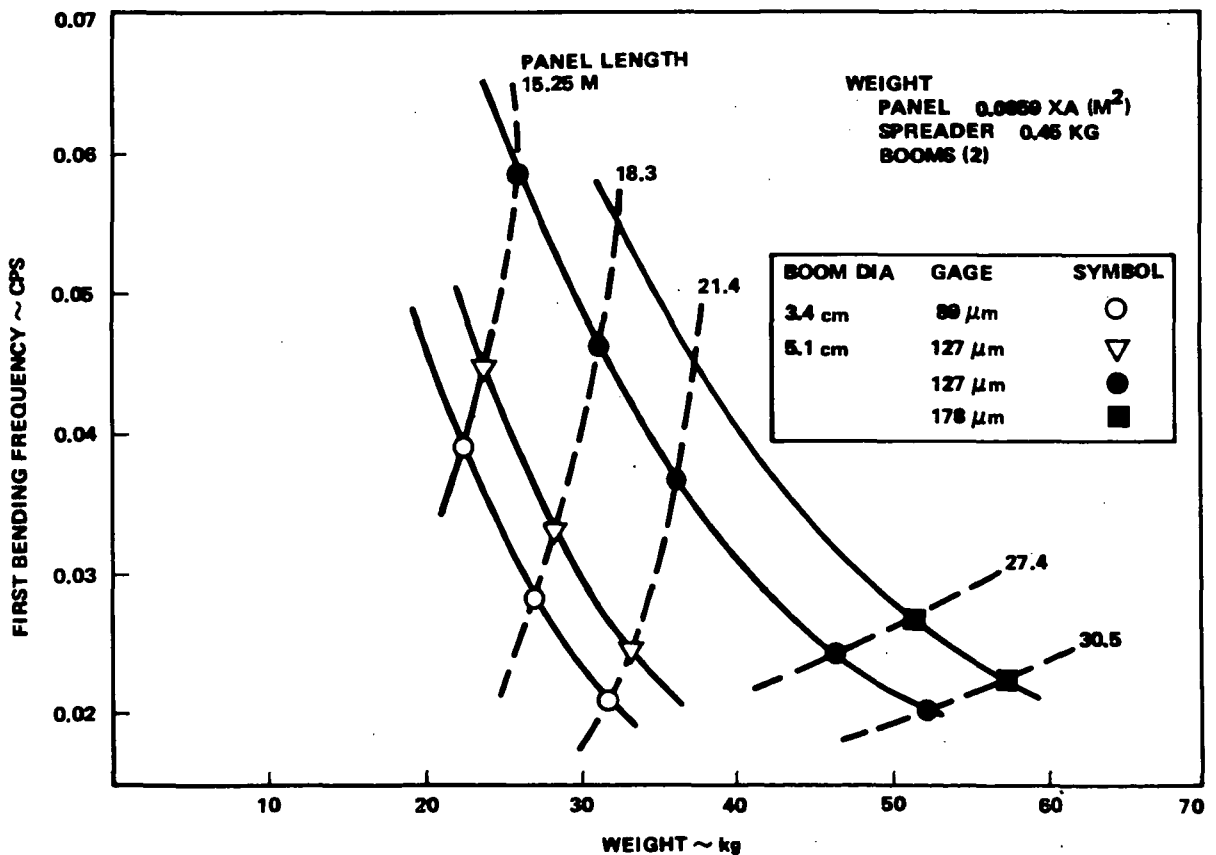
Figure 4.3-13. Modal Frequency for First Bending Mode

---

[*]Using a cantilevered mode analysis for this example.
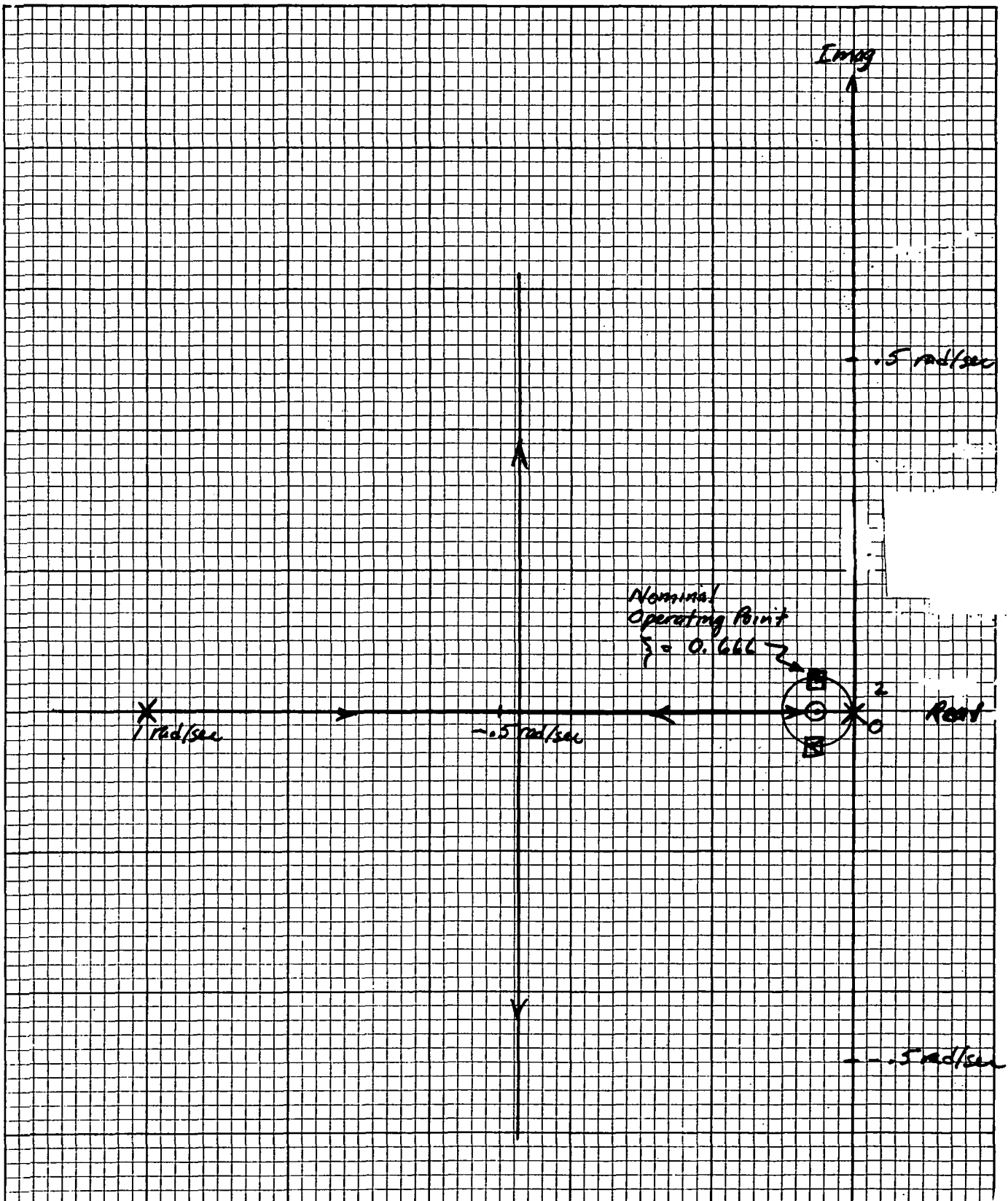
Figure 4.3-14. Root Locus Plot — Single Axis Wheel Loop, Rigid Body Only

Excluding the dipoles associated with the flexible dynamics, the loop is easily stabilized, and a reasonable degree of design freedom exists.

When the flexible body dipoles are added, the locus changes as indicated in Figure 4.3-15, and additional design constraints result from the closed loop damping and stability of the dipoles. Representative parameters for ATS/AMS are the following:

$$\tau_1 = 20 \text{ sec} \left.\vphantom{\begin{array}{c} \\ \\ \end{array}}\right\} \text{representative shaping to achieve adequate dynamic}$$
$$\tau_2 = 1 \text{ sec} \left.\vphantom{\begin{array}{c} \\ \\ \end{array}}\right\} \text{response}$$

$$I = 10.9 \times 10^3 \text{ Kg-m}^2$$

$$\Omega_1 = 0.222 \text{ rad/sec}$$

$$\mu_1 = 0.33$$

$$K_m = 34 \text{ N-m/rad}$$

As can be seen by comparison of Figures 4.3-14 and 4.3-15, the flexible body dynamics substantially alter the closed loop frequency response. However, the closed loop system is stable and the damping associated with the dipoles is enhanced by closed loop operation. For this example, the closed loop damping at a nominal operating gain (K = 24) is 1.6 percent, which is reasonable for a flexible structure considering the assumption of zero open loop structural damping.

In this example, the control frequency and the structural frequency are different, but not sufficiently separated to be neglected. The lowest structural mode is ~0.035 cps, and the closed loop ACS operating frequency is ~0.01 cps. As the dipole approaches the origin (the frequency decreasing as the panels become longer), frequency separation becomes nonexistent, but basic stability can still be maintained at the expense of somewhat degraded closed loop ACS damping.

The linearized example discussed here indicates the basic stability of the ATS/AMS system in the presence of flexible dynamics. A detailed study would be required, however, prior to or concurrent with the vehicle development to evaluate each of the three potential interaction paths, and to establish the actual dynamic responses under a typical mission profile.

Although basic stability can rather easily be established, the amplitude of the oscillations under repeated excitation should be established for both the vehicle and the array. This study is strongly recommended once a configuration is established and structural parameters of the array and vehicle can be generated. Techniques and tools are available at Hughes for performing such a study, and have been employed in similar design and analysis applications.
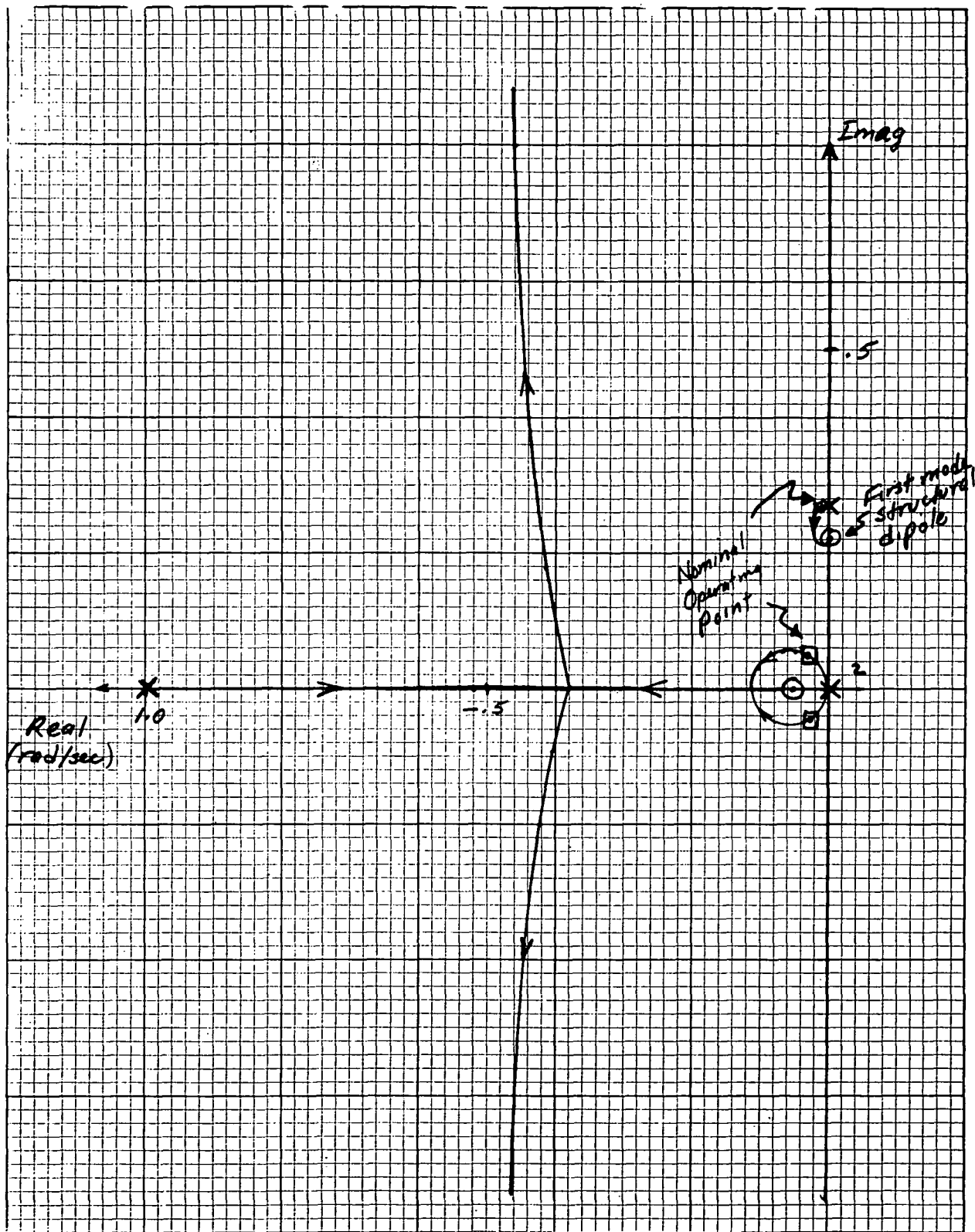
Figure 4.3-15. Root Locus Plot — Single Axis Wheel Loop, One
Structural Mode Included

4.3.5 Recommended Study Areas

As indicated above, the study of interactions between the attitude control system and both the flexible dynamics and control loop associated with the solar array requires further study. A large and complex simulation is required to thoroughly assess this area. However, similar problems have been evaluated at Hughes* as part of the development of the array (FRUSA) and its control system (OLSCA). It is expected that, for the low thrust levels and low torque levels of the electric propulsion thrusters and the momentum wheels, flexible interactions can be adequately isolated (in the frequency domain) so as not to create a stability problem. For the chemical propulsion application (Configuration B), there is more cause for concern. This general area of coupled interactions should be explored in depth, however, as part of a more detailed spacecraft design.

A second area for future evaluation is that of establishing dynamic torque (acceleration) requirements in order to acquire the desired orientation from a set of initial conditions representative of the mission.

_____

*Items 76-78, Appendix B

4.4 ELECTRIC PROPULSION SYSTEMS

Electric propulsion systems were considered in this study as possible alternatives for the two major mission functions of on-station attitude control and station-keeping and synchronous orbit injection or orbit raising. Detailed analyses of these requirements were presented in Sections 4.3 and 3.3, respectively. This section will present further system analyses and designs of electric propulsion systems to satisfy these mission requirements. For the attitude control and stationkeeping system, consideration will be given to the thrusters, propellant reservoirs, and power conditioning and control systems. However, in the case of the orbit raising system, only the thrusters and propellant reservoirs will be discussed. For this latter propulsion system, discussion of associated power processing and solar panel design options are given in Section 4.5.

Because of the performance gains offered by electric propulsion for both the satellite control and orbit raising function, it is appropriate to state the general design guidelines:

1) To establish system design credibility, state-of-the-art components and performance estimates were used wherever possible. Furthermore, in order to take advantage of the high state of development of Hg bombardment ion engines, this type of thruster will be employed for both functions under consideration.

2) To lend confidence to the final design, system reliability was established as an important design criterion; the design techniques by which high reliability was achieved (and determined) are discussed.

3) To minimize spacecraft program cost risks, components which require a minimum of technology advance and are presently under development have been used in all designs.

4.4.1 Attitude Control and Station-Keeping Ion Thruster Subsystem

The design of a synchronous satellite attitude control and station-keeping system (AK/SK) using ion thrusters which incorporate a thrust vectoring capability, depends on the choice of (1) general mode of operation (i.e., a definition of thrust vectors and duty cycle), (2) specific impulse, and (3) reliability requirements. In each case the choice must satisfy the vehicle control requirements as determined by a study of the perturbing forces and the disturbance torques, the specific spacecraft design, and the mission time. The vehicle control requirements which have been analyzed in detail and specified in Section 4.3 are summarized in Table 4.4-1.

Based on these requirements, a general discussion of the potential modes of operation and of the techniques employed to increase system reliability, along with a determination of optimum specific impulse, is given here prior to a description of the specific system design.

TABLE 4.4-1. VEHICLE CONTROL REQUIREMENTS*

Perturbation or Disturbance Direction	Magnitude
N-S	270 m/s
E-W	10.7 m/s
Perpendicular to each of 3-axes	214 m/s

*A-1 Configuration; five year mission
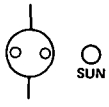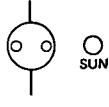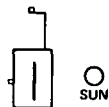
4.4.1.1 Attitude Control and Stationkeeping Control Mode Options

A number of attitude control and stationkeeping approaches using deflectable beam ion thrusters in combination with reaction wheels have been investigated during the course of this study. Four of the most promising thrust control modes considered are listed in Table 4.4-2 along with pertinent operational and subsystem evaluation data for each.

All of the control options presented are capable of (1) satisfying N-S and E-W stationkeeping requirements, (2) correcting for solar pressure (i.e., C.P. - C.M. solar torque and orbital eccentricity buildup), and (3) augmenting reaction wheel attitude control via thrust vectoring. However, as indicated, the total AC/SK system weight, control capability and thrust schedule can vary considerably among the options.

The comparative analyses on which Table 4.4-1 is based have shown that, on the basis of total subsystem weight, thruster location and general control flexibility, option 3 is the preferred approach. In option 3, N-S stationkeeping is unidirectional and performed during a 60-degree sector of the orbit at the time of maximum correction influence. While providing this stationkeeping, beam vectoring is used to produce 3-axis control torques to allow reaction wheel energy to be reduced. Periodically during the orbit (but not during N-S stationkeeping), the E-W thruster is operated to compensate for solar pressure and earth triaxiality effects. The major disadvantage in the baseline approach is that frequent on/off E-W thruster cycling is required. Because of this cycling requirement, as well as the long duration of the mission, reliability considerations have dictated that each thruster station be composed of three thrusters in a cluster. In this way, each control function has at least threefold thruster redundancy. The power conditioning unit associated with each thruster station is designed to operate a single thrust unit. In the event of a thruster failure, switching is provided to transfer the conditioned power to a standby. Power conditioning reliability is increased to the desired level by internal redundancy rather than by separate standby systems.

TABLE 4.4-2. SPACECRAFT CONFIGURATION "A" ATTITUDE CONTROL OPTIONS

Attitude Control Option	Number of Thrusters	Thrust Mode (No Thrust During eclipse)	Reaction Wheels	Propellant Mass (5 yrs.) KG	Thruster Mass KG	Peak Power Required Watts	Total Mass KG	Attitude Control Capability	Primary Disadvantages
1. SUN	2 Clusters of 4	Continuous throttled back during 2/3 of orbit	3 with 1.3-2.0 N-m-S capability M = 11 KG	24	9	290	44	Acceptable	Long thruster operating times Subsystem Mass
2. SUN	2 Clusters of 3	Continuous for 1/6 orbit - off for 5/6 orbit	2 with 1.3-2.0 N-m-S capability 1 with 11-13 N-m-S capability M = 18 KG	11	8	290	37	Acceptable	Once a month "down time" to utilize main thrusters for eccentricity
3. SUN	3 Clusters of 3	Bottom thrusters continuous for 1/6 orbit - off for 5/6 orbit Back thrusters used about 5 times per day for a total of 3 hours	3 with 1.3-3 N-m-S capability M = 13 KG	9	12	290	34	Excellent	Frequent ON/OFF cycling of thruster (may not present any difficulty)
4. SUN	3 Clusters of 3	Top and bottom thrusters each continuous for 1/6 orbit - off for 5/6 orbit. Back thruster used about 5 times a day for a total of 3 hours	3 with 1.3-3 N-m-S capability M = 13 KG	9	12	290	34	Good	Location of top thruster very awkward. Frequent ON/OFF cycling of thruster (may not present any difficulty)

4.4-3

4.4.1.2 Thruster Unit Characteristics

Based on the vehicle control requirements and the choice of mode of operation, the thrust level and deflection angle required by each individual thruster can be determined. For example, the N-S stationkeeping system operating at a duty cycle of 1/6 with two thrusters firing simultaneously produces the total required impulse if each thruster has a thrust level of 4 mN. In order to avoid the development of two types of thrusters, the E-W engine is also sized for 4 mN thrust with the thrust on-off time programmed to satisfy the control requirement. Finally, at the 4 mN thrust level and with the duty cycles presented in Table 4.4-2, a deflection angle capability of $\pm 10°$ is adequate to properly limit the energy storage requirement of the 3-axis reaction wheel system.

Once the thrust level and desired deflection angle have been defined, the only remaining characteristic to be specified is the specific impulse. Since ion thrusters can operate over a relatively wide range of specific impulse, its value can be chosen on the basis of minimizing total system weight. The optimization procedure involved is based on the fact that, for a given thrust level and thrusting time, the required Hg propellant decreases while the power and, therefore, power system weight increases with increasing specific impulse. These relationships are shown in Figure 4.4-1 for the two N-S stationkeeping thrusters (i.e., for a total thrust level of 8 mN operating for 1/6 duty cycle for 5 years).
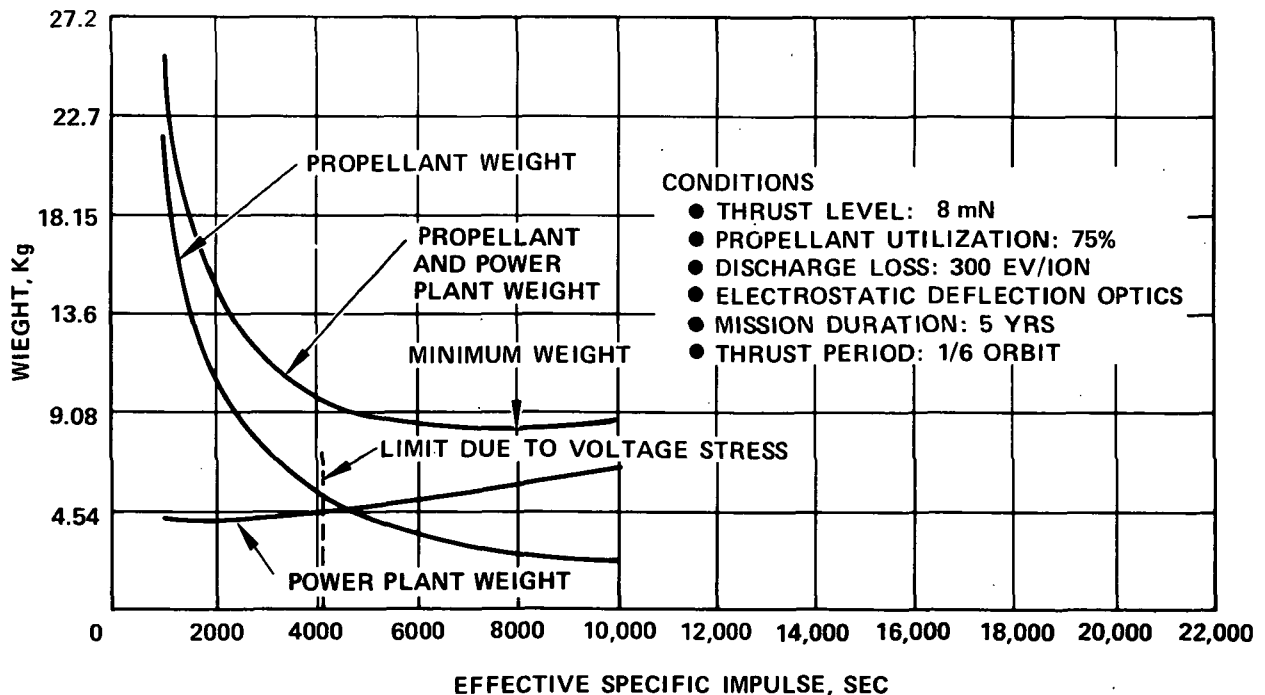
Figure 4.4-1. Optimum Specific Impulse Determination

From Figure 4.4-1, it can be seen that the optimum I_{sp} (i.e., minimum total system weight) occurs at ~8000 sec. However, Figure 4.4-1 also shows that the total system weight varies little over a I_{sp} range of 4000 sec to 10,000 sec. For this reason, it is possible to choose the operating specific impulse within this range on another important operational criterion; namely, holding beam voltage levels to reasonable values. On this basis, a beam voltage of 3000 volts was chosen which results in an effective specific impulse of 4100 sec.*

4.4.1.3 Thrust Vectoring Options

As noted previously, each ion thruster designed for stationkeeping and augmenting attitude control for spacecraft configuration A-1 must produce a thrust level of 4 mN and must incorporate a thrust vector deflection range of approximately ±10 degrees in two orthogonal axes.

In a recent study (NAS Contract NAS 3-14058), a number of techniques for controlling the direction of thrust from a Hg bombardment ion thruster were evaluated; the three most promising were found to be the electrostatic dual grid, the movable screen electrode, and the vectorable discharge chamber. Each of these thrust vectoring systems was developed and experimentally evaluated on a 5-cm Hg bombardment thruster.

A photograph of a dual grid electrostatic grid system is shown in Figure 4.4-2. This system was recently tested for over 150 hours under Contract NAS 3-15385. The test showed excellent ion optical system performance over the full beam current test range (20-35 mA; 25 mA nominal operating point) at deflection angles from zero to greater than 12 degrees. After 150 hours of testing over the above range, there was no significant erosion on any of the ion optical system components. This performance, coupled with the successful vibrational tests, verify the overall system design.

A conventional dual grid optical system, shown in Figure 4.4-3, in which the screen could be translated relative to the accelerator electrode, is an acceptable alternative to the dual grid electrostatic design. While such a system is inherently slower than the electrostatic system because of the thermomechanical actuators, it is possible to vector the ion beam more than ±15 degrees with no increase in accelerator electrode interception.

---

*The effective specific impulse (I_{spe}) of a Hg ion thruster is related to beam voltage (V_B) by the following equation: $I_{spe} = 100 \, \eta_m \, V_B^{1/2}$ where η_m is the thruster propellant mass utilization efficiency (typically 75% for small SOA thrusters).
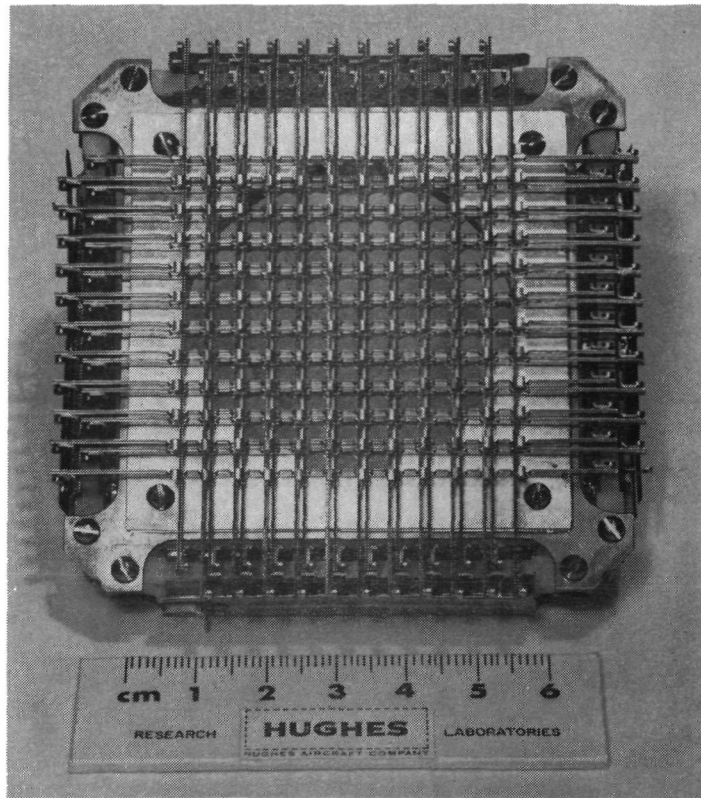
Figure 4.4-2. 5-Cm, Dual-Grid Electrostatic
Thrust Vectoring System
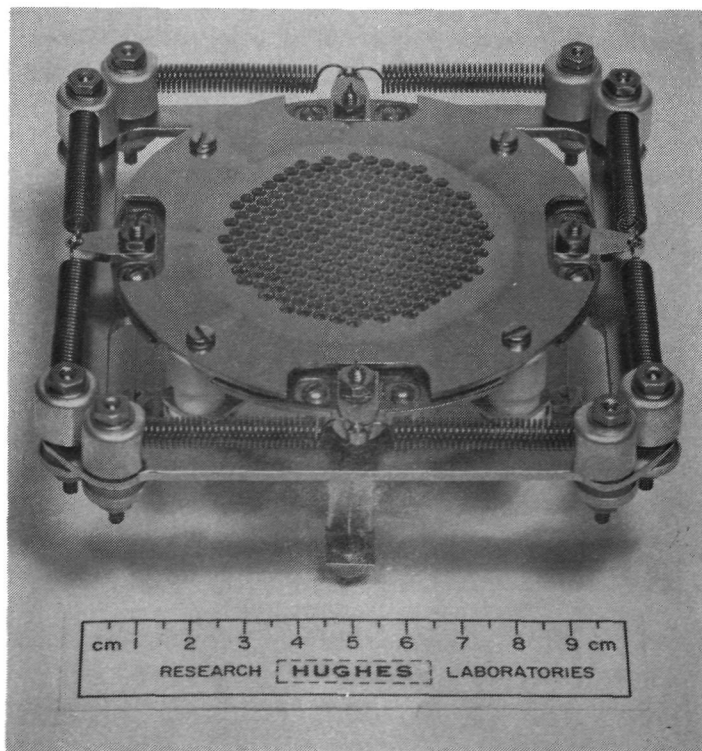
Figure 4.4-3. 5-Cm, Movable-Screen Electrode
Thrust Vectoring System

The basic design concept is shown in the photograph in Figure 4.4-3. The screen electrode is supported on four thin flexible columns which are strong in tension. The screen pole piece supports the electrode so that the columns cannot be compressed. This provides the necessary axial support without constraining the transverse flexibility. The electrode is held in static equilibrium by pairs of stretched coil springs whose axes are transverse to the supporting columns. In actual operation the screen electrode is moved by passing current through the desired spring(s). Approximately 10 degrees of deflection can be obtained with ~1 watt of spring heating power.

The vectorable discharge chamber system evolved from the promise that it would be easier to gimbal the relatively light discharge chamber and ion extraction system than to support and precisely control a complete thruster package, including the heavy propellant storage tank. Since the propellant feed line which connects the two is a thin flexible member, the two parts of the system are essentially mechanically decoupled, thus simplifying the design. The advantage of such a system is that the thruster performance should in no way be perturbed from that of a nonvectorable system.

A brief comparison of the three vectoring systems is given in Table 4.4-3. Although there is little subsystem weight and power requirement differences, the electrostatic deflection concept has been chosen as the baseline in this study because of its speed of response and absence of any moving parts.

4.4.1.4 System Layout and Description

Having selected the mode of operation, the degree of desired redundancy, the thruster characteristics and the type of thrust vectoring system to be employed, it is possible to describe the total AC/SK ion thruster subsystem and its integration with other major spacecraft subsystems.

Interface with Spacecraft Subsystems. A block diagram showing the attitude control and station-keeping thruster subsystem and its points of electrical interface with other A-1 spacecraft subsystems is presented in Figure 4.4-4.

The thruster power conditioning and control unit (PCU) consists of three integrated units which share common housekeeping bias supplies, sequential circuitry and drive electronics in order to reduce total power conditioning weight. It is anticipated that the PCU could be implemented with functional and electrical designs very similar to those presently under development for the 5-cm ion thruster mentioned above. Prime power for the PCU is derived from the 28 VDC bus.

Between the PCU and the three thruster stations is a switching matrix mechanized with latching relays. This allows rerouting of power to a redundant thruster within a given thruster station and provides a redundant station power conditioning capability (only a maximum of 2 of 3 power conditioners are required to operate at a given time) in the event of a partial

TABLE 4.4-3. COMPARISON OF THRUST VECTORING SYSTEMS

CRITERION	TYPE OF SYSTEM		
	DUAL GRID ELECTROSTATIC	MOVABLE SCREEN ELECTRODE	VECTORABLE DISCHARGE CHAMBER
Deflection Angle	Continuous deflection to greater than 10 deg	Continuous deflection to greater than 15 deg	Discrete deflection angles to 10 deg (continuous with modified design)
Deflection Azimuth	Continuous deflection to any azimuth	Continuous deflection to any azimuth	Deflection to discrete azimuths
Response Time	Electrical, $< 10^{-4}$ sec	Thermal, 10 to 100 sec	Mechanical $\sim$ 1 sec
Pointing Accuracy	High accuracy with closed loop control	High accuracy with closed loop control	Better than 1 deg (may change with time)
Lifetime	Little accel erosion at $\theta < 10$ deg. Interelectrode insulators susceptible to sputter deposition.	Little accel erosion at $\theta < 15$ deg	Approximately equal to a non-vectorable system
Thruster Performance	Discharge eV/ion increased	Discharge eV/ion increased	No effect
Adaptability	Tested on 5 cm thruster, mechanically difficult for 30 cm thruster	Adaptable to both 5 and 30 cm thrusters	Adaptable to 5 cm thruster; More difficult for 30 cm thruster
Tested Concept	Tested on 5 cm for 100 hours. No satisfactory design for 30 cm to date	Tested on 5 cm, mockup demonstrated for 30 cm	Tested on 5 cm mockup
Development Time and Cost	5 cm prototype design ready for qualification — 30 cm difficult	5 cm demonstrated — 30 cm prototype design ready at end of this contract	Prototype demonstrated for 5 cm thruster
Weight	Present 5 cm design Total grid weight = 210 g Added system weight = 3.9%	Present 5 cm grid design Total grid weight = 305 g Added system weight = 5.1%	Added system weight $\sim$ 500 g ($\sim$ 21%)
Power	Less than 1 W at $\theta = 10$ deg	Approximately 1 W at $\theta = 10$ deg	50 W, 50 msec pulse to actuate; steady-state - none
Reliability	No moving parts - possible failure mode - by accel erosion or insulator leakage	Spring and flexure deflection only motion required - no additional high voltage insulators	Mechanical actuators required
Power Conditioning Required	Two $\sim$ 1 kV power supplies required - Closed loop control desirable	Two low voltage heater supplies required - Closed loop control	Two pulse supplies required - Open loop control adequate
Thruster Design	No change in discharge chamber Minimal structural change	No change in discharge chamber Minimal structural change	No change in discharge chamber Modified mounting required

4.4-8
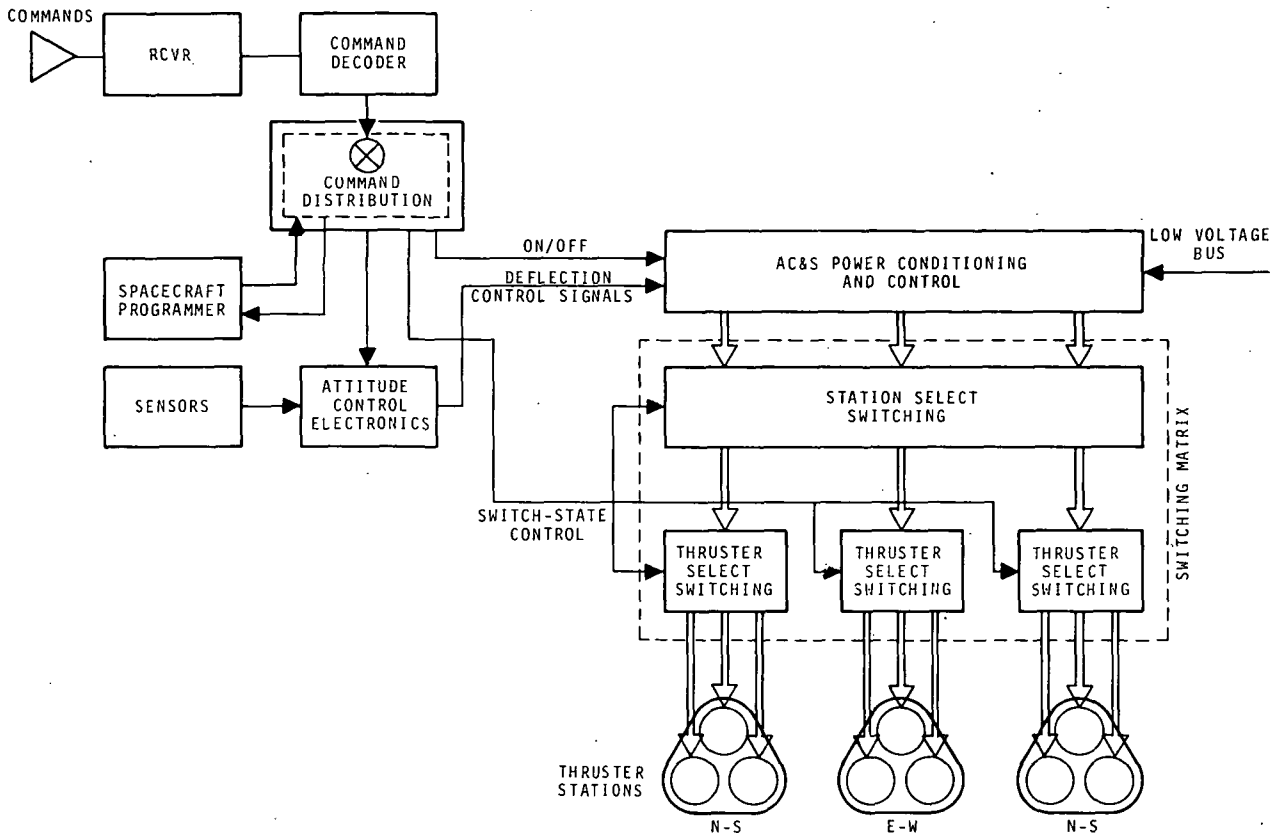
Figure 4.4-4.   Attitude Control and Stationkeeping Thruster
Subsystem Interface with Spacecraft

failure in the PCU.   To minimize thruster power cabling weight, the thruster
select switching would be located near its associated thruster station and the
station select switching would be located with the PCU.

Individual thruster on/off commands and switch-state controls are
issued from the command distribution circuitry.   Thruster beam vector
control signals from the attitude control electronics provide two axis deflec-
tion analog reference signals for the closed-loop electrostatic deflection
power supplies in the PCU.

Thruster Station.   As indicated above a total of three thruster stations
are provided for attitude control and station-keeping.   As shown in Fig-
ure 4.4-5 each station is equipped with three separate ion thruster units
which share a common liquid mercury feed system.   Only one thruster per
station is needed to fulfill mission thrust requirements, while two redundant
thrusters per station insure high propulsion reliability with minimal mass
penalty since the mercury reservoir constitutes the major mass contribution
of the thruster system.   The individual thruster units which have a mass of

SPACE CRAFT
STRUCTURE

THRUSTER SUPPORT
STRUCTURE

SIT-5 MERCURY
ION THRUSTERS

GAS PRESSURE
VESSEL

TANK BLADDER

BEAM DEFLECTION
EXTRACTION SYSTEM

PROPELLANT
MANIFOLD

MERCURY
TANK
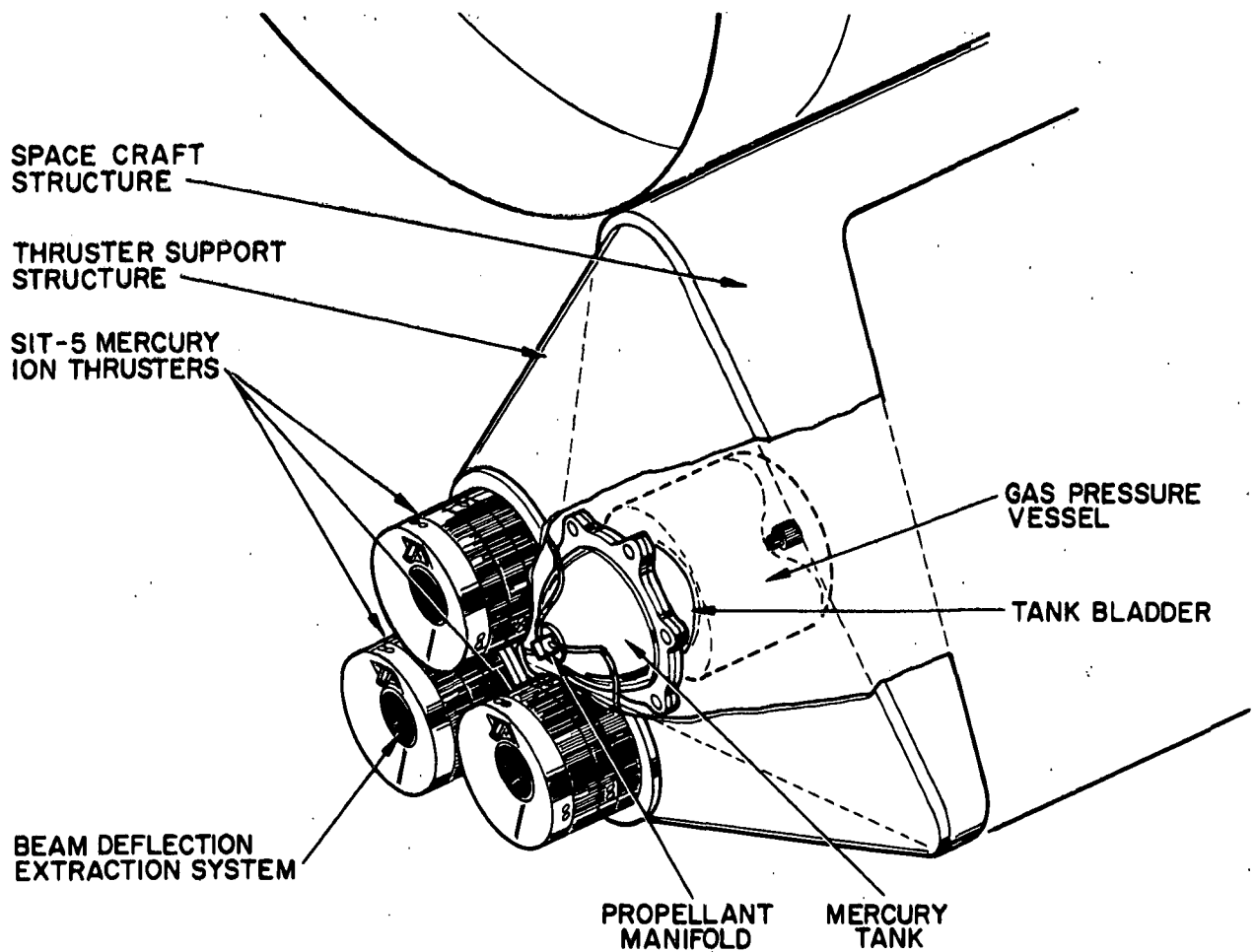
Figure 4.4-5. AC&S Thruster Station

0.7 kg each are adapted directly from the existing SIT-5 thruster system
shown in Figure 4.4-6.

At a given thruster station, each of the thruster units operate inde-
pendently of the other two. Propellant flowrate to the individual thruster is
regulated by a separate phase separator or vaporizer which provides the
necessary rate of vapor flow to the discharge chamber while preventing
direct transmission of liquid mercury. Electrical isolation from the
mercury supply is provided by separate high-voltage isolator subassemblies
located downstream of the propellant vaporizers. The system includes the
thrust vectorable ion-extraction system described earlier which is capable
of high angle (>10°) thrust vector control by electrostatic deflection.
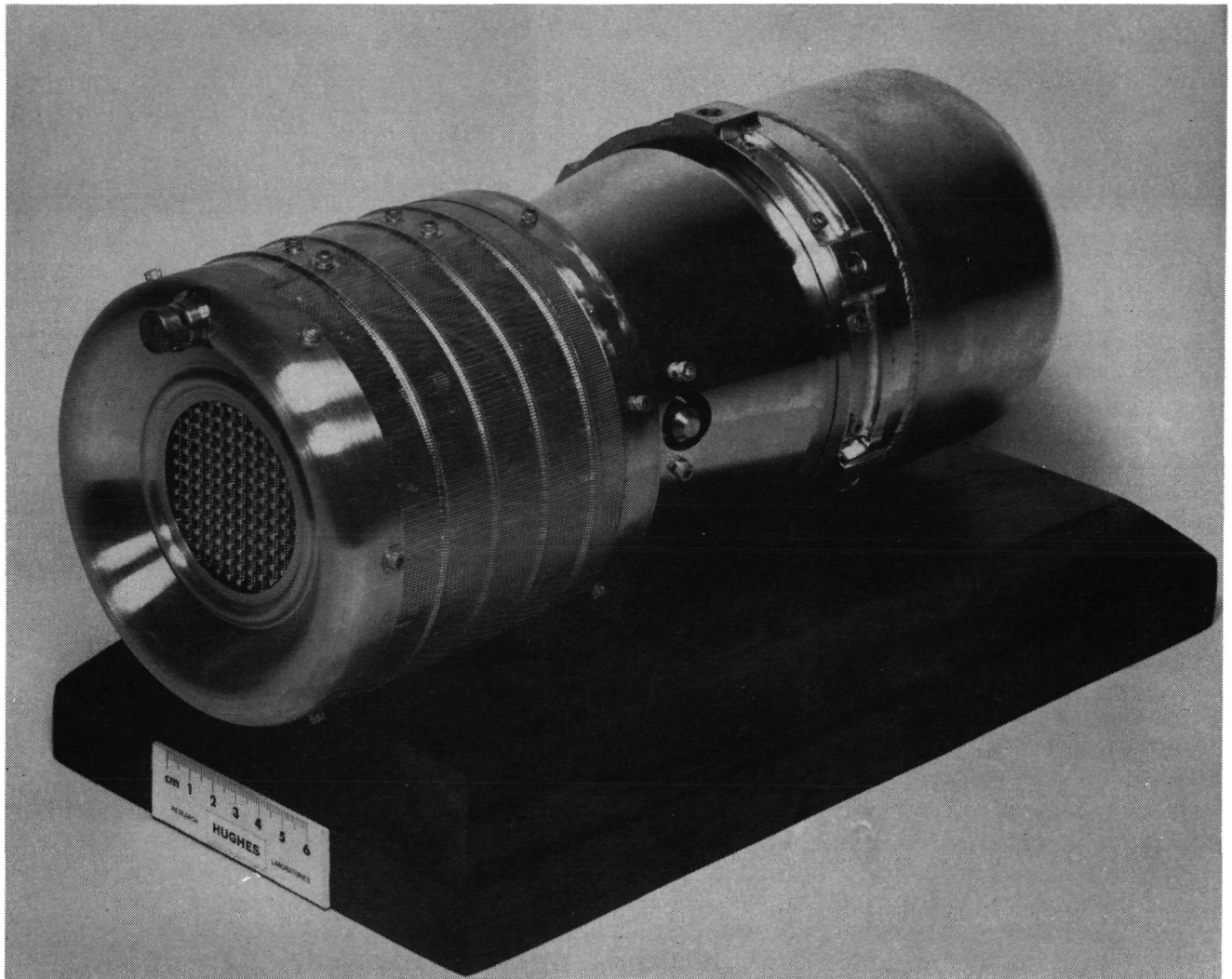
Figure 4.4-6. SIT-5 Thruster and Reservoir System

Each element of the SIT-5 system has been flight qualified by extensive test programs. Earlier models of both the thruster unit and the thrust-vectorable ion-extraction system have demonstrated their capability for booster launch by a rigorous series of shock and vibration tests. Structural integrity of the thruster system is demonstrated for shock (30 G), sinusoidal (9 G), and random (19 G^2/Hz) accelerations. Performance and reliability of system operation has been verified by testing in the vacuum environment. The most extensive test of the thruster system is currently underway at the NASA Lewis Research Center using SIT-5 hardware. As of February 1972, 3,000 hours of operation has been logged by one of the thrusters. For the first 2000 hours, the system was operated with the movable-screen deflection system; but the last 1,000 hours of operation has been logged without incident using the electrostatic vectorable optics.

The capabilities of thruster performance are well qualified by a recently completed program of discharge chamber modifications which optimized the systems performance profile for operation at the set point specified under NASA Contract NAS 3-15483. As shown in Table 4.4-4 the optimized system provides design thrust ($T = 2.1$ mN) at a net accelerating voltage ($V_B = 1600$ V) with a propellant utilization efficiency ($\eta_m = 76\%$) including neutralizer losses, and a system electrical efficiency ($\eta_E = 56\%$)

Only minimal modifications are required for reoptimization of SIT-5 thruster performance at the operating point suggested for the ATS/AMS application. Table 4.4-5 lists an earlier operating point demonstrated at conclusion of NASA Contract NAS 3-14129. The performance had been optimized at the suggested value ($I_B = 35$ mA) and efficient operation at beam currents (as high as $I_B = 45$ mA) were demonstrated during system optimization under NASA Contract NAS 3-15483. The increased beam, accelerating and deflection voltages suggested by Table 4.4-5 are within the capabilities of the existing design.

While only minor modifications are required to extend SIT-5 thruster performance to the 4 mN thrust level, choice of a somewhat larger thruster unit is also acceptable because of its relatively small size and mass compared to the entire satellite system. A similar thruster configuration of 8 cm anode diameter would provide the thrust suggested for the ATS/AMS application with no increase in current density or extraction voltage above the values listed in Tables 4.4-4 and 4.4-5 for the developed 5-cm system.

System Design Specification Summary. A summary of the specifications of the complete on-station ion thruster attitude control and station-keeping subsystem for spacecraft configuration A-1 is given in Table 4.4-6. As indicated, the total system weight for five year operation including three thruster stations, propellant, power conditioning and controls, and switching matrix is 13.8 Kg. Furthermore, the peak power requirement is 290 W, with two stations operating simultaneously. Finally, the system described in Table 4.4-6 is a conservative extension of SOA hardware to be flight tested on the Canadian Technology Satellite (April 1975 launch).

4.4.2 Orbit Raising (OR) Ion Thruster Subsystem

The design of the orbit raising ion thruster subsystem for the ATS/AMS must satisfy the overall design point established by the flight dynamics analyses. The specific design point required includes specification of the following:

1) Trajectory. The specific trajectory employed determines the variation of the initial design point with time and can affect thermal design considerations.

2) Power Level. The power level at 1 AU determines propulsion system size; its variation with time affects both reliability and power matching considerations. This variation for the ATS/AMS mission is discussed in this section (see Figure 4.4-11) and in Section 3.3.

4.4-12

TABLE 4.4-4. SIT-5 SYSTEM PERFORMANCE PROFILE
(FOR OPERATION AT THE DESIGN SET POINT
OF CONTRACT NAS 3-15483)

Nominal Operating Parameters	Operating Values (Test 102-TV-9)
Beam Voltage*, V	1600
Beam Current, mA	25.6
Accel Voltage*, V	800
Accel Drain Current, mA (at 0° deflection)	75
Discharge Voltage, V	45
Discharge Current, mA	260
Cathode Discharge Power, W	11.7
Keeper Voltage, V	18
Keeper Current, mA	365
Keeper Power, W	6.6
Heater Power, W	0
Vaporizer Voltage, V	3.2
Vaporizer Current, A	1.3
Vaporizer Heater Power, W	4.2
Neutralizer	
Keeper Voltage, V	17
Keeper Current, mA	365
Keeper Power, W	6.2
Heater Power, W	0
Vaporizer Voltage, V	2.3
Vaporizer Current, A	1
Vaporizer Heater Power, W	2.3
Coupling Voltage, V	11
Output Beam Power, W	40.3
Total Input Power, W	72.2
Thruster Propellant Flow Equivalent, mA (cathode flow)	31.1
Neutralizer Propellant Flow Equivalent, mA	2.6
Propellant Utilization Efficiency (Including neutralizer)	76
Electrical Efficiency, %	56
Over-all Efficiency, %	43
Discharge Loss, eV/ion	465
Thrust, mN	2.1
Specific Impulse, sec	3040
Power-to-Thrust Ratio, W/mN	34.6

*For experimental convenience, data for test 102-TV-9 were actually generated at a Beam and Accel voltage of 1200 V each, rather than the design point values listed above. Subsequent operation of the SIT-5 system at the design point demonstrated that no significant error was introduced by this expedient.

TABLE 4.4-5. COMPARISON OF ATS/AMS THRUSTER
AND DEVELOPED THRUSTER HARDWARE
OPERATING POINT (5 CM THRUSTER)

Parameter	Developed Thruster Operating Point (NASA Contract NAS 3-14129)	ATS/AMS Suggested Operating Point
Thrust, mN	2.5	4.0
Effective Specific Impulse, sec	2,500	4,100
Beam Voltage, volts	1,200	3,000
Beam Current, mA	35	35
Accelerator Voltage, volts	1,200	-1,000
Deflection Voltage for ±10 deg (2 dimensional capability), volts	±700	±1,200

TABLE 4.4-6. ATTITUDE CONTROL AND STATIONKEEPING ION THRUSTER SYSTEM SPECIFICATIONS

- **PROPULSION SYSTEM DEFINITION**
    - Thruster Stations = 3 (2 N-S, 1 E-W)
    - Reservoirs = 1/station
    - System Weight = 13.8 Kg
    - Propellant Weight = 9.1 Kg

- **THRUSTER STATION**
    - Thrusters/Station = 1 operation/2 standby
    - Reservoirs/Station = 1
    - Input Power = 145 watts
    - Thruster Diameter = 5 cm
    - Effective Specific Impulse = 4100 sec
    - Weight (less propellant) = 2.45 Kg

- **POWER CONDITIONING, SWITCHING & THRUSTER CONTROLS**
    - PC&C Units = 3
    - Efficiency ≥85%
    - Switching Matrix = 1
    - Minimum PC&C to operate = 2 of 3
    - Weight = 6.35 Kg

3) Solar Panel Bus Voltage. The initial bus voltage affects the basic power conditioner design; its variation with time affects voltage regulation requirements and reliability considerations.

4) Propellant Mass. The amount of propellant required affects the number and size of the propellant reservoirs employed.

5) Specific Impulse. The specific impulse chosen determines the ion beam voltage (screen electrode voltage) and affects the choice of thruster electrode system.

Since the power conditioning and control system designs for the orbit raising ion thruster subsystem are covered in Section 4.5, the effect of solar panel bus voltage on system design will not be considered here.

The design points for the proposed ATS/AMS vehicle with an orbit raising capability are:

Trajectory	(see Figure 4.4-7)
Initial Power (available to thrusters)	9.3 kw
Propellant Mass	54.5 kg
Specific Impulse	3500 sec

4.4.1 General Design Considerations

An approach or methodology, based on extensive analyses and system design considerations, has been developed for the purpose of designing prime electric propulsion systems for space vehicles. It is based on the design concept of seeking a minimum mass system while maintaining the system reliability at or above a given level. The methodology will be briefly reviewed here since it forms the basis of the propulsion system design definition.

Basic Tradeoffs

Because solar electric propulsion missions generally require long-duration component operation, it is obvious that system reliability is a major factor in system design. In general, reliability requirements dictate that such techniques as redundancy are necessary to increase the probability of mission success to acceptable levels. Redundancy techniques can, of course, lead to severe system mass penalties. Since increased mass is undesirable in any space system, it is important that these penalties be minimized.

Where redundant components must be employed to increase system reliability, an effective means of reducing the concomitant system mass penalty is the use of a modularized system concept: the replacement of a single large component with a number of smaller subsystem components. In such a subsystem the incorporation of a redundant component for reliability

purposes will, in general, result in a relatively small mass penalty. For
modularization to be considered, this reduction in mass penalty must com-
pensate for the increase in initial system mass which normally results
when a system is modularized.

A unique factor in the design of a solar-electric propulsion system is
the nature of the output characteristics of the solar panel power source.
First, the I-V characteristic and, thus, the maximum amount of power
available from the panel, is in general a function of time. Second, the
maximum power available will be delivered only when the ion engine load is
properly matched to the solar panel characteristic. Thus, it is apparent that
the ion engine system load must be continually and properly programmed
during the flight.

Reference 1 shows that the optimum procedure for programming an
ion engine load is a combination of varying the ion beam current (throttling
propellant flow rate) at constant beam voltage (constant specific impulse)
and switching ion engine modules. In general, the throttling of ion thrusters
can introduce a decrease in thruster efficiency (Figure 4.4-7). The degree
to which a thruster must be throttled for a given application is a function of
the number of thruster modules employed. Thus, the penalty associated with
power matching requirements is also determined by the degree of thruster
subsystem modularization.
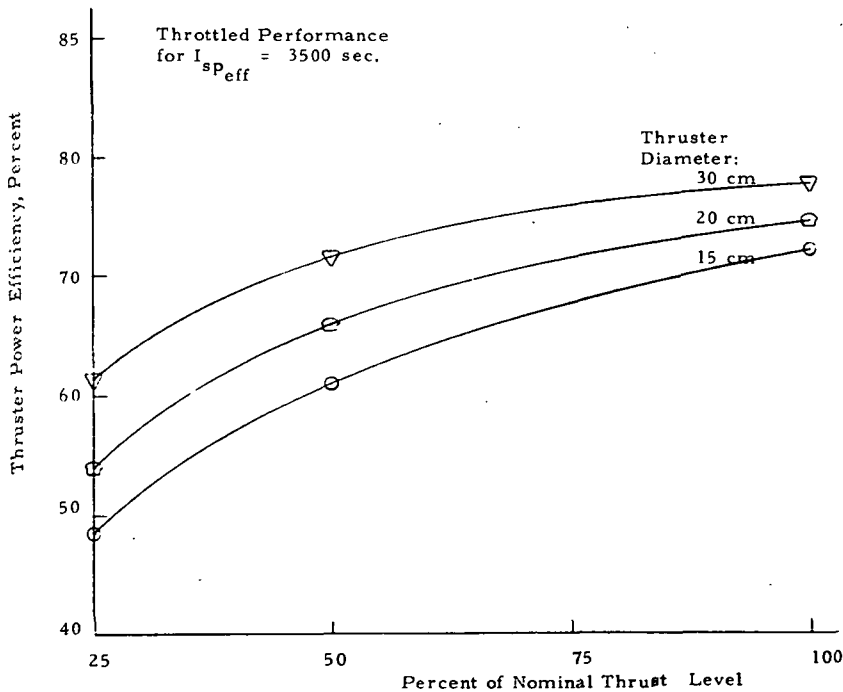
Figure 4.4-7. Throttled Thruster Power Efficiency

The above identified two basic tradeoffs involved in the design of a solar-electric propulsion system: system reliability versus system mass, and power matching versus system performance (the latter can be effectively related to system mass). In each case the number of modules employed in the system becomes the major design variable. Therefore, to minimize the system weight for a given application, the optimum number of modules must be determined.

System Configurations

In designing a modularized propulsion system, there are several ways in which the major subsystems (thrusters, power conditioners, and reservoirs) can be integrated. For example, each thruster could have its own reservoir and power conditioning and control system. In the other limit, by incorporating the proper cabling and switching matrix and manifolding and valving system, an individual thruster could be operated by any power conditioning panel and could be supplied with propellant by any reservoir. Between these two limiting designs several other possible configurations exist.

In this study the general configuration shown in Figure 4.4-8 has been assumed. In this case each operating thruster has its own assigned power conditioning and control system. In the event of a failure of an operating thruster, its power conditioner unit can be switched to any standby thruster. Furthermore, a single reservoir is employed which feeds propellant to a common manifold through which propellant is distributed to all operational engines. Because of the extreme penalty for the additional propellant involved, redundancy in the reservoir system is undesirable. Thus, it is assumed that the reliability of the reservoir subsystem is increased internally without reservoir redundancy and does not become part of the tradeoff studies discussed above. This configuration has been shown to be optimum (i.e., minimizes system weight) for most solar-electric spacecraft studies to date (e.g., see Ref. 2).

Thruster Switching Criterion

The thruster modules associated with a solar electric propulsion system must be both throttled and switched to provide the proper power or impedance matching capability. The throttling schedule for each module is obtained directly from the power-time relationship for a given mission and the switching times associated with the number of thruster modules under consideration. The choice of the times at which thrusters are switched also affects system reliability.

The thruster switching criterion which minimizes (Ref. 2) the penalty associated with power matching is shown in Figure 4.4-9. In this case the thruster switching time is selected by reference to the ion beam power. The solid curve represents the beam power as it would appear if there were no efficiency penalties associated with throttling. The dashed curve represents the actual beam power with the throttling penalties included. The dashed curve can be followed by switching off a thruster when the total beam power
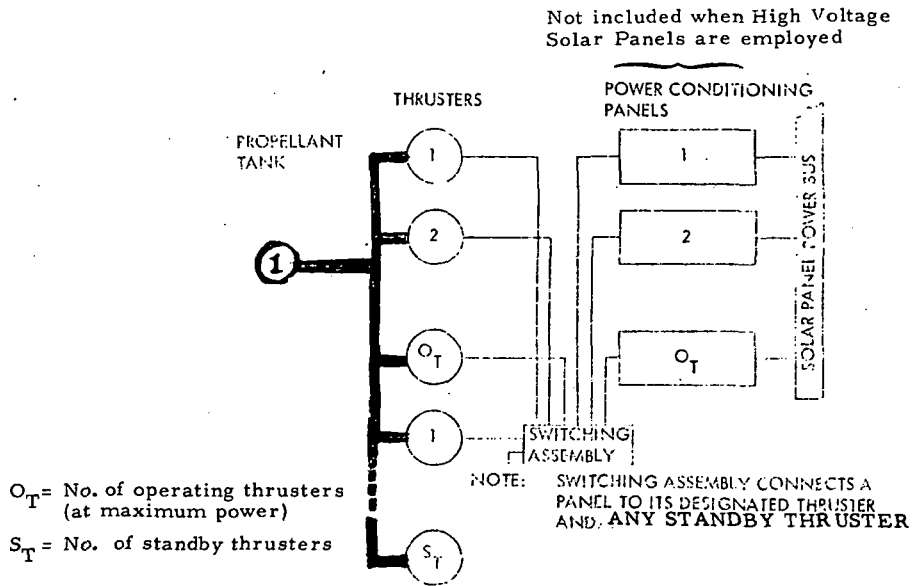
Figure 4.4-8. Generalized System Configuration

O_T = No. of operating thrusters (at maximum power)

S_T = No. of standby thrusters

NOTE: SWITCHING ASSEMBLY CONNECTS A PANEL TO ITS DESIGNATED THRUSTER AND ANY STANDBY THRUSTER

Not included when High Voltage Solar Panels are employed
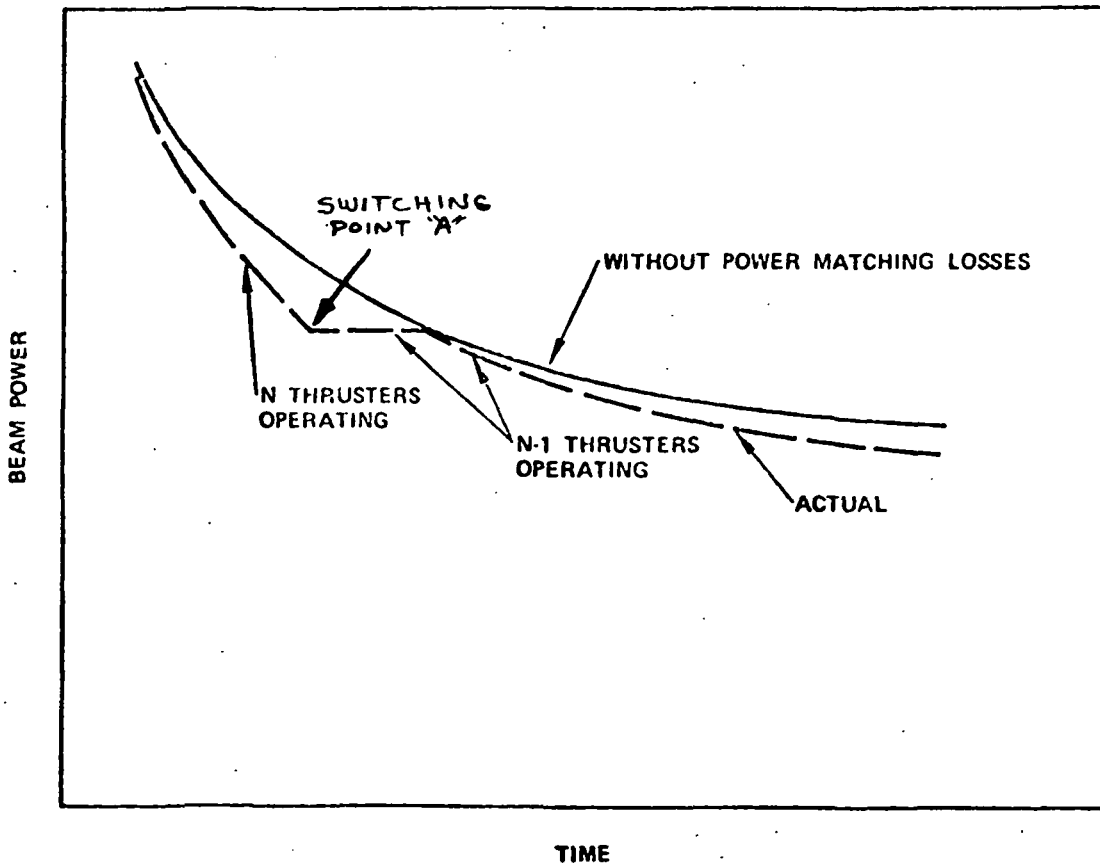
Figure 4.4-9. Power Matching Switching Criterion

for the throttled thruster array equals the nominal beam power of an array
minus one thruster. Since the thrusters cannot be operated at greater than
their nominal power, switching at these times (e.g., point A) in Figure 4.4-9
will result in the available power being larger than that which the thruster
array can handle. The power conditioning system is designed, however, to
allow the thruster array to operate under such conditions.

4.4.2.2 Thruster Module Size Determination

Using the overall design points obtained by the trajectory analysis, it
is necessary to design an electric propulsion system which meets these
requirement while satisfying such additional constraints as those imposed by
reliability and power matching considerations. Because of the availability of
detailed scaling studies (e.g., Figure 4.4-10) such a design definition is
reduced to the determination of the number and size of thruster modules.

Since only state-of-the-art hardware is to be considered, thrusters
with anode diameters of 30 cm, 20 cm, and 15 cm were evaluated. Fig-
ure 4.4-11 shows the solar panel power which is allocated to the orbit rais-
ing thruster system for three thruster module sizes. In each case, the power
is "clipped" for a few days at the start of the mission. This clipping is a
result of the mass/reliability optimization for each propulsion system design
based on the noted thruster size. In each case the horizontal part of the
power curve represents operating a given number of thrusters at full power,
i.e., two 30-cm thrusters, four 20-cm thrusters, and seven 15-cm thrusters.
Although this "clipping" results in "throwing away" power, the integrated
effect of losing this small amount of power for a short time is so small that
adding an additional thruster module to utilize this power without degrading
reliability is disadvantageous.
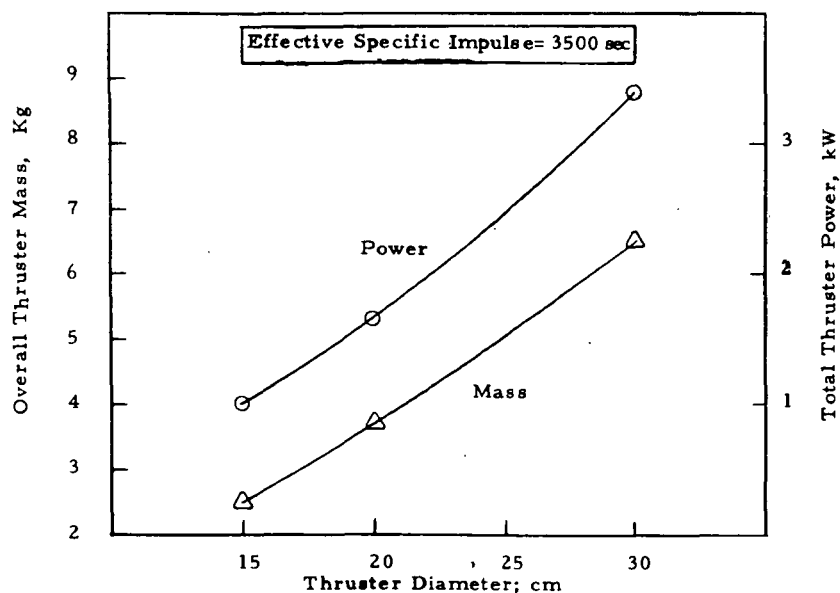
Figure 4.4-10. Thruster Module Power and Mass
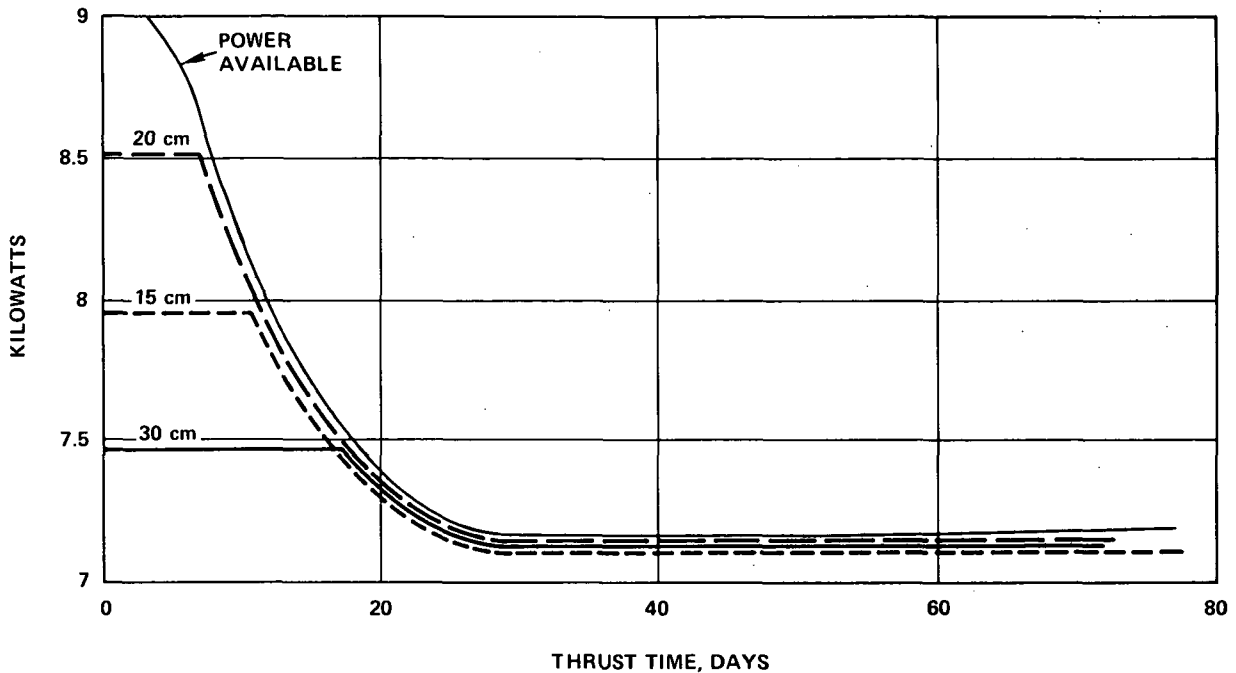
Figure 4.4-11. Solar Panel Power Allocated to Orbit Raising
Thruster System

Note that the total thrust time differs slightly between the three propulsion system designs. This variation is due not only to the different thrust/time profile, but also to the variation in thruster module efficiency with module size (e.g., see Figure 4.4-7). Mission time is eight days longer than thrust time due to eclipses.

The mass/reliability tradeoff for the thruster system is shown in Figure 4.4-12. The failure rates of the individual thruster sizes were determined in an earlier study (Ref. 1) and are shown in Table 4.4-7. The thruster failure rates are presumed constant throughout their lifetime.

In Figure 4.4-12 system reliabilities are shown both for the nominal failure rates and for failure rates 10 times these nominal values. The lower or nominal failure rate represents the minimum which is expected based on the studies in Ref. 1. The higher failure rate is estimated to be an upper bound on the failure rate which might be experienced. The effect of this wide range of thruster failure rates must be considered because experimentally provided statistical thruster failure data is unavailable at this time. Optimizing system mass and reliability requires that the best system be "above" and "to the left" of other systems on the figure, i.e., the system should have a high reliability and low mass. Although small thruster modules have higher reliability individually than larger thruster modules, thruster module systems made up of 30-cm thrusters are substantially superior for this mission when

4.4-21
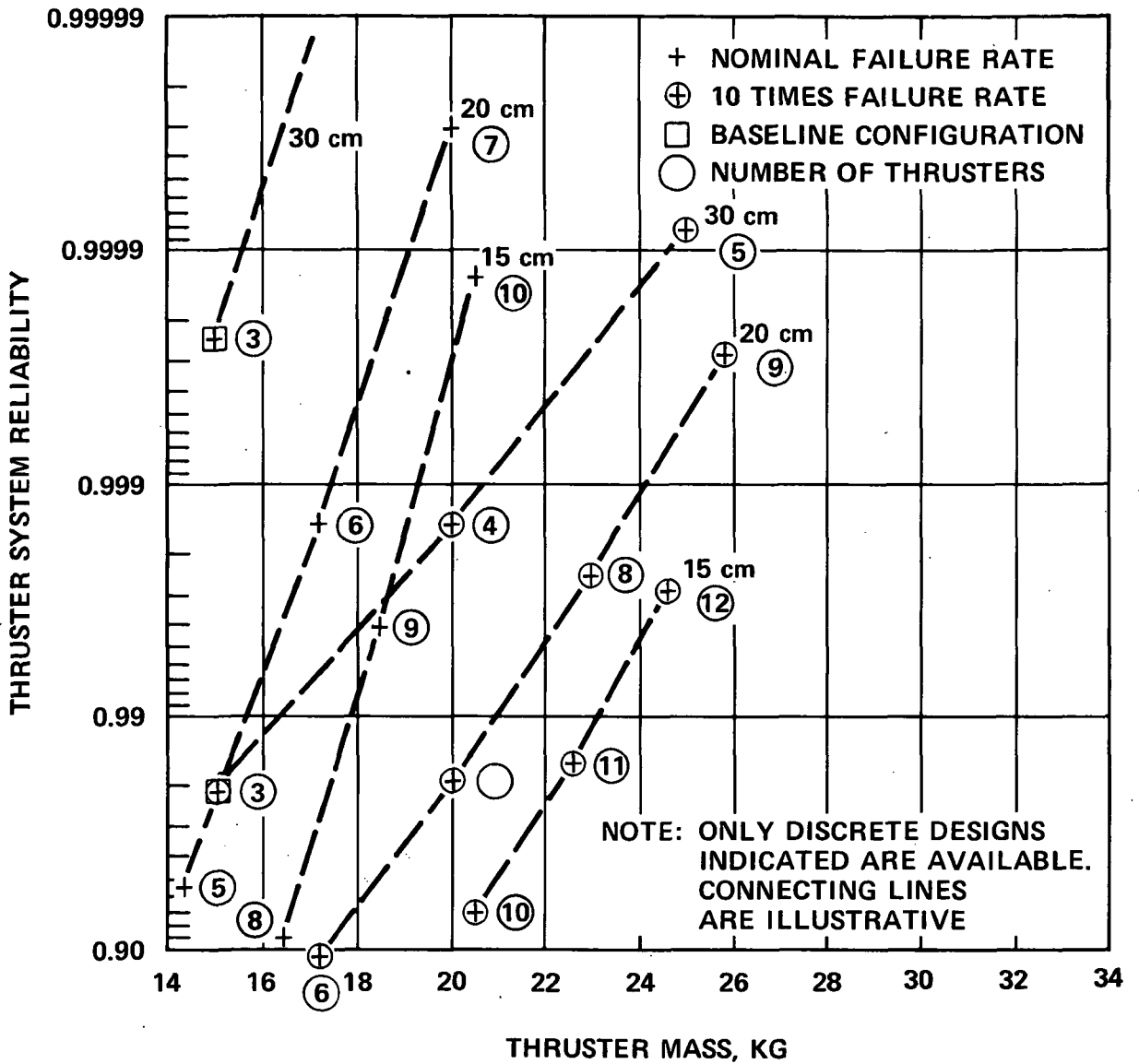
Figure 4.4-12. Thruster System Reliability vs Mass

TABLE 4.4-7. THRUSTER SUBSYSTEM FAILURE RATES
(FAILURES IN 10^6 HOURS)

Thruster Failure Rate	Thruster Size		
	15 cm	20 cm	30 cm
Minimum (nominal)	3.9	4.6	6.4

4.4-22

either nominal or 10 times failure rates are used, indicating that the 30-cm thruster module is the proper choice for the baseline design. The selected design has three 30-cm thrusters, only two of which are operating at any one time. The reliability estimate for this system design is about 98 percent when the thruster module failure rate is assumed to be 10 times the nominal value. Thrusters must operate less than 2000 hours and be throttled to no lower than 90 percent of nominal power. Both life and throttling requirements are well within the present state-of-the-art for the 30-cm thruster.

4.4.2.3 Module Designs

As a result of the studies and considerations presented above, the number, sizes, and designs of the thruster and reservoir modules to be used on the orbit raising ion thruster subsystem have been specified. Since the scaling laws used in these studies were based on state-of-the-art hardware, it is felt that the credibility of the results is established.

Thruster and Feed System Module. The thruster and feed system module proposed for all baseline designs is a 3.6 kW, 30-cm mercury bombardment ion engine operating at 3500 sec effective specific impulse. A schematic of the thruster and feed system showing overall dimensions and various components is provided in Figure 4.4-13, and a photograph of this thruster is shown in Figure 4.4-14.

A brief description of the operation of this device is as follows. The hollow cathode, located on center in the rear of the discharge chamber, emits electrons and some neutral mercury atoms. The magnets and magnetic end plates produce an approximately axial magnetic field in the discharge chamber. The electrons spiral around these field lines and are electrostatically reflected from the ends of the discharge chamber. They can thus reach the cylindrical anode only by scattering collisions with residual gas (mercury) atoms, ions, or other electrons. These collisions ionize the mercury atoms in the discharge chamber, creating the plasma from which the ions are extracted by the two-grid electrode system to form the beam. A mercury vapor hollow cathode neutralizer is used to neutralize the beam. Since the thruster operates at high voltage, propellant isolators are mounted immediately downstream of the cathode and main flow vaporizers to isolate the propellant reservoir electrically from the thruster. Thus, the Hg reservoir can be mounted at spacecraft ground.

A listing of the key operating and performance parameters and a component weight breakdown of the thruster and feed system are given in Tables 4.4-8 and 4.4-9, respectively.

The startup and shutdown procedures for the thruster showing the sequence and timing of the various power supplies are given in Table 4.4-10. The specific control modes employed for the various thruster electrical parameters are identified in Table 4.4-11.
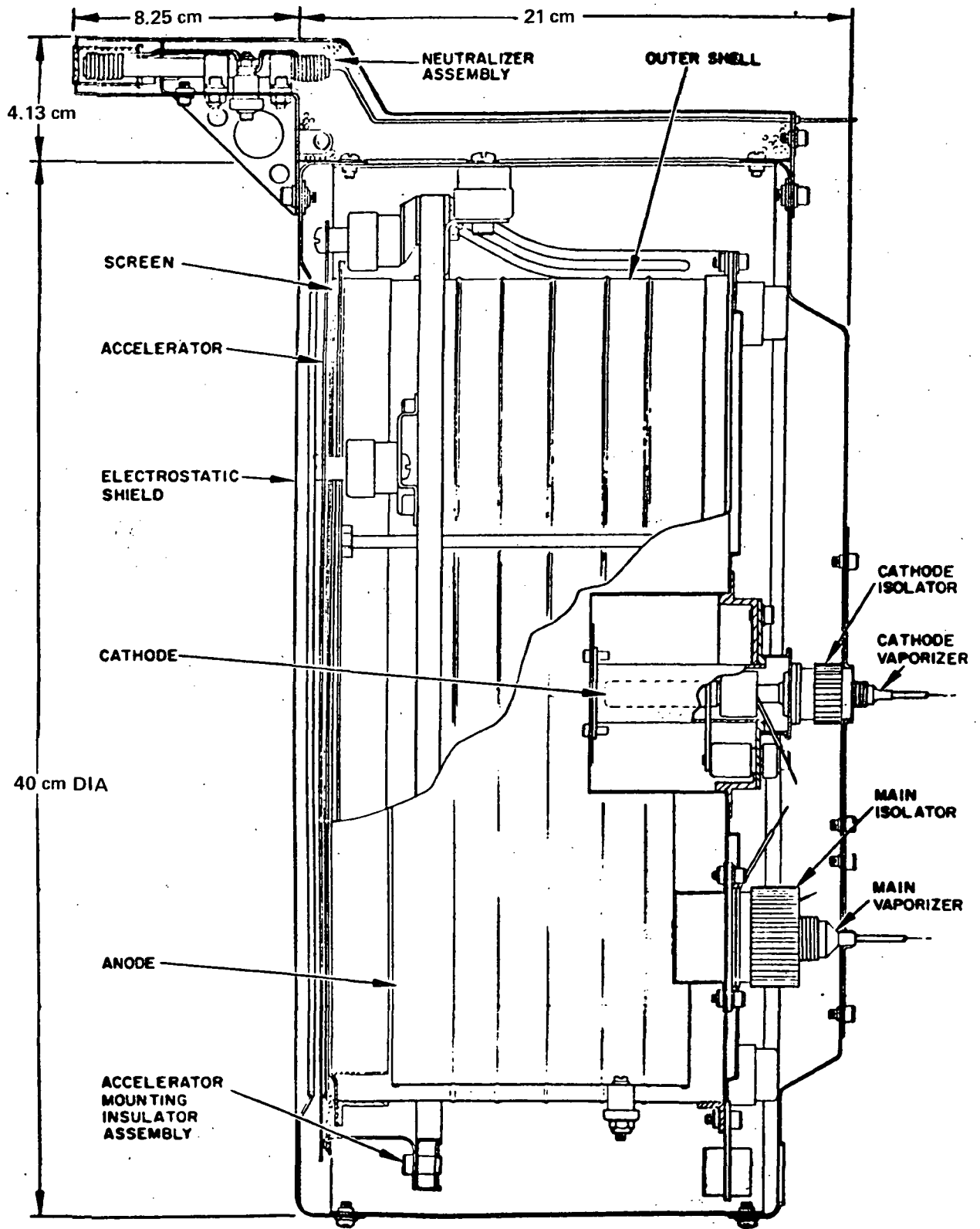
Figure 4.4-13. Schematic of Thruster and Feed System Module
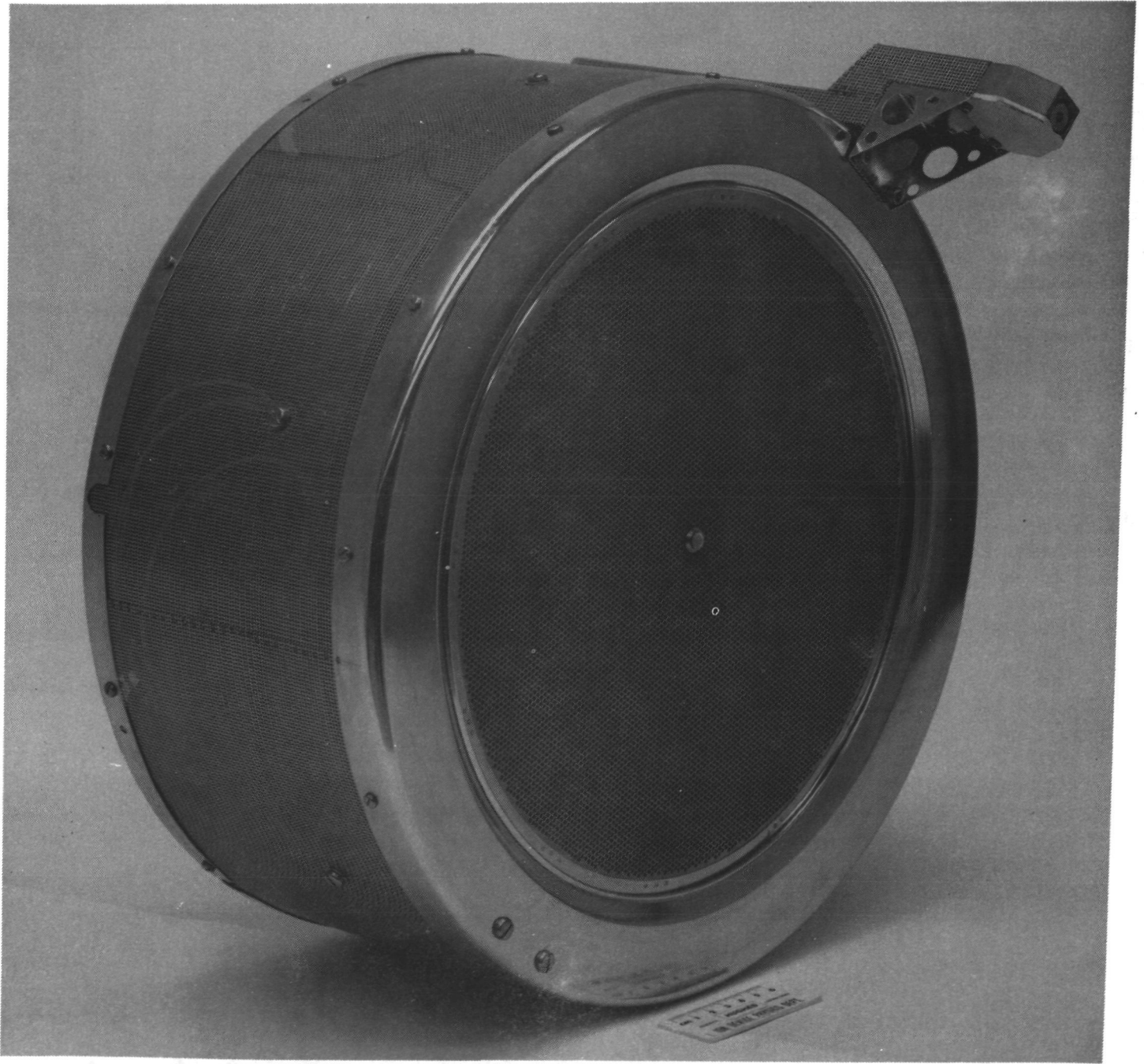
Figure 4.4-14. Photograph of HRL 30-cm Thruster and
Feed System Module

TABLE 4.4-8.   THRUSTER OPERATION PARAMETERS

Parameter	Current Performance	1973 ATS/ AMS Design
Effective Specific Impulse, sec	2840	3500
Input Thruster Power, W	2452	3560
Thruster Beam Power, W	1850	3020
Power Efficiency (at rated power), %	75.6	85
Discharge Losses (at rated power), eV/ion	260	220
Propellant Utilization Efficiency, %	90	90
Accel-Decel Ratio	2.5	2
Beam Current, A	1.85	2
Beam Potential, V	1000	1510
Thruster Power Losses, W		
Discharge	483	440
Fixed[1]	70	50
Neutralizer Coupling	37	40
Accelerator	12	10

[1] Fixed losses include all vaporizers, cathode heaters and keeper and isolators.

TABLE 4.4-9.   COMPONENT WEIGHTS OF 30 CM THRUSTER

Thruster Shell with 12 Magnets	1.12 Kg
Backplate Assembly with 8 Magnets	.68
Optics Assembly	1.62
CIV Assembly	.30
MIV Assembly	.14
Plenum Assembly	.34
Baffle Assembly	.20
Anode	.22
Ground Screen*	1.28
Neutralizer	.50
TOTAL	6.40 Kg

* Note: May be part vehicle structure in final configuration.

TABLE 4.4-10.   TIMING SEQUENCE FOR STARTUP AND SHUTDOWN FOR 30 CM THRUSTER

Automatic Startup Sequence

Automatic Startup Command

↓

Main Isolator Volt. ON - Start Level
Cathode Htr. Volt ON - Start Level
Neut Htr/Vap. Volt ON - Start Level

↓

T_1 = 30 Min.

↓

Cathode Vap. Volt ON - Start Level
Main Vap. Volt ON - Start Level
Cathode Keeper Volt ON - Start Level
Neut. Keeper Volt ON-Start Level

$I_{NK} \geq 0.5$ A $I_{KK} \geq 0.5$ A

Neut. Htr. -Vap Current
to Run Level

⊕

Discharge Volt ON - Start Level
Discharge Current Control Set to 10 A

↓

$I_I \geq 1$ A

↓

Close Δ V_I loop (cath. vap.)
Cath. Htr. to Run Setting

↓

T_2 = 10 Min.

↓

Screen Volt ON - Start Level
Accel Volt ON - Start Level
Activate Recycle Sequencer

↓

$I_B \geq 1.0$ A

↓

Close I_B loop (main vap.)
Initiate sequence to Increase I_B to 1.5 A

↓

I_B = 1.5 A

↓

Main Isol. Htr. Current to Run Setting
Cath. Keeper Current to Run Setting
Neut. Keeper Current to Run Setting
Close V_{NK} loop (neut. vap.)

↓

I_B = 1.5 A

I_{NE} = 1.5 A

↓

" Thruster Operating"

Automatic Shutdown Sequence

| Beam Off Command |

↓

Screen Voltage OFF
Accel Voltage OFF
Main Vap Current set to   A
Discharge Current set to 5 A
Neut. Htr. Current set to Start Level

↓

| Thruster OFF Command |

↓

Discharge Volt OFF
Main Vap Volt OFF
Cathode Vap Current set to   A (100 mA equiv.)
Cathode Htr. Volt set to Start Level
Cathode Keeper Current set to 0.5 A
Neut. Keeper Current set to 0.5 A

↓

T_2 = 10 Min.   (Manual hold possible here)

↓

Cathode Vap Volt OFF
Cathode Keeper Volt OFF
Neut. Htr. Volt OFF
Neut. Keeper Volt OFF

↓

T_3 = 60 Min.

↓

Cathode Htr. Voltage OFF
Main Isol. Voltage OFF

4.4-27

TABLE 4.4-11. THRUSTER PARAMETRIC CONTROL MODES

Parameter	Control Mode
1. Beam Voltage	Constant (manual setpoint).
2. Beam Current	Closed-loop controlled with main vaporizer. Level established by variable setpoint from throttling circuitry.
3. Discharge Voltage	Closed-loop controlled with cathode vaporizer (manual setpoint).
4. Discharge Current	Controlled in proportion to beam current. Level established by variable setpoint from throttling circuit.
5. Accel Voltage	Controlled in proportion to beam current over range of 0.68 A to 2.0 A. Level established by variable setpoint from throttling circuit.
6. Accel Current	Limited by overload detection circuitry.
7. Cathode Keeper Voltage	Regulates to provide constant current.
8. Cathode Keeper Current	Constant (manual setpoint).
9. Cathode Vaporizer Current I	Closed-loop controlled to maintain discharge voltage proportional to manual setpoint.
10. Main Vaporizer Current I	Closed-loop controlled to maintain beam current proportional to variable setpoint from throttling circuit.
11. Main Isolator Current I	Constant (manual setpoint).
12. Cathode Tip Heater Current I	Controlled in proportion to discharge current by variable setpoint from throttling circuit.
13. Neutralizer Tip and Vaporizer Heater Current I	Closed-loop controlled to maintain keeper voltage proportional to setpoint.
14. Neutralizer Keeper Voltage	Closed-loop controlled with neutralizer tip and vaporizer heater current (manual setpoint).
15. Neutralizer Keeper Current	Resultant of keeper supply level adjustment.
16. Magnetic Baffle Coil	Carries discharge current.

I   Internally current regulated power supplies

Mercury Propellant Reservoir. The basic requirement of the mercury tankage is that it reliably stores liquid mercury under a controlled pressure of approximately 2 atm. for the duration of the mission, including the launch phase. It is desirable that the weight of the tank itself be approximately 3% of the total weight of the system when full of mercury. This goal is made practical by the very high density of the mercury (13.6 g/cm^3).

As noted previously, the optimum reservoir system configuration for the orbit raising thrust subsystem consists of a single tank with redundancy in its expulsion system. To further increase reliability, the number of valves should be kept to a minimum (possibly one) to carry out system operation although redundant valves may be employed.

The reservoir concept employed for the NASA/LeRC SERT-II test flight was that of a spherical metal tank divided into two compartments by an elastomeric bladder. A representative design of such a tank is shown in Figure 4.4-15. One side is filled with mercury and the bladder is deformed to leave a relatively small void on the other side. This void is filled with a liquid (typically freon) in equilibrium with its vapor, and sealed. The pressure is then determined by the vapor pressure of the driving liquid and the ambient temperature, provided some material always remains in the liquid phase. This temperature may be artificially controlled if necessary. However, the operating pressure range over which the feed system will give satisfactory performance is such that a driving fluid may be chosen so that the ambient vehicle temperature will be sufficient.

The propellant is valved off near the tankage to avoid launching with flexible lines loaded with mercury. These valves would be opened prior to thruster-on commands. An orifice is used to restrict the propellant flow to prevent the momentum of the pressurized mercury from hammering the porous refractory metal vaporizers and damaging them. (There would be no gas cushion in the feedlines because of bleedout in space through the porous vaporizer).

Analysis on the tankage design itself has shown that spherical tanks of 6061 Aluminum 304 LC stainless steel or 6Al-4V Titanium meet the strength and weight requirements. Stainless steel has been chosen here because of reported attacks on both aluminum and titanium by mercury at high temperature and long exposures. For the mission under consideration in this study, 54.5 kg of mercury propellant is required. Table 4.4-11 lists the dimensions of the propellant tank which has the general configuration shown in Figure 4.4-15. The dimensions and weight shown in Table 4.4-12 allow for a 5 percent contingency in propellant and for a 6 percent tank ullage.
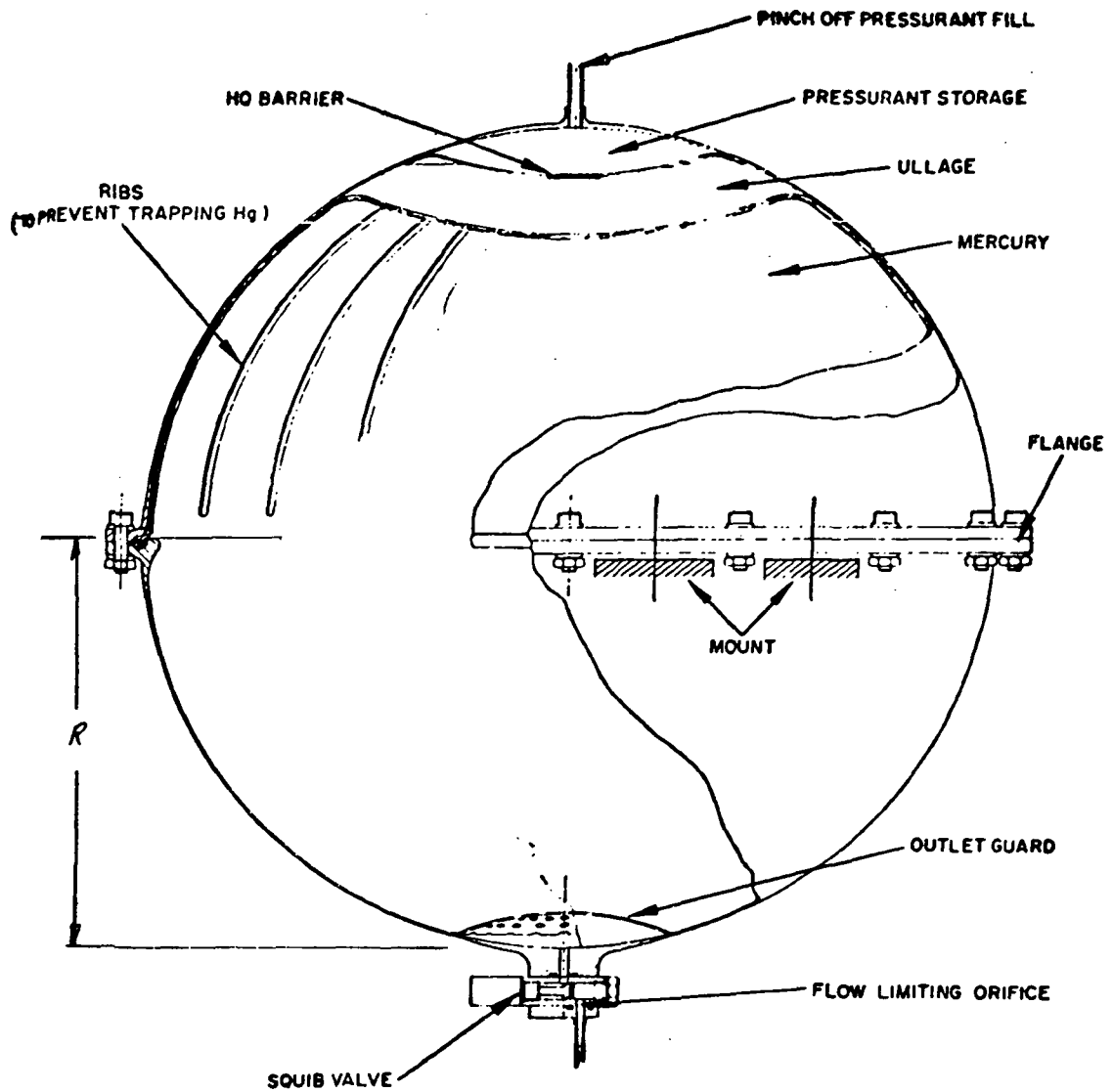
Figure 4.4-15.   Positive Expulsion Mercury Propellant Reservoir

TABLE 4.4-12.   TANK DIMENSIONS

Mercury Weight	57.2 Kg
Mercury Volume	4200 cm^2
Tank Volume	5000 cm^2
Tank Radius	10.6 cm
Tank Weight	1.68 Kg
Total Weight	59.1 Kg

4.4.2.4 Thrust Vectoring Options

The flight dynamics and spacecraft orientation control studies conducted during this program have shown that the prime propulsion system should be designed to remove orbital inclination and perform vehicle attitude control during the orbit raising thrusting phase. For this reason some thrust vectoring scheme must be included in the three 30-cm thruster array discussed above. Such a capability will also negate any potential unwanted thrust vector center of mass misalignment.

A number of techniques for achieving thrust vectoring in a 5-cm thruster were described earlier. For a 30-thruster the applicable techniques are:

1) Translator and Gimbals

2) Movable Screen Electrode

3) Dual Grid Electrostatic

Table 4.4-13 summarizes the important characteristics of these three basic types of thrust vectoring techniques as applied to a 30-cm O-R thruster module. The dual grid electrostatic system selected as baseline for the 5-cm thruster is beyond the state-of-the-art for a 30-cm thruster because of the great difficulty in fabricating the deflectable apertures over a 30-cm diameter. The translator and gimbals techniques which have been employed in numerous previous interplanetary studies is considered state-of-the-art. However, if the three 30-cm thruster modules were canted such that each would fire through the vehicle center of mass, no translator would be required. Thus, the necessary thrust vector control could be achieved by individual two degree of freedom thruster gimbaling with an acceptable attitude bias.

The movable screen electrode was selected as the baseline design for the O-R thrusters because of added weight and power of the gimbaling method and the additional complexity required by the use of flexible mercury feed lines. Under NASA Contract 3-15385, a 30-cm movable screen electrode system was developed and tested to demonstrate the applicability of vectoring a large beam by moving the screen electrode. The system, which is shown schematically in Figure 4.4-16, is a complete bench subassembly and is demountable from the thruster. The screen and accelerator electrodes are supported from a lightweight annular ring which provides a stable mounting base for the optics and a convenient interface to the mounting brackets on the thruster outer housing. The screen electrode is supported by six helical springs attached to the screen electrode mounting brackets and is also held by support wires at the periphery and by a center support. The helical springs, when heated by passing current through them, serve as a motion generating device. The flexible columns provide the proper axial spacing while allowing flexibility in the transverse direction with a minimum of resisting force. During recent tests of this system up to ±6 degrees of deflection was obtained at spring powers of 1.25 W, proving that the basic concept

TABLE 4.4-13. THRUST VECTORING TECHNIQUES

Technique	Comments
Translator and Gimbals	• Large O-R weight penalty ≥ 6.8 Kg
	• O-R operating power ≥ 12 watts
	• Complicates spacecraft booster structural interface for O-R
	• Requires flexible O-R propellant feedlines
	• O-R thruster array coordinates 1:1 with body axis
	• Present technology hardware
	• Limited life expectancy for 5 years AC&S mission
Movable Screen Electrode (Selected as baseline design for O-R thrusters)	• 30 cm prototype design presently under development
	• Thermal response time 10 to 100 sec
	• Deflection capability greater than 10 degrees
	• Spring and flecture deflection only motion required
	• Thrust vector not 1:1 with body axes - requires attitude bias
	• 2000 hr test on 5 cm thruster - approximately 1 W for 10 deg deflection
Dual Grid Electrostatic (Selected as baseline design for AC&S thrusters)	• Mechanical Designs for O-R thruster sizes difficult
	• Hardware developed and life tested on 5 cm AC&S thruster
	• Electrical response time less than 10^{-4} sec
	• Power less than 1 watt for 10 deg deflection
	• No moving parts
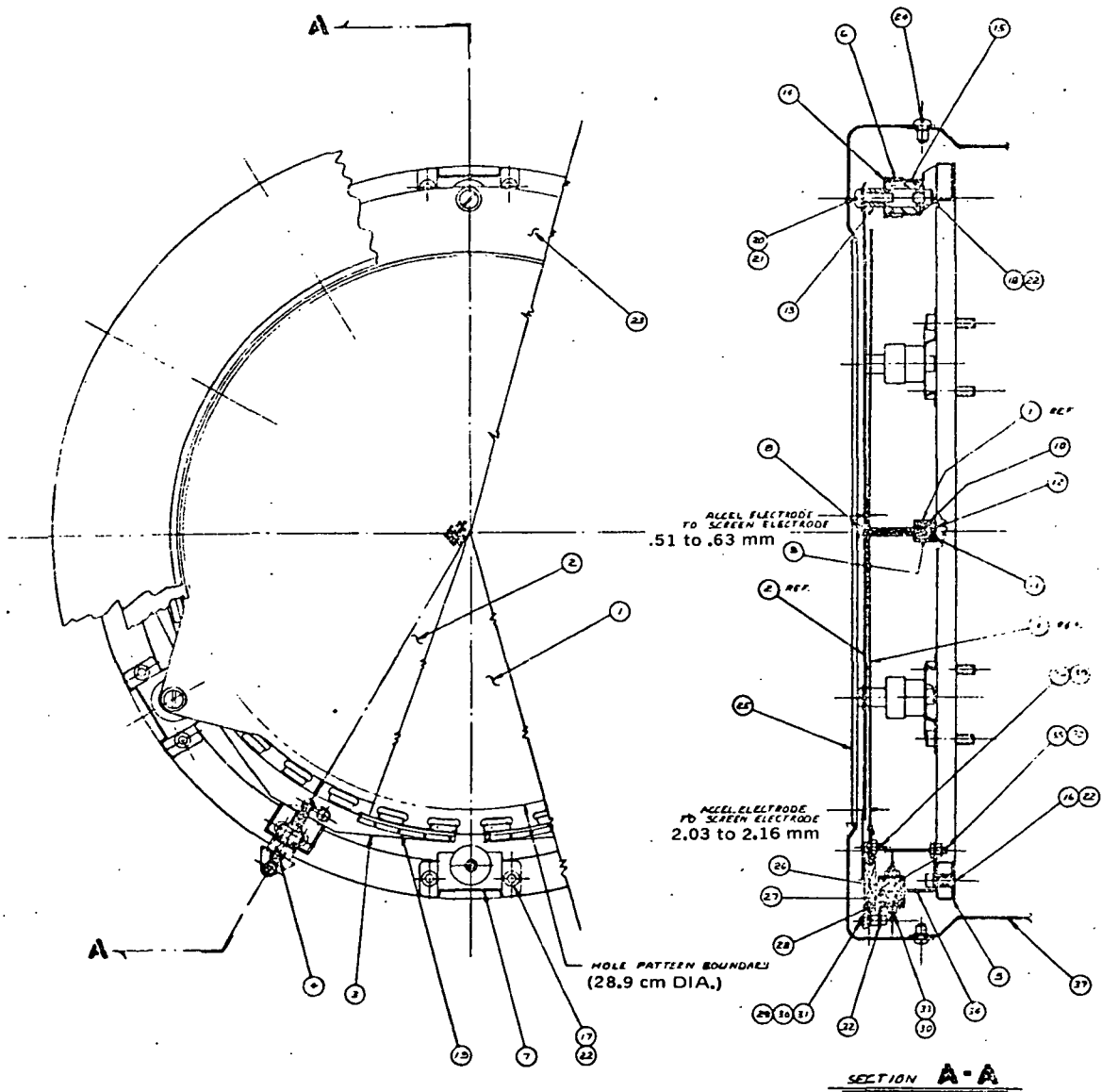
Figure 4.4-16. 30 Cm Movable Screen - Thrust Vectoring System

of a movable screen electrode is applicable to a 30-cm thruster. However, structural modifications will be required to improve the mechanical stability of the system to achieve reliable operation over the full power range. Development of this system is continuing.

4.4.2.5 Particle and Field Interactions*

The application of electric propulsion to near-earth spacecraft presents some potential problem areas that are not present with conventional high-thrust propulsion systems. Among the more important of these areas are the generation of magnetic and electric fields by thruster-ion beam system and its associated electrical circuitry, and the possible impingement on the spacecraft of neutral atoms and ions from the ion beam. The magnitude of the above effects must be determined and minimized before the propulsion system design is fixed.

Magnetic Fields. The primary source of the remnant magnetic field on the spacecraft is the axial permanent magnets mounted on each thruster. The contributions from currents flowing in the power supply and solar cells have been estimated to be at least three orders of magnitude weaker than the contributions from one thruster and thus will not be considered further. The thruster magnets produce an axial field of 5 to 10 gauss in the plane of the ion extraction grids over approximately the full 30-cm thruster diameter. For the Hughes 30-cm thruster, the resulting dipole moment was experimentally measured and found to be approximately 5 amp-M^{-2} gauss at a distance of 1 meter from the extraction grids. The overall contribution of the complete thruster array can be minimized by alternating the sense of the dipole moments to provide the maximum possible field cancellation. The resulting magnetic field strength should cause no interference with any systems or experiments proposed for the ATS/AMS vehicle.

Electric Fields. All the electric potentials, and hence electric fields associated with either an active or passive spacecraft, are determined by the equilibrium condition that no net current is interchanged between the vehicle and space plasma.

For the SERT-II vehicle, which was instrumented with a hot wire emissive probe to measure the spacecraft and ion beam potentials with respect to the ambient space plasma, it was found that the spacecraft potential varied from -12 to -28 volts with the thruster operating, and from -6 to -11 volts with the thrusters off. These spacecraft potentials were a function of the orbital position and the thruster operating parameters. It was also demonstrated on SERT-II that the spacecraft potential could be varied from 0 to -80 V by biasing the neutralizer with respect to the spacecraft. The above results should be applicable to the ATS/AMS spacecraft and should not cause any deleterious effects with any experiments associated with this mission.

---

*This discussion (including all conclusions) applies to the attitude control and station-keeping thruster subsystem presented in Section 4.4.1 as well as to the orbit raising system being considered here.

RFI. The radio frequency interference experiment flown by SERT-II to detect any noise generated by the SERT ion thruster in the 300-700, 1680-1720, and 2090-2130 MHz bands showed that there was no interference in these spacecraft communications bands (Ref. 3).

Similar results would be expected from the proposed cluster of three 30 cm ion thrusters since the local beam plasma density will be comparable to the SERT-II situation.

Particle Impingement and Disposition. Continued exposure of various vehicle subsystems (i.e., solar panels, antennas, etc.) to a flux of either direct or charge exchange ions or neutral particles could seriously degrade over-all system performance.

Figure 4.4-17 qualitatively describes the particle efflux from an ion engine. Beam ions, neutral mercury efflux, and sputtered material are, in general, emitted into a 2π steradian volume. The beam ions are highly directional with about 96 percent of the beam current emitted into a beam half angle of $\sim 20^{\circ}$. However, some of the more poorly focussed ions may have divergence angles approaching 90 degrees. On the other hand the un-ionized neutral propellant and the sputtered grid material are emitted in a cosine distribution so that there is an appreciable flux of these contaminates at large angles and a small percentage of neutrals can arrive at any space-craft component located downstream of the thruster exhaust plane. However, for the spacecraft under consideration, no component will be located down-stream of the exhaust plane of an operating thruster; therefore, beam impingement and neutral particle deposition can be neglected.

4.4.2.6 System Layout and Description

The introduction of a modularized ion thruster subsystem into a total space vehicle design is affected by a number of considerations other than those discussed above. Included in these considerations are the inter-faces between the thruster subsystem and other major subsystems such as the power system (i.e., solar panel, energy storage system, and power conditioning and control system) and the guidance and control system. In addition, the thruster modules and reservoir must be mechanically, ther-mally, and electrically integrated into the total spacecraft system.

Interface with Spacecraft Subsystems. The relation of the orbit raising thruster subsystem to other spacecraft electronic subsystems and components in the baseline design is presented in Figure 4.4-18 for the case where High Voltage Solar Arrays are employed.

During thruster operation the High Voltage Solar Array (HVSA) is configured to provide screen, accelerator, discharge and keeper starting power directly to two of the three thrusters in the thruster array. Regula-tion and sequential control of this power is performed by the on-board HVSA control electronics which issue digital control commands to the regulation and reconfiguration circuitry based on the general operational format required for the 30-cm thruster, the sensed thruster voltages and
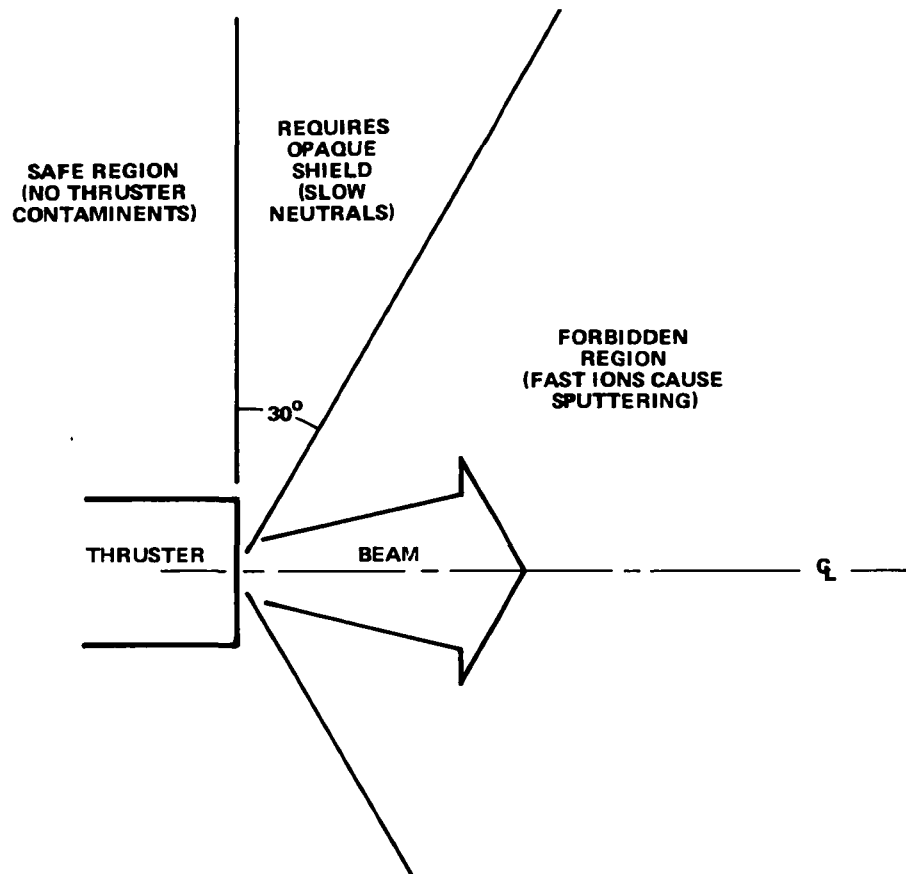
THRUSTER CONTAMINENTS	DESIGN CONSTRAINT
FAST IONS IN 60° HALF ANGLE CONE	AREA MUST BE LEFT CLEAR
NEUTRAL PARTICLES IN DOWN-STREAM HEMISPHERE	CAN PROTECT S/C WITH OPAQUE SHIELD

Figure 4.4-17.   Particle Impingement and Deposition on
Spacecraft Surfaces
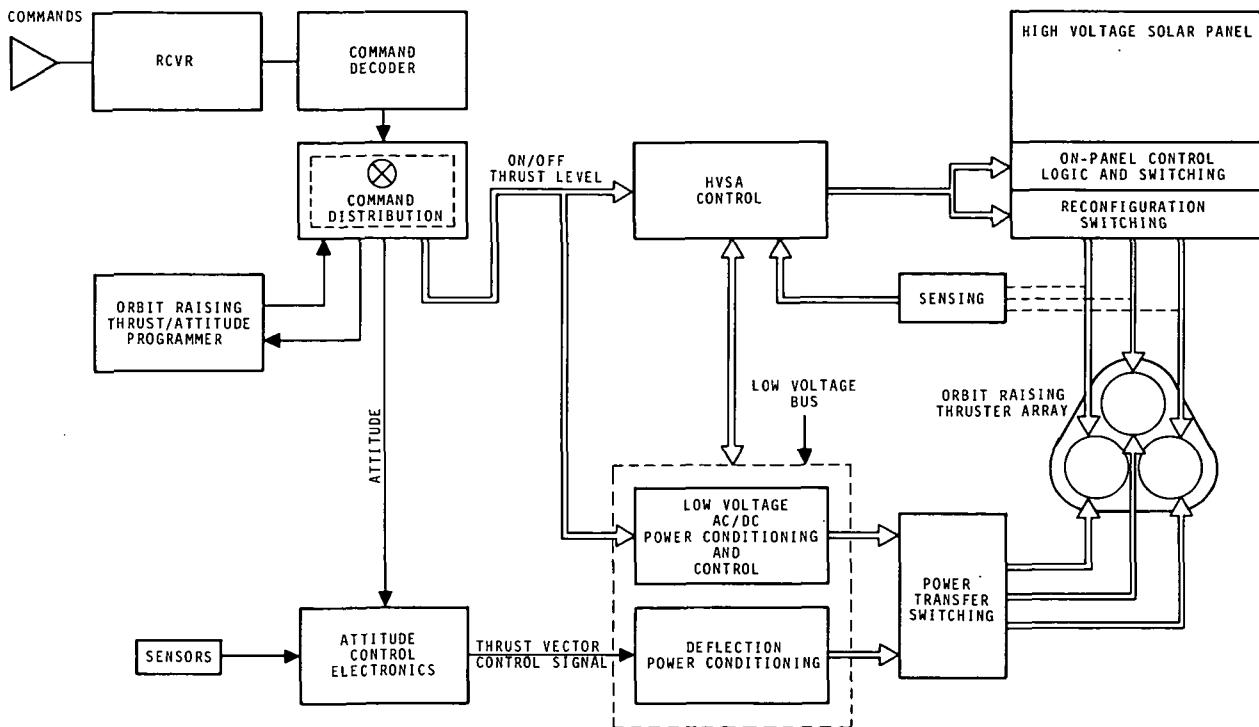
Figure 4.4-18. Orbit Raising Thruster Subsystem Interface
with Spacecraft

currents, and the thruster system command signals (preheat, startup,
thrust level, etc.) received from the spacecraft command distribution
electronics.

Additional conventional power conditioning operating from the 28 VDC
bus is required to provide conditioned low voltage power for heaters, vapor-
izers and keepers (at the run level) and for powering the movable screen beam
deflection system. In order to conserve weight this power conditioning is
designed to power only two thrusters; hence transfer switching is included to
allow rerouting the power to the standby thruster in the event of a failure.

Two-axis beam deflection of each operating thruster is accomplished
with analog thrust vector control signals received from the attitude control
electronics. These signals act as variable set point references in individual
deflection supply control loops.

The orbit raising thrust/attitude programmer which is up-dated once
each day, both directly and indirectly controls the operation of the thruster
system. It directly establishes the thruster on-off thrust profile by initiating
start-up and shut-down, and by setting beam current magnitude. It indirectly
determines the beam deflection (thrust vector) angles with the spacecraft
attitude profile issued to the attitude control electronics.

Although not explicitly shown, maximum power tracking circuitry similar to that suggested for ion propulsion systems powered with conventional power conditioning and a low voltage solar array (e.g., see Ref. 2), can be incorporated as part of the HVSA control logic with a negligible increase in weight.

Implementation of the tracker would be restricted to individual screen supplies which consist of configured solar cell power blocks. Since the thruster power use profile does not utilize the total maximum power during the earlier portions of the orbit raising mission, the tracker would actually function more as a monitor of power available to aid in determining allowable thrust/attitude programmer up-date levels.

The proximity of the commanded operating point (beam current level) to the maximum power point of the combined power blocks would be determined by injecting a low amplitude-low frequency dither signal into the beam current control loop. Then, by electrically monitoring the sensed screen voltage and current (already required for other control functions), an assessment of the operating point's position on the I-V characteristics would be made. This would establish whether a commanded beam current level could be achieved or what reserve existed between the commanded level and the maximum level.

Thruster Array Integration. Considerations of the mechanical, thermal, and electrical integration of the O-R ion thruster system into the A-1 spacecraft configuration have been covered in Sections 3.1, 4.6, and 4.5, respectively. Thus, only brief mention of the propulsion system requirements and constraints which effect these integration considerations will be given here.

The mechanical integration of three 30-cm thruster modules and single Hg propellant reservoir is relatively straightforward. As shown in Figure 4.4-19, each thruster is mounted to a thruster array shelf and canted such that its thrust vector is through the spacecraft center-of-mass. In order to minimize thrust loss (i.e., perpendicular thrust components) the cant angle is minimized by placing the thruster modules in a triangular array. This design also minimizes the overall array envelope and simplifies the spacecraft structural design at the spacecraft separation plane. The Hg reservoir is mounted directly to the equipment shelf from which structural supports emanate to both the thruster shelf and the sides of the spacecraft. In this way the major propulsion system weight (viz. the propellant reservoir) is rigidly mounted to the spacecraft.

From a thermal constraint standpoint, the allowable operating temperature limits for the thruster, Hg feed system, and Hg Reservoir are given in Table 4.4-14.
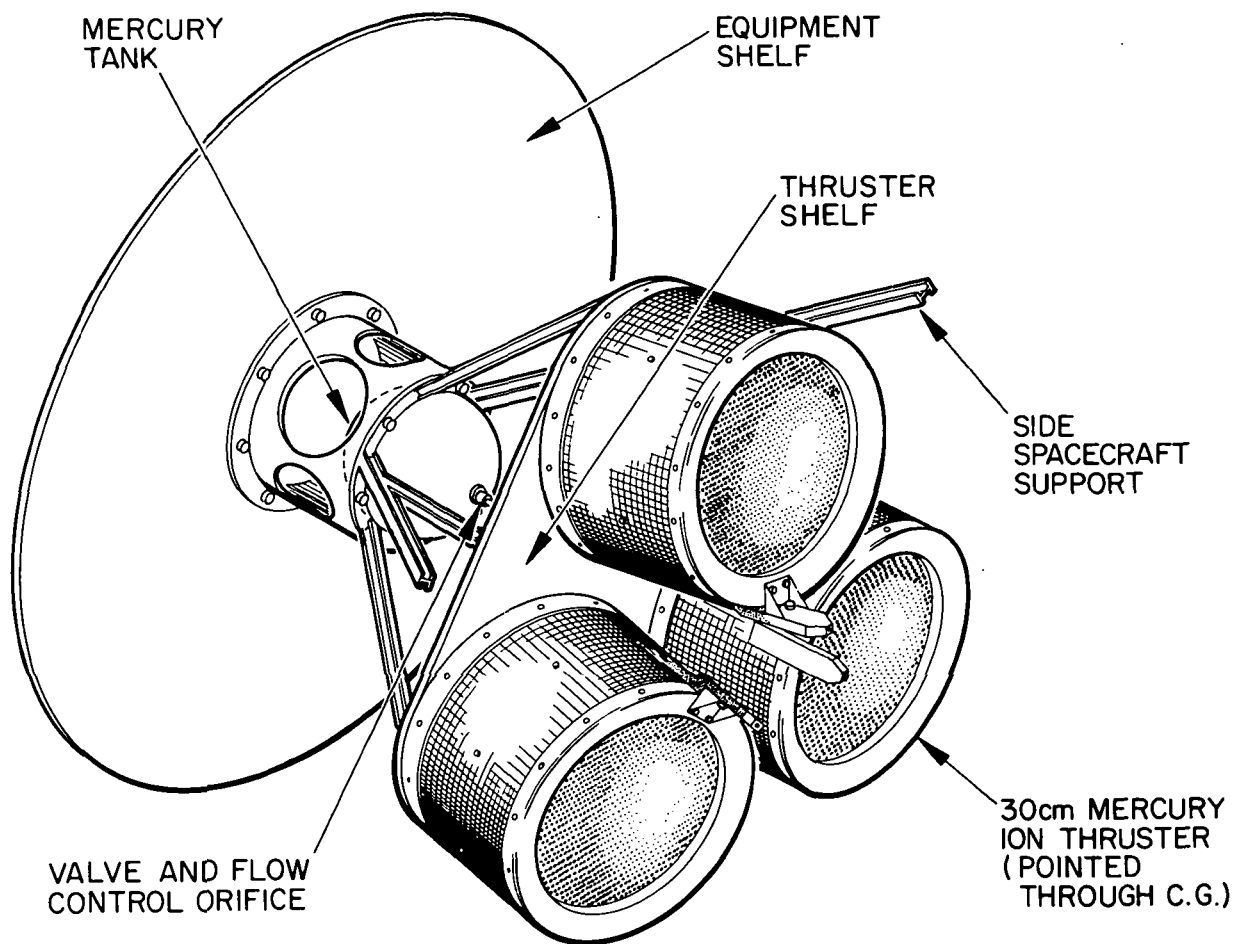
Figure 4.4-19. Orbit Raising Thruster Array

TABLE 4.4-14. ALLOWABLE TEMPERATURE

Subsystem	Operating Temperature, °K	
	Maximum	Minimum
Thrusters	673	-
Thruster Vaporizers	473	235
Mercury Reservoir	293	235
Mercury Feed Lines	473	235

A summary of the analyses which led to the general design specifications in Table 4.4-14 are as follows:

1) The critical thruster components are the permanent magnets mounted along the sides of the thruster cylinder. Above a critical temperature level (taken conservatively to be 673°K) they lose permanent magnetism. Aside from thruster redesign, which is not in the scope of this study, the only design parameter left open is thruster spacing. If the thrusters are tightly clustered, most of the heat generated at the anodes of the central thrusters must be radiated through the screen electrodes (i.e., in the direction of thrust). As the spacing between thrusters is increased, the cylinder sides have an increasing view to space and thruster temperatures decrease.

2) All components of the thruster feed system must be held at a temperature above the freezing point of mercury (234.1°K). In addition, there is an upper limit of 473°K for each of the three thruster vaporizers since the vaporizer heater must control the vaporizer temperatures between 523-623°K under normal operating conditions. The mercury reservoir must be held below the maximum permissible bladder temperature which is 393°K.

The electrical integration of the modularized ion propulsion system into the baseline spacecraft principally involves cable routing of thruster power from the slipring assembly (for HVSA power) and from the low voltage power conditioning via the standby transfer switching to terminations at the thruster array. The weight associated with the cabling (as well as the switching matrix) has been included in the electrical power subsystem breakdown given in Table 4.5-11.

System Design Specification Summary. A summary of the specifications of the complete orbit raising ion thruster subsystem including thruster array and propellant reservoir is given in Table 4.4-15. As indicated the total system weight including propellant is 75 Kg. The system requires a total initial power of 7.2 kW. By use of redundancy techniques system reliability is increased to levels greater than 0.99. Finally, the system design is based on a 30-cm thruster module which is scheduled for a 6000 hr life test during 1972 (NASA Contract No. NAS 3-15523).

TABLE 4.4-15. ORBIT-RAISING SUBSYSTEM DESIGN SPECIFICATIONS

PROPULSION SUBSYSTEM DEFINITION

- Thruster Array = 2 operating/1 standby

- Reservoir = 1

- Auxiliary Power Conditioning = 2.27 Kg

- System Weight = 20.4 Kg

- System Reliability ≥ 0.99

- Propellant Weight = 54.5 Kg

RESERVOIR

- Spherical Diameter = 21.2 cm

- Weight = 1.68 Kg

- Reliability ≥ 0.999

THRUSTER CHARACTERISTICS

Input Power	3.6 kW
Diameter	30 cm
Effective Specific Impulse	3500 sec
Mass Utilization	90%
Electrical Efficiency	85%
Beam Current Range	1.9 ±0.05A
Thrust Vector Technique	Movable screen electrode
Thrust Vector Capability	+10 degrees, 2 axes
Thruster Weight (including housing, feedlines, isolators, mounting interface, bulkhead-thruster cabling and movable screen mechanism)	5.5 Kg

REFERENCES
(Section 4.4)

1. Russell, K.J., Seliger, R.L., and Molitor, J.H., "Electric Propulsion Design Optimization Methodology," Journal of Spacecraft and Rockets, Vol. 7, No. 2, February 1970, pp. 164-169.

2. Schwaiger, L.E., Shollenberger, J.M., Jr., Molitor, J.H., and MacPherson, D., "Solar-Electric Propulsion Asteroid Belt Missions," Journal of Spacecraft and Rockets, Vol. 8, No. 6, pp. 612-617, June 1971.

3. Kerslake, W.R., Byers, D.C., Rawlin, V.K., Jones, S.G., and Berkopec, F.E., "Flight and Ground Performance of the SERT-II Thruster," AIAA Paper No. 70-1125, presented at the AIAA 8th Electric Propulsion Conference, Stanford, California, August 31-September 2, 1970.

4.5 ELECTRICAL POWER SUBSYSTEM

The electrical power subsystem designs for spacecraft configurations A-1, B-1 and B-5 are principally impacted by the end-of-life conditioned power required by the communication subsystem. The 1 kW (rf) Traveling Wave Tube (TWT) and the 2 kW (rf) Klystron which are common to the three configurations represent a load power demand of approximately 5 kW when both are operating simultaneously at saturation drive levels. By comparison the combined power requirements of other auxiliary subsystems, attitude control, orientation mechanisms, etc., are secondary and can be implemented in a standard manner typical of numerous spacecraft presently in operation.

The study effort concentrated on the TWT and Klystron requirements and the time phasing of power use for the A-1 configuration which employs 30-cm Hg bombardment ion thrusters for orbiting raising. For each of the baseline spacecraft configurations a corresponding power subsystem design was configured to satisfy total mission requirements. Trade studies were performed to judiciously select the best design approach from competing alternatives; however, as is clearly evident from a review of individual spacecraft configuration descriptions, the available power subsystem alternatives can be found distributed among the configurations. Therefore, to a great degree the approaches chosen to implement the electrical power subsystem design have contributed to making one spacecraft different and identifiable from another. A prime example of this is the use of a high voltage solar array with integral power conditioning on spacecraft B-5 and conventional power conditioning supplied from a medium voltage array on spacecraft B-1. Both are believed viable approaches for powering the communication system loads, but vary in the level of their technological development, weight, and cost.

A discussion of the various power subsystem tradeoffs considered can be found in Section 3.2.2 and a summary listing in Table 3-14. Table 3-5 in Section 3-1 presents the on-station baseline power budget requirements for the A-1, B-1 and B-5 spacecraft configurations and indicates the division of power for individual subsystem categories for both eclipse and non-eclipse conditions.

4.5.1 Spacecraft Electrical Power Subsystem Configurations

Configuration A-1 Power Subsystem

A power management block diagram of the electrical power subsystem for spacecraft configuration A-1 is shown in Figure 4.5-1. The rollout solar array is divided into two sections. The high voltage solar array (HVSA) section, which constitutes approximately 90 percent of the total array power, provides screen, accelerator, discharge and keeper starting power for the ion thrusters during orbit raising. Upon arrival on station the array power is rerouted through reconfiguration switches to the 1-kW TWT and to the 2-kW Klystron to provide the range of cathode and collector electronic
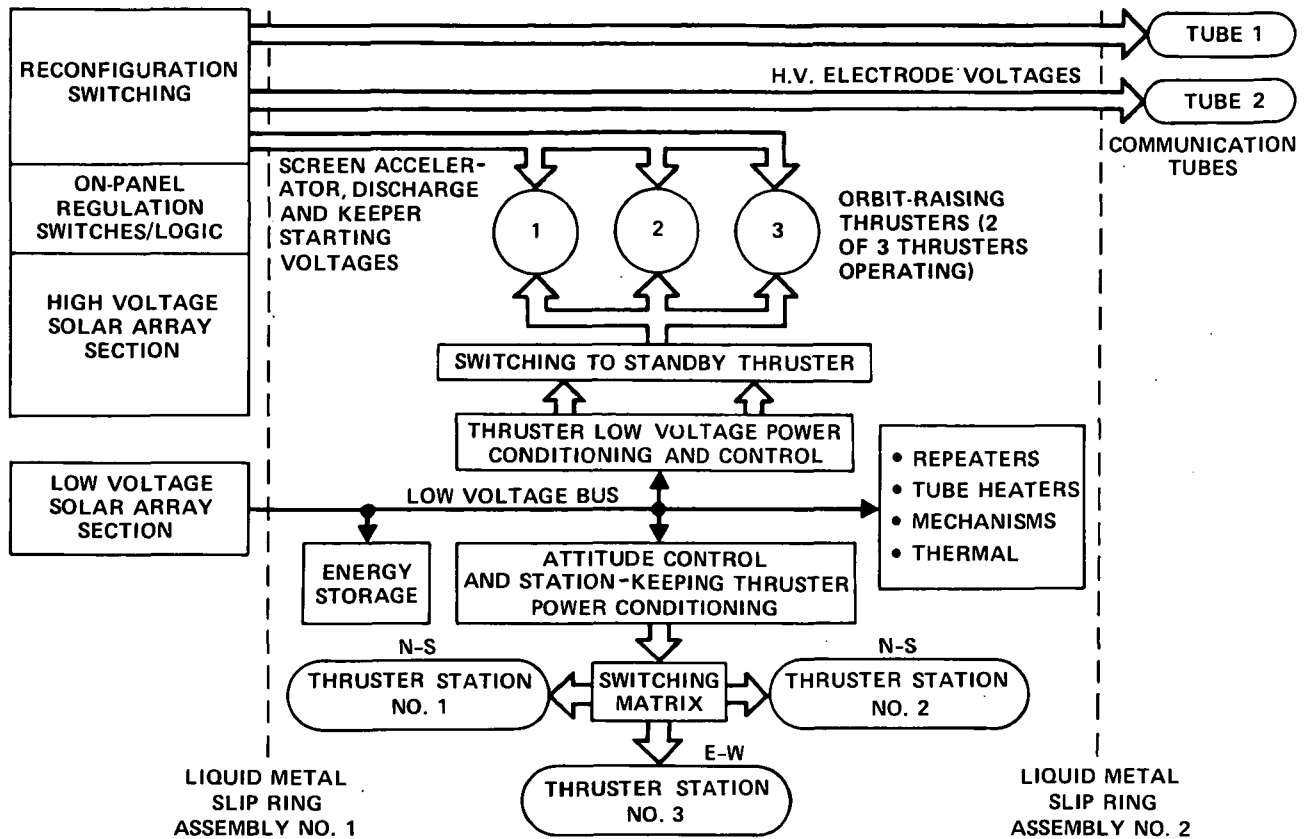
Figure 4.5-1. Power Management Block Diagram
Spacecraft Configuration Al

voltages required. Specific design considerations assumed for the HVSA are
based on previous studies conducted for NASA-LeRC*.

The low voltage solar array section provides a nominal 28 V power
bus for energy storage for the attitude control and station-keeping (AC/SK)
5-cm ion thrusters and for the various housekeeping functions. In addition,
during the orbit raising phase low voltage bus power is used to meet various
low voltage-low power needs of the orbit raising thrusters (vaporizers,
heaters and low voltage keeper sections). It is felt that this approach is a
more appropriate implementation for these low voltage-high current supplies
than using an extension of the HVSA concept to provide this power since the
number of slip rings and array/spacecraft cable runs would be greatly
increased.

Because of the wide range of spacecraft orientations possible during
orbit raising and the requirement for E-W panel orientation on-station to
allow body mounting of the AC/SK ion thrusters, two slip ring assemblies
are required. Liquid metal slip rings were selected for the A-1 configuration.

Energy storage is provided by two 6-ampere hour nickel cadmium
batteries.

---

*Contracts NAS 3-8996 and NAS 3-11535.

Configuration B-1 Power Subsystem

The power management block diagram of the electrical power subsystem for spacecraft configuration B-1 is shown in Figure 4.5-2. The solar array is again divided into two sections; one section provides a medium voltage bus (250 VDC nominal) for the TWT and Klystron conventional power conditioning and the other section functions as a low voltage bus (28 VDC nominal) for housekeeping, energy storage, and auxiliary use.

The selection of a medium voltage bus for powering the communication subsystem leads to a substantial saving in the project specific weight of the power conditioning, and to improved efficiency which becomes extremely important at the power levels required. Detailed design consideration for this power conditioning is given in Section 4.5.4.

Direct chemical spacecraft injection and N-S orientation of the solar panel lead to the necessity of a single slip ring assembly. Since spacecraft configuration B-1 was chosen to represent a more conservative and conventional spacecraft approach, a standard brush-on-ring assembly was selected for implementation.
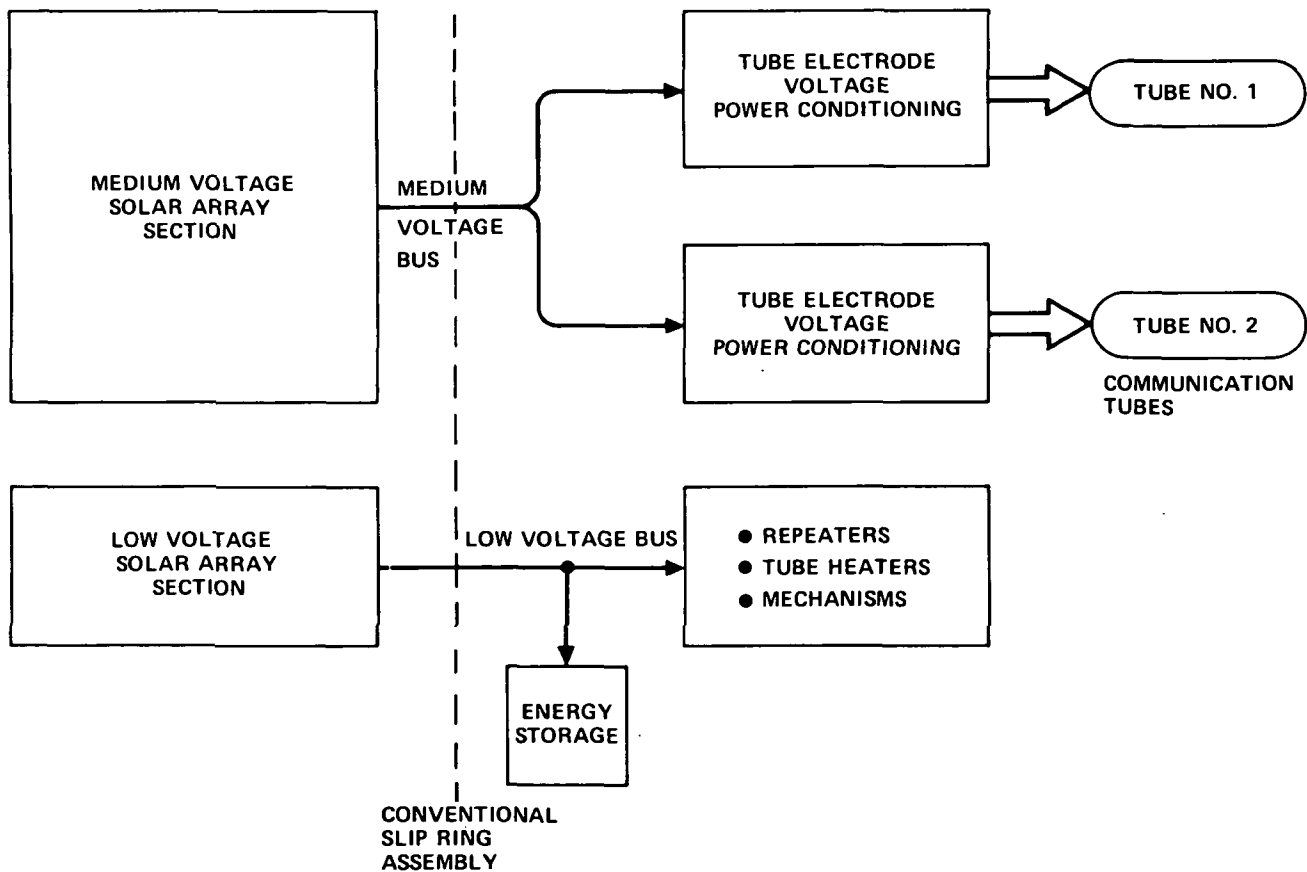
Figure 4.5-2. Power Management Block Diagram
Spacecraft Configuration B-1

4.5-3

Again, energy storage is provided by two 6 ampere-hour nickel cadmium batteries.

Configuration B-5 Power Subsystem

The power management block diagram for configuration B-5, shown in Figure 4.5-3, is essentially the same as that for configuration B-1 with the exception that a high voltage solar array with integral power conditioning replaces the medium voltage bus and the conventional power conditioning. A single liquid metal slipring assembly provides power transfer between the N-S oriented solar array and the spacecraft body, and two 6 ampere-hour nickel cadmium batteries provide energy storage.

```
┌─────────────────────────────┐                                    ╭──────────────╮
│                             │ ══════════════════════════════════>│  TUBE NO. 1  │
│    RECONFIGURATION          │                                    ╰──────────────╯
│    SWITCHING                │         H.V. ELECTRODE VOLTAGES
│                             │ ══════════════════════════════════>╭──────────────╮
├─────────────────────────────┤                                    │  TUBE NO. 2  │
│    ON-PANEL REGULATION      │                                    ╰──────────────╯
│    SWITCHES/LOGIC           │                                     COMMUNICATION
├─────────────────────────────┤                                     TUBES
│                             │
│    HIGH VOLTAGE             │
│    SOLAR ARRAY              │
│    SECTION                  │
│                             │
└─────────────────────────────┘                          ┌────────────────────────┐
                                                          │  ● REPEATERS           │
┌─────────────────────────────┐    LOW VOLTAGE BUS        │  ● TUBE HEATERS        │
│    LOW VOLTAGE              │ ─────────────────────────>│  ● MECHANISMS          │
│    SOLAR ARRAY             │                            │                        │
│    SECTION                 │                            └────────────────────────┘
│                           │                 ┌─────────┐
└─────────────────────────────┘               │ ENERGY  │
                                               │ STORAGE │
         LIQUID METAL                          └─────────┘
         SLIP RING
         ASSEMBLY
```
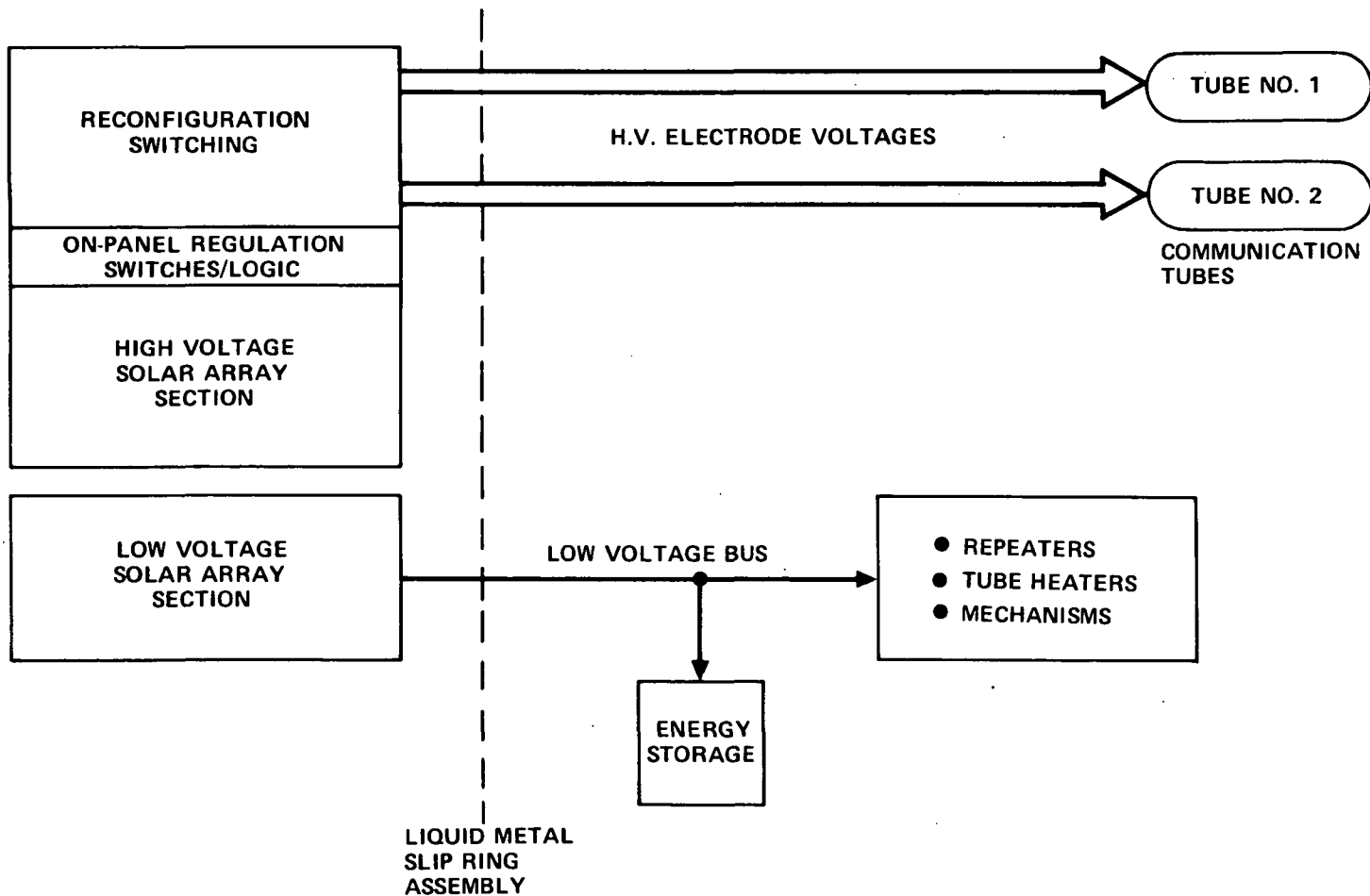
Figure 4.5-3. Power Management Block Diagram
Spacecraft Configuration B-5

4.5.2 Solar Arrays

The solar array in a typical spacecraft design represents a substantial portion of the total spacecraft weight. For high power communication satellites such as the ATS/AMS spacecraft where multikilowatts of array power are required, this is even more true. Therefore, during the study the array designs took a position of particular importance in the power system design and had significant impact on the total spacecraft design.

Selection of the ATS/AMS array design first involved an assessment of the current multikilowatt array state-of-the-art and a projection of anticipated near-future technology gains. The present rigid array state-of-the-art has reached a high level of sophistication. Cylindrical body-mounted arrays have been used at levels over 1 kilowatt (several kilowatt cell quantity on the cylinders). Also, rigid deployed arrays of several kilowatts in size have been used and larger multikilowatt arrays of the rigid oriented type are being readied for flight on the Apollo Applications Program.

With the recent successful flight of the 1-1/2 kilowatt FRUSA (Flexible Roll-Up Solar Array) system, however, a new generation of high power arrays has emerged. The FRUSA system already offers several times more power for a given weight than is available from rigid deployed arrays and further power/weight refinement is possible. Array systems based on FRUSA are being included in numerous advanced system designs and can be readily scaled to the 8-10 kilowatt range required of the ATS/AMS spacecraft. Furthermore, at the higher power levels the advantages of weight performance and stowage volume are enhanced. For these reasons the FRUSA system was selected as a firm, known baseline from which to gage other alternatives in a parametric performance design study. The FRUSA technology was also used extensively in detailed arrangement and mechanical design of the chosen ATS/AMS array system.

The result of the design effort was the selection of a high performance flexible array system consistent with a conservative extrapolation of present technology. The design is strongly based on the FRUSA, but incorporates lighter weight solar cells and covers, and capitalizes on the more weight-efficient performance possible at the higher power levels.

Solar Array Arrangement and Key Features

The solar array general arrangement chosen consists of two roll-out deployment drums, each carrying single panels of equal size and symmetrically attached to the spacecraft in either an E-W (S/C configuration A-1) or N-S (S/C configuration B-1 and B-5) panel axis orientation.

The roll-out drum storage technique was chosen after evaluation of other storage configurations, in particular, flat folding of flexible substrate arrays in "accordion" fashion. Structural weight of the flat fold storage package was not seen to offer significant advantage over the drum when all parts of the required mechanism system were taken into account. Most

importantly, the uncontrolled nature of the deployment of flat folded arrays is considered a serious deficiency in any but impractically small sizes. Based on experience with FRUSA, the predictable and controlled deployment possible with drum storage is an important feature. Because of this, the drum design has been used as baseline on all spacecraft configurations.

Key features of the drum and deployment mechanism applicable to all spacecraft configurations and the associated weights for the three baseline spacecraft configurations are shown in Table 4.5-1.

TABLE 4.5-1. WEIGHT AND KEY FEATURES OF THE ARRAY DEPLOYMENT SYSTEM

● Actuator Unit	Scaled existing flight designs
● Booms (two per drum)	5.08 cm diameter, 127 μm thick stainless steel
● Thermal Distortion	Less than 10° from deployment Plane
● Cushioning	Not required (single panel per drum)
● Retraction	Not required (permits deletion of boom length compensation)
● Power Transfer within Drum	By in-drum terminal connection after array deployment
● Minimum frequency	Greater than 0.035 Hz
● Dynamic Acceleration	0.01 g in deployed condition
● Array Weight Capability of Structure/Deployment System	Up to 1.1 kg/m^2
● Array Tension	0.545 Kg, deployed
● Drum	Composite fiber construction (graphite filament and epoxy composition)

	S/C Configuration		
	A-1	B-1	B-5
Drum, Deployment Mechanisms and Launch Retainer Weight (Kg)	57.3	49.5	51

Sizing Summary

The overall panel sizes shown in the array system summary presented in Table 4.5-2 will provide the system load power required for each of the final selected baseline spacecraft configurations with a reasonable power

TABLE 4.5-2. ARRAY SYSTEM SUMMARY

	Spacecraft Configuration		
	A-1	B-1	B-5
Orbit Raising/ Direct Injection	OR	DI	DI
Low Voltage/ High Voltage	HV	LV	HV
Panel/Sun Orientation	Fully oriented	23-1/2°	23-1/2°
Power Requirement (watts)	5985	5615	5655
End of Life Nominal Output, Constraining Season (kW)	6.5	6.0	6.0
Beginning of Life Nominal Output Oriented Median Solar Intensity (kW)	10.2	8.0	8.0
Total Array Area (m^2)	123	92.0	96.5
Total Array Weight Including Deployment and Storage Mech but not orientation (Kg)	138	107	114.5
Substrate Thickness (μm)	76 Kapton	25.4 fiberglass 25.4 Kapton	76 Kapton
Single Panel Length	23.8	18.9	19.8
Single Panel Width	2.59	2.44	2.44

contingency ranging from 515 to 345 watts. To supply the end-of-life (EOL), constraining-season load requirements (including conditioning losses) of 5615 to 5985 watts from the beginning-of-life (BOL) equinox array, design outputs are 8.0 kW for spacecraft configurations B-1 and B-5 and 10.2 kW for configuration A-1. Each of the two panels per spacecraft are configured in 2.4 to 2.6 m widths and 18 to 24 m lengths.

Seasonal variations of load requirements and panel outputs were examined to identify constraining design conditions, and the resulting seasonal factors were used in array sizing. For the missions selected, battery charge loads during the equinox season did not add to the fixed load requirements shown in the summary tabulation. This occurs for S/C configurations B-1 and B-5 since the worst-case seasonal condition is at summer solstice (23-1/2° spacecraft axis declination to sun, at a time within two weeks of lowest or aphelion solar intensity). Thus during the equinox season (from 0 to 10° axis declination and close to median sun intensity), about 8.3 percent more array output is available, which more than accommodates the equinox (eclipse season) battery charge load.

The A-1 mission is also constrained near summer solstice (actually at aphelion, about two weeks following summer solstice). This is because the complete sun-orientation of the panels for the E-W panel deployment eliminates all seasonal effect on panel output except the ±3-1/2 percent intensity variation due to earth-sun distance changes. However, in this case the minimum reserve power available (disregarding the 515 W contingency) at the start of eclipsing (about 23 days before autumnal equinox) is between 1 and 2 percent, or on the same order as the battery charge load.

The system-optimized solar array design was determined based on detailed quantitative performance and weight tradeoffs. These parametric data were keyed to the known power and weight features of the flight-proven FRUSA system. A wide variety of solar cell thicknesses, cover thicknesses, cell base resistivities, and cell performance features were examined. These were consolidated in six major configuration variables representative of the spectrum of viable alternatives. System sizing was then conducted for these six configurations to enable selection of the most favorable system, based on a weight optimization consistent with a sound design approach and a conservative technology extrapolation.

Performance of the six-cell cover types analyzed in detail for subsequent use in the system optimization is summarized in Figure 4.5-4. At this point, weight data (watts/Kg) includes only the cell/cover/substrate assembly. It is seen from the figure that configurations C and F (100 μm 10Ω-cm cell, 50 μm cover) appear at this stage to be most attractive in watts/Kg performance. Their advantage, however, diminishes when incorporated in the total system design. The watt/m^2 data also shown in the figure indicates that a counteracting weight effect exists at the system level for alternatives which, although offering high power/weight ratio on a cell/substrate assembly basis, require significantly larger array area.

Configuration Summary

Type	Base Res. Ω-cm	Cell μm mils.	Cover μm mils.
A	2	180	150
B	2	100	75
C	2	100	50
D	10	180	150
E	10	100	75
F	10	100	50
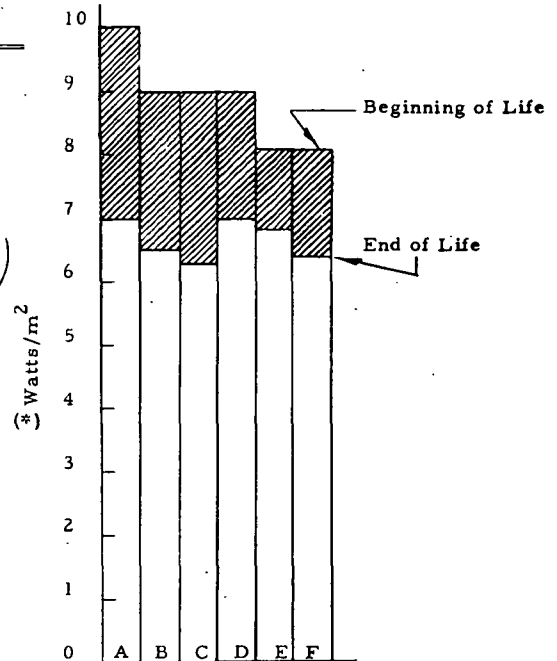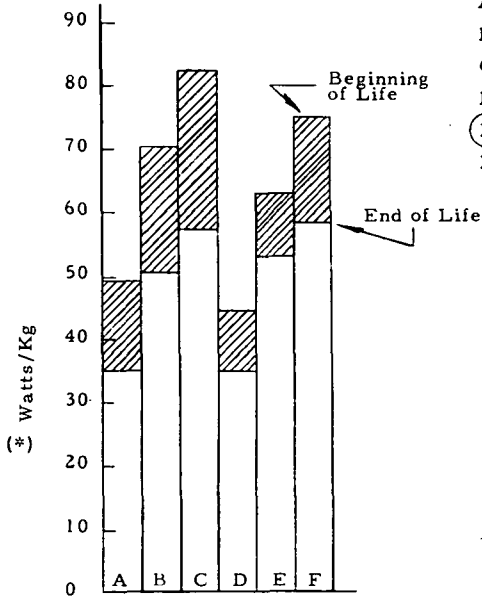
System Choice

(*) . Wts. for cell/substrate ass'y only;
. End-of-life data is for 5-year synchronous orbit, direct injection only
. Data is for 2000 cells/m^2, FRUSA substrate, median sun, oriented, no shadows, 328°K, P_m at slipring ass'y output, nominal.

Figure 4.5-4. Parametric Performance of Solar Cell Ass'ys for Array Design Optimization

Also developed were weight relationships for deployment mechanisms (drums, booms, activators, etc.). These data were used together with the preceding cell substrate assembly performance data to generate array system weights for the system optimization. The deployment mechanism weights are complex functions of detailed design features such as areas, aspect ratio, mounting method, etc. A number of restrictions were placed on the range of designs which could be considered. In particular, drum lengths were restricted due to spacecraft shroud limitations and this, in turn, leads to longer panel boom lengths requiring larger boom diameters of increased wall thicknesses in order to provide satisfactory fundamental bending mode frequencies. As a result 5 cm diameter booms of 130 μm thick stainless steel were selected for both the 8 kW and 10.2 kW array designs.

The first result of combining deployment system, solar cell/substrate, and launch retainer weight is the system weight data shown in Figure 4.5-5 for a BOL output of 8 kW for an array of low voltage design. These results are then summarized in Figure 4.5-6 in terms of BOL and EOL specific weights (Kgs/kW). The BOL data show configuration B (100 μm, 2-Ω2cm, 75 μm cover) to be favored, excluding the advanced alternatives C and F.
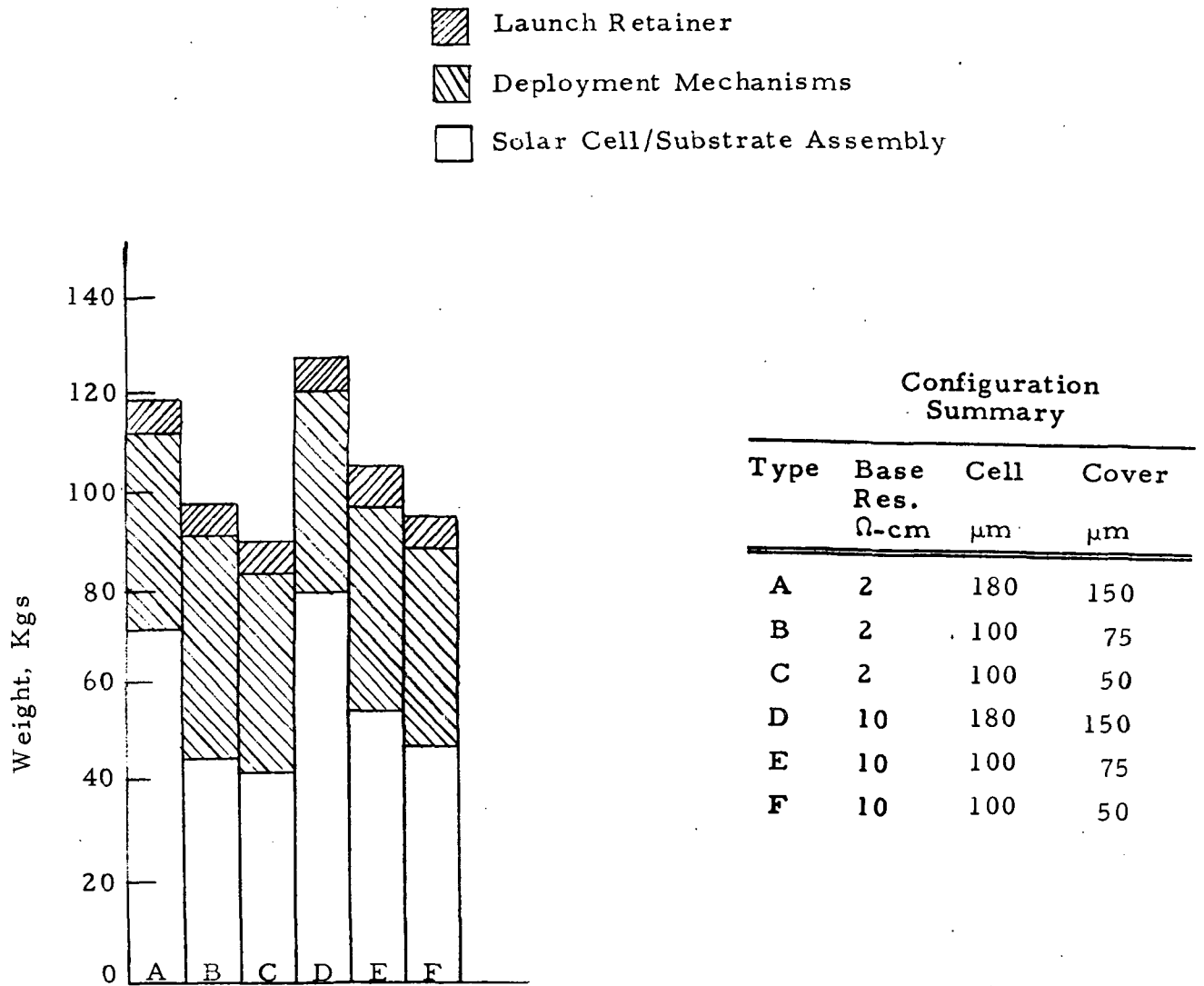
Figure 4.5-5. Solar Array System Weights for Various Cell/Cover
Combinations for Common 8 kW (BOL) Size
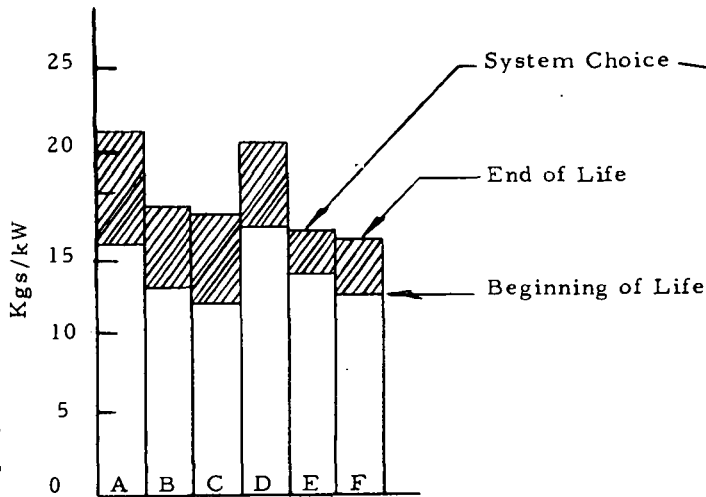
Configuration
Summary

Type	Base Res. Ω-cm	Cell μm	Cover μm
A	2	180	150
B	2	100	75
C	2	100	50
D	10	180	150
E	10	100	75
F	10	100	50

Figure 4.5-6. Solar Array System Specific Weights for Various
Cell/Cover Configurations in 8 kW (BOL) Range

However, the figure also shows that consideration of the five-year trapped
and flare radiation environment at synchronous altitude makes the E configu-
ration (10Ω-cm version of B) more favorable at EOL due to the performance
crossover between the 2Ω-cm and 10Ω-cm base resistivities. This cross-
over is, of course, even more prominent for the ion thruster orbit raising
mission. From the trajectory analysis, it was determined that the E config-
uration is also weight optimum and leads to a EOL radiation degradation
factor of 0.65 for the 100 μm, 10Ω-cm cell with 75 μm cover. This compares
to a radiation degradation factor of 0.85 for this same cell/coverslide com-
bination when used on the direct chemical injected spacecraft. Thus, the

parametric data and array system optimization yields an optimum choice of the 10Ω-cm, 100 μm thick cell and 75 μm thick cover.

Detailed Performance Analysis

The spacecraft configurations finally selected incorporates array designs with BOL powers of 8 kilowatts and 10.2 kilowatts, assuming performance measured at 1 astronomical unit and 328°K. During the early phases of the study, investigations were made of the solar array to obtain sizing data over a basic 4 to 8 kW range and later extended to include the 10.2 kW power level for the Thor/Delta A-1 configuration.

In developing detail design data for system optimization a wide range of candidate features were evaluated. Cell thicknesses from 100 μm to 200 μm were considered together with cover thicknesses from 50 to 150 μm. Both 2 ohm-cm, and 10 ohm-cm base resistivity cells were examined, with both being covered by integral and conventionally bonded coverglass.

Consideration was given to technology advancements which might be expected prior to a design freeze, such as possible efficiency improvement in thin solar cells using "gettered" base material, reflective back contacts and laminated FEP teflon covers. Some of these advancements are listed in Table 4.5-3, together with estimated performance gains associated with each. A conservative estimate is that less than half of the total gain indicated would be realized in time for inclusion in the ATS/AMS arrays. Also shown are important cost-saving advancements which may be realized in the near future. These generally will be able to be accommodated in present array design approaches and may eventually find application to the ATS/AMS system.

The results of cell and coverglass evaluations were consolidated into three basic alternative configurations summarized in Table 4.5-4. Other combinations are possible; however, the three configurations span the range of choice expected. With the 2Ω-cm/10Ω-cm base resistivity as a variable, these configurations represent the six designs previously considered in the system sizing optimization.

The first configuration is the proven FRUSA 180 μm cell/150 μm bonded cover. This configuration functioned as the comparison baseline to allow actual FRUSA production weight and performance data to be used in this study as a reliable proven point of departure for sizing and evaluating more advanced array designs.

The second configuration was chosen for all ATS/AMS spacecraft designs. It consists of a 100 μm cell with 75 μm bonded cover and is within existing technology although it has not yet been employed on a production basis. The present cost premium for the 100 μm cell/75 μm cover is expected to be much less significant when production experience is gained, and is felt to be appropriate for the time frame of the ATS/AMS spacecraft.

TABLE 4.5-3. FORECAST SOLAR CELL ADVANCEMENTS

Item	Estimated Percent Performance Gain End of Life	Source
A. Estimated Technology Advancements		
• Lithium doped P/N (or N/P) cells to reduce flare degradation	3	M. Wolf, IECEC, 1970
• Rear surface (P+, reflecting)	2	Centralab, July 1971
• Antireflection coating optimization on cover and cell	2	Internal Hughes Program
• TiOx cell coating	3, after temp. correction	US and European cell suppliers
• Wrap around contacts	2, or more	US and European cell suppliers
• "Gettering" per Telefunken, especially on thin cells	1	Telefunken data and US radiation tests
Total	13%	
B. Cost Savings Advancements		
• Cell Covers Integral cover		
Cerium doped glass		
Ribbon glass		
Teflon		
Optimization or elimination of cover coatings		
• Cells Large size (panel layout-related)		
Wrap-around contact (assembly ease)		
• Processes Welded interconnection, with silver-type or aluminum-type contacts		

TABLE 4.5-4. COMPARISON OF CELL/COVER CONFIGURATIONS

Class	Cell/Cover Thickness and Type	Cell/Cover Cost	Technical Status	Specific Performance Increase for Flexible Panel and Drum Assembly
Standard FRUSA	180 μm/150 μm bonded	Comparison baseline lowest.	FRUSA assembly completed successfully. Flight ready	Comparison baseline
High Performance Present Technology	100 μm/75 μm bonded	Approximately 50 percent cost increase over comparison baseline	Within present pilot line technology although not yet used in full production	Approximately 33 percent greater power/lb than comparison baseline
Projected Near Future Technology	100 μm/50 μm integral cover	Open	Integral covers will have been flown on several flight experiments, questionable stress compatibility with cells less than 200 μm at present time	Estimated 42 percent greater power/lb than comparison baseline

The third configuration is an example of further performance gains which might be possible if certain technical advancements are realized, namely, (1) integral glass or laminated FEP covers applied to thin 100 μm cells, and (2) power output improvements of the thin cells. Whether the design is equally applicable to low voltage and high voltage panel design is questionable. Studies to date are not conclusive as to the minimum cover thickness acceptable for array output voltages to 16 kV, however, in this study 75 μm covers have been judged acceptable.

The FRUSA data, together with the well established performance data acquired from Hughes rigid arrays in synchronous orbit, notably the low-energy proton-protected TACSAT, Intelsat IV's and ATS-E, provides a point from which to extrapolate to the 100 μm cell/75 μm cover combination with confidence. This accumulated experience has been incorporated in a periodically updated Hughes standard solar panel design procedure which was used as a basis for the ATS/AMS sizing. This proven procedure incorporates such items as anticipated procurable solar cell power output, temperature change effects, performance modeling methods and radiation degradation analysis techniques. The use of this procedure has resulted in consistent and reliable array sizing for the ATS/AMS spacecraft employing sound extrapolations of present proven experience.

The radiation environment at synchronous altitude used for this sizing was a 19th cycle flare summation and the ATS-1/Aerospace trapped electron measurement data. These environments have recently been used for Hughes synchronous satellite design on the Intelsat IV and the Canadian domestic Telesat programs. Both frontside and backside radiation damage were included.

Sizing data presented are for nominal performance. Statistical limits have been derived for various Hughes designs which are reflected in the use of nominal overdesign margins illustrated in the array system summary (Table 4.5-2).

Detailed weight data were generated to enable the system sizing optimization. A cross section and weight breakdown of the roll-out panel cell/substrate assembly is shown in Figure 4.5-7. The weight percentages

	WEIGHT	PANEL WEIGHT BREAKDOWN (PERCENTAGE)
150 μM MICROSHEET GLASS COVER ULTRAVIOLET AND ANTIREFLECTIVE COATINGS	0.150 gm /CELL*	34.65
ADHESIVE RTV 602	0.010 gm /CELL*	2.31
2 x 2 CM SOLAR CELL 180 μM THICK	0.190 gm /CELL*	43.86
ADHESIVE AND FIBERGLASS 25 μM	0.014 gm /CELL 0.0082 gm /CELL	3.24 1.90
SUBSTRATE 25 μM KAPTON	0.0169 gm /CELL	3.91
COLLECTORS AND BUS 175 μM COPPER WITH INTEGRAL KAPTON 25 μM OVERLAY	0.0214 gm /CELL	4.95
SOLAR CELL INTERCONNECT 50 μM ETCHED COPPER MESH	0.0224 gm /CELL	5.18

Figure 4.5-7. Panel Weight Breakdown

listed corresponds to a conventional low voltage design using 1.8 μm cells with bonded 150 μm covers. The 25 μm fiberglass/25 μm Kapton composite substrate employed on FRUSA has been retained for the low voltage panel (S/C configuration B-1); however, a thickness increase was felt warranted for the high voltage designs and has resulted in the selection of a 75 μm Kapton substrate for S/C configurations A-1 and B-5. This is discussed in greater detail in Section 4.5.2.

The array cross-section in Figure 4.5-7 does not show bypass diodes although addition of the diodes can be accommodated in the basic design when adapted to high voltage used. The bypass diodes may also be desirable in intermediate voltage designs based on "hot spot" analyses of the final cell arrangement.

Prototype versions of bypass diodes integral with solar cells have been evaluated by Hughes and cost appears reasonable. Discrete diodes used either as parallel bypass diodes or series blocked diodes on flexible arrays are also being developed on a Hughes roll up array program for the Air Force. Flat, array-mounted series blocking diodes have been fabricated and are undergoing test. These devices may also find application as bypass diodes at string fold points such as on the High Voltage Solar Cell Power Generation System (HVSCPGS) being constructed for NASA-LeRC by Hughes at the present time[*]. Development of the flat diodes will pave the way for incorporation of flexible-array-mounted semiconductor devices such as are planned for the high voltage arrays.

4.5.3 High Voltage Solar Array

The High Voltage Solar Array (HVSA) Concept for providing conditioned load power directly from blocks of solar cells has been studied by Hughes[**] and other companies under contracts from NASA-LeRC. These studies have considered both the space plasma-solar array interaction aspects of operating the array in a wide range of space environments, and the electrical configuration techniques best suited to provide regulation and means of reconfiguring and transferring the power to satisfy multiple load requirements.

The general consensus of all the studies was that HVSA's were feasible and potentially capable of superior performance in terms of efficiency, specific weight and reliability when compared to conventional power conditioning operating from a low voltage solar array.

Since the range of space environments and the types of loads considered in the previous HVSA studies are similar to those of the present ATS/AMS spacecraft missions, the HVSA study results to a large degree are applicable and were used as the basis of the investigations undertaken in this study.

The impact of HVSA design is to introduce incremental area and weight increases in comparison to a low voltage array with the same power

---

[*]Contract NAS 3-15826

[**]Contracts NAS 3-8996 and NAS 3-11535

level capability. This is due in part to increased border spacing of hard-wired solar cell modules to withstand high voltage stresses, area allowances for cable routing and electronics, and possible increases in panel substrate and cell coverslide thicknesses. The increases are apparent from the areas and weights previously given in Table 4.5-2 for the 8-kW (BOL) solar arrays of spacecraft configurations B-1 (low voltage) and B-5 (high voltage). The power control electronics which are considered an integral part of the HVSA electrically and physically, constitute an additional weight and are functionally comparable to electronics associated with conventional power conditioning when operated from a low voltage array.

HVSA's are incorporated in baseline spacecraft configurations A-1 and B-5. In configuration A-1 the solar cell power blocks are configured to provide most of the power required by 2 operating ion thrusters (with the exception of low voltage heater and keeper power) during orbit raising. Upon arrival on station the power blocks are reconfigured by miniature high voltage switches to an electrical circuit arrangement satisfying the voltage-current requirements of the TWT and Klystron. In configuration B-5, after an initial outgassing period in a low voltage condition, the power is configured and unclamped to directly provide all TWT and Klystron electrode and collector voltages as in configuration A-1.

Table 4.5-5 provides a listing of HVSA summary specifications and characteristics derived from previous studies or specifically determined in this study. All numerical values are considered to represent conservative designs and performance achievable within existing technology.

Several HVSA design considerations associated with specific mission use and the TWT and Klystron loads for spacecraft configurations A-1 and B-5 are discussed in following subsections. Of paramount importance is the relationship between solar cell maximum power current and the power matching efficiencies achievable with the NASA-LeRC specified tube loads.

Electrical Configurations

The HVSA power system consists of solar cell power blocks, on-panel regulation electronics, switches to reconfigure the power blocks, and on-board voltage and current sensors and control logic to establish closed-loop regulation and to direct reconfiguration sequencing.

The power blocks which subdivide the array power are sized in voltage and current capability according to the load requirements over the full mission length. Fine regulation is achieved within the power blocks by regulation switches which can short-circuit binary voltage-scaled solar cell subgroups. Digital control signals from on-board control logic, transmitted via photocouplers, command the state of the switches open or closed. In a general sense, each block can be considered a digital to analog power converter.

The collection of loads determined the number of power blocks required and their relative size in terms of the number of solar cells in series and in parallel. The manner in which the blocks are configured (electrically

TABLE 4.5-5. HIGH VOLTAGE SOLAR ARRAY SPECIFICATIONS AND CHARACTERISTICS

Panel Weight Penalty (Less Integral Pwr Cond)	10 percent	
Panel Area Penalty	5 percent	
Electrical Efficiency	99 percent	
Nominal Power Matching Efficiencies	90 percent	Communication tubes saturation drive (EOL)
	96 percent	Orbit raising ion thrusters (arrival on station)
Power Control Mechanization		
Reconfiguration and Load Switching		High voltage vacuum relays (magnetic latching)
		Switching functions: 102 (A-1, 63 (B-5)
Regulation		Solid-state shorting switches with intermediate on-panel switch drive logic. Binary weighted cell groupings
Control		Digital; control signals multiplexed; slip rings allotted, 10
HV Coupling Isolation		LED — phototransistor couplers
Integral Power Conditioning Weight		14 Kg (A-1), 12.7 Kg (B-5)

connected by hard-wiring or switches) is impacted not only by the loads, but by considerations of reliability and the general ease of array control under various operational extremes such as emergence from eclipse and overloads.

Figure 4.5-8 shows a representative switch arrangement for providing either beam power for an orbit raising ion thruster or the electrode voltages for the specified TWT. With the parallel-series switches open, solar cell power blocks B_1, ..., B_{10} are in parallel; when closed, all blocks are in series. Closure of both shorting switches clamps the array output
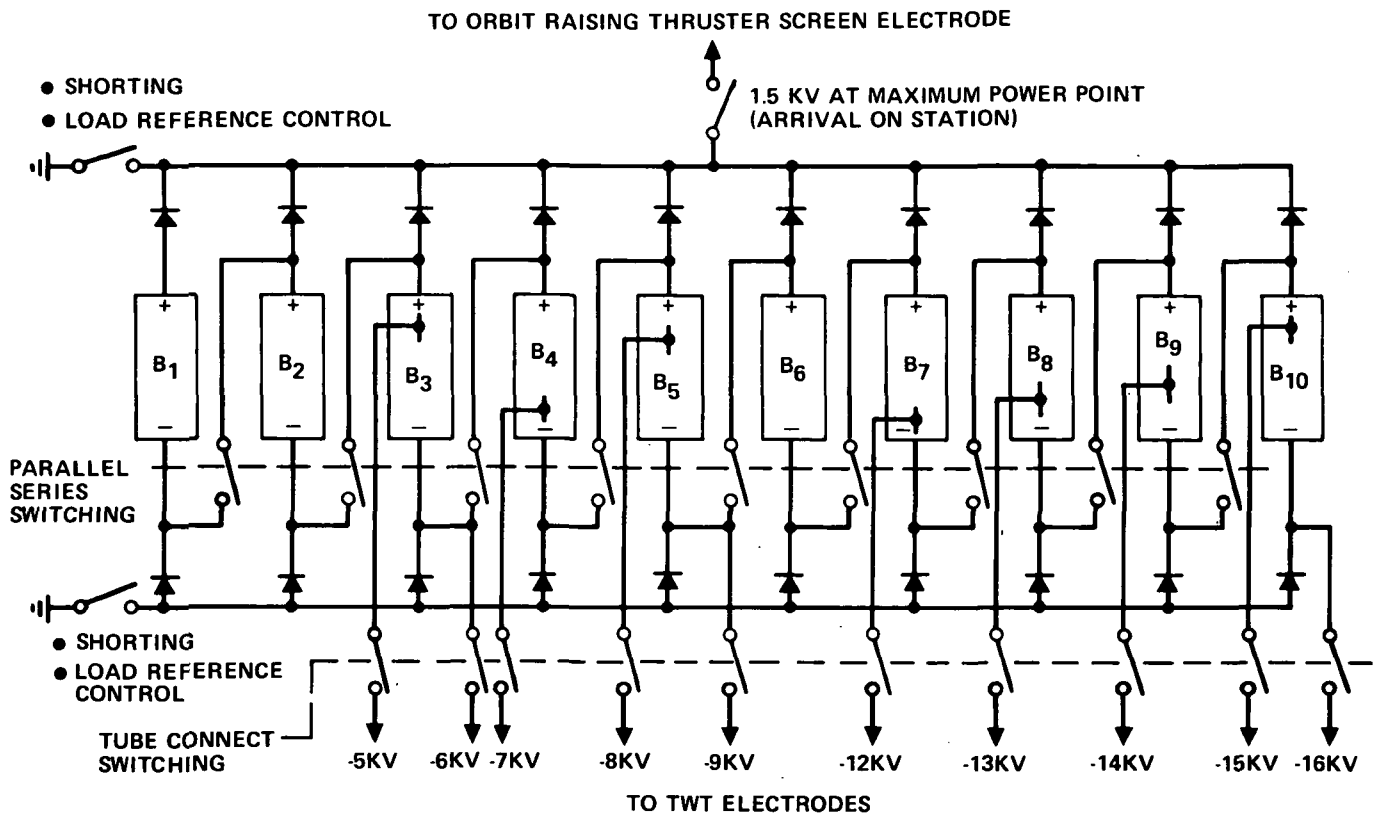
Figure 4.5-8. Typical HVSA Reconfiguration Switching Arrangement

voltage regardless of the state of other switches. These switches also allow the polarity of the array to be selected by closing one or the other shorting switches. Switches for connecting independent loads to the array power are also part of the reconfiguration switching subsystem.

An array power subdivision consisting of forty-four hard-wired solar cell blocks was used as the basis for projecting the HVSA integral power conditioning weight estimates presented in Table 4.5-6. The lower weight projected for the B-5 configuration is basically due to a reduced requirement for reconfiguration switches and sensors in the absence of the ion thruster system employed in configuration A-1.

It is clearly evident that the increased BOL high voltage power of configuration A-1 has negligible effect on the integral power conditioning weight. In fact, it is essentially axiomatic that the HVSA electronics weight is most directly impacted by the number of independent voltage outputs that must be regulated rather than by the total power controlled.

High Voltage Solar Array Power Efficiency

The effective power efficiency of a HVSA with integral power conditioning is determined by three independent power loss mechanisms: electronic

TABLE 4.5-6. HVSA INTEGRAL POWER CONDITIONING
WEIGHT ESTIMATES (KILOGRAMS)

Array Item	S/C Configuration	
	A-1	B-5
On-panel Regulation Electronics	4.98	4.98
Reconfiguration and Load Switching	2.72	2.04
Sensor Electronics	2.26	1.58
Blocking Diodes	1.81	1.81
Spacecraft Digital Control Electronics	2.26	2.26
Total Weight	14	12.7

circuit losses, space plasma drain currents and possible power mismatches between the configured array power and the load voltage-current requirements.

Electronic circuit losses are due to blocking and power steering diode voltage drops, power lead losses, electronic bias power required, etc. For the configurations considered in this study the losses in this area should be less than one percent of the output power at end-of-life.

The space plasma drain current losses result from the collection of space plasma ions or electrons at exposed conductor surfaces in the array's electrical system. For an uninsulated HVSA, fabricated using techniques similar to those used for low voltage arrays, the principal drain current collector is the open (uninsulated) tabs of the solar cells. The resultant array power loss due to the shunt loading effects of the plasma is a function of the array voltage magnitude and polarity and the plasma density (orbital altitude).

Figure 4.5-9 displays the percent power loss (determined analytically) for the maximum voltage range anticipated in a configuration A-1 type mission. The high power loss shown for the 1.5 kV ion thruster beam supply has been determined to have negligible influence on the mission because of the highly elliptical transfer orbit which leads to a required coast phase (thruster off) at the lower altitudes. In actual array operation the voltages would be clamped when not required and a high space plasma density existed. Losses at synchronous altitude, due to the application of high voltage to the TWT and Klystron, are shown to be less than 0.1 percent. It is concluded that the plasma current losses have insignificant impact on HVSA sizing for the planned modes of operation for spacecraft configurations A-1 and B-5.
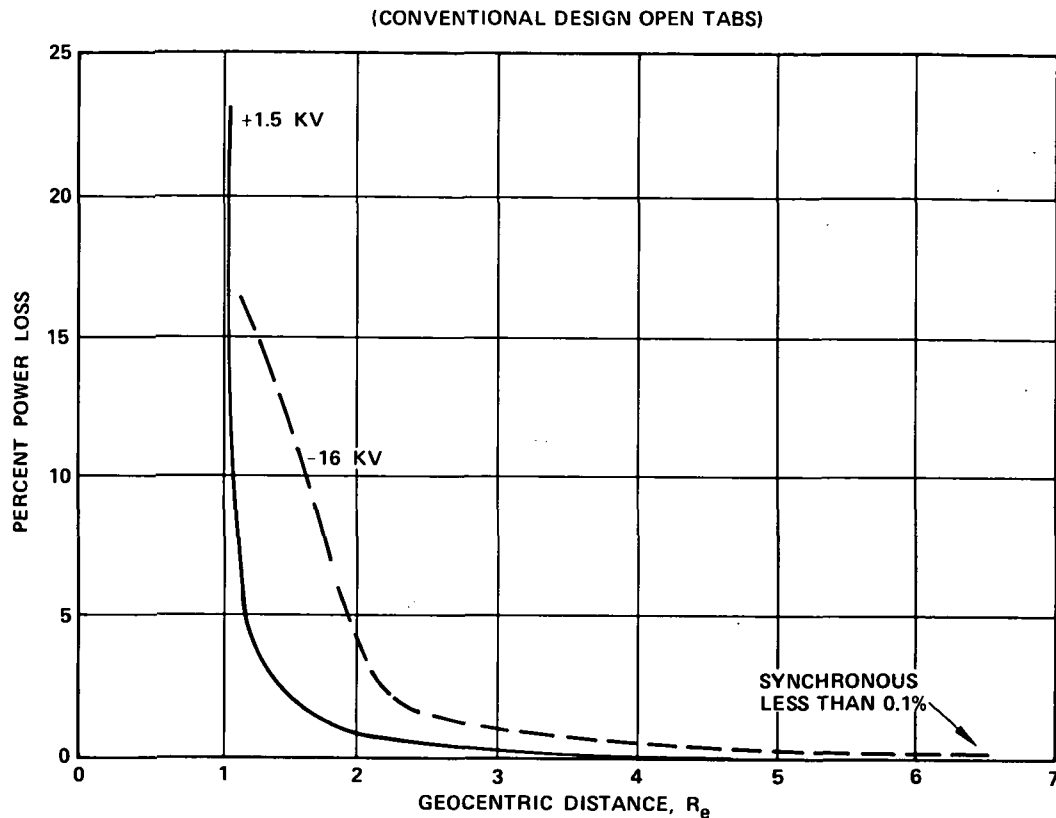
Figure 4.5-9. High Voltage Solar Array Power Loss
Due to Plasma Current Collection

The overall power efficiency of HVSA's can approach ninety-nine
percent. This can only occur, however, when the required load voltage-
current operating point falls at the maximum power point of the configured
solar cell I-V characteristics. When there is a mismatch the HVSA is unable
to deliver its full design power capability, hence, becomes an inefficient
power system requiring an overdesign with increased panel area and weight
to offset the inefficiency.

The voltage level of a solar cell power block can be sized in a fine
continuum of voltages because of the small voltage output per cell in com-
parison to a typical total output voltage. A similar statement cannot be said
about current for loads which require currents less than the capacity of a
single cell or in the range of a few cells in parallel.

When powering the orbit raising ion thrusters, the power matching
efficiency is relatively high since the current capability of a single series
string of the 2 x 2 cm solar cells selected to implement the array is small
compared to the current levels of the screen and discharge supplies which
represent the major portion of the thruster power. The efficiency value of
96 percent for the thruster should represent a very conservative estimate
since the thruster is throttlable.

The power matching capability of the HVSA when powering the NASA-LeRC specified 1-kW (rf) TWT and 2-kW (rf) Klystron was investigated in detail. The substantial number of independent collectors and electrodes requiring regulated voltages, which lead to the large integral power conditioning weight, also creates problems in achieving high efficiencies (particularly for the TWT) because of the low current levels for each voltage.

Figures 4.5-10 and 4.5-11 show the solar cell block configuration chosen to power the TWT and Klystron. On each figure is also shown the end of life power matching efficiencies for the orbit raising mission for power block implemented with 2 x 2 cm cells and with the best mix of 1 x 2 cm and 2 x 2 cm cells.

A detailed tabulation of power distributions for the two solar cell design implementations when powering the TWT are given in Table 4.5-7. It should be noted that not all blocks contain the same number of cells in series to achieve the 1-kV levels; however, the operating point on the I-V characteristic for each block is either at maximum power or to the open circuit side to assure satisfactory closed-loop regulation stability.

From a consideration of the relative power required by the TWT and the Klystron a combined efficiency of approximately 90 percent is possible for the given mission using only 2 x 2 cm cells. This was chosen as the baseline approach for all HVSA sizing in this study. By including 1 x 2 cm cells in the design, or special high voltage cells with comparable area efficiencies and maximum power current, a collective power matching efficiency near 97 percent could be achieved hence, the 90 percent power match used represents a very conservative judgement of the arrays potential capability.

4.5.4 Power Conditioning

Although only one of the three selected baseline designs (S/C configuration B-1) employs conventional power conditioning for the communication tubes, during the study power conditioning designs for both orbit raising ion thrusters and communication tubes were investigated in considerable depth. These two types of loads dominate the power demand for the extended total class of configurations considered; hence, they logically should be the determining factor in the section of the bus voltage when conventional power conditioning is used.

To have a fair comparison between conventional power conditioning and the advanced high voltage solar array concept, it was felt that more competitive power conditioning designs at the specific power levels in question should be generated which more accurately represented what could be achieved within existing technology. In generating and evaluating the conventional power conditioning configurations, past design experience in low power communication tube flight power supplies and in high power ion thruster flight prototype transistorized power conditioning was combined to arrive at design having attractive specific weight, efficiency and reliability specifications.
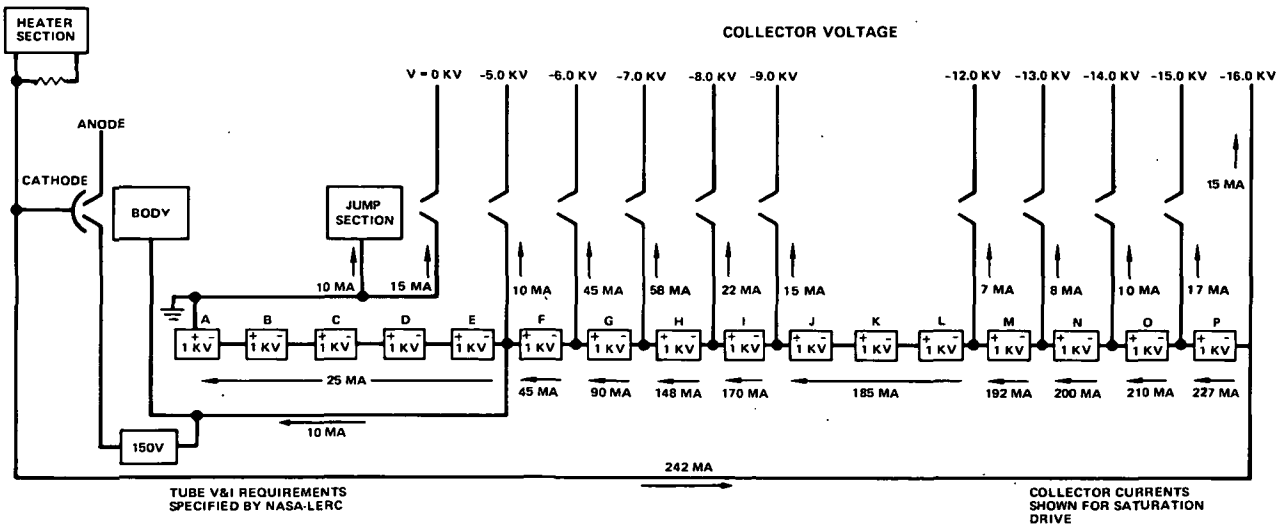
Figure 4.5-10. High Voltage Solar Panel Cell Block Configuration
for 1 kW (rf) TWT
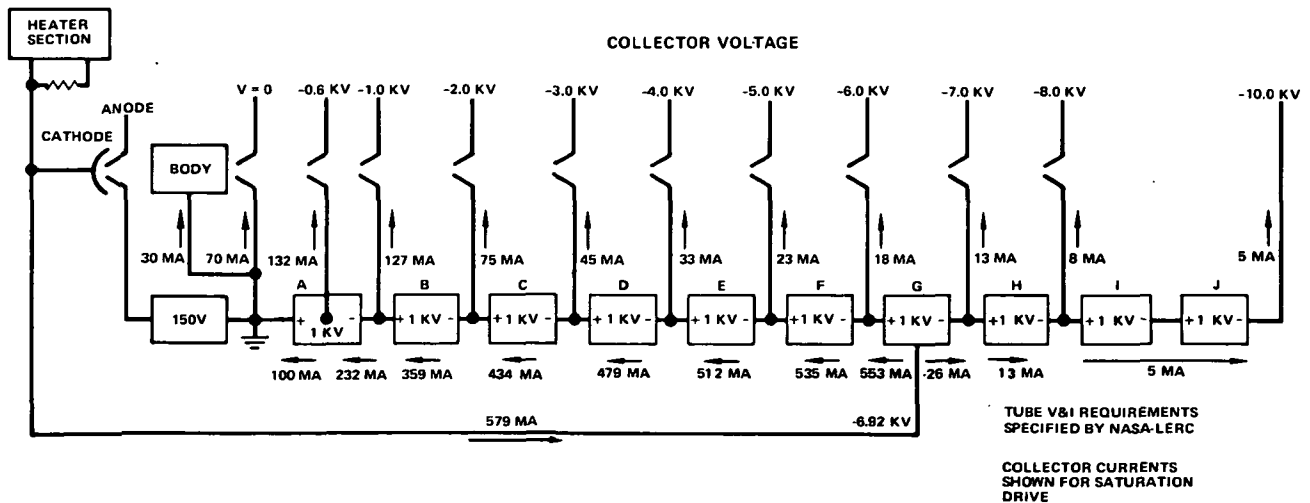
Figure 4.5-11. High Voltage Solar Cell Block Configuration
for 2 kW (rf) Klystron

TABLE 4.5-7. END-OF-LIFE POWER AND POWER MATCHING EFFICIENCIES HVSA POWERING 1 kW (RF) TWT AT SATURATION DRIVE

Supply	Saturation Rating Voltage (kV)	Saturation Rating Current (ma)	Required Power (W)	Design No. 1 Power (W)	Design No. 2 Power (W)
A	1	25	25	67	35
B	1	25	25	67	35
C	1	25	25	67	35
D	1	25	25	67	35
E	1	25	25	67	35
F	1	45	45	70	47
G	1	90	90	94	94
H	1	148	148	149	149
I	1	170	170	170	170
J	1	185	185	217	186
K	1	185	185	217	186
L	1	185	185	217	186
M	1	192	192	220	195
N	1	200	200	223	200
O	1	210	210	233	210
P	1	227	227	236	236
Total Power (W)			1962	2381	2034
Power Matching Efficiency (%)				82.4	96.5

Design No. 1   4 mil cells/3 mil cover, 10 cm, 2 x 2 cm assuming $P/P_o = 0.67$ and $I_f = 83$ ma

Design No. 2   4 mil cells/3 mil cover, 10 cm, best mix of 2 x 2 cm and 1 x 2 cm cells assuming $P/P_o = 0.67$ and $I_f = 83$ ma

Bus Voltage Selection

The power conditioning requirements for the communication tubes specified by NASA-LeRC and for the 30 cm ion thruster were reviewed in detail. Considering these requirements, efficiency and weight estimates for conventional power conditioning as a function of line voltage were determined. Figure 4.5-12 presents these estimates for designs ranging from 28 VDC to 300 VDC input bus voltages (Note that weight at a given line voltage is normalized with respect to the 28 VDC design.)

In deriving the normalized weight variations, the basic ground rules and assumptions included the following:

1) Designs based on modular transistor inverters.

2) Transformer step-up turns ratios limited to 15.

3) Maximum transistor collector current held constant with verying line voltage.
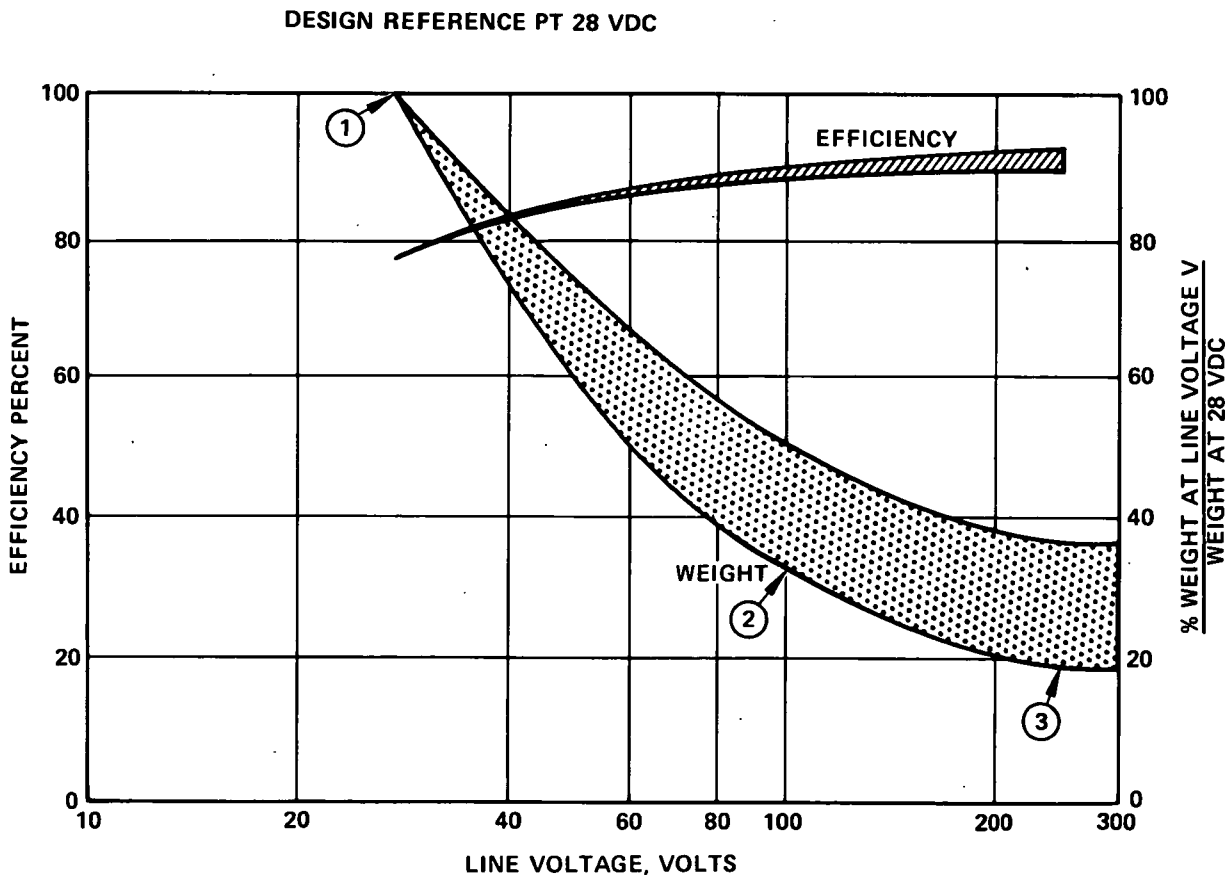
Figure 4.5-12. Efficiency and Weight of High Power Conventional Power Conditioning as a Function of Line Voltage

4)   Drive circuitry complexity per inverter power stage is constant with line voltage.

5)   Number of inverter power stages inversely proportional to line voltage.

6)   Electronic components (less magnetics) and power conditioning structure weight assumed to be twice the magnetic weight.

The resultant curve (Figure 4.5-12) and its spread, should not be construed as a universal result numerically applicable to all possible designs. The result is, however, in very close agreement with past flight prototype and experimental designs built by Hughes for multi-kilowatt ion thrusters using a modular transistorized power conditioning approach. For a specific weight of 13.6 Kg/kW at a 28 VDC bus (comparable to early thruster breadboard designs), the projected specific weight decreases to approximately 4.54 Kg/kW at 100 VDC (as typified by a developed 20-cm ion thruster power conditioner) and to 2.72 Kg/kW at 250 VDC (projected flight packaged weight of 30-cm ion thruster experimental laboratory power conditioner). Comparable weight improvements can be expected for high power communication conventional power conditioning and is discussed in considerable detail in a following subsection.

On the basis of present and projected near future high voltage transistor technology and the rate of diminishing specific weight ratios in the range of 200-300 VDC, a baseline medium voltage bus of 250 volts (nominal) was selected for configuration B-1.

Communication Tube Power Supply Design Considerations

Power supplies to provide the high voltages required by the high power TWT's and Klystrons can be implemented using conventional DC-DC converter techniques. The feasibility and anticipated performance of this approach is greatly increased by the relatively recent availability of high speed, high voltage, high current transistors and high Curie point, low loss, large size ferrite magnetic cores.

A medium voltage solar array bus in the range of 250 volts (nominal) makes possible the switching of 2 kilowatts in a single transistor at 10 amperes (as in a DC-DC converter or PWM* series chopper). Thus, transistors rated at 400 volts V_{CEO} and switching in 1/2 microsecond such as now available, permit high reliability (low stress) at a power level of 2 kilowatts per transistor switch. To complement the 1/2 microsecond transistor switching speed, ferrite converter transformers can be designed for use at 10 kHz. At this frequency, the newer ferrite alloys permit low transformer core loss at a relatively high flux density of 2 kilogauss. Cores with 500-watt power rating at 10 kHz are readily available with rounded cross section for low dielectric stress with high voltage windings. Thus, four 500-watt transformers may be

---

*Pulse Width Modulation

used in parallel on the output of a single bridge inverter with a medium voltage bus, and with a saturated transistor drop of 0.5 volts at 8 amps such as now available, the bridge inverter can maintain a high efficiency even though two transistors are in series with the load.

A further advantage of the medium voltage bus, resulting from the use of the bridge inverter, is the convenience of DC decoupling the output transformers with a series capacitor in the transformer primary, preventing bridge unbalance saturation of the transformer core. Also, the output transformer efficiency is improved for the same weight, compared to the center-tap primary connection used with push-pull inverter.

An additional consideration in the application of conventional techniques to the high voltage, high power TWT's and Klystrons is that of low weight magnetics design. At these voltages (up to 16 kV for TWT's), conventional space practice has been to oil-encapsulate for voltages over 5 kV. Such construction is very costly in the weight of the container and the volume of oil. Recent experience by NASA with SERT-II verifies the feasibility of vacuum dielectric, although only at 3.5 kV. Here, transformers used nickel-iron laminations in square or rectangular stack cross-sections. This experience, plus the geometry of available ferrite "U" cores with round cross section, has suggested the use of a hybrid transformer design, using separate epoxy-encapsulated and interleaved primary and secondary windings and terminals. Such a design would result in high voltage transformer specific weights comparable to weights achieved with low voltage, 10 kHz, ferrites.

The maximum size of available ferrite cores (500 watt) is also compatible with the maximum desirable step-up in the transformer for low distributed capacitance and associated low resonant ringing with leakage inductance. Thus, a step-up of only 1:5 will provide 1000 volts separately rectified for each 1-kV step in the TWT and Klystron electrode requirement.

The 250 medium voltage bus also acts as a determinant in the choice of regulation circuitry. It permits efficient PWM DC modulation on the input to the bridge inverters, with major filtering performed at low voltage (inductors and capacitors do not require high-voltage insulation). Also, since a single filter may supply power to four or more electrodes, the range of load variations on the filter will be less than that on any one electrode supply, permitting critical inductance to be achieved with a smaller inductor.

The modest step-up in the output transformer, combined with square-wave switching, will permit simple capacitor filtering on each 1-kV DC output, without the difficulty of high voltage insulation of an inductor, as required for PWM square-wave inverter output.

Although the power conditioning for the communication tubes has been configured in the preliminary investigation as separate TWT and Klystron supplies, a common housekeeping supply and clock can service both. In addition, the PWM chopper regulators, bridge inverters, and transformers, with a few minor exception, can be of the same electrical and physical design for both supplies.

TWT Power Supply

A functional diagram of the TWT supply is shown in Figure 4.5-13. The total power supply output required is approximately 1960 watts, at voltages in 1 kV steps from -5 kV to -9 kV, and from -12 kV to -16 kV. The current distribution and associated power distribution as shown is for the saturated rf drive condition. At this time, the precise current distributions for conditions from "zero drive" to "saturation" are not known, and may, when known, result in a more optimum distribution of power in the two (2) inverters shown; but it is doubtful that this will significantly affect the design philosophy and adequacy of two operating inverters.

The maximum power per transformer is 525 watts DC output, which supplies 185 mA for the 3 kV voltage from -9 kV to -12 kV in two rectifiers (this is the only transformer with other than 1 kV per rectifier). Three transformers, which provide electrode voltages from -12 kV to -16 kV with an efficiency of approximately 97 percent for the transformer-rectifier combination, requires 1425 W from the inverter. This power level corresponds to 7.56 A from a 188.5-Volt, 10-kHz square wave and would lead to less than a one half voltage/current stress for a presently available transistor such as the Transitron ST18007, which is rated at 400 V_{CEO}, 20 A I_C. These transistors have a typical saturation drop of 0.5 volts at 8 A, and a switching time of 0.5 to 0.7 μsec.

By using an efficient "energy storage" type drive for the bridge inverter, the inverter efficiency will typically be 97.7 percent. This circuit has been extensively used and tested at the 250 VDC bus level in a 30-cm thruster power conditioning and is considered "state-of-the-art."

Since it is expected that high-voltage arcing will be normal with the TWT, the circuit is protected against these arcs both by use of series chokes in the output to suppress current supplied by output capacitors, and by a current-transformer (CT), shown in the output of the inverter which will trigger the inverter off on an arc. Automatic restart after a delay would be provided in the control circuitry.

Each of the two operating inverters is supplied from separate PWM line regulators (DC chopper) which are modulated to compensate for line voltage variations and to provide load regulation to hold the cathode and jump voltages constant. With this technique of regulation, the DC-DC converter will be square-wave, not PWM, permitting simple output filtering and good load regulation, with lower bandwidth transformers. Load tracking of electrode voltages which are not directly regulated (as are the cathode and jump voltage) should be better than ±5 percent worst case.

The PWM line regulator also uses an "energy-storage" full-wave drive, providing optimum power match of drive circuit, eliminating higher drop of a Darlington connection, and lowering the power loss per transistor without the loss associated with parallel equalization. The resulting efficiency of 97.7 percent, including the output L-C filter, is equal to that of the bridge inverter.
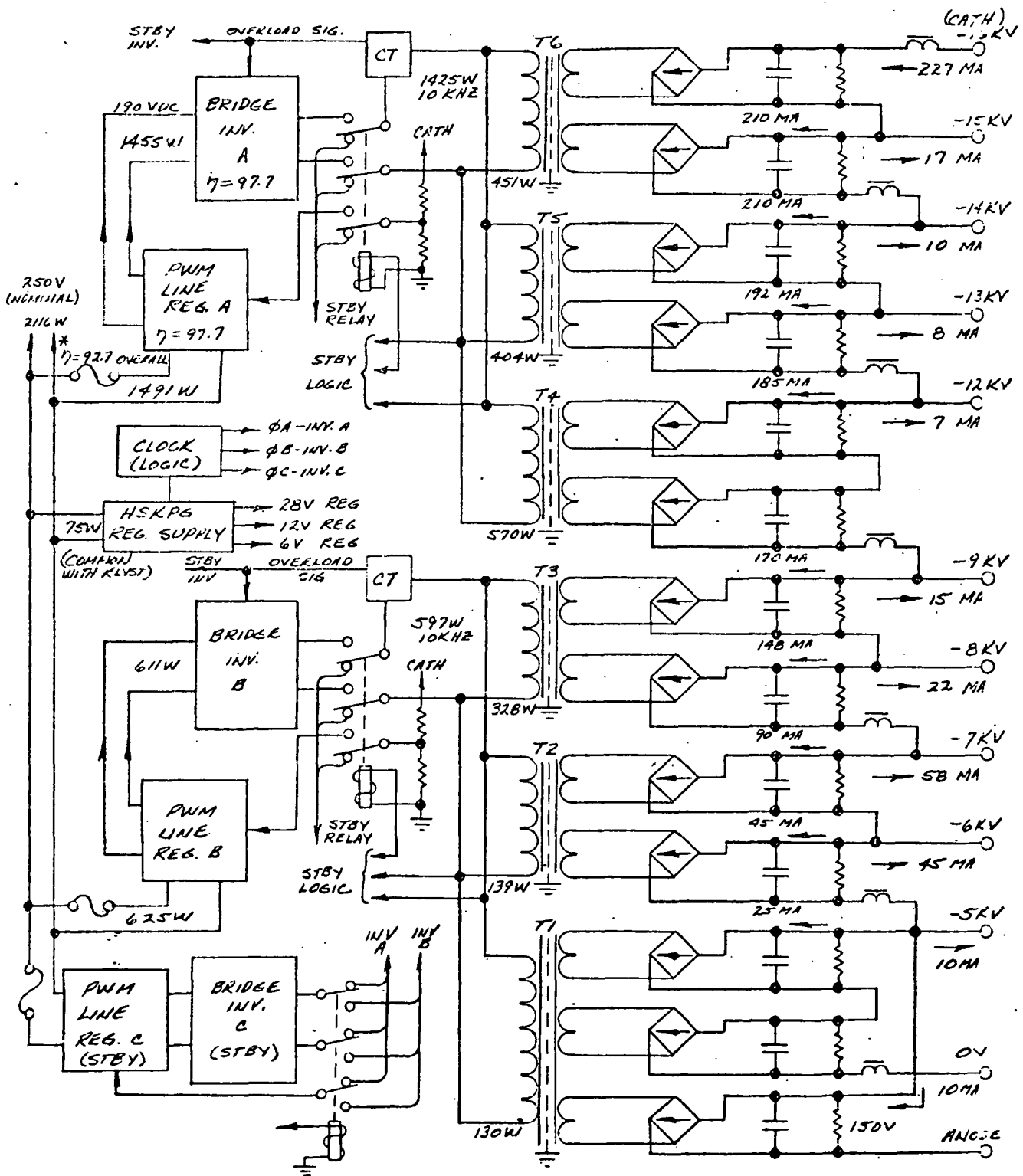
Figure 4.5-13. TWT Supply (Current Shown for Saturated RF Drive)

4.5-29

Klystron Power Supply

The Klystron supply functional diagram, shown in Figure 4.5-14, displays a great similarity to the TWT supply design. The principal difference is the higher maximum output power of 2980 watts required of the two inverters. Here, as with the TWT supply design, a more precise definition of variations in electride load currents, as the rf drive level is changed, may suggest a more optimum arrangement of transformers, and the different voltage levels in the high voltage series string which act as feedback to the individual PWM regulators, and different cathode voltages (-6.92 kV and -4 kV).

High Voltage Transformer Design

The power supply output transformer design is the key factor in determining whether an acceptable specific weight can be achieved with conventional power conditioning. The primary to secondary voltage stress level of 16 kV for the TWT represents a sizable departure from previous open-to-vacuum and encapsulated designs. There is a necessity, however, to break with traditional pressurized gas or oil-filled containers for the high voltage components since such an approach is prohibitive in weight at the multi-kilowatt level.

The proposed transformer design* uses some of the techniques of TV deflection transformers, but is dependent on vacuum dielectric (or sea-level air in test), with no dependence on encapsulant for HV insulation between secondary and primary. It does, however, use epoxy encapsulant for each winding independently for mechanical rigidity, thermal conductivity and surface sealing.

The design uses a Siemens "U" core manufactured with a high Curie point, low loss ferrite, having a round cross section and free from sharp edges and associated high dielectric stress. Primary and secondary are wound on separate bobbins machined from extruded nylon. The secondary is wound in four sections with a maximum of 500 volts in each section producing a low voltage per layer, a small area per layer and low distributed capacitance. The primary is wound in two sections on separate bobbins distributed on either side of the secondary for low leakage inductance. After winding, each bobbin is epoxy encapsulated in a diallyl-phthalate cup and then assembled on an epoxy-fiberglass tube with spacers between cups to increase creepage path. The joint between bobbins and tube, and tube and core is filled with RTV for thermal conductivity.

---

*The general design presented was implemented as part of an internal company program to investigate and extend High Voltage Technology. Preliminary tests substantiate feasibility.
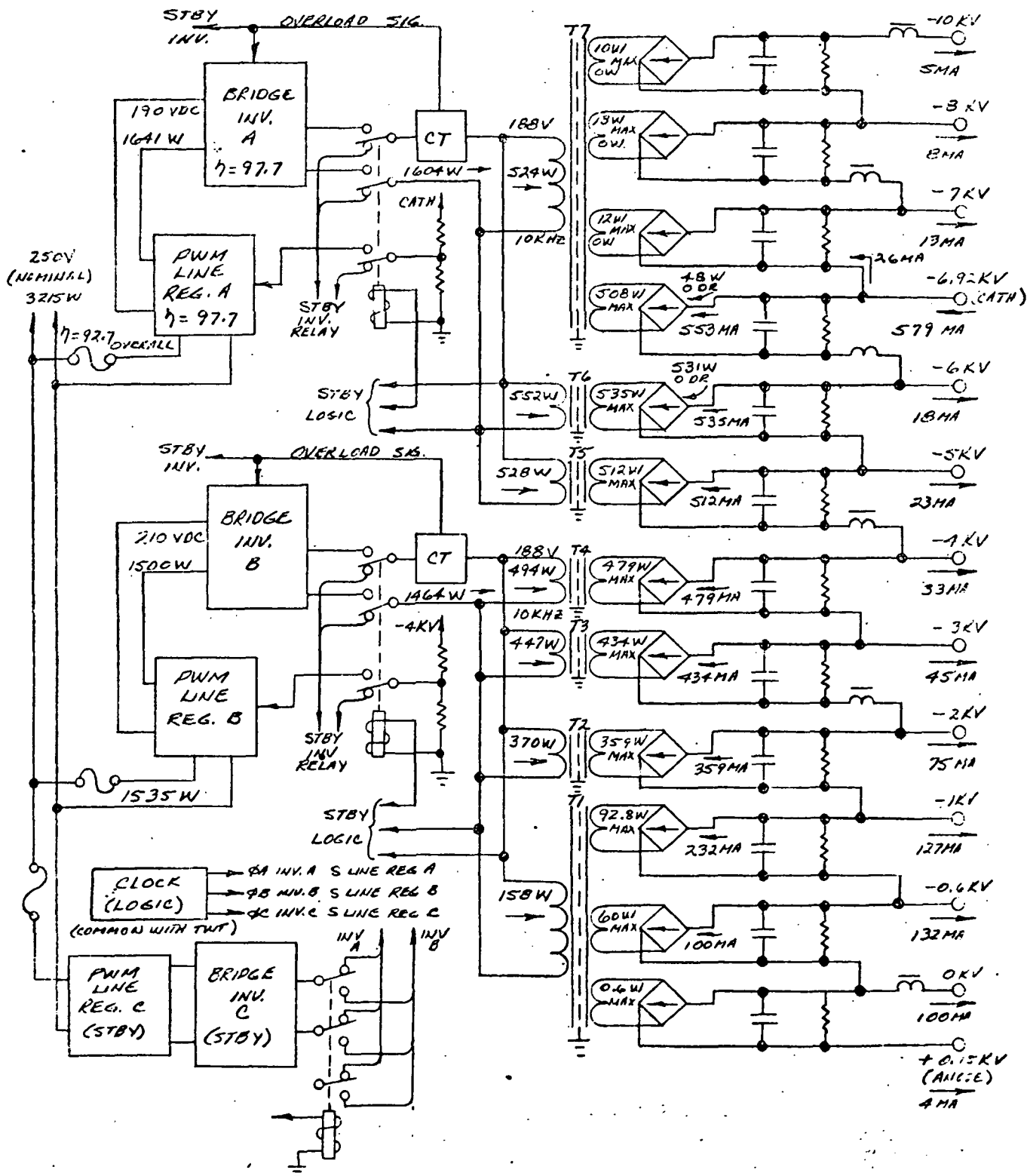
Figure 4.5-14. Klystron Supply (Current Shown for Saturated RF Drive)

Power Conditioning Specifications

The power conditioning system configured to provide TWT and Klystron conditioned power represents a substantial extrapolation from existing systems which operate at the required high voltages, particularly in terms of the physical layout and structural mounting of the open-to-vacuum high voltage portions of the system (transformers, rectifiers, filter capacitors, etc.).

Weight estimates based on the electrical designs shown in Figures 4.5-13 and 4.5-14, and on previous experience in fabricating high power ion thruster power conditioning panels which rely on direct radiation to space for cooling, produce a combined TWT and Klystron power system weight of less than 34 Kg, including housekeeping bias supplies, control logic, and transfer switching for bringing the standby inverters on line in the event of a failure.

There are a number of items which may impact on the system weight as further analysis and development are undertaken. Tighter collector voltage tracking (better than ±5 percent worst case) over the range of rf drive levels would probably require an increase in the number of inverters (but not transformers), hence their weight. A requirement for more rigid structural members than presently employed on ion propulsion power conditioning panels, or packaging techniques which do not use the thermal radiating panel can also contribute to increased weight of the power conditioner and the spacecraft thermal control system. In addition, although the system suggested uses staggered phase transistor switching to minimize array current ripple, sizable increases in line filtering and other EMI suppression filtering could contribute to yet another increase. Because of the above considerations a 50 percent contingency factor was used in specifying the ATS/AMS TWT and Klystron power conditioning weight. This leads to a weight estimate of 50 Kg.

An overall efficiency from solar panel to load of 91.4 percent was estimated for the combined supplies, and produces a total power loss of 460 watts. For direct radiation wity no solar incidence and a radiation temperature of 25°C, a loss density of 388 W/m^2 would require a thermal radiating area of 1.18 m^2. This area can be subdivided, with only minor restriction, into smaller panel sections for installation on the N-S surfaces of Spacecraft Configuration B-1. Panel thickness including an EMI back screen and connectors should be less than 10.2 cm.

A preliminary analysis of the failure rates of the system has shown that the greatest gain in reliability with minimum complexity is obtained by series-parallel redundancy of output rectifiers and output capacitors, and by circuit standby redundancy (2 of 3 required to operate) for the combined PWM line regulator and bridge inverter. The resultant reliability is 0.993 for five years excluding the housekeeping supply, clock, standby logic, and control. No difficulty is foreseen in obtaining a total system five-year reliability of 0.96 for the combined TWT and Klystron supplies including housekeeping, logic and control.

Table 4.5-8 presents summary specifications for the TWT and Klystron supplies and indicates both the calculated estimates and the very conservative

TABLE 4.5-8. TWT AND KLYSTRON POWER CONDITIONING
SPECIFICATIONS

Item	Calculated Estimates	ATS/AMS Baseline
Weight (Kg)	34	50
Efficiency (percent)	91.4	90
Radiating Panel Area (m^2)	1.18	1.21
5-year Reliability	0.96	0.96

ATS/AMS baseline values used where it impacted on total spacecraft weight or array power.

4.5.5 Power Transfer

Five means of transferring electrical power and electrical signals across rotating joints in spacecraft have been considered:

1)   Conventional brush-on-ring assemblies

2)   Flex cables with fast return

3)   Rotary transformers

4)   Non-sliding rotary electrical connectors

5)   Liquid metal slip rings.

For the baseline spacecraft configurations, power transfer is constrained by the requirements for continuous rotation, relatively high currents, and the need to transfer power at very high voltages in some spacecraft configurations.

Conventional brush-on-ring assemblies have been used extensively in prior spacecraft. Hughes has compiled three years of successful operation of large slip ring assemblies operating at over 50 rpm in the TACSAT and Intelsat IV dual-spin spacecraft. The advantages include well-developed technology and proven reliability in space; such slip ring assemblies have been chosen for configuration B-1. The disadvantages are high friction torque, electrical noise, and wear debris.

Flexible cables are often used where flexibility is required over a limited angular travel. For continuous rotation at slow speeds, a flexible cable can be designed to operate over a range of about 1 revolution with a mechanism to unwind the cable in a few seconds once each revolution. To avoid unwinding the cables by rotating the solar panels or spacecraft once each day, a slip ring assembly can be incorporated which operates only

during unwindings. The advantages over simple conventional slip rings are a reduction in electrical noise and the substitution of cable torques for friction torques. The disadvantages are the complexity, particularly where insulation for very high voltages is required, and the need to unwind the cable approximately once each day. The flexible cable with an unwinding mechanism has been proposed and may even be flying on other spacecraft. It is not being considered for the ATS/AMS application.

Rotary transformers have been studied under NASA contract[*] and found to be 99 percent efficient at frequencies near 10 kHz. A power of 500 watts dc was transferred at 97 percent overall efficiency with a 6.8 Kg rotary power transformer plus power conditioning. The major advantages are elimination of the friction and the wear-out mode of slip rings with its accompanying debris. Also, only one rotary transformer is required per circuit and dc isolation is achieved. Disadvantages are cost and complexity, particularly where direct current is being transferred and additional power conditioning is required. Rotary transformers might well be considered for signal transfer. Rotary transformers are presently in use on Intelsat IV.

A non-sliding rotary electrical connector is described by W. P. Fleming of MIT in AIAA Paper No. 70-458. This device has low electrical noise but appears to offer no advantages in low friction. It is in early stages of development and has not yet been qualified for space.

Liquid metal slip rings (LMSR) are being developed at Hughes under contract to NASA-LeRC,[**] with specifications directed towards use in solar array orientation mechanisms for high power communications satellites. The use of a liquid metal such as gallium to fill a narrow gap between concentric rotor and stator rings results in a power transfer means with extremely low resistance and thus negligible electrical noise and power loss. Stick-slip friction is replaced by viscous friction that is negligible at one revolution per day; it also eliminates a wear-out mode. Disadvantages include the need for temperature control so that the gallium can be frozen for containment during launch, and the need to maintain the slip rings in a strictly inert environment, such as argon gas or vacuum, from assembly through launch. The use of liquid metal slip rings on ATS is likely to be the first operational application of this technology, although it is expected that a LMSR experiment will fly before that time.

Conventional Slip Rings for Configuration B-1

The slip ring design for the solar array orientation mechanism of configuration B-1 is dominated by the large shaft which connects the two halves of the array through the body of the spacecraft. This shaft is likely to be 9.6 cm or greater in diameter and the slip rings must be mounted outside the shaft. It is estimated that the slip rings will have a diameter of 10.2 cm.

---

[*]Contract NAS-5-10459

[**]Contract NAS-3-11537 (complete) and NASA-3-13731 (in work)

For mounting locations on the end of a shaft, the diameter could be reduced to just enough to bring out the leads, about 5 cm or less.

Table 4.5-9 shows the slip ring complement using a conservative current allowance of 10 A per ring to provide for redundancy and to reduce electrical noise. Conventional slip rings carrying up to 30 A are in use on TACSAT.

The weight of this slip ring assembly is estimated as follows: Rings will be made of precious metal materials such as 90/100 coin silver for power circuits and Stackpole alloy SM476 for signal circuits. The ring must be heavy enough to carry current from the brush to the conductor attached to the ring without appreciable power loss. It must be wide enough for the brush to operate at low contact pressure for low wear, and it must be thick enough for dimensional stability and ease of connection to the conductor. A silver ring 10.2 cm in diameter, and 1.27 cm wide by 0.16 cm thick, will weigh 0.068 Kg. A signal ring might be only 0.0362 Kg, for a total weight (24 rings) of 0.86 Kg. Conductors will weigh this much again and insulation raises the weight on the shaft to about 3.6 Kg. The housing and brushes will weigh about 3.17 Kg for a total slip ring weight of 6.8 Kg, exclusive of shaft and bearings.

Friction is estimated based on a breakaway friction coefficient of 0.30 (typical for low pressure loadings used), a brush force of 28 grams for signal rings and 60 grams for power rings, and two brushes per ring. This results in a total friction torque of 28.2 newton-cm. By cutting the number of power rings to six, it can be reduced to 19 newton-cm. The friction level will be reduced very little when running at one revolution per day.

Electrical noise for conventional slip rings is estimated by considering a typical contact resistance to be three milliohms with a peak-to-peak variation during rotation of two milliohms. Thus, for a ten-amp circuit the expected voltage drop would be 30 millivolts with a power loss of 0.3 watts. The total

TABLE 4.5-9. SLIP RINGS FOR CONFIGURATION B-1

Function	Volts to Ground	Current	Number of Rings
Medium Voltage Bus	200 to 400	50 A	5
	0 (return)	50 A	5
Low Voltage Bus	28 to 50	20 A	2
	0	20 A	2
Controls	0 to 15	0.1 A	10
Total Rings			24
Estimated Weight (Slip rings, shaft, bearings, torques, etc.)			18.1 Kg

voltage drop and power loss including brushes, rings and leads might be considerably higher, depending upon specific design details. The electrical noise would be approximately 20 millivolts peak-to-peak, or 7 millivolts rms per ring.

The use of conventional slip rings for very high voltages should be considered as a backup. Slip rings used by Hughes in the proved designs for TACSAT and Intelsat IV have MoS_2 solid lubricant incorporated in the brush compound. Brush wear in the first year at 60 rpm is about 0.0089 cm, followed by steady wear at 0.00254 cm per year or less, based upon extensive vacuum testing. The debris from such wear must be contained by labyrinth seals to avoid formation of breakdown paths along lines of high electrical stress when used at 16 kV. However, the high current levels for which these rings were designed will not be required at high voltages. Oil-lubricated gold-wire brush designs, tested extensively by Hughes for currents up to 1 ampere, have shown no tendency to form wear particles. Labyrinths are used to retard loss of oil by evaporation. Application uncertainty hinges on the tendency for Paschen breakdown in the evaporated oil. There seem to be no overwhelming obstacles in the design of slip rings for very high voltage operation.

Liquid Metal Slip Rings for Configuration A-1 and B-5

LMSR design is also dominated by the through shaft. The weight of individual slip rings is determined by the same needs for electrical conductivity, dimensional stability and manufacturability. Slip rings for use with liquid metal cannot be made of silver, gold, copper, aluminum or beryllium because of the severe chemical reaction with gallium. Stainless steel, nickel and refractory metals such as tungsten and molybdenum are suitable. Therefore, despite the very low contact resistance, no great weight saving can be expected. The usual design of a LMSR utilizes a rotor and a stator ring for each line, and thus might be heavier for a given number of line functions that conventional slip rings. Liquid metal brush designs are being studied to reduce weight and complexity, and to increase environmental resistance.

The second slip ring assembly in Configuration A-1 connects the body of the spacecraft to the platform supporting the transmitter tubes and earth-pointing antenna. This assembly does not require a through shaft, permitting a significant reduction in weight. However, the design, fabrication and testing of two different designs is required. For this study, it is assumed that slip ring assemblies Nos. 1 and 2 have many common parts, including housing and slip rings.

Slip ring requirements for spacecraft configurations A-1 and B-5 are shown in Table 4.5-10. The slip ring complements do not exceed the 116 rings required in a liquid metal slip ring/solar array orientation mechanism for which preliminary designs have been accomplished under contract to NASA-LeRC.* The weight goal for this mechanism is 18.1 Kg. Housing, thermal

---

*Contracts NAS-3-11537 and NAS-3-13731

TABLE 4.5-10. SLIP RINGS FOR CONFIGURATION A-1 OR B-5

Function	Volts to Ground (Volts)	Current (Amps)	No. of Rings, Slip Ring Assy. No.	
			1	2*
Orbit Raising Thrusters	+1 kV to +2 kV	10 A	3	0
	+1 kV to +2 kV	1A to 2A	3	0
	-1 kV to -2 kV	0.1 A	3	0
	0 (return)	6 A	1	0
Low Voltage Bus	28 V to 50 V	20 A	1	1
	0	20 A	1	1
Controls	0 to 15	0.1 A	10	10
Traveling Wave Tube	0	0.25 A	1	1
Collectors	-5 kV to -16 kV	0.25 A	10	10
Heater	-16 kV	2 A	0	0
Anode	-5 kV	0.25 A	0	1
Klystron	0	0.25 A	1	1
Collectors	-5 kV to -11.1 kV	0.25 A	11	11
Heater	-7.4 kV	0.25 A	0	2
Anode	150 V	0.25 A	0	1
Total Rings			45	41

Estimate Total Weight (slip rings, shaft, bearings, torques, etc.).	Configuration A-1	45.3 Kg		
	B-5	22.6 Kg		

*Slip Ring Assembly No. 2 is not required in spacecraft configuration B-5.

shroud, 7.63 cm diameter through shaft, bearings, two large brushless torquers and a brushless pick-off are included. The actual slip ring assemblies are estimated to weigh only 5.98 Kg of the total. Although this is an extremely tight weight budget for a 116-ring assembly, it could be met with relative confidence for the lower numbers of rings required for this application.

Gallium is used in the liquid metal slip rings because of its low vapor pressure. Mercury has excessive evaporation. The 303°K freezing point of gallium is convenient to allow freezing for retention during launch. The surface tension of 0.00735 newton/cm allows retention during orbital conditions and testing.

The viscous friction in the liquid metal slip rings can be calculated if the geometry of the ring is known. Viscous coupling in a radial gap is

$$C = 2\pi\mu R^3 w/h$$

where

μ = 0.016 poise   viscosity of gallium

R = radius to gap

w = width of gap

h = radial gap

Assuming a ring of 10-cm radius, 1-cm width and a gap of 0.025 cm, the viscous coupling is

$$C = 4.02 \times 10^{-2} \text{ newton-cm per (rad/sec) per ring}$$

Using the conservative approach that all rings are this size, an 86 ring assembly has a torque, at 1 revolution per day, of

$$T = 0.292 \times 10^{-5} \text{ newton-cm}$$

This friction torque is clearly inconsequential.

The electrical noise and voltage drop through the liquid gallium is similarly inconsequential. The resistivity of the gallium is 28 microhm-cm. The surface resistance through the interface from gallium to nickel is less than 0.1 microhm-cm^2 when the nickel is well-wetted by the gallium. For the ring described above, the resistance would be:

$$R = (28 \times 10^{-6} \text{ ohm-cm})(0.25 \text{ cm})/(20\pi \text{ cm}^2) + 2(0.1 \times 10^{-6} \text{ ohm-cm}^2)/(20\pi \text{ cm}^2)$$

$$= (11.14 + 3.18) \times 10^{-9}$$

$$= 1.43 \times 10^{-8} \text{ ohm}$$

The variation of this resistance with rotation would be a sinusoid due to eccentricity with an amplitude of about 1/10 of the average resistance.

The liquid metal brushes use a much smaller contact area. With a "brush" tip 0.318 cm by 0.318 cm, and a gap of 0.254 cm, the resistance becomes 9.2 microhms.

The superiority of liquid metal as the contact in slip rings is readily seen.

The most serious problem remaining in the development of LMSR for spacecraft is the film which forms on gallium when exposed to air. This film is very thin but quasi-plastic in nature. It tears when the rings are rotated, and rolls up, forming a debris which may escape from the rings or which may mix with the liquid gallium to form a sludge. This characteristic has prevented the use of gallium for slip rings in an air environment.

The film does not form in the absence of air and water vapor. If the slip rings can be assembled in an argon atmosphere with less than 10 parts per million oxygen or water vapor, they should be free of film. This has not yet been accomplished. However, it has been noted that the film does not continue to form during slip ring testing in high vacuum.

The conclusion is that, to be film free, the LMSR assembly must have a gas-tight seal and must be purged with pure argon or kept at high vacuum during assembly, test, transportation and launch. The gas-tight seals around the shaft where it exits the assembly should be gallium with suitable labyrinths to retain the external debris which may be generated during testing. As an alternative, the seal might utilize magnetic fluids such as the ferrometric rotary vacuum feedthrough seal by Ferrofluidics, Inc. The gallium feed-through seal would be frozen during launch and might function as a launch lock.

Another alternative would be to permit the gallium slip ring assembly to contact air only when frozen, when the surface activity is much less. Testing and rotation of the rings would be allowed only after outgassing in a vacuum. Provisions could be made to trap the small amount of residual debris in labyrinth seals on each ring, as would be required for conventional slip rings in very high voltage applications.

Large diameter slip rings may be required with through shafts and many slip rings. The gallium cannot reasonably be retained in such rings by surface tension forces during testing unless the rings remain in a relatively horizontal plane. Therefore, the liquid metal slip ring assembly must be maintained with a vertical axis whenever the gallium is liquid. This restriction will not be required if the liquid metal brush is employed.

Although the need for continuing studies into liquid metal slip ring operational characteristics is evident, the initial promise of low friction and electrical noise makes them an attractive candidate for this application.

4.5.6 Energy Storage

The energy storage system provides power during the launch phase prior to solar panel deployment, power for housekeeping operation during eclipse, and additional power for peak load requirements to the low voltage bus during sunlight operation such as igniting squibs, etc. The demand varies from a few watts during the launch phase to approximately 125 watts during the on-orbit eclipse operation. For the spacecraft configuration A-1, the solar panels are deployed within one hour of liftoff so the total energy consumed before deployment is less than required for on-orbit eclipse operation. For the B-1 and B-5 spacecraft, however, the launch and transfer orbit lasts approximately six hours and imposes a moderate constraint on energy storage. The equipment operating during this time will be minimized to make the total energy requirement approximately an equivalent to an on-orbit eclipse period.

The above requirements can best be satisfied for a 5-year mission lifetime with nickel-cadmium battery cells. These cells have been proved on many previous missions. They are available in reliably sealed individual cells with rugged electrode construction.

The housekeeping bus in general will be run at a low voltage of approximately 28 volts. However, in one of the spacecraft configurations considered (C-1), it is desirable to run an eclipse bus at 250 volts to provide power for one high-power communication tube. Since the reliability of "unprotected" strings of battery cells decreases exponentially with voltage, individual cell protection is required as well as careful cell matching to avoid battery failures due to capacity and voltage divergence. Another problem inherent in medium voltage systems requiring energy storage is the packaging inefficiency associated with a large number of small cells. The ratio of active materials to hardware (case, terminals, battery hardware) increases as cell capacity increases. Since the three baseline spacecraft do not require energy storage at medium bus voltages, detailed analysis of this problem was not pursued.

Degradation with time is sensitive to many factors. Temperature extremes, amount of reconditioning, depth of discharge, and operating rates all influence the rate of degradation. However, over a 5-year period, battery degradation will not affect performance if operating temperature extremes are held between 283°K and 308°K, periodic reconditioning is performed, and depth of discharge does not exceed 50 percent.

Baseline Approach

Based on the requirements of the baseline spacecraft configurations, a battery system composed of two 6-ampere-hour nickel-cadmium batteries appears adequate; this system can supply all mission needs at a depth of discharge of approximately 50 percent. Charging of the batteries is accomplished with the low voltage solar panel section, achieving a lightweight, reliable approach to providing a constant charge current. Attainment of full charge for the batteries is detected by signal electrode cells in each battery which act on a switch in the respective charge controller to terminate charge. Charge termination can also be effected by ground command.

Battery power is provided to the eclipse bus through diode coupling. Series resistance is provided to ensure good current sharing between the two batteries, but the system can operate on one battery in a failure mode condition. In this event, certain eclipse loads could be removed by ground command to reduce the total battery drain. The output bus voltage is approximately 28 VDC. Any further regulation and/or power conditioning is provided by the using subsystem.

4.5.7 Power Subsystem Weight Summary

The weights of individual electrical power subsystem units for the three baseline spacecraft configurations are presented in Table 4.5-11.

TABLE 4.5-11. POWER SUBSYSTEM WEIGHT SUMMARY

Unit	Configuration		
	A-1	B-1	B-5
High Voltage Solar Array	304		252
Integral Power Conditioning	31		28
Low Voltage Solar Array		236	
Communications Conventional Power Conditioning	10	120	10
AC&S Ion Thruster Power Conditioning	14		
Orbit Raising Ion Thruster Power Conditioning	5		
Liquid Metal Slip Rings	100		50
Conventional Slip Rings		40	
Batteries and Electronics	50	50	50
Orientation Electronics	15	15	15
Totals (kilograms)	529	461	405

4.6 THERMAL CONTROL

4.6.1 Introduction

The primary objective of the thermal control design effort during the study has been to establish workable methods for handling the very high system power dissipations. The key conclusions which have evolved from this effort are the following:

1)   High temperature, direct radiating TWT and klystron collector designs are essential. The radiator area inherently available in the various configurations is not sufficient to handle the approximately 2 kw of thermal dissipation at ambient temperatures.

2)   Large amounts of localized power dissipation (with saturated tube operation) within the spacecraft require the use of heat pipes to provide adequate energy distribution. Particularly significant thermal loads are the RF output switches, filters and lines, which result in 590 watts of thermal dissipation for 3 kw of RF output, and must be temperature controlled in the range from $273^{\circ}K$ to $338^{\circ}K$.

3)   On-orbit temperature control when tubes are operating below saturation can be provided through active heating without penalizing the power system design. The operating characteristics of the multistage collector tubes are such that ample power becomes available for active temperature control purposes when the tubes are operated in a backed off mode.

4)   Transfer orbit temperature control can be provided through active heating for the electric propulsion configurations. Ejectable radiator covers are required for the apogee motor configurations, since no prime power is available.

Feasible thermal control design approaches have been established for each configuration examined and the thermal characteristics of the various configuration options are summarized in Table 4.6-1. The use of electric propulsion, high voltage arrays and liquid metal sliprings are recognized as offering significant additional complexity to the thermal design. However, this increase in complexity must be considered as part of the overall hardware development/mission performance tradeoff.

Although the thermal design approach varies among the several options due to these factors, there do not appear to be system thermal control weight, complexity or developmental differences sufficient to play a major role in the configuration selection process. The key system elements are the development and integration of the direct radiating TWT and the heat pipe radiator system required for distribution and rejection of other spacecraft heat loads. These items are common to all configurations.

TABLE 4.6-1. KEY THERMAL FEATURES

	Configuration			
	A-1	B-1	B-5	C-1
Transfer orbit	a) 200 watts of active heating b) 40 watts of continuous	Ejectable radiator covers	Ejectable radiator covers	a) 400 watts of active heating b) 40 watts of LMSR heating
On-orbit operations	Use excess system power for active heating when tubes are operated in the backed-off mode 80 watts of continuous LMSR heating (2 assemblies)	Passive 10 watts RCS heating	Passive a) 10 watts active RCS heating b) 40 watts LMSR heating	Use excess system power for active heating when tubes are operated in the backed-off mode 80 watts of LMSR heating (2 assemblies)
Power system demands, watts	240	10	50	440
Thermal Control Weight (kg / lb)				
● Apogee motor insulation		0.9 / 2	0.9 / 2	
● Low temperature insulation	2.6 / 6	3.6 / 8	3.6 / 8	3.6 / 8
● High temperature insulation (ion engines and tube collectors)	4.5 / 10	0.9 / 2	0.9 / 2	4.5 / 10
● RCS heaters	0.9 / 2	1.4 / 3	1.4 / 3	
● LMSR heaters	2.3 / 5		0.5 / 1	0.9 / 2
● Second surface mirror radiator finish		6.8 / 15	4.5 / 10	3.6 / 8
● Internal paint	1.4 / 3	1.4 / 3	1.4 / 3	1.4 / 3
TOTAL	11.8 / 26	14.1 / 31	12.3 / 27	14.1 / 31

The balance of this section presents the system thermal design requirements, a discussion of key design elements, and a thermal design description for each of the prime configuration candidates.

4.6.2 Requirements

Orbital Environment

The external thermal environment in synchronous equatorial orbit consists of direct solar irradiation and the deep space surroundings. Earth emitted radiation and albedo are negligible compared to the direct solar flux.

Solar energy incident on the spacecraft is proportional to the projected area normal to the solar vector. Thus, variation in incidence angle between the sunline and vehicle must be considered. Yearly angular variations resulting from the inclination of the earth's spin axis is shown in Figure 4.6-1.

The geometry is such that the north and south facing spacecraft surfaces are the most useful as thermal radiators, due to the minimal solar illumination. The average value of the solar constant is approximately 126 watts/ft^2 with a variation of ±3.5 percent due to the eccentricity of the earth's orbit. The variation of the solar constant over the year is shown in Figure 4.6-2.

During the equinox season, the spacecraft will experience a daily eclipse caused by the earth's shadow. This will occur for a period of approximately 45 days, with a maximum eclipse time of 72 minutes during this period.

The transfer orbit thermal environment is significantly different, depending on the method of final orbit injection to be used. For those options which employ a conventional apogee motor, the sun angle with respect to the spacecraft is controlled to within desired limits by proper selection of the daily launch window. On injection into the transfer orbit the spacecraft would
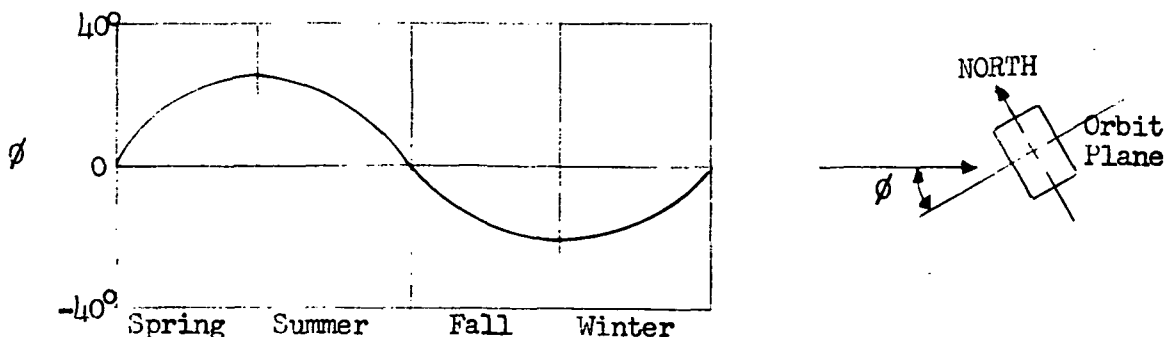
Figure 4.6-1. Yearly Flux Angle Variation

4.6-3
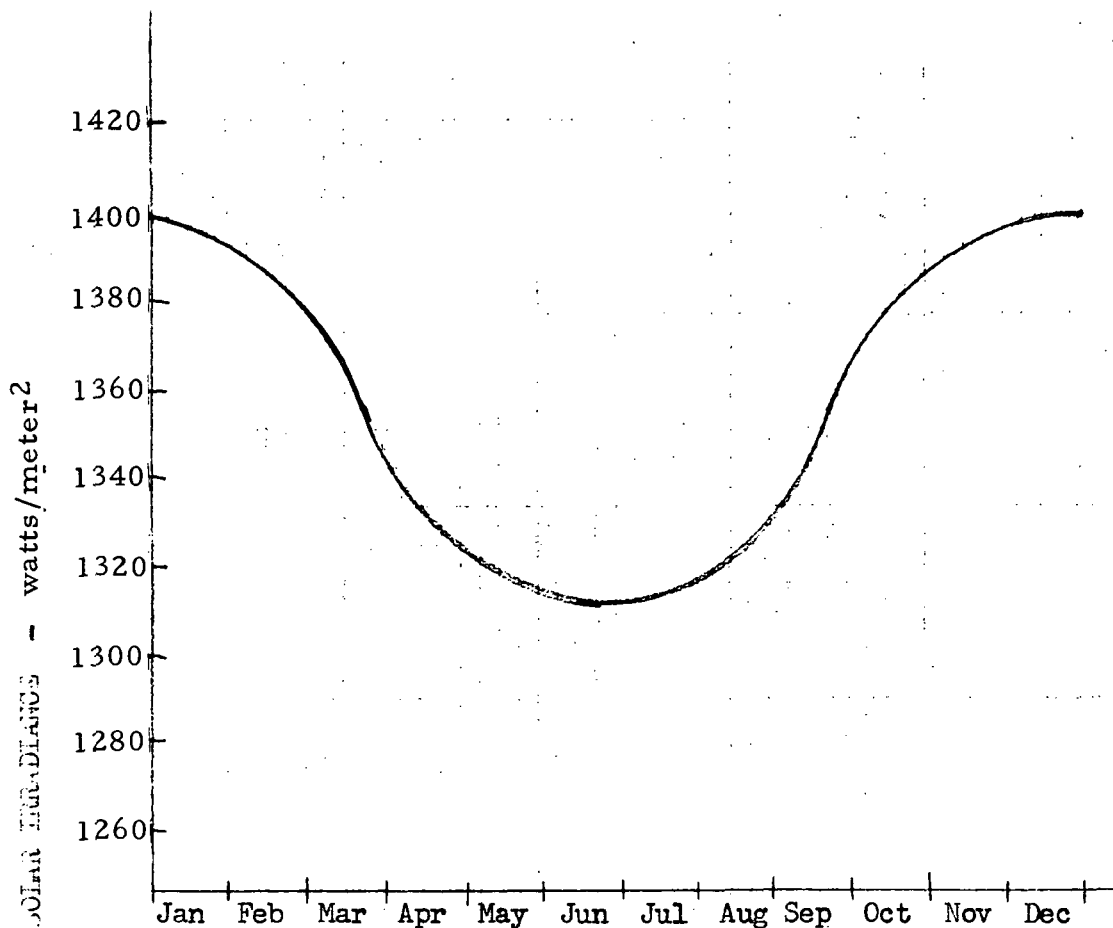
Figure 4.6-2. Seasonal Variation of Solar Irradiance

be spun up about the apogee motor thrust axis, and injection into synchronous orbit would be planned to occur at first apogee, approximately 5-1/2 hours after launch. However, it is desirable to permit the option to complete an additional revolution in the transfer orbit if, for example, the motor alignment is not satisfactory at first apogee. Thus, the thermal design should be capable of protecting the equipment for up to 18 hours in the transfer orbit environment.

For those options which use electric propulsion, about 3 months is required to achieve the final orbit. During this time the sun will transverse a varying path about the spacecraft body in the plan normal to the solar panel axis as the thrust vector direction is varied to achieve the optimum combination of orbit raising and inclination change. This difference must be accounted for in the overall thermal design.

Equipment Temperature Requirements

Table 4.6-2 shows the temperature limits required by the major elements of the spacecraft. In general, for electronics, attitude control and power subsystem equipment, the limits shown are consistent with past practice. The temperature requirements for the ion engine subsystem are based on current mercury hollow cathode thruster technology. The 1273°K limit for the tube collectors assumes the use of molybdenum collector discs and ceramic isolators, and is based primarily on the tube design work done at NASA-Lewis.

The turn-on limits refer to the minimum permissible temperature at which the equipment can be turned on without incurring permanent damage. This requirement is applicable when the spacecraft is exiting eclipse. The survival/storage limits refer to both ground and on-orbit exposure of equipment with no power applied.

TABLE 4.6-2. EQUIPMENT TEMPERATURE REQUIREMENTS

Subsystem/Elements	Design Temperature Limits for the S/C Mounting Surface, °K	Turn-on Minimum, °K	Storage Minimum, °K	Comments
Transponder				
TWT or klystron Collector	*Up to 1273 Collector temperature		203	Assumes multistage molybdenum collector
Tube barrel	273 to 373	258	233	
RF filter, switches and waveguide	273 to 338	258	233	
Electronics (tube drivers and receivers	273 to 313	258	233	
T&C	273 to 313	258	233	
Power				
Electronics	273 to 313			
Batteries	*273 to 308	268	258	
Solar panel	*93 to 438	93	93	
Power conditioning	273 to 338	258	233	
Attitude Control				
Gyros, wheels, and control electronics	273 to 313	258	233	Gyros equipped with active heating
LMSR	*308 to 323	308		Gallium melts at ~303°K
Propulsion - tanks, lines and valves - thruster	*278 to 338 ≠263 to combustion temp	268 263	268 263	Active heating required
Ion Engines				
Stationkeeping	273 to 673		233	
Orbit raising	273 to 673		233	Will operate continuously in the transfer orbit
*Unit temperatures.				

Equipment Power Dissipation

    Table 4.6-3 summarizes the sources of thermal dissipation within the several spacecraft options, excluding the TWT and klystron collector dissipations. This tabulation represents the maximum amount of heat which must be rejected from the spacecraft body. The minimum operational dissipations would correspond to zero drive to the TWT and klystron tubes, or a reduction of 590 watts. A further reduction of the power conditioning loss would occur in Configuration B-1 in the backed-off operating modes. Figure 4.6-3 shows the power consumption as a function of RF output based on operating characteristics which have been calculated for the TWT. The klystron would be expected to exhibit similar characteristics. It is apparent from Figure 4.6-3 that ample power for the active heating required in Configurations A-1 and C-1 becomes available during backed-off operating modes to compensate for the correspondingly reduced RF losses within the spacecraft.

TABLE 4.6-3. RADIATOR POWER DISSIPATION REQUIREMENTS

	A-1	B-1	B-5	C-1
TWT/klystron tube cavities	150	150	150	150
RF losses (switches, filters)	590	590	590	590
Repeater electronics	100	100	100	100
TT&C	20	20	20	20
Power distribution (housekeeping)	45	45	45	45
Attitude control	55	55	55	55
Liquid metal slipring active heating	80	-	40	80
Power conditioning	-	545	-	-
Total (watts)	1040	1505	1000	1040
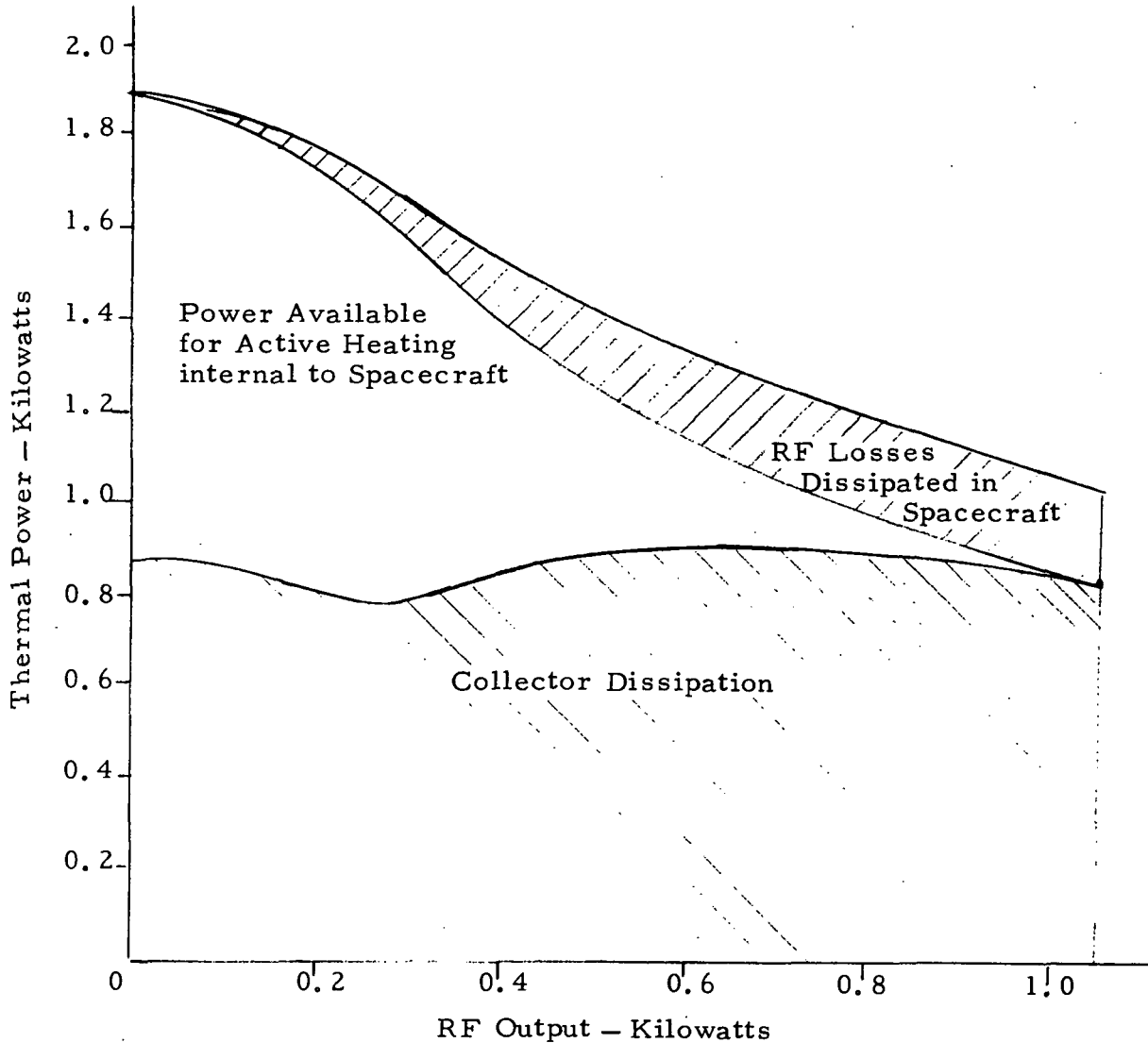
Figure 4.6-3. TWT Power Consumption Characteristics
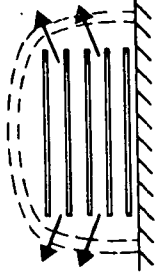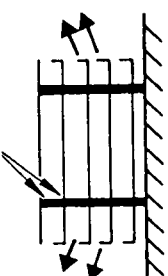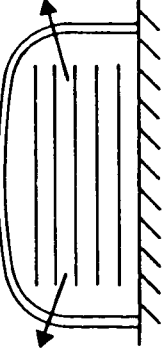
4.6.3 Design Approach

Direct Radiating TWT and Klystron Collectors

Table 4.6-4 presents the several potential options for achieving a direct radiating design. The third approach, which uses an envelope over the collector elements, seems to be the most reasonable.

The second option offers the most efficient design in that direct radiation from the collector plates is achieved both in ground test and on-orbit without requiring a ground test envelope to be jettisoned after launch.

TABLE 4.6-4. TWT COLLECTOR THERMAL DESIGN

	OPERATING TEMPERATURE	ADVANTAGES	DISADVANTAGES
Open Envelope, Direct Radiator	Up to 1273°K	• Minimum weight and complexity. • Space vacuum pumped.	• Large temperature excursion in eclipse. • Imposes ground test constraints. • Must provide for in-orbit mechanical removal of ground test envelope.
Sealed Envelope, Direct Radiator Vacuum Seals	Up to 1273°K	• Ease in ground test. • Can be space vacuum pumped (seals must hold only in ground environment).	• Many seals exposed to temperature cycling. • Large temperature excursion in eclipse.
Sealed IR Opaque or Transparent Envelope	Up to 1273°K	• Ease in ground test. • Can be space vacuum pumped. • Envelope seal exposed to less severe temperature cycling (single seal).	• Less weight efficient than direct radiator.
Sealed Envelope, Low Temperature Radiator	373 to 573°K	• Existing experience.	• Heavy. • Large radiator area required.

The practical disadvantage is the necessity for maintaining 22 ceramic-to-metal vacuum ring seals throughout the ground test life of the tube. The advantages of this design can be realized in the third option, where only one seal is required, if the envelope can be retained on-orbit. Provision can be made for puncturing the envelope on-orbit to permit space pumping. Figure 4.6-4 summarizes the computed peak disc dissipations as a function of tube operating point. The peak dissipation per collector disc is 200 watts, or approximately twice the average value per collector. Figure 4.6-5 represents the calculated bulk collector disc and envelope temperatures as a function of total

Output Power Levels:

- • Saturation (0 dB)
- X -3 dB
- O -6 dB
- △ Zero Drive
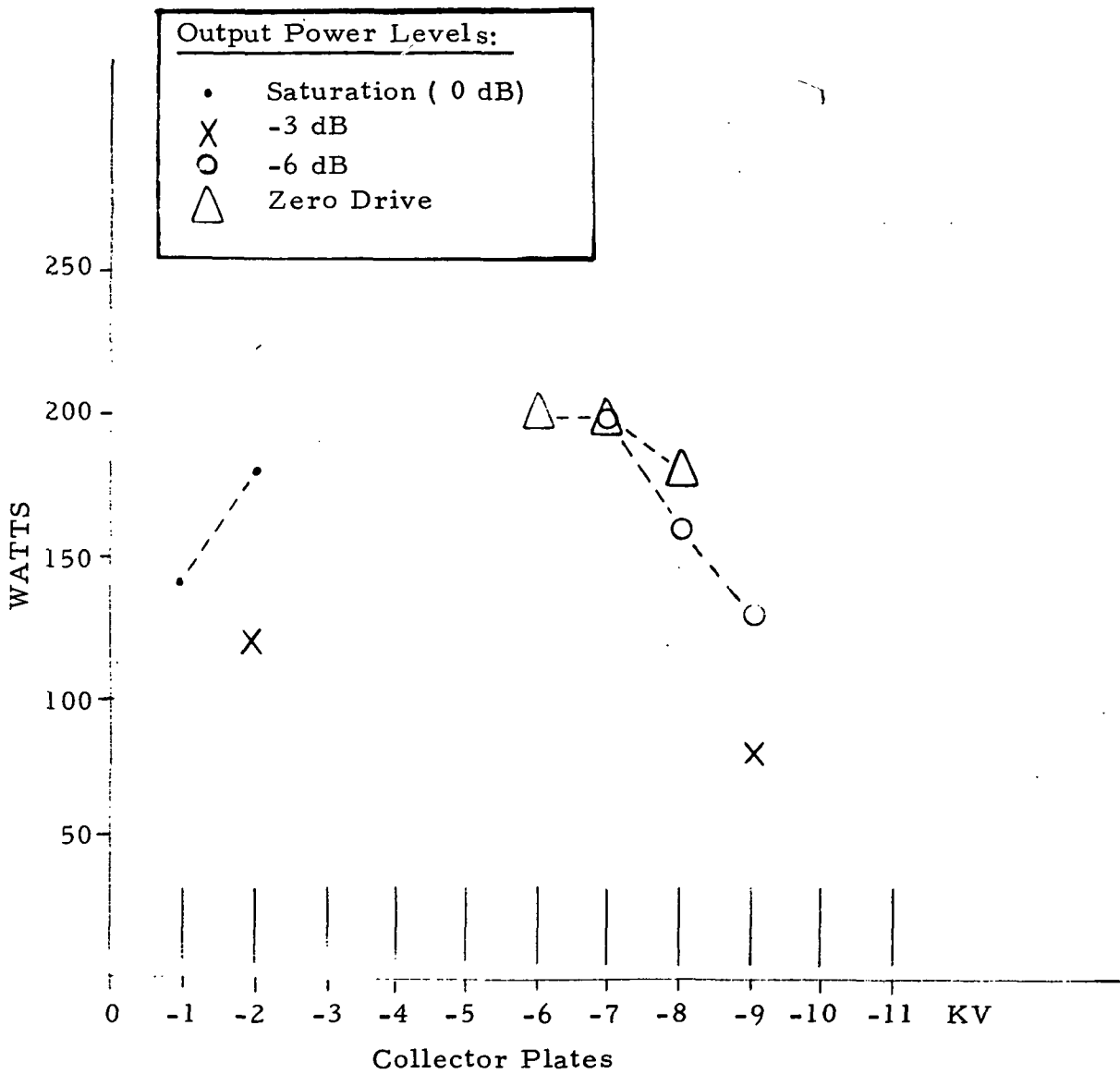
Figure 4.6-4. TWT Collector Dissipation
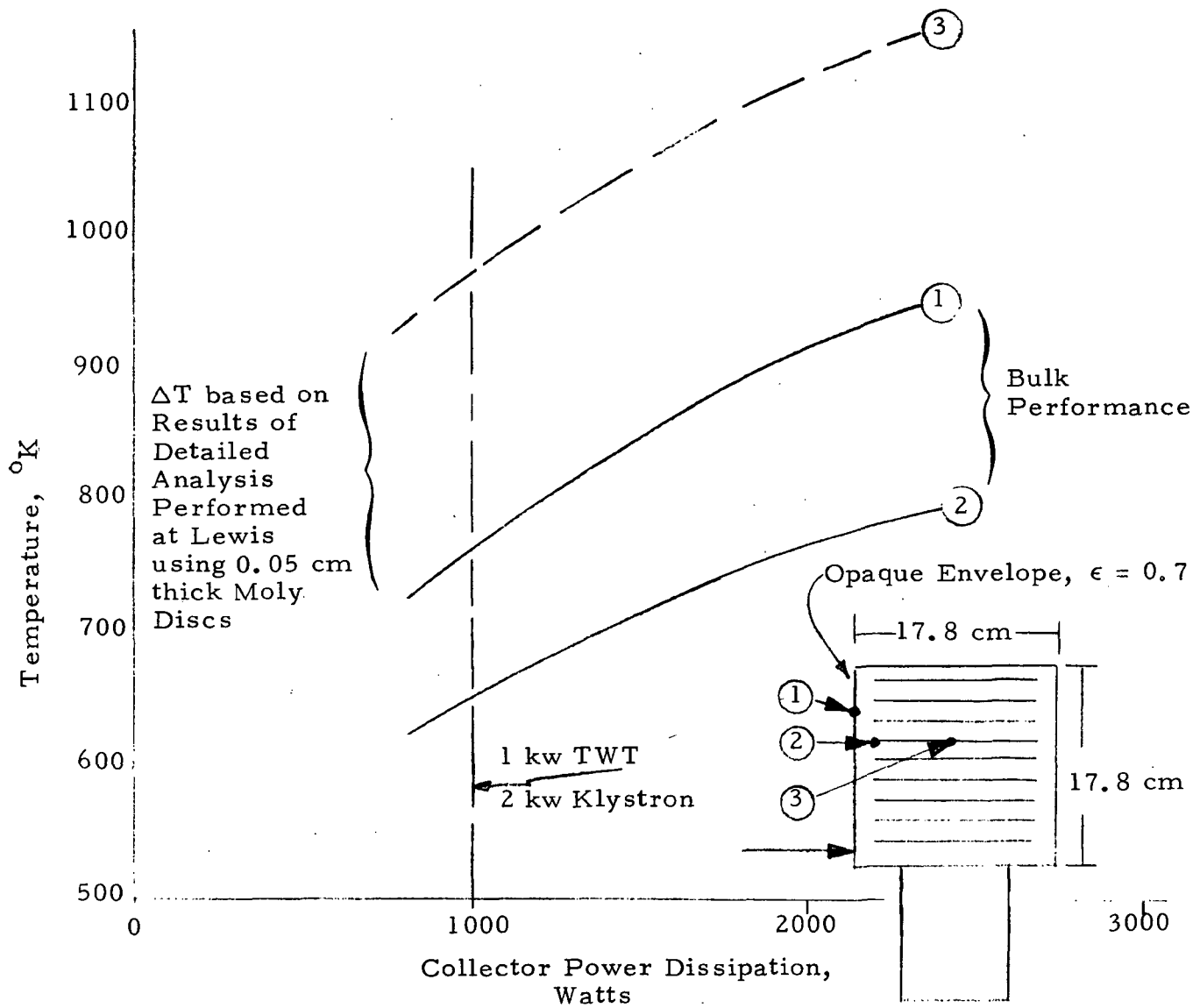
Figure 4.6-5. Tube Collector Power-Temperature Performance

dissipation. For the bulk model, the peak local dissipation of 200 watts per collector is conservatively equivalent to a 2 kw total dissipation. For this conservative assumption, the figure shows that the tube collector of interest can be kept at acceptable temperatures when housed in an opaque envelope. Provisions can be made to puncture the envelope while on-orbit, to effect space pumping, and partially transmitting envelope materials can be considered as a means of dropping the operating temperature of the discs without having to jettison the envelope.

The integration of the tube into the spacecraft requires a) local protection of the spacecraft around the hot collector, and b) provision for dissipating the tube cavity power (50 to 100 watts) at 338°K or lower. The arrangement of the tube in the spacecraft skin which satisfies these requirements is shown in Figure 4.6-6.

4.6-10

Approximately 0.186 m^2 of
Dedicated Radiation Area

Heat Pipes

Multilayer
High Temperature
Insulation

Spacecraft North Face

$T_{bulk} = 1273^{\circ}K$

Heat Flux, Collector
to Skin < 0.155w/cm^2
at R $\simeq$ 12"

Heat Pipes for Removal
of Cavity Dissipation
($\sim$100 watts)
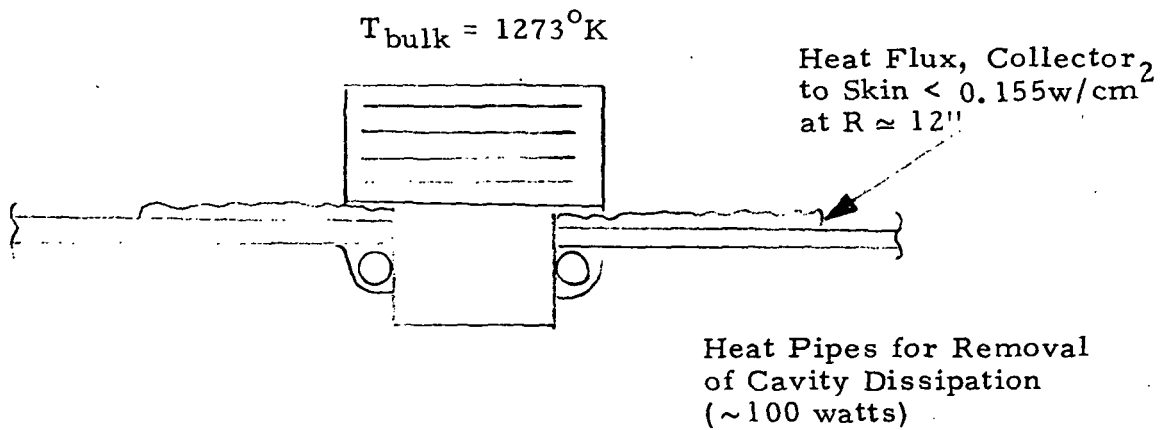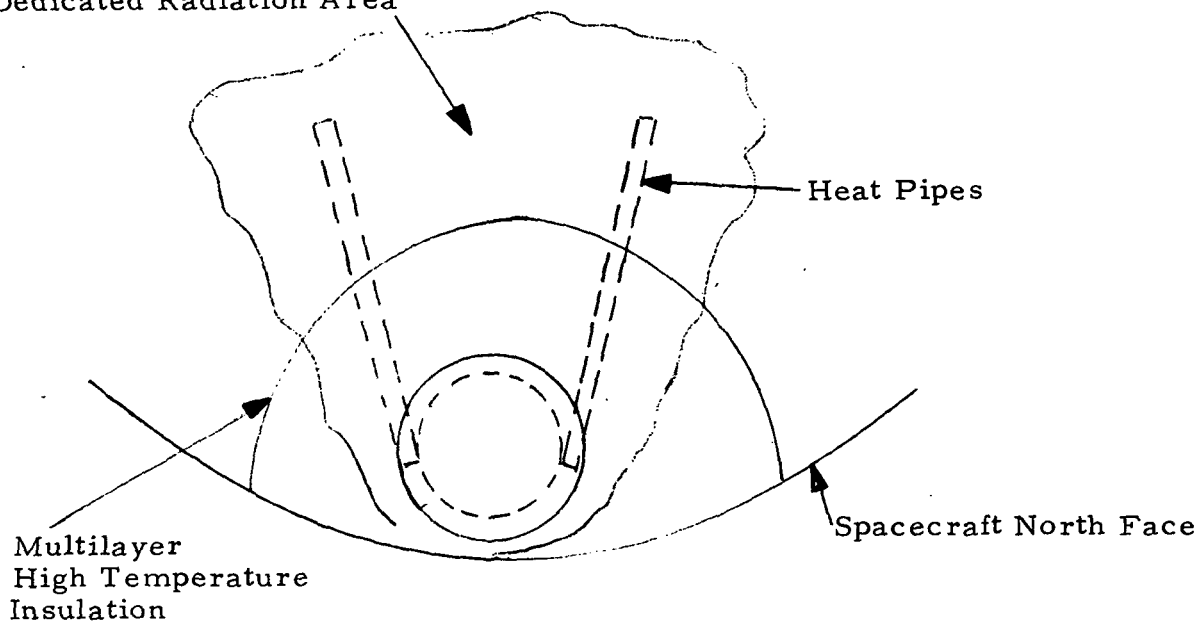
Figure 4.6-6.   Tube Integration

High temperature insulation is provided locally to protect the spacecraft structure. In order to maintain the desired cavity temperature of 338°K or less, special purpose heat pipes would be used to provide a path for energy transport from the tube cavity to a useful portion of the radiator beyond the insulation.

Equipment Radiator Design

All configurations must handle significant amounts of power dissipation associated with RF losses generated within the output switches, filters, and lines. To control these components to a maximum of 338°K, with a reasonable expenditure in weight, heat pipes were selected for the energy distribution purposes. Figure 4.6-7 shows a typical segment of a radiator which was designed and built as part of an internal R&D study. The heat pipes are 0.05 cm wall aluminum with screen wicks and would utilize either ammonia or acetone as the working fluid. The segment and heater shown closely approximates the arrangement required to control an RF switch dissipating approximately 60 watts.

The maximum capability of the available radiator area is realized in all spacecraft configurations by using second surface silvered quartz mirrors as the external finish. The silvered quartz offers the lowest solar absorptance achievable, thereby minimizing the absorbed sun loads at the solstice. Figure 4.6-8 shows the relationship between radiator weight and the number of heat pipes used, based on the configuration shown in Figure 4.6-7. Selecting a near optimum pipe spacing of 5 cm yields a representative specific weight of 5.6 kg/m². Allowing for the second surface glass mirrors and the adhesive, the total design weight becomes 6.35 kg/m². For purposes of summarizing weights, all panel weight has been included as structure, and only the glass mirrors have been included as thermal control weight.

Liquid Metal Slipring Assemblies

Requirements for thermal integration of the LMSR into the spacecraft are two-fold: a) the Gallium must remain frozen throughout the initial ascent and during synchronous orbit injection for options using chemical apogee motors, and b) provisions must be made to maintain the Gallium in the liquid state continuously after all high structural loading events have occurred. Since the freezing point of Gallium (approximately 300°K) is very near typical spacecraft operating temperatures, active heating is required while on-orbit to insure that freezing does not occur. This heating demand is dictated primarily by the thermal path presented by the electrical cabling entering and exiting the assembly, and the radiation losses via the open ends of the assembly.

Figure 4.6-9 shows heater-power/temperature characteristics expected for the Hughes LMSR design. The selection of 40 watts as the heater size is somewhat conservative in that some thermal closure of the ends will probably be possible, and the number of wires assumed is an upper bound.

Heat Pipe Specs

1.26 cm O.D. , 0.05 cm wall, 91.5 cm long, Al
1 layer 50 mesh Al (5054) screen
11 cc Acetone

Bond to Facesheet

or

Al Adaptor

Detail

Insulation Blanket

Facesheets
0.0305 cm

Two 10.2 x 10.2 cm 60^w
Blanket Heaters

20.3 cm

91.5 cm

40.6 cm

Heat Pipes
(see Detail)
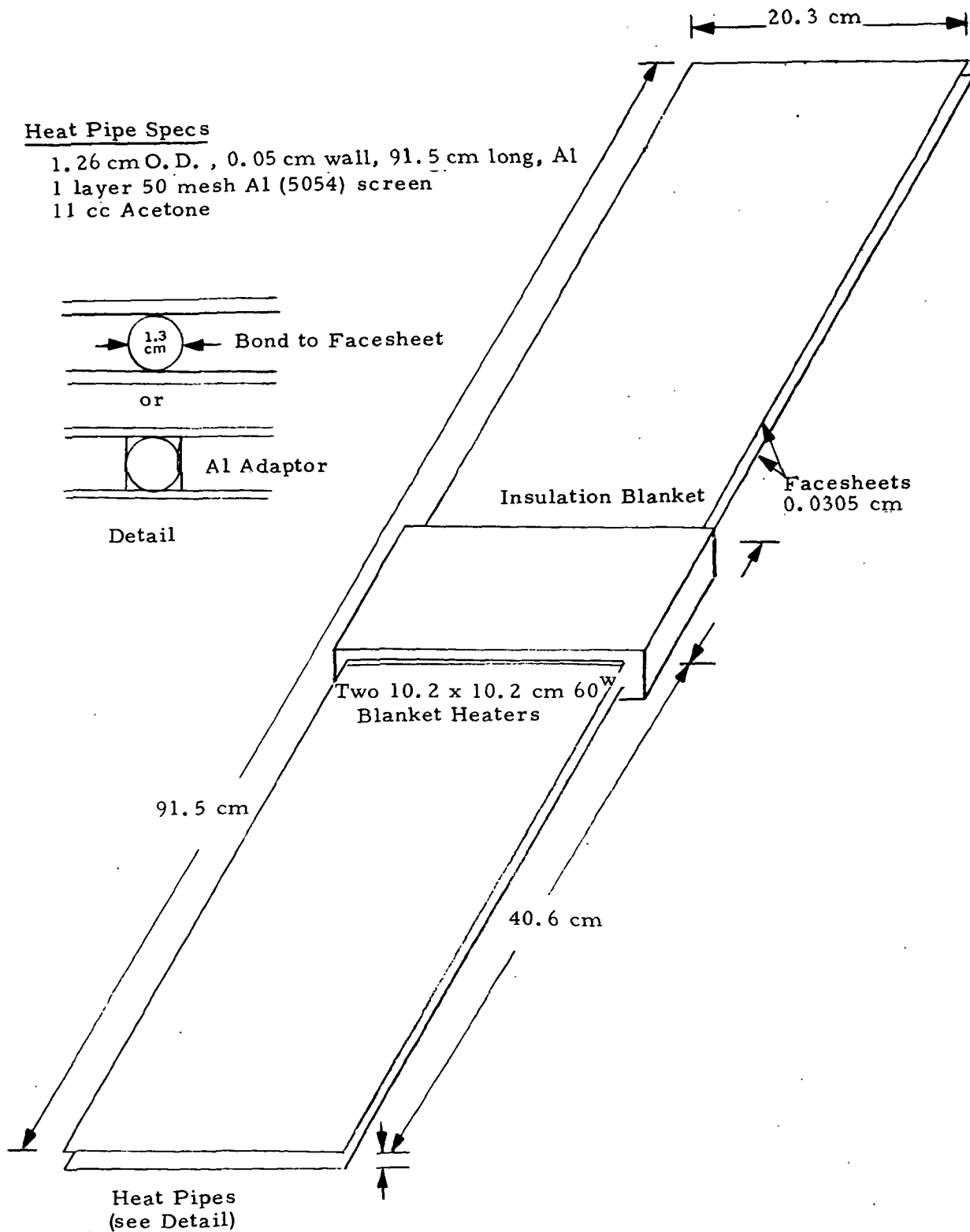
Figure 4.6-7.   Heat Pipe Radiator Assembly
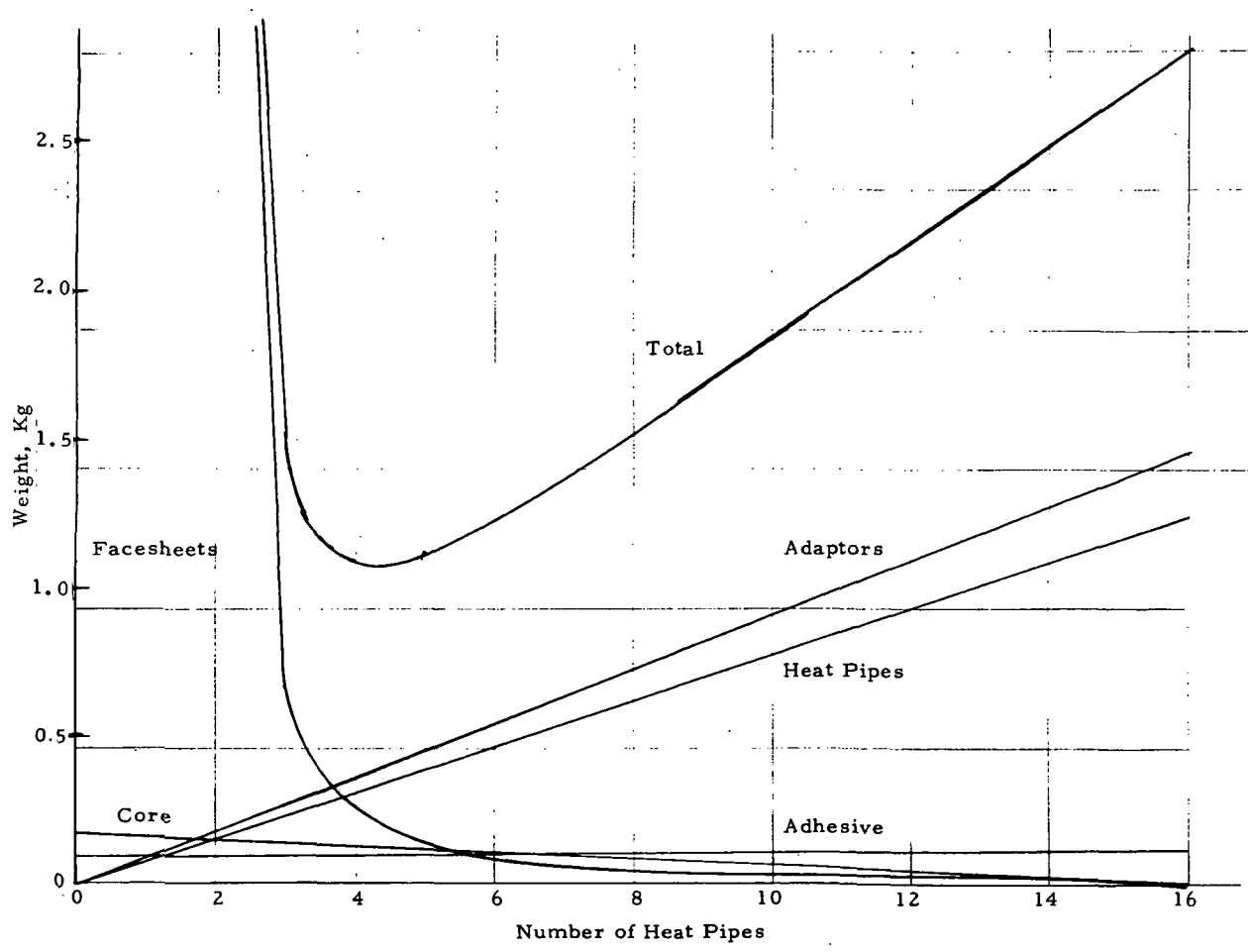
Figure 4.6-8.   Thermal System and Component Weights
vs Number of Heat Pipes
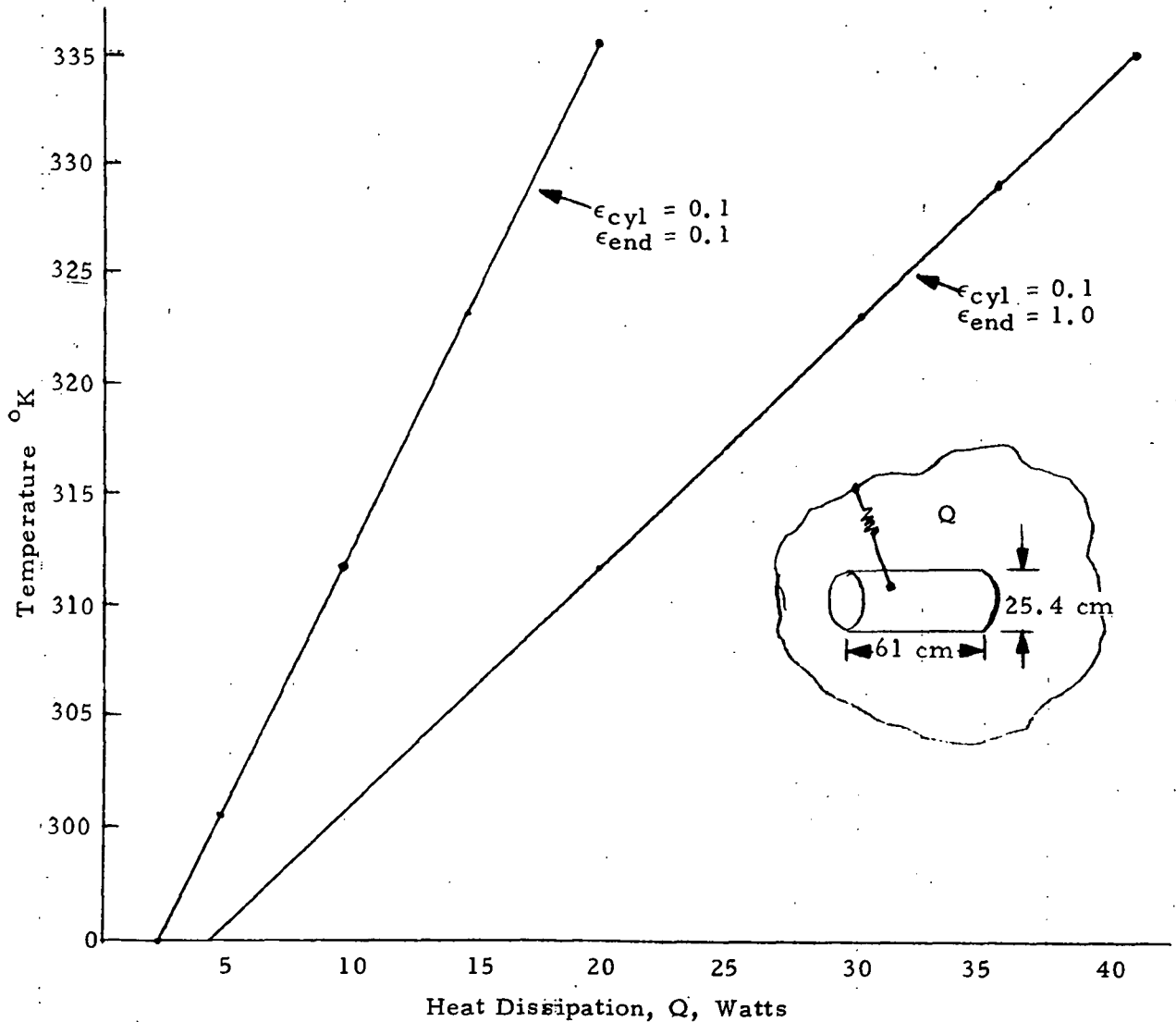
Figure 4. 6-9. Bulk Equilibrium Temperature of LMSR
$$T_{s/c} = 293^{\circ}K$$

Figure 4. 6-10 shows the response of the spacecraft cavity and the liquid metal slipring assembly during the maximum eclipse period of 72 minutes. This preliminary transient analysis indicates that active heating of the LMSR during eclipse need not be considered in sizing the spacecraft battery system.

The LMSR can be kept in the frozen state during initial boost into the transfer orbit by providing on-pad precooling and then depending upon the long effective thermal time constant relative to the several minutes of powered flight. For those configurations which use apogee kick motors, a
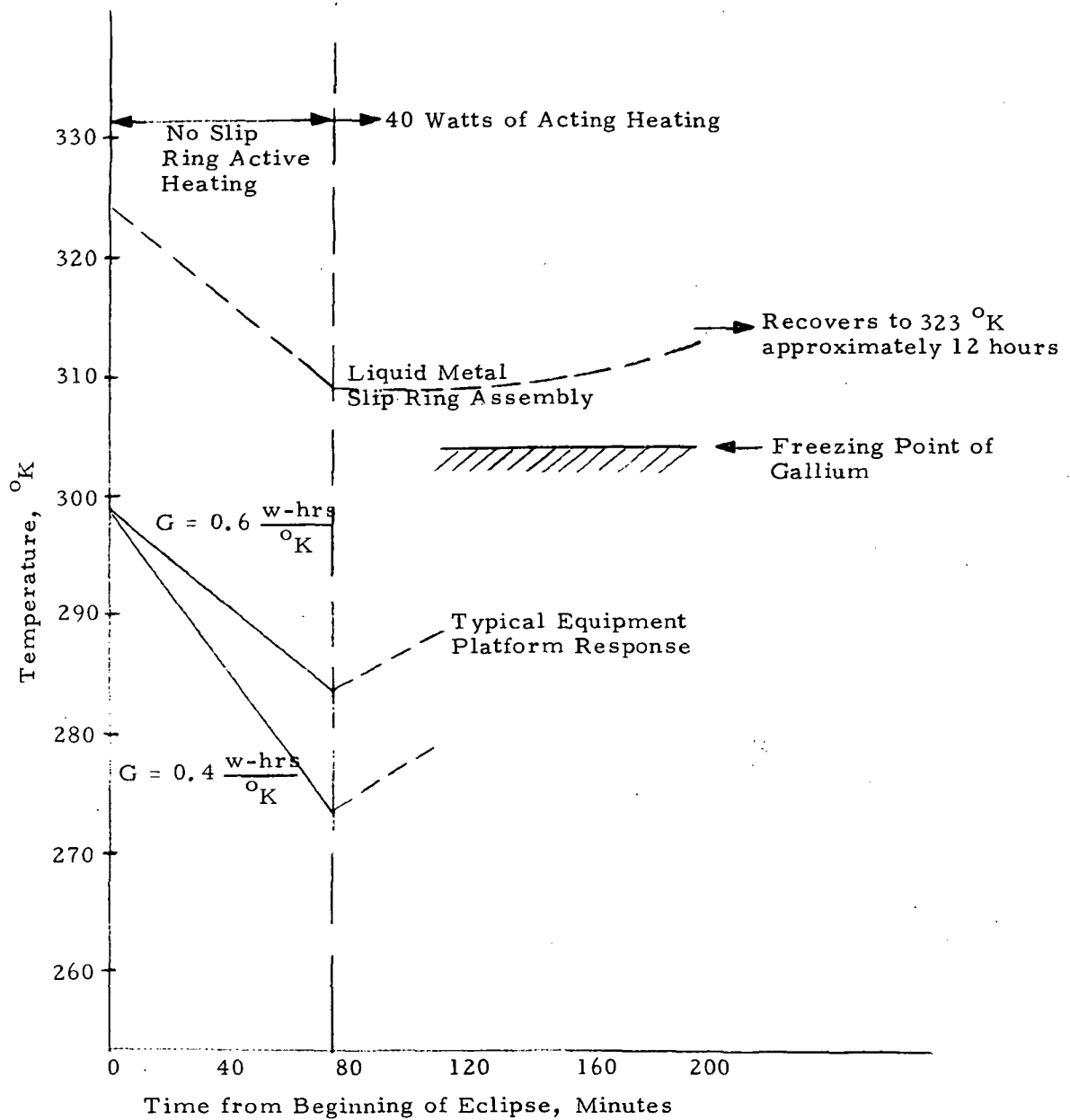
Figure 4.6-10. LMSR Eclipse Temperature Response

bulk spacecraft transfer orbit temperature will be established which is compatible with storage/survival of the communications equipment, but sufficiently low to preclude thawing of the LMSR prior to injection.

Ion Thrusters

The critical thruster components are the permanent magnets mounted along the sides of the thruster cylinder. Above a critical temperature level of approximately 673°K, they lose their permanent magnetism. Aside from thruster redesign, which is not within the scope of this study, the only remaining design parameter is thruster spacing. If the thrusters are tightly clustered, most of the heat generated at the anodes of the central thrusters must be radiated through the screen electrodes, i.e., in the direction of thrust. As the spacing between thrusters is increased, the cylinder sides have an increasing view to space, and thruster temperatures decrease. Practically speaking, there is little freedom to do anything other than cluster the thrusters rather tightly, in either of Configurations A-1 or C-1.

Assuming that heat is generated uniformly along the anode surface, at 400 watts per thruster, and that the electrode screens are 50 percent porous, temperatures of the external cylinders (which are also approximately the temperatures of the magnets) were found to be 583°K for a tight cluster. It is interesting to note that, despite the tight clustering, the radiation path from the sides of the interior thrusters is as effective as the path through the electrode screen.

Also examined, in a rather simplified fashion, were the effects of non-uniform anode heat generation on external cylinder temperature. It was assumed that all the heat was generated in one half of the anode area at the screen end. The resultant local cylinder temperature increase is approximately 50°K, from 583°K to 633°K, and is still below the allowable maximum of 673°K.

4.6.4 Integrated Spacecraft Thermal Designs

Configuration A-1 Design Description

Figure 4.6-11 describes the thermal design features of the A-1 configuration. All of the communications related equipment, which represents 840 watts of internal dissipation, is mounted to the north facing deck, and the dissipation is distributed by a radial array of heat pipes of similar design to those previously described. The power temperature performance of this radiator is shown in Figure 4.6-12. It is evident that supplemental heating is required to maintain acceptable temperatures as the tubes are backed-off from saturated operation. As previously discussed, more than sufficient power becomes available for this purpose as the RF output is decreased.

The transfer orbit, however, presents a separate problem since as much prime power as possible is to be used to operate the ion propulsion system. At least 200 watts of array power must be allocated to active heating of the top deck during this period, since there is no communications system dissipation available.

High Temperature Collector

High Temperature Multilayer Insulation
(Molybdenum or Steel Foil)

- Radiator for Low Temperature
  Portion of the Transponder
  (Second Surface Silvered Quartz)

- Low Temperature Insulation
  (2 layers Aluminized Mylar)

- East-West Radiators (Second
  Surface Teflon) for Dissipation
  of Spacecraft Housekeeping
  Power

- High Temperature Insulation
  (Molybdenum or Steel Foil)

- ~ 2 kw Radiated Aft through
  Thruster Openings during
  Orbit Raising

Figure 4.6-11.   A-1 Thermal Configuration
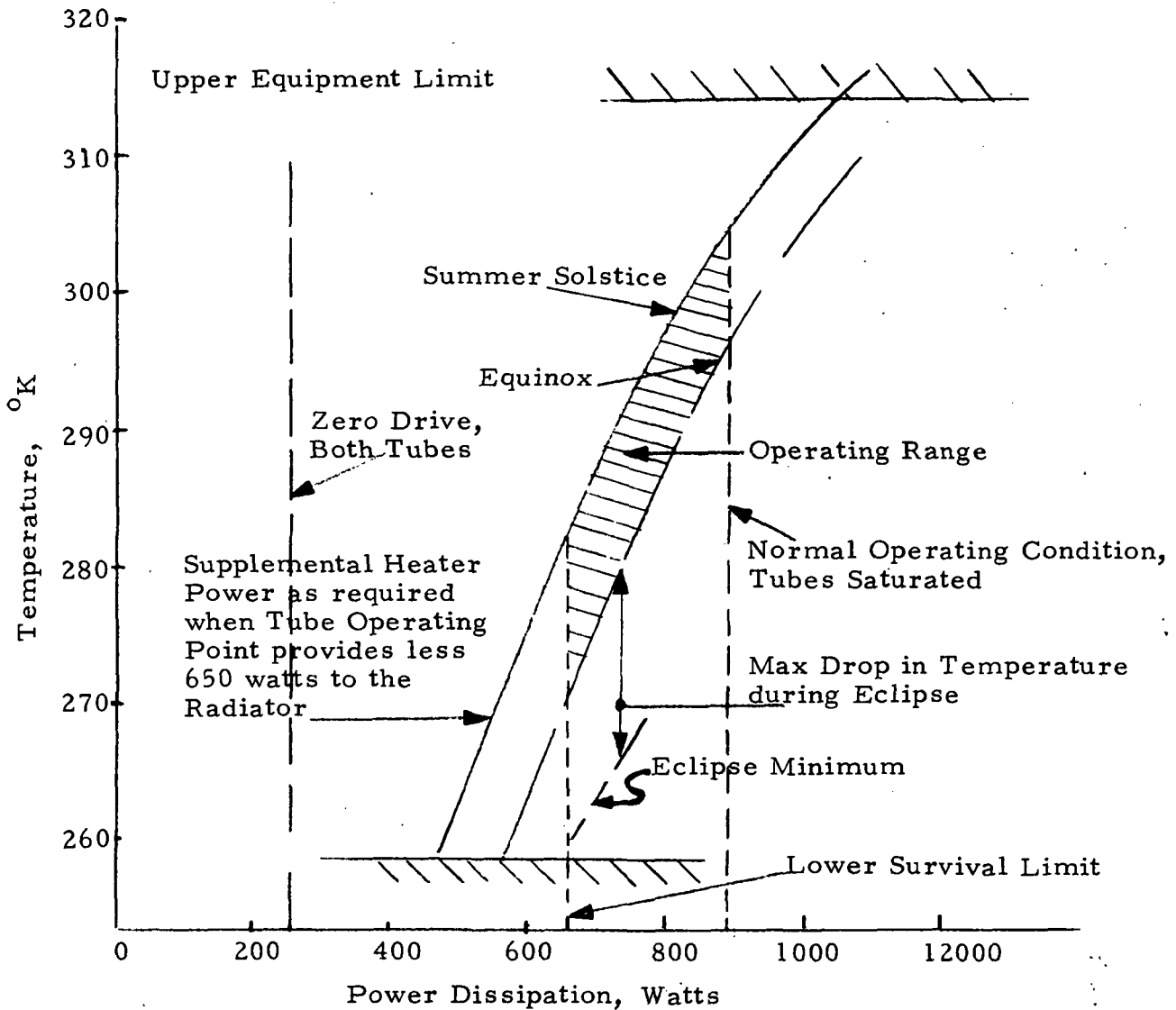
Figure 4. 6-12. Configuration A-1 North Radiator Performance

The cylindrical walls of the communications platform are insulated to minimize equipment temperature oscillations over the daily sun cycle. This insulation system consists of multilayered aluminized mylar with performance characteristics as shown in Figure 4. 6-13. An effective emittance of 0. 02 is sufficient to keep transverse temperature differences to $10^{\circ}K$ or less, and can be achieved with a 20 to 30 layer insulation blanket.

The sun-oriented spacecraft body contains the spacecraft housekeeping equipment, and utilizes the face directed perpendicular to the sun line as equipment radiator area. The balance of the area is insulated in a manner similar to that of the earth pointing portion of the spacecraft.

EXPERIMENTAL DATA

PER SHEET THICKNESS
0.000635 CM

DENSITY
100 SHEETS/INCH

TEMP RANGE
300°K TO -27°K FOR
ALL DATA GIVEN

□ 91.5 CM DIA SPHERE MINIMAL PENETRATIONS (SURVEYOR)
☆ 152 CM DIA X 152 CM LONG, INCLUDING LARGE NUMBER OF
  PENETRATIONS. (APPLICATIONS TECH SATELLITE)
△ 91.5 X 122 CM FLAT SURFACE, LARGE NUMBER OF PENETRATIONS
◉ 91.5 X 122 CM FLAT SURFACE, NEGLIGIBLE PENETRATIONS
○ 45.7 X 45.7 CM BOX, LARGE NUMBER OF PENETRATIONS
  (SURVEYOR)
▽ 45.7 X 3.05 CM ELLIPTICAL TANK, NEGLIGIBLE PENETRATIONS
  (SURVEYORS)
◇ 10 LAYERS, DOUBLE ALUMINIZED, DACRON SEPARATOR,
  (INTELSAT IV)
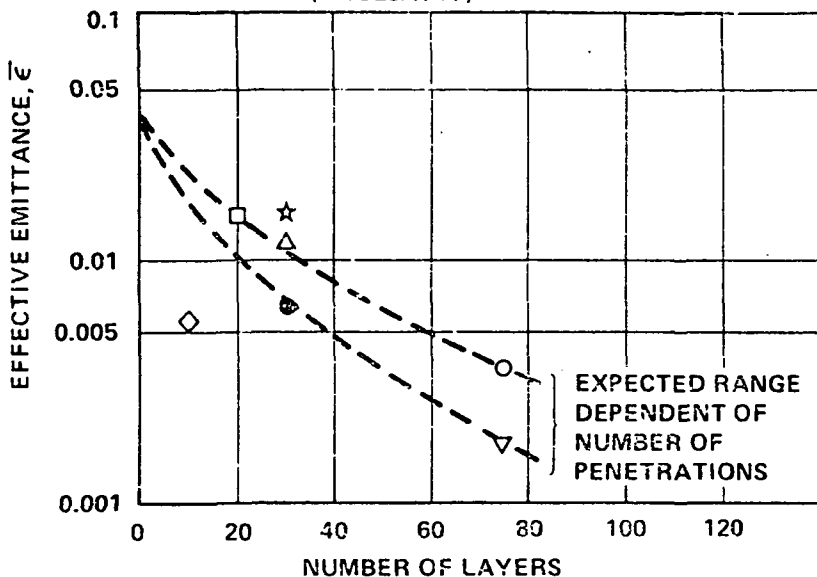
Figure 4. 6-13. Performance of Multi-Layer Insulation

The electric propulsion module is thermally separated from the spacecraft body by a high-temperature, multilayered insulation system. Figure 4. 6-14 describes the kind of performance which has been achieved using a composite metal foil/refrasil blanket. This particular blanket has been used for protecting spacecraft structures from rocket motor exhaust plume heating and weights approximately 733 kg/m^2 per layer.

A five layer blanket is sufficient to limit the heat flow into the space-craft to approximately 100 watts during ion engine operation during orbit raising. This heat flow, together with the 100 watts of spacecraft equipment power dissipation, is sufficient to maintain acceptable temperatures in the sun oriented spacecraft body.

The internal structural elements would be painted black to maximize internal radiation coupling. The liquid metal slipring assembly is provided with a low emittance finish and 40 watts of active heating to preclude freezing
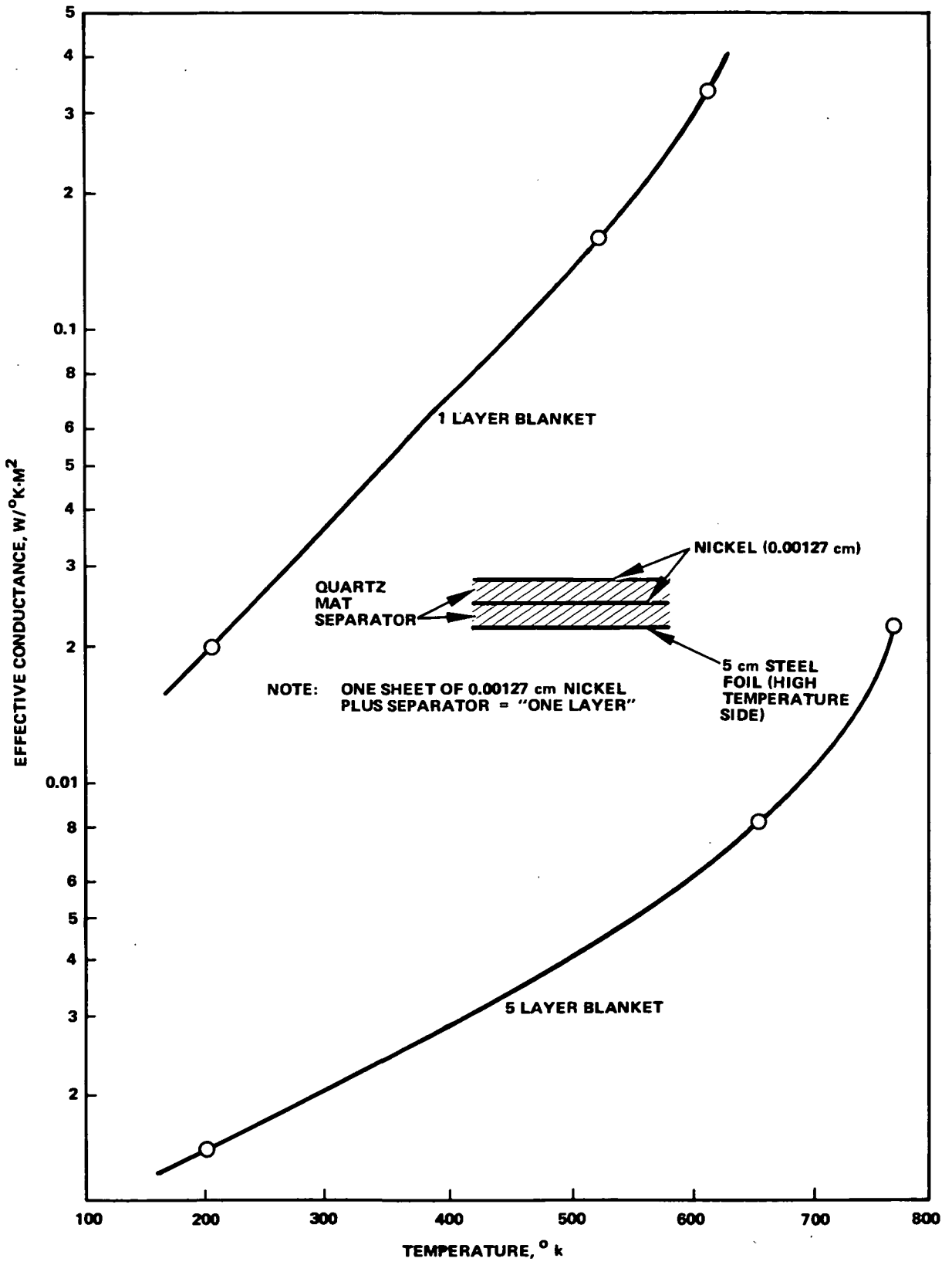
Figure 4.6-14. High Temperature Insulation Measured Performance

of the Gallium. Table 4.6-5 summarizes the thermal finishes which have been identified in the design. All are space-qualified finishes used in previous spacecraft designs at Hughes.

Configuration B-1

Figure 4.6-15 shows the passive thermal control arrangement for Configuration B-1. The predominantly non-sun facing north and south surfaces are used as the equipment radiators. Heat pipes are incorporated into the radiator/mounting structure to minimize lateral temperature gradients, and to allow the total thermal mass of the system to act together during eclipse. All other surfaces are insulated to prevent excessive internal temperature gradients as the body rotates with respect to the sun. Insulation and radiator surface treatments are similar to those employed in Configuration A-1. The TWT and Klystron collectors are placed on the insulated faces such that they possess a relatively unobstructed field of view. High temperature insulation (.e.g, nickel foil) is provided locally to prevent overheating of the surrounding structure.

TABLE 4.6-5. THERMAL CONTROL

Radiation Properties			Measured Radiation Properties*				Usage	Reason
Material/Finish			Solar Absorptance			Infrared Emittance		
	α_{BOL}	$\Delta\alpha_{UV}$	$\Delta\alpha_{p^++e^-}$	α_{EOL}**	ϵ_N at $294^\circ K$	ϵ_N at High Temperature		
Mirrors Quartz/Ag	0.06	0.01		0.07 (estimated)	0.84	DNA***	Primary north/south equipment radiators.	Maximum utilization of available radiator area
2 mil Teflon (FEP)/VDA 2 mil aluminum foil	0.16	0.03 (7500 SEH)	0.05 to 0.12	~0.30	0.68	DNA	East/west housekeeping equipment radiators.	Adequate to meet needs and is less complex than glass.
Kapton/VDA a) (1/2 mil) b) (1 mil)	0.34 0.36	0.01 to 0.03 (1000 SEH)		<0.40 (estimated) <0.44 (estimated)	0.56 0.65	DNA DNA	Outer layer of insulation blankets.	Space stability with adequate radiative properties.
Sperey VHT Black	0.85	Neg.	Neg.	0.85	ϵ_H 0.59 to 0.65	$\epsilon_H \geq 0.80$ at $593^\circ K$	High temperature insulation blankets for ion engines and tube collector integration.	Special material and processes needed for high temperature survival.
Gold (Hanovia type 6518 over black oxide)	DNA	DNA	DNA	DNA	0.04	≤ 0.18 (estimated)		
Nickel foil	DNA	DNA	DNA	DNA	0.04	0.1 at $427^\circ K$		
Black paint CTL 15	DNA	DNA	DNA	DNA	0.91	DNA	Internal spacecraft structure.	Maximize internal radiation coupling to minimize gradients.

*Radiation properties for room temperature conditions are measured values obtained on Hughes Gier Dunkle heated Hohlraum and integrating sphere. High temperature ϵ values obtained from TRW high temperature equipment.

**α_{EOL} defined as $\alpha_{BOL} + \Delta\alpha_{UV} + \Delta\alpha_{p^++e^-}$ where EOL = 10 years. (BOL) is beginning of life and EOL is end of life.

***DNA Does Not Apply.
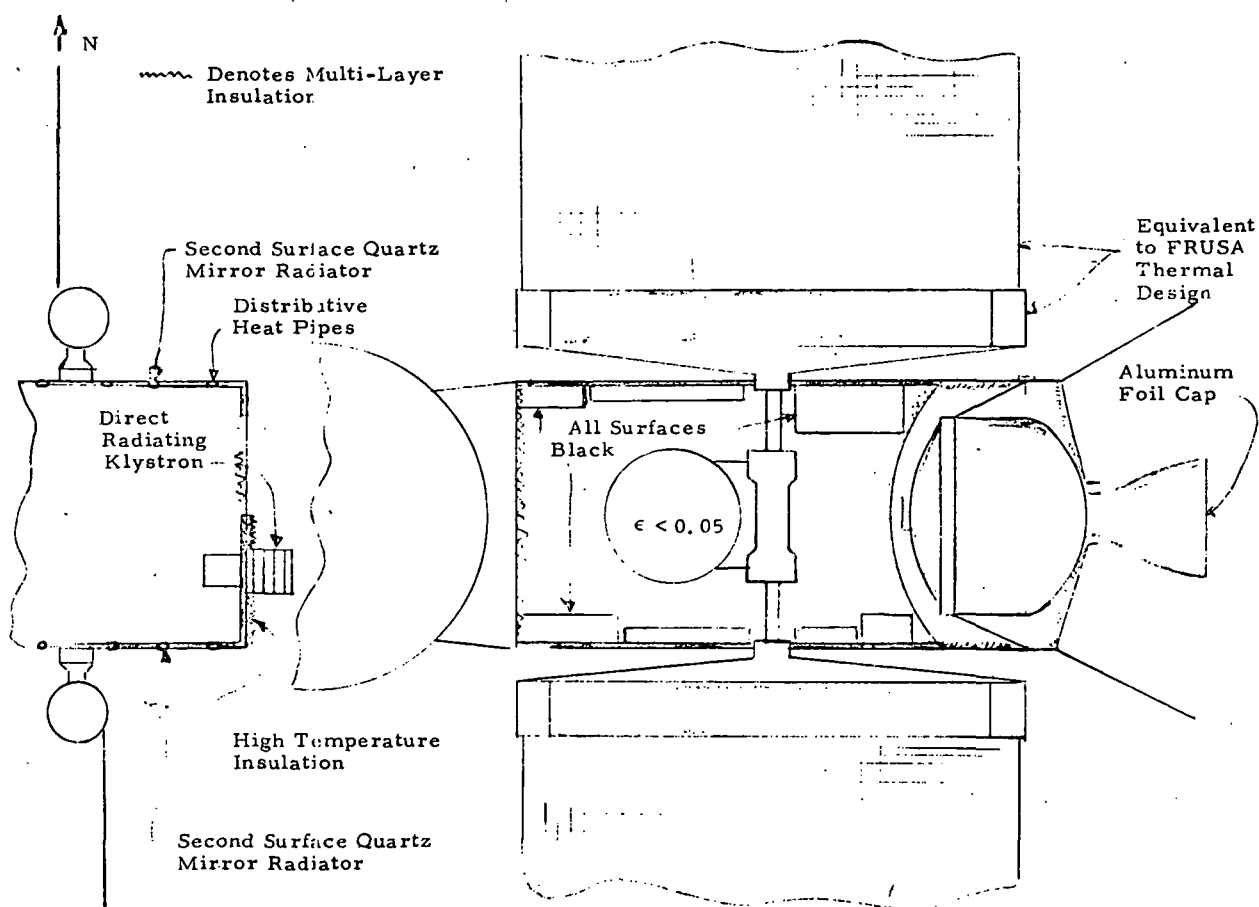
Figure 4.6-15 Configuration B-1 Thermal Design Arrangement

The power dissipation distribution within the body of the spacecraft is itemized in Table 4.6-6. The breakdown shown provides a reasonable power balance between the north and south radiators. Analysis of the radiator capability, including the solar panel effects, yields an average dissipation capability of 134.5 watts/m^2 at 300°K and summer solstice. The radiator areas required are 6.14 m^2 and 51.2 m^2, for the north and south radiators, respectively. The additional area in excess of the 41.8 m^2 north and south faces can be provided within the fairing constraints. This, or either of the other methods shown in Figure 4.6-16 will provide adequate performance with the third method being preferred on the basis of design simplicity.

Figure 4.6-17 shows that for the power-temperature performance achieved, the passive north-south radiator concept is sufficient to provide reasonable flexibility in the operation of the communications equipment. As noted, the RF output can be reduced to zero without causing internal equipment temperatures to become excessively low. This is due to the stabilizing effect of the external heat load from the solar panels which is not present in the A configuration.

TABLE 4.6-6. B-1 SPACECRAFT POWER DISSIPATION SUMMARY

Equipment	Power Dissipation, Watts
Klystron	
Tube Cavity	100
RF Losses in output (switch, filter, line)	400
Power Conditioning	330
Sub Total =	830 North Radiator
TWT	
Tube Cavity	50
RF Losses	190
Power Conditioning	215
Repeater	100
Attitude Control	75
TT&C	20
Housekeeping Power Distr.	45
Sub Total =	695 South Radiator

Extend Solar Panel Drum Outboard

0.61 cm
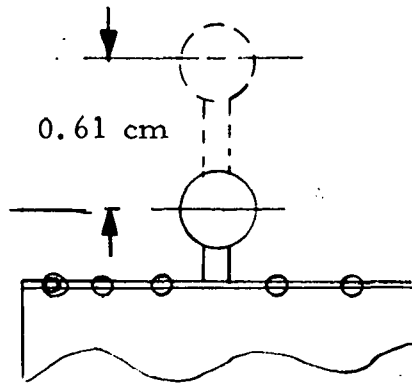
Provide Fixed Extensions
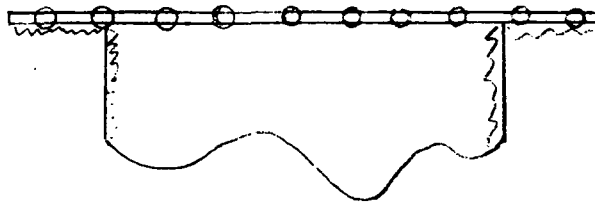
Extend Radiator to Sun Sides

Baseline
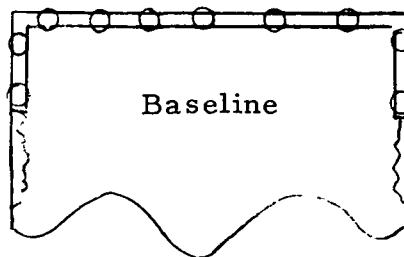
Figure 4.6-16. Radiator Design Options
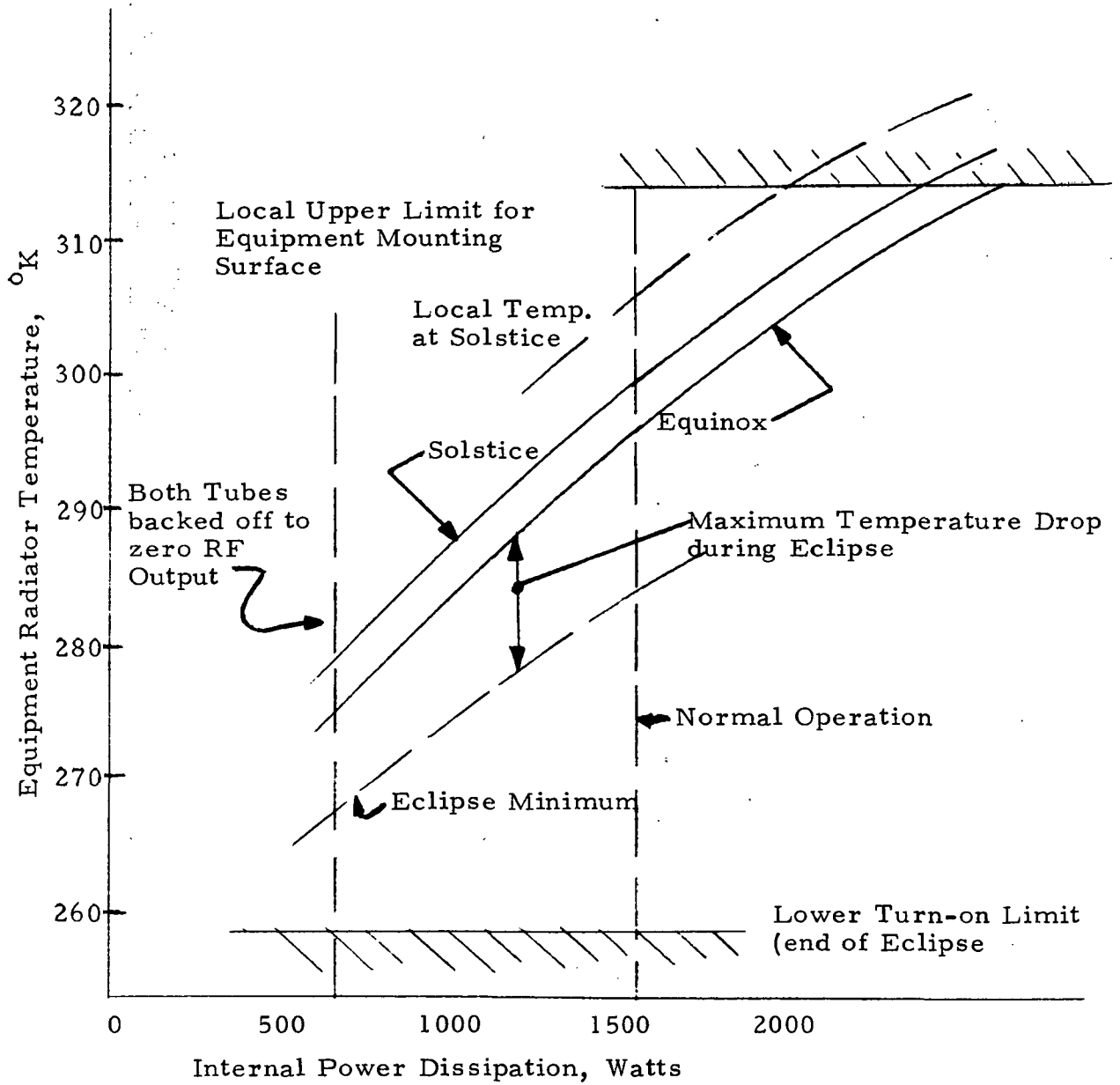
Figure 4.6-17. Configuration B-1 Radiator Performance

Examination of the heat balance in the spinning mode during the transfer orbit yields equipment temperatures below 200°K if the radiator capability is not reduced. A simple removable radiator shielding system can be used to maintain acceptable survival temperatures during the transfer orbit. The external finish of these covers would be adjusted to provide an acceptable equilibrium survival temperature for the communications equipment, and yet remain sufficiently below 300°K to insure that the Gallium in the LMSR remains frozen at least until completion of apogee motor burn.

Configuration B-5

Configuration B-5 is equivalent in all thermal respects to Configuration B-1 except that the use of a high voltage array eliminates the power conditioning losses from the internal spacecraft heat dissipation requirement. The reduced radiator requirement makes this configuration a somewhat simpler design than B-1. The performance over the operational range of the communications system remains essentially equivalent to B-1.

Configuration C-1

Configuration C is equivalent in overall thermal concept to Configuration A except that dimensions and internal power dissipations are significantly increased. The solar oriented portion of the body has more than sufficient available radiator area facing along the solar panel axis to dissipate the housekeeping power. The communications equipment dissipations must all be handled by the north facing surface of the earth pointed communications platform. These loads and the required radiator area are as follows:

Tube Cavities = 200

Power Conditioning* = 150

RF Losses = 790

Repeater Electronics = 100

$$\text{Required radiator area} = \frac{1240}{215 \text{ w/m}^2 \text{ (at solstice)}} = 5.76 \text{ m}^2$$

The necessary radiator area is provided by extending the north face beyond the diameter of the main body. The required area of 5.76 m² requires a significant overhang, but it is within the allowable shroud clearance. Again, as in configuration A-1, distributive heat pipes would be used on the platform to allow effective use of the available radiator area.

---

*The one klystron which is operated during eclipse is always operated with conventional power conditioning.

4.7 TELEMETRY, TRACKING, AND COMMAND (TT&C) SUBSYSTEM

4.7.1 Overall Requirements

The major requirements for the ATS/AMS TT&C subsystem are as follows:

- Monitor experiment and housekeeping functions and transmit the data to the ground control station.

- Enable ground tracking and determination of the spacecraft orbit.

- Receive, store, and implement ground generated commands for control of spacecraft equipment.

- Provide timing information for synchronization of spacecraft functions.

The TT&C subsystem has been configured to meet the requirements, with the same basic design used for all of the spacecraft configurations. The design is based on previous spacecraft experience and uses existing hardware for the most part. Since the ATS/AMS is experimental in nature, the need for a large and flexible telemetry and command capacity is envisioned. The subsystem must be compatible with the existing NASA Satellite Tracking and Data Acquisition Network (STADAN), which is to be used for receiving data and sending commands during the launch and orbit raising phase as well as for on-orbit operations.

Each of the ATS/AMS subsystems impose requirements on the TT&C subsystem, as summarized in Table 4.7-1. The communication subsystem will require monitoring of operational status of the various units, including gains, power levels, etc. The attitude control and stationkeeping subsystem requires monitoring of sensor status as well as processing of the data from these sensors for onboard and/or ground determination of spacecraft attitude. A moderate amount of data will be generated in the electrical power subsystem. This includes monitoring of currents, voltages, and temperatures. The roll-out solar panels will require monitoring of the position orientation mechanism.

Preliminary command requirements of the various subsystems are also listed in Table 4.7-1. The communications subsystem will require commands for equipment on/off control, gain control, and bandwidth changes. The attitude control and stationkeeping subsystem will require commands for control of the sensor status and for updating the orbit-raising thrust profile. The electrical power subsystem requires discrete commands for solar panel deployment, control of battery charge, solar panel array switching, etc.

TABLE 4.7-1. ATS/AMS T&C REQUIREMENTS

Subsystem	Command		Telemetry	
	Realtime	Stored	Analog	Digital
Communications/Antenna	20		20	20
ACS	15	600 10-bit words	15	15
Electrical Propulsion	20		10	20
Electrical Power	20		15	20
Thermal	5		10	5
Miscellaneous	5		5	5
Total	85	600 10-bit words	75	85

4.7.2 Subsystem Description

The block diagram for the TT&C subsystem is shown in Figure 4.7-1. It consists of two central encoders (redundant) with eight remote multiplexers, two 5 watt VHF telemetry transmitters, connected by diplexers to a dual hybrid balun, an eight element (whip) T&C VHF antenna, two VHF command receivers, two central demodulator/decoders, a command processor, a spacecraft clock, and a squib driver assembly. This subsystem provides all the data handling and control functions currently envisioned for the ATS/AMS spacecraft, and is compatible with the STADAN.

The eight remote multiplexers monitor the telemetry inputs to the subsystem. Each remote multiplexer can be connector programmed to accept combinations of data varying from all analog to all digital; this flexibility permits changing the telemetry format almost to the time of spacecraft launch.

The remote multiplexer channels are sequentially interrogated by means of a channel address code from the central encoder. Interrogation timing in the remote multiplexer is derived from the spacecraft clock. Data appearing at the selected channel (or channels in the case of digital data) is transferred to the central encoder. Analog data is converted into 8-bit words and biphase modulated prior to being shifted to the telemetry transmitter. When digital data is received by the central encoder, the A/D conversion process is bypassed. The capacity of the subsystem is 128 analog and 128 digital signals, which is adequate for ATS/AMS needs.
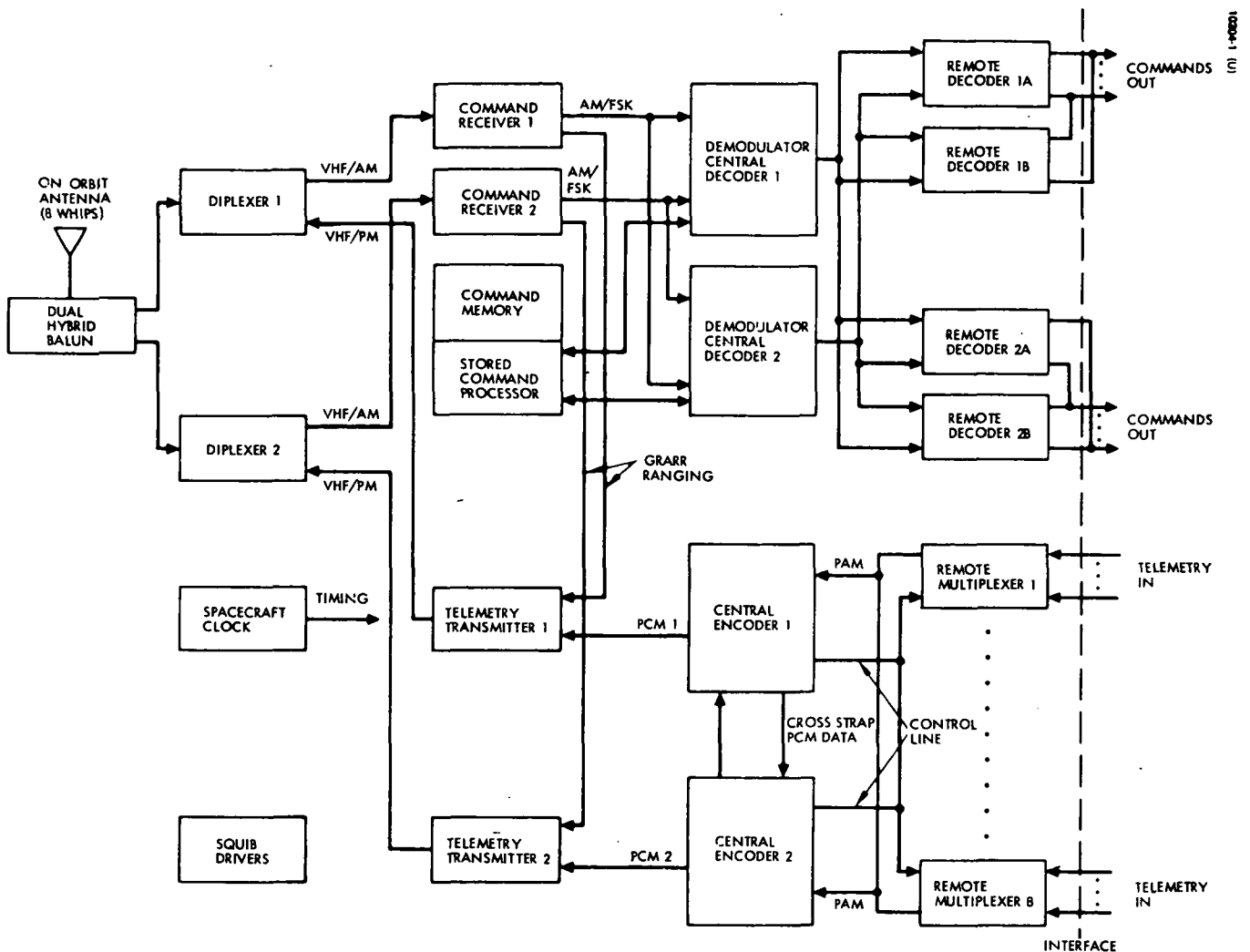
Figure 4.7-1. T&C Block Diagram

By ground command, the data output from the redundant central encoder can be gated to either telemetry transmitter, e.g., central encoder 1 can be commanded to drive telemetry transmitter 2. The pulse code modulation (PCM) data stream from each central encoder (500 bps) is phase modulated on a VHF carrier by the telemetry transmitter. VHF isolators provide isolation between the two transmitters, thus preventing the generation of beat notes that could jam the command receivers. The output of the isolator drives the diplexer, where the telemetry transmitter and command receiver are coupled, through the dual hybrid balun, to the common antenna line. The antenna provides near omnidirectional coverage during all phases of spacecraft operations.

Earth generated command signals received by the antenna are split into redundant paths in the hybrid. The VHF carrier signal passes through the diplexer to the command receiver where the amplitude modulation/ frequency shift keying (AM/FSK) command data is detected. These data

4.7-3

signals from the receiver drive both demodulator/central decoder units. Circuits within the demodulators will cause them to lock to whichever receiver is providing a valid output signal, providing redundancy in the event of a receiver failure.

The demodulator section accepts the AM/FSK data and detects the resulting information. The signal is demodulated into one, zero and clock information, at a 512 bps data rate. This data is shifted into the central decoder section where the spacecraft address is decoded. If the decoded address matches that for a particular central decoder, the remainder of the data message is processed. A parity check is performed on the command message. If the check is not valid, the command is rejected. If the command is valid, the central decoder decodes the address of the selected remote decoder and serially transfers the remainder of the command to the address unit for exeuction. Each remote decoder of the two redundant pairs is individually addressable, and provides capability for 64 discrete and 4 magnitude commands.

The remote decoder identifies the incoming data as defining a discrete command or one of four magnitude commands. For a magnitude command, the 8-bit magnitude word, together with a parity bit, is transferred to the selected user. A discrete command word is stored by the remote decoder. Upon completion of a parity check of the stored word, it is decoded into one of 64 discrete commands and a pulse provided on the selected command line.

The modular remote approach utilized in this subsystem provides flexibility to accommodate changing data handling requirements. Increased telemetry channels can be implemented by simply adding five wires to the spacecraft harness and changing a programming plug. Conversely, should subsequent circumstances eliminate the need for data points, unused units can be deleted, thereby eliminating the burden of carrying excess telemetry capability.

Each of the two telemetry transmitters provide 5 watts of RF power at 136 MHz. One of the spacecraft transmitters will be on continuously, permitting tracking and data acquisition whenever the spacecraft is in view of the ground support network during the orbit raising period. Sufficient residual carrier power exists in the RF signal to permit use of the GSFC-STADAN mini-track system for orbit determination simultaneously with data acquisition.

The two command receivers operate at 148 MHz. Both receivers will be operated continuously. Any pair consisting of one of the VHF transmitters and one of the receivers functions as a GRARR transponder to enable accurate ranging information to be obtained so as to determine the final orbit.

The command memory/stored command processor provides the capability to store a programmed thrust vectoring profile for the ion engines during the orbit raising phase. The demodulator/central decoder recognizes a special "memory load" address which transfers data to be stored via the

stored command processor into the command memory. This memory has the capability for 1024 stored, time-tagged (time initiated) commands. When coincidence occurs between the stored command time tag and the spacecraft clock time code, the stored commands are processed through the demodulator/central decoder and the remote decoders in a manner similar to a ground-generated command. The memory can be loaded via the STADAN in less than three minutes. In addition, the contents can be telemetered via the VHF transmitter for ground verification in less than three minutes. This stored command capability should provide for ATS/AMS operation for more than a day during the orbit raising period.

The spacecraft clock provides time references to execute time tagged stored commands and can be used to provide time references to experiments, if required.

The squib drivers fire pyrotechnic devices required for reliable unlocking of mechanical devices that deploy the solar panel, unlock the despin bearing assembly, etc. As a critical failure criteria, all squib drivers require a two-command sequence input before a command is executed.

Table 4.7-2 indicates the weight and power requirements of constituent components for the TT&C subsystem. Table 4.7-3 indicates the design similarity to past programs. No new conceptual developments are required since virtually all components of the subsystem are variants of existing designs. Key features of the command subsystem are listed in Table 4.7-4.

TABLE 4.7-2.   SUMMARY OF TT&C SUBSYSTEM
PHYSICAL CHARACTERISTICS

Unit	Size	Unit Weight, kilograms	Number Required (Normally ON)	Power per Spacecraft, Watts
VHF Antenna				
Multiple Whip (including balun)	53.4 cm	0.68 total		None
VHF RF Equipment				
Transmitter	19 x 14.6 x 3.56 cm	0.40	2 (1)	5.0
Receiver	19.7 x 19 x 3.81 cm	0.50	2 (2)	2.4
Diplexer	15.2 x 10.1 x 2.54 cm	0.186	2	None
Digital Hardware				
Encoder (central)	3160 cm^3	2.45	2 (1)	3.6
Remote Multiplexer	246 cm^3	2.5	8 (1)	2.0
Demodulator/Decoder	3160 cm^3	2.27	2 (2)	6.0
Remote Decoders	458 cm^3	0.272	2 (0)	Negligible
Command Memory	2130 cm^3	2.72	1	0.2
Command Processor	1475 cm^3	1.36	1	0.4
Spacecraft Clock	1070 cm^3	0.91	1	2.0
Squib Drivers	17.8 x 14.7 x 7.1 cm	1.36	1	Negligible

TABLE 4.7-3. COMPONENT DEVELOPMENT STATUS

Component	Hardware Genealogy
Command Receiver	Similar to ATS command receiver modified to provide GRARR capability.
Demodulator/Central Decoder	Similar to OSO.
Remote Decoder	Identical to MOS-LSI remote unit used on OSO.
Stored Command Processor	Similar to OSO.
Command Memory	Existing unit from memory manufacturers.
Multiple Squib Drivers (redundant pair/unit)	Circuits similar to those used on Intelsat IV.
Spacecraft Clock	Similar to OSO spacecraft clock.
PCM Encoder	Similar to OSO central encoder design.
Remote Multiplexer	Similar to OSO.
VHF Transmitter	ATS transmitter modified to provide GRARR capability.
Diplexer	Identical to ATS diplexer.
VHF Antenna	Identical to ATS antenna.

TABLE 4.7-4. SUMMARY OF KEY CHARACTERISTICS

FEATURES	REMARKS
TELEMETRY	
Distributed Remote Multiplexers	Accept both analog and digital data.
Modular Growth Capability	Changes in telemetry requirements accommodated by addition or deletion of remote multiplexers.
Efficient Use of Spacecraft Volume	Small remote components will fit into recesses near telemetry source which normally cannot be used.
Low Harness Weight and Complexity	Provides ease of harness management.
Signal Conditioning	Transducer constant current source provided when desired. Current source applied as stimulus to passive transducer while transducer is being sampled, thus allowing resultant voltage to be measured.
COMMAND	
Distributed Remote Decoders	Provide both pulse and serial digital commands.
Modular Growth Capability	Command subsystem capacity may be increased by the addition of remote decoder components without affecting design of any component.
High Reliability	Redundant components cross-strapped such that failure in one unit will not affect operation of remaining units.
Efficient Use of Spacecraft Volume	Small remote components will fit into recesses near command user which normally cannot be used.
Low Harness Weight and Complexity	Provides ease of harness management.
Nonvolatile Memory	Not affected by power dropouts.
Failsafe Checks	Command parity checks, plus redundant address check circuits.
Greater than one day of autonomous spacecraft operation during orbit raising	Stored commands are time initiated.
Power supply fault protection	Suppresses false command execution due to undervoltage/overvoltage conditions.

5. PROGRAM PLANNING

5.1 INTRODUCTION

During the latter part of this study, an estimate of resource requirements was requested from each of the responsible engineering activities. It was from these inputs that the Master Phasing Schedule was formulated. The Rough Order of Magnitude (ROM) cost data were prepared and a preliminary analysis of facility requirements was also performed with inputs from these activities.

The Master Phasing Schedule is realistic if it is assumed that approximately one year of further system definition and advanced development on critical subsystem technology, such as the high voltage tubes and liquid metal sliprings, precedes the starting date of the system hardware program. This topic is discussed in more detail in Section 5.2. Discussed in Section 5.3 are the facilities requirements. The facility requirements for the handling of frozen liquid metal sliprings, and the facility requirement to test a sealed high power transmitter tube during spacecraft test, offers some unusual challenges. Section 5.4 discusses the program cost and the method used to derive these costs.

5.2 MASTER PHASING SCHEDULE

The Master Phasing schedule has been prepared by taking the individual engineering subsystem plans and systems plans and time phasing the activities. A 30-month schedule has been calculated as a reasonable time span to accomplish the ATS/AMS Hardware Program. However, it must be recognized that advanced development work would have to commence much earlier (probably a year earlier) than the program go-ahead in at least the following areas:

1)   High power transmitting tube

2)   Liquid metal slipring

Beneficial advanced work should also be started in the following areas:

1) Ion engines

2) Electrical power

3) Antenna

If the lens antenna design is adopted, advanced development work should also commence about a year prior to the system contract go-ahead.

Apogee motor development on an optimized design should also be started somewhat prior to the 30-month spacecraft program.

On the Master Phasing Schedule, Figure 5-1, are depicted the completion times for the engineering, qualification and flight models. The allocated time spans and the choice of types of models is based upon Hughes' satellite experience. It is this experience that determines that the qualification model could be refurbished as a backup to the flight vehicle. It is this experience that directs that the engineering models to be complete in 11 months, the prototypes in 16 months, and the qualification program to be completed in 20 months.

The Master Phasing Schedule also shows the importance that Hughes places on test programs. The test program is virtually continuous from the tenth month after go-ahead until the completion of flight model acceptance test. Note in the Master Phasing Schedule a gap in the test program from the completion of qualification testing until the start of flight acceptance tests. This time gap is so situated to allow for the incorporation of any engineering changes that might occur as the result of qualification testing.

5.3 FACILITIES

The facility requirements necessary to fabricate and test the subsystems and to assemble and test the ATS/AMS spacecraft offer some unique challenges. Each previous spacecraft series has required major changes and/or modifications to the existing facilities. The most recent change at Hughes was the construction of the high bay spacecraft assembly and test area as a result of the need to handle large spacecraft such as TACSAT and Intelsat IV.

5.3.1 System Facilities

The facility requirements for assembly and tests of the ATS/AMS spacecraft present some unique problems. Spacecraft assembly facility requirements can be met in straightforward fashion and involve techniques

Figure 5-1. ATS/AMS Preliminary Master Phasing Schedule

which have been used on many other earlier programs. However, it is necessary to make special preparations for the following:

1) LMSR to be kept below $300^{\circ}K$ and not rotated.

2) No electrical power to be applied to the ion engines.

3) Solar panels to be locked closed in order to prevent accidental deployment.

Spacecraft testing does, however, present some interesting challenges:

1) When the communication subsystem is operated, the high power transmitting tube must be cooled.

2) The ion engine cannot be operated at the system level.

3) In order to verify at the system level that the LMSR and the electrical power bus can handle the high voltage, the LMSR shall be unfrozen and operated in a vacuum environment.

5.3.2 Subsystem Facilities

ATS/AMS subsystem facility requirements are also unique in several areas:

Ion Engines - Ion engine development and testing requires the dedication of a vacuum chamber. This has already been accomplished at Hughes. A vacuum chamber in the El Segundo facility has been dedicated to testing of 30-cm class ion engines. The mercury handling problem is not considered serious, as proper handling, loading and storage procedures have been instituted. It is also recognized that the spacecraft will have, after installation of the ion engines, about 63.5 kilograms of mercury onboard. This is not considered a problem, but requires an awareness that proper handling procedures must be employed.

High Power Transmitting Tubes - There are no unique facilities requirements for the manufacture of high power TWT's. The requirement for special test equipment at the correct operating frequencies is satisified in a straightforward manner per prior experience. The facilities considerations regarding operation of the high power transmitting tube after installation on the spacecraft must include supplemental cooling equipment.

Electrical Power - Electrical power will be provided by batteries plus two very long Flexible Rolled-Up Solar Arrays (FRUSA). The solar arrays present a facilities requirement that is unusual, namely, a 30.5 meter long, 1.83 meter wide water table. The water table is used to perform solar panel deployment tests.

Preceding Page Blank

The assembly and testing of the solar panel will be done in 1 kw sections, similar to that shown in Figure 5-2. This is a photograph of a 1.5 kw FRUSA that was manufactured for the Air Force and flown successfully on a technology spacecraft.

Liquid Metal Slip Rings (LMSR) - The technique for the fabrication and assembly of LMSR has progressed to the point that a clear definition can be given for facility requirements. To assemble a liquid gallium slip rings, one needs an oxygen free environment (glove box) and temperature controlled plates. In the assembly process, it is necessary to freeze the gallium ring. This is accomplished by dropping the temperature below $300^{\circ}K$. An assembled LMSR requires a handling container whose temperature can be kept below $300^{\circ}K$.

Antenna - If a standard parabolic antenna is specified on ATS/AMS, the necessary facilities for development and testing are already in existence. If the lens antenna design is specified, consideration must be given to the tooling requirements.

The fabrication tooling requirements and the alignment requirements are the only requirements requiring special consideration.

In summary, it can be stated that the facility requirements for the ATS/AMS program can be met with some specialized subsystem and system facilities and some modification to existing test facilities.

5.4 COST

This subsection presents the estimated cost. Cost estimates were prepared by the engineering activities using the Master Phasing Schedule, Figure 5-1, the Work Breakdown Structure, Figure 5-3, and the Hardware List, Table 5-1. These costs estimates have been prepared, using past experience in the design and manufacture of communication satellites, and knowledge gained during the study phase of ATS/AMS, to arrive at a valid estimate. The major hardware quantities that are included in the cost summaries in Table 5-2 are as follows:

1) One (1) qualification model to be refurbished as a backup flight model

2) One (1) flight vehicle

3) One (1) thermal/structural test model

4) Engineering models and/or breadboards as required for development

5)   Spares in accordance with policy of prior programs of similar
     scope.

The cost totals in Table 5-2 are given for the three baseline con-
figurations A-1, B-1 and B-5.   These costs are in 1971 dollars and would
have to be adjusted upward for the actual time period of such a program.

Figure 5-2. Flexible Rolled-Up Solar Array

NOTE: See Hardware List for Quantities

COMMUNICATION SUBSYSTEM

| PROGRAM MANAGEMENT | SYSTEM ENGINEERING | INTEGRATION AND ASSEMBLY | PRODUCT EFFECTIVENESS | SYSTEM TEST | LAUNCH SUPPORT AND ORBITAL OPERATIONS | SUPPORT EQUIPMENT | REPEATER SUBSYSTEM | TRANSMITTER TUBES -GFE- | ANTENNA SUBSYSTEM | ATTITUDE CONTROL SUBSYSTEM | ELECTRICAL PROPULSION SUBSYSTEM | REACTION CONTROL SUBSYSTEM | APOGEE MOTOR | ELECTRICAL POWER SUBSYSTEM | TELEMETRY AND COMMAND (RF) | DIGITAL ELECTRONICS (T&C) | STRUCTURE SUBSYSTEM | | |

PROGRAM MANAGEMENT:
System Engineering
9. System Engineering
10. Structural and Thermal Test

SYSTEM ENGINEERING:
1. System Analysis
2. Dynamics & loads
3. Stress Analysis
4. Thermal Analysis
5. Mass Properties
6. Orbit Analysis
7. Attitude Control Analysis
8. Communication Anal

INTEGRATION AND ASSEMBLY:
1. Design Integration
2. Assembly & Integration

PRODUCT EFFECTIVENESS:
1. Reliability
2. Quality Assurance
3. Components and Material

SYSTEM TEST:
1. Test Planning
2. System Functional Tests
3. System Qualification tests
4. System Acceptance Tests

LAUNCH SUPPORT AND ORBITAL OPERATIONS:
1. Launch Operations
2. Orbital Operations and Test

SUPPORT EQUIPMENT:
1. Electrical Test Equip
2. Mechanical Test Equip
3. Test Planning

REPEATER SUBSYSTEM:
See Hardware List for Details

TRANSMITTER TUBES -GFE-:
1. 1-kw TWT
2. 2-kw Klystron

ANTENNA SUBSYSTEM:
1. 1.83 Meter Dish

ATTITUDE CONTROL SUBSYSTEM:
1. Control Electronics
2. Earth Sensor
3. Sun Sensor
4. Reaction Wheels
5. Gyro
6. Bearing & Slip Ring Assembly
7. Antenna Earth Pointing Control
8. Solar Panel Control and Attachment

ELECTRICAL PROPULSION SUBSYSTEM:
1. Ion Thrusters 30 CM
2. Ion Thrusters 5 CM
3. Power Conditioning

REACTION CONTROL SUBSYSTEM:
1. Hydrazine System

ELECTRICAL POWER SUBSYSTEM:
1. Solar Cell Blanket
2. Deployment Apparatus
3. Stowage Apparatus
4. Batteries
5. Electronics

TELEMETRY AND COMMAND (RF):
1. Transmitter
2. Receiver
3. Diplexer
4. Whips

DIGITAL ELECTRONICS (T&C):
See Hardware List for Details

STRUCTURE SUBSYSTEM:
1. Structures
2. Adapter
3. Wire Harness

Figure 5-3. ATS/AMS Preliminary Work Breakdown Structure

TABLE 5-1. ATS/AMS HARDWARE LIST

Subsystem	Quantity			Comments
	A-1	B-1	B-5	
Communications				
Repeater				
Antenna Switching Network	1	1	1	Receive
Preamplifier	7	7	7	
Receiver Switching Network	1	1	1	
Receiver	2	2	2	
Reference Generator	1	1	1	
Driver Amplifier	2	2	2	
Xmtr Switching Network	1	1	1	
Antenna Switching Network	1	1	1	Transmit
Transmitter Tubes				
TWT -	1	1	1	1-kw, GFE
Power Conditioner		1		250 VDC Input
Klystron -	1	1	1	2-kw, GFE
Power Conditioner		1		250 VDC Input
Antenna	1	1	1	1.83 meter dish
Attitude Control and Station Keeping				
Rate Integrating Gyro	1	1	1	
Reaction Wheels	1	1	1	
Attitude Control Electronics	1	1	1	
Earth Sensor (with electronics)	1	1	1	Quantic
Sun Sensor (with electronics)	1	1	1	Adcole
Antenna Earth Pointing Control Electronics	1	1	1	
Solar Panel Control Electronics	1	1	1	
Bearing and Slip	2		1	LMSR
Ring Assembly		1		Conventional

Preceding Page Blank

TABLE 5-1. (Continued)

Subsystem	Quantity			Comments
	A-1	B-1	B-5	
Reaction Control System				
Hydrazine Thrusters		8	8	0.0453 kg
Hydrazine Tanks, Lines		1	1	
Electric Propulsion				
30 Centimeter Thruster	3			
Tank, Lines	1			
5 Centimeter Thruster	9			
Tank, Lines	3			
Power Conditioner	6			
Electrical Power				
Solar Panel Assembly	HV 10 kw	LV 8 kw	HV 8 kw	HV Arrays Includes Integral Power Cond.
Batteries	2	2	2	6 Ampere-Hour Cells
Electronics	2	2	2	Battery Controllers, Charging/Discharging Sensor
Telemetry and Command				
RF Equipment				
Transmitter	2	2	2	5 watt
Receiver	2	2	2	GRARR Ranging
Diplexer	2	2	2	ATS
VHF Antenna	1	1	1	ATS (Including Balun)
Digital Hardware				
Central Encoder	2	2	2	
Remote Multiplexer	8	8	8	128 Analog/ 128 Digital
Demodulator/Decoder	2	2	2	
Remote Decoder	2	2	2	128 Discrete/ 8 Magnitude

TABLE 5-1. (Continued)

Subsystem	Quantity			Comments
	A-1	B-1	B-5	
Command Memory	1	1	1	OSO
Command Processor	1	1	1	OSO
Spacecraft Clock	1	1	1	Similar to ATS
Squib Drivers	1	1	1	Similar to IT4
Solenoid Drivers		8	8	
Structure Subsystem				
Structure	1	1	1	
Adapter	1	1	1	
Wire Harness	1	1	1	
Solar Panel Structure	1	1	1	
Booster Assembly				
Main Booster	1			Thor-Delta 2914
		1	1	Atlas-Centaur
Shroud	1			218 cm Thor-Delta
		1	1	IT4
Apogee Motor		1	1	New Motor

TABLE 5-2. ATS/AMS COST COMPARISON
(Dollars in Millions at Sales Price)

Description	A-1	B-1	B-5
Spacecraft Development	57. 5	52. 2	53. 8
Thor Delta (2914) Launch Vehicle	6. 0		
Atlas-Centaur Launch Vehicle		16. 0	16. 0
Total Program Cost	63. 5	68. 2	69. 8
Recurring Cost for each Additional Spacecraft (including L/V)*	20. 4	29. 0	29. 5
Recurring Cost Delta (Relative to A-1)		+8. 6	+9. 1
1971 Dollars			
*Assuming a user procurement of eight operational spacecraft.			

APPENDIX A

STATEMENT OF WORK

EXHIBIT "A" TO Contract NAS 3-14359

EXHIBIT "A"

1.0 SCOPE OF WORK

The Contractor shall provide the personnel, facilities, materials, supplies and other resources necessary to accomplish the effort as set forth below.

2.0 OBJECTIVES

2.1 Mission Objectives

The mission objectives for the satellites to be considered in this study are:

2.1.1 To demonstrate high power communications technology using transmitter output of one kilowatt or more in space in the frequency band of 11.7 - 12.2 GHz. Specific technologies to be demonstrated are high power transmitting devices, a high power solar array as the power source, high voltage power conditioning (15 kilovolt range), efficient methods for rejecting to space waste heat of up to 50% of the solar array power, attitude control and station keeping for extended periods of time, and efficient, reliable methods of transmitting power across rotating joints.

2.1.2 To develop the technology for the controlled illumination of desired areas of the earth, with shaped multibeam transmission, using antennas with major beam dimensions of up to 7°, minor beam dimensions as small as ½°, and having axial ratios less than 3.

Superceded by new Paragraph 2.1.2 shown on Page A-7

2.1.3 To demonstrate the use of the spacecraft technologies of 2.1.1 and 2.1.2 for the development of information networking systems comprised of small user terminals.

2.2 Study Objectives

The major objective of this mission study is to provide sound technical plans for an Application Technology Satellite by examining technical alternatives, comparisons and tradeoffs. Specifically, the study outputs shall include:

2.2.1 Definition of three (3) possible spacecraft approaches and associated prime experiments that satisfy the mission objectives.

2.2.2 Analysis of the possible approaches and determination of the technical and economic merits of each.

2.2.3 Definition of additional experiments which would utilize the technological capabilities of the spacecraft.

2.2.4 Identification of the critical research and development required to meet the mission objectives.

2.2.5 Determination of the hardware and facilities' requirements for manufacturing, testing, and support.

2.2.6 Determination of gross schedules for implementation and gross estimates of the resources required, including facilities, manpower, and finances.

3.0 MISSION CONSTRAINTS

3.1 The projected first launch date shall be 1976.

3.2 The contractor shall consider in his designs the following launch vehicle combinations:

1. Titan III C (operational)

2. SLV3C Centaur

3. TAT (9C)/DELTA (transtage engine)

Apogee kick motors, Burner II, or electric third stage shall be considered for final orbit injection.

3.3 The spacecraft will be placed in a geostationary orbit.

3.4 The spacecraft shall be designed to have a two years minimum lifetime in orbit with all subsystems operating within specifications.

3.5 The microwave amplifiers considered shall be klystrons and traveling wave tubes which have efficiencies of 50% or greater.

3.6 Energy storage will be provided for the necessary housekeeping functions and for operation of the power amplifier cathode heater at 50% nominal power level during periods of solar eclipse.

3.7   The spacecraft shall have sufficient station keeping capability to meet the requirement of +0.2° for both North-South and East-West station keeping for 5 years.

3.8   Attitude control shall be sufficiently accurate to permit antenna beam pointing accuracy of ±0.2° for latitude and longitude at the sub-satellite point and ±0.2° in rotation about the boresight axis for five years.

3.9   The spacecraft shall have a mimimum ΔV of ~~100 ft~~/sec for station repositioning capability.   30.48 m

3.10   The prime power source shall be photovoltaic cell array. Both high voltage and low voltage configurations shall be used.

3.11   The spacecraft configuration shall be compatible with the venting of the microwave amplifier to space vacuum, i.e., open envelope tube operation.

3.12   The spacecraft configuration shall use space vacuum for high voltage insulation whenever possible.

3.13   Angle modulation format shall be used. The output signal level will range from saturated output to 6 dB below saturation.

3.14   The spacecraft shall be capable of repeater-type operation.

3.15   The spacecraft shall incorporate the following experiments:

        3.15.1 <u>Experiments</u>

                1. Generation of microwave power of 1.0 kW in space in the frequency band of 11.7 to 12.2 GHz.

Superceded by new   2. ~~Controlled illumination of desired areas on earth by space-~~
Paragraph 2 under   ~~borne antennas having multibeam, shaped patterns.~~
3.15.1, as shown
on Page A-7   3. Power generation by a highpower (>2 kW) solar array.

                4. Methods of efficiently transferring the power from the solar array to the spacecraft body using a gallium liquid metal slip ring.

                5. Demonstrate efficient heat rejection from the transmitter power amplifier.

                6. Multi-beam transmission to and from small ground terminals.

                7. Power generation from chains of photovoltaic elements, biased to 5 kV, 10 kV, and 15 kV with respect to spacecraft ground. (This experiment is not required for approaches using high voltage solar array's).

3.15 In defining additional experiments (Section 4.4) consideration shall be given among others to the following:

1. Satellite-to-satellite communications.

2. Optical communications between spacecraft and earth and/or station sensing by optical methods.

4.0 TASKS

4.1 Review the literature concerning potential small terminal users and information networking flight experiments, considering user needs, feasibility, benefits, and required spacecraft technology. Based on the review, determine the spacecraft requirements necessary to support both these needs and the mission objectives of Section 2.

4.2 Define 3 spacecraft approaches for accomplishing the mission objectives of Section 2 within the constraints of Section 3.

4.2.1 Determine the technical merits of each approach and the associated programmatic costs.

4.2.2 Define experiment execution and the required instrumentation.

4.2.3 Determine the advantages and disadvantages of the selected approaches from the standpoint of redundancy and complexity of experiment execution.

4.3 Evaluate the technology required to meet the mission objectives and determine the advanced technology requirements. Define the required research and development.

4.4 Define additional experiments that may be conducted utilizing the special capability developed for this mission. Evaluate those experiments listed in 3.16 for compatibility.

4.5 Define the gross schedule for implementation and gross estimate of the resources required, including financial, manpower, and facilities.

4.6 Determine the required manufacturing, testing, end support hardware and facilities.

4.7 Perform preliminary designs of the spacecraft and spacecraft subsystems determined in 4.2.

Perform an analysis of spacecraft subsystems and determine the interrelationships among them. Optimize the tradeoffs between the interrelate subsystems. The primary subsystems considered shall be:

1. Power System

2. Communications System

　　　　3.　Antenna and Feed System

　　　　4.　Attitude, Station Repositioning, and Station keeping Systems

　　　　5.　Thermal Control System

4.8　Define ascent trajectories and launch sequences through injection into the required orbit.

4.9　Determine the required ground support system for transmitting up to the spacecraft and for the receiving of the spacecraft signals and evaluation of spacecraft performance.

4.10　Determine the ground support equipment required from launch through orbit injection.

4.11　Provide the following for each spacecraft configuration:

　　　　1.　Artists drawings of the spacecraft in orbit.

　　　　2.　Slides of (1.) above.

4.12　Two presentations will be made at LeRC.

　　　4.12.1　An informal mid-term review.

　　　4.12.2　A formal presentation within 30 days after the completion of the study. This presentation will include a summary of all the work done during the contract period, giving the study results and conclusions. The presentation shall be implemented by charts, graphs, and/or diagrams. Such documentation shall be furnished to the NASA Project Manager in 50 copies at the time of the presentation.

5.0　DELIVERABLE ITEMS

The Contractor shall deliver the items made under 4.11 to LeRC within fifteen (15) days after completion of the contract.

6.0　REPORTING REQUIREMENTS

6.1　Technical, financial and schedular reporting shall be in accordance with the attachment entitled "Reports of Work (with contract progress schedule form NASA-C-63)", which is hereby made a part of this contract.

6.2　The monthly report submission date shall be 20 days after the closing date of the Contractor's accounting month.

6.3 The number of copies to be submitted for each monthly report is as follows:

6.3.1 A maximum of 20 copies of Monthly Technical Narratives

6.3.2 A maximum of 20 copies of Contract Progress Schedule

6.3.3 A maximum of 5 copies of Contractor Financial Management Report

6.4 The categories for the Schedular (NASA-C-63) and the Financial Management (NASA 533b) reporting shall be:

6.4.1 Schedular (NASA Form C-63)

1. Mission Analysis   2. Primary Experiment Design
3. Spacecraft Design   4. Program Planning

6.4.2 Financial Management (NASA Form 533b)

Total direct cost and man-hours for each of the items in 6.4.1

Overhead

Other costs

G & A

Fee

6.5 <u>Final Report</u>

6.5.1 Ten (10) copies of the rough draft of the final report shall be submitted to NASA for review and approval within ten (10) days of the conclusion of the technical effort. Change first sentence in Paragraph C.1. FINAL REPORT of Reports of Work attachment to read ten (10) in lieu of four (4) copies and ten (10) in lieu of thirty (30) days.

6.5.2 It is desired that the final report be issued in less than seven (7) months from the date of award of contract.

6.5.3 A maximum of 150 copies of the final report shall be issued by the Contractor at the direction of NASA.

The following changes to the Statement of Work were made in accordance with Supplemental Agreement No. 1, dated 10 December 1971 to Contract NAS 3-14359:

1. On Page 1 of EXHIBIT "A" of the contract delete paragraph 2.1.2 in its entirety and substitute therefor the following:

   "2.1.2 To develop the technology for the controlled illumination of desired areas of the earth, which shaped multibeam transmission, using antennas producing contoured beam patterns having maximum contour curvature of 0.1 radian and minimum contour curvature of 0.004/radian."

2. On page 3 of EXHIBIT "A" of the Contract delete 3.15.1 "EXPERIMENTS" paragraph 2 in its entirety and substitute therefor the following:

   "3.15.1 EXPERIMENTS

   2. Controlled illumination of desired areas on earth by spaceborne antennas having multibeam, contoured patterns. The contoured patterns shall be other than circular or elliptical and have contour curvature not greater than 0.1 radian and a minimum contour curvature of 0.008 radian. Contour curvature shall be defined as $\frac{1}{d}$ where r is the radius of curvature of the half power contour measured in a plane normal to the direction of propagation and located at a distance d from the source."

APPENDIX B

REFERENCES AND BIBLIOGRAPHY

APPENDIX B   ATS/AMS BIBLIOGRAPHY

1 FOSDICK, G.E., MORGENTHALER, G.W., CERVI, J.E.,(MARTIN CORP.)
   -THE IMPACT OF INFO SAT. ON EVERYDAY LIVING
   -PAPER PRES. AT OPER RESEARCH SOC. OF AMER. MTG., NOV. 6-9, 1968

2 MARSTEN, R.B. AND GUBIN, S.(RCA)
   -A DIRECT-TO-HOME TV SATELLITE SYSTEM FOR 1970 (AIAA 66-30_)
   -PAPER PROPOSED FOR AIAA AT WASH. D.C., MAY 2-4, 1966

3 BERGIN, P.A.(CONVAIR/GEN. DYNAMICS)
   -A TELEVISION BROADCAST SATELLITE SYSTEM FOR ETV/ITV -AIAA 70-452
   -PAPER PRES. AT AIAA MTG. AT LOS ANGELES, APRIL 6-8, 1970

4 KIESLING, JOHN D. AND MEYERHOFF, HENRY J.(COMSAT LAB.)
   -TV SATELLITE DIST. AT FREQ. ABOVE 10 GHZ (AIAA 70-454)
   -PAPER PRES. AT AIAA MTG. AT LOS ANGELES, APRIL 6-8, 1970

5 FREEMAN, K.G., JACKSON, R.N.(MULLARD RESEARCH LAB., ENGLAND)
   -SOME ASPECTS OF DIRECT TELEVISION RECEPTION FROM SAT.
   -PAPER PUB. IN PROC. IEE, VOL. 117, NO. 3, MARCH 1970

6 LOWENHAR, HERMAN (ASSOC. ED., SPACE/ASTRONAUTICS)
   -TV DISTRIBUTION FROM SPACE
   -PAPER PUB. IN SPACE/ASTRONAUTICS MARCH 1969

7 MARSTEN, R.B.(RCA)
   -OPERATIONAL TELECASTING BY SPACECRAFT AFTER 1975
   -PAPER PRES. AT AMER. ATRONAUT. SOC. MTG. FEB. 21-23 1966

8 JANSEN, J. AND JORDAN P.L.(TRW INC.)
   -TELEVISION BROADCAST SATELLITE STUDY (NASA CR-72510)
   -DOC. PREPARED FOR NASA LEWIS(R.E. ALEXOVICH) OCT. 24, 1969

9 HESSELBACHER, R.W. (GE)
   -TV BRDCST SAT. STY. R. AND TEC. IMPLIC. RPT.(NASACR-72511)
   -DOC. PREP. FOR NASA LEWIS(R.E. ALEXOVICH) OCT. 6, 1969

10 HERRON, B.G., CREED, D.E., OPJORDEN, R.W., TODD, G.T.,(HUGHES)
   -HIGH VOLTAGE SOLAR ARRAY CONFIGURATION STUDY(NASA CR-72724)
   -DOC. PREP. FOR NASA LEWIS(B.L.SATER) JULY 1970

11 CLARK, RICH(HUGHES)
   -PROP. FOR LIQ. METAL SLIP RING EXP. FOR ATS-G S/C(SSD-90361P)

12 WOLFF, GEORGE (HUGHES)
   -SECOND SEMI. LARGE RETRACT. SOLAR CELL ARRY PRES.(SSD-90278B)

13 WOLFF, GEORGE (HUGHES)
   -FOURTH SEMI. FLX. ROLLED-UP SOL. CELL ARRY PRES.(GA-07185)

14 CLARK, RICH (HUGHES)
   -PROP. TO DEV., DSGN., AND FAB. LIQ. MTL. SLIP RNG/SOL. ARRAY
   -MECH.(SSD-00282P) (JUNE 1970)

15 WOLFF, GEORGE (HUGHES)
   -LARGE RETRACT. SOL. CELL ARRY PWR SYS. FOR ATS-G S/C(SSD 90473P)

16 WALP, ROBERT (HUGHES)
   -HIGH PWR 12GHZ EXP. FOR ATS-G S/C (SSD 00246P) (MAY 1970)

17 BERGIN, P. (CONVAIR-G/D)
   -TELEVISION BROAD. SAT. STUDY, MID. PRESENTATION
   -DOC. PREP. FOR NASA MARSHALL(E.C. HAMILTON) JULY 1969

18 GENERAL ELECTRIC DOCUMENT
   -MULTIKILOWATT TRANS. STUDY FOR SPACE COMM. SAT.(DOC.NO.68SD4268)
   -DOC. PREP. FOR NASA MARSHALL, JUNE 1968

19 HAC PROPOSAL
   -LARGE SPACE STA. SOL. ARRY TECH. EVAL. PROG.(SSD 00075P) FEB 70

20 PAWLIK, E.V., COSTOGUE, E.N., FERRERA, J.D., MACIE, T.W.(JPL)
   -SOLAR ELECTRIC PROPULSION SYSTEM EVALUATION
   -PAPER PUB. IN J. SPACECRAFT, VOL 7, NO. 8

21 RUTSTEIN, IRVING (GE)
   -KEY TECHNOLOGIES FOR HIGH POWER BROADCAST SATELLITES-AIAA69-1069
   -PAPER PRES. AT AIAA MTG. AT ANAHEIM, OCT 20-24, 1969

22 WOLFF, GEORGE (HUGHES)
   -ORIENTED FLEXIBLE ROLLED-UP SOLAR ARRAY (AIAA 70-738)
   -PAPER PRES. IN LOS ANGELES, APRIL 6-8, 1970

23 BELOHOUBEK, E., PRESSER, A., STEVENSON, D., ROSEN, A., (RCA)
   -S-BAND CW POWER MODULE FOR PHASED ARRAYS
   -PUB. IN THE MICROWAVE JOURNAL, JULY 1970

24 HARDEMAN, LYMAN J. (ASSOC. ED., MICROWAVES)
   -PHASED ARRAYS SCAN RAPIDLY TOWARDS GROWTH IN THE 70'S
   -PUB. IN MICROWAVES, JUNE 1970

25 GLASSOW, FRANK (HUGHES)
   -DESPIN TECH. AND APPLICATIONS FOR COMM. SAT. (AIAA 70-459)
   -PAPER PRES. IN LOS ANGELES, APRIL 6-8, 1970

26 READER, P.D. AND REGETZ, J.D.,JR. (NASA LEWIS)
    -A DELTA BOOSTED, ELECTRICALLY RAISED, HIGH PWR. SYNC. SATELLITE
    -PAPER PROPOSED FOR AIAA MTG AT ANAHEIM, OCT 20-24, 1969

27 GHOSH, R. AND HUSON, G. (COMSAT)
   -ACHIEVEMENT OF SYNCHRONOUS ORBIT USING ELECTRIC PROPULSION
   -PAPER PRES. AT AIAA MTG. AT WILLIAMSBURG, VIRGINIA, MAR 3-9,1969

28 RUBIN, P.A., (HUGHES)
   -ETV SATELLITES FOR DEVELOPING NATIONS (AIAA 68-424)
   -PAPER PRES. AT AIAA MTG. AT SAN FRANCISCO, APR 8-10, 1968

29 SWENSEN, R.D., (COMSAT)
   -ECONOMIC COMPARISONS OF DOMESTIC SAT. TV DIST. SYS.(AIAA 68-410)
   -PAPER PRES. AT AIAA MTG. AT SAN FRAN., APR 8-10, 1968

30 GOLDMAN, ALFRED M. JR. (CONVAIR-G/D)
   -A SYSTEM ANAL.OF A UHF TV BROAD. SAT. WITH EMPHASIS ON GND REC.
   -REQ.(AIAA 68-420), PAPER PRES. AT S.F., APRIL 8-10, 1968

31 MCCLANNAN, G.B. AND HECKERT, G.P. (PHILCO)
   -A SATELLITE SYSTEM FOR CATV
   -PAPER PUB. IN PROC. OF IEEE, VOL. 58, NO. 7, JULY 1970

32 BARTZ, DONALD R. (JPL) AND HORSEWOOD, J.L. -ANALYTICAL MECH. ASS.
   -CHAR., CAP., AND COSTS OF SOL. ELEC. S/C FOR PLAN. MISS.(AIAA 69
   -1103), PAPER PRES. AT ANAHEIM, OCT. 20-24, 1969

33 KRAEMER, ROBERT S. (NASA HEADQUARTERS)
   -A FORECAST OF ELECTRICALLY-PROPELLED S/C APP. (AIAA 69-1108)
   -PAPER PRES. IN ANAHEIM, OCT 20-24, 1969

34 SARKAR, S.K.   (PTT RESEARCH LABS., BERNE, SWITZERLAND)
   -TV BROADCAST SATELLITE DIRECT-TO-HOME
   -21ST INT. ASTRONAUT. CONG., WEST GERMANY, OCT. 4-10, 1970

35 COWAN, J.H., ZIERMAN, C.A., (PHIHCO-FORD)
   -A MULTI-BEAM ANTENNA SYSTEM FOR A REGIONAL COMM. SAT.
   -IEEE PROCEEDINGS, SAN FRANCISCO, JUNE 8-10, 1970, VOL. 2

36 HESLER, J.P., WHITE, O.S., (GENERAL ELECTRIC CO.)
   -LOW COST GROUND CONVERTERS FOR HIGH POWER COMM. SATELLITES
   -AIAA 70-440, LOS ANGELES, APR. 6-8, 1970

37 JANKOWSKI, H. (GENERAL ELEC. CO.)
   -HIGH POWER TRANSMITTERS FOR SPACE
   -AIAA 70-436, LOS ANGELES, APR. 6-8, 1970

38 RAMINS, P. (NASA LEWIS)
   -TUBES FOR HIGH POWER MICROWAVE TRANSMISSION IN SPACE
   -AIAA 70-435, LOS ANGELES, APR. 6-8, 1970

39 LIPSCOMP, E.T. (CONVAIR, G/D)
   -HI-PWR SPACEBORNE TV XMTR DESIGN TRD/OFFS FOR 1970-1985 PERIOD
   -AIAA 70-434, LOS ANGELES, APR. 6-8, 1970

40 FOSTER, D.E., HANSON, K.L., RASMUSSEN, R., WEINBERGER, S.M. (GE)
   -PWR SOURCES, TRANSFER, AND COND. FOR HIGH PWR COMM. SATTELITES
   -AIAA 70-433, LOS ANGELES, APR 6-8, 1970

41 HUGHES DOCUMENT
   -REPEATER TECHNOLOGY STUDY APPROACH FOR ADVANCED MULTI-FUNCTIONAL
   -COMM. SATELLITES, SCG 10069R, MARCH 1971

42 PRASADA, B., SINGH, J.P. (INDIAN INST. OF TECHNOLOGY)
   -ACME- A HYBRID AIRBORNE SAT. TV AND COMM. SYSTEM FOR INDIA
   -AIAA 70-472, LOS ANGELES, APR 6-8, 1970

43 SIMMONS, N. (BRITISH INTERPLANETARY SOCIETY)
   -SOME POSS. CONCEPTS FOR A 2ND PHASE OF COMM. SAT. DEV. IN EUROPE
   -9TH EUROPEAN SPACE SYMPOSIUM, LONDON, MAY 14-16, 1969

44 GILBERT, P.C., JEFFERIS, A.K., POPE, D.G.(GEN. POST OFF.,LONDON)
   -SAT. TV DIST.- SERVICE FROM GEOSTAT. SAT. TO COMMUN. ANT. IN
   -MULTI-COVERAGE AREAS, IEE PROC., VOL 116, PP. 1501-1504

45 SITARAM, H. (INST. OF ENG., INDIA)
   -A PROP. NAT. SYS. FOR TV DIST. THROUGH SAT. FOR INDIA
   -JOURNAL, ELEC. AND TELECOM. ENG. DIV., VOL. 49, PP. 50-53

46 CONFERENCE RECORD
   -COMM. IN THE SPACE AGE- THE USE OF SAT. BY THE MASS MEDIA
   -UNESCO CONFERENCE, PARIS, DEC 19, 1965

47 ROSEN, H.A. (HUGHES)
   -SAT. SYSTEM FOR EDUCATIONAL TV
   -UN CONF. ON THE EXPLOR. AND PEACE. USES OF OUTER SPACE, VIENNA,
   -AUSTRIA, AUG. 14-27, 1968

48 NAGARAJAN, M.S., NERURKAR, B.Y., RAO, B.S. , SITARAM, H., VEPA,P.
   -SAT. TV- A SYS. PROPOSAL FOR INDIA
   -UN CO. ON EX. AND PE. USES OF OU. SP., VIENNA, AUG. 14-27, 1968

49 OLDEKOP, W., QUAST, A., RASCH, W., SCHARF, W.
   -CONC. STDY. OF SAT. FOR DIR. TV BCST. WI. INCORE-THERMIONIC-REAC
   -AND ELEC. PROP, UN CO. ON EX. AND PE. USES OF OU.SP., AUG. 1968

50 KOCH, G.M., (RCA, CANADA)
   -HIGH POWER AMP. IN SAT. COMM. SYS.
   -PROC. 6TH INTER. CONF. ON MICRO. AND OPTICAL GEN. AND AMPL.,
   -CAMBRIDGE, ENGLAND, SEP. 12-16, 1966

51 MORENO, T. (VARIAN ASSOC.)
   -HIGH-PWR. LINEAR-BEAM TUBES
   -WEST. ELEC. SHOW AND CONV., LOS ANGEL., AUG. 23-26, 1966 (PAPER)

52 CHADWICK, G.G., KORVIN, W. (NASA GODDARD)
   -LATEST WORD IN SPACE TALK- IT CAN COME FROM ANYWHERE
   -ELECTRONICS, VOL. 39, MAY 30, 1966

53 BRANCH, G.M. (GEN. ELEC.)
   -CIRC. EFF. ENHANCEMENT STUDIES AT 12GHZ
   -FINAL REPORT, NASA-CR-72696

54 JANSEN, J. (TRW SYSTEMS)
   -TV BCAST. SAT. STUDY RESEARCH AND TECH. IMPLIC. RPT.
   -REPORT, NASA-CR-72637

55 TRANSLATION FROM FRENCH
   -PRELIMINARY TECHNICAL STUDY OF A DIRECT TELECAST SAT.
   -PARIS, CNES, 1968

56 REPORT NASA-CR-101406
   -USEFUL APPLICATIONS OF EARTH-ORIENTED SATELLITES
   -NAT. ACAD. OF SCIENCES- NAT. RESEARCH COUN., WASH. DC

57 DUCK, K.I., BARTLETT, R.O., AND SULLIVAN, R.J. (NASA)
   -EVAL. OF AN ION PROP. SYS. FOR A SYNC. SPACECRAFT MISSION
   -AIAA 67-720,NEW YORK, SEPT. 1967

58 BRANCH, G.M., MIHRAN, T.G. (GEN. ELECTRIC)
   -ANAL. DESIGNS OF A SPACE-BORNE MAG. FOCUSED KLYS. AMP.
   -REPORT NASA-CR-72461, OCT. 25, 1968

59 STANFORD UNIV. REPORT
   -ADVANCED SYS. FOR COMM. AND ED. IN NAT. DEV.
   -FINAL REPORT, JUNE 1967

60 HULT, J.L. (RAND CORP.)
   -SAT. AND FUTURE COMM., INCLUDING BROADCAST
   -13TH ANN. MTG. OF AMER. ASTRONAUTICAL SOC., DALLAS, MAY 1-3,1967

61 BARTLETT, H.E., AND OISHI, R.K. (RADIATION, INC.)
   -STUDY OF SPEC. BEAMSPADING ANT.
   -3RD QUART. RPT., 1 MAR- 31 AUG. 1965

62 FELDMAN, N.E. (RAND CORP.)
   -COMM. SAT. OUTPUT DEVICES
   -RPT. ASA-CR-70037 JUNE 1965

63 HUFF, R. (OHIO STATE UNIV.)
   -ARRAY APP. TO SAT. COMM. PROB.- PHASED TRANS.AND MULT. ACC. TECH
   -FINAL REPORT- 11 JAN 65- 25 JAN 1967

64 BURT, E.G.C. (ROYAL AIRCRAFT ESTABLISHMENT)
   -ON SPACE MANOEUVRES WITH CONTINUOUS THRUST
   -PAPER PUB. IN ARS JOURNAL, VOL. 31, NO. 8, AUG. 1961

65 ALLEN, R.D., WILLIAMS, R.E., LAKE, B., AND WELLMAN, A.J.(RYAN C.)
   -FEASIBILITY STUDY, 30 WATTS PER POUND ROLL-UP SOLAR ARRAY
   -REP. 40067-4, NASA CR-97205, JUNE 1968

66 SHEPARD, N.F. (GEN. ELECTRIC CO.)
   -FEASIBILITY STUDY,30 WATTS PER POUND ROLL-UP SOLAR ARRAY
   -REP. 68SD4301,NASA CR-96230, JUNE 1968

67 DILLARD, P.A. (TRW SYSTEMS)
   -40 WATTS/POUND SPACECRAFT SOLAR ARRAYS
   -PROCEEDINGS OF THE 4TH INTERSOC. ENER. CONVERSION ENG CONF SEP69

68 PHILCO-FORD CORP.
   -ANTENNA PATTERN SHAPING, SENSING, AND STEERING STUDY
   -REP. TR-DA2052, MAY 1968 (NASA CONTRACT NAS3-11525)

69 SYLVANIA ELECTRIC PRODUCTS, INC.
   -ANTENNA PATTERN SHAPING, SENSING, AND STEERING STUDY
   -REPORT, MAY 1969 (NASA CONTRACT NAS3-11524)

70 HUGHES PROPOSAL
   -A HIGH POWER 12GHZ TRANS. EXP. FOR PARTICIPATION IN ADVANCED
   -APPLICATIONS FLIGHT EXPERIMENTS(AAFE), MARCH 1971

71 NASA-LEWIS RESEARCH CENTER TECHNICAL REPORT
   -DISASTER WARNING SATELLITE STUDY
   -MARCH, 1971

72 F.W. FIELD (HUGHES)
   -USER ANAL. SUMM., LAW ENFORCEMENT W/B INFO. TRANSFER
   -RPT. 4092.2/001, 11 NOV 70, CONTRACT NAS 2-5571

73 PROPOSAL FOR A GIGABIT CO2 COMMUNICATIONS EXPERIMENTS FOR PARTICI-
   PATION IN ADVANCED FLIGHT EXPERIMENTS (AAFE)
   -HUGHES REF. NO. 71(41)-2382/C4106-SCG 10118P   MARCH 1971

74 EGGERT, DENNIS
   -STUDY OF A LOW ALTITUDE SATELLITE UTILIZING A DATA RELAY SATELLITE
     SYSTEM
   -PHASE 1 / FINAL REPORT   CONTRACT NO. NAS 5-11602
   -HUGHES REFERENCE NO. B6560 - SSD 90008R

75 KLESTADT, B. - IDC 4113.10/11   APRIL 2, 1971
   -APPLICATION OF 'STARS' TO PRECISION ATTITUDE SENSING AND CONTROL
     IN SYNCHRONOUS ORBIT.

76 KRIMGOLD, D. B. — IDC 2223/3423   6 NOVEMBER 1969
  —DIGITAL SIMULATION OF A GAS JET CONTROLLED VEHICLE WITH N
  APPENDAGE, ORIENTABLE IN TWO AXES RELATIVE TO THE VEHICL .

77 FISCHER, J. IDC HS-207/J/MI   6 NOVEMBER 1969
  —ANALOG SIMULATION OF LRSCA-AGENA VEHICLE INTERACTIONS

77 OLSCA — ORIENTATION LINKAGE FOR A SOLAR CELL ARRAY
  —TECHNICAL REPORT AFAPL-TR-68-76,   JULY 1968

APPENDIX C

TRANSMISSION PERFORMANCE CALCULATIONS

APPENDIX C

TRANSMISSION PERFORMANCE CALCULATIONS

A.   Analog Television Transmission

The discussion in this report is based upon the U.S. 525-line NTSC color system with a 4.2 MHz baseband. Performance calculations could be carried out just as well for any other subcarrier color system and base bandwidth; however, the numerical results obviously would be expected to be different.

In the NTSC color television system, the demodulated baseband signal strongly resembles the standard monochrome signal. Color information is added to the basic black and white luminance signal in the form of a chrominance subcarrier, the sidebands of which modulate the luminance components. The instantaneous phase of the subcarrier relative to a color burst transmitted once every line indicates the exact hue of the scanned object at any instant. Furthermore, the amplitude of the subcarrier determines the degree of saturation of the resulting color, e.g., light pink or dark crimson.

In monochrome transmission, the main portion of the signal energy is concentrated at the lower end of the baseband. Therefore, a minor aberration in the frequency characteristics of the transmission medium at the higher end of the band does not cause serious degradation of the reproduced image. In color transmission, however, the frequency components of the added chrominance signal lie near the upper end of the baseband and therefore any high frequency defects of the medium degrade the faithful reproduction of the color information. In order to reduce these effects on the reproduction of color television, the technique of pre-emphasis is used. By this means, the low frequency high amplitude components of the signal, the most important contributors to luminance amplitude, are somewhat reduced and the color subcarrier, although increased, causes the frequency modulated carrier to deviate more nearly about the center of the FM bandwidth thereby improving linearity of transmission of the color subcarrier. The degree of improvement achieved in this fashion is commonly quoted as 3 dB.

The Bell System has found by practical experience and by a number of subjective tests that the signal-to-noise ratio requirement for NTSC signals is the same as that already derived for monochrome signals. For monochrome the overall Bell System network signal-to-weighted noise requirement is 53 dB peak-to-peak video (including sync tips) to weight RMS noise. In terms of the actual delivered information, the 53 dB number converts to 50 dB peak-to-peak picture. The CCIR objective for a hypothetical reference circuit is 6 dB higher, that is, 56 dB peak-to-peak picture to weighted RMS noise. Although no agreed upon CCIR objective exists for color television, it is assumed, as the Bell System does, that color signal-to-noise requirement is no higher than monochrome. (Table 1 gives the relationship between several SNR standards and Table 2 explains the TASO quality standards.

The overall signal-to-noise ratio is (SNR) = net carrier-to-noise ratio plus FM improvement factor plus miscellaneous fixed improvement and conversion factors. The last term in this equation will now be evaluated.

The desired quantity, SNR, is stated in terms of peak-to-peak picture. Calculations are more easily performed, however, in terms of a hypothetical sinusoid whose peak-to-peak amplitude corresponds to the maximum radio frequency swing, i. e., that produced by the total video including the sync tips. Therefore, a part of the miscellaneous conversion factor can be accounted for as follows:

peak-peak picture/peak-peak video = -3 dB
peak-peak/RMS = +9 dB

The weighting factor is usually the amount by which noise, having a triangular voltage spectrum, would be reduced in passing through a network designed to simulate the filtering effect of human vision. The standard noise weighting factor for U.S. television transmission is 10.2 dB.

The peak-to-peak picture to weighted RMS noise ratio now is:

TABLE 1.

Conversion of TV SNR Definitions (in dB) for AM Transmission

From \ To	Bell System	CCIR	DCA	EIA	TASO	TRW
Bell System	0	-2.9	-5.8	-2.2	-3.6	-3.6
CCIR	+2.9	0	-2.9	+0.7	-0.7	-0.7
DCA	+5.8	+2.9	0	+3.6	+2.2	+2.2
EIA	+2.2	-0.7	-3.6	0	-1.4	-1.4
TASO	+3.6	+0.7	-2.2	+1.4	0	0
TRW	+3.6	+0.7	-2.2	+1.4	0	0
Table 1 $(\frac{P}{N_o W})$	+2.0	-0.9	-3.8	-0.2	-1.6	-1.6

P = peak RF power

N_o W = mean-square noise in channel bandwidth

TABLE 2.

TASO Quality Grades

Grade	Description	Signal-to-noise ratio (db) adequate for given percentage of viewers		
		25%	50%	75%
Excellent	Extremely high quality	38	44	50
Fine	High quality, enjoyable viewing, but perceptible interference	30	34	38
Passable	Acceptable quality, interference not objectionable	25	27	30
Marginal	Poor quality. Improvement desirable, interference somewhat objectionable	21	23	25
Inferior	Very poor quality, could be watched, interference definitely objectionable	15	17	19
Unusable	Picture too bad to be watched	12	14	16

$(SNR)_w$ = RMS signal-to-unweighted, unpre-emphasized RMS noise ratio + 9 dB (peak-peak/RMS) - 3 dB (picture/video) + 13.2 dB (pre-emphasized and weighted)

For the 4 MHz NTSC system, the performance objective equation can be stated as:

$$(SNR)_w = 10 \log (B_{rf} - 8 \times 10^6)^2 + 10 \log (C/N)_{IF} + 10 \log B_{rf} - 185.8$$

For the CCIR and TASO performance objectives previously cited, the relationship between net predetection carrier-to-noise ratio and RF bandwidth occupancy is shown in Figure 1. The figure shows that for any practical demodulator bandwidths, i.e., up to 40 MHz for CCIR quality, the system must always operate, to a greater or lesser extent depending on the bandwidth used, above the demodulator thresholds to achieve the performance quality objective. This is shown clearly in Figure 2 for several RF bandwidths. Note, however, that the lower SNRs will permit operation at or near the thresholds.

Figure 2 also shows the required predetection carrier-to-noise ratio required for any other performance quality criterion one might wish to choose.

One further area of interest which remains to be accounted for is the connection between the previously discussed parameters and signal quality and the pertinent satellite and earth station parameters. Certain assumptions are made regarding the characteristics of the satellite and earth station in order to calculate the combinations of EIRP and earth station G/T as functions of the RF bandwidth employed.

The values assumed are as follows:

Total downlink path loss at 12 GHz	-205.2 dB
Additional path loss to stn at 37° N. lat.	- 0.4 dB
Additional atmospheric attenuation exceeded 0.1% of the time	- 3.0 dB

Earth station antenna pointing loss (function of diameter) for 2' dish	- 0.3 dB
Receiver RF loss	- 1.0 dB
Spacecraft RF loss	- 1.0 dB
Demodulator thresholds:	
Discriminator	10.0 dB
Phase locked loop	6.0 dB

Using these assumptions and reiterated link calculations, one obtains a useful set of design curves as shown in Figure 3.

B. Digital Data Transmission

To determine the relationship between spacecraft RF power and transmitted data rate, we first assume a bit error probability of 10^{-5}. With PCM/PSK transmission, a realistically practical bit energy-to-noise density ratio (E_b/N_o) is 11 dB.

The relationship is given as follows:

$$\frac{E_b}{N_o} = \frac{P_T\, G_S\, A\text{ eff}}{K\, T\, 4\pi d^2\, r} = \frac{P_T\, G_S\, (0.55)\, \pi D^2/4}{K\, T\, 4\pi d^2\, r}$$

where:

r = data rate (variable)

$P_T\, G_S$ = EIRP (variable)

E_b/N_o = 9.55 dB (theoretical); 11 dB (practical) = 12.6 (numerics)

d = 41,200 km

K = 1.38 x 10^{-23} watts/$^\circ$K Hz

$$12.6 = \frac{(0.55)\,(\text{EIRP})\,(D)^2}{(1.38 \times 10^{-23})\,(16)\,(T)\,(4.12 \times 10^7)^2\,(r)}$$

$$\boxed{8.5 \times 10^{-6}\,(r) = (\text{EIRP})\,D^2/T}$$

Figure 4 shows this relationship graphically. A 3-dB atmospheric attenuation allowance and 1 dB each for transmit and receive RF loss has been included.

525- LINE NTSC COLOR TELEVISION
    4.2 MHZ BASEBAND
    FM TRANSMISSION

PICTURE QUALITIES:

$$\frac{PEAK\text{-}TO\text{-}PEAK \ PICTURE \ SIGNAL}{WEIGHTED, \ PRE\text{-}EMPH. \ RMS \ NOISE} = \begin{array}{ll} 56 \ dB & FOR \ CCIR \\ 44.7 \ dB & FOR \ TASO \ 1 \\ 34.7 \ dB & FOR \ TASO \ 2 \end{array}$$
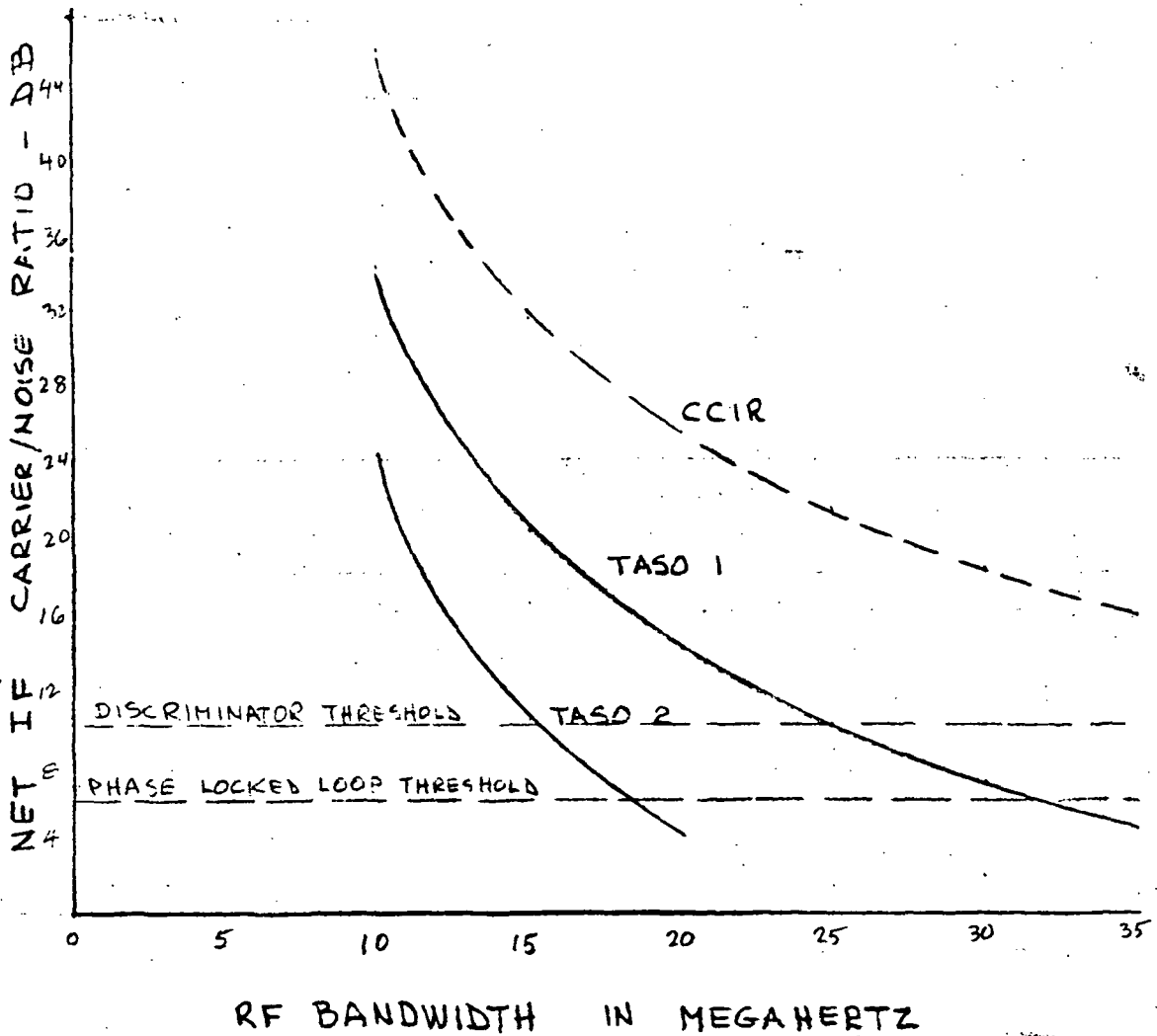
Figure C-1. Television Quality vs RF Channel Performance

NTSC COLOR TV USA SYSTEM
4.2 MHz BASEBAND
S/N vs C/N
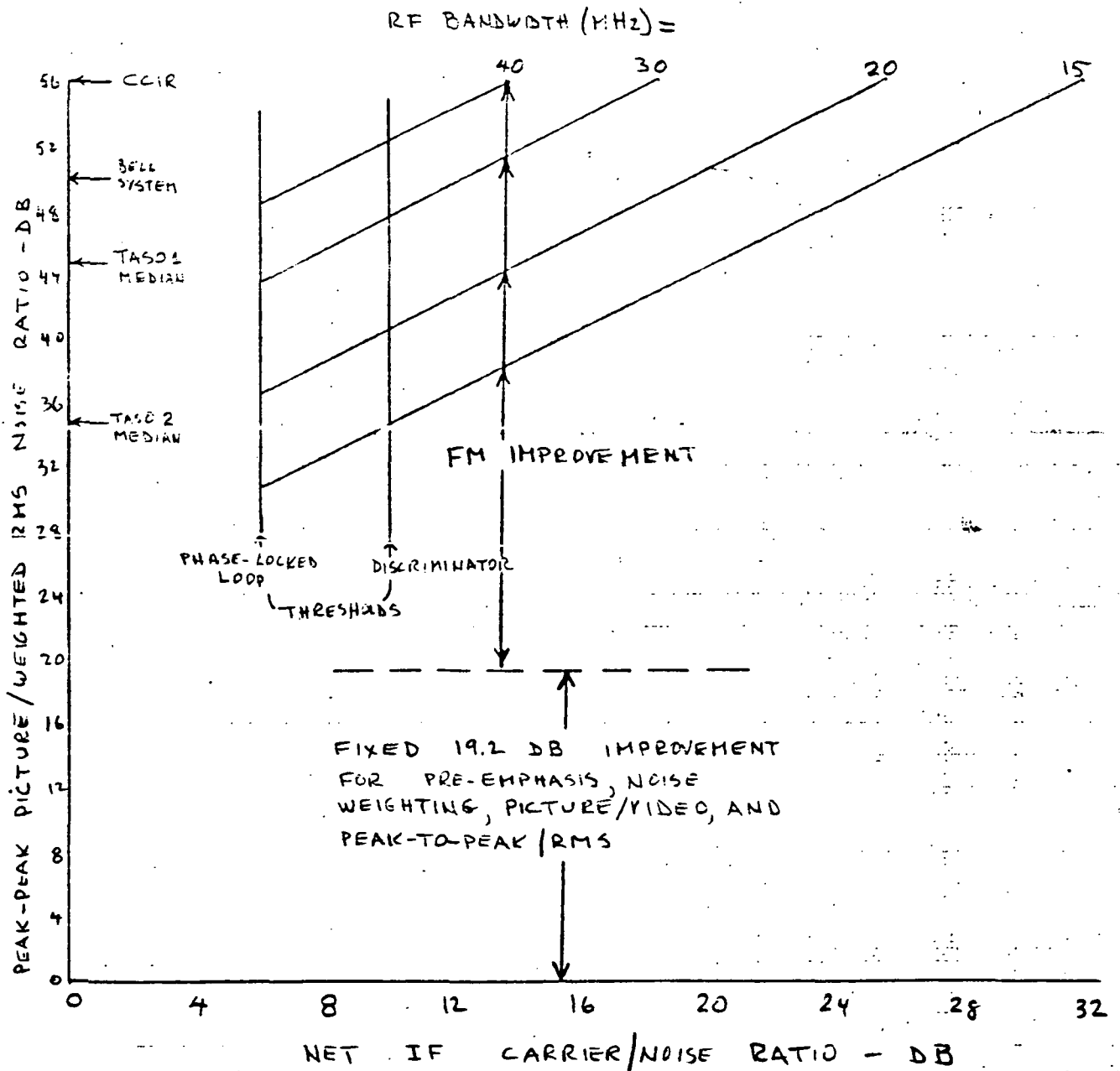
RF BANDWIDTH (MHz) =

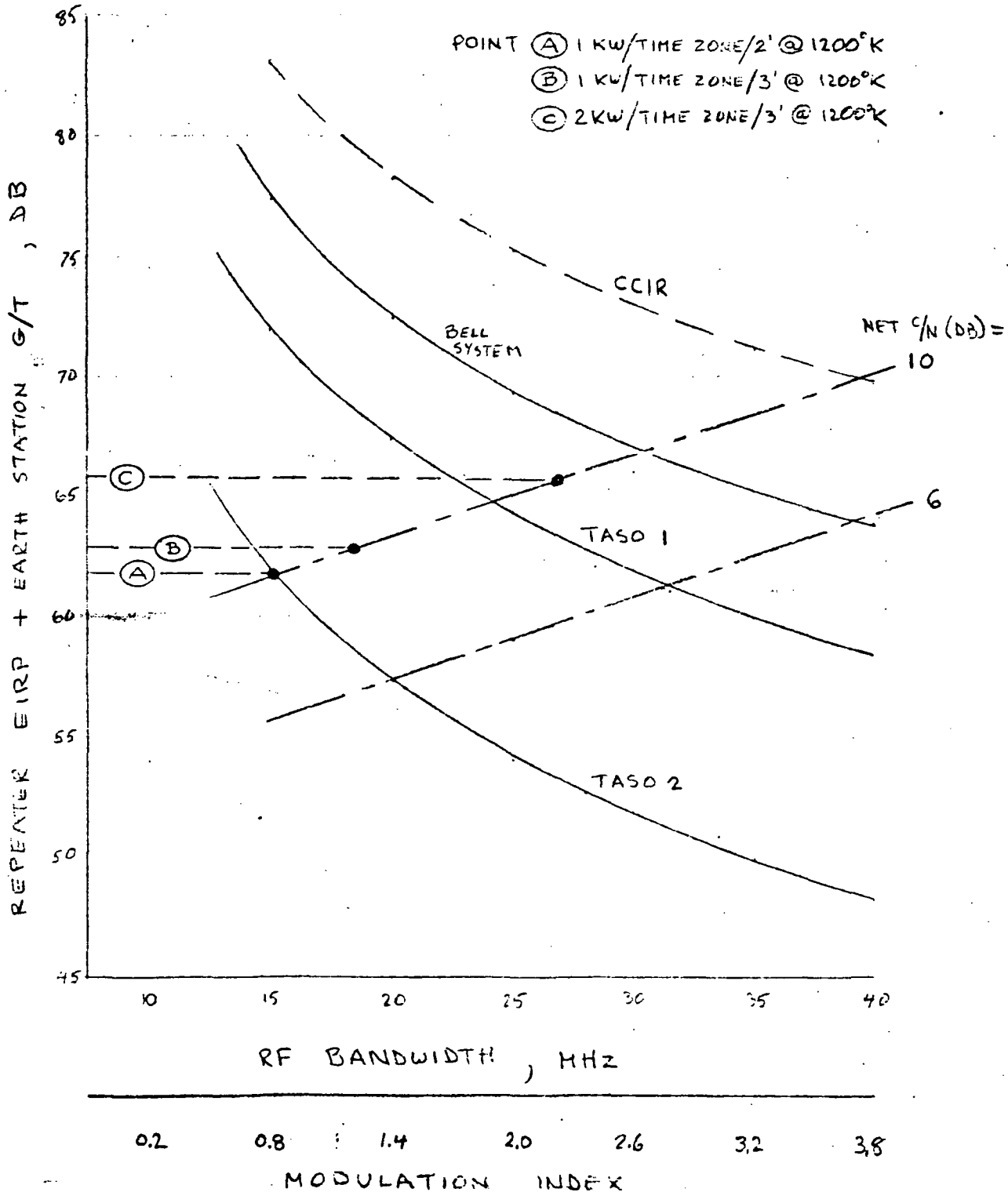Figure C-2. Television Channel Performance vs RF Bandwidth
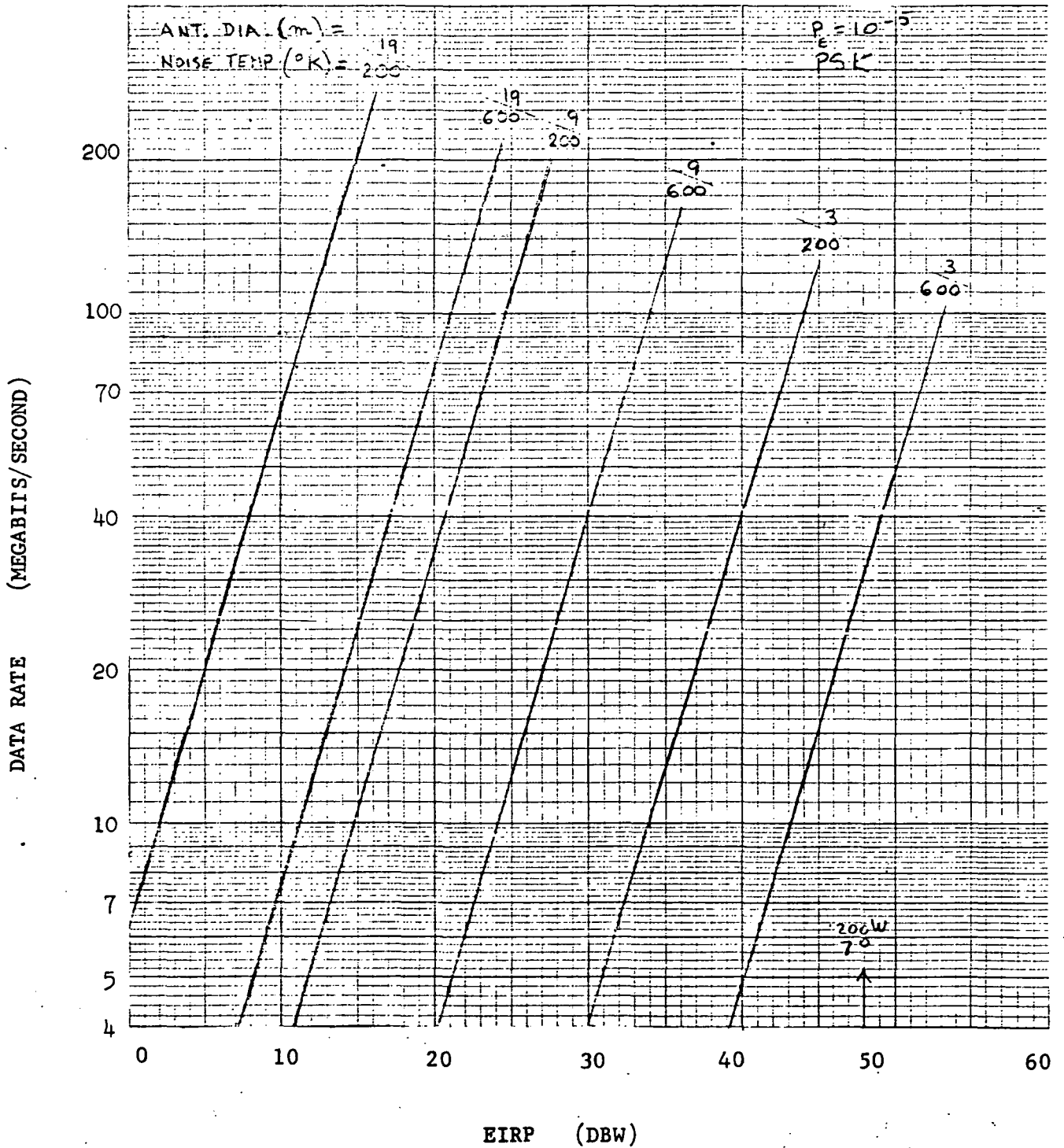
Figure C-3. Television Channel Performance at 12 GHz

Figure C-4.   Digital Communications System Performance